FINAL TECHNICAL REPORT

National Aeronautics and Space Administration
Grant NSG-3048: ALTERNATIVES FOR JET ENGINE CONTROL
March 1, 1975 - May 31, 1985

Volume 1: Modelling and Control Design with Jet Engine Data

Michael K. Sain

ABSTRACT

This document compiles a comprehensive list of publications supported by, or related to, National Aeronautics and Space Administration Grant NSG-3048, entitled "Alternatives for Jet Engine Control". Dr. Kurt Seldner was the original Technical Officer for the grant, at Lewis Research Center. Dr. Bruce Lehtinen was the final Technical Officer. At the University of Notre Dame, Drs. Michael K. Sain and R. Jeffrey Leake were the original Project Directors, with Dr. Sain becoming the final Project Director.

Publications cover work over a ten-year period. The Final Report is divided into two parts. Volume 1, "Modelling and Control Design with Jet Engine Data", follows in this report. Volume 2, "Modelling and Control Design with Tensors", has been bound separately.

TABLE OF CONTENTS BY TITLE

BIBLIOGRAPHY

1. V. Seshadri, "Compensation of Multivariable Control Systems", Masters Thesis, Department of Electrical Engineering, University of Notre Dame, Notre Dame, Indiana, May 1976.

2. Raghvendra R. Gejji, "Polynomial Techniques Applied to Multivariable Control", Masters Thesis, Department of Electrical Engineering, University of Notre Dame, Notre Dame, Indiana, May 1976.

3. M.K. Sain, R.J. Leake, R. Basso, R. Gejji, A. Maloney, and V. Seshadri, "Alternative Methods for the Design of Jet Engine Control Systems", Proceedings Fifteenth Joint Automatic Control Conference, Pages 133-142, July 1976.

4. Anthony J. Maloney III, "Graphics Analysis of Dominance in Jet Engine Control Models", Masters Thesis, Department of Electrical Engineering, University of Notre Dame, Notre Dame, Indiana, August 1976.

5. Raghvendra R. Gejji and Michael K. Sain, "A Jet Engine Control Problem for Evaluating Minimal Design Software", Proceedings Nineteenth Midwest Symposium on Circuits and Systems, Pages 238-243, August 1976.

6. V. Seshadri and M.K. Sain, "Interaction Studies on a Jet Engine Model by Characteristic Methodologies", Proceedings Nineteenth Midwest Symposium on Circuits and Systems, Pages 232-237, August 1976.

7. Peter W. Hoppner, "The Direct Approach to Compensation of Multivariable Jet Engine Models", Masters Thesis, Department of Electrical Engineering, University of Notre Dame, Notre Dame, Indiana, May 1977.

8. R. Michael Schafer, "A Graphical Approach to System Dominance", Masters Thesis, Department of Electrical Engineering, University of Notre Dame, Notre Dame, Indiana, May 1977.

9. R.M. Schafer, R.R. Gejji, P.W. Hoppner, W.E. Longenbaker, and M.K. Sain, "Frequency Domain Compensation of a DYNGEN Turbofan Engine Model", Proceedings Sixteenth Joint Automatic Control Conference, Pages 1013-1018, June 1977.

10. R.R. Gejji and M.K. Sain, "Application of Polynomial Techniques to Multivariable Control of Jet Engines", Proceedings Fourth Symposium on Multivariable Technological Systems, International Federation of Automatic Control, Pages 421-429, July 1977.

11. R. Gejji, R.M. Schafer, M.K. Sain, and P. Hoppner, "A Comparison of Frequency Domain Techniques for Jet Engine Control System Design", Proceedings Twentieth Midwest Symposium on Circuits and Systems, Pages 680-685, August 1977.

12. R. Michael Schafer and Michael K. Sain, "Some Features of CARDIAD Plots for System Dominance", Proceedings IEEE Conference on Decision and Control, Pages 801-806, December 1977.

13. Michael K. Sain, Joseph L. Peczkowski, and James L. Melsa, Editors, Alternatives for Linear Multivariable Control, Chicago: National Engineering Consortium, 1978.

14. M.K. Sain, "The Theme Problem", Alternatives for Linear Multivariable Control, M.K. Sain, J.L. Peczkowski, and J.L. Melsa, Editors, National Engineering Consortium, 1977, Pages 20-30.

15. R.M. Schafer and M.K. Sain, "Input Compensation for Dominance of Turbofan Models", Alternatives for Linear Multivariable Control, M.K. Sain, J.L. Peczkowski, and J.L. Melsa, Editors, National Engineering Consortium, 1977, Pages 156-169.

16. J.L. Peczkowski and M.K. Sain, "Linear Multivariable Synthesis with Transfer Functions", Alternatives for Linear Multivariable Control, M.K. Sain, J.L. Peczkowski, and J.L. Melsa, Editors, National Engineering Consortium, 1977, Pages 71-87.

17. R.M. Schafer and M.K. Sain, "CARDIAD Design: Progress in the Four Input/Output Case", Proceedings Sixteenth Annual Allerton Conference on Communication, Control, and Computing, Page 567, October 1978.

18. Michael K. Sain and R. Michael Schafer, "Alternatives for Jet Engine Control", Proceedings Propulsion Controls Symposium, NASA Conference Publication 2137, Pages 129-138, May 1979.

19. J.L. Peczkowski, M.K. Sain, and R.J. Leake, "Multivariable Synthesis with Inverses", Proceedings Eighteenth Joint Automatic Control Conference, Pages 375-380, June 1979.

20. R. Michael Schafer and Michael K. Sain, "Frequency Dependent Precompensation for Dominance in a Four Input/Output Theme Problem Model", Proceedings Eighteenth Joint Automatic Control Conference, Pages 348-353, June 1979.

21. R. Michael Schafer and Michael K. Sain, "CARDIAD Approach to System Dominance with Application to Turbofan Engine Models", Proceedings Thirteenth Annual Asilomar Conference on Circuits, Systems, and Computers, Pages 78-82, November 1979.

22. Raghvendra R. Gejji, "On the Total Synthesis Problem of Linear Multivariable Control", Ph.D. Dissertation, Department of Electrical Engineering, University of Notre Dame, Notre Dame, Indiana, May 1980.

23. R. Michael Schafer, "On the Design of Dynamical Compensation for Diagonal Dominance", Ph.D. Dissertation, Department of Electrical Engineering, University of Notre Dame, Notre Dame, Indiana, May 1980.

24. Joseph L. Peczkowski and Michael K. Sain, "Control Design with Transfer Functions: An Application Illustration", Proceedings Twenty-Third Midwest Symposium on Circuits and Systems, Pages 47-52, August 1980.

25. Michael K. Sain and Abraham Ma, "Multivariable Synthesis with Reduced Comparison Sensitivity", Proceedings Nineteenth Joint Automatic Control Conference, Paper WP-8B, August 1980.

26. R. R. Gejji, "Reliable Floating Point Computation of Minimal Bases", Proceedings Nineteenth Joint Automatic Control Conference, Paper WA-8B, August 1980.

27. M.K. Sain, R.M. Schafer, and K.P. Dudek, "An Application of Total Synthesis to Robust Coupled Design", Proceedings Eighteenth Annual Allerton Conference on Communication, Control, and Computing, Pages 386-395, October 1980.

28. Joseph L. Peczkowski and Michael K. Sain, "Scheduled Nonlinear Control Design for a Turbojet Engine", Proceedings IEEE International Symposium on Circuits and Systems, Pages 248-251, April 1981.

29. Stephen Yurkovich, Thomas A. Klingler, and Michael K. Sain, "Tensor Ideas for Nonlinear Modeling of a Turbofan Jet Engine: Preliminary Studies", Proceedings Twelfth Annual Pittsburgh Conference on Modeling and Simulation, Pages 1423-1428, May 1981.

30. Michael K. Sain and Joseph L. Peczkowski, "An Approach to Robust Nonlinear Control Design", Proceedings Twentieth Joint Automatic Control Conference, Paper FA-3D, June 1981.

31. Thomas A. Klingler, Stephen Yurkovich, and Michael K. Sain, "An Application of Tensor Ideas to Nonlinear Modeling of a Turbofan Jet Engine", Proceedings Thirteenth Annual Pittsburgh Conference on Modeling and Simulation, Pages 45-54, April 1982.

32. Michael K. Sain and Joseph L. Peczkowski, "Nonlinear Multivariable Design by Total Synthesis", Proceedings American Control Conference, Pages 252-260, June 1982 .

33. Thomas A. Klingler, "Nonlinear Modeling of a Turbofan Jet Engine: A Tensor Method Application", Masters Thesis, Department of Electrical Engineering, University of Notre Dame, Notre Dame, Indiana, August 1982.

34. T.A. Klingler, S. Yurkovich, and M.K. Sain, "A Computer-Aided Design Package for Nonlinear Model Applications", Preprints Second Symposium on Computer Aided Design of Multivariable Technological Systems, International Federation of Automatic Control, Pages 345-353, September 1982.

35. Kenneth P. Dudek, "The Total Synthesis Problem for Linear Multivariable Systems with Disturbances", Ph.D. Dissertation, Department of Electrical Engineering, University of Notre Dame, Notre Dame, Indiana, May 1984.

36. Joseph L. Peczkowski and Michael K. Sain, "Design of Nonlinear Multivariable Feedback Controls by Total Synthesis", Proceedings American Control Conference, Pages 688-697, 1984.

37. Joseph L. Peczkowski and Michael K. Sain, "Synthesis of System Responses: A Nonlinear Multivariable Control Design Approach", Proceedings American Control Conference, June 1985.

38. Michael K. Sain and Joseph L. Peczkowski, "Nonlinear Control by Coordinated Feedback Synthesis with Gas Turbine Applications", Proceedings American Control Conference, June 1985.

COMPENSATION OF MULTIVARIABLE CONTROL SYSTEMS

A Thesis

Submitted to the Graduate School of the
University of Notre Dame in Partial Fulfillment
of the Requirements for the Degree of

Master of Science in Electrical Engineering

by

V. Seshadri, B.Tech.

Michael K. Sain
Director

Department of Electrical Engineering
Notre Dame, Indiana

May, 1976

COMPENSATION OF MULTIVARIABLE CONTROL SYSTEMS

Abstract

by

V. Seshadri

This study addresses two possible approaches to the problem of linear multivariable control system design. The first approach belongs to the class of exact model matching designs; the second approach makes use of the characteristic methodologies of MacFarlane.

In the exact model matching case, we consider the problem of finding stable solutions G(s) to the transfer function matrix equation

$$G_1(v)\ G(v) = G_2(v)$$

where all matrices have their elements in the quotient field R(v) formed from the ring R[v] of polynomials in the indeterminate v with coefficients in the real number field R. Our viewpoint on this equation is the free R[v]-module structure presented by Sain in 1975. Previous work has made clear how to answer questions such as whether G(v) can be proper and minimal. Herein we present some tools and partial results oriented to the question of whether G(v) can be stable.

In the MacFarlane methodologies case, we have considered the problem of compensating a two-input, two-output, five-state jet engine model in the class described by Michael and Farrar. Inputs chosen were main burner fuel flow and jet exhaust area; outputs were thrust and high turbine inlet temperature. Software was developed for constructing characteristic loci and a number of related parameters, and an effort was made to use the ideas of noninteraction, integrity, and accuracy to achieve an introductory jet engine control design. The results are positive in nature, although we feel that more attention is needed in this theory toward the actual design of reasonable compensators.

TABLE OF CONTENTS

POLYNOMIAL TECHNIQUES APPLIED TO MULTIVARIABLE CONTROL

A Thesis

Submitted to the Graduate School of the
University of Notre Dame in Partial Fulfillment
of the Requirements for the Degree of

Master of Science in Electrical Engineering

by

Raghvendra Ramchandra Gejji, B. Tech.

Michael K. Sain
Director

Department of Electrical Engineering
Notre Dame, Indiana

May, 1976

POLYNOMIAL TECHNIQUES APPLIED
TO MULTIVARIABLE CONTROL

Abstract

By

Raghvendra R. Gejji

One way to approach the design of linear multivariable control systems is by means of exact model matching, where desired closed loop performance is expressed in terms of a specified transfer function matrix. One question which is often raised about such an approach involves the practicality of specification of such a desired, closed loop performance matrix.. Another, related, question concerns the possibility of determining the existence of compensators to achieve such a performance, as well as giving a finite enumeration of them and selecting those which are, for example, minimal or stable.

This study addresses itself to these points, in reverse order. Research by Sain in 1975 has established that determination of the existence of compensators and a finite enumeration of them is possible within the context of free modules over polynomial rings. Algorithms to accomplish this in theory are also available. The first purpose of this work was to construct straightforward computer software to check the workability of these theoretical algorithms. This has been accomplished in both FORTRAN and PL1, with listings for the former included herein. It was found that these programs were successful on the sort of small problems which often appear in the literature. The second purpose of the work was to evaluate these first-generation software efforts on a realistic practical problem. This has been accomplished in the context of multivariable control of models derived from the F100 turbofan engine by Michael and Farrar. It was established that specification of desired closed loop performance matrices is a reasonable idea for this application, and in fact that in at least one case it has

already been done. This means that exact model matching is not a vacuous idea, at least for jet engines. Efforts were then expended to determine if the first-generation software would compute compensators —— which had been proven to exist. The results here were promising but inconclusive. Though the software would yield answers of the degree expected (a definitely nontrivial achievement), eigenvalue tests and other checks initiated to verify accuracy were decidedly disappointing.

Two conclusions are possible: (1) that some oversight remains undetected in the software or (2) that straight forward computer software is unequal to this application. The second of these possibilities appears to be the more probable at this time, though the first cannot be eliminated with certainty. Studies are under way to develop more sophisticated software.

In any event, the results in terms of problem formulation are promising enough, and the computer results close enough, to suggest that further work on this problem would be worthwhile.

omit to p. 9

TABLE OF CONTENTS

PRODUCTIVITY . . .

Proceedings
of the

1976
Joint Automatic Control Conference

Purdue University,
West Lafayette, Indiana
July 27-30, 1976

SPONSORING SOCIETIES:
- AMERICAN INSTITUTE OF CHEMICAL ENGINEERS
- AMERICAN SOCIETY OF MECHANICAL ENGINEERS
- INSTITUTE OF ELECTRICAL AND ELECTRONICS ENGINEERS
- INSTRUMENT SOCIETY OF AMERICA
- SOCIETY OF MANUFACTURING ENGINEERS

PARTICIPATING SOCIETIES:
- AMERICAN INSTITUTE OF AERONAUTICS AND ASTRONAUTICS
- INSTITUTE OF TRAFFIC ENGINEERS
- SOCIETY FOR INDUSTRIAL AND APPLIED MATHEMATICS
- TECHNICAL ASSOCIATION OF THE PULP AND PAPER INDUSTRY

Published on behalf of the American Automatic Control Council by

THE AMERICAN SOCIETY OF MECHANICAL ENGINEERS

United Engineering Center • 345 East 47th Street • New York, N. Y. 10017

ALTERNATIVE METHODS FOR THE DESIGN OF JET ENGINE CONTROL SYSTEMS

M. K. Sain, R. J. Leake, R. Basso, R. Gejji,
A. Maloney, and V. Seshadri

Department of Electrical Engineering
The University of Notre Dame
Notre Dame, Indiana

ABSTRACT

This paper is a report on research being carried on at the University of Notre Dame Department of Electrical Engineering on alternatives to current Jet Engine Control System design methods which rely heavily on linear quadratic and Riccati equation techniques. The main alternatives are classified into two broad categories

1) Nonlinear Global Mathematical Programming Methods
2) Linear Local Multivariable Frequency Domain Methods

Specific studies within these categories which are described briefly in the paper include model reduction, the Eigenvalue Locus Method, the Inverse Nyquist Method, Polynomial Design, Dynamic Programming and Conjugate Gradient approaches. The studies are being carried out with the objective of arriving at a design to be tested on the DYNGEN jet engine simulator.

NOMENCLATURE

A_7 - nozzle area
C_C - compressor specific heat
C_F - fan specific heat
C_{LT} - low turbine specific heat
C_{HT} - high turbine specific heat
h - enthalpy
F - thrust
I_C - compressor moment of inertia
I_F - fan moment of inertia
J - mechanical equivalent of heat
N_C - compressor rotor speed
N_F - fan rotor speed
P_4 - main burner pressure
P_7 - afterburner pressure
P_{50} - high turbine pressure
R - gas constant
T_4 - high turbine inlet temperature
T_7 - afterburner temperature
T_{21} - fan output temperature
T_{50} - low turbine input temperature
T_{55} - low turbine output temperature
u_i - control variable
V_{COM} - combustor volume
V_{LT} - low turbine volume
WAC - compressor flow
WFB - main burner fuel flow
WG55 - low turbine flow
x_i - state variable
α - duct bleed ratio
β - high turbine bleed ratio
γ - ratio of specific heats
η - main burner efficiency
ρ_B - main burner density
ϕ^B - compressor bleed ratio

INTRODUCTION

A large share of the current work (1), (2), (3) on jet engine control system design involves linear quadratic and Riccati equation methods at specified operating points, with global nonlinear controllers being produced by scheduling and gain interpolation between operating points. In this work we briefly examine several alternatives to this approach. It is anticipated that designs obtained by combining one or more of these alternatives will be tested on a simulated turbofan engine resembling the Pratt and Whitney F-100 model, using DYNGEN (4), (5), a computer program developed at NASA Lewis Research Center for simulating a variety of engine configurations.

The alternatives which are considered can be categorized broadly into Nonlinear Global Mathematical Programming methods and Linear Local Multivariable methods. In each case it is desirable to have a relatively low order analytical model of the engine in order to carry out the associated design procedure. As an initial attempt to realize such a model, the configuration of Figure 1 was chosen with no duct or afterburning, and 23 differential equations were specified; 3 for each volume unit, and 1 for each rotor. The method employed corresponds closely to that described in (6), (7), (8).

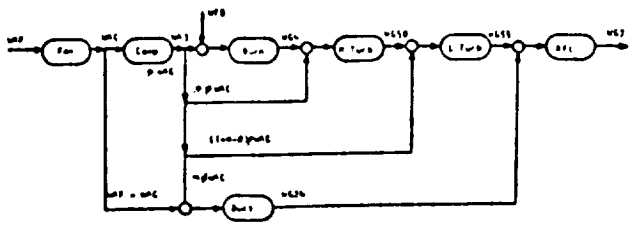

Fig. 1. Assumed Engine Configuration

It is well known that the essential dynamics of a turbofan engine can be retained by eliminating certain differential equations which correspond to high frequency response characteristics. We do this by replacing the dynamical condition by its associated equilibrium condition. As an illustration, we choose fan turbine inlet temperature $x_1 = T_{50}$, main burner pressure $x_2 = P_4$, fan speed $x_3 = N_F$, high compressor speed $x_4 = N_C$, and afterburner pressure $x_5 = P_7$, as the essential state variables. As control inputs we choose jet exhaust area $u_1 = A_7$ and main burner fuel flow $u_2 = WFB$. The outputs are taken as thrust $y_1 = F$ and high turbine inlet temperature $y_2 = T_4$. These choices correspond to those used in (1), and provide an opportunity for relating a fifth order nonlinear model to well known linear models. The usual approach to obtain linear models is to employ an identification scheme (1), (9), (10), based on system measurements. The analytical nonlinear model provides an alternative through partial differentiation and is expected to yield additional insight into the system structure.

Using the methods of (6), (7), (8), and taking into account the flow relations of Fig. 1, the following equations are obtained.

$$\frac{dT_{50}}{dt} = \frac{RT_{50}}{V_{LT}P_{50}}(\gamma T_{55}-T_{50})[(1-\alpha\phi)WAC+WFB-WG55] \tag{1}$$

$$\frac{dP_4}{dt} = \frac{R\gamma}{V_{COM}}\left[(T_3-T_4)(1-\phi)WAC+\eta\frac{h_B}{C_B}WFB\right] \tag{2}$$

$$\frac{dN_F}{dt} = \left(\frac{30}{\pi}\right)^2\frac{J}{N_F I_F}[C_F(T_2-T_{21})(A_7\bar{W}_7-WFB) + C_{LT}(T_{50}(WFB+(1-\alpha\phi)WAC)-WG55\ T_{55})] \tag{3}$$

$$\frac{dN_C}{dt} = \left(\frac{30}{\pi}\right)^2\frac{J}{N_C I_C}[C_C(T_{21}-T_3)WAC + C_{HT}((T_4-T_{50})(WFB+(1+\beta\phi-\phi)WAC))] \tag{4}$$

$$\frac{dP_7}{dt} = \frac{R\gamma T_7}{V_{AF}}[WG55-WFB-(1-\alpha\phi)WAC] \tag{5}$$

where T_{50}, P_4, N_F, N_C, P_7 are states; A_7 and WFB are inputs; P_{50}, T_{55}, WAC, WG55, η, T_{21}, $WG7 = A_7\bar{W}_7$, and T_7 are nonlinear functions of the inputs and state variables determined by component characteristics; and finally the outputs F and T_4 are also nonlinear functions.

In the next four sections, we discuss methodologies relevant to the analysis and design of linearized models of equations such as these.

LINEAR MULTIVARIABLE SYSTEMS

In this section we wish to provide some general background relevant to the problem of controlling linear multivariable systems. Keeping in line with the theme of "alternative methods", we shall bypass the common topics of state feedback approaches, including the ubiquitous Riccati equation. Instead we shall focus upon input/output descriptions. Of particular interest at this point are what we mean by a linear multivariable system and what issues arise when we close loops around such systems.

Denote by R the field of real numbers, and by R[s] the commutative ring of polynomials in s with coefficients in R. Because R[s] is an integral domain, there is a field of quotients (11) associated with it. Denote this field by R(s), and note that this is the usual "field of rational functions in s". For our purposes herein, a linear multivariable system is just an rxm matrix G(s) each of whose elements is in R(s). In accordance with the customary conventions, we refer to an element in R(s) as a "transfer function" and to G(s) as a "transfer function matrix".

Turning now to the closed loop topology, we consider an interconnection of linear multivariable systems as shown in Fig. 2. Here we regard the linear

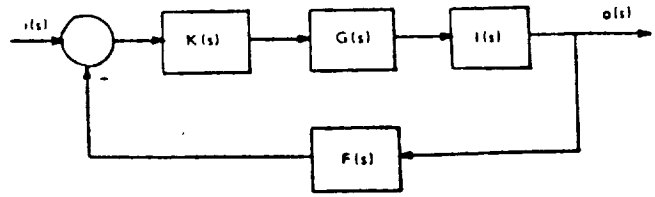

Fig. 2 Feedback Interconnection

multivariable systems F(s), K(s) and L(s) as compensators, whereas G(s) is assumed to be the object of control. Working on the premise that o(s) is to be compared with i(s), the system F(s) is taken as square. The composite system in the forward path is denoted by

$$Q(s) = L(s)\ G(s)\ K(s). \tag{6}$$

Insofar as Figure 2 is concerned, one of the most central questions of interest centers upon the relation between the "poles" of the closed loop configuration and how they relate to those of the open loop configuration.

A number of issues pertain to this relationship. Given Q(s) alone, it is clear that we cannot determine the nature of any modes which cancelled when it was constructed; accordingly, we concentrate upon the knowledge available from Q(s) itself. By the characteristic polynomial $T_Q(s)$ of Q(s) we shall mean the least common multiple of all the "denominators" of all the minors of the matrix Q(s). A corresponding meaning is attached to $T_F(s)$. Then the open loop characteristic polynomial $T_{OL}(s)$ is defined by

$$T_{OL}(s) = T_Q(s)\ T_F(s). \tag{7}$$

In many situations it happens that the feedback compensator system F(s) can be represented by the identity matrix; then (7) simplifies to

$$T_{OL}(s) = T_Q(s). \tag{8}$$

Because of space limitations, we shall use (8) in our further discussions. Next we recall the closed loop system H(s) given by

$$H(s) = (I + Q(s))^{-1}\ Q(s) \tag{9}$$

and denote its characteristic polynomial by $T_H(s)$. Within the context of our present assumptions, it is realistic to understand $T_H(s)$ as the closed loop characteristic polynomial $T_{CL}(s)$.

Now the "poles" of the open loop system may be taken as the zeros of $T_{OL}(s)$, and the "poles" of the

closed loop system may be taken as the zeros of $T_{CL}(s)$. Central, then, to the treatment of this section and of the two sections which follow is the identity

$$T_{CL}(s) = |I + Q(s)|\, T_{OL}(s), \tag{10}$$

where the vertical bars stand as usual for a calculation of the determinant. This relation is by now quite well known (12), (13), (14), (15). A consequence of (10) is that a Nyquist plot of

$$|I + Q(s)| \tag{11}$$

suffices, as in the classical case, to inform the designer about closed loop stability. There are various ways to attack the construction of a Nyquist plot for (11), and we shall briefly examine two of these in the next two sections, in the context of the following jet engine example.

Let G(s) be a 2x2 transfer function matrix describing linearized F-100 turbofan jet engine dynamics at a power lever angle of 47 degrees. The inputs are main burner fuel flow and jet exhaust area; the outputs are thrust and high turbine inlet temperature; and the states, five in number, are high compressor speed, fan speed, fan turbine inlet temperature, main burner pressure, and afterburner pressure. We have selected this model to correspond to a linearization of (1), (2), (3), (4), (5). The data for our model has been taken from a report by Michael and Farrar (1). The power lever angle chosen is about midway between the engine idle condition and maximum non-afterburning power. G(s) is found to be

$$\frac{\begin{bmatrix} (.018s^5+.145s^4-92.05s^3 & (.546s^5+71.9s^4+2247s^3 \\ -396.9s^2+29801s+95491) & -1943s^2-16855s-12495) \\ (-.086s^5+31.63s^4+3321.5s^3 & (-.013s^5-.437s^4+68.2s^3 \\ +25500s^2+76068s+78277) & +1703.3s^2+1742.9s-3532.2) \end{bmatrix}}{s^5+140.7s^4+5337.6s^3+38691s^2+119690s+133389} \tag{12}$$

THE EIGENVALUE APPROACH

We have mentioned in the preceding section that interest in closed loop stability can center upon the determinant (11). Here we want to illustrate one approach to the construction of a Nyquist plot of (11). This approach is due to MacFarlane (15), and all the curves presented are taken from a thesis by Seshadri (16).

The basic idea is this: for each particular value of s on a Nyquist contour, the determinant (11) is the product of its eigenvalues in the manner

$$|I + Q(s)| = \prod_{i=1}^{k} e_i(I + Q(s)), \tag{13}$$

where $e_i(A)$ denotes the ith eigenvalue of the matrix A. Moreover, from the evident relation

$$e_i(I + Q(s)) = 1 + e_i(Q(s)), \tag{14}$$

we find that

$$|I + Q(s)| = \prod_{i=1}^{k} (1 + e_i(Q(s))). \tag{15}$$

Recalling that the argument of a product of complex numbers is the sum of the arguments of its factors, and noting that each of the factors in (15) resembles the function which is plotted in Nyquist studies of single-input, single-output systems, one is motivated to make k individual Nyquist plots, in a manner suggested by the right member of (15), in place of the one, more complicated, Nyquist plot of its left member. This is the idea suggested by MacFarlane.

From a computational point of view, the idea is attractive, requiring only eigenvalue routines---which are available ---which accept arbitrary square complex matrices. We can illustrate this construction on the jet engine problem given numerically in (12). One allows s to follow a clockwise Nyquist contour, and computes the eigenvalues of (12) for each value of s. The locus of one eigenvalue of $G(j\omega)$ is shown in Fig. 3 for positive values of ω. To the analyst experienced

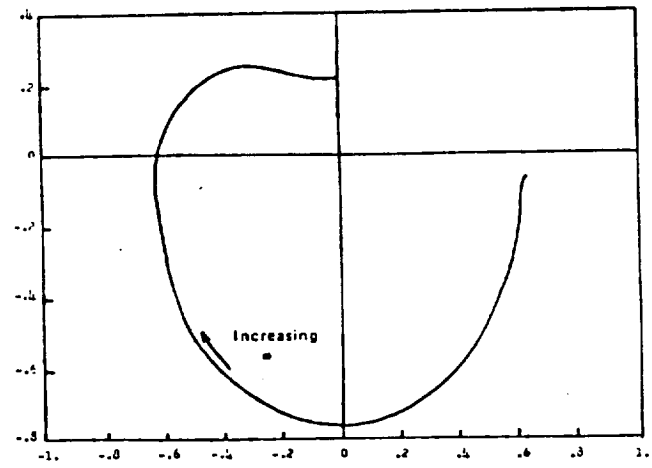

Fig. 3 First Eigenvalue Locus of (12)

in Nyquist plots of single-input, single-output systems, there is one very noticeable feature of the locus in Fig. 3; and that is the fact that it does not begin ($\omega = 0$) on the real axis. In fact, of course, it is easy to see that the points of beginning for the loci are determined by the eigenvalues of the matrix which

$$\frac{\begin{bmatrix} 95491 & -12495 \\ 78277 & -3532.2 \end{bmatrix}}{133389}, \tag{16}$$

is found from (12) upon placing s equal to zero. Similarly, the loci need not end on an axis either, or be asymptotic to one. This is not as easy to see from Fig. 3, where the scale tends to prevent us from seeing that the locus ends at .0025 + .216j, which is one of the eigenvalues of

$$\lim_{s \to j\infty} G(s) = \begin{bmatrix} .018 & .546 \\ -.086 & -.013 \end{bmatrix}. \tag{17}$$

Generally speaking, the eigenvalues of which we speak are solutions to the equation

$$r_2(s)\,\lambda^2 + r_1(s)\,\lambda + r_0(s) = 0 \tag{18}$$

for $r_i(s) \in R(s)$, $i = 0, 1, 2$. If (18) is satisfied for a particular pair (s, λ), then clearly it will also be satisfied for the pair (s^*, λ^*), where we use the superscript (*) for conjugation. Thus we know that the locus conjugate to that in Fig. 3 will be the negative-ω locus for an eigenvalue plot. Inspection of Fig. 3, however, shows clearly that the locus and its conjugate do not combine to form a closed curve for the Nyquist test. To see why this is the case, we examine the second eigenvalue locus of (12), which is portrayed in

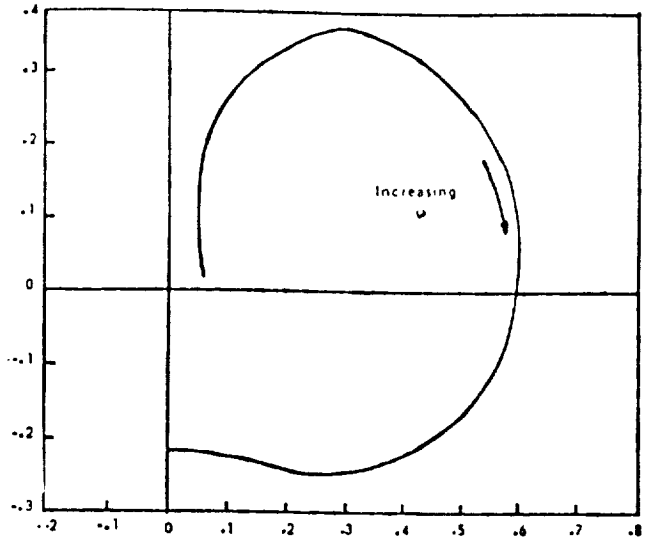

Fig. 4 Second Eigenvalue Locus of (12)

Fig. 4. Now it can be seen that the conjugate of the second locus fits together with the first locus to form a closed curve; and, similarly, the conjugate of the first locus fits together with the second. From Fig. 3 and 4, then, we can piece together two closed Nyquist loci, neither of which encloses the point -1 + j0. Thus we would consider concluding that the system (12) is stable under unity negative feedback.

Some quite delicate questions are associated with this method. Among these is the matter of whether or not (13) is sensible when both members are regarded as functions of the complex variable s. This existence question has been solved (17). More crucial for Nyquist considerations is the behavior of the functions $e_1, e_2, \ldots, e_k$ in the right-half plane $\mathrm{Re}\{s\} \geq 0$. Barman and Katzenelson (18) have shown that, for stable systems such as the jet engine model under study here, the exceptional points to be heeded in $\mathrm{Re}\{s\} \geq 0$ are those points for which (18) has zeros of multiplicity greater than one. Seshadri (16) has determined that there are three of these points in our example, all on the real axis. Generally speaking, it is the presence of such points that causes us to have to piece together the conjugate of Fig. 4 with Fig. 3 to form a closed locus, instead of being able to fit the conjugate of Fig. 3 together with Fig. 3 itself. This feature precludes any easy approach to identifying "individual" closed-path eigenvalue functions, although by addition of branch cuts from the exceptional points, together with a corresponding modification of the Nyquist contour, it is possible to achieve this goal (18). The problem, however, is that computation of exceptional points off the imaginary axis, as well as the branch cuts, presents an added computational burden. It seems much easier, instead, to use the above approach of "piecing together" the various loci.

Further insights can be gained by making similar plots for the strictly proper part of (12). To do this, G(s) is written as the sum of (17) plus a remainder matrix, which is the strictly proper part. Fig. 5 shows the first eigenvalue locus for this situation. A notable feature of the plot is its beginning and ending on the real axis. As a result, its conjugate can be combined with itself to give a closed "individual" eigenvalue locus. A similar observation obviously holds for Fig. 6. It can be shown that no exceptional points are present for this example, which is also stable under unity feedback.

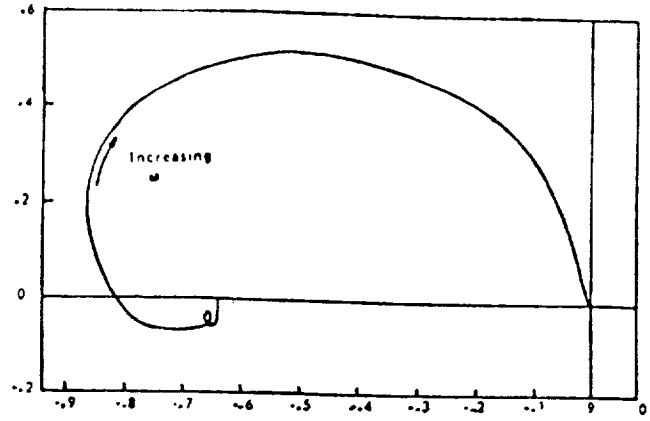

Fig. 5 First Eigenvalue Locus for Strictly Proper Part of (12)

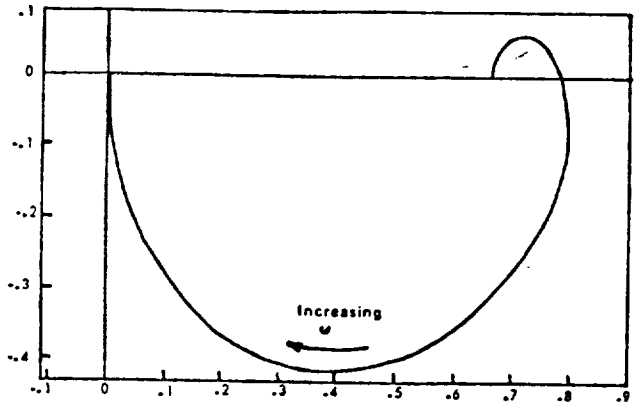

Fig. 6 Second Eigenvalue Locus for Strictly Proper Part of (12)

Considerable care is advisable in considering this tool when F(s) is not proportional by an element of R(s) to the identity matrix. Rosenbrock and Cook have exhibited (19) counterexamples when F(s) is diagonal with differing elements. Such a difficulty can be anticipated from (14).

The eigenvalue approach does, therefore, seem to add insight to the analysis of jet engine control models. Preliminary efforts, however, to compensate the models with introductory techniques (15) have led to the tentative conclusion (16) that the theory of eigenvalue compensation may be in need of some extension for the jet engine control problem. Moreover, the proportionality restrictions on F(s) appear to represent a notable limitation which suggests care in assessing the physical nature of the feedback to be employed. In many digital control situations, the assumptions would seem to be sound; however, simulation is always a desirable check.

THE DOMINANCE APPROACH

We have commented earlier that a Nyquist plot of (11) is central to the linear, multivariable feedback control problem. One approach to the treatment of such a determinant has been described in the preceding section. We now turn to another approach, which is due to Rosenbrock (12).

Here the idea is to recognize that the calculation of (11) would reduce to k single-input, single-output problems if Q(s) were diagonal, or equivalently if the forward path system had negligible interaction. Instead, however, of seeking exact noninteraction, Rosenbrock has set up a theory based upon "approximate" noninteraction. The keystone in the theory is the result of Gershgorin, which states that the eigenvalues of an kxk complex matrix Z lie in the union of the discs

$$|s - Z_{ii}| - \sum_{\substack{j=1 \\ j\neq i}}^{k} |Z_{ij}| \leq 0, \quad i = 1,2,\ldots,k \tag{19}$$

and also in the union of the discs

$$|s - Z_{ii}| - \sum_{\substack{j=1 \\ j\neq i}}^{k} |Z_{ji}| \leq 0, \quad i = 1,2,\ldots,k. \tag{20}$$

Clearly, $|Z|$ is nonzero if the intersection of the disc sets (19) and (20) does not include the origin. The feature of excluding the origin is called "dominance" by Rosenbrock. In particular, if

$$|Z_{ii}(s)| - \sum_{\substack{j=1 \\ j\neq i}}^{k} |Z_{ij}(s)| > \varepsilon, \quad i = 1,2,\ldots,k \tag{21}$$

for every s on a Nyquist contour having on it no poles of $Z_{ij}(s)$, i = 1,2,...,k, then Z(s) is said to be column dominant; again, if (21) is replaced by

$$|Z_{ii}(s)| - \sum_{\substack{j=1 \\ j\neq i}}^{k} |Z_{ji}(s)| > \varepsilon, \quad i = 1,2,\ldots,k, \tag{22}$$

then Z(s) is termed row dominant. Either (21) or (22) is sufficient to ensure that the number of times that a Nyquist locus of $|Z(s)|$ encircles the origin can be determined by forming a net sum of the number of times that Nyquist loci of $Z_{ii}(s)$, i = 1,2,...,k, encircle the origin.

If we denote by H(s) the matrix

$$(I + Q(s))^{-1}Q(s), \tag{23}$$

then

$$|I + Q(s)| = |H^{-1}(s)|/|Q^{-1}(s)|, \tag{24}$$

provided that Q(s) has an inverse. When both $Q^{-1}(s)$ and $H^{-1}(s)$ are, for example, row dominant, Nyquist locus behavior of their determinants in (24) can be computed from the Nyquist locus behavior of the elements on their diagonal. Moreover, because

$$H^{-1}(s) = Q^{-1}(s) + I, \tag{25}$$

diagonal elements of $H^{-1}(s)$ are just corresponding elements of $Q^{-1}(s)$ shifted by unity.

From these ideas, Rosenbrock has developed a number of graphical strategies here for our jet engine example. For each i, i = 1,2,...,k, construct the Nyquist locus of $(Q^{-1}(s))_{ii}$; at each s, construct a circle with center $(Q^{-1}(s))_{ii}$ and radius

$$\sum_{\substack{j=1 \\ j\neq i}}^{k} |Q^{-1}(s))_{ij}| \tag{26}$$

If neither the point -1 + j0 nor the origin lie in the union of these circles, then $Q^{-1}(s)$ and $H^{-1}(s)$ are column dominant and stability can be studied by examining the Nyquist loci of $(Q^{-1}(s))_{ii}$, i = 1,2,...,k.

Fig. 7 and 8 show such plots for the cases i = 1 and i = 2, respectively, when Q(s) is equal to the G(s) specified in (12). The small arrow in these figures indicates the direction of increasing ω as ω goes from zero to infinity. Fig. 7 is quite satisfactory; however, Fig. 8 indicates poor dominance at low frequencies.

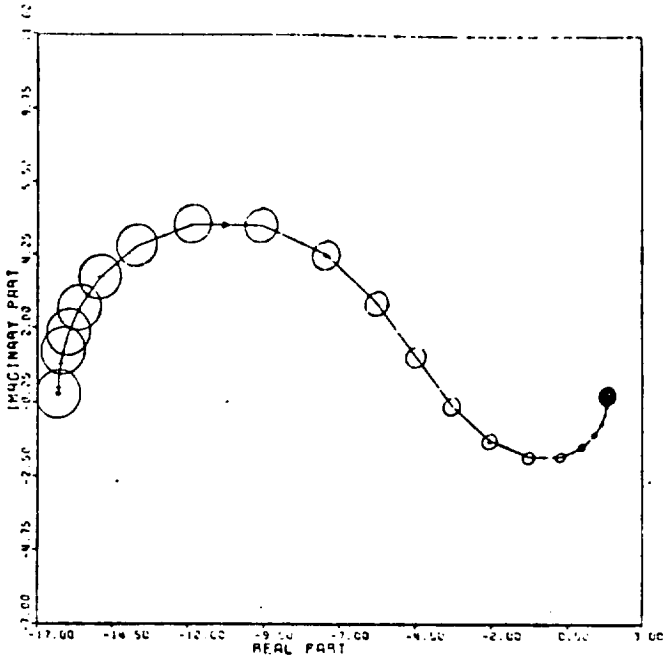

Fig. 7 First Gershgorin Band Plot Corresponding to (12)

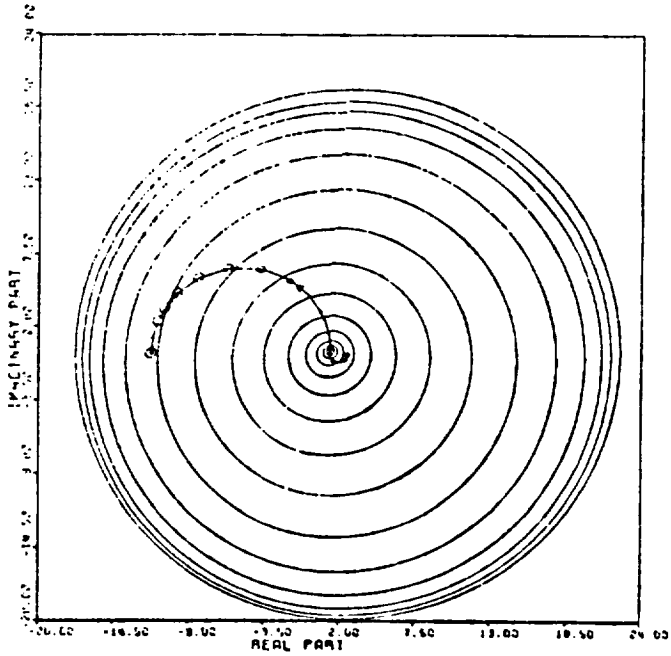

Fig. 8 Second Gershgorin Band Plot Corresponding to (12)

This leads us, then, to the basic question of how to achieve dominance. In a real sense, this may be the central issue in the present approach to analysis and design. From the jet engine control problem viewpoint, it would be very desirable if any compensators K(s) and L(s) chosen to achieve dominance were constant. Because of the presence of a number of physical variables upon which a parameterization might be based, it might then be possible to choose constant compensators at a family of operating points and then to interpolate between them according to the action of a suitable physical variable. For this presentation, then, we took an introductory look at constant compensators to achieve dominance.

In view of Fig. 8, it seems promising to try a compensator $G^{-1}(0)$ for K. Such a choice results in perfect dominance at zero frequency. As expected, the new plots, Figs. 9 and 10, reflect this improvement at low frequencies. Note that, although Fig. 9 indicates

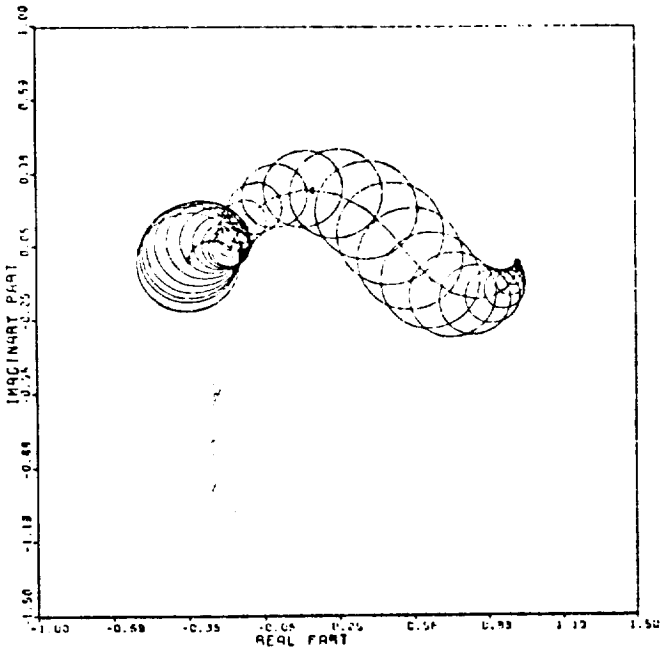

Fig. 9 First Plot for System Compensated at Zero Frequency

dominance, the dominance situation in Fig. 10 remains unsatisfactory, with least dominant behavior now occurring at high frequencies in contrast to such behavior which was seen at low frequencies in Fig. 8.

We have space here for one more illustration. Using an optimization method termed "pseudo-dominance" by Rosenbrock (12), we chose a constant compensator K designed to improve row dominance near unity angular frequency. The results are shown in Figs. 11 and 12. Though not easily checked visually, the Gershgorin bands exclude the origin; stability could thus be established by gain adjustment in the feedback path. (Although the compensator K was chosen for row dominance for $Q^{-1}(s)$, we have plotted bands corresponding to column dominance. This was necessary because this K did not achieve row dominance of $Q^{-1}(s)$. Fortunately, however, it did help with column dominance. For consistency, then, we have plotted Fig. 7-10 also in column band form. All six plots are due to Maloney (20)).

Once dominance is achieved, this methodology leads rather quickly to designs of compensators in the individual input or output channels. Principal

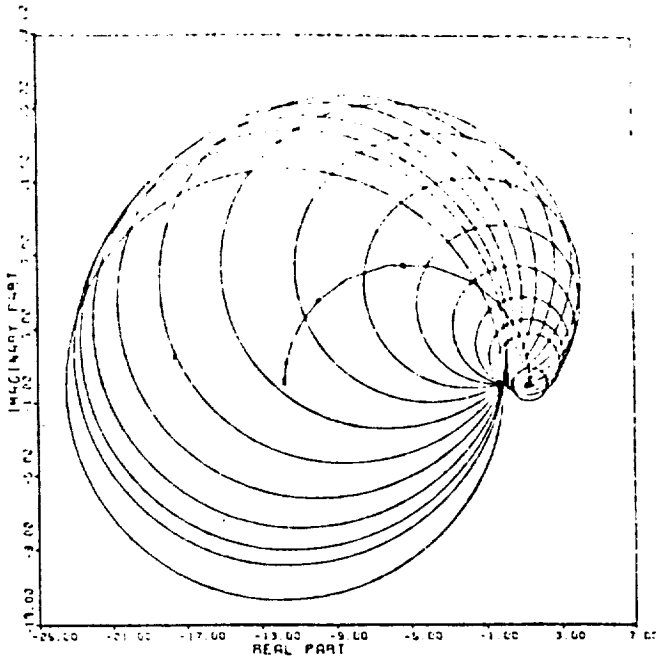

Fig. 10 Second Plot for System Compensated at Zero Frequency

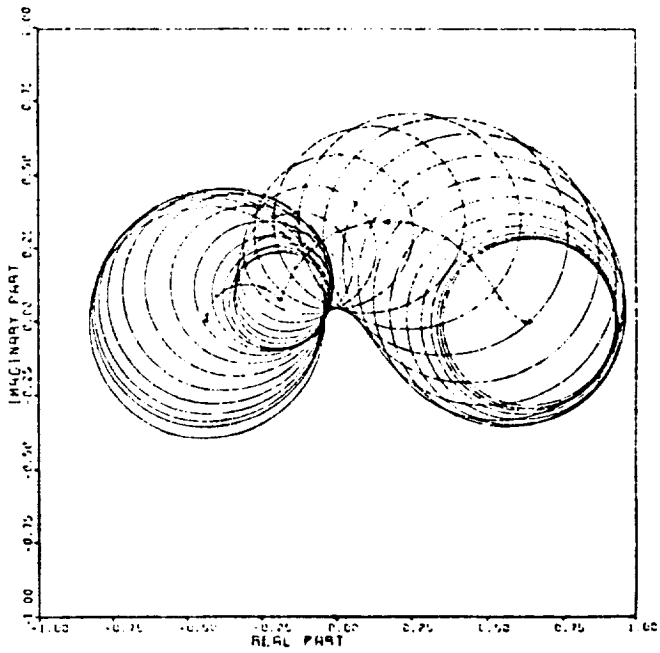

Fig. 11. First Plot for System Compensated at Unit Frequency

interest, then, attaches to the achievement of dominance. Though our examples here are definitely introductory, they do serve to show that typical jet engine models do not yield trivial dominance questions. These observations have been borne out on studies at power lever angles of 35 and 60 degrees as well, for models up to five inputs and five outputs (1).

A preliminary conclusion seems to be that dynamic compensation may be needed to achieve dominance in jet engine models. This would of course add to the complexities of building up a global controller from multiple local linear controllers.

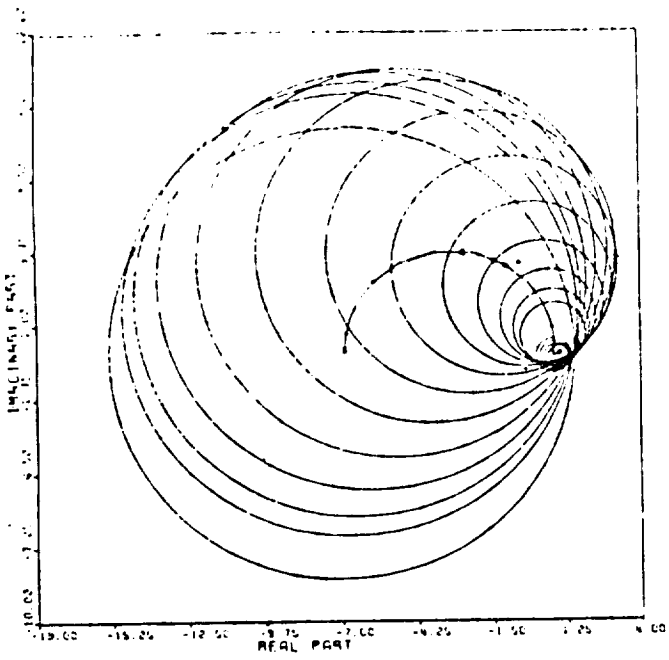

Fig. 12. Second Plot for System Compensated at Unit Frequency

POLYNOMIAL DESIGN

This section concludes our discussion of linear design alternatives. Unlike the previous two sections, the discussion here takes place outside the Nyquist context. Rather, it is based almost entirely on polynomial algebra.

Problem formulation is deceptively simple. Given two matrices $G_1(s)$ and $G_2(s)$ each of whose elements is in R(s), we seek to find and enumerate all matrices G(s) which satisfy the equation

$$G_1(s)\ G(s) = G_2(s). \tag{27}$$

and which also have elements in R(s). Other aspects about G(s) which are of considerable interest include whether or not it is proper (which translates into linear dynamical realizability), whether or not the number of dynamical elements required to realize it is a minimum among proper solutions to (27), and the location of its poles. In the literature, (27) has come to be known as the "exact model matching problem". Our purpose here is not to give an historical survey of the literature, but we can comment in passing on one of the more recent approaches to solving this problem (21). Basically, one expresses

$$G_i(s) = (b_i(s)I)^{-1}\ A_i(s),\ i = 1,2, \tag{28}$$

where $b_i(s)I$ and $A_i(s)$ are polynomial matrices. Then it can be shown that solution to (27) amounts to a calculation of the kernel of the matrix

$$[b_2(s)\ A_1(s) \quad -b_1(s)\ A_2(s)], \tag{29}$$

regarded as defining a morphism of free R[s]-modules (11). From the basis of this kernel, which amounts to the desired enumerative description of possible G(s), it is possible to determine minimal proper solutions and to address pole location. Gejji (22) has developed "KERPO" software for finding the KERnel of POlynomial matrices, both in FORTRAN and PL1. He has further studied applicability of the technique to the jet engine model (12).

The situation is as shown in Fig. 13. The engine

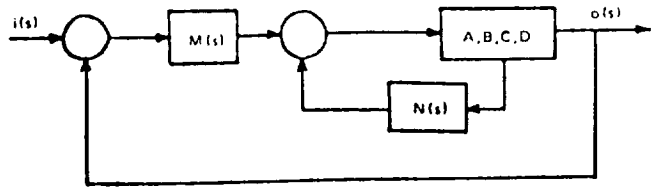

Fig. 13 Polynomial Design Configuration

model (12) is represented by a minimal realization (A,B,C,D), as in (1). A desired transfer function matrix $T^*(s)$ is specified such that

$$o(s) = T^*(s)\ i\ (s). \tag{30}$$

It is desired to enumerate all possible proper compensators M(s) and N(s), the latter operating upon the states realizing (12), in Fig. 13 such that (30) is achieved. It can be shown (22) that this problem reduces to computing a kernel for the matrix

$$[M(s) \quad -d(s)\ I], \tag{31}$$

where

$$(d(s)I)^{-1}\ M(s) = [Q^T(s) \quad -P^T(s)], \tag{32}$$

superscript "T" denoting transposition, for

$$P(s) = (sI - A)^{-1}B, \tag{33}$$

$$Q(s) = [(T^*(s))^{-1} - I]\ G(s). \tag{34}$$

$T^*(s)$ was determined in a manner similar to (1), with (31) becoming a 2x9 matrix having polynomial entries of degrees as high as thirteen.

The purpose of this study was to determine whether straightforward implementation of known algorithms such as (21) would succeed computationally on these typical jet engine problems or whether more sophisticated softwares would be required. Results indicate that success will probably be achievable with software using rational arithmetic, while the use of real arithmetic is less promising.

Of course, the principal difficulty in exact model matching designs is generally specification of $T^*(s)$. Of greater interest, then, might be the inversion of these methods to describe achievable $T^*(s)$.

The utility of linear design methods in jet engine control appears to lie in piecing linear designs together to get a global nonlinear design. Of course, a direct approach to global nonlinear design based on the equations (1)-(5) is also possible, and we turn now to some alternatives in this regard.

MATHEMATICAL PROGRAMMING APPROACH

The linear multivariable approaches of the previous sections aim at various criteria common to good regulation about design equilibrium points. They depend on scheduled nominal inputs for large excursions which are often part of the engine design itself. A global nonlinear approach actually takes scheduling and local control action into account simultaneously by specifying the total control, and in this manner,

overlaps the control and engine design problems.

As a preliminary global study, the problem is taken as one of going from idle to a high thrust design equilibrium point in minimum time, while observing side constraints on surge margin and high turbine inlet temperature.

The usual approaches of Optimal Control (23), (24), (25) have been considered, but only within the more modern, more systematic, and more general framework of Mathematical Programming (26), (27), (28). If side constraints are included through penalty and barrier methods, the control problem can be viewed as an unconstrained minimization of an objective function $J(\underline{u})$ where

$$\underline{u} = \begin{bmatrix} u(0) \\ u(1) \\ \vdots \\ u(N-1) \end{bmatrix} \tag{35}$$

and

$$J(\underline{u}) = K(x(N)) + \sum_{t=0}^{N-1} L(x(t),u(t),t) \tag{36}$$

with the differential equation approximation

$$x(t+1) = x(t) + f(x(t),u(t)). \tag{37}$$

Standard algorithms such as the Fletcher-Reeves Conjugate Gradient (26), (29) and the modified Davidon-Fletcher-Powell quasi-Newton algorithm with self-scaling and automatic restart (26), (27) can be applied directly to this problem with $J(\underline{u})$ being evaluated by solving (36), (37) for $t = 0,1,\ldots,N-1$. The gradient

$$\nabla_{\underline{u}} J = [\nabla_{u(0)} J \ \nabla_{u(1)} J \ \cdots \ \nabla_{u(N-1)} J] \tag{38}$$

is determined by solving the adjoint equations

$$\lambda(t) = \lambda(t+1) + \lambda(t+1)\nabla_x f(x(t),u(t)) + \nabla_x L(x(t),u(t),t) \tag{39}$$

$$\lambda(N) = \nabla_x K(x(N))$$

for $t = N-1, \ldots, 2, 1$ and observing that

$$\nabla_{u(t)} J = \lambda(t+1)\nabla_u f(x(t),u(t)) + \nabla_u L(N(t),u(t),t) \tag{40}$$

Each of the algorithms mentioned above requires a line search for minimization of

$$h(\alpha) = J(\underline{u}+\alpha\underline{d}), \quad h'(0) = \nabla_{\underline{u}} J(\underline{u}) \tag{41}$$

along directions $\underline{d}$, (usually not the gradient direction) determined by the particular algorithm. A cubic approximation of $h(\alpha)$ depending on $h(0)$, $h'(0)$ and two other values $h(a)$, $h(b)$ as suggested by Lasdon (29) seems to be an efficient basis for carrying out a fairly simple line search in one step. Refinements of this approach are being sought, as it is essential that the number of evaluations of $J(\underline{u})$ and $\nabla_{\underline{u}} J(\underline{u})$ be kept to a minimum due to the amount of computation required.

Let us now consider a simple computational example. The two spool turbofan engine of Fig. 1 can be specialized to a single spool turbojet engine by zeroing out certain terms. If we also choose burner density ρ_B as a state variable a simple third order model is

$$\frac{d\rho_B}{dt} = \frac{1}{V_{COM}} (WAC+WFB-WG4) \tag{42}$$

$$\frac{dp_4}{dt} = \frac{R\gamma}{V_{COM}} \left(T_3 WAC + T_4 (WFB-WG4) + \frac{nh_B}{C_B}\right) \tag{43}$$

$$\frac{dN_C}{dt} = \left(\frac{30}{\pi}\right)^2 \frac{J}{N_C I_C} [C_C WAC(T_{21}-T_3) + C_{HT} WG4(T_4-T_7)] \tag{44}$$

If the variables are normalized about a high thrust design point and certain simplifications (8), are assumed for the nonlinear functions involved, a complete numerical model which has the essential characteristics of the engine studied in (7) is

$$\frac{d\hat{\rho}_B}{dt} = 37.78\ \hat{WAC} - 38.448\ \hat{P}_4 + .66849\ \hat{WFB} \tag{45}$$

$$\frac{d\hat{P}_4}{dt} = 21.435\ \hat{WAC}\ \hat{T}_3 - 53.86\ \frac{\hat{P}_4^2}{\hat{\rho}_B} + (31.486 + .93586\ \frac{\hat{P}_4}{\hat{\rho}_b})\hat{WFB} \tag{46}$$

$$\frac{d\hat{N}_C}{dt} = 1.258\ \{\frac{\hat{P}_4^2}{\hat{\rho}_B \hat{N}} - \hat{WAC}\ \hat{N}\} \tag{47}$$

with

$$WAC = 1.3009\ N_C - .139825\ \hat{P}_4 - .13982\ \sqrt{\hat{P}_4^2 + .41688\ \hat{N}_C^2 - .0899\ \hat{P}_4\ \hat{N}_C} \tag{48}$$

$$\hat{T}_3 = .64212 + .35788\ \hat{N}_C^2 . \tag{49}$$

The single control variable is $\hat{WFB}$ and the problem is to drive the system from idle (actually windmill here with $\hat{WFB} = 0$)

$$\hat{\rho}_B = 1.774 \quad \hat{P}_4 = .5384 \quad \hat{N}_C = .5461 \tag{50}$$

to design (with $\hat{WFB} = 1$) and

$$\hat{\rho}_B = 1 \quad \hat{P}_4 = 1 \quad \hat{N}_C = 1 \tag{51}$$

in minimum time subject to surge margin and turbine inlet temperature constraints approximated respectively (30) by

$$\hat{P}_4 \leq 1.25\ \hat{N}_C \tag{52}$$

$$\hat{P}_4 \leq 1.25\ \hat{\rho}_B . \tag{53}$$

Notice that a good second order approximation to the problem can be obtained by considering only the dynamical equations (45) and (47) and taking $\hat{P}_4$ as a control variable. Once the optimal $\hat{P}_4$ is obtained, equation (46) is used to determine the $\hat{WFB}$ necessary to yield P_4. This technique was used (30) to obtain a Dynamic Programming solution to the problem with time step size $\Delta t = .002$ as indicated in Figs. 14 and 15. Generally there are three regions of control:

(1) $\hat{P}_4$ rides the surge margin constraint boundary ($\hat{P}_4 = 1.25\ \hat{N}_C$).
(2) $\hat{P}_4$ switches and rides the inlet temperature constraint boundary ($P_4 = 1.25\ \hat{\rho}_B$)
(3) $\hat{P}_4$ leaves the inlet temperature constraint boundary and adjusts to get all states to final design equilibrium value of unity.

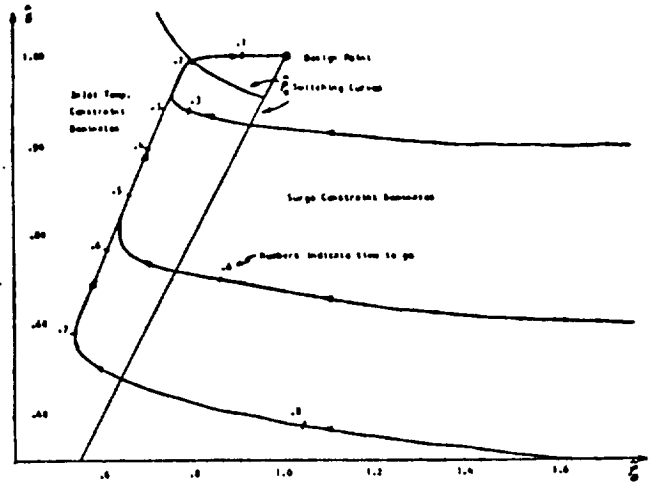

Fig. 14 $\hat{P}_4$ Switching Regions For Minimum Time From Idle to Design

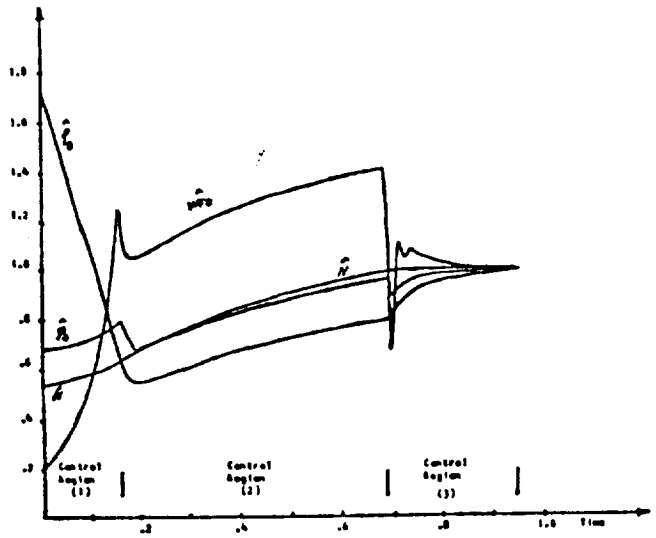

Fig. 15 Dynamic Programming Open Loop Optimal Time Trajectories

The optimal time from idle to design is slightly less than 1 second. Many more details are given in (30).

A preliminary open loop solution using a conjugate gradient algorithm with time variable penalty functions to account for state constraints and terminal condition is shown in Fig. 16. The constraint violations which occur in $\hat{P}_4$ are due to exterior penalty functions. Feasible direction and barrier approaches are being studied to remedy this effect.

The fact that the problem is time optimal and the optimal number of steps N is initially unknown does not appear to offer any real difficulty as a few rough computational runs quickly give one a good estimate of N.

Future studies will involve experimentation with various conjugate gradient and quasi-Newton algorithms in combination with penalty, barrier, and augmented Lagrangian techniques. Also, it appears that the state constraints can be taken to be of very simple form (such as $x_i(t) \geq 0$) and this should open the way for the development of simple feasible direction methods to handle the hard side constraints.

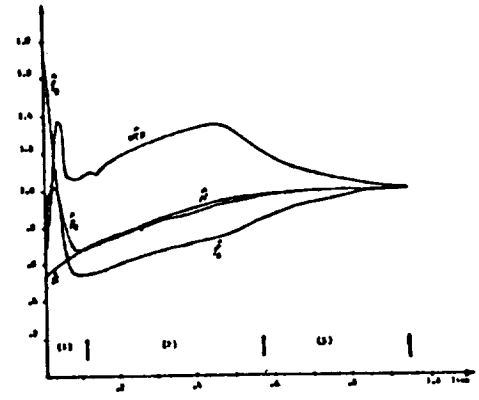

Fig. 16 Conjugate Gradient Open Loop Optimal Time Trajectories

SUMMARY

The objective of this work is to report on various alternatives to linear quadratic design methods for jet engine control systems. The principal global considerations are problem formulation, simple analytical models, the DYNGEN engine simulator, and Mathematical Programming methods. The principal linear multivariable approaches are the Characteristic Locus Method of MacFarlane, the Inverse Nyquist Method of Rosenbrock and Polynomial Methods as studied by Sain (21).

Even though the number of system states is moderate, the multivariable nature of the problem presents considerable difficulty and pushes current computer software to the limit in numerical efficiency. It is anticipated that both global nonlinear and local linear considerations will be essential to a good design approach to jet engine control systems, and that both areas will require new innovations in the development of computer software and effective numerical procedures.

ACKNOWLEDGEMENTS

The authors would like to thank the National Aeronautics and Space Administration for their support of this study under NASA NSG 3048, and the National Science Foundation for their support under NSF GK 37285.

REFERENCES

(1) Michael, G. J., et al., "An Analytical Method for the Synthesis of Nonlinear Multivariable Feedback Control," AD-762 797, June 1973.

(2) Sevich, G. J., and Beattie, E. C., "Integrated Flight Propulsion Control Design Techniques Starting with the Engine," Society of Automotive Engineers, Air Transportation Meeting, Dallas, Texas, paper 740481, May 1974.

(3) Geyser, L. C., and Lehtinen, B., "Digital Program for Solving the Linear Stochastic Optimal Control and Estimation Problem," NASA TN D-7820, Lewis Research Center, March 1975.

(4) Sellers, J. F., and Daniele, C. J., "DYNGEN-A Program for Calculating Steady-State and Transient Performance of Turbojet and Turbofan Engines," NASA TN D-7901, Lewis Research Center, April 1975.

(5) Shearer, J. C., "An IBM 370/158 Installation and User's Guide to the DYNGEN Jet Engine Simulator," M.S. Thesis, University of Notre Dame, Department of Electrical Engineering, November 1975.

(6) Seldner, K., Mihaloew, J. R., and Blaha, R. J., "Generalized Simulation Technique for Turbojet Engine System Analysis," NASA TN D-6610, Lewis Research Center, February 1972.

(7) Seldner, K. et al., "Performance and Control Study of a Low-Pressure-Ratio Turbojet Engine for a Drone Aircraft," NASA TM X-2537, April 1972.

(8) Brennan, T. C., "Simplified Simulation Models for Control Studies of Turbojet Engines," M.S. Thesis, University of Notre Dame, Department of Electrical Engineering, November 1975.

(9) "Low Order Linearized Models of Turbine Engines," Performance Analysis Branch, Directorate of Propulsion and Power Engineering, Aeronautical Systems Division ASD-TR-75-24, Wright-Patterson AFB, July 1975.

(10) Liu, R. and Suen, L. C., "Minimal Dimension Realization and Identifiability of Input/Output Sequences," Memorandum, University of Notre Dame, Dept. of Electrical Engineering, April 1975.

(11) MacLane, S. and Birkhoff, G., Algebra, Macmillan, New York, 1967.

(12) H. H. Rosenbrock, Computer-Aided Control System Design, Academic Press, New York, 1974.

(13) H. H. Rosenbrock, State-Space and Multivariable Theory, Wiley, New York, 1970.

(14) A. G. J. MacFarlane, "Relationships Between Recent Developments in Linear Control Theory and Classical Design Techniques," University of Manchester Institute of Science and Technology, Manchester M60 1QD, England.

(15) A. G. J. MacFarlane, "Notes on the Vector Frequency Response Approach to the Analysis and Design of Multivariable Feedback Systems," University of Manchester Institute of Science and Technology, Manchester M60 1QD, England, August 1972.

(16) V. Seshadri, "Compensation of Multivariable Control Systems," M.S. Thesis, Department of Electrical Engineering, University of Notre Dame, Notre Dame, Indiana 46556, May 1976.

(17) E. Hille, Analytic Function Theory, Vol. II, Chelsea, New York, 1962.

(18) John F. Barman and Jacob Katzenelson, "A Generalized Nyquist-Type Stability Criterion for Multivariable Feedback Systems," International Journal of Control, Vol. 20, No. 4, pp. 593-622, 1974.

(19) H. H. Rosenbrock and P. A. Cook, "Stability and the Eigenvalues of G(s)," International Journal of Control, Vol. 21, No. 1, pp. 99-104, 1975.

(20) A. Maloney, "Multivariable Techniques Applied to Jet Engine Control," M.S. Thesis, Department of Electrical Engineering, University of Notre Dame, Notre Dame, Indiana 46556, August 1976.

(21) Sain, M. K., "A Free-Modular Algorithm for Minimal Design of Linear Multivariable Systems," Preprint, Sixth IFAC World Congress, Part IB, pp. 9.1-1-9.1-7, August 1975.

(22) Gejji, R. R., "Polynomial Techniques Applied to Multivariable Control," M.S. Thesis, Univ. of Notre Dame, Dept. of Electrical Engineering, March 1976.

(23) Bryson, A.E., and Ho, Y.C., "Applied Optimal Control: Optimization, Estimation, and Control," Wiley and Sons, New York, Revised Printing, 1975.

(24) Jacobson, D. H., "A Transaction Technique for Optimal Control Problems with a State Variable Constraint," IEEE Trans. Automatic Control, October 1969.

(25) Larson, R., "State Increment Dynamic Programming," American Elsevier Publishing Co., 1968.

(26) Luenberger, D., "Introduction to Linear and Nonlinear Programming," Addison-Wesley, 1965.

(27) Pierre, D. A. and Lowe, M. J., "Mathematical Programming Via Augmented Lagrangians," Addison-Wesley, 1975.

(28) Rockafeller, R. T., "Augmented Lagrange Multiplier Functions and Quality in Nonconvex Programming," SIAM Journal on Control, Vol. 12, pp. 268-285, May 1974.

(29) Lasdon, L. S., "The Conjugate Gradient Method for Optimal Control Problems," IEEE Trans. Automatic Control, April, 1967.

(30) Basso, R., "Alternative Methods to Obtain Time Optimal Jet Engine Control," M.S. Thesis, Univ. of Notre Dame, Dept. of Electrical Engineering, in progress.

D4

GRAPHICS ANALYSIS OF DOMINANCE IN JET ENGINE CONTROL MODELS

A Thesis

Submitted to the Graduate School of the
University of Notre Dame in Partial Fulfillment
of the Requirements for the Degree of

Master of Science in Electrical Engineering

by

Anthony Joseph Maloney III, B.S.E.E.

Michael K. Sain
Director

Department of Electrical Engineering
Notre Dame, Indiana
August, 1976

GRAPHICS ANALYSIS OF DOMINANCE IN JET ENGINE CONTROL MODELS

Abstract

Modern control systems design must necessarily address the control of objects having more than one input and output. For the better part of a decade, now, the most widely available tool in the linear case has been LQG (Linear, Quadratic, Gaussian) Theory, a powerful approach which remains nonetheless indirect --- a consequence of its spinoff from the theory of optimal control.

In the last few years, however, new alternatives to the LQG Theory have been brought forward. More than one of these is related to generalizations of the classical approaches of Nyquist. An example of this type of activity is the dominance approach of Rosenbrock. Within about the same span of time, it has become increasingly apparent in the jet engine control industry that the workhorse hydromechanical technique for control was reaching a plateau in terms of being able to respond to future needs. As attention has turned to the possibilities of having a digital computer take over some of these tasks, interest has grown in determining the applicability of linear multivariable methods to families of jet engine models.

This study is one of several of such type. Using the Rosenbrock methodologies, we have examined a two-input, two-output, five-state jet engine model in the class described by Michael and Farrar. Inputs chosen are jet exhaust area and main burner fuel flow; outputs are thrust

and high turbine inlet temperature; states are high compressor speed, fan speed, fan turbine inlet temperature, main burner pressure, and afterburner pressure. Software has been developed in the Speakezy Language for graphics display and hard copy on the University of Notre Dame IBM 370/158 system.

The main result seems to be that achieving dominance in typical jet engine models is a nontrivial task. Our main example does turn out to be diagonally dominant; however we encountered definite difficulties in trying to achieve row or column dominance, which was the main objective. There seems to be a real need for additional research in frequency dependent compensation, both of the type which achieves dominance and of the type that modifies dynamic behavior when neither row nor column dominance is attained.

TABLE OF CONTENTS

PROCEEDINGS OF THE

NINETEENTH MIDWEST SYMPOSIUM ON CIRCUITS AND SYSTEMS

AUGUST 16-17, 1976

Edited by
J. D. McPherson

A JET ENGINE CONTROL PROBLEM FOR EVALUATING MINIMAL DESIGN SOFTWARE*

Raghvendra R. Gejji and Michael K. Sain
Department of Electrical Engineering
University of Notre Dame
Notre Dame, Indiana 46556

Abstract

The problem of designing feedforward and feedback compensators to achieve a specified closed loop performance matrix is shown to reduce to a minimal design problem. Existing results for the F100 turbofan engine can be interpreted to yield the closed loop specifications for the associated control problem--and also a possible solution. All possible solutions can be enumerated by computing the kernel of a polynomial matrix. It is shown how this matrix can be obtained from the formulation of the minimal design problem.

1. INTRODUCTION

The design of compensators in multivariable control problems often leads to the minimal design problem (MDP), which can be represented by the equation

$$G_1(v)\, G(v) = G_2(v). \qquad (1)$$

Here, G_1, G_2 and G are all matrices over the field F(v) of rational functions in the indeterminate 'v' and with coefficients from the field F. G_1 and G_2 are known, while G represents the compensator to be designed. The problem is to enumerate all realizable G's which satisfy (1) and have a minimum number of dynamical elements.

In recent years, considerable research has been directed toward the minimal realization problem. We cite, for example, studies by Popov [1], Forney [2] and Wolovich [3]. But the focus here is on the minimal design problem instead. This latter problem has been studied by Wang and Davison [4], by Forney [2], and by Sain [5], who showed how it can be transformed into a problem of finding the kernel of a linear operator over free F[v]-modules, (where F[v] is the ring of polynomials in 'v' over F) and proposed an algorithm for its solution in that structure. First generation software has been written [6,9] to find the kernel of a polynomial operator.

Later application studies [7] have shown that when F is the field of real numbers and 'v' the complex frequency 's', the computational aspect of the problem becomes quite demanding. Numerical challenges increase with the size of the matrix, the degrees of the polynomials and the variation in magnitude of the coefficients.

We propose to describe herein a minimal design problem which is academically tractable, sufficiently challenging to be relevant to researchers in this area, and of such potential application as to be of more than academic interest. We will show how the problem is reduced to the form (1) and further to a form suitable for solution by kernel calculating software.

We have selected a version of the problem studied by Michael and Farrar [8] for control of the F100 turbofan engine. The problem is one of selecting feedback and feedforward compensators in order to make the overall transfer function matrix exactly equal to some desired $T^*(s)$. The desired $T^*(s)$ is selected by state-space optimization techniques similar to those described in Reference [8]. In this paper, we propose to outline briefly the techniques and also present the numerical results obtained.

2. MDP AND POLYNOMIAL EQUATIONS

2.1 SOME POLYNOMIAL MODULE CONCEPTS

*This work was supported in part by the National Science Foundation under Grant ENG 75-22322 and in part by the National Aeronautics and Space Administration under Grant NSG 3048.

Before we examine the solution of MDP via polynomial equations, it is necessary to explain some of the terminology. The reader may wish to refer to a standard text on algebra [10] or multivariable linear systems [11] for further discussion.

Recall that, depending on the choice of basis, any element in the free polynomial module $(F[v])^n$ can be represented by a list of n ring elements. In vector space terminology this is familiar as a column vector. A correspondence between such a list and an element of the module is implicit.

The column degree of a list is the maximum of the degrees of all the elements occurring in it.

The column degree rank of an mxn matrix R(v) is obtained thus. Form the mxn F-matrix R; the i^{th} column of R is formed from the coefficients in the i^{th} column of R(v), corresponding to its i^{th} column degree. The rank of R is the column degree rank of R(v).

For $p \leq n$, the set $\{b_1, b_2, \ldots, b_p\}$, of elements in $(F[v])^n$, is said to be reduced if the matrix

$$[b_1, b_2, \ldots, b_p]$$

has column degree rank p. If, in addition, the last p rows of the above matrix have column degree rank p, then the set is said to admit a linear dynamical interpretation [5].

A matrix D(v) of polynomials is unimodular if the determinant $|D(v)|$ is nonzero in the field F.

2.2 MDP AND POLYNOMIAL MODULES

We return, once again, to the minimal design problem (MDP) of linear multivariable systems, which can be stated as follows. Determine whether there exist rational proper solutions for G(v) in

$$G_1(v)\, G(v) = G_2(v), \tag{2}$$

where G_1 and G_2 are matrices of rational functions; and if so, find one that yields a realization with the minimum number of dynamical elements. To do this, we go through the following mathematical manipulation. Let

$$G_1(v) = \frac{N_1(v)}{d_1(v)} \tag{3}$$

$$G_2(v) = \frac{N_2(v)}{d_2(v)}, \tag{4}$$

and use the matrix fraction representation for G

$$G(v) = N(v)\, D^{-1}(v) \tag{5}$$

where N_1, N_2, N and D are matrices over F[v] and d_1 and d_2 are polynomials in F[v]. Also, we assume that G_1 is k x m and G_2 is k x n, which requires G to be m x n. Making the above substitution, we get (6),

$$\frac{N_1(v)}{d_1(v)} \cdot N(v)\, D^{-1}(v) = \frac{N_2(v)}{d_2(v)} \tag{6}$$

which can easily be reduced to (7),

$$d_2(v)N_1(v)N(v) = d_1(v)\, N_2(v)\, D(v) \tag{7}$$

or (8).

$$[d_2(v)N_1(v) \vdots -d_1(v)N_2(v)] \begin{bmatrix} N(v) \\ D(v) \end{bmatrix} = [0] \tag{8}$$

The last equation can be viewed in a manner analogous to that of a standard linear equation with coefficients in a field.

$$Ax = b \tag{9}$$

where $A \in F^{kxm}$, $x \in F^m$, $b \in F^k$. Complete solution of (9) requires us to calculate bases for the kernel and image of A viewed as a linear operator from the space F^m to the space F^k. Similarly, we look at the first matrix in the left member of (8) as a linear operator from the free F[v]-module $(F[v])^{m+n}$ to the free F[v]-module $(F[v])^k$. Then, in any solution $\begin{bmatrix} N \\ D \end{bmatrix}$ of (8), each of the n columns will be contained in the kernel of the polynomial operator. All solution pairs (N,D) can thus be built up from kernel elements. How can we tell if a solution pair (N,D) will yield a minimal G(v)?

Although we cannot go into the theory of the answer to the last question, we present some observations which should be helpful in clarifying the mechanics of the solution. The idea is to assume that for any candidate pair (N,D), the n columns of the matrix $\begin{bmatrix} N \\ D \end{bmatrix}$ form a reduced set.

This can be done without loss of generality, because if this is not the case, it is a straightforward procedure to remove from (N,D) a greatest common right divisor R and obtain an equivalent pair $(\hat{N},\hat{D})$ such that (10), (11) and (12) hold,

$$N(v) = \hat{N}(v)\, R(v) \tag{10}$$
$$D(v) = \hat{D}(v)\, R(v) \tag{11}$$
$$N(v)D^{-1}(v) = \hat{N}(v)\hat{D}^{-1}(v) \tag{12}$$

and R is non-unimodular. Then we make the following points, which are offered without proof.

(1) $N(v)D^{-1}(v)$ can be realized by a linear dynamical system if the columns of the matrix D(v) are reduced. In such a case $N(v)D^{-1}(v)$ is proper and there exists a minimal realization A,B,C,E, over F such that

$$G(v) = N(v)\, D^{-1}(v) = C(vI-A)^{-1}B + E \tag{13}$$

This condition was previously defined for the columns in $\begin{bmatrix} N \\ D \end{bmatrix}$ to have a linear dynamical interpretation.

(2) If property (1) is satisfied, then the determinant $|D(v)|$ is the characteristic

polynomial $|vI-A|$, possibly scaled by a field element; and

(3) the sum of the column degrees of D(v) is the number of dynamical elements required to realize G(v).

The problem of finding proper solutions for G(v) is thus equivalent to one of selecting kernel elements which admit a linear dynamical interpretation.

2.3 THE MDP ALGORITHM

The solution to MDP [5] is obtained by systematically applying the following steps. Let T(v) represent the k x (m+n) matrix of polynomials whose kernel is to be calculated. We assume that k is less than m+n, or in other words, the kernel is non-zero. Apply the following steps.

(1) Obtain a basis for Ker T in this manner. Adjoin an (m+n) x (m+n) identity matrix to T to get the (k+m+n) x (m+n) matrix

$$\begin{bmatrix} T(v) \\ I \end{bmatrix}$$

By applying unimodular column operation type transformations, reduce the first k rows to a column echelon form. Let the final form of the matrix be

$$\begin{bmatrix} E_{11} & 0 \\ E_{12} & E_{22} \end{bmatrix}$$

(2) The columns of E_{22} are a basis for Ker T. Obtain a reduced basis set from these by further application of suitable unimodular transformations.

(3) From the elements of the reduced basis, select (if possible) n elements that admit a linear dynamical interpretation, such that the sum of the column degrees is the least possible.

Failure of the algorithm indicates no solution existing to MDP, and success yields a solution automatically. The importance of the algorithm arises from the fact that all possible solutions can be built from the reduced basis alone.

3. MDP IN JET ENGINE CONTROL

3.1 PROBLEM DESCRIPTION

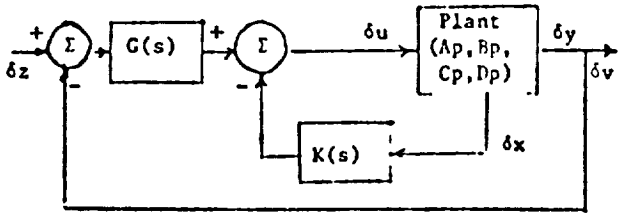

Figure 1. Compensation Problem

In Figure 1, the plant is the linearized model of the F100 jet engine. This is a 2-input, 5-state, 2-output model. The model holds for small variations around a steady state obtained at a power level angle (PLA) of 47°, which corresponds to a point approximately midway between idle and maximum nonafterburning power. Ap, Bp, Cp and Dp represent the corresponding state description matrices. These were obtained from data given in Reference [8] and are listed in Table I. The underlying dynamics are represented by the equations (14) and (15).

$$\delta\dot{x} = Ap\delta x + BP\delta u \quad (14)$$
$$\delta y = Cp\delta x + Dp\delta u \quad (15)$$

TABLE I

STATE DESCRIPTION MATRICES FOR JET ENGINE (PLA=47°)

Matrix	Matrix Elements				
Ap	-57.096	3.613	-10.211	-5.481	-2.715
	19.832	-72.34	30.295	40.972	15.327
	0.66	4.496	-3.601	-0.011	-2.808
	1.326	2.313	-0.809	-3.032	-0.821
	0.882	0.703	2.922	1.471	-4.596
Bp		1.017		39.792	
		-0.125		4.181	
		-0.077		-0.382	
		-0.088		-0.565	
		-3.563		-0.785	
Cp	-0.037	0.031	-0.016	-0.042	1.368
	1.081	0.149	-0.057	0.001	-0.096
Dp		0.546		0.018	
		-0.013		-0.086	

The inputs are (1) jet exhaust area and (2) main burner fuel flow. The five states are (1) high-compressor speed, (2) fan speed, (3) fan turbine inlet temperature, (4) main burner pressure and (5) after burner pressure. The two outputs are (1) thrust and (2) high turbine inlet temperature.

δx represents the states being fed back through the dynamic compensator K(s). G(s) is the compensator in the forward path.

The design problem is to find G(s) and K(s) such that δv is related to δz by some desired transfer function matrix $T^*(s)$. The optimal integral control configuration of Michael and Farrar [8] is a specific solution, which requires ideal integrations in G(s). The optimal integral control configuration is subsequently discussed in this paper. The advantage of reformulating the problem as in Figure 1 is that it leads to MDP, and thence a kernel problem which yields all solutions of a particular class. For example, it may be possible to have a G(s) that does not call for ideal integrators. If so, hopefully it can be found using the polynomial techniques.

Before we proceed with the problem it may be well to consider whether specification of closed loop performance matrices is a sound idea with regard to jet engines. In the next section we will show that at least in one instance, the essence of the idea has already been used in the literature for designing controllers. We will choose the same result as a basis for obtaining closed loop specifications for our problem.

3.2 MATHEMATICAL FORMULATION

In order to formulate mathematically the above "exact model matching" problem, we redraw Figure 1 as Figure 2.

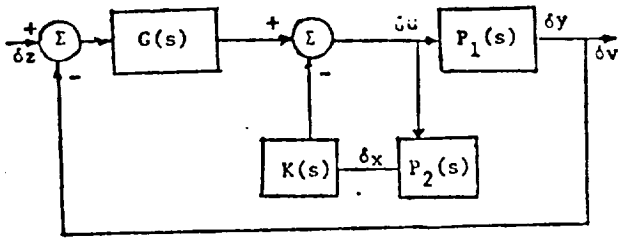

Figure 2. Plant As Two Transfer Functions

With $P_1(s)$ and $P_2(s)$ as in (16) and (17), and I in each case the conformal identity matrix,

$$P_1(s) = C_p(sI - A_p)^{-1} B_p + D_p \tag{16}$$

$$P_2(s) = (sI - A_p)^{-1} B_p \tag{17}$$

it follows immediately that

$$\delta y = P_1\, \delta u \tag{18}$$

$$\delta x = P_2\, \delta u \tag{19}$$

The design goal then translates into the equation (20),

$$(I + P_3(s))^{-1} P_3(s) = T^*(s) \tag{20}$$

where

$$P_3(s) = P_1(s)(I + K(s)P_2(s))^{-1} G(s) \tag{21}$$

If we assume all necessary inverses to exist, (20) can be simplified to (22)

$$P_3^{-1}(s) = T^{*-1}(s) - I \tag{22}$$

and further, by substitution of (21) to (23),

$$G^{-1}(s)(I + K(s)P_2(s))\, P_1^{-1}(s) = T^{*-1}(s) - I \tag{23}$$

or (24).

$$(I + K(s)P_2(s)) = G(s)(T^{*-1}(s) - I)\, P_1(s) \tag{24}$$

If we set

$$(T^{*-1}(s) - I)P_1(s) = P_4(s) \tag{25}$$

(24) becomes (26),

$$P_4^T(s)G^T(s) - P_2^T(s)K^T(s) = I \tag{26}$$

where superscript T denotes matrix transposition. Equation (26) is reduced to familiar MDP form to yield

$$\left[P_4^T(s) \vdots - P_2^T(s)\right] \begin{bmatrix} G^T(s) \\ K^T(s) \end{bmatrix} = I \tag{27}$$

Perform the obvious next step. Let

$$\left[P_4^T(s) \vdots - P_2^T(s)\right] = \frac{M(s)}{d(s)} \tag{28}$$

$$\begin{bmatrix} G^T(s) \\ K^T(s) \end{bmatrix} = N(s)D^{-1}(s) \tag{29}$$

where M, N and D are matrices over R[s] and d is a polynomial in R[s]. It can be shown [6] how to realize both G and K with one set of dynamics governed by D(s) . Now we have (30).

$$\frac{M(s)}{d(s)} \cdot \left[N(s)D^{-1}(s)\right] = I \tag{30}$$

or (31).

$$\left[M(s) \vdots - d(s)I\right] \begin{bmatrix} N(s) \\ D(s) \end{bmatrix} = [0] \tag{31}$$

Equation (31) is a standard kernel problem suitable for solution by kernel calculating software. We note that P_4 is 2x2 and P_2^T is 2x5, which tells us that the matrix

$$T(s) = \left[M(s) \vdots - d(s)\, I\right] \tag{32}$$

would be 2x9.

4. CLOSED LOOP SPECIFICATIONS FOR A JET ENGINE CONTROL PROBLEM

4.1 THE APPROACH OF MICHAEL AND FARRAR

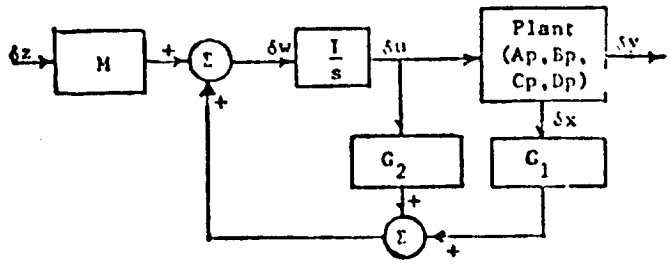

Figure 3. Linear Optimal Control

The standard linear optimal control configuration is shown in Figure 3. G_1 and G_2 are obtained as outlined in Reference [8] to minimize a performance index of the type

$$J = \tfrac{1}{2}\int (\delta y^T Q \delta y + \delta \dot{u}^T R \delta \dot{u} + \delta \dot{y}^T S \delta \dot{y})dt \qquad (33)$$

The problem is transformed to a linear state feedback law by considering the δu's and the δx's as states of an extended system having δw as its input vector.

The matrices Q, R and S for our problem are listed in Table II.

TABLE II

WEIGHTING MATRICES WITH OPTIMAL INTEGRAL CONTROL SOLUTION

Matrix	Matrix Elements				
Q	50,000		0		
	0		10,000		
R	550		0		
	0		175		
S	0		0		
	0		20,000		
L	0.509	0.268	1.979	2.171	2.098
	-2.137	-0.377	-0.223	-0.776	-0.227
H	8.329		-1.126		
	2.811		-1.842		

The optimal integral control configuration is shown in Figure 4.

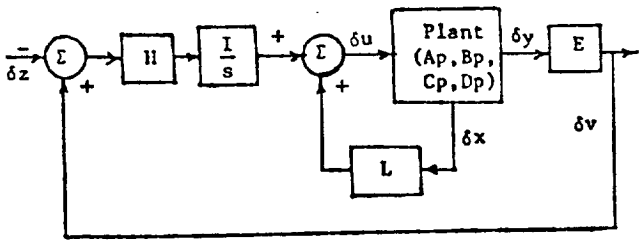

Figure 4. Optimal Integral Control

It has been shown in [8] that the H and L matrices are related to the G_1 and G_2 matrices of Figure 3. The resulting L and H matrices as obtained from G_1 and G_2 are shown in Table II. The advantage of the control scheme of Figure 4 comes from the added dynamics of the integrators. This causes the steady state error to go to zero, even in the presence of plant parameter variation.

4.2 EXACT MODEL MATCHING APPLIED TO THE PROBLEM

It is shown here that the problem of going from linear optimal control to optimal integral control is esentially one of matching closed loop transfer function matrices.

The transfer function $T^*(s)$ relating the output δv to the input δz can be shown to be as (See Figure 3) in (34), if $\delta v = E\delta y$,

$$T^*(s) = EP_5(s)\,[sI - P_6(s)]^{-1}\,M \qquad (34)$$

where

$$P_5(s) = Cp(sI - Ap)^{-1}\,Bp + Dp \qquad (35)$$

$$P_6(s) = G_1(sI - Ap)^{-1}\,Bp + G_2 \qquad (36)$$

In the actual problem being considered, E is taken to be be the 2x2 identity matrix and its presence as a factor is ignored.

Next, we use the relation given in [8], that is,

$$M = -H \qquad (37)$$

$$[L \;\; H]\begin{bmatrix} Ap & Bp \\ ECp & EDp \end{bmatrix} = [G_1 \,;\, G_2] \qquad (38)$$

and thereby continue the proof. First, it is seen that in Figure 3,

$$T^*(s) = -EP_5(s)[sI - P_6(s)]^{-1}\,H \qquad (39)$$

Second, we see from Figure 4, that

$$T^*(s) = -EP_5(s)[sI - P_7(s)]^{-1}\,H \qquad (40)$$

where

$$P_7(s) = HE\,P_5(s) + sL(sI - Ap)^{-1}\,Bp \qquad (41)$$

It is easy to show that both equations for $T^*(s)$ are the same, by comparing $P_7(s)$ and $P_6(s)$, with the aid of (37) and (38).

Thus, the systems in Figures 3 and 4 have the same overall transfer function matrices.

5. DISCUSSION OF THE KERNEL PROBLEM

In the preceding sections, we have shown how, starting with the state matrices for the plant, and the compensator matrices L and H in the optimal integral control scheme, we arrive at a standard kernel problem. In the final analysis, the design problem of Section 3 yields a 2x9 matrix of polynomials, whose kernel must be computed for a complete solution of the problem. We cannot reproduce the entire matrix here due to lack of space. However, we mention that a typical element in the matrix is a 13th degree polynomial as shown in Figure 5. Further, we see a wide range of variation in the magnitude of the coefficients. This makes the problem just large enough to give a thorough test to kernel calculating software such as [6].

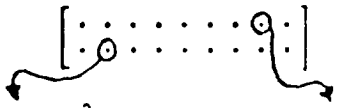

1.17	E10	s^3	-1.37	E10	s^2
+4.40	E10	s^4	-4.99	E10	s^3
+4.06	E10	s^5	-4.21	E10	s^4
+1.18	E10	s^6	-1.07	E10	s^5
-1.24	E9	s^7	+1.49	E9	s^6
-1.26	E9	s^8	+1.99	E9	s^7
-2.07	E8	s^9	+1.99	E8	s^8
-5.55	E6	s^{10}	+6.93	E6	s^9
-4.80	E4	s^{11}	+8.33	E4	s^{10}
-7.09	E1	s^{12}	+2.38	E2	s^{11}
+4.5	E-1	s^{13}	-1.00	E0	s^{12}

Figure 5. Polynomial Matrix

We now show how the results of Michael and Farrar can be interpreted to establish the existence of a solution to the MDP problem that has been formulated. To do this compare Figures 1 and 4. Then Figure 4 is seen as a possible solution to the problem of Figure 1. This happens because in Figure 4 we are able to achieve the closed loop specification $T^*(s)$ by setting

$$G(s) = \frac{-H}{s} \tag{42}$$

$$K(s) = -L \tag{43}$$

Combine (42) and (43) with the matrix fraction representation

$$\begin{bmatrix} G^T(s) \\ \hline K^T(s) \end{bmatrix} = N(s)D^{-1}(s) \tag{44}$$

We can now identify

$$N = \begin{bmatrix} -H^T \\ \hline -sL^T \end{bmatrix} \tag{45}$$

$$D = sI \tag{46}$$

Then the two columns $(\text{in}(F[s]))^9$ of the matrix $\begin{bmatrix} N \\ \hline D \end{bmatrix}$ formed from (45) and (46) will both be in the kernel of the polynomial matrix T(s) obtained from the problem. This assures existence of a solution to the kernel problem we have formulated.

6. CONCLUSION

We have presented a kernel problem which we believe will be most interesting to researchers in the area. So far the attempts for mechanizing the solution of such problems have been of a preliminary nature [6]. Existing problems in the literature tend to be of an academic nature. Elliott [9] has reported good success, but the problems that have been tried are of very limited conplexity. We feel that the problem presented here is challenging and worthwhile of numerical study.

We have mentioned before, that when the kernel calculating software of [6] was used, a perfect solution was not obtained. As a sketch of our numerical experience we should like to record that out of seven elements in the reduced basis, five were of first degree. However, this solution was not conclusive, because attempts to generate the solution of (45) and (46) from these five columns have not yet been successful.

7. REFERENCES

1. Popov, V.M., "Some Properties of Control Systems with Irreducible Matrix Transfer Functions," in Seminar on Differential Equations and Dynamical Systems (Lecture Notes in Mathematics, Number 144), pp. 250-261, New York: Springer, 1970.
2. Forney, Jr., G.D., "Minimal Bases of Rational Vector Spaces, with Applications to Multivariable Linear Systems," SIAM Journal on Control, Vol. 13, pp. 493-520, May 1975.
3. Wolovich, W.A., "The Determination of State-Space Representations for Linear Multivariable Systems," Automatica, Vol. 9, pp. 97-106, January 1973.
4. Wang, S.H. and Davison, E.J., "A Minimization Algorithm for the Design of Linear Multivariable Systems," IEEE Transactions on Automatic Control, Vol. AC-18, pp. 220-225, 1973.
5. Sain, M.K., "A Free Modular Algorithm for Minimal Design of Linear Multivariable Systems," Preprints Sixth IFAC World Congress, pp. 9.1-1--9.1-7, Boston, August 1975.
6. Gejji, R.R. and Sain, M.K., "Polynomial Techniques Applied to Multivariable Control of Jet Engines," Technical Report No. EE-761, Dept. of Electrical Engineering, University of Notre Dame, Notre Dame, Indiana, March 1976.
7. Sain, M.K., Leake, R.J., et.al., "Alternative Methods for the Design of Jet Engine Control Systems," Joint Automatic Control Conference, Purdue University, Lafayette, Indiana, 1976.
8. Michael, G.J. and Farrar, F.A., "An Analytical Method for the Synthesis of Nonlinear Multivariable Feedback Control," United Aircraft Research Laboratories Report M941338-2, East Hartford, Connecticut, June 1973.
9. Elliott, H., "Implementation of Computer Algorithms Related to Multivariable Systems Theory," Division of Engineering Technical Report No. NSF-Eng73-03846AOI/3, Brown University, Providence, Rhode Island, May 1975.
10. MacLane, S. and Birkhoff, G., Algebra. London: Macmillan, 1967.
11. Rosenbrock, H.H., State Space and Multivariable Theory. New York: Wiley, 1970.

omit

Preprint of paper to be presented at the
1976 Midwest Symposium on Circuits and
Systems, University of Wisconsin,
Milwaukee, August 16-17, 1976.

INTERACTION STUDIES ON A JET ENGINE MODEL BY CHARACTERISTIC METHODOLOGIES

V. Seshadri and M. K. Sain
Department of Electrical Engineering
University of Notre Dame
Notre Dame, Indiana 46556

Abstract

Conflicting requirements of stability and non-interaction can present demanding design questions in control studies on jet engine models. It is shown that a step-by-step solution exists, at least in some cases. However, in some situations, interaction-free design is very difficult to achieve. The features of both these possibilities are illustrated with the aid of MacFarlane's characteristic locus.

1. INTRODUCTION

The Bode [1] and Nyquist [2] classical frequency response approaches for the analysis and design of single-input, single-output systems resulted in a very flexible and useful design technique because it allowed the conflicting requirements of stability and accuracy to be treated simultaneously by means of a single form of representation - the open-loop frequency response function of a complex variable. Then came the state-space methods which moved the focus away from graphical techniques towards optimization methods. The potential and elegance of state-space methods stems from the systematized utilization of the properties of linear vector spaces. The trade-off, of course, is that one loses a considerable portion of the design intuition which is of the essence in the classical frequency-response approach.

MacFarlane [3] has attempted to combine the essence of the two abovementioned approaches by adopting, as his basic tool, linear vector spaces defined over the complex field. In this way he has developed a general vector frequency response approach to the analysis and design of multivariable feedback systems, with the classical scalar design approach as just a special case of this general approach.

In this paper, we will introduce the generalized characteristic locus method developed by MacFarlane [3], and show how this method can be used for a step-by-step design of multivariable compensators. We will not discuss the theoretical basis of the design method in much detail, due to limitations of space; for that, the reader is referred to [3], [10]. Instead, since a major test of the effectiveness of a design method is how viable a tool it is for the actual design of reasonable compensators in real-world situations, we will illustrate, here, the use of the generalized locus method by means of a jet engine example.

2. THE PLANT

The basic plant that we have selected is the F-100 turbofan engine, as described by Michael and Farrar [4]. Specifically, we consider a two-input, two-output, five-state linearized model at a power lever angle (PLA) of 47°, which corresponds to a region roughly midway between the engine idle condition and maximum nonafterburning power. The inputs being considered are jet exhaust area and main burner fuel flow, the outputs are thrust and high turbine inlet temperature, and the five states are high-compressor speed, fan speed, fan turbine inlet temperature, main burner pressure and afterburner pressure.

The A, B and C matrices for this linearized jet engine model, at a PLA of 47°, are shown in Figure 1. Actually, the system that we are first considering is a simplification obtained by excluding the D

matrix. Next, the plant transfer function matrix is obtained by means of the Fadeeva algorithm [5], and is given by

$$G(s) = \frac{\begin{bmatrix} (-4.9s^4-667.3s^3 & (-2.4s^4-188.1s^3 \\ -23068s^2-82206s & -1093.3s^2+27647s \\ -85325) & +93090) \\ (1.4s^4+137.6s^3 & (43.7s^4+3780.5s^3 \\ +2206.3s^2+3298.9s & +28827s^2+86361s \\ -1798.1) & +89748) \end{bmatrix}}{s^5+140.7s^4+5337.6s^3+38691s^2+119690s+133389} \quad (1)$$

3. THE FEEDBACK SCHEME

The feedback scheme that we employ is based on the input-output approach to compensation. In Figure 2, G(s) is the plant that we just described. K(s) is the feedforward compensator to be designed. With respect to our example, the compensator K(s) would be represented by a 2x2 matrix, each of whose elements belongs to R(s), the field of real rational functions in s. Note also that since we will be dealing with the generalized Nyquist approach to design, Figure 2 shows a unity feedback scheme. Considerable care is advisable in considering this tool when the feedback matrix is not proportional by an element of R(s) to the identity matrix [6].

4. THE DESIGN PROCEDURE

The design procedure attempts to strike a balance between four conflicting objectives: stability, integrity, interaction and accuracy. How each of these individual aspects of the closed-loop performance is determined is elaborated below.

4.1 STABILITY

Let Q(s) denote the composite system in the forward path, that is,

$$Q(s) = G(s)\ K(s). \quad (2)$$

The closed-loop transfer function matrix T(s) is given by

$$T(s) = [I + Q(s)]^{-1}\ Q(s). \quad (3)$$

Based on MacFarlane's approach [3] to the problem, we have the stability theorem that the difference between the number of right half-plane poles of the closed-loop configuration and those of the open-loop configuration is equal to the sum of the number of clockwise encirclements of the "usual" critical (-1,0) point by the characteristic loci of Q(s), where, by the term "characteristic loci" of a particular matrix we mean the loci of the eigenvalues of that matrix for all values of s on a "usual" Nyquist contour.

For a detailed discussion of the above theorem, the reader is referred to [3], [10]; here, we illustrate the theorem by applying it to the jet engine problem given by Equation 1. We let s follow the usual clockwise Nyquist contour, and compute the eigenvalues of (1) for each value of s. Thus we obtain the characteristic loci $q_i(s)$ of G(s); these loci, for $s = j\omega$ with ω varying from 0 to ∞, are shown in Figure 3(a) and (b).

To analyze these curves in terms of closed loop system stability, we first note that the open-loop characteristic polynomial (OLCP) is given by

$$s^5+140.7s^4+5337.6s^3+38691s^2+119690s+133389. \quad (4)$$

The zeros of the OLCP are found to be:

$$-79.207, -53.135, -2.389, -2.967+j2.113, -2.967-j2.113. \quad (5)$$

Since all the zeros of the OLCP are in the left half-plane, the system is open-loop stable. From the stability theorem then, the corresponding closed-loop system will be stable if and only if the net sum of critical point encirclements by the characteristic loci of G(s) is equal to zero.

Referring once again to Figure 3(a) and (b), and taking the critical point as (-1/k,0), (that is, with equal gains k in each loop) we deduce the following stability conditions:

(i) For $0<k<1.27(=1/.79)$, the closed-loop system is stable.

(ii) For $k\geq 1.27$, the locus (a) contributes clockwise encirclements of the critical point; thus the closed-loop system is unstable for $k\geq 1.27$.

4.2 INTEGRITY

A multivariable feedback system is said to be of high integrity if it remains stable under a stipulated set of failure conditions. Consistent with MacFarlane's concept of interaction-free system design [3], we will focus upon loop-failure conditions, that is, we will be designing compensators so that an output depends mainly upon one particular input, so our integrity test will involve testing the stability of the system with feedback only around a particular loop (and with all other loops open).

A measure of this stability is obtained by applying the Nyquist encirclement theorem to the frequency response loci of each of the diagonal elements of G(s). For detailed tables and figures, the reader is referred to [10]; for purposes of brevity, we merely state here that on applying this integrity test to the jet engine example of Equation 1, we find that the stable region is limited mainly because the integrity, with loop 2 open, is poor. This is intuitively pleasing in terms of an inspection of the 1-1 element of G(s); it would appear that the application of high gains around loop 1 will produce a positive feedback because of the minus signs. To remedy the situation, we change the sign of this feedback loop by means of an elementary compensator matrix

$$K_1 = \begin{bmatrix} -1 & 0 \\ 0 & 1 \end{bmatrix}. \quad (6)$$

This greatly improves the system integrity under loop-failure conditions; the resultant open-loop transfer function matrix is

$$Q_1(s) = G(s)\,K_1. \qquad (7)$$

Note that we have once again to perform a stability check on the new open-loop transfer function matrix (7). The steps of this calculation are shown in [10] and lead to the conclusion that, subject to the bound that k should be positive, the closed-loop system is now stable for high gains. Hence it is fair to surmise that the relatively poor stability properties were primarily due to lack of integrity; having corrected this, we next consider interaction.

4.3 INTERACTION

Consider once again the closed-loop multivariable feedback system of Figure 2. Now, if we apply $r_i(s)$ to the ith input, we will obtain some response from each of the controlled outputs $\{c_j(s): j=1,2,\ldots,n\}$. In interaction-free system design, one desires a specific output $c_i(s)$ to respond to $r_i(s)$ and all the other outputs $\{c_j(s): j=1,2,\ldots,n; j\neq i\}$ to remain "small". Thus the term "interaction" signifies the set of relationships that influence the way in which a particular input $r_i(s)$ affects the set of outputs $\{c_j(s): j=1,2,\ldots,n; j\neq i\}$.

It has been shown [3] that closed-loop interaction at low frequencies will be suppressed provided the moduli of the characteristic loci of Q(s) are sufficiently large, and that high-frequency interaction will be suppressed provided the angular misalignment $\theta_i(s)$ is small between the characteristic direction set of Q(s) and the standard basis direction set in R^n, where the "characteristic direction set" is just the set of eigenvectors associated with the characteristic loci, and the "standard basis direction set" is

$$\{(100\ldots0)^t,(010\ldots0)^t,\ldots,(00\ldots01)^t\}. \qquad (8)$$

Thus it is convenient to consider interaction over the whole frequency range by means of two sets of graphs:

(a) the moduli of $q_i(j\omega)$ versus ω
(b) the misalignment angles $\theta_i(j\omega)$ versus ω.

Figures 4(a) and (b), 5(a) and (b) show plots of the moduli of the characteristic loci versus frequency and of the angular misalignment of the characteristic directions versus frequency for the open-loop transfer function matrix $Q_1(s)$, (7), of our example. An inspection of these plots shows that there are interaction difficulties mainly at low frequencies. To compensate this, we use Rosenbrock's diagonal-dominance ideas [7], [8] and insert the controller factor

$$K_2(s) = Q_1^{-1}(0)/s, \qquad (9)$$

where

$$Q_1(0) = \frac{\begin{bmatrix} 85325 & 93090 \\ 1798.1 & 89748 \end{bmatrix}}{133389}. \qquad (10)$$

The modified open-loop transfer function matrix is

$$Q_2(s) = Q_1(s)\,K_2(s) \qquad (11)$$

which, hopefully, will display better interaction characteristics at low frequencies. Figures 6(a) and (b), 7(a) and (b) show that this is indeed the case; whereas the alignment of the characteristic directions has remained practically unchanged, the moduli of the characteristic loci are larger at low frequencies, so that the design is quite satisfactory with respect to both low-frequency and high-frequency interaction.

Figures 8(a) and (b) show the characteristic loci of the current open-loop transfer function matrix $Q_2(s)$. They are of particular interest, since they typify the situation in which the transfer function matrix has an "s" in the denominator, corresponding to an open-loop pole at the origin. Thus, to find out the direction in which the characteristic loci of Figures 8(a) and (b) close, we must exclude this pole by means of an indentation (say, a small counter-clockwise semi-circle) at the origin.

Figures 9(a) and (b) give two families of curves corresponding to semi-circles of different radii at the origin, where ω varies from 0- to 0+. It is noteworthy that the curves are topologically consistent. From Figures 8(a) and (b), 9(a) and (b), we see that both characteristic loci "close" in the clockwise direction and that the system is stable; so we proceed to the final stage to adjust the overall performance.

4.4 ACCURACY

The overall percentage error of the closed-loop system of Figure 2 is defined as

$$\frac{||e(j\omega)||}{||r(j\omega)||} \times 100\% \triangleq \frac{\langle e(j\omega),e(j\omega)\rangle^{1/2}}{\langle r(j\omega),r(j\omega)\rangle^{1/2}} \times 100\%. \qquad (12)$$

Briefly, good closed-loop accuracy may be obtained by injecting gain along the characteristic directions [3]. Since, in our example, the characteristic directions are well-aligned to the standard basis directions, especially at higher frequencies, we can effectively inject gain along the characteristic directions by employing the simpler procedure of increasing the column gains. Selecting a diagonal "gain-injecting" controller factor

$$K_3 = \begin{bmatrix} 100 & 0 \\ 0 & 10 \end{bmatrix} \qquad (13)$$

we have the resultant open-loop transfer function matrix

$$Q_3(s) = Q_2(s)\,K_3$$

$$= \frac{\begin{bmatrix} (790.8s^4+107250s^3 & -(117.7s^4+13921s^3 \\ +3690229s^2+13049634s & +399034s^2+942715s \\ +13338558) & +15.3) \\ -(363.68s^4+34097s^3 & (687.23s^4+59726s^3 \\ +444918s^2+803767s & +474602s^2+1366945s \\ +9.73) & +1333912) \end{bmatrix}}{s^6+140.7s^5+5337.6s^4+38691s^3+119690s^2+133389s} \qquad (14)$$

The time response curves of the two outputs of the

final compensated system, to a unit step in each of the inputs by turn, are illustrated in Figure 10. From this figure, we see that interaction is negligible and that the time responses are fast and accurate. Hence our design is complete.

5. SOME FEATURES OF GENERALIZED LOCI

Now that we have worked through the design of a multivariable compensator using the generalized Nyquist loci, we are in a position to comment on certain features which characterize them. One trivial difference between these loci and the familiar single-variable Nyquist loci is that in the former case, the characteristic loci need not start from the real axis on the complex plane for s=0, since a matrix all of whose elements are real can have complex eigenvalues. Another difference is that, since the system may have a non-zero D matrix, that is, there may exist a direct coupling between the input and the output, the characteristic loci need not end on the real axis for s=j∞ either.

Another interesting exercise is to deduce the loci for s =-j∞ to s=0- from the loci for s=0+ to s=j∞. A little thought shows us how to deduce them, depending on the eigenvalues at 0 and ∞. If the eigenvalues of both matrices G(0) and G(∞) are real, the loci for s=-j∞ to s=0- are mirror images about the real axis of the loci for s=0+ to s=j∞. On the other hand, if these eigenvalues are complex conjugate pairs, the "positive" half of one locus will be the mirror image of the "negative" half of another locus, and vice-versa.

Yet another crucial question for Nyquist considerations is the behavior of the loci in the complex right half-plane. Barman and Katzenelson [9] have shown that, for stable systems such as the jet engine model under study here, there are exceptional points to be heeded in Re(s)>0. This feature precludes any easy approach to identifying "individual" closed-path characteristic loci, although, by the addition of branch cuts from the exceptional points, together with a corresponding modification of the Nyquist contour, it is possible to achieve this goal [9]. The problem, however, is that computation of exceptional points off the imaginary axis, as well as the branch cuts, presents an added computational burden. It seems much easier, instead, to use the above approach of "piecing together" the various loci; but this may not always be possible, as the following extended jet engine example indicates.

The extended example that we now present includes the D matrix also (at PLA=47°) from Figure 11 in addition to the A, B and C matrices included earlier. The control inputs are the main burner fuel flow and the jet exhaust area; the outputs are thrust and the high turbine inlet temperature. The transfer function matrix of the resultant two input-five state-two output plant is given by

$$G(s) = \frac{\begin{bmatrix} (.018s^5+.145s^4 & (.546s^5+71.9s^4 \\ -92.05s^3-396.9s^2 & +2247s^3-1943s^2 \\ +29801s+95491) & -16855s-12495) \\ (-.086s^5+31.63s^4 & (-.013s^5-.437s^4 \\ +3321.5s^3+25500s^2 & +68.2s^3+1703.3s^2 \\ +76068s+78277) & +1742.9s-3532.2) \end{bmatrix}}{s^5+140.7s^4+5337.6s^3+38691s^2+119690s+133389} \quad (15)$$

In conformity with the procedure that we followed in the earlier example, we first obtain the characteristic loci of G(s), as shown in Figures 12(a) and (b). Note that, in contradistinction to the previous example, the loci do not end at the origin, because we have a non-zero D matrix with complex eigenvalues in this case. Furthermore, our earlier approach of "piecing together" two individual loci does not work here; in fact, only one closed, properly parameterized curve can be formed from these figures. This curve is shown in Figure 13 and requires use of Figures 12(a) and (b) as well as their mirror images about the real axis.

A question that now arises concerns the information that we can derive from such an unusual situation, that is, that the locus of Figure 13 cannot be separated into two individual loci. It is easy to see when such a situation will occur. It occurs, for our 2-5-2 case, if and only if one of the matrices

$$G(\infty),\ G(0)$$

has distinct real eigenvalues while the other has complex conjugate eigenvalues.

Equally important to us, however, is what this situation of non-decomposability into individual loci tells us. When we proceeded, with this jet engine example, to try to simultaneously achieve low interaction and good transient response, we encountered considerable difficulty. We could achieve one or the other, but not both. It is interesting to make the conjecture, then, that the difficulty in achieving low interaction while simultaneously obtaining good transient response is related to the fact that the locus of Figure 13 cannot be decomposed. If that is true, a possible design strategy could be to apply a pre-compensator to modify the eigenvalues at 0 and ∞ and then proceed with the design steps in the usual way.

6. ACKNOWLEDGMENTS

This work was supported in part by the National Aeronautics and Space Administration under Grant NSG-3048 and in part by the National Science Foundation under Grant ENG75-22322.

7. REFERENCES

1. H. W. Bode, Network Analysis and Feedback Amplifier Design. New York: Van Nostrand, 1945.

2. H. Nyquist, "Regeneration Theory," Bell System Technical Journal, vol. 11, pp. 126-147, 1932.

3. A. G. J. MacFarlane, "Notes on the Vector Frequency Response Approach to the Analysis and Design of Multivariable Feedback Systems," Department of Electrical Engineering and Electronics, University of Manchester Institute of Science and Technology, Manchester, August 1972.

4. G. J. Michael and F. A. Farrar, "An Analytical Method for the Synthesis of Nonlinear Multivariable Feedback Control," United Aircraft Research Laboratories Report M941338-2, East Hartford, Connecticut, June 1973.

5. L. A. Zadeh and C. A. Desoer, Linear System Theory. New York: McGraw-Hill, 1963.

6. H. H. Rosenbrock and P. A. Cook, "Stability and the Eigenvalues of G(s)," International Journal of Control, vol. 21, no. 1, pp. 99-104, 1975.

7. H. H. Rosenbrock, State Space and Multivariable Theory. New York: Wiley, 1970.

8. H. H. Rosenbrock, Computer-Aided Control Systems Design. New York: Academic Press, 1974.

9. J. F. Barman and J. Katzenelson, "A Generalized Nyquist-type Stability Criterion for Multivariable Feedback Systems," International Journal of Control, vol. 20, no. 4, pp. 593-622, 1974.

10. V. Seshadri, "Compensation of Multivariable Control Systems," M.S. Thesis, Department of Electrical Engineering, University of Notre Dame, Notre Dame, Indiana, May 1976; also available as Technical Report No. EE-763, May 9, 1976.

11. M. K. Sain, R. J. Leake, et al., "Alternative Methods for the Design of Jet Engine Control Systems," 1976 Joint Automatic Control Conference, Purdue University, Lafayette, Indiana, July 1976.

A	-57.096	3.613	-10.211	-5.481	-2.715
	19.832	-72.34	30.295	40.972	15.327
	0.66	4.496	-3.601	-0.011	-2.808
	1.326	2.313	-0.809	-3.032	-0.821
	0.882	0.703	2.922	1.471	-4.596
B		1.017		39.792	
		-0.125		4.181	
		-0.077		-0.382	
		-0.088		-0.565	
		-3.563		-0.785	
C	-0.037	0.031	-0.016	-0.042	1.368
	1.081	0.149	-0.057	0.001	-0.086

FIGURE 1. Jet engine model.

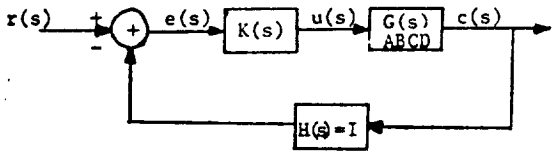

FIGURE 2. Multivariable feedback system.

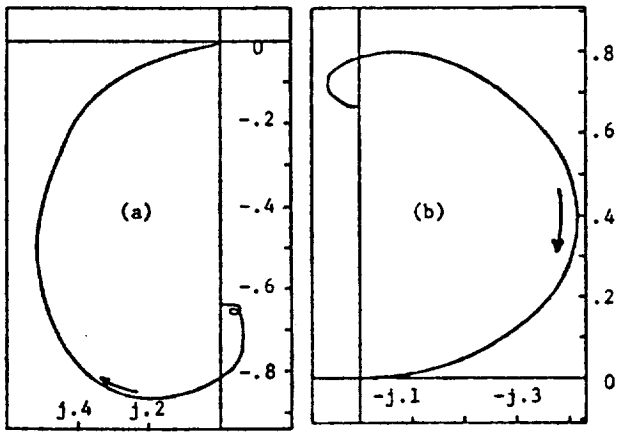

FIGURE 3. Characteristic loci of G(s).

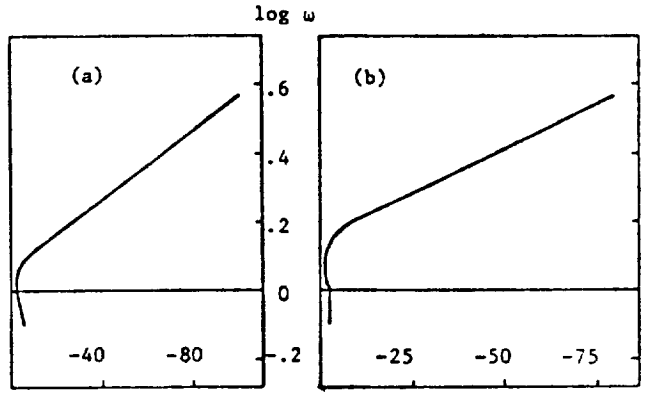

FIGURE 4. Log moduli of loci for $Q_1(s)$.

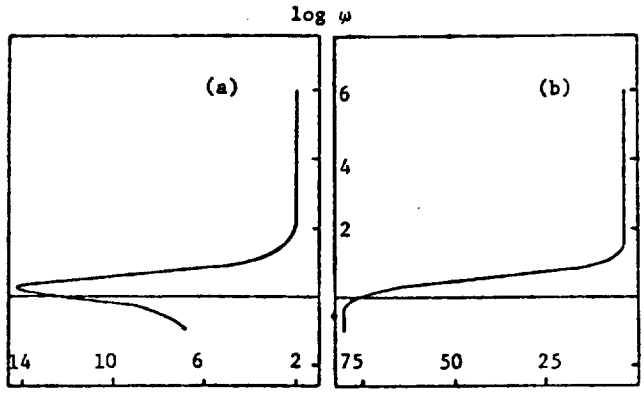

FIGURE 5. Misalignment degrees of characteristic directions of $Q_1(s)$.

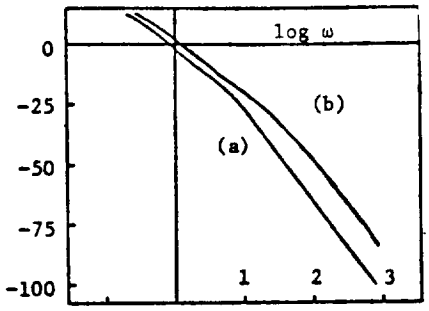

FIGURE 6. Log moduli of loci for $Q_2(s)$.

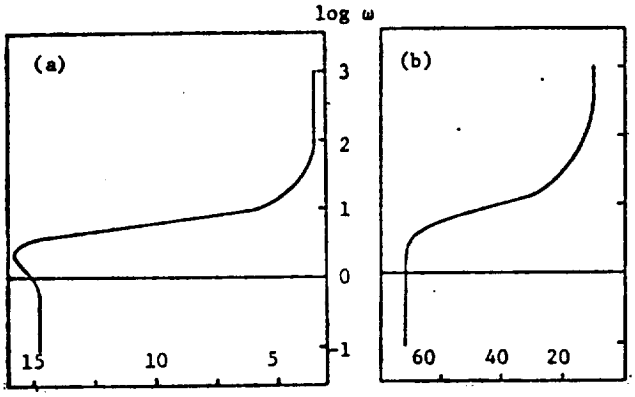

FIGURE 7. Misalignment degrees of characteristic directions of $Q_2(s)$.

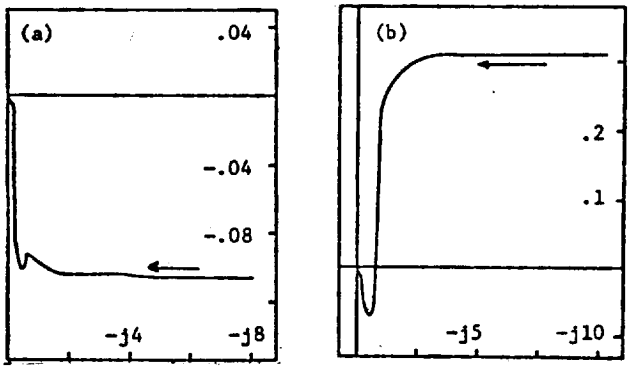

FIGURE 8. Characteristic loci of $Q_2(s)$.

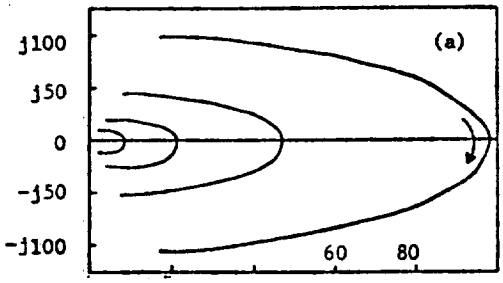

FIGURE 9. Closure loci for Figure 8(a). A similar set of curves is true for Figure 8(b).

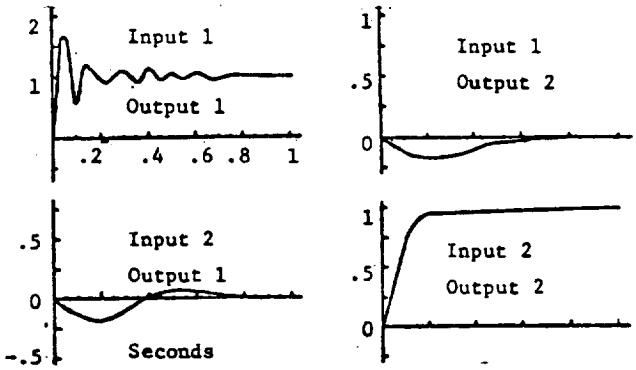

FIGURE 10. Time responses.

B^T	39.792	4.181	-.382	-.565	-.785
	1.017	- .125	-.077	-.088	-3.563
D		.018		.546	
		-.086		-.013	

FIGURE 11. Matrices B, D; see Figure 1 for matrices A, C.

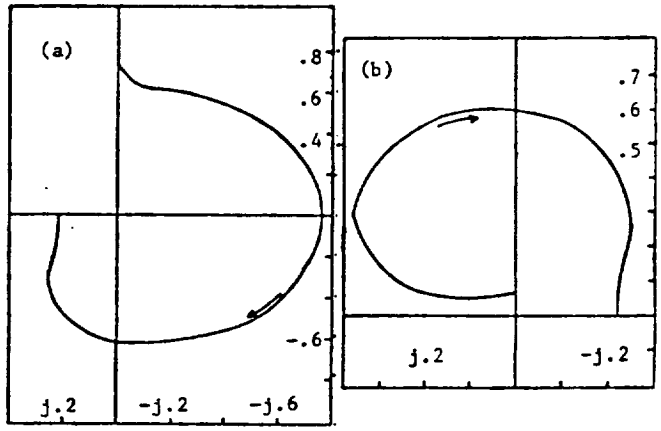

FIGURE 12. Characteristic loci of G(s).

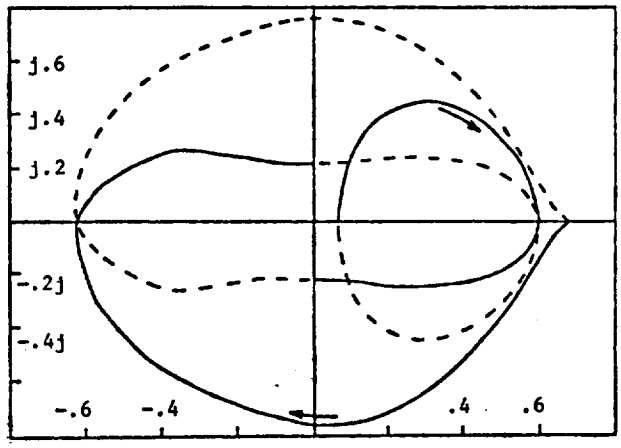

FIGURE 13. Complete locus.

THE DIRECT APPROACH TO COMPENSATION OF MULTIVARIABLE JET ENGINE MODELS

A Thesis

Submitted to the Graduate School of the
University of Notre Dame in Partial Fulfillment
of the Requirements for the Degree of

Master of Science in Electrical Engineering

by

Peter W. Hoppner, B.S.E.E.

Michael K. Sain
Director

Department of Electrical Engineering
Notre Dame, Indiana

May, 1977

THE DIRECT APPROACH TO COMPENSATION OF MULTIVARIABLE JET ENGINE MODELS

A Thesis

Submitted to the Graduate School of the
University of Notre Dame in Partial Fulfillment
of the Requirements for the Degree of

Master of Science in Electrical Engineering

by

Peter W. Hoppner, B.S.E.E.

Michael K. Sain
Director

Department of Electrical Engineering
Notre Dame, Indiana

May, 1977

Abstract

The use of the Nyquist criterion has been a valuable tool in designing single input-output control systems. This work addresses itself primarily to the problem of applying this criterion to the multi input-output system. The concept of the return difference and its determinant play an important role in this study.

The purpose of this work is to investigate the Direct Approach method for the design of multivariable control systems and to apply this method to a jet engine model.

TABLE OF CONTENTS

A GRAPHICAL APPROACH TO SYSTEM DOMINANCE

A Thesis

Submitted to the Graduate School of the
University of Notre Dame in Partial Fulfillment
of the Requirements for the Degree of

Master of Science in Electrical Engineering

by

Robert Michael Schafer, B.S.E.E.

Michael K. Sain
Director

Department of Electrical Engineering
Notre Dame, Indiana

May, 1977

A GRAPHICAL APPROACH TO SYSTEM DOMINANCE

Abstract

by

Robert Michael Schafer

In recent years, increased attention has been paid to the use of frequency domain techniques as applied to multivariable control systems. Particular emphasis has been given to the problem of achieving low system interaction.

This thesis presents a graphical approach to the problem of achieving system dominance, one such criterion for low interaction. The method is successfully applied to a series of jet engine control problems.

TABLE OF CONTENTS

D7A

FREQUENCY DOMAIN COMPENSATION OF A DYNGEN TURBOFAN ENGINE MODEL*

R. M. SCHAFER, R. R. GEJJI, P. W. HOPPNER,
W. E. LONGENBAKER and M. K. SAIN
Department of Electrical Engineering
University of Notre Dame
Notre Dame, Indiana 46556

Abstract

Following Rosenbrock's ideas regarding the advantages of dominance in linear multivariable control systems, a new graphical technique is used for the design of compensators that achieve dominance. The technique is illustrated with an application to the problem of designing compensators for a linear turbofan-engine model. The resulting design is put into perspective by examining it in the light of two other multivariable frequency-domain methods. One, MacFarlane's method of characteristic loci, is used to realize a final design for stability and low interaction. The other is a direct technique based upon the algebraic expansion of the determinant of the return difference in terms of it's elements. Results from simulations carried out on the NASA DYNGEN software are included.

1. Introduction

Recent years have witnessed a renewal of interest in frequency domain design methods for linear multivariable control systems. The preponderance of these ideas are closely related to classical Nyquist constructions on the determinant of return difference. In this paper, we use three such methods to design a compensator for a two-input, five-state, two-output linear model of a modern two-spool turbofan jet engine obtained from the DYNGEN digital jet engine simulation.

Rosenbrock [1] has related the classical Nyquist construction on the determinant of return difference to corresponding classical constructions on the diagonal elements of the return difference--provided these diagonal elements "dominate" their rows or columns in an appropriate manner. Focussing the design interest on achieving dominance in this sense, Section 3 presents a new graphical technique to help with this aspect of design. Next, Section 4 utilizes the generalized Nyquist plots to obtain an acceptable compensator design. The ideas of generalized Nyquist plots were introduced by MacFarlane [2], who related the determinant of the return difference to it's spectrum when regarded as an appropriate linear operator.

In Section 5, we utilize a direct technique which emphasizes the algebraic relationship between the elements of the return difference and it's determinant. Typically, when it achieves user satisfaction, this method does so with greater speed, and fewer concepts, than it's competitors. The jet engine model is introduced in Section 2, which also establishes the notation for succeeding sections. Finally, in Section 6, we give results of simulations to evaluate the performance of the system.

* This work was supported in part by the National Science Foundation under Grant ENG 75-22322 and in part by the National Aeronautics and Space Administration under Grant NSG 3048.

2. Jet Engine Model and Return Difference Determinant

The linear model used for the study is based upon data obtained from a DYNGEN simulation. It is specified by the equations

$$\dot{x} = Ax + Bu \tag{1}$$

$$y = Cx + Du \tag{2}$$

where x, u, y denote the state, input and output vectors respectively. The inputs are fuel flow and nozzle area; the five states are compressor rotor speed, fan rotor speed, burner exit pressure, afterburner exit pressure and high pressure turbine inlet energy; while thrust and high pressure turbine inlet temperature constitute the two outputs.

We next consider the problem of designing controllers for the plant. The underlying feedback control scheme is shown in Fig. 1. G(s), the plant,

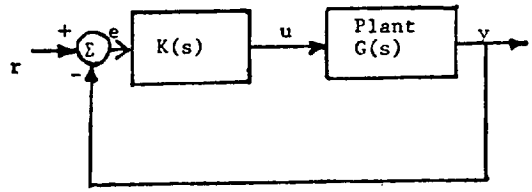

Fig. 1 Feedback Control Scheme

represents the jet engine model, that is,

$$G(s) = C(sI - A)^{-1}B + D. \tag{3}$$

K(s) represents the rational compensator to be designed. G(s) can be computed as:

$$G(s) = \frac{\begin{bmatrix} -502s^5-3.64E5s^4 & 4104s^5+1.93E6s^4 \\ -1.78E7s^3+6.15E9s^2 & +1.69E8s^3-1.44E10s^2 \\ +1.26E11s+6.25E11 & -6.77E10s+6.59E10 \\ -14.554s^5+1.33E5s^4 & 20.46s^5+1.69E4s^4 \\ +4.96E7s^3+3.7E9s^2 & +7.03E6s^3+1.12E9s^2 \\ +2.82E10s+4.95E10 & +5.63E9s+5.41E8 \end{bmatrix}}{s^5+609.57s^4+1.184E5s^3+7.3E6s^2 +6.52E7s+1.62E8} \tag{4}$$

Central to the application of Nyquist type ideas to multivariable systems is the return difference matrix, which in this case becomes [I+G(s)K(s)]. It's principal use arises from the relation of the closed loop characteristic polynomial (CLCP) to the open loop characteristic polynomial (OLCP) which can be stated, in the manner of [1], as

$$\frac{CLCP}{OLCP} = \det[I+G(s)K(s)], \tag{5}$$

where equality is understood up to a real constant. Of primary concern here is the behavior of det(I+GK) for values of s on the standard Nyquist contour (SNC), which encircles the open right half plane clockwise with indentations into the left half plane around poles and zeros on the imaginary axis. In practice, plots are made for values of s on the positive imaginary axis. Stability can then be determined from plots of det(I+GK) in conjunction with knowledge of the open loop characteristic polynomial. Also interesting, of course, is the use of such plots to aid in the choice of a suitable K(s).

3. CARDIAD Plots and Dominance [3,4]

The CARDIAD (Compensator Acceptability Region for DIAgonal Dominance) plot is a graphical approach to the problem of choosing a compensator that will achieve system dominance. A system is said to be row (column) dominant [1] if the magnitude of each diagonal element of the open loop transfer function matrix is greater than the sum of the magnitudes of the off diagonal elements of the row (column) at all frequencies. In the 2x2 case being considered in this paper, the dominance condition reduces to the magnitude of the diagonal element being greater than the magnitude of the off diagonal element of the row (column). Consonant with the Rosenbrock approach, the CARDIAD plot analysis is applied to the inverse of the plant G(s). As a notational point, the inverse plant transfer function matrix will be denoted by $\hat{G}(s)$ and the inverse precompensator by $\hat{K}(s)$.

The specific application to the jet engine design problem involves trying to find a compensator $\hat{K}(s)$ such that $\hat{K}(s)\hat{G}(s)$ is row dominant. Without loss of generality, the form of $\hat{K}(s)$ will be restricted to

$$\hat{K}(s) = \begin{bmatrix} 1 & \beta_1(s) \\ \beta_2(s) & 1 \end{bmatrix} \tag{6}$$

where

$$\beta_i(s) = x_i(s) + jy_i(s), \quad i = 1,2. \tag{7}$$

If $\hat{G}(s)$ and $\hat{K}(s)$ are each evaluated at a frequency jw_o, the equation for dominance of the i^{th} row of $\hat{K}(s)\hat{G}(s)$ becomes a function $f_i(x_i,y_i)$ which describes a paraboloid in three-space. The intersection of this paraboloid and the complex plane is a circle which is the locus of the values of x_i and y_i such that the magnitude of the diagonal element of the i^{th} row of $\hat{K}(s)\hat{G}(s)$ is equal to the magnitude of the off diagonal element of the row. Minima and maxima analysis of the function f_i reveals that values of x_i and y_i on one side of the circle will make the system dominant, whereas values which lie on the other side of the circle will not. In the CARDIAD plots, this differentiation is made by drawing a solid circle if the acceptable values of x_i and y_i lie inside and dashed circles if the acceptable region is outside.

If the above procedure is repeated over a range of frequencies for each row of the system, and the circles of intersection drawn, a plot describing the acceptable values of the complex number $x_i + jy_i$ for each frequency results. In this way, the acceptable range of the function $\beta_i(s)$ such that the i^{th} row of $\hat{K}(s)\hat{G}(s)$ is dominant is described.

The analysis of the CARDIAD plot for a given row of $\hat{G}(s)$ proceeds as follows. If the origin of the plot is contained inside all solid circles and is excluded by all dashed circles, the row of $\hat{G}(s)$ is dominant uncompensated. If the row of $\hat{G}(s)$ is not dominant uncompensated, the CARDIAD plot is next checked to see if there is a constant entry β_i that will make $\hat{K}(s)\hat{G}(s)$ dominant at all frequencies. For this to be the case, there must be a point on the real axis that is included in all solid circles and excluded by all dashed circles.

If there exists no constant β_i such that the i^{th} row of $K(s)\hat{G}(s)$ is dominant at all frequencies, the CARDIAD plot is used as a guide to design a frequency dependent $\beta_i(s)$ that will achieve dominance. This is accomplished by realizing a function $\beta_i(s)$ whose value at jw_o lies inside the circle associated with the same frequency in the CARDIAD plot if that circle is solid, or outside if that circle is dashed. This approach is illustrated by considering the DYNGEN problem.

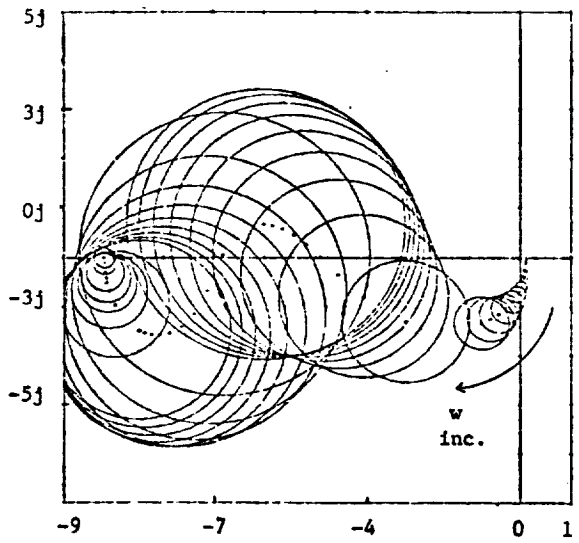

Fig. 2 CARDIAD Plot Row 1 Uncompensated

The initial CARDIAD plots of $\hat{G}(s)$ indicate that row 2 of $\hat{G}(s)$ is dominant uncompensated since the plot consists only of dashed circles, which all exclude the origin. The plot for row 1, however, shows that this row is not dominant uncompensated and also that there is no constant entry in the off diagonal element of row 1 of $\hat{K}(s)$ that will make the row dominant at all frequencies. This is easily seen since all the circles in this plot are solid and there is no point on the x axis that is included in all the circles. Moreover, the plot hints that there will be difficulty finding a $\beta_1(s)$

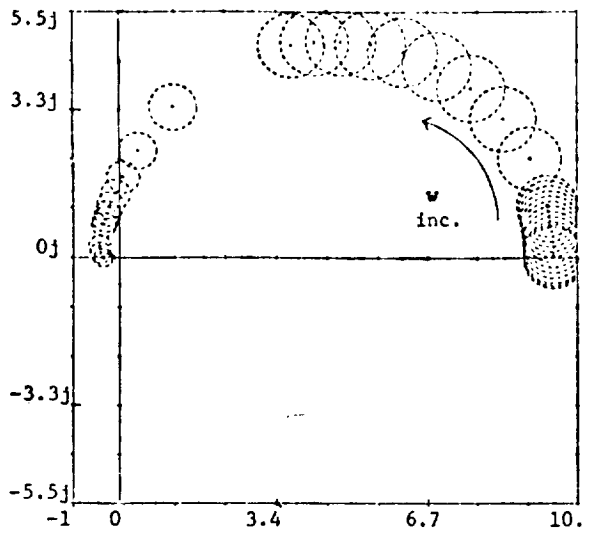

Fig. 3 CARDIAD Plot Row 2
Uncompensated

that will make this row of $\hat{K}(s)\hat{G}(s)$ dominant because of the complexity of the plot and the small radii of the low frequency circles which necessitate a very close fit.

To facilitate the process of finding a compensator that will make $\hat{K}(s)\hat{G}(s)$ dominant, the system was first precompensated with

$$\hat{K}_1 = \begin{bmatrix} 0 & 1 \\ 1 & 0 \end{bmatrix}.$$

Space limitations do not allow the CARDIAD plots of $\hat{K}_1\hat{G}(s)$ to be included, but the new plots are the same shape as the CARDIAD plots of $\hat{G}(s)$ with two major changes. The row 1 plot of $\hat{K}_1\hat{G}(s)$ is the same shape as the row 2 plot of $\hat{G}(s)$ with dashed circles changed to solid circles. Similarly, the row 2 plot of $\hat{K}_1\hat{G}(s)$ is the same shape as the row 1 plot of $\hat{G}(s)$ with the solid circles changed to dashed circles.

The problem of finding a $\hat{K}_2(s)$ such that $\hat{K}_2(s)\hat{K}_1\hat{G}(s)$ is dominant is now simplified. Since row 2 of $\hat{K}_1\hat{G}(s)$ is now dominant uncompensated, the off diagonal term in the second row of $\hat{K}_2(s)$ is left a zero, with the provision that if it later proves helpful in compensation, the entry may be chosen to be any constant that lies outside all of the circles. To make row 1 of $\hat{K}_1\hat{G}(s)$ dominant, the off diagonal entry in row 1 of $\hat{K}_2(s)$ must follow the semicircular path through the complex plane described by the CARDIAD plot for this row. A fit was made to this shape and the resulting $K_2(s)$ was

$$\hat{K}_2(s) = \begin{bmatrix} 1 & \dfrac{9.4798 + 0.2494s}{1. - 1.2359s} \\ 0 & 1 \end{bmatrix} \qquad (8)$$

The CARDIAD plots of $\hat{K}_2(s)\hat{K}_1\hat{G}(s)$ are considerably more complex than the previous plots. The plot for row 2 shows that the row is dominant at all frequencies since the origin is included by all solid circles and excluded by all dashed circles. The CARDIAD plot for row 1 shows that the row is clearly not dominant at all frequencies. Dominance is lost

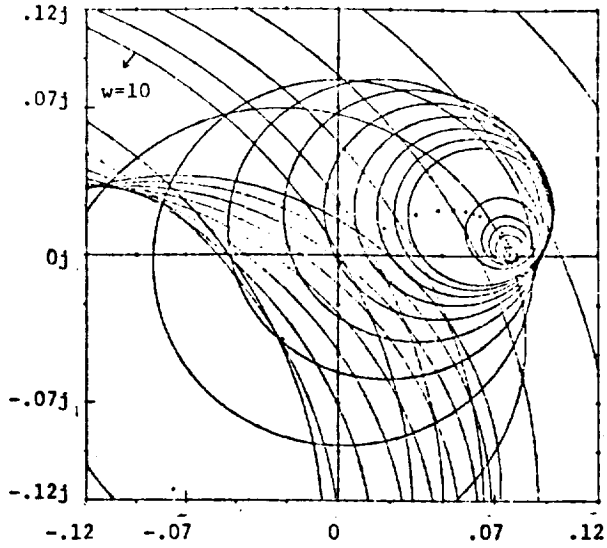

Fig. 4 CARDIAD Plot Row 1
Compensated

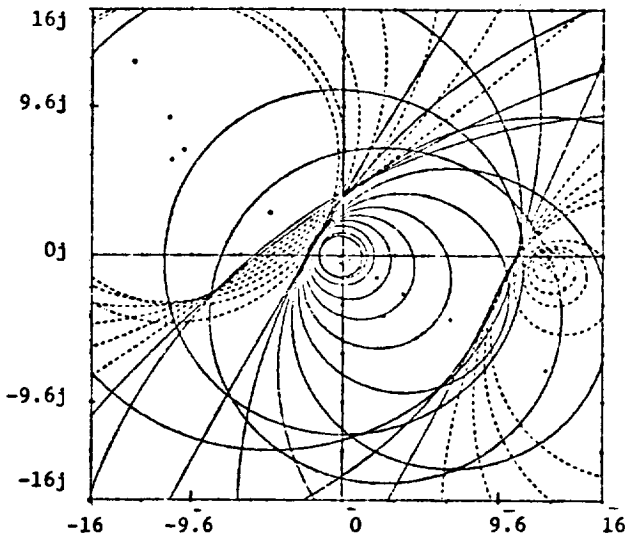

Fig. 5 CARDIAD Plot Row 2
Compensated

at w=10, is regained as w=90, and is lost again at w=700. It is perhaps possible to find a better choice of $K_2(s)$ that will make row 1 dominant at all frequencies, but the dominance achieved by the above $K_2(s)$ proved to be sufficient.

An interesting feature of the CARDIAD plot is illustrated in the final plot for row 2. Close analysis of this plot shows that there are three occurrences of solid circles changing to dashed circles or dashed circles changing to solid. When these transitions occur, the paraboloid is inverting and the circle of intersection degenerates to a line. These lines occur when the other row changes from being dominant to not dominant or vice versa. Thus, each change in dominance of row 1 causes a change in the type of circle being drawn in the plot of row 2.

4. Design Using Characteristic Loci

Another approach to design, due to A.G.J.MacFarlane, uses the locus of the eigenvalues of G(s)K(s), called the characteristic loci (C.L.), for values of s on the SNC. This method is based on the relation of the determinant of the return difference to eigenvalues of G(s)K(s). In order to assess stability from the C.L. plots, for s=jw, w positive, one must count the clockwise encirclements of the critical point (-1,0) made by the C.L. plots and sum all these up. The closed loop system is stable if this sum equals -po, where po is the number of zeros of OLCP enclosed by the SNC. As an approximate measure of interaction, we compare the eigenvalue plots with plots of the diagonal elements of Q(s)=G(s)K(s). For a noninteracting system with Q(s) a diagonal matrix, these would be identical. In our design example, Q(s) is a 2x2 matrix, and therefore we will be looking at plots of two eigenvalues $\lambda_1(s)$, $\lambda_2(s)$ and the two diagonal elements $q_{11}(s)$, $q_{22}(s)$.

First, an examination of the C.L. plots of the uncompensated system revealed that, without compensation, the closed loop system is unstable. The plots are not included due to lack of space, but conclusions drawn from them are given. Control problems for the uncompensated model were complicated by the existence of considerable interaction, and large gains at high frequencies. An additional difficulty was that one of the eigenvalues was negative at zero frequency. This tended to limit the response speed of the closed loop system. It appeared on the C.L. plots that, from a stability viewpoint, the frequency range of interest is in the vicinity of 10 rps. This gives justification for use of the compensator given in the previous section. As a practical matter, our goal is to achieve as rapid a response as possible to a step input, without suffering any overshoot. Heavy emphasis is placed also on steady state accuracy.

To remove the right half plane pole in $\hat{K}_2$, we choose K_3 arbitrarily as diag (1/s,(-1+1.2359s)/s). The resulting $K(s)=K_1*K_2*K_3$ becomes

$$K(s) = \frac{\begin{bmatrix} 0 & -1+1.2359s \\ 1 & 9.4798+0.2494s \end{bmatrix}}{s} \qquad (9)$$

The diagonal nature of $K_3(s)$ does not affect dominance. Moreover, an examination of the (1,1) and (1,2) elements of G(s) reveals that if the 0 in K(s) is changed to 9, we can significantly reduce the high frequency magnitude of $q_{11}(s)$ while simultaneously boosting the low frequency magnitude. This is in accordance with the freedom specified for $\hat{K}_2$ previously. The modified K(s) gives rise to the plots of Fig. 6 and 7.

Since dominance is not affected by diagonal compensators, the problem becomes that of independently shaping q_{11} and q_{22} by means of single loop techniques. In order to reduce high frequency gain in q_{22} without appreciably affecting low frequency behavior, we use lag compensation. A little bit of cut and try led finally to $K_4(s)$=diag.(0.44E-4, (-s-0.1)/(2000s+10)). The plots corresponding to $K=K_1*K_2*K_3*K_4$ are not shown. The λ_1 and q_{11} plot is essentially that of λ_1 in Fig. 6 scaled by a factor of 0.44E-4. Similarly, the q_{22} plot inverted and scaled by 0.0005. (By inversion we mean reflection through both axes.) The plot for λ_2 is shown in Fig. 8.

5. The Direct Method of Analysis

Direct methods of multivariable Nyquist analysis concern themselves with the algebraic relationship between the elements of return difference and its determinant. For an NxN return difference, the most basic of these relationships is

$$\det(I+GK) = 1+\sum_{i=1}^{N}\{\sum ixi \text{ principal minors of } GK\}. \qquad (10)$$

For the example of this paper, (10) takes the form

$$1+\{(G_{11}K_{11}+G_{12}K_{21})+(G_{21}K_{12}+G_{22}K_{22})\} + \det(GK). \qquad (11)$$

In (10) and (11) we note the advantage of minute detail and the disadvantage of nonrecursive construction. Considerable interest attaches to the removal of this disadvantage, which can be accomplished by methods drawn from the results of exterior algebra [5]. Consider the recursion (where tr denotes trace)

$$\alpha_0 = 1 \qquad (12a)$$

$$\alpha_r = -\frac{1}{r}\sum_{p=0}^{r-1}\alpha_p \,tr(GK)^{r-p} \qquad (12b)$$

for $1 \le r \le N$. It can be shown that

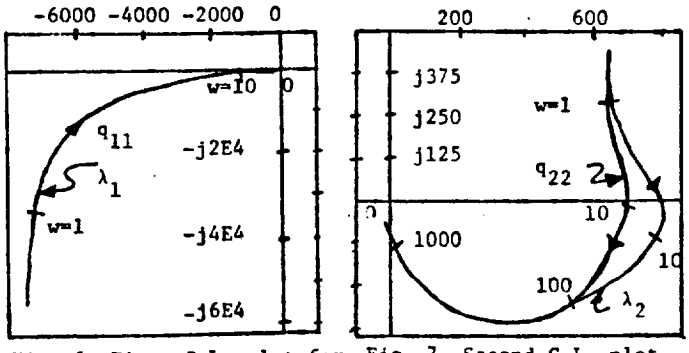

Fig. 6 First C.L. plot for $GK_1K_2K_3$.

Fig. 7 Second C.L. plot for $GK_1K_2K_3$.

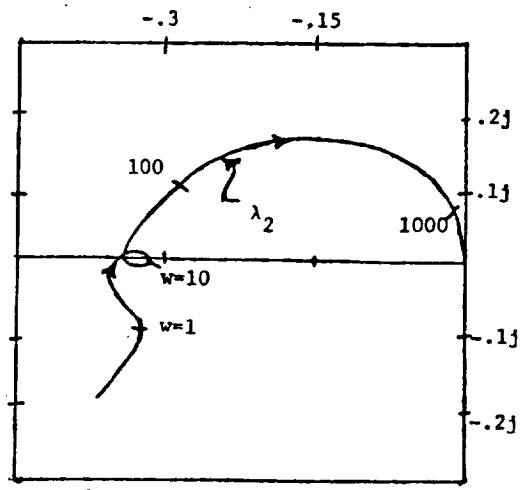

Fig. 8 Second C.L. plot for $GK_1K_2K_3K_4$.

$$\det(I+GK) = \sum_{i=0}^{N} (-1)^i \alpha_i . \qquad (13)$$

The direct approaches differ appreciably from methods described in preceding sections, in that they address themselves directly to the image of det(I+GK) on the SNC, without any particular concern for such issues as dominance or interaction. Alternate insights accrue from such plots, which we illustrate here for the engine design example. All plots are drawn for the final return difference as developed in the sections preceding.

Fig. 9 indicates the five constituents of a det(I+GK) plot as developed in (11), while Fig. 10 presents the corresponding two constituents according to (13). Fig. 11 contains the total Nyquist plot, which is obtained by adding the individual curves in either of the two prior figures. Revealed in this plot, Fig. 11 is a feature not so readily noticeable in the earlier plots, namely conditional stability. It appears, therefore, that the availability of a variety of graphical tools is in the multivariable case every bit as valuable as in the more classical, one-input, one-output situation.

It is readily seen in Fig. 11 that the plot encircles -1+j0 twice in a counterclockwise direction. Therefore, the system is shown to be stable because the open loop characteristic polynomial has a double zero at the origin.

Further exploratory studies of direct methods as design aids are available elsewhere [6].

6. Simulation Results

Closed-loop time responses were obtained both by using the linear model simulation and by implementing the compensator on DYNGEN, a jet engine simulation program developed by the NASA Lewis Research Center [7].

DYNGEN is a versatile digital program which analyzes steady-state and transient performance of turbojet and turbofan engines. It uses a sixteenth order system to model this example, and solves the state differential equations by a modified Euler method. The user need only supply appropriate component performance maps and design-point information, and then write the control subroutines. Implementation of the compensator required first order functions to perform integration and lead-lag compensation.

The linear model used in this study was also obtained from DYNGEN. By utilizing a special control subroutine written by NASA, called DYGABCD [8], models can be derived using whatever states the user desires. DYNGEN thus possesses the capability to determine linear models for the engine with any order up to sixteen.

Fig. 12 shows the response of the linear model to a step input in the first channel. Thrust has a rise time (10%-90%) of 1.04 seconds with no overshoot occurring. High pressure turbine inlet temperature increases to a maximum of 0.105 at approximately 0.9 seconds, then gradually decreases.

Similar, and even better, results occur when the compensator is employed in the DYNGEN simulation using a one percent step. Thrust rise time is 0.88 seconds, and the turbine temperature reaches a maximum increase of 0.097.

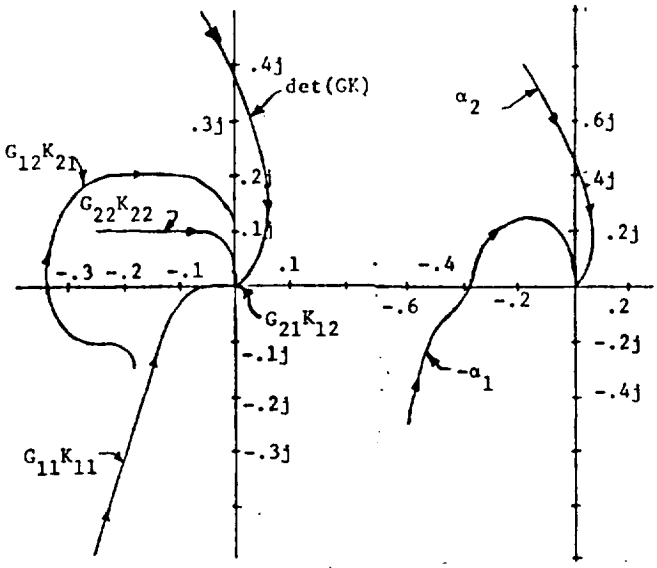

Fig. 9 The Nyquist Plot of the Elements of Det(I+GK), According to Expansion Eq. (11).

Fig. 10 The Nyquist Plot of the Elements of Det(I+GK) According to Expansion, Eq. (13).

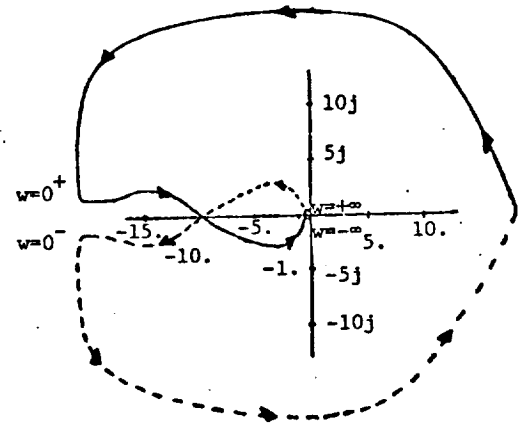

Fig. 11 Nyquist Plot of Det(I+GK).

The linear and nonlinear responses were not in such close agreement for a step input in the second channel. The linear model shows turbine temperature slowly ramping up (Fig. 13) as the change in thrust is held to a minimum. DYNGEN produces similar results for the turbine temperature response; however thrust experiences a strong decrease before rising to zero. At this writing, it is believed that the five states chosen for the DYGABCD model do not adequately describe local engine behavior for the second channel equipped with the present controller.

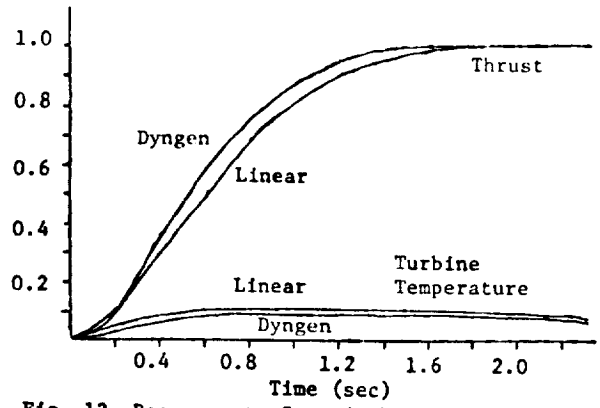

Fig. 12 Response to Step in First Channel

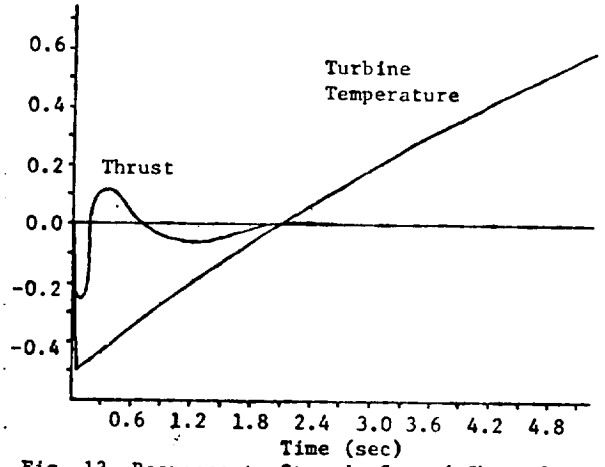

Fig. 13 Response to Step in Second Channel

7. Conclusions

This paper has demonstrated the usefulness of the new CARDIAD plot approach to designing compensators for complex plants. The DYNGEN simulation for a step in channel 1 has shown that acceptable responses can be obtained using linear compensators. An ordered collection of these may make global control feasible. For steps in channel 2, conclusive evidence was not obtained. We suspect that this is due to inadequacy of the linear model in describing the plant. This important factor of selecting an appropriate linear model is often overlooked. But, as we have seen, it turns out to be crucial in practical applications.

The method of CARDIAD plots can be generalized to plants with more than two inputs and outputs by considering a family of compensators with 1's on the diagonal and only one non-zero off-diagonal term. As stated in [1], except for changes in the ordering of inputs or outputs, such a study is exhaustive.

8. References

[1] H. H. Rosenbrock, Computer-Aided Control System Design.London: Academic Press, 1974.

[2] A. G. J. MacFarlane, and J. J. Belletrutti, "The Characteristic Locus Design Method," Automatica, Vol. 9, No.5, pp. 575-588, September 1973.

[3] R. M. Schafer, W. E. Longenbaker and M. K. Sain, "System Dominance," Preliminary Report Department of Electrical Engineering, University of Notre Dame, Notre Dame, Indiana, November 1976.

[4] R. M. Schafer, "A Graphical Approach to System Dominance," M. S. Thesis, Department of Electrical Engineering, University of Notre Dame, Notre Dame, Indiana, May 1977.

[5] W. H. Greub, Multilinear Algebra. New York: Springer, 1967.

[6] P. W. Hoppner, "The Direct Approach to Compensation of Multivariable Jet Engine Models," M. S. Thesis, Department of Electrical Engineering, Notre Dame, Indiana, May 1977.

[7] J. F. Sellers and C. J. Daniele, "DYNGEN-A Program for Calculating Steady-State and Transient Performance of Turbojet and Turbofan Engines," NASA Technical Note, NASA TN D-7901, Washington, D.C., April 1975.

[8] L. C. Geyser, "NASA Preliminary Report on DYGABCD," April 1976.

APPLICATION OF POLYNOMIAL TECHNIQUES TO MULTIVARIABLE CONTROL OF JET ENGINES*

R. R. Gejji and M. K. Sain

Department of Electrical Engineering, University of Notre Dame, Notre Dame, Indiana, U.S.A. 46556

SUMMARY

This paper describes a complete case study of the application of the theory of minimal design to multivariable control of jet engines. The minimal design problem is approached from the viewpoint of polynomial modules, and computational experience with PL/I and FORMAC-PL/I software is discussed. The complete minimal design solution exhibits flexibilities not apparent in early industry studies, and a new approach to pole assignment can be used to advantage in this situation.

1. INTRODUCTION

One way to approach the design of linear multivariable control systems is to express system specifications in terms of a desired closed loop transfer function matrix. A question which is often raised about such an approach is the practicality of making such a specification. Another, related, question concerns the possibility of determining the existence of realizable compensators to achieve the specification. When such compensators do exist, there are the very practical issues of giving a finite enumeration of them, of determining whether they have fixed poles, and of assigning one or more of the non-fixed poles. Of special interest, as it turns out, for the issue of pole assignment is the idea of minimality, in the state-space sense, of a proposed solution in the context of all possible solutions.

This paper provides a thorough case study of such a design approach when applied to realistic numerical models associated with an F-100-like turbofan engine. Specifications are accomplished by means of the methods of linear optimal control theory, according to procedures already worked out in the jet engine industry. The remaining tasks are addressed by regarding the design as a problem in free polynomial modules. A special feature of the application lies in its attention to compensators of simple structure, with a view to the use of a graded collection of them for the purpose of global engine control.

Section 2 describes the basic design problem, once specifications are made. Section 3 provides the discussion of the jet engine application, with particular attention paid to the manner of making the specifications and to the formulation of the main design problem for the jet engine application. Section 4 explains how to cast the design problem in terms of free polynomial modules, and Section 5 describes floating point computational experience gained in applying extended precision PL/I software to solve the jet engine problem in the free module context. Section 6 outlines the corresponding experience associated with an exact rational calculation made with FORMAC-PL/I software.

The results of Section 6 show that considerably greater compensator design freedom is available than had been apparent from early industry studies. Using these results, a new pole placement design procedure based on alternating multilinear algebra achieves in Section 7 a minimal pole placement solution not possible by those earlier industry methods.

Section 8 closes with remarks designed to place the work in historical perspective, to reference the literature, and to assess the merits of polynomial methods for control system design in the near term.

2. THE MINIMAL DESIGN PROBLEM

Suppose that F is a given field. For the jet engine control problem, F is taken to be R, the field of real numbers; however, a great deal of the algorithmic nature of the discussion is more general than that, and is so stated. The set of polynomials which are of interest is F[s], namely those polynomials in the variable s with coefficients in the field F. The fact that F[s] is a principal ideal domain ring is well known, as is the equally pertinent fact that F[s] has a quotient field F(s). More intuitively, F(s) is often described as the field of rational functions in s having coefficients in F.

The design problems of interest in the sequel are conventionally stated in terms of F(s); however, Section 4 explains how such problems may be re-converted back to a corresponding F[s] form.

Principal interest centers upon the minimal design problem (MDP), which can be described as follows. Let $G: V_1 \to V_2$ be a linear operator for finite-dimensional F(s)-vector spaces V_1 and V_2. G is regarded as realizable if its matrix is proper. Now let $G_1: V_2 \to V_3$ and $G_2: V_1 \to V_3$ be given linear operators, where V_3 is also a finite-dimensional F(s)-vector space. MDP consists in determining whether there are realizable linear operators G which make the diagram in fig. 1 commute and, if so, to find one whose minimal realization is of least dimension among all such realizable operators. Intuitively,

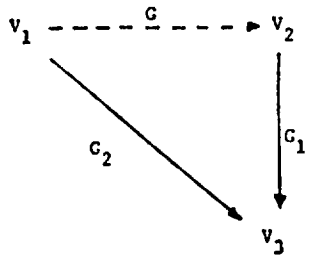

Fig. 1. Minimal Design Problem

the operators G_1 and G_2 derive from the given plant and from the specifications, while G represents the compensators to be designed.

Beyond the basic MDP, several additional issues are of practical importance. Among these should be included

* This work was supported in part by the National Science Foundation under Grants GK-37285 and ENG 75-22322 and in part by the National Aeronautics and Space Administration under Grant NSG 3048.

(i) a finite enumeration of all possible solutions, (ii) determination of any fixed poles in the matrix of G, and (iii) methods for assigning the poles of G which are not fixed. The answers to these questions resolve such issues as the availability of solutions with varying degrees of integration. From a conceptual viewpoint, these ideas are developed further in Sections 4 and 7, whereas the computational issues are discussed in Sections 5 and 6.

Next in order of presentation, however, is the statement of a minimal design problem for jet engine control.

3. JET ENGINE APPLICATION

In this section, we demonstrate the practicality of the minimal design approach in the context of jet engine control. The basic plant is a version of the F-100 turbofan engine. Inputs are jet exhaust area and main burner fuel flow; states are fan inlet temperature, main burner pressure, fan speed, high compressor speed, and afterburner pressure; and outputs are thrust and high-turbine inlet temperature. The linearized model approximates the small signal behavior of these engine variables in a neighborhood of 47° Power Lever Angle (PLA). This corresponds to a point approximately midway between engine idle and maximum nonafterburning power. The plant is specified by the four matrices A_p, B_p, C_p, D_p in (1) and (2).

$$\dot{\delta x} = A_p\, \delta x + B_p\, \delta u \tag{1}$$

$$\delta y = C_p\, \delta x + D_p\, \delta u \tag{2}$$

Table 1 lists these matrices for our example. The attempt to design simple compensators for linear control over a specified region is part of a strategy for global control of the engine using a graded collection of these.

Table 1

State Description Matrices for Jet Engine (PLA=47°)

Matrix	Matrix Elements				
A_p	-57.096	3.613	-10.211	- 5.481	- 2.715
	19.832	-72.34	30.295	40.972	15.327
	0.66	4.496	- 3.601	- 0.011	- 2.808
	1.326	2.313	- 0.809	- 3.032	- 0.821
	0.882	0.703	2.922	1.471	- 4.596
B_p		1.017		39.792	
		- 0.125		4.181	
		- 0.077		- 0.382	
		- 0.088		- 0.565	
		- 3.563		- 0.785	
C_p	- 0.037	0.031	- 0.016	- 0.042	1.368
	1.081	0.149	- 0.057	0.001	- 0.086
D_p		0.546		0.018	
		- 0.013		- 0.086	

We next examine how engine control specifications can be obtained from linear optimal control theory. In fig. 2, the compensators.

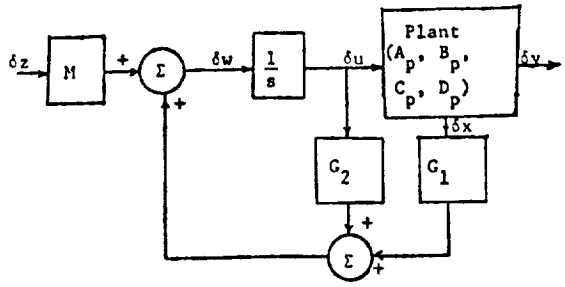

Fig. 2. Linear Optimal Control

specified by gain matrices G_1 and G_2 are chosen with the objective of minimizing the performance index of (3).

$$J = \frac{1}{2}\int_0^\infty (\delta y^T Q \delta y + \delta \dot{u}^T R \delta \dot{u} + \delta \dot{y}^T S \delta \dot{y})dt \tag{3}$$

where superscript T denotes matrix transposition. The weighting matrices Q,R, and S are listed in table 2.

Table 2

Weighting Matrices
with Optimal Integral Control Solution

Matrix	Matrix Elements				
Q	50,000	0			
	0	10,000			
R	550	0			
	0	175			
S	0	0			
	0	20,000			
L	0.509	0.268	1.979	2.171	2.098
	-2.137	-0.377	- 0.223	- 0.776	- 0.227
H	8.329		- 1.126		
	-2.811		- 1.842		

At this point, a minimal design problem can be brought into play. The control scheme of fig. 3 is seen to be more desirable because it incorporates output feedback and enjoys the concomitant advantage of zero steady state error, even in the presence of plant parameter variation.

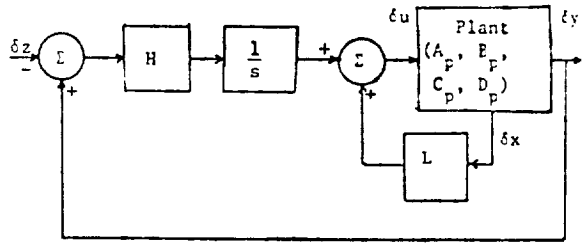

Fig. 3. Optimal Integral Control

One relates the performance of the two control schemes by equating, in both, the Laplace transform of the variable δu, as written in terms of the respective state variables. This leads to the following equations, which may be solved for L and H, the values of which have been listed in table 2.

$$M = -H \tag{4}$$

$$[L:H]\left[\begin{array}{c:c} A_p & B_p \\ \hdashline C_p & D_p \end{array}\right] = [G_1 \vdots G_2] \tag{5}$$

That this is nothing but a form of the minimal design problem can be seen by evaluating the 2x2 closed loop transfer function matrices T(s) and T'(s) for the two systems in figs. 2 and 3. In fig. 2,

$$T(s) = P_1(s)\,[sI - P_2(s)]^{-1} M \tag{6}$$

where

$$P_1(s) = C_p(sI-A_p)^{-1} B_p + D_p \tag{7}$$

$$P_2(s) = G_1(sI-A_p)^{-1} B_p + G_2. \tag{8}$$

In fig. 3, on the other hand,

$$T'(s) = -P_1(s)\,[sI-P_3(s)]^{-1} H \tag{9}$$

where

$$P_3(s) = HP_1(s) + sL(sI-A_p)^{-1} B_p. \tag{10}$$

Now, rewrite (6) using (4) as

$$T(s) = -P_1(s)\,[sI-P_2(s)]^{-1} H. \tag{11}$$

The relationship between (9) and (11) now depends upon that between (8) and (10).

Comparison of $P_3(s)$ and $P_2(s)$, with the aid of (5) and (7), establishes the equality of the two transfer functions $T(s)$ and $T'(s)$.

We can then pose questions regarding the existence of compensators other than H and L to achieve the same performance as attained in fig. 3, and what, if any, advantages such compensators would have over that scheme. To do this, we consider fig. 4, which is a more general scheme of control based on fig. 3.

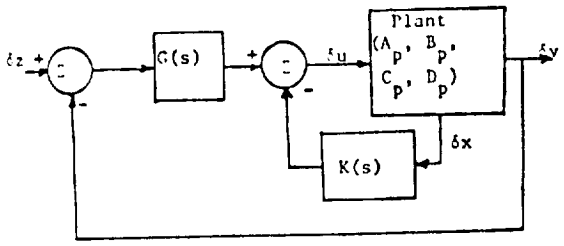

Fig. 4. Generalized Compensation Scheme

Our objective is to design compensators G(s) and K(s) to achieve exactly the transfer function $T(s) = T'(s)$ between δz and δy. This means that we must have

$$(I + P_4(s))^{-1} P_4(s) = T(s) \tag{12}$$

where we have introduced

$$P_4(s) = P_1(s)\,(I+K(s)P_5(s))^{-1}\,G(s) \tag{13}$$

and

$$P_5(s) = (sI-A_p)^{-1}\,B_p. \tag{14}$$

From (12), we obtain the equivalent condition

$$P_4(s) = (I+P_4(s))\,T(s), \tag{15}$$

which can be restated in the manner

$$P_1(I+KP_5)^{-1}G = (I+P_1(I+KP_5)^{-1}G)T. \tag{16}$$

From table 1, D_p is clearly invertible; and so the linear dynamical system P_1 has a unique linear dynamical inverse system P_1^{-1}, which we designate $\hat{P}_1$. Thus (16) is equivalent to

$$G(I-T) - K\,P_5\hat{P}_1T = \hat{P}_1T \tag{17}$$

which in turn can be written

$$[(I-T^T) \,\vdots\, -T^T\hat{P}_1^TP_5^T]\begin{bmatrix}G^T\\ \cdots\\ K^T\end{bmatrix} = T^T\hat{P}_1^T. \tag{18}$$

Some simplification can be achieved at this point if we take advantage of the fact that the matrix $T^T(s)$ has an inverse $\hat{T}^T(s)$. Then (18) can be cleared in its right member so that

$$[P_1^T(\hat{T}^T-I) \,\vdots\, -P_5^T]\begin{bmatrix}G^T\\ \cdots\\ K^T\end{bmatrix} = I \tag{19}$$

Now compare (19) with fig. 1, from which it becomes clear that G_2 is the identity map, or that our control system minimal design problem turns out to be a version of the minimal inverse system problem. Writing

$$\begin{bmatrix}G^T(s)\\ \cdots\\ K^T(s)\end{bmatrix} = N(s)D^{-1}(s), \tag{20}$$

and

$$[P_1^T(s)(\hat{T}^T(s)-I) \,\vdots\, -P_5^T(s)] = \frac{M(s)}{d(s)}, \tag{21}$$

where N(s), D(s), and M(s) are matrices over R[s], and where $d(s) \in R[s]$, we can put (21) in the polynomial form

$$[M(s) \,\vdots\, -d(s)I]\begin{bmatrix}N(s)\\ \cdots\\ D(s)\end{bmatrix} = 0 \tag{22}$$

Equation (22) is a polynomial "kernel" problem, equivalent to the design problem of fig. 4. By comparing figs. 3 and 4, we can trivially establish that a solution to the problem does indeed exist. Our goal in the sequel is to give a finite enumeration of all possible solutions and to study their pole assignment possibilities relative to the structure of fig. 4.

We remark here on a special feature of (20), in that it implies a common set of dynamics for both compensators. Suppose that a suitable solution of (22) leads us to matrices A_g, B_g, C_g, D_g and A_k, B_k, C_k, and D_k such that

$$G(s) = C_g(sI-A_g)^{-1}B_g + D_g \tag{23}$$

$$K(s) = C_k(sI-A_k)^{-1}B_k + D_k. \tag{24}$$

In a typical situation, $D_g = 0$; and it can be shown that

$$A_g = A_k; \qquad C_g = C_k.$$

Fig. 5 then shows how such a control scheme can be realized.

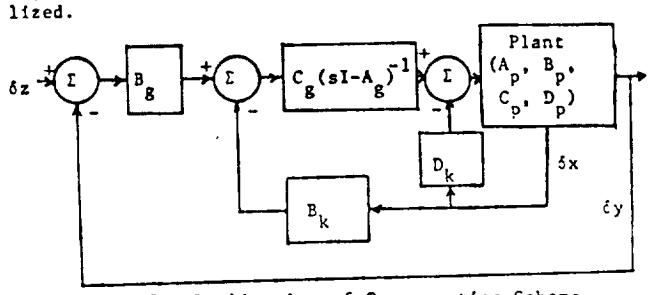

Fig. 5. Realization of Compensation Scheme

Finally, we make the observation that (22) can be completely solved, and a minimal solution computed by algorithms given in the Appendix. The next section deals with the theoretical foundation of these algorithms; and subsequent sections describe their application to (22).

4. FREE MODULAR APPROACH TO MDP

In matrix form, the minimal design problem of fig. 1 reduces to solving an equation

$$G_1(s)G(s) = G_2(s) \tag{25}$$

for the various realizable G(s), where $G_1(s)$ and $G_2(s)$ are given. Section 3 provided a nontrivial illustration of (25) in (19), where

$$G_1(s) = [P_1^T(s)\{\hat{T}^T(s)-I\} \,\vdots\, -P_5^T(s)] \tag{26}$$

$$G_2(s) = I, \tag{27}$$

and where the field F was R, the real numbers.

The free modular approach to MDP is based upon the recognition that, as a set,

$$F(s) \subset F[s] \times F[s],$$

which, in turn, suggests that it may be possible to express (25) in terms of F[s]. A convenient way to bring this about, as illustrated in (20), is to write

$$G(s) = N(s)\,D^{-1}(s), \tag{28}$$

where N(s) and D(s) have their elements in F[s]. It is easy to see that every G(s) has representation in the form (28). Similar representations could be adopted for $G_i(s)$, $i = 1,2$, but the presentation can be simplified if the choice

$$G_i(s) = \frac{M_i(s)}{d_i(s)} \qquad i = 1, 2 \tag{29}$$

is made, with $d_i(s) \in F[s]$, $i = 1,2$ and $M_i(s)$ having elements in F[s], $i = 1,2$. Equation (25) is then clearly the same as

$$\frac{M_1(s)}{d_1(s)}\,N(s)D^{-1}(s) = \frac{M_2(s)}{d_2(s)}, \tag{30}$$

which, in turn, is equivalent to

$$[d_2(s)M_1(s) \,\vdots\, -d_1(s)M_2(s)]\begin{bmatrix}N(s)\\ \cdots\\ D(s)\end{bmatrix} = 0, \tag{31}$$

an equation written over F[s]. For the jet engine

problem, (22) corresponds to (31). Let

$$\hat{t}_i(s) = \begin{bmatrix} \hat{n}_i(s) \\ \hline \hat{d}_i(s) \end{bmatrix} \tag{32}$$

denote the ith column of

$$\begin{bmatrix} N(s) \\ \hline D(s) \end{bmatrix}.$$

Then

$$[d_2(s)M_1(s) \vdots -d_1(s)M_2(s)]\ \hat{t}_i(s) = 0, \tag{33}$$

and every candidate to construct a solution (28) can be traced to such $\hat{t}_i(s)$.

Thus MDP is quite closely related to the homogeneous equation

$$[d_2(s)M_1(s) \vdots -d_1(s)M_2(s)]\ t(s) = 0. \tag{34}$$

The purpose of this section is to explain briefly an appropriate algebraic interpretation of (34). This interpretation is based upon generalizing the notion of the n-dimensional F(s)-vector space $F(s)^n$ to that of a rank-n F[s]-module $F[s]^n$. As a vector space, $F(s)^n$ satisfies the usual axioms, with scalars taken from the field F(s). As a module, $F[s]^n$ satisfies exactly the same set of axioms, but with scalars taken from the principal ideal domain ring F[s]. Despite this close similarity, F[s]-modules do not behave in exactly the same way as vector spaces. But there is a class of them, known as finite-rank free modules, which have a great similarity to finite-dimensional vector spaces in that they have a basis, which can be defined in the usual way using concepts of span and independence. $F[s]^n$, for example, is said to be free on the basis

$$\{(0, \ldots, 0, \underset{\substack{\uparrow \\ \text{ith position}}}{1}, 0, \ldots, 0);\ i = 1,2,\ldots,n\}. \tag{35}$$

Morphisms of F[s]-modules are defined analogously to linear operators on vector spaces; and, when domain and codomain are finite-rank free modules, the basis concept is used in the usual way to define a matrix for the morphism. This, then, is the interpretation to be given to the $p \times q$ matrix

$$[d_2(s)M_1(s) \vdots -d_1(s)M_2(s)] \tag{36}$$

in (34), namely the interpretation of a morphism

$$M: F[s]^q \to F[s]^p \tag{37}$$

of finite-rank free F[s]-modules. As a submodule of the finite-rank free module $F[s]^q$ over the principal ideal domain F[s], the kernel of M is also free, and thus the solution to (34) is tantamount to finding a basis for this kernel. The process for calculating such a basis is provided by Algorithm 1 in the Appendix.

If a basis

$$t_1(s), t_2(s), \ldots, t_\rho(s) \tag{38}$$

for Ker M has been computed, MDP solution then depends upon a determination of whether these basis elements can be used, through (32) and (28), to construct realizable G(s) matrices---and, if they can, to find G(s) whose minimal realizations are smallest and to assign poles wherever possible. It turns out to be convenient to answer these questions in terms of a reduced basis, whose definition is as follows. Let

$$t_i(s) = \sum_{j=0}^{k_i} t_{i,j} s^j \tag{39}$$

where $t_{i,j} \in F^q$, $t_{i,k_i} \neq 0$, and $i = 1,2,\ldots,\rho$. Then the basis (38) is said to be reduced if the matrix

$$[t_{1,k_1} \vdots t_{2,k_2} \vdots \cdots \vdots t_{\rho,k_\rho}] \tag{40}$$

has rank ρ. Algorithm 2 in the Appendix reduces a basis.

With these notions, the MDP Algorithm in the Appendix solves MDP. The issue of pole assignment is taken up in Section 7.

5. FLOATING POINT EXPERIENCE

In view of the material presented in the previous section, we are ready to take a closer look at (22). The matrix [N(s) ⋮ -d(s)I] turns out to be a 2 x 9 matrix of polynomials in R[s]. Lack of space prevents us from reproducing all the numbers here, but fig. 6 shows that the typical element is a thirteenth degree polynomial. We also note the large variation in the magnitudes of the coefficients of the polynomials.

1.17 E10 s^3	-1.37 E10 s^2
+4.40 E10 s^4	-4.99 E10 s^3
+4.06 E10 s^5	-4.21 E10 s^4
+1.18 E10 s^6	-1.07 E10 s^5
-1.24 E9 s^7	+1.49 E9 s^6
-1.26 E9 s^8	+1.99 E9 s^7
-2.07 E8 s^9	+1.99 E8 s^8
-5.55 E6 s^{10}	+6.93 E6 s^9
-4.80 E4 s^{11}	+8.33 E4 s^{10}
-7.09 E1 s^{12}	+2.38 E2 s^{11}
+4.5 E-1 s^{13}	-1.00 E0 s^{12}

Fig. 6. Polynomial Matrix

In this section, we report on FORTRAN and PL/I softwares developed to implement the MDP Algorithm on a digital computer, and our experience in the application of the software to the jet engine control problem described earlier in the paper. Both the programs use floating point arithmetic to implement the MDP Algorithm, considered over the field of real numbers. The FORTRAN version, using double precision arithmetic, affords 15 digits of precision (decimal) on an IBM 370/158 computer. The PL/I version, using extended precision arithmetic, carries 33 significant digits. Our jet engine minimal design problem comes down to the question of determining the rank-seven kernel of a module morphism whose domain has rank nine, and whose matrix representation in the usual basis contains thirteenth degree polynomials. In our experience, the principal difficulties arise from roundoff error occurring as a result of finite representation of real numbers in the computer.

There are two noteworthy features of the floating point KERPO (KERnel of a Polynomial Operator) software. First, it provides the user some control over the number of digits considered significant during internal computer arithmetic. In actual problems, this appeared as the critical factor in obtaining acceptable solutions from the computer. Second, it performs a verification of the computed results up to four significant digits. Any discrepancy so pointed up, one attempts to rectify by varying the number of digits considered significant. In the case of the jet engine problem, after making several runs, we obtained an (apparently) acceptable solution from the PL/I version by setting the threshold for loss of significance near eleven digits. We can compare this solution with the known solution to the problem, represented by fig. 3. To do this, we proceed as follows.

The complete solution to the kernel problem appears in the form of seven elements in a rank nine module, which are the required reduced basis for the kernel. Represented in the usual manner, five of these contained polynomials of degree k_i one or less. It is interesting to note that the existence of such elements can be predicted by the following argument. We interpret fig. 3

to yield a solution to the kernel problem, of the form (41).

$$\begin{bmatrix} N \\ \hline D \end{bmatrix} = \begin{bmatrix} -H^T \\ \hline sL \\ \hline sI \end{bmatrix} \qquad (41)$$

On the assumption that all solutions can be generated from the kernel basis, the logical conclusion is that the two columns of (41) can be represented as a linear combination of the five first degree elements in the reduced kernel basis. Interestingly enough, the question of determining this transformation can itself be represented as another kernel problem in polynomial modules. However, attempts to generate such a transformation turned out to be unsatisfactory.

As an alternative approach to verifying the KERPO solution, we used two of the five first degree basis elements to realize a second order dynamical control scheme for the jet engine, along the lines of fig. 5. From fig. 5, we could then obtain a state description for the overall closed loop system, which we then compared with the corresponding optimal integral control scheme system of fig. 3. This comparison was based on the first few Markov parameters. Table 3 shows this comparison for two of these parameters.

Table 3

Comparison of KERPO Results with Optimal Integral Control

Markov Parameter	KERPO Solution	Optimal Integral Control
CB	-4.4968 0.64815 -0.13348 -0.17304	-4.4969 0.64814 -0.13348 -0.17305
CAB	2631.6 1348 20693 10890	70.451 3.544 129.15 95.573

We note that our solution appears to have identified the B and C matrices correctly, while it is in error so far as the A matrix is concerned. On the basis of this evidence, we conjecture that roundoff error incurred in implementing the Euclidean division algorithm has the most serious impact on the correctness of the solution. This is because, intuitively, the effect of the A matrix in the state space corresponds to multiplication by 's' in the module. Since, in our case, the factors by which the matrix columns are multiplied are computed via the division algorithm, we hypothesize this to be the source of the error.

In order to solve the jet engine minimal design problem, then, one has the option of developing floating-point software which has increased sophistication or of switching to softwares which permit exact rational calculations. The next section reports on the latter method.

6. EXACT RATIONAL SOLUTION

One way to avoid the difficulties of finite machine representation of real numbers is to consider the numbers of table 1 as being rational instead of real numbers. It is then possible to get an exact solution to the jet engine problem, using softwares such as FORMAC or ALTRAN. These have the capability of rational and symbolic manipulation with an essentially unlimited degree of precision. Naturally, as the calculation proceeds, one would expect the integer size to increase quite a bit. As a consequence, the storage requirements and computer time needed to manipulate these would also be substantial. In this section we give evidence as to the magnitude of these, especially to contrast with the requirements for the floating point calculations. This yields valuable insight into the tradeoffs involved in terms of computer usage needed to solve typical realistic jet engine control problems from the polynomial approach. The results reported here are based upon FORMAC software written to implement, in rational arithmetic, the procedure of the Appendix, on an IBM 370/158 computer.

Starting with the numbers of table 1, together with the L and H matrices of table 2, we go through the calculations outlined in Section 3, and arrive at an exact rational-coefficient version of the kernel problem of (22). By applying the MDP Algorithm, conceived now over the field Q of rational numbers, we are led finally to an exact reduced basis for the corresponding exact 2 x 9 matrix over Q[s]. The seven basis elements turn out to contain polynomials of degree k_i equal to one and no polynomials of higher degree. Note that this means the floating point software missed at least two elements of first degree in the reduced basis. Rounded to fit in the available space, the seven basis elements obtained from exact software are indicated in table 4.

We would now like to compare the computer resources needed for the floating point calculation with those required for the exact calculation.

In the floating point software, a sort of trial and error process was used to optimize the calculation by varying the threshold for loss of significance. Though this software did not reach a satisfactory answer for the jet engine problem, we have allotted from our experience about seven runs of two CPU minutes each to this calculation. Each run occupied 400K bytes of memory.

Next consider the exact calculation. This software occupied 300K bytes of memory and executed the jet engine calculation in 135 minutes CPU time. However, the great majority of this time turns out to be consumed in Algorithm 2, which computes a reduced basis. This suggests strongly that more research on the reduction process---a common one in the literature ---could have a considerably greater than average effect on practical applications of the method. Except for the reduction, the remaining part of the calculation is just about an order of magnitude away from being very reasonable; and improvements of that order can be expected to occur in the near term, either through hardware or software advances.

A comparison is made in table 5. Here it is seen

Table 5

Comparison of Floating Point and Exact Solutions

Resource	Floating Point Algorithms 1 and 2	Exact Algorithm 1	Exact Algorithm 2
Memory	400K bytes	300K bytes	300K bytes
CPU	14 minutes(average)	18 minutes	117 minutes

that, on the average, the difference between floating point and exact softwares was about an order of magnitude in computing time.

For the exact solution, it is of interest also to examine integer sizes at various stages in the calculation. Such a summary has been made in table 6. Note

Table 6

Integer Size During Exact Solution

Stage of Computation	No. of Decimal Digits in Typical Integer
1. State Matrices For Plant	4
2. Plant Transfer Function	14
3. Inverse of Closed Loop System (T)	33
4. Kernel Problem (2 x 9 matrix)	45
5. After Algorithm 1	150
6. 20% through Algorithm 2	270
7. 60% through Algorithm 2	250
8. Final Reduced Basis	160

Table 4

(Rounded) Reduced Basis from Exact Solution

2.443E-3	0.0	0.0	0.0	0.0	0.0	0.0
1.601E-3	0.0	0.0	0.0	0.0	0.0	6.565E-4
-3.824E-2 1.125E-3s	-7.199E-5 -6.649E-6s	4.494E-4 1.288E-5s	4.146E-4 1.188E-5s	4.146E-4 5.151E-6s	4.146E-4 5.834E-6s	0.0 5.806E-4s
-7.898E-3 1.87 E-4s	-6.41 E-4 -1.331E-5s	0.0 3.653E-6s	0.0 3.322E-6s	0.0 -2.571E-6s	0.0 -1.768E-6s	0.0 8.467E-5s
-1.526E-3 6.54 E-4s	9.685E-5 -6.621E-5s	2.893E-6 -4.642E-5s	0.0 -4.423E-5s	0.0 -2.416E-5s	0.0 -1.847E-5s	0.0 -1.314E-4s
0.0	5.081E-4	4.794E-4 1.843E-4s	4.479E-4 1.713E-4s	0.0 -4.245E-5s	0.0 -3.076E-5s	0.0 1.279E-5s
0.0	0.0	0.0	-2.217E-6	-3.491E-5 +3.131E-6s	0.0 7.438E-6s	0.0 -1.421E-4s
0.0	0.0	0.0	0.0	0.0	1.622E-5	0.0 9.972E-5s
2.935E-2 8.69 E-4s	2.949E-4	-4.416E-4	-4.068E-4	-2.25 E-4	-2.434E-4	0.0 2.955E-4s

that integer size before and after Algorithm 2 is about the same, while it nearly doubles during Algorithm 2. This also suggests that improvements in the efficiency of Algorithm 2 may be possible.

Finally, we summarize by commenting that the floating point software used on the order of 4×10^8 byte seconds of computing power, but eventually did not yield an acceptable solution. On the other hand, the exact rational software required on the order of 2.4×10^9 byte seconds of computing resources and led to an exact solution.

7. COMPENSATOR POLE ASSIGNMENT

The exact rational software discussed in Section 6 obtained the reduced basis, $t_i(s)$, $1 \le i \le 7$, with

$$t_i(s) = \begin{bmatrix} n_i(s) \\ d_i(s) \end{bmatrix} \tag{42}$$

of table 4. From (20), where $G^T(s)$ is 2 x 2 and $K^T(s)$ is 5 x 2, we see that the matrix N(s) must be 7 x 2 while D(s) is 2 x 2. Accordingly,

$$\begin{bmatrix} N(s) \\ \hline D(s) \end{bmatrix}$$

is a 9 x 2 matrix, which means from (32) that two kernel elements

$$\hat{t}_i(s) = \begin{bmatrix} \hat{n}_i(s) \\ \hline d_i(s) \end{bmatrix}, \quad i = 1,2 \tag{43}$$

must be chosen to effect a design. These elements (43) will be linear combinations of the reduced basis elements (42). If

$$[\hat{t}_1(s) \vdots \hat{t}_2(s)]$$

has a linear dynamical interpretation as described in the Appendix, then $N(s)D^{-1}(s)$ has a minimal realization whose state matrix has a characteristic polynomial

$$|D(s)| = |\hat{d}_1(s) \vdots \hat{d}_2(s)|. \tag{44}$$

Now let

$$\hat{d}_i(s) = \sum_{k=1}^{7} f_{ik}\, d_k(s), \quad f_{ik} \in R, \ i = 1,2. \tag{45}$$

Then

$$|D(s)| = \Big| \sum_{k=1}^{7} f_{1k}\, d_k(s) \vdots \sum_{j=1}^{7} f_{2j} d_j(s) \Big| = \sum_{k=1}^{7} \sum_{j=1}^{7} f_{1k} f_{2j}\, |d_k(s) \vdots d_j(s)|, \tag{46}$$

by elementary properties of determinants. This shows that the characteristic polynomial of the state matrix in a minimal realization of $N(s)D^{-1}(s)$ can be viewed as a linear combination of the determinants $|d_k(s) \vdots d_j(s)|$.

Table 4 makes it clear that $|D|$ must have degree at least two; and so, since

$$|d_1 \vdots d_6| = -1.4092974E\text{-}8s - 4.7599915E\text{-}7 \tag{47a}$$

$$|d_1 \vdots d_7| = -8.6656773E\text{-}8s^2 - 2.9268875E\text{-}6s \tag{47b}$$

$$|d_6 \vdots d_7| = 2.9060023E\text{-}8s, \tag{47c}$$

with the polynomials in (47) serving as a basis for $R_2[s]$, the R-subspace of R[s] consisting of polynomials of degree two or less, it is possible to construct an arbitrary polynomial

$$|D(s)| = b_1 s^2 + b_2 s + b_3, \tag{48}$$

for $b_i \in R$, $i = 1,2,3$ by forming an appropriate linear combination

$$\beta_1 |d_1 \vdots d_6| + \beta_2 |d_1 \vdots d_7| + \beta_3 |d_6 \vdots d_7|; \tag{49}$$

$\beta_i \in R$, $i = 1,2,3$. The β_i's are uniquely determined by the b_i's. To complete a minimal design (48), it is only necessary to calculate f_{1k} and f_{2j} for k and $j = 1,6,7$. But certain results from the exterior algebra, referenced in Section 8, permit the calculation of (f_{11}, f_{16}, f_{17}) and (f_{21}, f_{26}, f_{27}) as the basis of the kernel of the matrix $[\beta_3, -\beta_2, \beta_1]$. Space precludes a complete treatment of the theory, so we turn to the jet engine example.

We make the selection

$$|D(s)| = s^2 + 2s + 2, \tag{50}$$

not so much because these dynamics are most desirable, but rather because the industry methods described in Section 3 could not be used to achieve (50) in a minimal design. Thus, by solving this case, we establish potential superiority for MDP over existing industry techniques.

Starting then, with (50) and working backwards, we can calculate β_i, $i = 1,2,3$ and thence (f_{11}, f_{16}, f_{17}) as well as (f_{21}, f_{26}, f_{27}). These calculations were performed using exact arithmetic again. The results are presented here after rounding. First we obtain,

$$\beta_1 = -4.202E6 \tag{51a}$$

$$\beta_2 = -1.154E7 \tag{51b}$$

$$\beta_3 = -1.095E9. \tag{51c}$$

Next, the needed f_{ij}'s are obtained from the basis for the kernel of $[\beta_3, \beta_2, \beta_1]$. A workable set of f_{ij}'s is,

$$f_{11} = \beta_2/\beta_3 \quad (52a)$$

$$f_{21} = -\beta_1/\beta_3 \quad (52b)$$

$$f_{16} = f_{27} = 0 \quad (52c)$$

$$f_{26} = f_{17} = 1 \quad (52d)$$

The f_{ij}'s were, in our application, further scaled by a factor of 10^5 to obtain the compensator gains as reasonable numbers. This can be done without upsetting the compensator pole placement to be achieved. Eqs. (45) and (42) can then be solved for t_1 and t_2 of (43). The 9 x 2 matrix $[t_1 \vdots t_2]$, which represents our solution, is seen to be,

$$\begin{bmatrix} 2.573 & -0.937 \\ 1.687 & 65.039 \\ 1.769s + 1.183 & 57.634s + 14.665 \\ 0.0202s - 8.32 & 8.395s + 3.029 \\ -1.158s - 1.607 & -13.396s + 0.585 \\ -3.076s & 1.279s \\ 0.744s & -14.214s \\ 1.622 & 9.972s \\ 0.915s + 6.582 & 29.213s - 11.258. \end{bmatrix} \quad (53)$$

A number of procedures exist which lead directly from the matrix $[t_1 \vdots t_2]$ to a state-space realization for the compensators G(s) and K(s). Referring then to fig. 5 and eqs. (23) and (24), we find the matrices A_g, B_g, C_g, B_k and D_k for a final solution of the problem. These are listed in Table 7, after rounding.

Table 7

Compensator Realizations

Matrix	Elements				
A_g	-2.0	-0.1626			
	12.298	0			
B_g	2.5732	1.686			
	-0.9369	65.039			
C_g	-3.2	0.1			
	1.092	0			
B_k	-11.727	-9.725	2.888	5.944	0.824
	36.416	3.28	-13.66	-37.83	9.147
D_k	0.119	0.777	2.363	9.973	-3.806
	1.932	0.022	-1.265	-3.36	0.813

The solution given in table 7 was verified by comparing the corresponding Markov parameters for the closed loop systems of figs. 5 and 3. An exact calculation comparing the first two Markov parameters, showed these to be identical for both systems. Another, non-exact calculation, which verified the first six Markov parameters, showed agreement to four digits. The first two of these were listed in the second column of table 3.

Step responses obtained from the closed loop system of fig. 5, using the numbers of table 7, are shown in fig. 7.

A visual comparison of fig. 7, with similar plots obtained for the optimal integral control system of fig. 3 showed them to be identical. Hence the latter set is not included here. It might be interesting to examine the distribution of closed loop poles, which is given below.

$$-138.43 \qquad -4.47 \pm 0.986\, i$$
$$-78.38 \qquad -1.678 \pm 0.238\, i$$
$$-0.136.$$

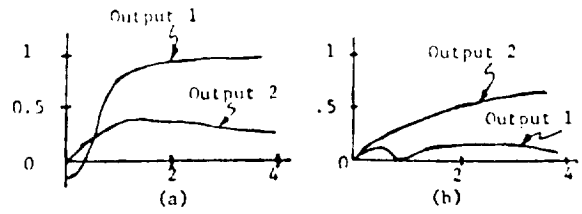

Fig. 7 Unit Step Responses. (a) Step on Input 1 (b) Step on Input 2.

As a final note in this section, it can be pointed out that the fixed poles in a compensator solution are the zeros of the greatest common divisor of the polynomials $\{|d_i \vdots d_j|,\ i, j = 1,2,\ldots,7\}$. It is clear from the pairings (1,6), (1,7), (6,7) of our example that this GCD is 1, and thus that there are no fixed poles in the jet engine application.

8. REMARKS

8.1 Conclusions

Considerable work has been done in the control systems area on polynomial design methods. Regardless of which viewpoint one takes toward the definition of such problems, their solution is usually assumed to proceed according to algorithms of the type described in the Appendix. Conceptually, this theory has achieved considerable maturity, and so it seems appropriate to conduct an extensive case study of its application to a realistic problem. This is the reason for the jet engine control analyses carried out in this paper.

The conclusions are generally positive in nature, though with some temporary limitations. On the positive side, Sections 3 and 7 show that MDP is a problem relevant to the jet engine control industry and that the MDP Algorithm offers a significant improvement in flexibility of design over existing algorithms in that industry. The application problem detailed herein provides a realistic and nontrivial test case for workers in the area of computer solution of polynomial problems. A first limitation clearly occurs in Algorithm 2, which is a popular and well known theoretical algorithm. Both in terms of integer growth and relative CPU time, this reduction algorithm points to a need for further research. Following such an improvement, it would appear that the second limitation is overall CPU time for an exact solution. Though the cost of such time would be a small part of overall design cost, it appears desirable to reduce this time by an order of magnitude. Since such a reduction seems to be a near-term possibility by hardware or software advances, it would seem that polynomial methods may soon be ready to play a greater role in everyday practical design.

8.2 Historical Remarks

The original stimulus for this work was the paper of Wang and Davison [1] in 1973, in which a minimal inverse system problem was solved. That work subsequently led to the algorithm of Forney [2] phrased in rational vector spaces. Together, these works then led to the free-modular MDP Algorithm [3] which has been applied here. The jet engine application has been motivated by Michael and Farrar [4], whence arose our numerical data. A report on KERPO in double-precision FORTRAN has been presented [5], as has a more complete treatment of the pole assignment approach [6] in Section 7. Background reading on the algebraic aspects of the paper is available in [7]; and the exact proposition needed in Section 7 can be found in Chapter XV, Section 8, Proposition 15 of [8]. Further references to related

polynomial works have been cited in [3].

REFERENCES

1. S. H. Wang and E. J. Davison, "A Minimization Algorithm for the Design of Linear Multivariable Systems," IEEE Transactions on Automatic Control, Vol. AC-18, pp. 220-225, June 1973.
2. G. D. Forney, Jr., "Minimal Bases of Rational Vector Spaces, with Applications to Multivariable Linear Systems," SIAM Journal on Control, Vol. 13, pp. 493-520, May 1975.
3. M. K. Sain, "A Free-Modular Algorithm for Minimal Design of Linear Multivariable Systems," Proceedings IFAC 6th World Congress, Part IB, pp. 9.1-1--9.1-7, August 1975.
4. G. J. Michael and F. A. Farrar, "An Analytical Method for the Synthesis of Nonlinear Multivariable Feedback Control," Report M941338-2, United Aircraft Research Laboratories, June 1973.
5. R. R. Gejji, "A Computer Program to Find the Kernel of a Polynomial Operator," Proceedings Fourteenth Allerton Conference on Circuit and System Theory, September 1976.
6. V. Seshadri and M. Sain, "An Approach to Pole Assignment by Exterior Algebra," Proceedings Fourteenth Allerton Conference on Circuit and System Theory, September 1976.
7. M. K. Sain, "The Growing Algebraic Presence in Systems Engineering: An Introduction," IEEE Proceedings, Vol. 64, pp. 96-111, January 1976.
8. S. MacLane and G. Birkhoff, Algebra. London: The Macmillan Co., 1967.

APPENDIX

Let

$$M : F[s]^q \to F[s]^p \tag{A.1}$$

be a morphism of free modules. In the appendix, we describe how a reduced basis for the kernel of M can be obtained and used to solve MDP. For a more complete discussion, the reader is referred to [3]. Solutions are obtained in the form of the $q \times \ell$ matrix

$$\begin{bmatrix} N(s) \\ \hline D(s) \end{bmatrix} \tag{A.2}$$

over $F[s]$.

We change notation slightly by letting M be the $h \times q$ matrix representing the morphism M. The technique is to choose $q \times q$ unimodular $F[s]$-matrices to post-multiply M. A matrix is unimodular if it has a non-zero determinant that is an element of F. Mathematically,

$$U : F[s]^q \to F[s]^q \tag{A.3}$$

is unimodular if $|U| \neq 0, \in F$. Such an operation is equivalent to a change of basis in $F[s]^q$ and leads to a representation of M in the new basis. The following elementary column operations are examples of such transformations. The column operations are, (1) interchanging two columns of M; (2) adding an $F[s]$-multiple of one column of M to another; (3) multiplication of a column of M by a non-zero element of F.

Given the $p \times q$ matrix M, the following algorithm leads to a basis for Ker M. The basis elements are represented in the usual manner.

Algorithm 1

Step 1. To the $p \times q$ matrix M, adjoin a $q \times q$ identity matrix to form

$$\begin{bmatrix} M \\ \hline I \end{bmatrix}. \tag{A.4}$$

Step 2. By elementary column operations, reduce (A.4) to the form

$$\begin{bmatrix} E_{11} & 0 \\ \hline E_{21} & E_{22} \end{bmatrix} \tag{A.5}$$

where E_{11} has p rows, has no zero columns and is in an echelon form.

Step 3. Then the columns of E_{11} are a basis for the image of M, and the columns of E_{22} are a basis for the kernel of M (Ker M).

Now, let b_i, $i = 1,2,\ldots,\rho$ be the columns of E_{22} obtained from Algorithm 1 as a basis for Ker M. Then by application of further unimodular transformations, we can get an equivalent basis for Ker M which is reduced in the sense of Section 4. Notice that we have introduced the notation b_i for elements of the basis before reduction, to avoid confusion with t_i, $i = 1,2,\ldots\rho$, which was assumed to be a reduced basis in Section 4. The algorithm below is used to reduce the kernel basis. However, the procedure is more general in nature and can be used to reduce ρ linearly independent elements in $F[s]^q$ regardless of their origin. This one is typical of procedures described in the literature for doing these kinds of calculations. However, as has been pointed out in the paper, it is this part of the computation that consumes the major portion of computer time. Any research aimed at achieving efficiency in the reduction process is, therefore, the most likely to have a significant payoff in terms of making the MDP method of control system design tractable in the near term.

Algorithm 2

Write each b_i, $i = 1,2,\ldots,\rho$ in the manner

$$b_i = \sum_{j=0}^{\ell_i} b_{i,j} s^j \tag{A.6}$$

where $b_{i,j} \in F^q$ and $b_{i,\ell_i} \neq 0$. We shall say the list $b_1, b_2,\ldots, b_\rho$ is reduced if the matrix

$$[b_{1,\ell_1}\ b_{2,\ell_2} \cdots b_{\rho,\ell_\rho}] \tag{A.7}$$

has rank ρ. Then, perform:

Step 1. If the list $b_1, b_2,\ldots, b_\rho$ of linearly independent elements is reduced, stop; otherwise, continue.

Step 2. Determine field elements f_i in F, $1 \leq i \leq \rho$, which are not all zero and which satisfy

$$\sum_{i=1}^{\rho} f_i\, b_{i,\ell_i} = 0. \tag{A.8}$$

Step 3. For the set of integers i having f_i non-zero, determine an i, denoted by i_{max}, for which ℓ_i is a maximum, denoted by ℓ_{max}.

Step 4. Perform the elementary column operation: Replace $b_{i_{max}}$ by

$$\sum_{i=1}^{\rho} f_i\, b_i s^{(\ell_{max}-\ell_i)}$$

Return to Step 1.

The question that remains is how the reduced basis may be used to obtain linear dynamical solutions to MDP. Let MDP take the form (A.9) when stated over $F[s]$.

$$M \begin{bmatrix} N \\ \hline D \end{bmatrix} = 0. \tag{A.9}$$

Now, in any solution

$$\begin{bmatrix} N \\ \hline D \end{bmatrix}$$

of (A.9), each of the ℓ columns will be contained in the kernel of M. All solutions pairs (N,D) can, thus, be built up as linear combinations of elements in a basis for Ker M. Under what conditions will a solution pair (N,D) yield a minimal solution?

Without loss of generality, we may assume that for any candidate pair (N,D) the ℓ columns of

$$\left[\frac{N}{D}\right]$$

are reduced, because if they are not, a unimodular transformation V on $F[s]^{\ell}$, chosen according to Algorithm 2, will produce an equivalent pair $(\hat{N},\hat{D})$ such that the columns of

$$\left[\frac{\hat{N}}{\hat{D}}\right]$$

are reduced and

$$ND^{-1} = NV(DV)^{-1} = \hat{N}\hat{D}^{-1}. \tag{A.10}$$

Then, we make the following comments, offered without proof.

(1) $N(s)D^{-1}(s)$ can be realized by a linear dynamical system if ND^{-1} is a matrix of proper rational functions. In such a situation, there exists a realization A,B,C,E, all matrices over F, such that

$$\begin{aligned} G(s) &= N(s)D^{-1}(s) \\ &= C(sI-A)^{-1}B + E. \end{aligned} \tag{A.11}$$

Equivalently, we also say that a pair (N,D) has a linear dynamical interpretation if the ℓ columns of

$$\left[\frac{N}{D}\right]$$

are reduced and furthermore, letting the i^{th} column be

$$\hat{t}_i = \left[\frac{\hat{n}_i}{\hat{d}_i}\right], \quad i = 1,2,\ldots,\ell, \tag{A.12}$$

these ℓ columns, when expressed as

$$\hat{t}_i = \sum_{j=0}^{m_i} \hat{t}_{i,j} s^j, \quad \hat{t}_{i,m_i} \neq 0 \tag{A.13}$$

are such that the last ℓ rows of the matrix

$$[\hat{t}_{1,m_1} \; \hat{t}_{2,m_2} \cdots \hat{t}_{\ell,m_\ell}] \tag{A.14}$$

have full rank.

Being concerned with finding a realization with the least order of dynamics, we state two more properties.

(2) If the property in (1) is satisfied, then the determinant $|D(s)|$ is related to the minimal realization, being an F-multiple of the corresponding characteristic polynomial $|sI-A)|$. Also,

(3) The columns of

$$\left[\frac{N}{D}\right]$$

when expressed as in (A.13), yield the number of dynamical elements in the minimal realization as

$$\sum_{i=1}^{\ell} m_i.$$

With these notions, let t_i, $i = 1,2,\ldots,n$ be the ordered basis obtained from Algorithm 2. Then, MDP reduces to generating ℓ elements in Ker M which have a linear dynamical interpretation, with minimum order dynamics. For this, we can use the MDP Algorithm.

MDP Algorithm

Step 1. Apply Algorithm 1 to obtain a basis

$$b_i, \quad 1 \leq i \leq n \tag{A.15}$$

for Ker M.

Step 2. Apply Algorithm 2 to the elements of (A.15) to form a reduced basis,

$$t_i, \quad 1 \leq i \leq n. \tag{A.16}$$

Step 3. Express the reduced basis (A.16) in this manner

$$t_i = \sum_{j=0}^{k_i} k_{i,j} s^j, \quad t_{i,k_i} \neq 0 \tag{A.17}$$

for $i = 1,2,\ldots,n$. Form the matrix

$$[t_{1,k_1} \; t_{2,k_2} \cdots t_{n,k_n}]. \tag{A.18}$$

If the rank of the matrix formed from the last ℓ rows of (A.18) is not equal to ℓ, stop; MDP has no solution; otherwise, continue.

Step 4. From the elements of (A.16) in the reduced basis select ℓ elements

$$t_{i_1}, t_{i_2}, \ldots, t_{i_\ell}$$

with the properties

(i) the rank of the matrix formed from the last ℓ rows of

$$[t_{i_1,k_{i_1}} \; t_{i_2,k_{i_2}} \cdots t_{i_\ell,k_{i_\ell}}]$$

is equal to ℓ; and

(ii) $\sum_{j=0}^{\ell} k_{i_j}$ is a minimum.

As a matter of fact, more solutions to MDP may be possible. Any elements $\hat{t}_1, \hat{t}_2, \ldots, \hat{t}_\ell$ in Ker M, which admit a linear dynamical interpretation and achieve the minimum order dynamics predicted in (ii) above, are a solution to MDP through the equations

$$\left[\frac{N}{D}\right] = [\hat{t}_1 \; \hat{t}_2 \cdots \hat{t}_\ell] \tag{A.19}$$

and

$$G(s) = N(s)D^{-1}(s). \tag{A.20}$$

Now, in the jet engine problem, n is 7 and ℓ is 2. The two needed columns of

$$\left[\frac{N}{D}\right]$$

were generated in Section 7 to satisfy the pole placement requirement.

MICHAEL K. SAIN
Department of Electrical Engineering
UNIVERSITY OF NOTRE DAME
[illegible] INDIANA 46556 U.S.

20th
MIDWEST SYMPOSIUM
ON
CIRCUITS AND SYSTEMS

AUGUST 15-17, 1977

Edited by
K.S. CHAO/R. SAEKS

TEXAS TECH UNIVERSITY

59

A COMPARISON OF FREQUENCY DOMAIN TECHNIQUES FOR JET ENGINE CONTROL SYSTEM DESIGN

R. Gejji, R. M. Schafer, M. K. Sain, & P. Hoppner
Department of Electrical Engineering
University of Notre Dame
Notre Dame, Indiana 46556

Abstract

Present research efforts in the area of linear multivariable control systems include activities which will probably reestablish frequency domain methods as frequently used tools for design. Two notable branches of this activity are polynomial methods and return-difference-determinant methods. This paper sketches some features of these approaches, in the context of a numerical example from turbofan engine control.

1. INTRODUCTION

State variable methods for the design of linear multivariable control systems are well established as a major tool in the applications. Variants of the linear quadratic regulator theory are probably the most successful, with a variety of other techniques such as pole placement, decoupling, and geometric regulator theory also available. Even today, however, linear quadratic regulator theory still requires a somewhat indirect thought process, a feature it shares with many optimization methods; and much of the remaining technique is synthesis oriented instead of design oriented.

Accordingly, some modern re-emergence of frequency domain thought has occurred---especially for design. Broadly depicted, this work involves polynomial methods and return-difference-determinant methods. This paper records certain studies of these ideas, on a common illustration from turbofan engine control. Brevity precludes in-depth treatment; we rely instead on the illustrations and the references.

2. ILLUSTRATIVE PROBLEM

The turbofan engine model chosen for the illustrations has two control inputs--fuel flow and exhaust area, five states--fan turbine inlet temperature, main burner pressure, fan speed, high compressor speed, and augmentor pressure, and two outputs--thrust and high turbine inlet temperature. In traditional (A,B,C,D) form, the state description [1] is given by the matrices at the top of the following column, at a power lever angle of 47°. For the sequel the corresponding matrix G(s), namely $C(sI-A)^{-1}B+D$, is recorded.

The design problem is to select compensators for G(s), in a loop under unity negative feedback of the plant outputs. Fast step responses with small overshoot are of interest.

$$A = \begin{bmatrix} -57.096 & 3.613 & -10.211 & -5.481 & -2.715 \\ 19.832 & -72.340 & 30.295 & 40.972 & 15.327 \\ .660 & 4.496 & -3.601 & -.011 & -2.808 \\ 1.326 & 2.313 & -.809 & -3.032 & -.821 \\ .882 & .703 & 2.922 & 1.471 & -4.596 \end{bmatrix}$$

$$B = \begin{bmatrix} 39.792 & 1.017 \\ 4.181 & -.125 \\ -.382 & -.077 \\ -.565 & -.088 \\ -.785 & -3.563 \end{bmatrix} \qquad D = \begin{bmatrix} .018 & .546 \\ -.086 & -.013 \end{bmatrix}$$

$$C = \begin{bmatrix} -.037 & .031 & -.016 & -.042 & 1.368 \\ 1.081 & .149 & -.057 & .001 & -.086 \end{bmatrix}$$

3. POLYNOMIAL METHODS [2]

Polynomial methods take advantage of the fact that action of the A-matrix and the s-variable are closely related in a module theoretic sense [3]. Not yet well advanced computationally, polynomial methods nonetheless offer considerable insight into system structure. As is to be expected, they resemble the geometric methods in this regard.

$$G(s) = \frac{\begin{bmatrix} (.018s^5 + .145s^4 - 92.05s^3 & (.546s^5 + 71.9s^4 + 2247s^3 \\ -396.9s^2 + 29801s + 95491) & -1943.s^2 - 16855s - 12495) \\ (-.086s^5 + 31.63s^4 + 3321.5s^3 & (-.013s^5 - .437s^4 + 68.2s^3 \\ + 25500s^2 + 76068s + 78277) & + 1703.3s^2 + 1742.9s - 3532.2) \end{bmatrix}}{s^5 + 140.7s^4 + 5337.6s^3 + 38691s^2 + 119690s + 133389}$$

As an example, consider the selection of $K_1(s)$ and $K_2(s)$ in Figure 1 in order to achieve a specified closed loop performance T(s). Such a specification is, of course, a nontrivial issue in its own right. A complete treatment of such a specification can be found in [2]. Relying upon the algebraic interpretation of a transfer function as a pair of polynomials, such a design problem can be converted to a kernel calculation in R[s]-modules, where R[s] denotes polynomials in s with coefficients in the real number field R. Considerable manipulation must be carried out to set up this kernel problem, which turns out to involve a 2x9 matrix of polynomials up to the thirteenth degree, as shown below.

[. . . . . ⊙ .]
[. ⊙ . . . . .]

1.17 E10 s^3	-1.37 E10 s^2
+4.40 E10 s^4	-4.99 E10 s^3
+4.06 E10 s^5	-4.21 E10 s^4
+1.18 E10 s^6	-1.07 E10 s^5
-1.24 E9 s^7	+1.49 E9 s^6
-1.26 E9 s^8	+1.99 E9 s^7
-2.07 E8 s^9	+1.99 E8 s^8
-5.55 E6 s^{10}	+6.93 E6 s^9
-4.80 E4 s^{11}	+8.33 E4 s^{10}
-7.09 E1 s^{12}	+2.38 E2 s^{11}
+4.5 E-1 s^{13}	-1.00 E0 s^{12}

Solution involves automorphic transformations on the domain of the map represented by this matrix to determine seven "reduced basis" elements, shown below which serve to describe the kernel. From these, construction of $K_1(s)$ and $K_2(s)$ involves two linear combinations of these seven module elements, and standard realization methodology. Using first, sixth, and seventh elements, and the assumptions

$$C_{K_1} = C_{K_2} \quad A_{K_1} = A_{K_2}, \quad D_{K_1} = 0,$$

realizations can be found in the manner

Compensator Realizations

Matrix	Elements				
A_{K_1}	-2.0	-0.1626			
	12.298	0			
B_{K_1}	2.5732	1.686			
	-0.9369	65.039			
C_{K_1}	-3.2	0.1			
	1.092	0			
B_{K_2}	-11.727	-9.725	2.888	5.944	0.824
	36.416	3.28	-13.66	-37.85	9.147
D_{K_2}	0.119	0.777	2.363	9.973	-3.806
	1.932	0.022	-1.265	-3.36	0.813

Responses to unit steps in the two reference channel are shown in Figures 2 and 3.

Solution of a problem by polynomial methods involves at this time nontrivial computational overhead, which is discussed in greater detail in [2]. It is likely, however, that advances in software and hardware will soon reduce this overhead. Advantages of the method include a finite enumeration of all solutions for a given T(s), and perhaps eventually a finite description of all possible performances.

2.443E-3	0.0	0.0	0.0	0.0	0.0	0.0
1.601E-3	0.0	0.0	0.0	0.0	0.0	6.565E-4
-3.824E-2	-7.199E-5	4.494E-4	4.146E-4	4.146E-4	4.146E-4	0.0
1.125E-3s	-6.649E-6s	1.288E-5s	1.188E-5s	5.151E-6s	5.834E-6s	5.806E-4s
-7.898E-3	-6.41 E-4	0.0	0.0	0.0	0.0	0.0
1.87 E-4s	-1.331E-5s	3.653-6s	3.322E-6s	-2.571E-6s	-1.768E-6s	8.467E-5s
-1.526E-3	9.685E-5	2.893E-6	0.0	0.0	0.0	0.0
6.54 E-4s	-6.621E-5s	-4.642E-5s	-4.423E-5s	-2.416E-5s	-1.847E-5s	-1.314E-4s
0.0	5.081E-4	4.794E-4	4.4794E-4	0.0	0.0	0.0
		1.843E-4s	1.713E-4s	-4.245E-5s	-3.076E-5s	1.279E-5s
0.0	0.0	0.0	-2.217E-6	-3.491E-5	0.0	0.0
				+3.131E-6s	7.438E-6s	-1.421E-4s
0.0	0.0	0.0	0.0	0.0	1.622E-5	0.0
						9.972E-5s
2.935E-2	2.949E-4	-4.416E-4	-4.068E-4	-2.25 E-4	-2.434 E-4	0.0
8.69 E-4s						2.955E-4s

4. RETURN-DIFFERENCE-DETERMINANTS [4]

The present computational situation for polynomial methods makes alternate frequency domain approaches of interest.

If we set K_2 to zero and denote K_1 by K, we have the archetypal unity negative feedback precompensation problem. If K is assumed to have state description (A_K, B_K, C_K, D_K), then a combined state description (A_C, B_C, C_C, D_C) for

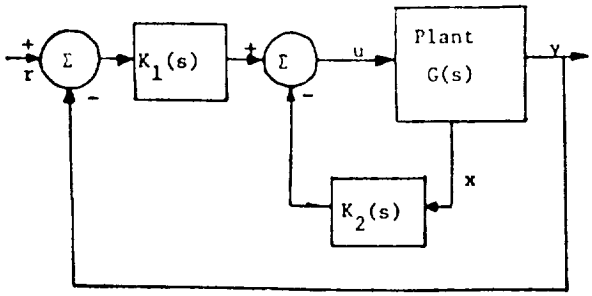

Fig. 1
Compensation Scheme for Polynomial Design

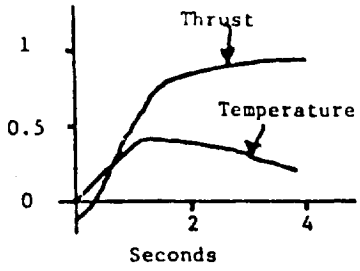

Fig. 2
Closed Loop Response to Unit Step in Commanded Thrust; Polynomial Design

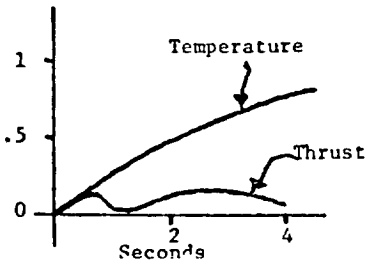

Fig. 3
Closed Loop Response to Unit Step in Commanded Temperature; Polynomial Design

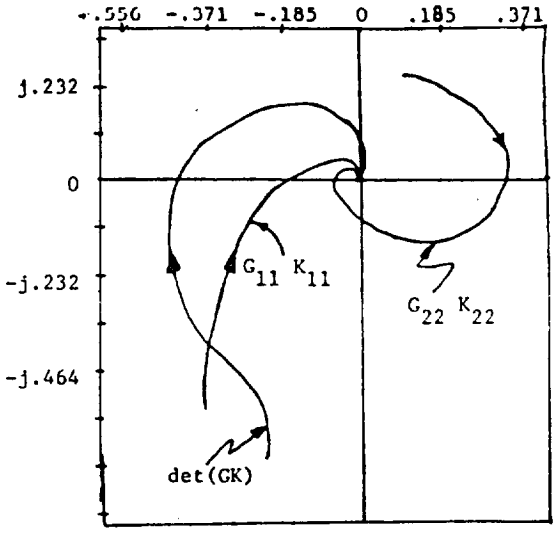

Fig. 4
Nyquist Plots for Compensated System; Direct Expansion

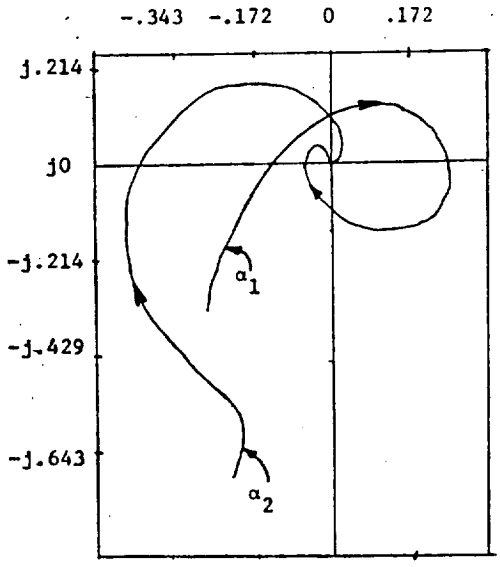

Fig. 5
Nyquist Plots for Compensated System; Alpha Expansion

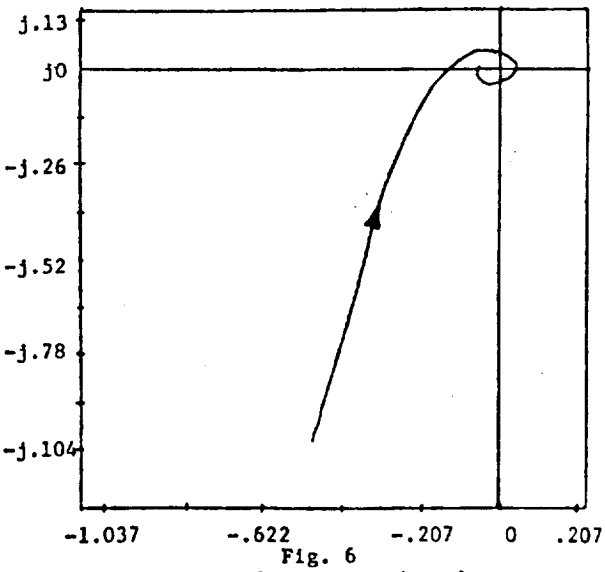

Fig. 6
Nyquist Plot for det(I+GK)

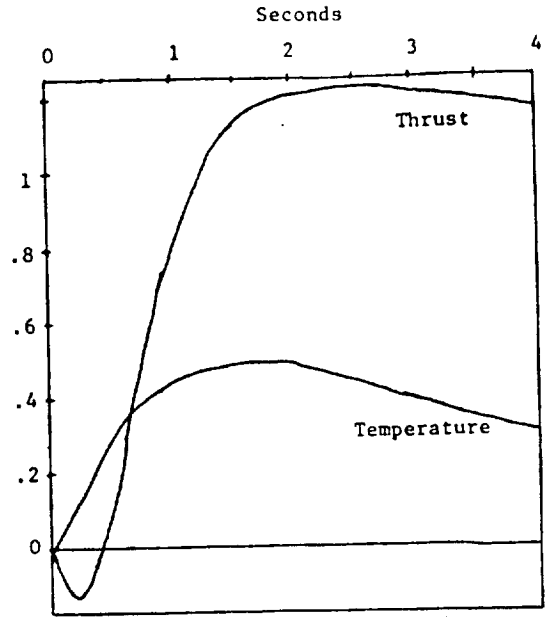

Fig. 7
Same as Fig. 2 for Direct Approach Design

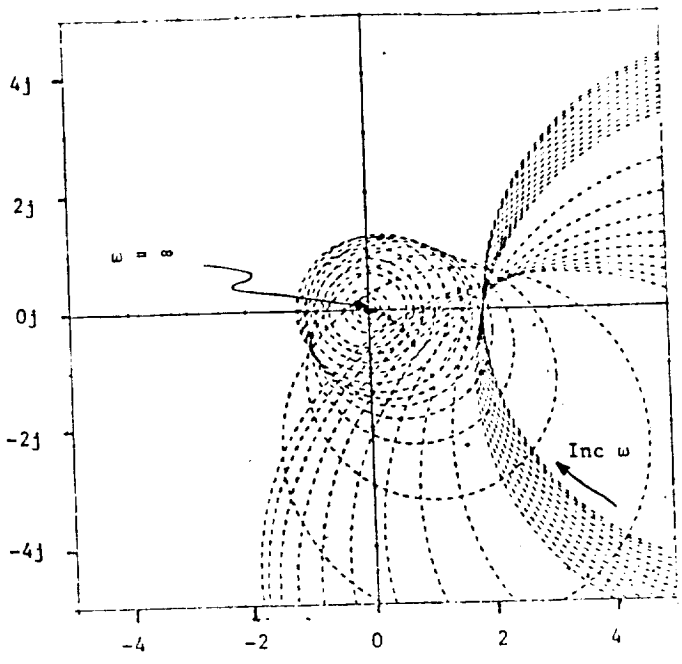

Fig. 9
CARDIAD Plot, Column 1, Uncompensated

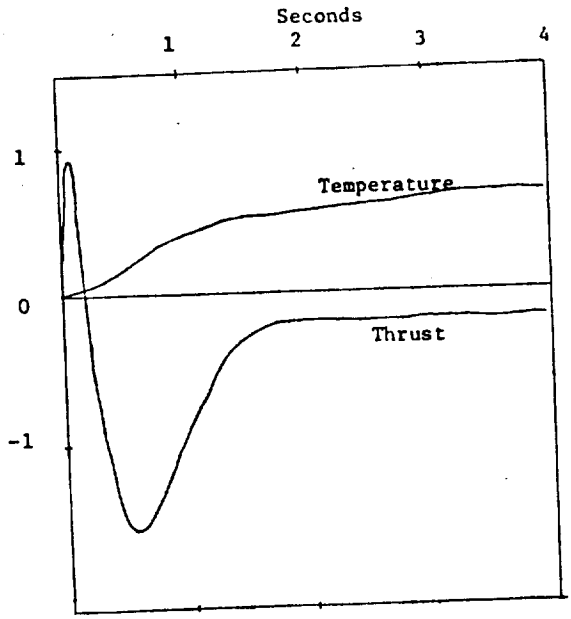

Fig. 8
Same as Fig. 3 for Direct Approach Design

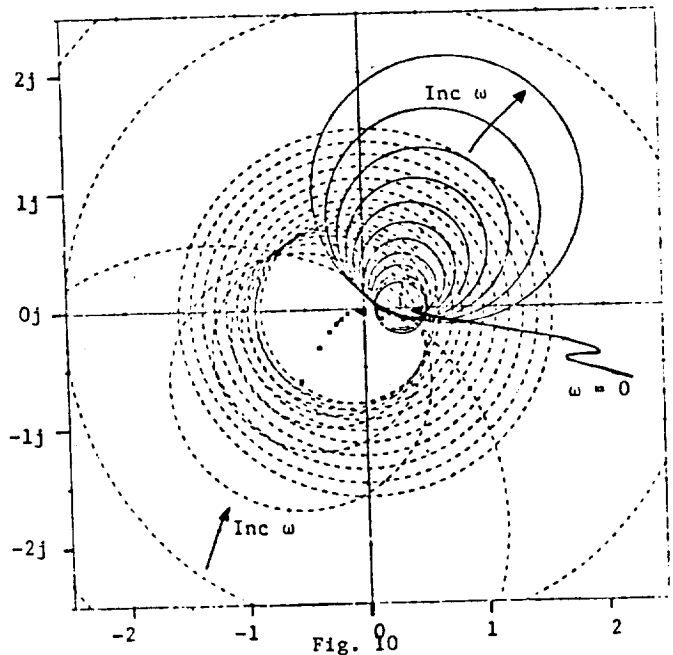

Fig. 10
CARDIAD Plot, Column 2, Uncompensated

the loop can be obtained by an isomorphism on the product of the state spaces X and X_K associated with the plant and compensator, respectively, provided that the gain matrix DD_K has no negative unit eigenvalues. For this situation, one has the important relationship that

$$|I+DD_K|\ |sI-A_C| = |I+CK|\ |sI-A|\ |sI-A_K|,$$

upon which a Nyquist study can be based. We refer

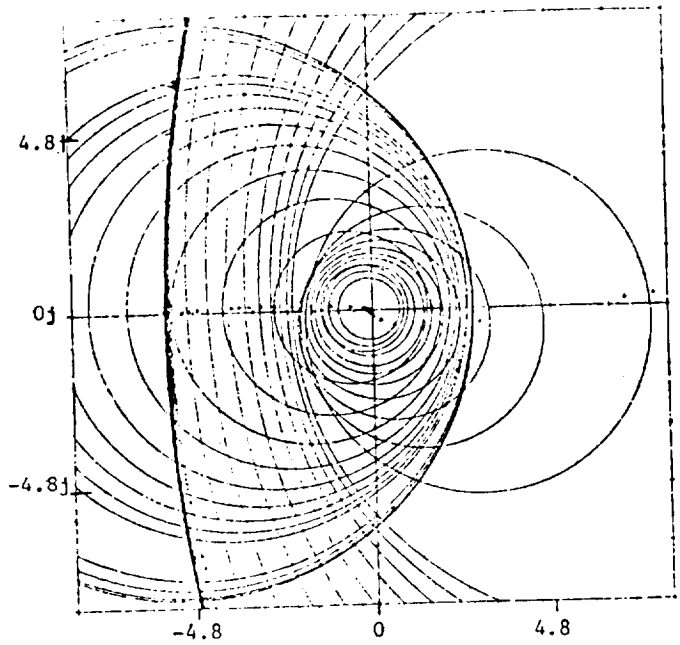

Fig. 11
CARDIAD Plot, Column 1, Compensated System

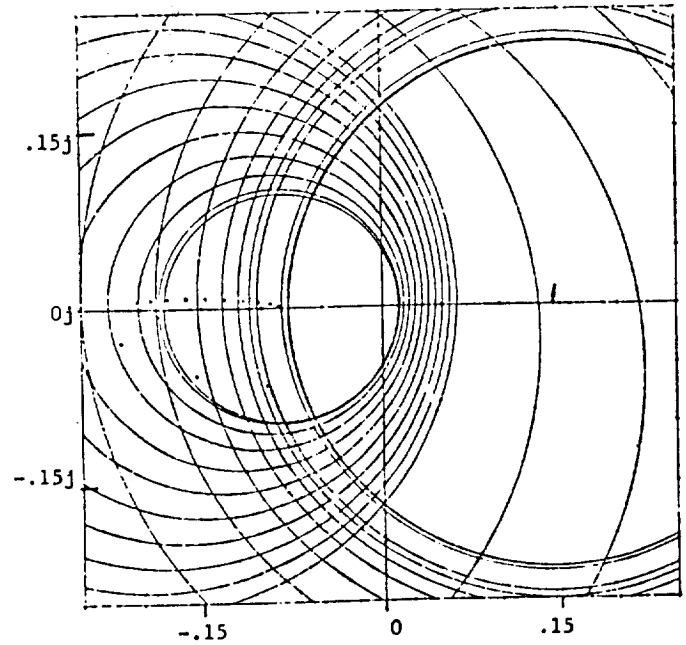

Fig. 12
CARDIAD Plot, Column 2, Compensated System

to such studies as return-difference-determinant methods, because of the presence of |I+GK| in a key role.

Construction of a Nyquist plot is related to the expansion chosen for the return-difference-determinant. The obvious expansion, shown for the present illustrative case, is

$$1 + G_{11}K_{11} + G_{12}K_{21} + G_{21}K_{12} + G_{22}K_{22} + |GK|;$$

and a less obvious, more recursive expansion in an NxN case is

$$\sum_{i=0}^{N} (-1)^i \alpha_i,$$

where

$$\alpha_0 = 1,$$

and

$$\alpha_i = (-1/i) \sum_{p=0}^{i-1} \alpha_p \, \mathrm{trace}(GK)^{i-p},$$

for $i \geq 1$.

Design based upon Nyquist plots of |I+GK| is made challenging by the intricate way in which the compensator K relates to the determinant. At present, only introductory design studies based upon the expansions above have been made [4]. An illustration is the compensator

$$K(s) = \begin{bmatrix} \frac{1}{s} & 0 \\ 0 & \frac{1000(s+1)}{s(s+200)} \end{bmatrix},$$

which was chosen by a cut-and-try method to increase the speed of response of the second output. Figures 4 and 5 show the terms in the "obvious" and "α" expansions for the compensated system, with Figure 6 indicating the sum, exclusive of the unit term in each expansion. Closed loop responses to reference steps in each channel are shown in Figures 7 and 8. Though the temperature response in Figure 8 is acceptable, the thrust response in Figure 7 exhibits overshoot; and considerable interaction is evident.

In current practice, plots such as Figure 6 tend to be the most useful. Design technique tends to focus upon reducing the interaction evident in these results, which brings us to the next topic.

5. CARDIAD--A DOMINANCE APPROACH [5]

In making a Nyquist plot of the determinant of return difference, H. H. Rosenbrock, [7] has established that |I+GK| encirclements can be counted as the algebraic sum of the encirclements of the diagonal elements of return difference (I+GK)--provided that a condition of "dominance" holds on (I+GK). This means, in our case, that the off-diagonal element in a column is smaller in magnitude than the diagonal element, as a function of frequency ($s=j\omega$). Related to this stability oriented usage of the dominance idea is a corresponding requirement on the loop transmission GK, which is used to help with decoupling closed loop performance.

Selection of K(s) for this latter purpose, so that $G(j\omega)K(j\omega)$ is dominant on its columns, has been widely studied for the case in which K(s) is restricted to be a constant matrix. Much less has been accomplished relative to the choice of a dynamic K(s).

A new technique for this purpose is the CARDIAD

plot, acronymed for Compensator Acceptability Region for Diagonal Dominance. Compensators

$$K(j\omega) = \begin{bmatrix} 1 & x_2(j\omega)+jy_2(j\omega) \\ x_1(j\omega)+jy_1(j\omega) & 1 \end{bmatrix}$$

are assumed, without loss of generality for precompensation. A CARDIAD plot for column one of the uncompensated system is shown in Figure 9. Each circle corresponds to a particular frequency ω, and acceptable (x_1,y_1) pairs must be outside dashed circles at the frequency in question. Note that $y_1 = 0$ and x_1 suitably negative will be acceptable for all frequencies. Figure 10 shows a CARDIAD plot for column two. Acceptable (x_2,y_2) pairs must be inside solid circles at the frequency in question.

The simple compensator

$$K(s) = \begin{bmatrix} 1 & \dfrac{.7s + .44}{.05s + 1} \\ -10 & 1 \end{bmatrix}$$

achieves dominance at all frequencies in both columns, as can be seen in Figures 11 and 12, which consist only of solid circles each of which includes the origin.

More detailed information about an application of this method to design and simulation of a turbofan engine control can be found in [6].

6. DISCUSSION

Recent activities in frequency domain analysis and design of linear multivariable control systems suggest a certain resurgence of this viewpoint in useful new ways. Though somewhat limited by space constraints, we have tried to give a glimpse of some of these methods in the context of a numerical model from the turbofan engine area. Focus has been on polynomial methods, which bear close resemblance to geometric control methods in an abstract algebraic sense, and upon methods related to the determinant of return difference. The CARDIAD plot, a new dynamical approach to dominance, has been illustrated.

ACKNOWLEDGMENTS

This work was supported in part by the National Science Foundation under Grant ENG 75-22322 and in part by the National Aeronautics and Space Administration under Grant NSG 3048.

REFERENCES

1. G. J. Michael and F. A. Farrar, "An Analytic Method for the Synthesis of Nonlinear Multivariable Control," United Technologies Research Laboratories, Report M941338-2, East Hartford, Connecticut, June 1973.

2. R. R. Gejji and M. K. Sain, "Application of Polynomial Techniques to Multivariable Control of Jet Engines," Preprints Fourth IFAC International Symposium on Multivariable Technological Systems, pp. 421-429, June 1977.

3. S. MacLane and G. Birkhoff, Algebra. London: The Macmillan Co., 1967.

4. P. W. Hoppner, "The Direct Approach to Compensation of Multivariable Jet Engine Models," Tech. Rept. EE-779, Notre Dame, Indiana, April 25, 1977.

5. R. M. Schafer, "A Graphical Approach to System Dominance," Tech. Rept. EE-778, Notre Dame, Indiana, March 26, 1977.

6. R. M. Schafer, R. R. Gejji, P. W. Hoppner, W. E. Longenbaker, and M. K. Sain, "Frequency Domain Compensation of a DYNGEN Turbofan Engine Model," Proc. 1977 Joint Automatic Control Conference, pp. 1013-1018.

7. H. H. Rosenbrock, Computer-Aided Control System Design. New York: Academic Press, 1974.

10
11

SOME FEATURES OF CARDIAD PLOTS FOR SYSTEM DOMINANCE*

R. Michael Schafer
Department of Electrical Engineering
University of Notre Dame
Notre Dame, Indiana 46556

Michael K. Sain
Department of Electrical Engineering
University of Notre Dame
Notre Dame, Indiana 46556

Abstract

Recently, the CARDIAD (Complex Acceptability Region for DIAgonal Dominance) plot has been introduced and applied to the problem of designing dynamical precompensation to achieve column dominance. This paper illustrates several basic features of the method while using it to design a single, low-order dynamical compensator which achieves dominance at five operating points of a realistic two-spool turbofan digital simulation.

1. Introduction

The CARDIAD (Complex Acceptability Region for DIAgonal Dominance) plot is a graphical technique for choosing dynamical compensators to achieve diagonal row or column dominance, as defined by Rosenbrock [1]. Without essential loss of generality, the compensator is assumed to have its diagonal elements equal to unity, and a typical CARDIAD plot describes the acceptable range of the real and imaginary parts of the off-diagonal elements such that dominance is achieved. The basic graphical building block is the circle. Each circle represents the acceptable range at a specific frequency. Solid circles are drawn if acceptable real and imaginary pairs correspond to points inside the circle, and dashed circles are drawn if acceptable pairs correspond to points outside the circle. Plotted as a function of frequency, these circles describe the acceptable range of the compensator element in question, considered as a complex function of frequency.

Recently, CARDIAD plots have been shown to be an effective design tool in dynamical precompensation of multivariable plants to achieve dominance [2, 3, 4, 5]. This paper focuses upon another aspect of the CARDIAD plot, namely its ability to assist with the classification of various operating points of a nonlinear system with regard to their dominance possibilities and to help with the design of compensators which achieve dominance of multiple operating points.

*This work was supported in part by the National Aeronautics and Space Administration under Grant NSG 3048 and in part by the National Science Foundation under Grant ENG 75-22322.

2. Specific Assumptions

Plant models used to construct the plots in the sequel have been generated from the general purpose digital jet engine simulator DYNGEN [6] under a load which provides behavior similar to that of the F-100 two-spool turbofan engine at sea level static conditions. The models have two inputs, five states, and two outputs. They are linearizations of DYNGEN obtained with the aid of the DYGABCD package [7] under development at NASA Lewis Research Center. Physical description of the states can be found in the references [3]. The inputs are fuel flow and exhaust area; the outputs are thrust and high turbine inlet temperature. Parameterization is accomplished through the nominal value of the fuel flow WFB, which takes the five values 2.145, 2.31, 2.475, 2.64, and 2.75 LBM/SEC, ranging from a low thrust condition to high thrust without augmentation. All the models have been normalized.

Thus the plant transfer function matrix has two rows and two columns, and exhibits transfer functions of degree five in both numerator and denominator. Space limitations preclude their presence in this manuscript.

Denote the plant by G(s). Then the issue is to select a precompensator K(s) in such a way that G(s) K(s) is column dominant [1]. In particular, it is desired to select one K(s) so that column dominance is maintained over all five nominal fuel flow conditions.

3. General CARDIAD Features

If the origin of the CARDIAD plot for a given column is included by all solid circles and excluded by all dashed circles, that column of the system is dominant without further compensation, in as much as the origin represents unity compensation. Thus, the eventual goal of compensation using the CARDIAD plot method is to arrive at a system where all the CARDIAD plots have this feature. If there exists a point on the real axis such that the point is included by all solid circles and excluded by all dashed circles in the CARDIAD plot for a given column, then the choice of the value of this point in the off-diagonal

entry which the CARDIAD plot represents will make the column dominant at all frequencies. If there is no such point the CARDIAD plot describes the range of a frequency dependent off-diagonal entry which will make the column dominant.

CARDIAD plots for two input, two output systems have some interesting features. A circle at a specific frequency in the CARDIAD plot for one column will be solid if and only if the other column is dominant at that frequency. Thus, when a system is dominant at all frequencies, all the circles in the CARDIAD plots will be solid and all will contain the origin. Another interesting feature is the effect of a column switch, that is, multiplication by a matrix with the only non zero elements being ones on the off-diagonal. The effects of such a switching of the inputs are that all the solid circles become dashed, all the dashed circles become solid, and the shapes of the column one and two plots are switched. This fact will be used in the next section to achieve dominance in the various set point models.

4. Design Example

The CARDIAD plots of the five uncompensated models are all very similar in shape. This great similarity suggests that one compensator might be found that will make all of the models column dominant. The uncompensated plots also show that a column switch would make the first column of each of the models dominant at all frequencies without further compensation. Thus, K_1 was chosen to be

$$\begin{matrix} 0 & 1 \\ 1 & 0 \end{matrix}.$$

Figures 1 - 10 are the CARDIAD plots of $G(s)K_1$ for the five models. The repetition of the general shapes of the plots, which is unaffected by the column switch, is very apparent. The plots also show that the first column of each of the models is now dominant. This can be ascertained either by the fact that the origins of the column one plots are included by all solid circles and excluded by all dashed circles or by noting that all of the circles in the column two plots are solid.

To achieve dominance in the second columns of the models, it is clear that some sort of frequency depentent compensation will be necessary because there exist no points on the real axes of the plots which lie inside all of the solid circles. A first choice of a function to fit the paths of the circles could be a simple first order function which traces a semicircle through the complex plane as the frequency varies. However, it is desired that one such function be found that will work on all five of the models; so, a second order compensator will be used to fit better the shape of the circles at the hihger frequencies. Two things that should be noted about the shapes of the circles in the column two plots are that the circles tend to be larger for the lower values of fuel flow and that in general, the center of the lowest frequency (largest) circles moves toward the origin as the nominal value of the fuel flow increases. Since there is more margin for error in the lower nominal value of fuel flow models, a compensator which is fit to a rough average of the five plots and which tends to be closer to the higher nominal value of fuel flow models, might achieve dominance in all five models.

The average value of the center of the lowest frequency circle of the five plots is -9.81. This suggests that designing a compensator to fit the nominal fuel flow of 2.75 model which has as the center of the lowest frequency circle the value of -9.59 might achieve dominance in all of the models. The second order funtion that was chosen is

$$\frac{-.742s - 9.59}{.014s^2 - .998s + 1.}$$

and the next compensator, $K_2(s)$, is

$$K(s) = \begin{matrix} 1 & \dfrac{-.742s - 9.59}{.014s^2 - .998s + 1} \\ 0 & 1 \end{matrix}.$$

Thus, the overall compensation is K(s) given by

$$K(s) = \begin{matrix} 0 & 1 \\ 1 & \dfrac{-.742s - 9.59}{.014s^2 - .998s + 1.} \end{matrix}.$$

Figures 11 - 20 are the CARDIAD plots of G(s)K(s) for the five models. It is clear that they are all dominant at all frequencies since all of the circles are solid and all include the origin. Thus, one compensator has been found which will make all five of the models considered in this paper dominant.

5. Conclusions

Through the use of CARDIAD plots, it has been possible to achieve dominance over a range of operating points of a jet engine simulation. The compensator given above also achieves dominance at all but a very narrow range of frequencies in the model of another operating point. The results suggest two things. First, using the CARDIAD plots as a guide, it could be possible to design a compensator which varies with the nominal value of the fuel flow and achieves global dominance over a wide range of operating points. This is currently being studied. Second, the repetitive shape of the CARDIAD plots over the range of operating points suggests that the CARDIAD plot might be a useful tool in the classification of operating points with regard to interaction. Such a feature could be quite helpful in analysis of which models to use over flight envelopes varying from sea level to high altitude and from low through high thrust.

Acknowledgment

The authors thank R. R. Gejji for his assistance in obtaining the linear models used for these plots.

References

1. H. H. Rosenbrock, Computer Aided Control System Design. London: Academic Press, 1974.

2. R. Michael Schafer, "A Graphical Approach to System Dominance," Technical Report No. 778, Department of Electrical Engineering, University of Notre Dame, March 26, 1977.

3. R. M. Schafer, R. R. Gejji, P. W. Hoppner, W. E. Longenbaker, and M. K. Sain, "Frequency Domain Compensation of a DYNGEN Turbofan Engine Model," Preprints 1977 Joint Automatic Control Conference, Volume Two, pp. 1013-1018.

4. R. Gejji, R. M. Schafer, M. K. Sain, and P. Hoppner, "A Comparison of Frequency Doman Techniques for Jet Engine Control System Design," Proc. 20th Midwest Symposium on Circuits and Systems, Part 2, pp. 680-685, August 1977.

5. R. M. Schafer and M. K. Sain, "A Dynamical Approach to Diagonal Dominance, with Illustrations for a Turbofan Engine Model," Proc. 1977. NEC International Forum on Alternatives for Linear Multivariable Control, October 1977.

6. J. P. Sellers and C. J. Daniele, "DYNGEN - A Program for calculating Steady State and Transient Performance of Turbojet and Turbofan Engines," NASA TN D-7901, April 1975.

7. L. Geyser, "DYGABCD - A Program for Calculating Linear A, B, C, and D Matrices from a Nonlinear Dynamic Engine Simulator," private Communication.

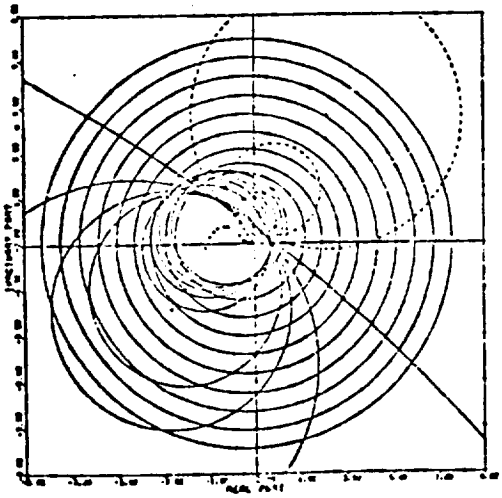

Fig. 1. WFB=2.145, $G(s)K_1$, Column 1.

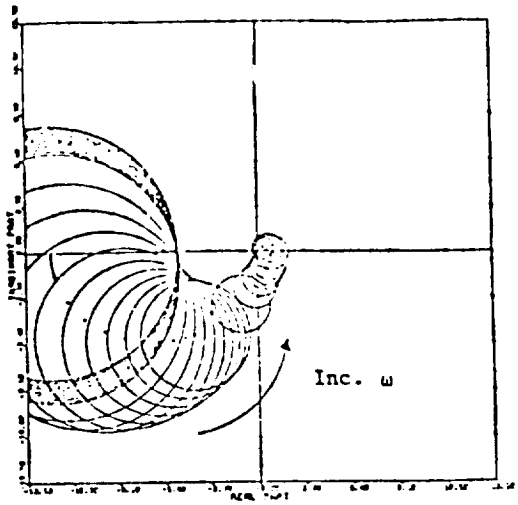

Fig. 2. WFB=2.145, $G(s)K_1$, Column 2.

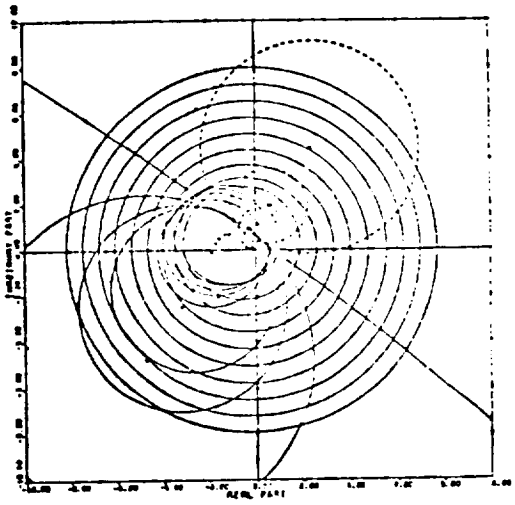

Fig. 3. WFB=2.31, $G(s)K_1$, Column 1.

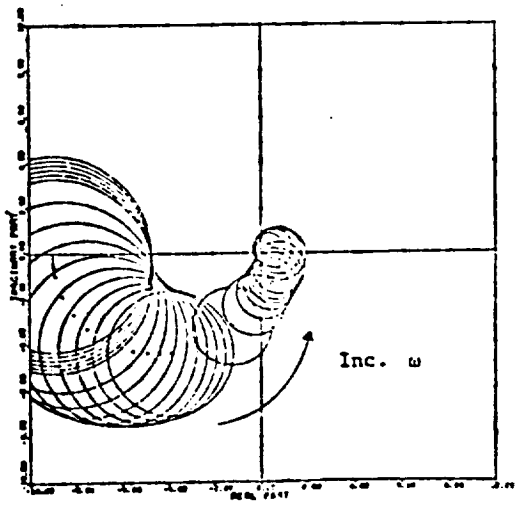

Fig. 4. WFB=2.31, $G(s)K_1$, Column 2.

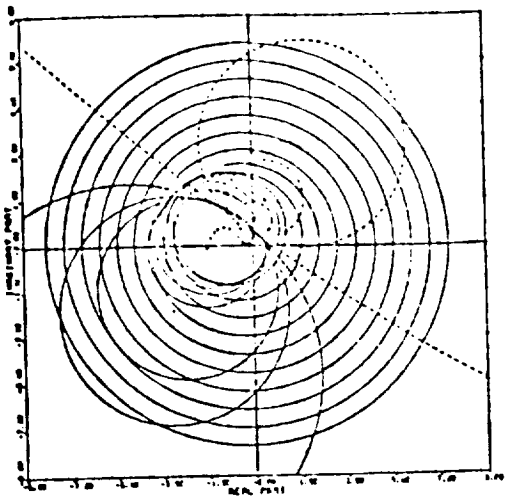

Fig. 5. WFB=2.475, $G(s)K_1$, Column 1.

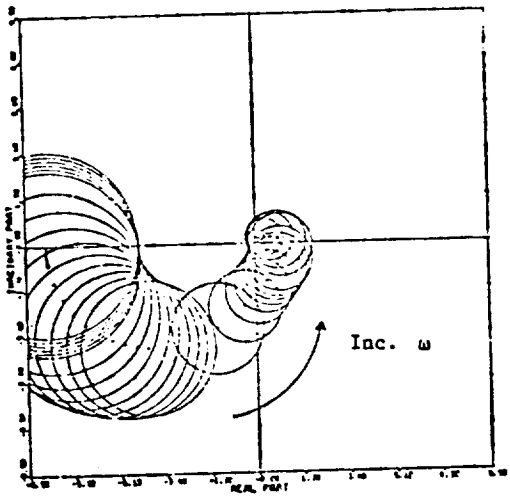

Fig. 6. WFB=2.475, $G(s)K_1$, Column 2.

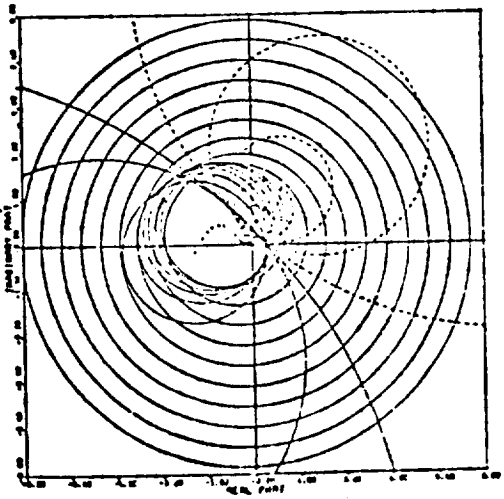

Fig. 7. WFB=2.64, $G(s)K_1$, Column 1.

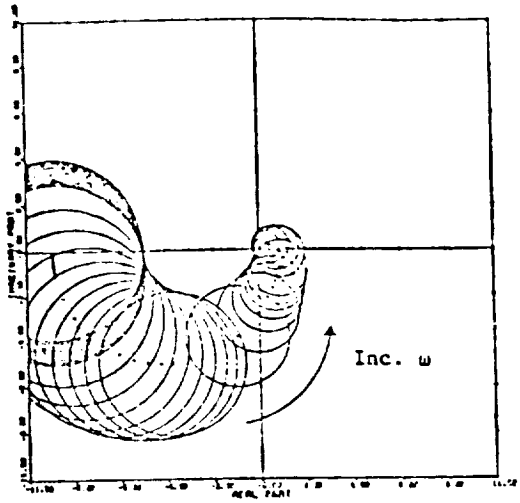

Fig. 8. WFB=2.64, $G(s)K_1$, Column 2.

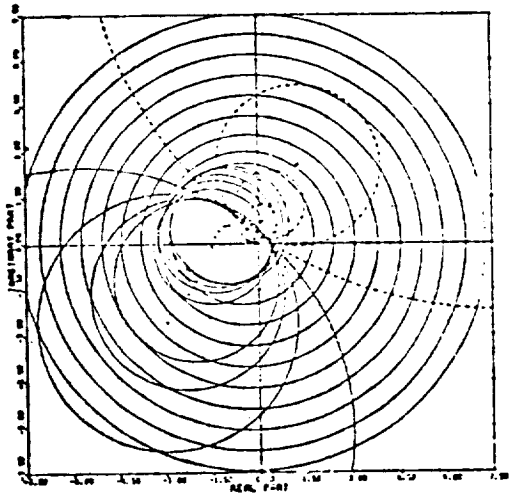

Fig. 9. WFB=2.75, $G(s)K_1$, Column 1.

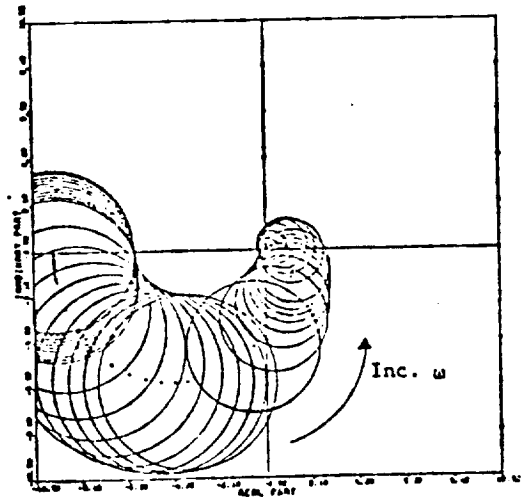

Fig. 10. WFB=2.75, $G(s)K_1$, Column 2.

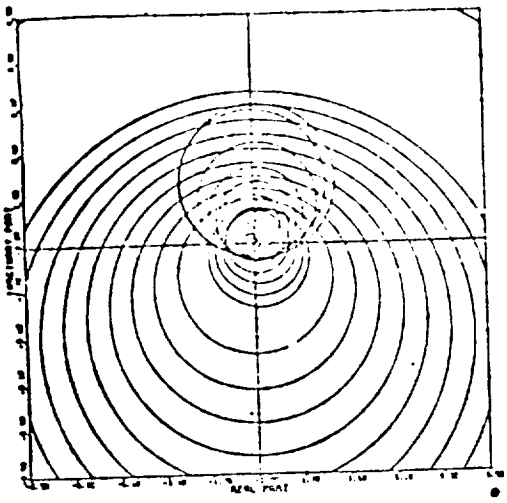

Fig. 11. WFB=2.145, G(s)K(s), Column 1.

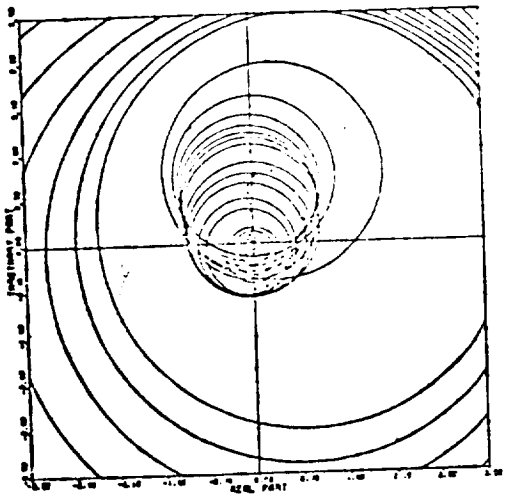

Fig. 12. WFB=2.145, G(s)K(s), Column 2.

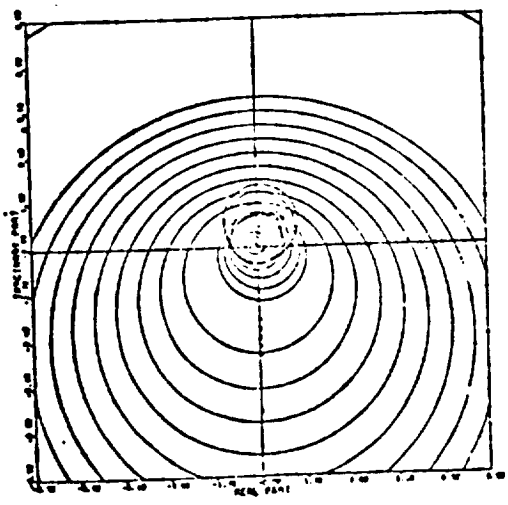

Fig. 13. WFB=2.31, G(s)K(s), Column 1.

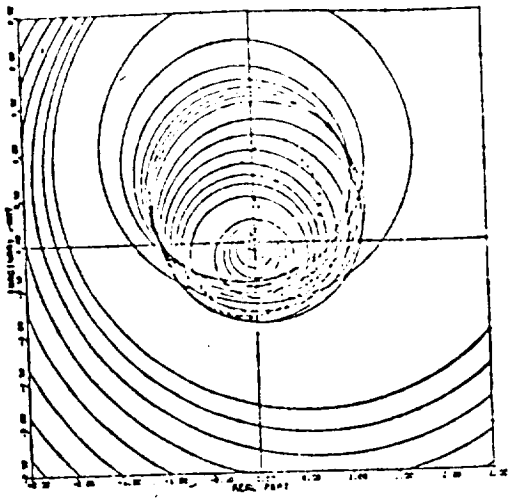

Fig. 14. WFB=2.31, G(s)K(s), Column 2.

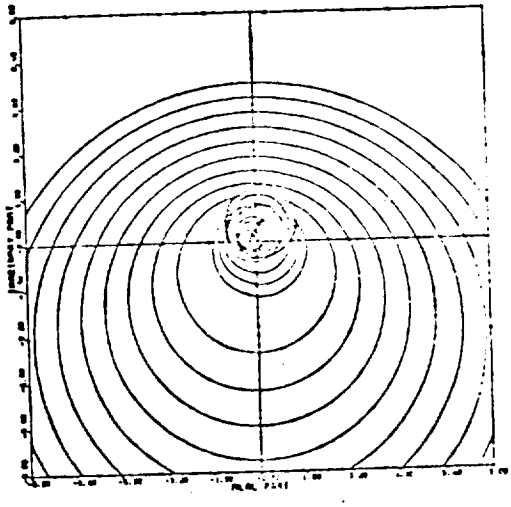

Fig. 15. WFB=2.475, G(s)K(s), Column 1.

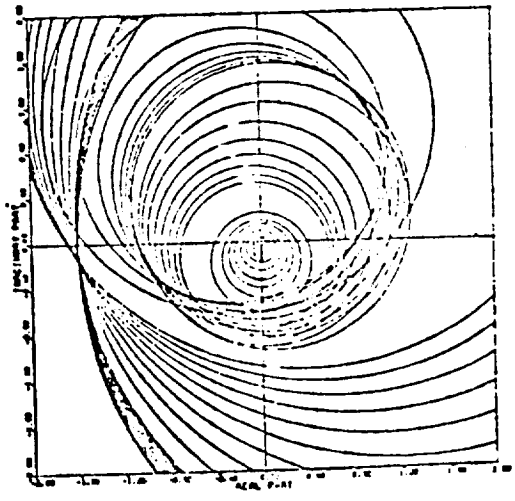

Fig. 16. WFB=2.475, G(s)K(s) Column 2.

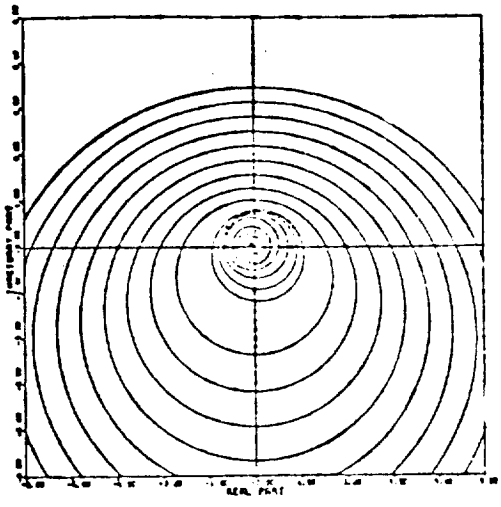

Fig. 17. WFB=2.64, G(s)K(s), Column 1.

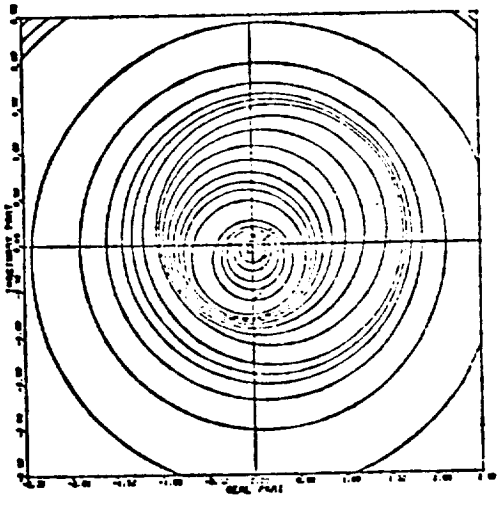

Fig. 18. WFB=2.64, G(s)K(s), Column 2.

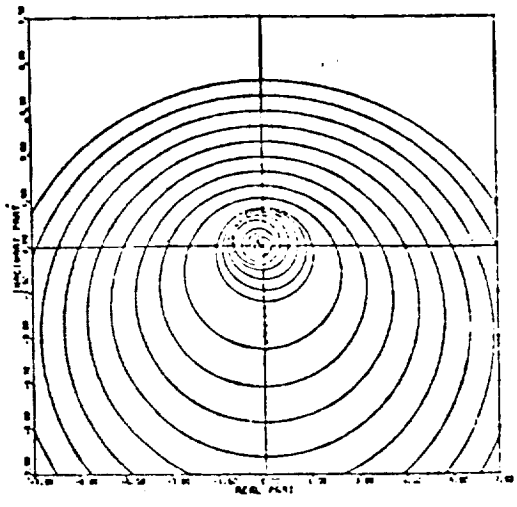

Fig. 19. WFB=2.75, G(s)K(s), Column 1.

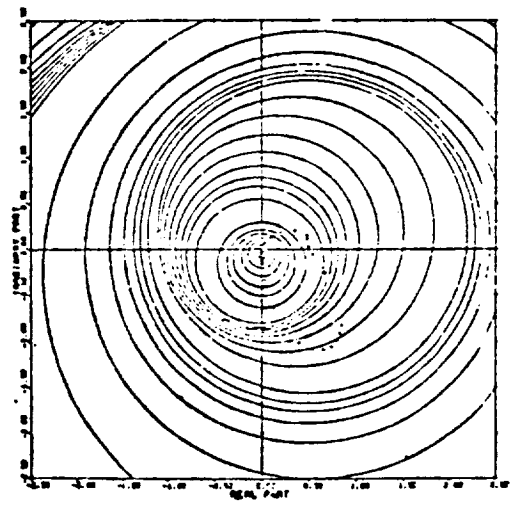

Fig. 20. WFB=2.75, G(s)K(s), Column 2.

ALTERNATIVES FOR LINEAR MULTIVARIABLE CONTROL

with TURBOFAN ENGINE THEME PROBLEM

MICHAEL K. SAIN
Department of Electrical Engineering
University of Notre Dame

JOSEPH L. PECZKOWSKI
Energy Controls Division
The Bendix Corporation

JAMES L. MELSA
Department of Electrical Engineering
University of Notre Dame

EDITORS

NATIONAL ENGINEERING CONSORTIUM, INC., CHICAGO, 1978

CONTENTS

I/0

1.2

THE THEME PROBLEM

Michael K. Sain

Department of Electrical Engineering
University of Notre Dame
Notre Dame, Indiana

Foreword

From the outset, the use of a Theme Problem has posed certain challenges. Authors from academic backgrounds tend to be in need of highly detailed information about plant and specifications, while workers in industry and laboratories must often be satisfied with indirect information and sometimes with none at all. We have tried to arrange a reasonable compromise somewhere on middle ground. Our decision to select a problem related to a realistic modern turbofan engine had special ramifications of its own, not the least of which was the fact that certain types of additional data were precluded for proprietary or other reasons. We believed all along that the advantages of data realism outweigh the disadvantages of incomplete information.

The chronology of the Theme Problem begins in late summer, 1976, during discussions with J. L. Melsa. Subsequent contacts with several potential Forum participants led to the drafting of a Tentative Theme Problem Description, which was sent out to various workers for critique in early 1977. When evaluations were in hand, a Theme Problem Description was prepared on March 1, 1977 and became the working document for authors preparing papers for the meeting. Communications with several additional researchers established the need for minor modifications and clarifications, which were decided at a committee meeting held during the Joint Automatic Control Conference at San Francisco in June, 1977. These decisions formed the basis for an addition Theme Problem Memorandum mailed to all participants on July 18, 1977.

All these adjustments are included in the Final Theme Problem Description, which is included here.

Any clarity which may be present in this final problem description is due in large part to the valued advice of many colleagues, among whom I must especially mention R. L. DeHoff, R. D. Hackney, B. Lehtinen, W. C. Merrill, J. L. Peczkowski, C. A. Skira, and H. A. Spang, III. Credit for any and all obscurities must, of necessity, accrue to the author.

ABSTRACT

The theme design problem should serve the Forum goals in at least three ways. First, it should help to unify the presentations and, thus, make them more useful for group study after publication. Second, it should help to make the Forum relevant to the present-day design world by focusing upon a real system of considerable current interest. Third, it should help to delineate the state of computational readiness of the various design viewpoints, and so help to point out where additional numerical researches would be useful.

Caveat: It is important to recognize the generally positive intent involved with the use of this problem. It is not intended that the theme problem usage degenerate into a computational contest.

1. INTRODUCTION

A very important developing area for linear multivariable control has arisen because of recent increases in the complexity of aircraft turbine engines. Engines in use today have, essentially, the one control variable of fuel flow, though some make use of a variable nozzle area which is not unlike the iris diaphragm that controls aperture settings in a camera. Engines in the not-so-distant future can be expected to permit control of vanes in the stator portions of the various compressor stages. Further down the development line are engines with enough variable geometry to receive the informal designation of "rubber engines" by research engineers in the industry.

It is widely accepted that the older, workhorse, hydromechanical control methods are not equal to these new tasks and that they will, therefore, give way to electronic digital control. The entrance of the digital computer opens up vast numbers of new design possibilities, which are now beginning to receive increased attention in the industry. The central role played by the aircraft turbine engines in civil and military aviation makes clear the economic import of these trends. It would be hard to select a more timely theme design example for comparison of linear control alternatives than the jet engine.

In the United States, a joint study is now underway on the Pratt & Whitney F100-PW-100 afterburning turbofan, a low-bypass-ratio, twin-spool, axial-flow engine. Sponsored by the Air Force and by the National Aeronautics and Space Administration, this study focuses on the linear quadratic regulator theory, applied at multiple operating points in the control regime.

One effect of the theme usage of such a plant in the NEC Forum should be a broadening of the design discussion to include other design viewpoints as well.

2. PLANT

The numerical model of the jet engine is supplied in (A,B,C,D) form on Attachment 1. For the A and C matrices, note that columns 9-16 are listed below columns 1-8. This model is for zero altitude and for a power lever angle (PLA) of 83 degrees, which is near maximum non-afterburning power. The motivation for choosing this operating point comes from the fact that every engine has to pass through this condition, as, for example, on takeoff. Also supplied is a list of the input, state, and output variables associated with this model. These two pages are taken from the report

R. J. Miller and R. D. Hackney, "F100 Multivariable Control System Models/ Design Criteria," Pratt and Whitney Aircraft Group, United Technologies Corporation, West Palm Beach, Florida, November 1976.

Because a number of the techniques which will be discussed at the Forum have graphical aspects, it is planned to facilitate the inclusion of curves in the publication by limiting the plant to three control inputs. In consultation with numbers of our Theme Problem Advisory Committee, we have selected U_1, U_2, and U_3 as these inputs. Workers who feel an absolute necessity to use all five inputs are welcome to do so; however, we would ask that in such a case they provide a comparison of the effect of using five inputs over and above that of using only three. This request is designed to increase the comparability of the various design results.

Actuator information for the three control inputs is given in Attachment 2. Also provided is information associated with the actuation of U_4, if that input is used in addition to U_1, U_2, and U_3. Finally, should U_5 be used in addition to U_1, U_2, and U_3, a servo time constant of 0.02 sec. can be assumed for actuation. Various rate limits on the actuators can be noted, as in Table A.

Table A
Actuator Rate Limits

U_1	15,800	(lb/hr)/sec.
U_2	3.6	Ft^2/sec.
U_3	48	Deg/sec.
U_4	40	Deg/sec.

The actuators have some limits, also, which will be mentioned here. On U_3, it may be assumed that the limit is $\pm$ 6°. On U_2, a limit arises because the nozzle area is pretty well down to its minimum at this operating point; the limit is assumed to be about 1 square feet in that direction.

The Theme Problem models are in absolute, unnormalized form, without any mention of the set point values. This makes it difficult to size inputs. The committee worked out a proposal to supply "ballpark" set point values so that the model could be normalized. Unfortunately, it was not possible to obtain even such approximate information.

A consequence of this fact is that the absolute rate limits of Table A have meaning only in relationship to the size of reference commands assumed. Because we are unable to supply the suggested reference command, the effect of actuator rate limits can be treated only hypothetically; and we have to leave the issue of whether to do this, and how to do this, in the hands of the authors.

Turning now to the sensed variables, we have available X_1, X_2, X_3, X_5, and (X_{12} + X_{13}), the last of which is denoted FT1T for "fan turbine inlet temperature." Sensor time constants in seconds are listed in Table B.

Table B

Sensor Time Constants

X_1	0.03
X_2	0.05
X_3	0.05
X_5	0.05

Sensing of FTIT is a bit more elaborate and is indicated on Attachment 3.

3. ENVIRONMENT

Measurement noise is on the order of 1%; and state noise is negligible. Therefore it is not planned to supply any noise data. Authors wishing to make noise studies must make their own assumptions. This is not unrealistic for the present stage of discussion. Though some techniques may well make use of observers or dynamical output feedback, no formal stress on filters is anticipated. The Forum, then, is visualized primarily as a control meeting, although contributed papers in the stochastic area will be accepted if they contribute to the Forum theme.

Practice in the industry involves the use of multiple linear models at various operating points from sea level to high altitude and from low to high thrust. As operation transitions from the neighborhood of one operating point to the neighborhood of another, these models change in consonance with some physical variable. Parameter variation is, therefore, an aspect of design.

But publicly available neighboring linear models are not near enough to the Theme Problem model to provide meaningful data on parametric variation. This fact, combined with lack of set point information, led the committee to suggest a 5% change in eigenvalues as one, hopefully useful, measure of such variation. Because normalization of the model is a similarity transformation, this characterization is independent of set point.

4. REDUCED ORDER MODELS

Approximate eigenvalues of the Theme Problem plant are -577, -176, -59.2, -50.7, -47.1, -38.7, $-21.3 \pm i1.822$, $-17.3 \pm i4.78$, -19.0, $-6.71 \pm i1.31$, -2.62, -1.91, -.648. It is the nature of the jet engine control problem that these can usually be well identified with physical variables. For example, -.648 associates with X_{10}, -1.91 associates with X_{13}, -2.62 associates with X_2, and so forth. X_1 is related to the eigenvalue pair $-6.71 \pm i1.31$. This type of information can be deduced from a study of the eigenvectors corresponding to a particular eigenvalue. It can be expected that actuator modes, such as that involved with fuel flow, will enter into this list. Some discussion on this point can be found in R. L. DeHoff and W. E. Hall, Jr., "Design of a Multivariable Controller for an Advanced Turbofan Engine," Proceedings 1976 IEEE Conference on Decision and Control, page 1002.

In the interest of offering some assistance to authors who might be having computational difficulty with the full size problem, the following reduced model has been made available by Dr. DeHoff of Systems Control, Inc. (Vt.). It is a model which neglects sensor dynamics, augments the plant by the dominant actuator dynamics, and then reduces to fifth order. The resulting five states are

$\hat{X}_1$ = Fan Speed (rpm)

$\hat{X}_2$ = Compressor Speed (rpm)

$\hat{X}_3$ = "Augmentor" Pressure (psia)

$\hat{X}_4$ = Fuel Flow (lb./hr.)

$\hat{X}_5$ = Burner Pressure (psia)

Note that the "Augmentor" Pressure $\hat{X}_3$ is not to be identified with X_5; the quantities are not defined at the same physical location. Note also that $\hat{X}_5$ was not one of the original states.

Remark: The U_3 Actuator diagram shows a Servo System gain of 2.4. It has come to our attention that a more realistic number for this gain would be about 12.0. The effect of this gain change is to take the dominant CIVV position actuator eignevalue from a location of high dominance in the overall plant-actuator system to a location of considerably less dominance. It is not necessary for authors to make this change if they have already completed their calculations, inasmuch as the 2.4 gain apparently is one of those "glitches" which crept in an uninvited manner. Some authors may choose to compare the effect of the gain 12.0 with the gain 2.4, if time and space permits. We have included this remark here so that the reduced order model, which has the same controls and outputs as the full size system, may be more understandable.

A (5 x 5)

-.3245E+01	-.2158E+01	-.9155E+03	.5731E+00	.1342E+03
.1642E+01	-.5941E+01	-.2816E+03	.1897E+00	.5705E+02
.1685E-01	-.2554E-01	-.1003E+02	.7994E-02	.5807E+00
.0000	.0000	.0000	-.1000E+02	.0000
-.2163E+01	.6862E+01	.7405E+03	.1195E+01	-.1715E+03

B (5 x 5)

.1432E-01	-.3553E+03	-.9906E+02	-.1549E+02	.2220E+05
.2871E+00	.7286E+03	.2514E+02	-.6487E+02	.8122E+04
-.2469E-02	-.1030E+03	.6333E+00	-.3213E+00	-.7418E+02
.1000E+02	.0000	.0000	.0000	.0000
-.1311E+00	.3295E+03	-.2500E+02	.6257E+02	-.6445E+05

C (5 x 5)

.1662E+01	-.1768E+01	.7999E+02	-.1890E+00	.3771E+02
.1383E-01	.3142E-05	-.1060E-01	.1289E-03	-.1839E-06
.1694E+00	-.1129E+00	-.4959E+01	.7386E-01	-.1835E+00
.7590E-04	.3269E-05	-.1477E-01	.2284E-05	.4315E-04
-.4859E-04	.1381E-03	.1140E-01	.1951E-04	-.2688E-02

D (5 x 5)

.1302E+00	.1992E+03	.4802E+02	-.1503E+02	.1083E+05
.1449E-06	.3395E+00	.6806E+00	.2812E-03	.3204E-03
.2967E-01	.7927E+02	.2567E+01	-.7631E+00	.2066E+04
.1046E-05	-.7720E-02	-.5814E-02	.1157E-03	.6605E-01
-.8395E-05	-.7897E-02	-.6841E-03	-.9643E-03	-.2815E+00

5. SPECIFICATIONS

The overall viewpoint of the controller is quite simple. The pilot has one lever, which we might intuitively call the throttle and which sets what is called in the industry the "power lever angle." Basically, the pilot increases the lever angle to obtain more thrust. All the other variables must be controlled so as to achieve the new thrust quickly, but without overshoot and without violating some important physical considerations. An example of one of these is the temperature at the inlet to the "high" turbine just aft of the burner. This temperature is ordinarily scheduled very near its maximum safe value, and temperature increases are not welcome because the turbine elements are thin, respond very fast, and can be permanently damaged or create a need for more frequent engine overhauls. Another example of a constraint is the various undesirable stall conditions in the compressor.

This problem comes down to us in the following form. Assuming a step change in power lever angle, we want to move the engine to a slightly different operating point in the above described acceptable dynamic fashion. The power lever angle change is converted by a master engine scheduler into a reference input for our linearized feedback model. The nature of this reference input is not highly specific. Step inputs are commonly studied. It is not likely that highly detailed information about these references will be available, but we can try to firm up any particular issues which may be crucial to one paper or another. The exact nature of these references gets one into the exact nature of the schedulers. It does not seem too productive in a linear meeting to go very far into such "global" issues. If greater reference variety is needed, it can probably be safely assumed. It would be good, however, if each paper tried to discuss at least the reference step.

For purposes of design, we can group the variables into two families. Y_1, Y_2, X_1, and X_2 are desired to respond fast without overshoot. Y_4 should not decrease more than $-.05$; Y_5 should not decrease more than .15.

Remark: The decrease limits on Y_4 and Y_5 are to be regarded in the same spirit as the U_3 actuator gain change in the preceding section. If calculations are complete, there is no requirement to incorporate it. Some authors may wish to study its effect, however.

6. VIEWPOINT

We believe that the theme problem should appear in each presentation as the major, and probably the only, illustration of the particular design methodology being described. We visualize each paper as an exposition of design viewpoint, with jet engine illustration. We do not visualize the paper as an exposition of jet engine design. In other words, the theme problem will be an apparent thread through the fabric of the Forum, but the pattern of the fabric will be set by the various linear control alternatives as entities in themselves. Put in yet another way, the Forum is on "Alternatives for Linear Multivariable Control" and is not upon "Various Approaches to Jet Engine Control."

F100 MODEL ALT=0.0 PLA=83

THE A MATRIX

-4.328	.1714	5.376	401.6	-724.6	-1.933	1.020	-.9820
-.4402	-5.643	127.5	-233.5	-434.3	26.59	2.040	-2.592
1.038	6.073	-165.0	-4.483	1049.	-82.45	-5.314	5.097
.5304	-.1086	131.3	-578.3	102.0	-9.240	-1.146	-2.408
.8476E-02	-.1563E-01	.5602E-01	1.573	-10.05	.1952	-.8804E-02	-.2110E-01
.8350	-.1249E-01	-.3567E-01	-.6074	37.65	-19.79	-.1813	-.2962E-01
.6768	-.1264E-01	-.9683E-01	-.3567	80.24	-.8239E-01	-20.47	-.3928E-01
-.9696E-01	.8666	16.87	1.051	-102.3	29.66	.5943	-19.97
-.8785E-02	-.1636E-01	.1847	.2169	-8.420	.7003	.5666E-01	6.623
-.1298E-03	-.2430E-03	.2718E-02	.3214E-02	-.1246	.1039E-01	.8395E-03	.9812E-01
-1.207	-6.717	26.26	12.49	-1269.	103.0	7.480	36.84
-.2730E-01	-.4539	-52.72	198.8	-28.09	2.243	.1794	9.750
-.1206E-02	-.2017E-01	-2.343	8.835	-1.248	.9975E-01	.8059E-02	.4333
-.1613	-.2469	-24.05	23.38	146.3	1.638	.1385	4.486
-.1244E-01	.3020E-01	-.1198	-.4821E-01	5.675	-.4525	19.81	.1249
-1.653	1.831	-3.822	113.4	341.4	-27.34	-2.040	-.6166
.9990	1.521	-4.062	9.567	10.08	-.6017	-.1312	.9602E-01
11.32	10.90	-4.071	-.5739E-01	-.6063	-.7488E-01	-.5936	-.9602E-01
-.9389E-02	.1352	5.638	.2246E-01	.1797	.2407E-01	1.100	.2743E-01
-3.081	-4.529	5.707	-.2346	-2.111	-.2460	-.4686	-.3223
.2090E-02	-.5256E-01	-.4077E-01	-.9182E-02	-.8178E-01	.3428E-01	.4995E-02	-.1256E-01
-.1953E-01	-.1622	-.6439E-02	-.2346E-01	-.2201	-.2514E-01	-.3749E-02	-.3361E-01
.1878E-01	-.2129	-.9337E-02	-.3144E-01	-.2919	-.3370E-01	.8873E-01	-.4458E-01
.2253E-01	.1791	.8371E-02	.2645E-01	.2560	.2835E-01	-.3749E-01	.3635E-01
-49.99	.6760E-01	39.46	.4991E-02	.8983E-01	.5349E-02	.0	.1372E-01
-.6666	-.6657	.5847	.6654E-04	.1347E-02	.7131E-04	.0	.2057E-03
.2854	2.332	-47.65	.3406	3.065	.3624	-.4343	.4681
-9.627	-9.557	38.48	-50.01	.1011	.1203E-01	-.4686E-01	.1715E-01
-.4278	-.4245	1.710	-2.000	-1.996	.5349E-03	-.1999E-02	.7544E-03
-4.414	-4.354	17.66	-3.113	-3.018	-19.77	-.4999E-01	.1509E-01
-.1127E-02	-.6760E-02	.1835E-01	-.9981E-03	-.1347E-01	-.1070E-02	-20.00	-.2057E-02
.5004	-.1437	-2.416	-.1073	-1.078	30.63	19.89	-50.16

THE B MATRIX

-.4570E-01	-451.6	-105.8	-1.506	851.5
.1114	-546.1	-6.575	-107.8	3526.
.2153	1362.	13.46	20.14	-.6777E+05
.3262	208.0	-2.888	-1.653	-269.1
.9948E-02	-98.39	.5069	-.1940	-94.70
.2728E-01	71.62	9.608	-.3160	-184.1
.1716E-01	71.71	8.571	.7989	-515.2
-.7741E-01	-141.2	-.8215	39.74	1376.
.3855E-01	-7.710	-.4371E-01	-.1024	-6684.
.5707E-03	-.1144	-.6359E-03	-.1432E-02	-99.02
5.727	-1745.	-8.940	-17.96	.8898E+05
.1392	-24.30	-.2736	-.3403	-6931.
.6172E-02	-1.082	-.1183E-01	-.1452E-01	-307.7
.6777E-01	16.60	.3980	.2311E-01	-2588.
.1880E-02	9.147	-.8241	.8984E-01	-32.31
.1677	435.8	-89.94	4.900	-295.5

THE C MATRIX

.4866	-.6741	5.392	95.42	24.03	10.52	.8190	-.4492
.1383E-01	.2789E-05	.0	.0	-.1081E-01	-.5545E-04	.4722E-04	.0
.0	.0	.0	.0	.0	.0	.0	.0
.7418E-04	.5496E-05	.4790E-05	.1478E-03	-.1504E-01	-.6503E-04	.8820E-04	.4999E-05
.1538E-04	.1201E-03	-.2579E-02	-.1609E-03	.1618E-01	-.1071E-02	-.9561E-04	-.5503E-05
.5195	.8437	-1.863	.5709E-01	.4815	3.428	2.161	.7681E-01
.0	.0	.0	.0	.0	.0	.0	.0
.0	.0	1.000	.0	.0	.0	.0	.0
.3434E-05	.2727E-04	.1128E-05	.4002E-05	.3673E-04	.4290E-05	-.4958E-05	.5609E-05
-.3732E-05	-.2996E-04	-.1234E-05	-.4380E-05	-.4024E-04	-.4721E-05	.5324E-05	-.6103E-05

THE D MATRIX

-.6777E-01	-420.5	32.97	-1.824	1245.
.1282E-03	.3353	.6804	-.5605E-04	-.1199E-01
.0	.0	.0	.0	.0
.1030E-05	-.1193E-01	-.5806E-02	.6015E-04	.4463E-01
.8109E-05	.2328E-01	.1178E-03	-.5538E-02	-.1039

1. Engine State Variables

X_1 = Fan Speed, SNFAN (N_1) - rpm

X_2 = Compressor Speed, SNCOM (N_2) - rpm

X_3 = Compressor Discharge Pressure, P_{t3} - psia

X_4 = Interturbine Volume Pressure, $P_{t4.5}$ - psia

X_5 = Augmentor Pressure, P_{t7m} - psia

X_6 = Fan Inside Diameter Discharge Temperature, $T_{t2.5h}$ - °R

X_7 = Duct Temperature, $T_{t2.5c}$ - °R

X_8 = Compressor Discharge Temperature, T_{t3} - °R

X_9 = Burner Exit Fast Response Temperature, T_{t4hi} - °R

X_{10} = Burner Exit Slow Response Temperature, T_{t4lo} - °R

X_{11} = Burner Exit Total Temperature, T_{t4} - °R

X_{12} = Fan Turbine Inlet Fast Response Temperature, $T_{t4.5hi}$ - °R

X_{13} = Fan Turbine Inlet Slow Response Temperature, $T_{t4.5lo}$ - °R

X_{14} = Fan Turbine Exit Temperature, T_{t5} - °R

X_{15} = Duct Exit Temperature, T_{t6c} - °R

X_{16} = Duct Exit Temperature, T_{t7m} - °R

2. Engine Inputs

U_1 = Main Burner Fuel Flow, WFMB - lb/hr

U_2 = Nozzle Jet Area, A_j - ft^2

U_3 = Inlet Guide Vane Position, CIVV - deg

U_4 = High Variable Stator Position, RCVV - deg

U_5 = Customer Compressor Bleed Flow, BLC - %

3. Engine Outputs

Y_1 = Engine Net Thrust Level, FN - lb

Y_2 = Total Engine Airflow, WFAN - lb/sec

Y_3 = Turbine Inlet Temperature, T_{t4} - °R

Y_4 = Fan Stall Margin, SMAF

Y_5 = Compressor Stall Margin, SMHC

ATTACHMENT 2

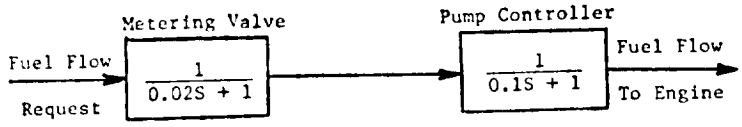

U_1 Actuator

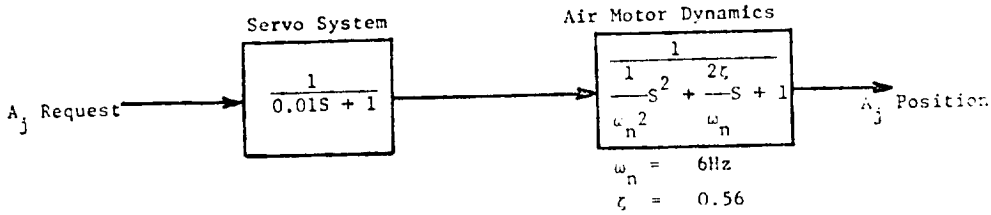

U_2 Actuator

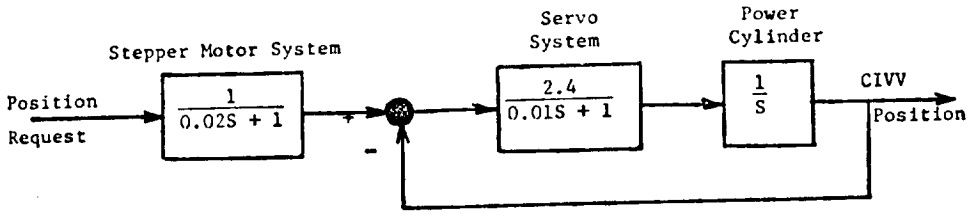

U_3 Actuator

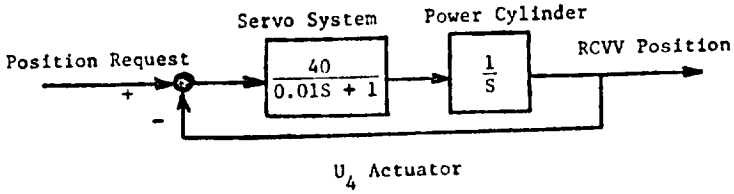

U_4 Actuator

29

ATTACHMENT 3

FTIT Sensor

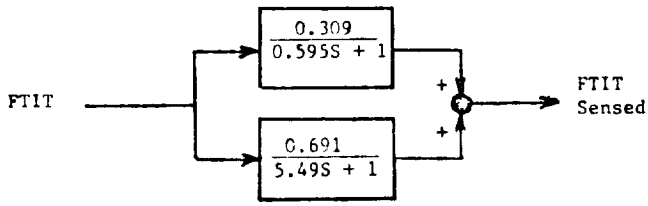

MICHAEL K. SAIN
Department of Electrical Engineering
UNIVERSITY OF NOTRE DAME
NOTRE DAME, INDIANA 46556 USA

13

INPUT COMPENSATION FOR DOMINANCE OF TURBOFAN MODELS

R. M. Schafer and M. K. Sain

Department of Electrical Engineering
University of Notre Dame
Notre Dame, Indiana 46556
U.S.A.

ABSTRACT

The determinant of return difference establishes a crucial link between open and closed loop characteristic polynomials in multivariable feedback control systems. As a result, Nyquist constructions on this determinant carry important design information. One way to extract this information is by achieving diagonal dominance. This paper presents a method which uses dynamical input compensation to achieve column dominance. Application to the Theme Problem is included.

1. INTRODUCTION

Recent advances in the generalized Nyquist theory for linear multivariable feedback control systems have brought about very substantial new opportunities for research in the area of frequency domain control design. Most of these advances are predicated upon the relationship between closed loop and open loop characteristic polynomials--as embodied in the determinant of return difference. Features of the Nyquist diagram of this determinant are important aids to control system design.

It is apparent that a diagonal return difference will decompose the return difference determinant into a product of its diagonal elements, thus reducing a multivariable problem to classical single-input, single-output form. Less apparent, but of much greater practical significance is the fact that an approximately diagonal return difference can have essentially the same reducing effect on a multivariable problem, when regarded from a generalized Nyquist viewpoint. The best known of these approximately diagonal conditions has come to be described as diagonal dominance. A productive design strategy can be mounted, therefore, in two steps. First, achieve diagonal dominance; second, apply classical single-input, single-output techniques [1].

Unfortunately, methods to attain diagonal dominance have been rather slow to advance. For the most part, they have been restricted to the selection of constant real compensators, the entries of which are typically obtained by procedures of optimization that do little to preserve some of the classical advantages, such as insight, afforded by the frequency domain approach. Much work needs yet to be done on the theory of attaining diagonal dominance by use of frequency dependent, dynamical compensation.

This paper considers the application to the Theme Problem of a useful new design aid called the CARDIAD Plot. In its present form, this method deals with the design of a dynamic precompensator for the plant, in such a way that column dominance is achieved. An important feature of the approach is the enhancement of designer insight toward the coupling present in a plant.

Section 2 introduces the CARDIAD method for two-input, two-output plants, and Section 3 provides an illustration of certain basic features of the method, in the context of a jet engine plant related to the Theme Problem. Section 4 gives a generalization of the idea to three inputs and three outputs, and Section 5 applies these results to the Theme Problem. Conclusions appear in Section 6.

2. GRAPHICAL APPROACH

The i^{th} column of a matrix $Z(s)$ is said to be dominant if

$$\left|z_{ii}(s)\right| - \sum_{\substack{j=1 \\ j\neq i}}^{n} \left|z_{ji}(s)\right| > 0 \tag{1}$$

for all s on a Nyquist contour D. A similar definition can be made for row dominance.

For a two-input, two-output system, Eq. (1) can be equivalently written

$$\left|z_{ii}(s)\right|^2 - \left|z_{ji}(s)\right|^2 > 0 \qquad i \neq j \tag{2}$$

for all s on D.

Consider a two-input, two-output system having only precompensation. The open loop transfer function of the system is

$$Q(s) = G(s)K(s). \tag{3}$$

Let $K(s)$ be restricted to the form

$$K(s) = \begin{bmatrix} 1 & \alpha_2(s) \\ \alpha_1(s) & 1 \end{bmatrix}. \tag{4}$$

Since any matrix having nonzero entries on its main diagonal may be put into this form by multiplication with a diagonal matrix, and since multiplication by a diagonal matrix does not affect dominance, this can be done without essential loss of generality.

Let $G(s)$ be evaluated at a specific frequency ω. Then

$$Q(j\omega) = \begin{bmatrix} r_{11} + i_{11}j & r_{12} + i_{12}j \\ r_{21} + i_{21}j & r_{22} + i_{22}j \end{bmatrix} \begin{bmatrix} 1 & x_2 + y_2j \\ x_1 + y_1j & 1 \end{bmatrix}. \tag{5}$$

Performing the indicated matrix multiplication, the four entries in the matrix $Q(s)\Big|_{s=j\omega}$ are

$$q_{11} = r_{11} + i_{11}j + (r_{12} + i_{12}j)(x_1 + y_1j), \tag{6}$$

$$q_{12} = r_{12} + i_{12}j + (r_{11} + i_{11}j)(x_2 + y_2j), \tag{7}$$

$$q_{21} = r_{21} + i_{21}j + (r_{22} + i_{22}j)(x_1 + y_1j), \tag{8}$$

$$q_{22} = r_{22} + i_{22}j + (r_{21} + i_{21}j)(x_2 + y_2j). \tag{9}$$

From Eq. (2), the first column of $Q(s)\Big|_{s=j\omega}$ will be dominant if

$$\left|q_{11}\right|^2 - \left|q_{21}\right|^2 > 0. \tag{10}$$

Performing the indicated subtraction results in what will be referred to as the dominance inequality for column 1. The form of this inequality is

$$f_1(x_1,y_1) = ax_1^2 + ay_1^2 + 2bx_1 + 2cy_1 + d \quad 0,$$

where the constants are defined as

$$a = r_{12}^2 + i_{12}^2 - r_{22}^2 - i_{22}^2 \tag{11}$$

$$b = r_{11}r_{12} + i_{11}i_{12} - r_{21}r_{22} - i_{21}i_{22}, \tag{12}$$

$$c = r_{12}i_{11} + r_{21}i_{22} - r_{11}i_{12} - r_{22}i_{21}, \tag{13}$$

$$d = r_{11}^2 + i_{11}^2 - r_{21}^2 - i_{21}^2. \tag{14}$$

Note that each constant is composed of complex field elements which come from evaluation of G(s) at a specific frequency ω.

The function $f_1(x_1,y_1)$ is a paraboloid in three-space and is normal to the x_1-y_1 plane. If this paraboloid intersects the x_1-y_1 plane, the intersection will be a circle. Standard maximum-minimum analysis gives that the maximum or minimum of the dominance function occurs at

$$x_1 = -b/a \qquad y_1 = -c/a \tag{15}$$

To determine if the point that was found is a minimum or a maximum, the hessian is formed. If the hessian is negative definite, the point found is a maximum. If the hessian is positive definite, the point found is a minimum. The hessian of the dominance equation for column one is

$$\begin{bmatrix} 2a & 0 \\ 0 & 2a \end{bmatrix} \tag{16}$$

so that the second derivative test reduces to a test on the sign of a.

Proceeding from this analysis, there are four possible cases. The point that was found was a positive maximum, positive minimum, negative maximum, or negative minimum. The two cases that are of interest are the positive maximum and the negative minimum since it has been shown [2] that the other two cases cannot occur. In each of the cases of interest, the positive maximum and the negative minimum, there is an intersection of the x_1-y_1 plane. Recalling that the column will be dominant if $f_1(x_1,y_1)$ is positive, the analysis of the two cases is as follows. In the positive maximum case, the values of x_1 and y_1 which will result in solution of the dominance inequality are those points which lie inside the intersection of $f_1(x_1,y_1)$ and the x_1-y_1 plane, that is the circle which is the solution of $f_1(x_1,y_1) = 0$. In the negative minimum case, the choices of x_1 and y_1 which result in solution of the dominance inequality are those points which lie outside the circle of intersection. Thus, the intersection of the dominance function $f_1(x_1,y_1)$ for column one and the x_1-y_1 plane defines the acceptable range of x_1 and y_1 such that the system will be dominant in the first column at the specific frequency at which the analysis was performed. In like fashion, the second column of the system may be analyzed, and the acceptable choices of x_2 and y_2 may be determined.

If this dominance analysis is repeated over a range of frequencies, and the resulting circles of intersection plotted, a CARDIAD (Complex Acceptability Region for DIAgonal Dominance) Plot is produced. A solid circle is drawn if the acceptable choice of x and y lie inside the circle, and a dashed circle is drawn if the acceptable region is outside the circle of intersection. Associated with each CARDIAD plot is a locus of centers plot, which indicates the centers and labels the frequency of each. Space limitations do not allow the locus of centers plots to be included with the CARDIAD plots in this paper, but they will be mentioned and referenced as necessary.

3. ILLUSTRATION

Figs. 1 and 2 are CARDIAD Plots of a two-input, five-state, two-output model of a jet engine. The model is derived from a jet engine simulator called DYNGEN [3,4] and represents an F-100 turbofan jet engine with a fuel flow of 2.75 Lbm/sec. (full

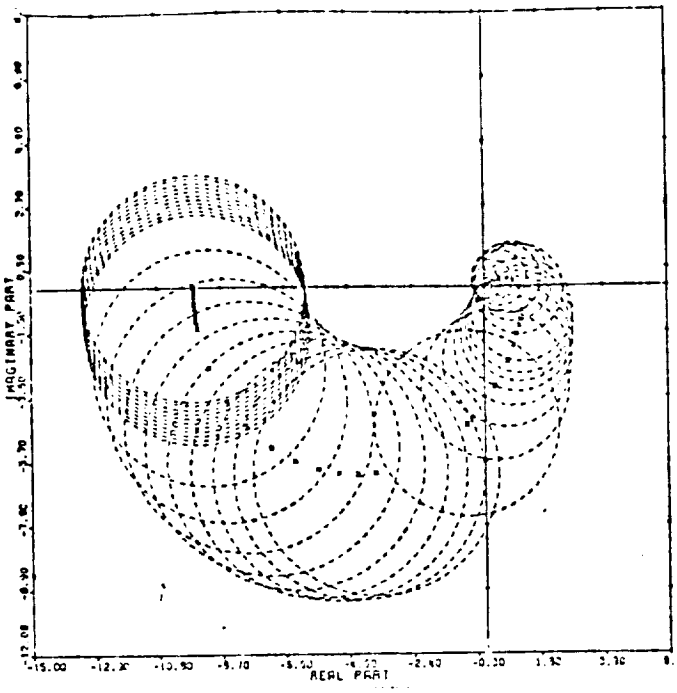

Fig. 1. Column 1, Uncompensated

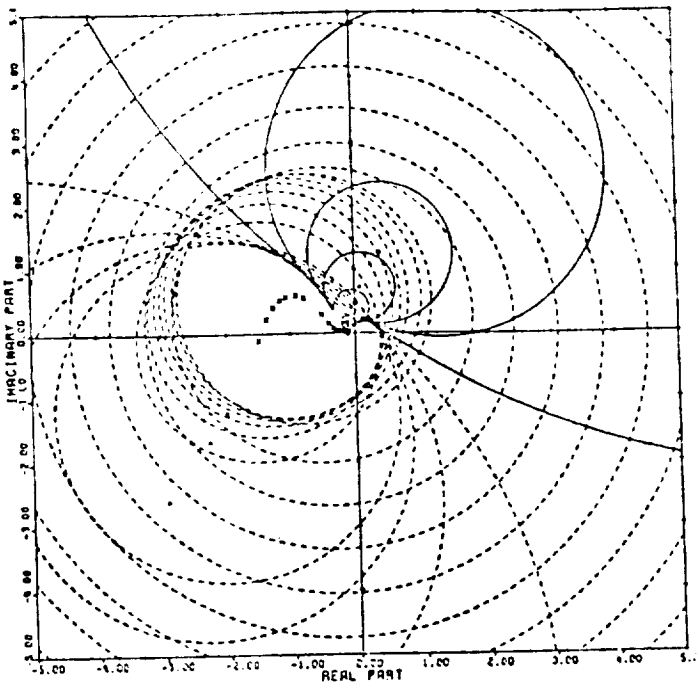

Fig. 2. Column 2, Uncompensated

throttle without afterburners). The inputs are fuel flow and exhaust area and the outputs are thrust and high turbine inlet temperature. This model is one of a series of such models presently being used in a set point study of an F-100 like jet engine.

The analysis of CARDIAD plots proceeds as follows. Recall that, at any given frequency, the acceptable region is outside the circle if the circle is dashed or inside if the circle is solid. The first question of interest is whether the columns of the system are dominant uncompensated. For this to be the case, the origin of the CARDIAD plot must be included in all solid circles and excluded by all dashed circles, since the origin represents identity compensation of the column. This is not the case for either of the two CARDIAD plots of this system. The next question is whether the system can be made dominant by constant real precompensation. If this is the case, there will exist a point on the real axis which lies inside all solid circles and outside all dashed circles. Fig. 1 shows that the first column of the system can be made dominant at all frequencies by the choice of any constant x_1 which lies outside all the dashed circles of the CARDIAD plot. Fig. 2 shows that there exists no constant value that will make the second column of the system dominant at all frequencies. Thus, some form of frequency dependent precompensation will be necessary.

Before proceeding with dominating this system, some of the features of CARDIAD plots should be mentioned. One property is that a circle at a specific frequency in the plot for one column will be solid if the other column is dominant at that frequency and will be dashed if the other column is not dominant. From this fact it follows that the transition from one type of circle to the other in the CARDIAD plot for one column occurs when there is a change in dominance in the other column. Once again considering Figs. 1 and 2, these facts indicate that the second column is not dominant at any frequency since all of the circles in the CARDIAD plot for the first column are dashed and that the first column is dominant at low frequencies (until ω=7) because the circles in the CARDIAD plot for the second column are solid for this and all lower frequencies.

A second feature of the CARDIAD Plot is the effects of a column switch on the plots,

that is, premultiplication by a matrix with the only nonzero entries being off-diagonal 1's. The effects of such a switching of the inputs are that all solid circles become dashed circles, all dashed circles become solid, and the shapes of the column one and two plots are switched. The CARDIAD plots of the system with this type of compensation are given in Figs. 3 and 4. Note that the first column is now dominant at all frequencies without further compensation. This fact can be ascertained

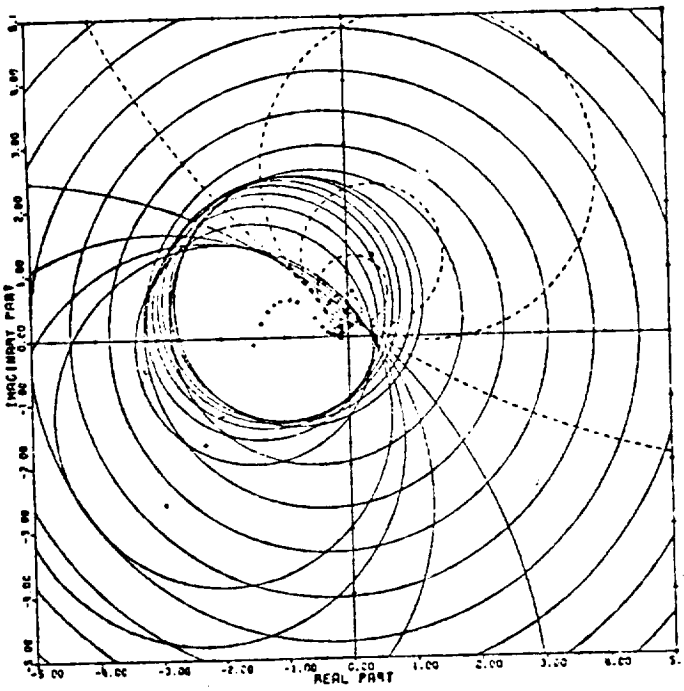

Fig. 3. Column 1, $G(s)*K_1$

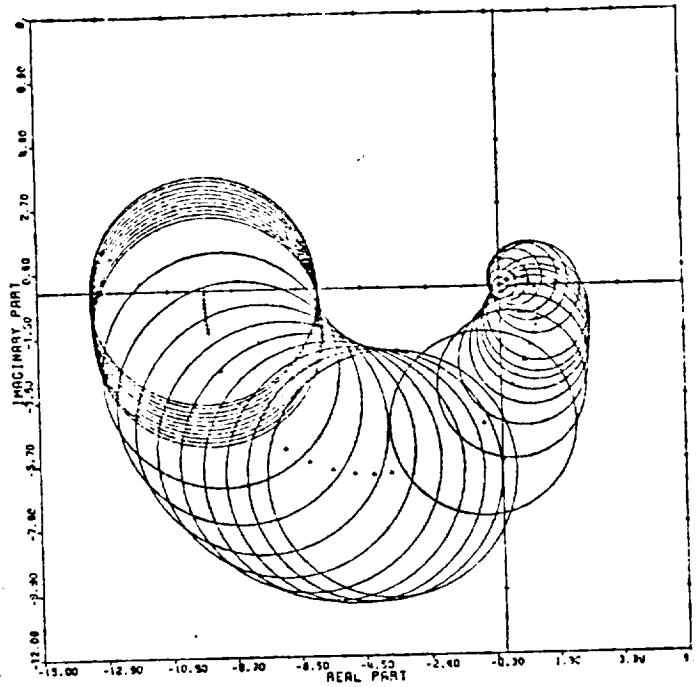

Fig. 4. Column 2, $G(s)*K_1$

either from the fact that the origin in the CARDIAD plot for column one is included by all solid circles and excluded by all dashed circles, or from the fact that all of the circles in the CARDIAD plot for the second column are solid.

Since switching the inputs makes one column dominant uncompensated, it seems a logical first step in compensating for dominance at all frequencies. Thus, K_1 is chosen to be

$$K_1 = \begin{bmatrix} 0 & 1 \\ 1 & 0 \end{bmatrix}. \tag{17}$$

It is still necessary to make the second column of the system dominant. From the CARDIAD plot for this column (Fig. 4), it is apparent that frequency dependent compensation will be necessary since there exists no point in the real axis which is included in all the solid circles of this plot. To design such a compensator, a function of s is fitted to the shape of the CARDIAD plot so that, at any given frequency, the compensator lies inside the solid circle associated with the same frequency in the CARDIAD plot. While it is possible to find a first order compensator that will make this column dominant, a second order compensator has been used because this same compensator could also achieve dominance at four other set points of the model. $K_2(s)$ is the compensator that achieves dominance in the second column of $G(s)*K_1$.

$$K_2(s) = \begin{bmatrix} 1 & \dfrac{-.742s - 9.59}{.014s^2 - .998s + 1.} \\ 0 & 1 \end{bmatrix} \tag{18}$$

The overall compensation is $K_1 * K_2(s) = K(s)$ given below.

$$K(s) = \begin{bmatrix} 0 & 1 \\ 1 & \dfrac{-0.742s - 9.59}{.014s^2 - .998s + 1.} \end{bmatrix} \tag{19}$$

The CARDIAD plots of the system with this compensator are given in Figs. 5 and 6. It is obvious either from the fact that only solid circles appear in the plots or from the fact that all the solid circles include the origin that each column of the system is now dominant at all frequencies.

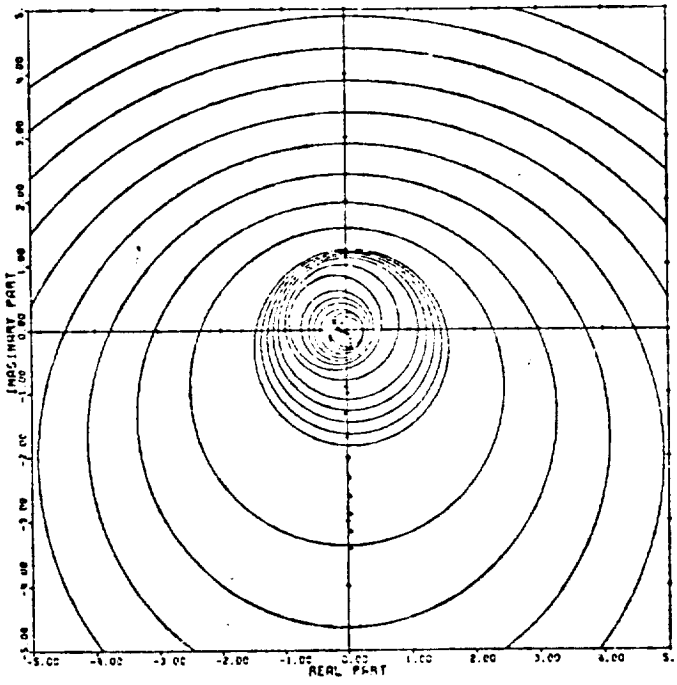

Fig. 5. Column 1, G(s)*K(s)

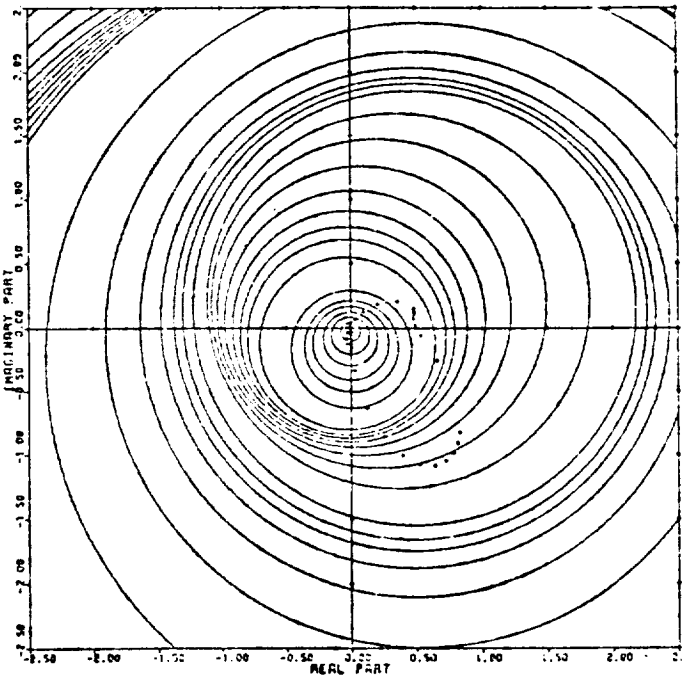

Fig. 6. Column 2, G(s)*K(s)

4. GENERALIZATION

The CARDIAD Plot approach to system dominance in the three-input, three-output case is similar to the approach in the two-input, two-output case.

The actual condition for dominance in the 3 x 3 case is the i^{th} column of a matrix Z(s) will be dominant if

$$|z_{ii}(s)| > \sum_{\substack{j=1 \\ j \neq i}}^{3} |z_{ji}(s)| \tag{20}$$

for all s on D. If both sides of this inequality are squared as in the 2 x 2 case, then an equivalent condition is

$$|z_{ii}(s)|^2 > \left[\sum_{\substack{j=1 \\ j \neq i}}^{3} |z_{ji}(s)| \right]^2 . \tag{21}$$

Using inequality (21), the condition for dominance in, say, the first column is

$$|z_{11}(s)|^2 > |z_{21}(s)|^2 + |z_{31}(s)|^2 + 2|z_{21}(s)||z_{31}(s)|. \tag{22}$$

The cross term produced by squaring adds non-integral power terms to the dominance

inequality for the 3 x 3 system. To circumvent this problem, the last term of inequality (22) is replaced by an upper bound. Since

$$|z_{21}(s)|^2 + |z_{31}(s)|^2 \geq 2|z_{21}(s)||z_{31}(s)| \tag{23}$$

with equality when $|z_{21}(s)| = |z_{31}(s)|$, it is convenient to replace the last term of inequality (22) with the left member of inequality (23). This yields a sufficient condition for dominance. For column 1, the condition is

$$|z_{11}(s)|^2 - 2|z_{21}(s)|^2 - 2|z_{31}(s)|^2 > 0; \tag{24}$$

and the general form is

$$|z_{ii}(s)|^2 - 2\sum_{\substack{j=1 \\ j\neq i}}^{3} |z_{ji}(s)|^2 > 0, \quad i = 1,2,3. \tag{25}$$

From inequality (24), the derivation of the dominance equation for the 3 x 3 case proceeds analogously to the 2 x 2 derivation. The general form of the compensator used in the analysis is

$$K(s) = \begin{bmatrix} 1 & \alpha_{12}(s) & \alpha_{13}(s) \\ \alpha_{21}(s) & 1 & \alpha_{23}(s) \\ \alpha_{31}(s) & \alpha_{32}(s) & 1 \end{bmatrix} \tag{26}$$

where $\alpha_{ij}\Big|_{s=j\omega} = x_{ij} + y_{ij}j$.

Once again, the open loop transfer function matrix G(s) and the general form (26) of the compensator are evaluated at a specific frequency and multiplied to form Q(jω). Then, using inequality (25), a dominance inequality for each of the three columns of Q(jω) can be formed. For example, the first column of Q(jω) will be dominant at the frequency ω if

$$|q_{11}|^2 - 2|q_{21}|^2 - 2|q_{31}|^2 > 0 \tag{27}$$

and the dominance function for column 1 is

$$\begin{aligned} f_1(x_{21},y_{21},x_{31},y_{31}) = {} & c_1 + x_{21}^2 c_2 + y_{21}^2 c_2 + x_{31}^2 c_3 + y_{31}^2 c_3 \\ & + 2x_{21}c_4 + 2y_{21}c_5 + 2x_{31}c_6 + 2y_{31}c_7 + 2x_{21}x_{31}c_8 \\ & + 2y_{21}y_{31}c_8 + 2x_{21}y_{31}c_9 - 2x_{31}y_{21}c_9 > 0 \end{aligned} \tag{28}$$

where the constants c_1-c_9 are functions of G(s) evaluated at the frequency ω. Similar dominance functions can be derived for the other two columns.

The maximum-minimum analysis is performed in two different ways. In the first approach, which will be referred to as the standard analysis, the variables of the dominance inequality are first paired by the entry in the compensator which they represent; and the maximum-minimum analysis is performed on each pair assuming that the other pair is zero. The resulting maximums or minimums are

$$x_{21} = -c_4/c_2; \quad y_{21} = -c_5/c_2,$$

$$x_{31} = -c_6/c_3; \quad y_{31} = -c_7/c_3.$$

The hessian for each pair of variables is diagonal and the second derivative test once again reduces to a sign test.

The dominance analysis is repeated over a range of frequencies and CARDIAD plots result. There is one plot for each off-diagonal entry in the compensator and each entry is plotted assuming that the other off-diagonal entry in the column is zero. Using CARDIAD plots generated by the standard analysis, dominance is achieved by setting one of the off-diagonal entries to zero while the other is chosen as was the case in the 2 x 2 design.

There does not always exist a value in one off-diagonal entry of a column of the compensator that will make the column of the system dominant when the other off-diagonal entry in that column of the compensator is zero. When this occurs, the maximum-minimum analysis is performed by finding the full gradient of the dominance function. The hessian is no longer diagonal but the eigenvalues of the hessian are all negative in Section 5, so the point that is found is a maximum. Design which is performed on plots generated by the full gradient analysis involves both of the off-diagonal entries of a column of the compensator, and functions must be fit to each to achieve dominance.

A new symbol appears in the plots. At any given frequency, unless dominance can be achieved at that frequency with the other entry zero, a small triangle is drawn which shows the best that can be done towards achieving dominance. It should be noted that the triangle can appear in plots generated by either analysis. In the standard analysis CARDIAD plots, if triangles appear in one plot for a column but not the other, dominance can be achieved by keeping the entry in which the triangles appeared zero and using the other entry to achieve dominance. In the full gradient analysis plots, triangles appearing in both plots do not mean that dominance cannot be achieved. Given that one entry in the compensator is chosen exactly on the triangle at a certain frequency, there is a radius of points around the triangle in the other plot that will achieve dominance; but since the size of the circle is a function of how well the other entry is fit to the triangles, such a circle could easily be misleading. Both of these points will be illustrated in the next section.

5. THEME PROBLEM ANALYSIS

The following design is performed on the reduced order model of the theme problem with state feedback. The states being fed back are the two turbine speeds and the pressure P_b. Dominance will be achieved using only precompensation.

The plots for the uncompensated system using the standard dominance analysis showed that the first two columns of the system could be made dominant with one off-diagonal entry in each of the first two columns of the compensator zero. The third column, however, could not be made dominant at any frequency with either one of the off-diagonal entries in the third column zero. Physically, this indicates that the principal effects of all three inputs (fuel flow, exhaust area, and guide vanes) are on the two speed states. To facilitate achieving dominance, a column switch was done by choosing the first compensator to be

$$K_1 = \begin{bmatrix} 0 & 1 & 0 \\ 0 & 0 & 1 \\ 1 & 0 & 0 \end{bmatrix}.$$

Figs. 7-12 are the CARDIAD plots of the system with this compensator and use the standard dominance analysis. The plots for the entries in the first column, Figs. 7 and 8, show that the first column is dominant without further compensation, since the origin of each plot is included inside all solid circles and excluded by all dashed circles. Figs. 9 and 10 are the CARDIAD plots for the second column. Fig. 10, the plot for the 3,2 entry, has several triangles in it, indicating that, at

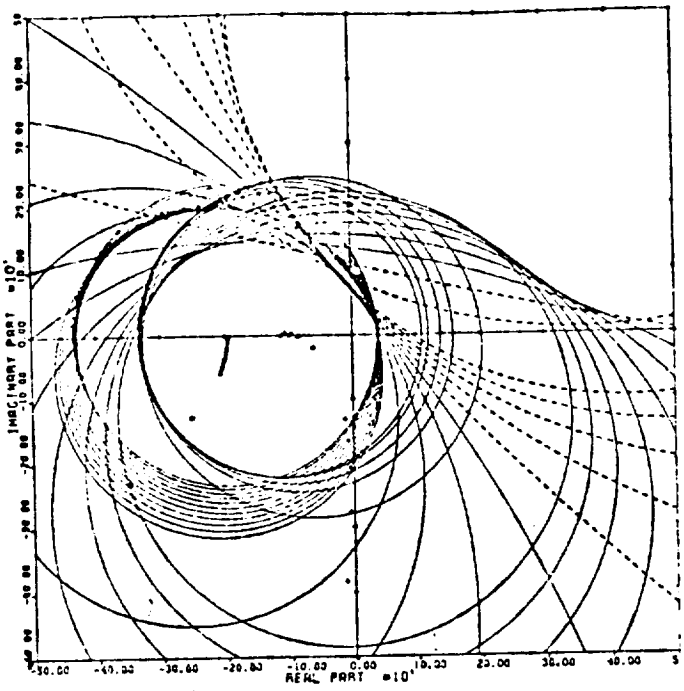

Fig. 7. $G(s)*K_1$, 2,1 Entry

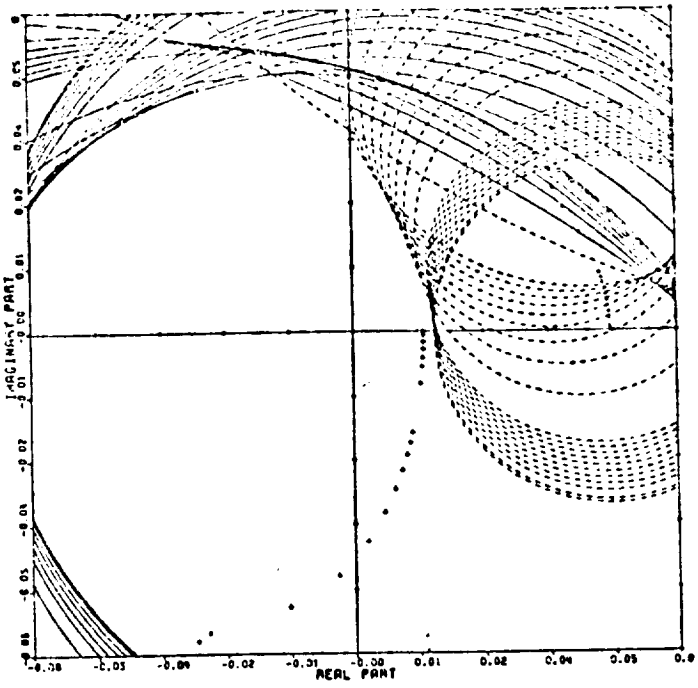

Fig. 8. $G(s)*K_1$, 3,1 Entry

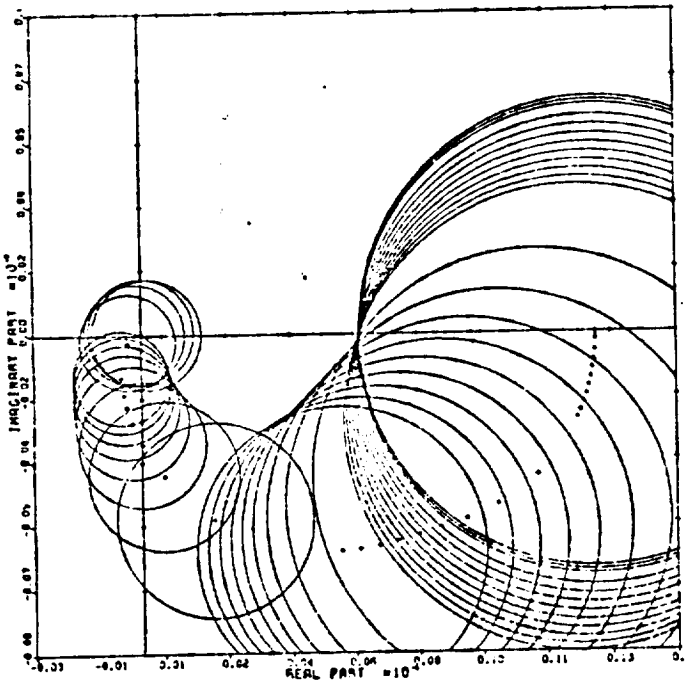

Fig. 9. $G(s)*K_1$, 1,2 Entry

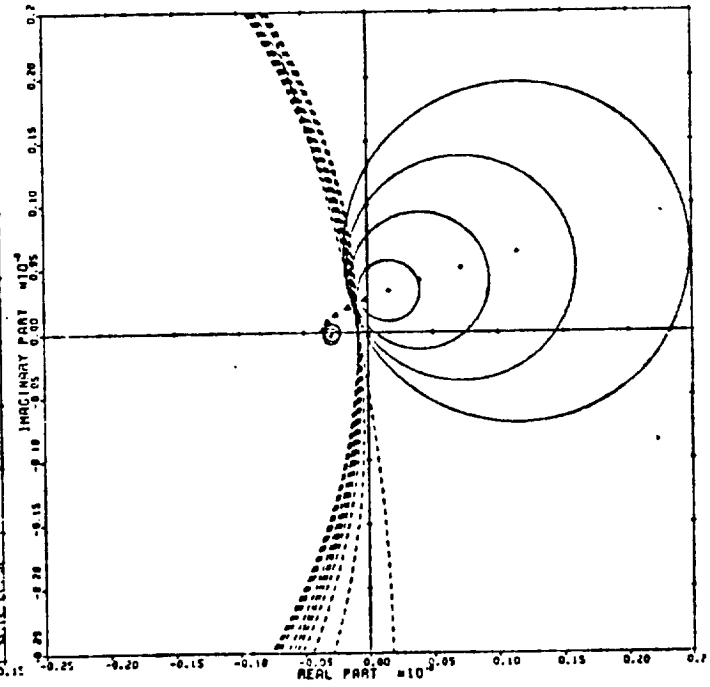

Fig. 10. $G(s)*K_1$, 3,2 Entry

the frequencies where they occur, there is no value in the 3,2 entry that will make the column dominant with the 1,2 element zero. However, Fig. 9 shows that there are no such triangles in the 1,2 entry; so, if a function is fit to the shape of the solid circles of this plot and if the 3,2 entry is kept at zero, dominance can be achieved. Figs. 11 and 12 are the CARDIAD plots for the third column. The 1,3 entry is all triangles and the 2,3 entry has triangles at lower frequencies. Thus, there is no way to make this column of the system dominant with one of the off-

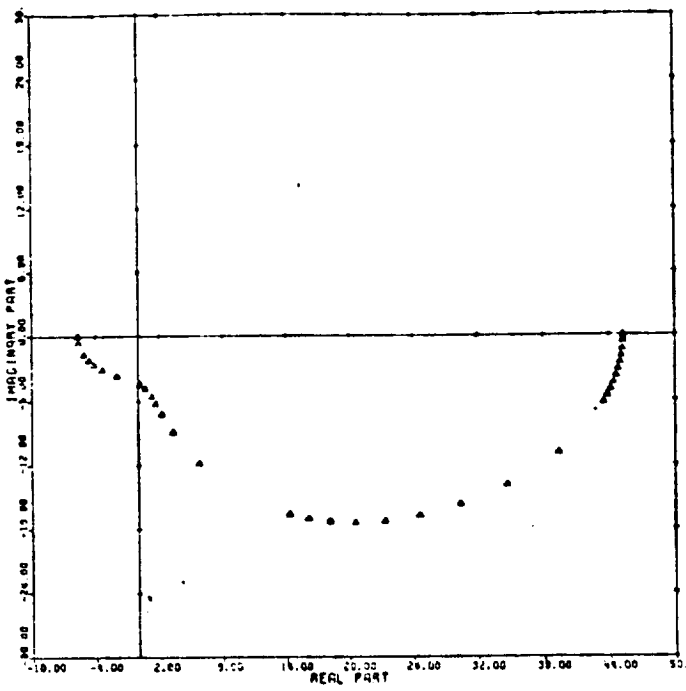

Fig. 11. $G(s)*K_1$, 1,3 Entry

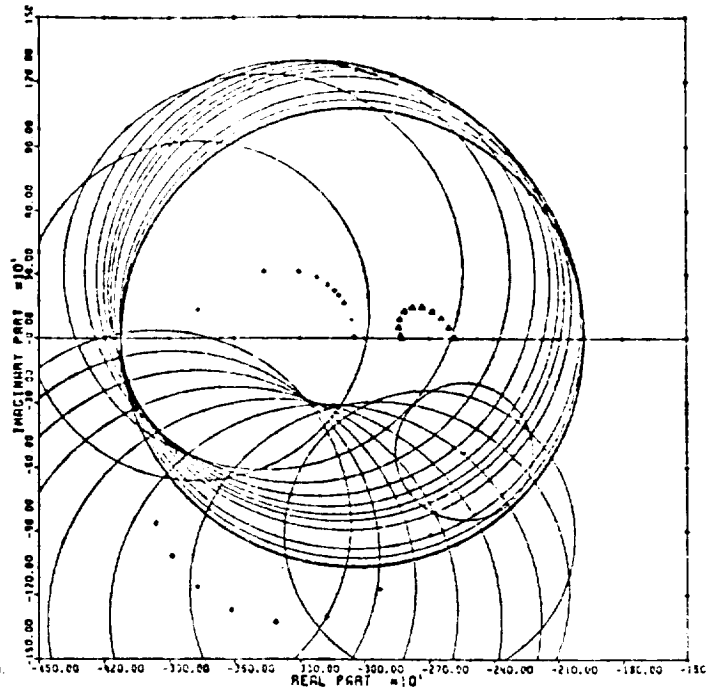

Fig. 12. $G(s)*K_1$, 2,3 Entry

diagonal entries in the compensator zero.

Figs. 13 and 14 are the plots for the third column using the full gradient rather than the standard analysis. The solid circles which appear at high frequencies in Fig. 14 are very important. Recall that the circle will only be drawn if dominance can be achieved while the other entry is zero. This means that by staying inside these solid circles, dominance can be achieved at the frequencies at which they occur while the 1,3 entry in the compensator is zero. Thus, in designing the 2,3

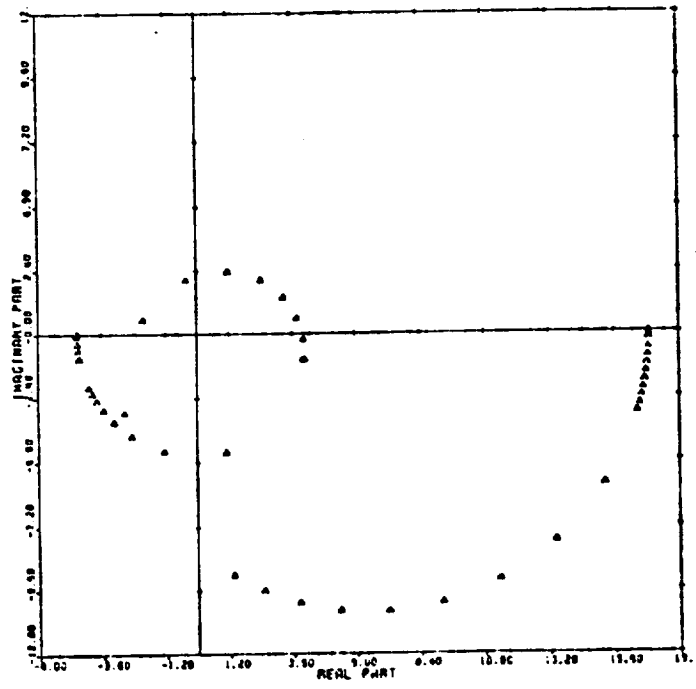

Fig. 13. $G(s)*K_1$, 1,3 Entry (Gradient)

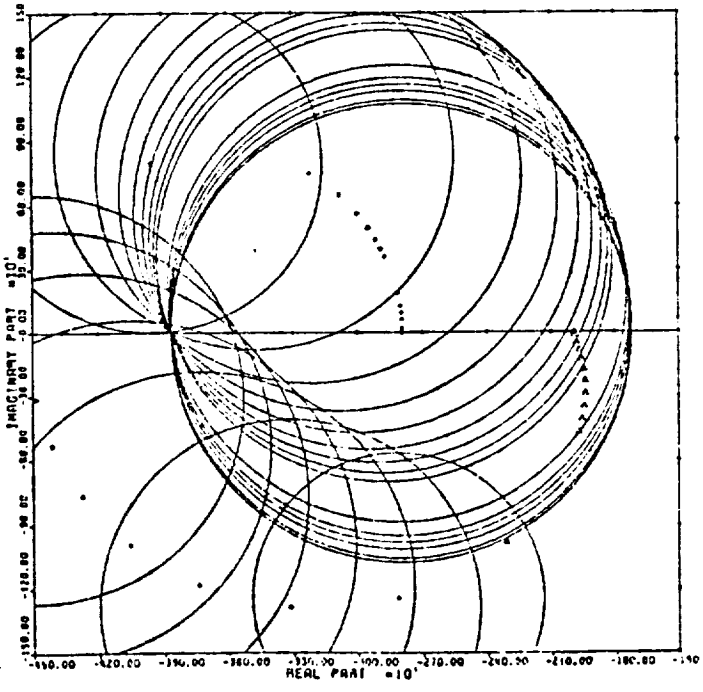

Fig. 14. $G(s)*K_1$, 2,3 Entry (Gradient)

entry, the strategy that is employed is to follow the triangles at low frequencies and stay inside the solid circles at the higher frequencies. If this is done, the design of the 1,3 entry will be simplified because it will only be necessary to fit the entry to the low frequency triangles and have the function go to zero at higher frequencies.

Utilizing this strategy, a lag compensator was designed to fit the 2,3 entry as described previously. The compensator entry that was chosen is

$$k_{23}(s) = \frac{-129.4s - 1940.2}{.0365s + 1.} .$$

At the same time, another lag compensator is fit to the solid circles in Fig. 9, the CARDIAD plot for the 1,2 entry. This was chosen to be

$$k_{12}(s) = \frac{.0127}{.1162s + 1.} .$$

Defining this compensator as $K_2(s)$ with all the other off-diagonal entries zero, the overall compensation thus far is $K_3(s) = K_1K_2(s)$.

$$K_3(s) = \begin{bmatrix} 0 & 1 & \frac{-129.4s - 1940.2}{.0365s + 1} \\ 0 & 0 & 1 \\ 1 & \frac{.0127}{.1162s + 1.} & 0 \end{bmatrix}$$

Figs. 15-20 are the CARDIAD plots of $G(s)K_3(s)$ using the standard dominance analysis. The plots show that the first two columns of the system are dominant at all frequencies since in Figs. 15-18 the origin of each plot is contained by all solid circles and excluded by all dashed circles. Fig. 19 shows that the strategy applied in the design for the 2,3 entry was successful. To make the third column dominant, it is now only necessary to fit a compensator to the shape of the solid circles in Fig. 19

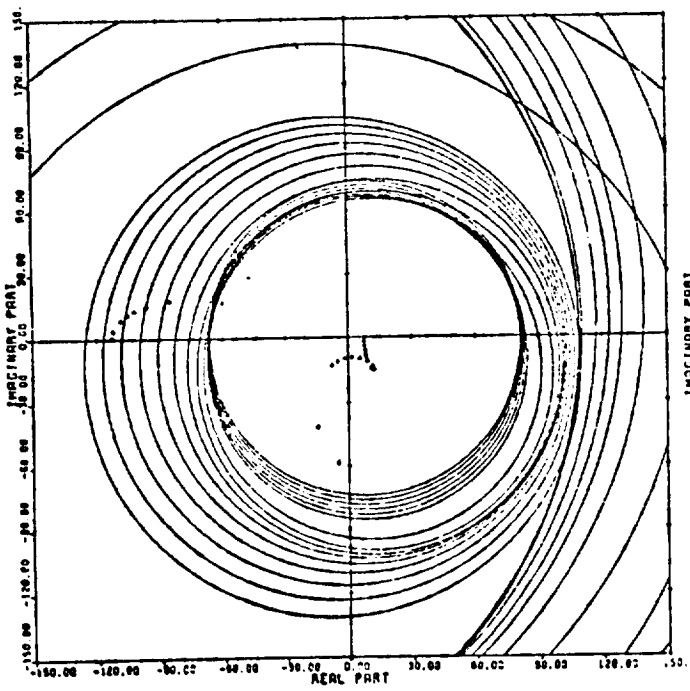

Fig. 15. $G(s)*K_3(s)$, 2,1 Entry

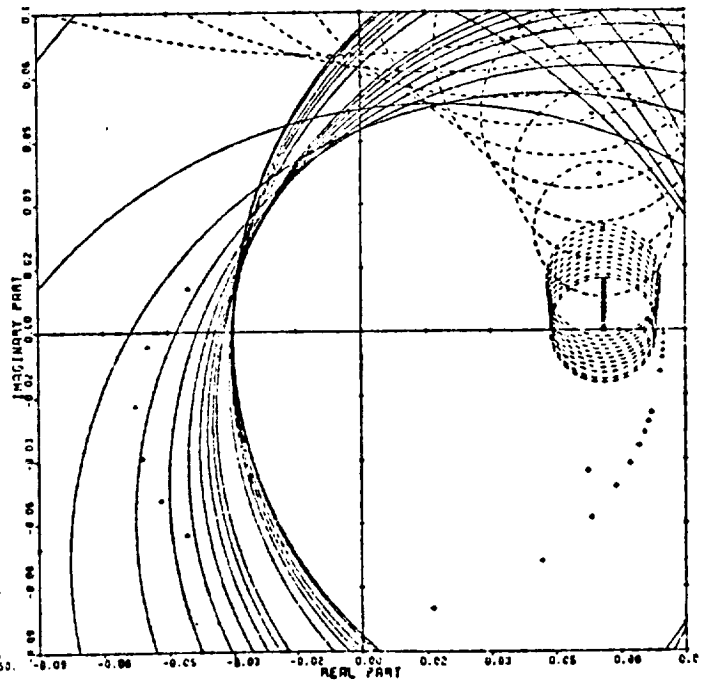

Fig. 16. $G(s)*K_3(S)$, 3,1 Entry

and have it go to zero at higher frequencies. The function that was chosen is

$$k_{13}(s) = \frac{.532s + 16.917}{.0127s^2 + .1986s + 1.}$$

The only change this has on the overall compensator is that the zero in the 3,3 entry is replaced by this function. When the third column is replotted using this compensator and standard dominance analysis, Figs. 21 and 22, the CARDIAD plots show that the third column is now dominant at all frequencies. Thus, the system is now dominant at all frequencies.

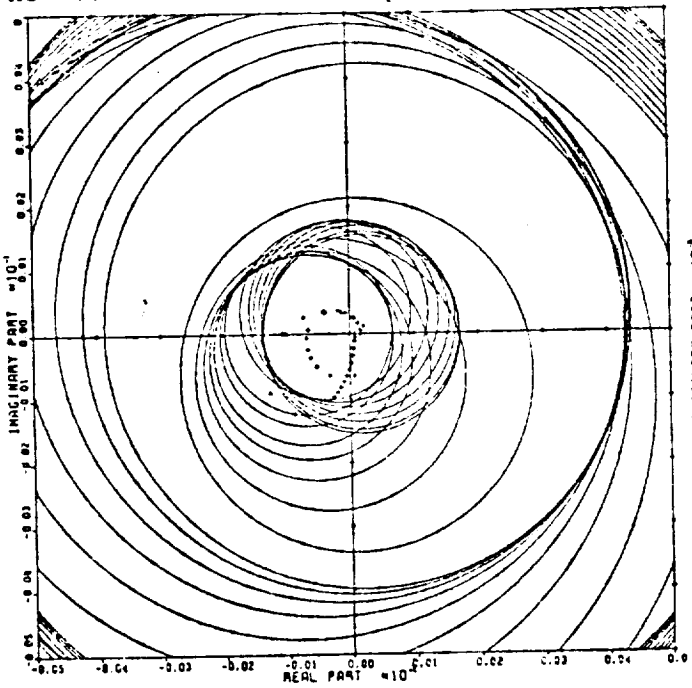

Fig. 17. $G(s)*K_3(s)$, 1,2 Entry

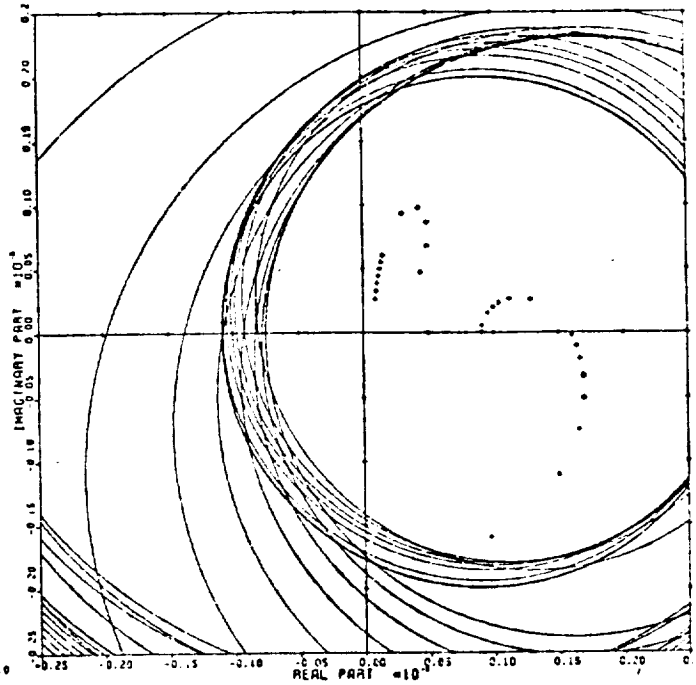

Fig. 18. $G(s)*K_3(s)$, 3,2 Entry

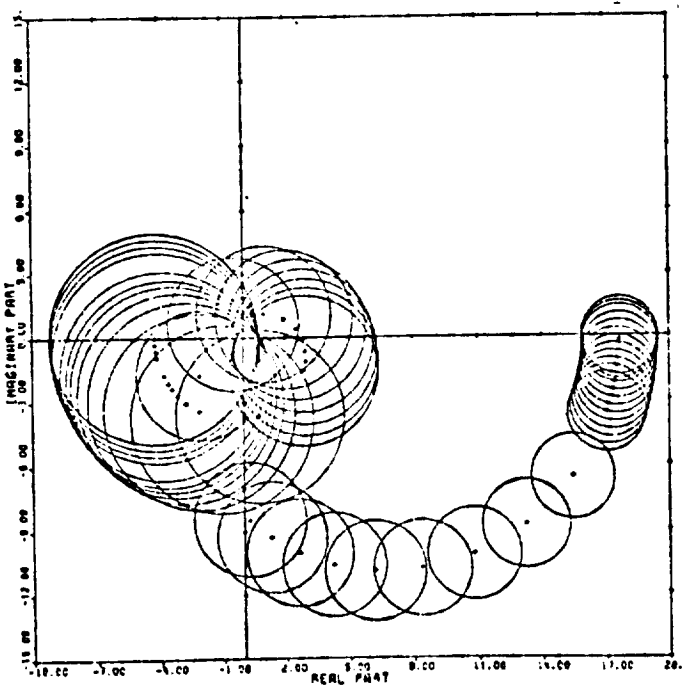

Fig. 19. $G(s)*K_3(s)$, 1,3 Entry

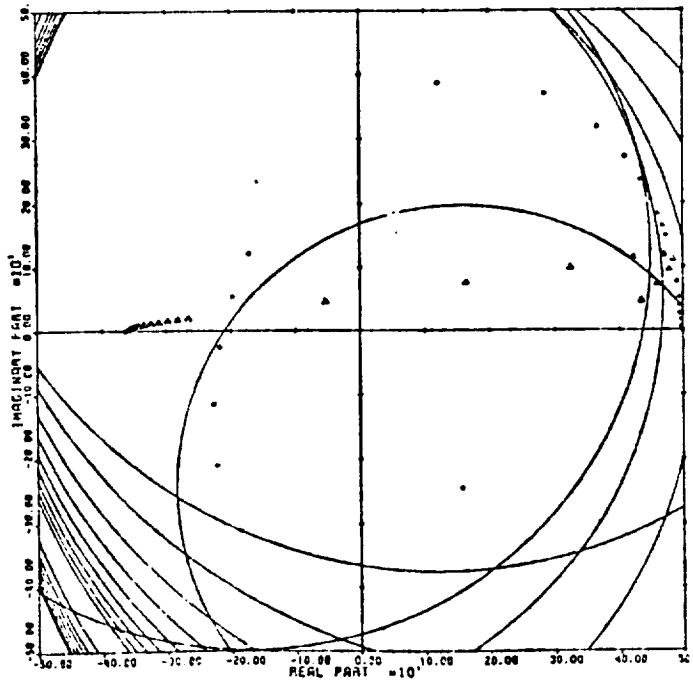

Fig. 20. $G(s)*K_3(s)$, 2,3 Entry

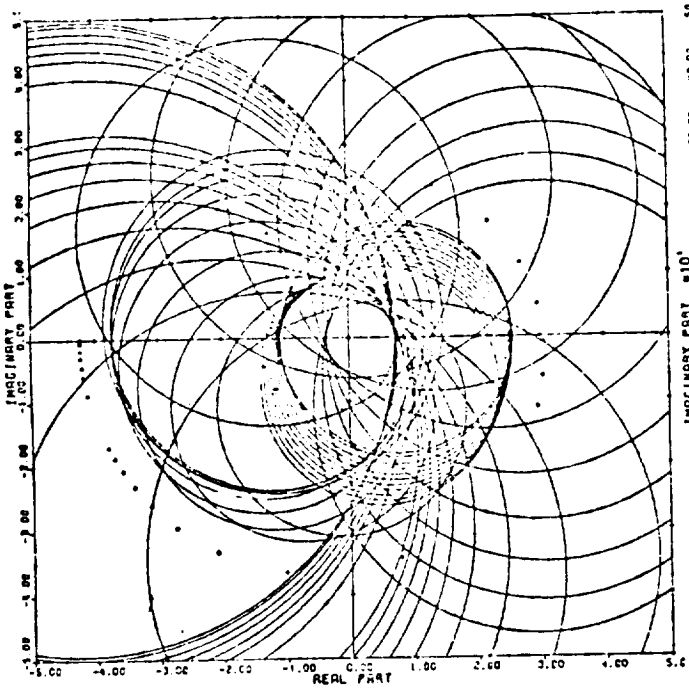

Fig. 21. G(s)*K(s), 1,3 Entry

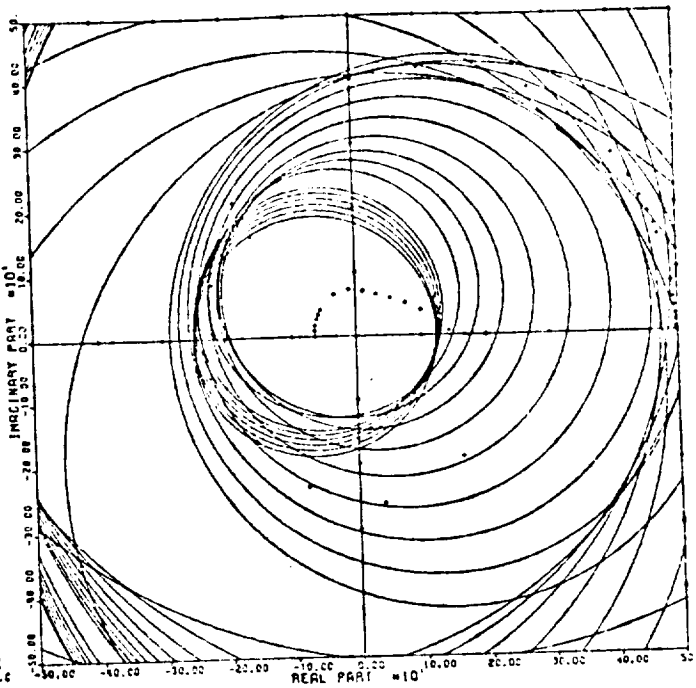

Fig. 22. G(s)*K(s), 2,3 Entry

6. CONCLUSIONS

The graphical CARDIAD method described in this paper has been effective on the Theme Problem. The authors' experience indicates that it is an easily learned design aid which can be quite helpful in achieving dominance for realistic plants. A special advantage of the CARDIAD approach lies in the way in which it provides insight to the designer. The plots indicate whether or not it will be possible to achieve dominance with simple, lead-lag compensators. Examples up to this time suggest that, over the useful bandwidth, simple compensators are often successful in this regard.

It should be noted that this paper illustrates only compensator selection for dominance. Completion of the design is by classical means. For an example, see [5]. Of particular note is the fact that compensator denominators having right half plane zeros do not necessarily lead to unstable controllers. This may also be seen in [5].

Continued research on this class of graphical, interactive methods is in progress.

7. ACKNOWLEDGMENT

This work was supported in part by the National Science Foundation under Grant ENG 75-22322 and in part by the National Aeronautics and Space Administration under Grant NSG 3048.

8. REFERENCES

1. H. H. Rosenbrock, Computer Aided Control System Design. New York: Academic Press, 1974.

2. R. M. Schafer, "A Graphical Approach to System Dominance," M.S. Thesis, Department of Electrical Engineering, University of Notre Dame, Notre Dame, Indiana, May 1977.

3. J. F. Sellers and C. J. Daniele, "DYNGEN--A Program for Calculating Steady-State

and Transient Performance of Turbojet and Turbofan Engines," NASA Tehcnical Notes, NASA TN D-7901, Washington, D.C., April 1975.

4. L. C. Geyser, "NASA Preliminary Report on DYGABCD," April 1976.

5. R. M. Schafer, R. R. Gejji, P. W. Hoppner, W. E. Longenbaker, and M. K. Sain, "Frequency Domain Compensation of DYNGEN Turbofan Engine Model," Proc. Joint Automatic Control Conference, pp. 1013-1018, June 1977.

D13-14

LINEAR MULTIVARIABLE SYNTHESIS WITH TRANSFER FUNCTIONS

Joseph L. Peczkowski

Energy Controls Division
The Bendix Corporation
South Bend, Indiana

Michael K. Sain

Department of Electrical Engineering
University of Notre Dame
Notre Dame, Indiana

ABSTRACT

This paper re-examines the use of transfer functions for linear multivariable synthesis. Traditionally offering high intuitive appeal, as well as enhanced designer insight and involvement in the synthesis process, transfer functions now appear to present a nontrivial alternative to the state variable oriented algebraic methodologies. A great deal of their usefulness stems from a unique synthesis equation and the classical feature of approximate cancellation, a convenience as yet not fully provided in a computational sense by highly precise modern algebraic techniques.

INTRODUCTION

The concept of transfer function has been a workhorse of engineering technique. Nonetheless, about the mid-century, the transfer function idea began to encounter difficulties as designers created matrices of them by transforming entire systems of differential equations. Practical computation with transfer function matrices was not an easy issue to resolve at that time, and still remains as a lesser challenge today. The question of how to extend performance specifications to matrices of transfer functions posed yet another riddle, the intricacies of which have only recently begun to come to light with new definitions of the zeros of multivariable systems [1, 2, 3].

Accordingly, it is hardly surprising that the advent of the state variable point of view, together with the methods of optimal control, so profoundly affected the subsequent course of multivariable control. The beginnings of the digital era and numerical integration advances provided a computational alternative; and the idea of a performance index avoided the specification difficulties. Most influential on linear control systems have been the quadratic regulator ideas, which for the engine control problem have been applied by various investigators [4, 5, 6, 7]. But these methods generally provide relatively little insight to the designer on the physical and dynamical characteristics of the plant and feedback control system.

This paper is about multivariable transfer function synthesis. The philosophy and viewpoint adopted is that the control engineer is an essential part of the design process and a synthesis technique should illuminate for the designer key relationships and characteristics of both plant and controller. The synthesis procedure is based on a matrix design equation which reflects the simple notion that a controller is a function of the given plant and the desired performance.

Significant features of the proposed synthesis method are :

- Selection of controlled and output variables
- Choice of closed loop structure
- Selection of closed loop response
- Calculation of the controller
- Verification

A primary objective is to maintain physical insight during the design process, so that the designer may interact with the system in a direct, integrated manner. This work is offered in the same spirit as that of other investigations [8, 9, 10, 11, 12] which are making transfer function design more relevant to modern multivariable control problems.

TRANSFER FUNCTION DESIGN

In this section we review the algebraic aspects of the transfer function design problem and point out the current relevance of certain aspects of classical approximate calculation. It is assumed that a controllable and observable state variable description (A_p, B_p, C_p, D_p) is given for the plant, which then has an essentially equivalent description by its transfer function matrix P(s). Also, it is required that the plant be output regulatable [13] for all appropriate sensed and output variables. Briefly, output regulatability requires that any desired steady state output can be achieved with a bounded control. Moreover, for an output regulatable plant, appropriate inverses exist and complete output regulation including noninteractive control is possible. Selection of closed loop structure and specification of a closed loop response matrix T(s) then typically lead to a design equation of the type

$$f(P, G) = T \tag{1}$$

where G(s) is the matrix of a part of the controller to be designed. Algebraically, it is frequently possible and highly desirable to convert (1) to the more tractable form

$$G_1 G = G_2 \tag{2}$$

$$G_i = f_i(P, T), \qquad i = 1, 2 \tag{3}$$

which also reflects the intuitive notion that a controller is determined by functions of the plant and specified response.

The idea of transfer function design by solution of (1) is not new. It was under intensive investigation about twenty years ago when techniques of optimal control began to hold sway [14, 15, 16, 17]. A very interesting historical note is that those early investigations were also motivated by jet engine control [18, 19] . At that time, there were substantial difficulties associated with computation, specification, and the understanding of loop stability. These are no longer so formidable.

Theoretically, the solution of (2) can proceed in one of basically two ways. First, regard (2) as a linear equation over R(s), the field of rational functions in s with coefficients in the real number field R, and find particular and complementary solutions. In floating point arithmetic, this method suffers from undesirable degree growth. It can be accomplished, however, with exact rational softwares. Second, "clear denominators" in (2) and regard the problem as one of polynomials. This can be accomplished conceptually within the context of free $R[s]$ - modules, where $R[s]$ is the principal ideal domain ring of polynomials in s with coefficients in R. At present, the free modular approach appears to offer advantages when dealing with issues such as the realizability, stability, or minimality of G(s). We assume the reader to be familiar with the first method. For an introduction to the second, see [20, 21] .

Studies of the solution of (2) by the second method on a turbofan engine illustration have been made [22] . Computationally, these show that existing exact rational softwares can solve the problem successfully, but not with acceptable cpu time. Thus the exact rational approach must await hardware advances. Moreover, while documenting these facts, the exact rational approach demonstrated numerical inefficiencies both in computation time and degree growth for a key reduction algorithm found in the literature. Thus theoretical improvements appear warranted as well. These observations, together with the fact that model numbers are only approximately rational, argue for floating point numerical arithmetic. The same studies indicate greatly improved cpu time, but difficulties with numerical stability for floating point implementations of the second method. It seems likely, however, that some of the obstacles can be at least partially overcome in the near term by means of the application of more sophisticated theoretical and numerical technique, as for example the singular value decompositions.

A great deal of the numerical challenge which occurs in the application of modern algebraic technique is the result of its paying too much attention to detail. It has as yet no convenient way to make the observation that

$$\frac{(1.1\,s+1)}{(2\,s+1)(s+1)} \cong \frac{1}{2s+1} \qquad (4)$$

In view of this, the present paper re-examines the first method for solving (2), with a format that makes a step (4) accessible.

MULTIVARIABLE CONTROL SYNTHESIS

The basic design idea of the paper is easy to understand. Consider Figure 1, which is a block diagram for a unity negative feedback servomechanism problem with no disturbances. References, error, plant input, and plant output are designated r, e, u, and y respectively.

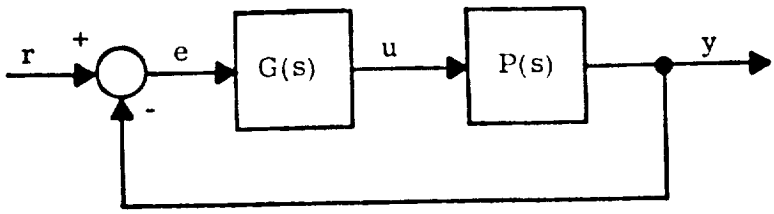

Fig. 1. Elementary Servo Mechanism

The plant P(s) and the controller G(s) have been introduced in the preceding section. It is desired to design G(s) so that a response T(s) indicated in Figure 2 is achieved.

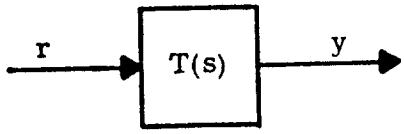

Fig. 2. Desired Response

This is, of course, a version of the problem (1) with

$$f(P,G) = (I + PG)^{-1} PG \tag{5}$$

For a servomechanism problem, there are numerous ways to argue that T(s) must have full column rank over R(s). A simple way to do this is to consider a class of reference inputs, such as steps. By partial fraction expansion of the output y resulting from an arbitrary reference step, it is easy to see that T(0) must have full column rank over R, for otherwise nonzero references could lead to zero responses. But this implies that the columns of T(s) are indeed linearly independent over R(s), as desired. From (1) and (5), moreover, it follows that P(s) G(s) must have the same column rank property, as well as being square. When the plant has equal numbers of inputs and outputs, this requires in turn that P(s) have an inverse and that G(s) be uniquely given by

$$G = P^{-1} T (I - T)^{-1} \tag{6}$$

For convenience, define a matrix

$$Q = T (I - T)^{-1} \tag{7}$$

and name it the performance matrix. Note that the performance matrix Q has the same decoupling properties (diagonal, block-diagonal, triangular, etc.) as the response matrix T. It also accurately portrays the usual servoinduced constraints on loop dynamics. For example, if

$$t_{ii}(s) = 1 / (\tau s + 1) \tag{8}$$

then

$$q_{ii}(s) = 1/(\tau s), \tag{9}$$

i.e., asymptotic tracking of a step requires an integrator. Obvious generalizations of this observation are many in number. For example, if

$$T = ND^{-1} \tag{10}$$

is a coprime polynomial matrix factorization of the response T(s), then

$$Q = N(D - N)^{-1}, \tag{11}$$

so that T(s) and Q(s) have the same "numerator dynamics", as indicated by the polynomial matrix N(s). This well known classical response limitation can be very important in turbofan engine models, where the thrust and high turbine inlet temperature responses of linearized models often involve right-half plane zeros.

In terms of the performance matrix, (6) becomes

$$G = P^{-1}Q \tag{12}$$

This relationship is considered a synthesis equation for controllers G(s) under the unity feedback structure of Figure 1. Though some wisdom is useful in specifying T(s), (12) shows that controller design primarily focuses upon the properties of $P^{-1}(s)$ and how they interact with Q(s). This has implications for control synthesis. Note also that an unstable inverse $P^{-1}(s)$ in (12) need not result in an unstable controller G(s) if the performance matrix Q(s) takes due account of the non-minimum phase nature of the plant. Neither need it result in an unstable loop, as shown shortly.

More General System Representation

Plant dynamics define the characteristics of the primary devices, machines or structures which are to be controlled, as for example, a jet engine, automotive engine or nuclear reactor. However, to effect control of a plant, it is necessary to use actuators to drive inputs and to use sensors to track and measure outputs. Moreover, sensors and actuators usually impose significant dynamic effects into the signal paths of the basic plant.

Now assume that diagonal actuator and sensor matrices A(s) and S(s) are introduced into the problem of Figure 1, and add a feedback matrix H(s). This leads to Figure 3, in which the output y is still assumed to be completely sensed. The real servo error, of course, is y - r; but if we assume that H(s) compensates primarily for S(s), then an approximate error is $\tilde{e}$ as indicated. The plant input request u_r and sensed outputs y_s are also shown.

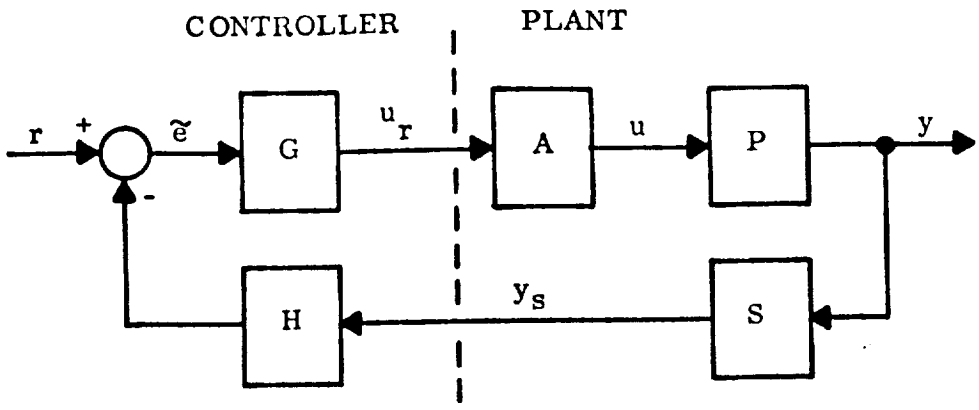

Fig. 3. Generalized Servomechanism

In this more general case,

$$f(P,G) = (I + PAGHS)^{-1} PAG, \tag{13}$$

and a performance matrix

$$Q = T (I - HST)^{-1} \tag{14}$$

is easily identified. The design equation (12) becomes

$$G = A^{-1} P^{-1} Q \tag{15}$$

for Q as in (14). This is a synthesis equation for systems as depicted in Figure 3.

CONTROLLING INACCESSIBLE OUTPUTS WITH MEASURED VARIABLES

It often occurs in practice that outputs of interest sometimes are not sensed. In such circumstance, the control of desired, but inaccessible, outputs is obtained indirectly using known, inherent plant coupling. For example, two gas turbine output variables of paramount importance which are not sensed, and thus not available for direct feedback, are turbine inlet temperature and thrust. These outputs are usually inferred by control of sensed parameters such as rotor speeds and turbine outlet temperature.

If plant outputs differ from the variables which are sensed, then plant dynamics may be modelled in a system block diagram as shown in Figure 4.

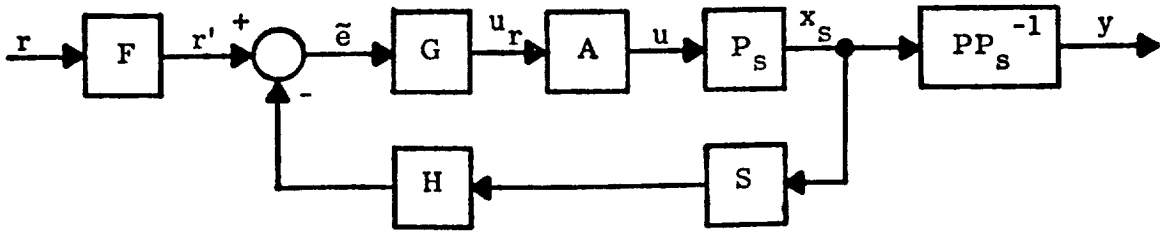

Fig. 4. Extension to Non-sensed Outputs

Observe that the plant transfer matrix is restructured into two matrices to define the transfer characteristics from the inputs u to the sensed parameters x_s and from x_s to the desired outputs y. The transfer matrix P_s is obtained from the state space description of the plant by defining another output equation, namely

$$x_s = C_s x + D_s u \tag{16}$$

Technically, it is assumed that (C_s, A_p) is an observable pair. Thus the transfer matrix P_s is given by

$$P_s = C_s (sI - A_p)^{-1} B_p + D_s \tag{17}$$

From (17) we note that the characteristic equations of P_s and P are identical. The condition that P_s have an inverse is required in application; it is, as it turns out, a necessary condition to assure total closed loop regulatability. The matrix F(s) is an added prefilter.

Having defined P_s, it is possible, via the synthesis equation, to design controllers to achieve prescribed closed loop response T_s between a request vector r' and the sensed plant variable vector x_s. The system in Figure 4 now becomes

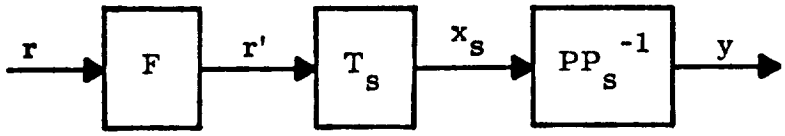

Fig. 5. Overall System

It is desired that the overall response of the system be y = Tr. From Figure 5 it readily follows that

$$T = P P_s^{-1} T_s F \tag{18}$$

For a given plant, P and P_s^{-1} in (18) are known and two elements of the system, the closed loop T_s and the prefilter F, are available to the designer to shape the overall response T. On the one hand, if a closed loop response is selected, the prefilter to obtain an output response T is

$$F = T_s^{-1} P_s P^{-1} T \tag{19}$$

On the other hand, if a prefilter is selected, the closed loop response which shapes the output response T is

$$T_s = P_s P^{-1} T F^{-1} \tag{20}$$

In this latter case, the performance matrix Q_s is determined from T_s and the synthesis equation is applied. Some aspects and utility of these ideas and calculations can be better judged in the design example later in this paper.

SPECIFICATIONS

In this section, we discuss briefly some aspects of the specification problem.

Plant : At the outset it is necessary, of course, to determine if a plant is capable of being regulated. Output regulatability [13] conditions guarantee that finite, desired output time functions can be obtained with bounded input functions. It turns out that for proportional plants, similar to the design example, the existence of appropriate plant transfer matrix inverses assure complete output regulatability.

Controller : Consider performance matrix (11) and synthesis equation (12). Write P(s) in coprime polynomial matrix form $N_p(s)\, D_p^{-1}(s)$ and combine the equation to give

$$G = D_p N_p^{-1}\, N\, (D - N)^{-1} \tag{21}$$

Stability of G is affected by $|N_p|$ and $|D - N|$. The latter determinant is sometimes forced to have factors with closed right half plane zeros for servo-mechanism purposes. An example is seen in (8) and (9). Right half plane zeros of $|N_p|$, however, represent definite nonminimum phase limitations which are often incompatible with the combined requirements of loop stability and tracking. Accordingly, factors of $|N_p|$ having such zeros are usually eliminated from G by appropriate choice of N. In this regard, it is important to realize that cancellations occurring in (21) do not create hidden modes, but merely serve as guidelines for controller design.

Loop Stability : In any design, it is necessary to check for loop stability. This is especially so in servo problems with nonminimum phase plants. Relative to Figure 4, this can be accomplished perfunctorily with an eigenvalue check on the loop state matrix A_L , or with added insight by a Nyquist interpretation of the equation

$$|sI - A_L| = |I + P_S AGHS|\, |sI - A_{P_S}||sI - A_A|\, |sI - A_G|\, |sI - A_H||sI - A_S| \tag{22}$$

where $A_\alpha, \alpha \in \{P_S, A, G, H, S\}$, is the state matrix associated with the transfer function matrix $\alpha(s)$. If A_α is part of a given description $(A_\alpha, B_\alpha, C_\alpha, D_\alpha)$ for any part of the loop in Figure 4, then it should be used in (22) whether or not (A_α , B_α) is controllable and (C_α , A_α) is observable. If only $\alpha(s)$ is given, however, the A_α used in (22) should correspond to minimal realization of $\alpha(s)$.

Equation (22) assumes the infinite - frequency return ratio to be zero around the loop. This is appropriate for our example where states are being sensed. Otherwise (22) would involve an additional constant of proportionality. If we assume plant, actuators, and sensors to be stable, and H(s) to be stable by choice, then loop stability can revolve around a Nyquist diagram of the determinant of return difference, with open loop right-half plane zeros of $|sI - A_G|$ properly counted.

Performance : If decoupling is the design choice, it is reasonably easy to conclude from Nyquist arguments based on (22) that loop stability and transient response will tend to be robust properties of the control system for small variations in parameters of A, P, and S in Figure 3. A similar statement could be made for variations in P(s) relative to asymptotic tracking of, say step references, in Figure 1.

Moreover, care should be taken to avoid linear designs which attempt superlative response; this may lead out of the validity region of the linear model itself.

ILLUSTRATIVE EXAMPLES

Some aspects of multivariable synthesis with transfer functions are illustrated by applying the approach to the theme problem : the F 100 gas turbine engine at sea level, 83 degree power lever conditions. The following features are highlighted :

- unique transfer matrix descriptions
- model reduction
- selection of feedback structure
- selection of desired response
- shaping of inaccessible output response
- verification

This section starts with a description of engine model reduction and selection of sensed and output variables. Next, actuator and sensor dynamics are established. The response specification of the theme problem is noted. Finally, the design approach for the illustrative examples is highlighted : choosing the feedback structure, selection of closed loop response and performance matrix, 3 input- 3 output example, 4 input - 4 output example.

Verification of all controllers was done by a digital time simulation of the system using step commands. The plant used in the simulation included a 6th order engine model and complete actuator and sensor dynamics.

The Engine : The F100 engine theme example is a 16 state, 5 input, 5 output model. In addition five actuators are given with quadratic or cubic dynamics and five sensors are provided, four with first order lags and the fifth with slow quadratic response. The sixteen eigenvalues of the engine were determined to be approximately : -577, -175, -58, -51, -48, -39, $-21.4 \pm .9i$, -18.6, $-17.8 \pm 4.2i$, $-5.8 \pm 5i$, -3.8, -2, -.68.

A reduced order plant was obtained [25] by eliminating all eigenvalues beyond the frequency range of interest, namelv all real parts less than -17.8. This gave a fifth order model. However since FTIT is a sensed variable, the fast response eigenvalue of FTIT (-51) was also included. Correspondence of eigenvalues with engine physical variables was determined. A sixth order reduced engine model was established with eigenvalues and state variable correspondence as follows :

-.68	$-T_{41o}$, Burner Exit Slow Response (x_6)
-2.0	$-T_{4.5lo}$, Fan Turbine Inlet Slow Response (x_5)
-4.06	$-N_2$, Compressor Speed (x_2)
$-5.4 + 4.7i$	N_1 , Fan Speed (x_1)
$-5.4 - 4.7i$	P_7 , Augmentor Pressure (x_3)
-51	$T_{4.5\ hi}$, Fan Turbine Inlet Fast Response (x_4)

The fan speed and augmentor pressure are coupled by a complex root pair. All of the sensed variables, except compressor discharge pressure, appear in the reduced

model. A state description of the reduced engine model is $\dot{x} = A_p x + B_p u; y = C_p x + D_p u;$ $x_s = C_s \underline{x}$

$$x = (N_1, N_2, P_7, T_{4.5\,hi}, T_{4.5\,lo}, T_{4lo})$$

$$u = (WFMB, A_j, CIVV, RCVV, BLC)$$

$$y = (FN, WFAN, T_4, SMAF, SMHC)$$

$$x_s = (N_1, N_2, P_7, FTIT)$$

and

$$A_p = \begin{bmatrix} -5.62 & 3.61 & -192 & 9.60 & 9.58 & -.832 \\ .291 & -3.09 & -122 & .066 & .686 & 13.0 \\ .087 & -.004 & -7.41 & -.014 & -.090 & -.070 \\ 3.83 & -2.27 & -591 & -50.0 & .771 & -10.1 \\ .170 & -.101 & -26.3 & -2.00 & -1.97 & -.449 \\ .006 & -.003 & -1.07 & .0002 & .003 & -.665 \end{bmatrix} \quad B_p = \begin{bmatrix} .467 & 237 & -126 & 13.1 & -35745 \\ .877 & -174 & 6.97 & -84.1 & -20138 \\ .012 & -95.0 & .535 & -.176 & -247 \\ 4.36 & -702 & 45.3 & 59.0 & 41611 \\ .194 & -31.2 & 2.01 & 2.62 & 1849 \\ .008 & -1.33 & .080 & .104 & 72.6 \end{bmatrix}$$

$$C_p = \begin{bmatrix} .923 & .030 & 180 & -.508 & -.271 & -.588 \\ .014 & .000003 & -.011 & 0 & 0 & 0 \\ .103 & -.064 & -17.9 & .004 & .044 & .032 \\ .00007 & .000007 & -.015 & .000003 & .00004 & .00002 \\ -.000007 & .00002 & .002 & -.000004 & -.00005 & -.00003 \end{bmatrix} \quad C_s = \begin{bmatrix} 1 & 0 & 0 & 0 & 0 & 0 \\ 0 & 1 & 0 & 0 & 0 & 0 \\ 0 & 0 & 1 & 0 & 0 & 0 \\ 0 & 0 & 0 & 1 & 1 & 0 \end{bmatrix}$$

$$D_p = \begin{bmatrix} .336 & -239 & 37.3 & 5.50 & -5615 \\ .0001 & .335 & .680 & -.00005 & -.013 \\ .130 & -22.7 & 1.31 & 1.43 & 1451 \\ .000003 & -.012 & -.006 & .0001 & .043 \\ -.000008 & .004 & -.0002 & -.006 & .839 \end{bmatrix}$$

Actuators : Actuator dynamics are expressed by a separate diagonal transfer function matrix A(s) such that $\underline{u} = A\,\underline{u_r}$. The vector $\underline{u}$ is the input vector and $\underline{u_r}$ is the input request vector.

To save space, dynamic factors of transfer functions shall be represented by a compact form omitting the usual s and +1 notations as follows :

$$\frac{K(T_1 s+1)}{s(T_a s+1)(a_2 s^2+a_1 s+1)(T_b s+1)} \triangleq \frac{K(T_1)}{s(T_a)(a_2, a_1)(T_b)} \tag{24}$$

The actuator dynamics are specified in the theme problem : A(s): $a_{11} = 1/(.1)(.02)$, $a_{22} = 1/(.01)(.0007,03)$, $a_{33} = 1/(.02)(.071)(.012)$, $a_{44} = 1/(.00025, 025)$, $a_{55} = 1/(.02)$ Bleed control and actuator a_{55} are not used in the examples. For design purposes the above actuator dynamics will be approximated by the diagonal matrix :

$$A(s) : a_{11} = 1/(.12),\ a_{22} = 1/(.04),\ a_{33} = 1/(.1),\ a_{44} = 1/(.03) \tag{25}$$

Sensors : Sensor dynamics are described in a diagonal matrix S(s)

$$S(s) : s_{11} = 1/(.03),\ s_{22} = 1/(.05),\ s_{33} = 1/(.05),\ s_{44} = (2)/(5.5)(.6) \tag{26}$$

These elements define the N_1, N_2, P_7 and FTIT sensors respectively.

Response Specification : It is required that the engine thrust, FN, and the turbine inlet temperature, T_4 respond fast without overshoot and that the fan stall margin, SMAF, and the compressor stall margin, SMHC shall not decrease by more than .05 and .15 respectively. It is also given that the above output variables are not sensed and therefore, are not available for direct feedback to a controller.

System Design

In the illustrative examples control of the sensed variables is first accomplished. Decoupled, noninteracting control of the sensed variables is demonstrated. Then decoupling and control of inaccessible outputs is illustrated.

Feedback Structure : The engine-control system structure used in the examples is pictured in Figure 4. Essentially, a unity feedback configuration is obtained by compensating sensor dynamics with the feedback matrix H(s) such that $H \cong S^{-1}$. Thus, the controller feedback matrix is diagonal :

$$H(s) : h_{11}=(.03)/(.003),\ h_{22} = h_{33} = (.05)/(.005),\ h_{44}=(5.5)(.6)/(2)(.006) \quad (27)$$

For the 3 input - 3 output example, the first three elements are used.

The Response Matrix : Closed loop response is selected to produce the following characteristics :

- stable, essentially first order response
- settle in 1 second
- decoupled
- zero steady state error

These characteristics suggest a diagonal response matrix of the form $t_{ii}=1/(.25)(\ \cdot\ )$. The gain of 1 implies no steady state error and the .25 time constant assures 1 second settling. The parentheses (•) indicate other, smaller, acceptable time constants used to effect realizeability, or smoothing or simplification.

Example 3 input - 3 output

Here we choose to control three sensed engine variables $x_S = (N_1, N_2, P_7)$ with three inputs u = (WFMB, A_j, CIVV). First, decoupled response of the sensed variables is demonstrated. Then, decoupled response of three inaccessible but desired outputs y = (FN, T_4, SMAF) is illustrated. The situation is as pictured in Figure 4 with $HS \cong I$.

The transfer function matrices of the engine are :

$$P_s = \frac{\begin{bmatrix} .19\ (.007)(.040,\ .37)(.49)(1.4) & 614\ (.0002,.02)(.24)(.5)(1.4) & -14\ (.02)(.120)(.320)(.5)(1.5) \\ .20\ (.020)(.025,\ .27)(.50)(1.3) & 300\ (.02)(.20)(-.02)(.5)(1.2) & 5.4\ (.02)(.007,\ -.01)(.5)(1.3) \\ .003\ (.040)(.040)(.20)(.50)(1.4) & -6.2\ (.02)(.20)(\ .35)\ (.5)(1.5) & -.10\ (.02)(.340)(-.07)(.5)(1.5) \end{bmatrix}}{(.02)\ (.02,\ .21)(\ 25)(.5)(1.47)} \quad (28)$$

$$P = \frac{\begin{bmatrix} 1.10\ (.02)(.006,.12)\ (.21)(.5)(1.4) & -826(.0002,.031)(.22)(.44)(.56)(1.6) & 6.0\ (.02)(.08)(.42,\ 1.04)(.5)(1.3) \\ .075\ (.02)(.02,\ .26)\ (.34)(.5)(1.5) & 132(.02)(.19)(-.014)(.31)(.50)(1.5) & 1.3\ (.02)(.01,\ -.05)(\ .39)(.5)(1.5) \\ -.00003(.001,.05)(-.04)(.21)(.5)(1.5) & .13(.02)(-.009)(.18)(.28)(.50)(1.5) & -.005(.02)(.11)(.05,\ .40)(.5)(1.5) \end{bmatrix}}{(.02)\ (.02,\ .21)(.25)(.50)\ (\ 1.47\ )} \quad (29)$$

$$P_s^{-1} = \frac{\begin{bmatrix} .059(.02)(.36)(.55)(3.1) & 2.55(.02)(.34)(.50)(1.5) & 135(.02)(-.01)(.5)(1.3) \\ .0007(.02)(-.05)(.50)(1.3) & .0005(.02)(.29)(.50)(1.5) & -.068(.02)(.16)(.50)(1.3) \\ -.04(.02)(.20)(.50)(1.3) & .058(.007)(.2)(.50)(1.4) & -1.16(.02)(.03)(.50)(1.3) \end{bmatrix}}{(.02)\,(.50)\,(1.3)} \tag{30}$$

$$P^{-1} = \frac{\begin{bmatrix} .74(.02)(.18)(.32)(-.013)(.50)(1.5) & 3.1(.0005,.045)(.15)(.46)(.58)(1.6) & 1589(.02)(-.007)(.18,.81)(.50)(1.5) \\ -.0003(.02)(.09)(.10,.63)(.50)(1.5) & .005(.02)(.007,.15)(.21)(.50)(1.4) & .85(.02)(.07)(.40)(-.70)(.50)(1.5) \\ -.012(.02)(.10)(.31)(-.009)(.50)(1.5) & .10(.02)(-.007)(.08)(.20)(.50)(1.5) & -177(.02)(.008)(.23)(.28)(.50)(1.5) \end{bmatrix}}{(.017)\,(.02)\,(.125)\,(.3)\,(.5)\,(1.5)} \tag{31}$$

From (28) and (29) one obtains the insight that the longest time constants, (1.47) and (.5), and shortest time constant (.02) of the engine are not dynamically significant since they essentially cancel out of the matrices. Thus the engine is primarily 3rd order. Moreover, the unique transfer functions indicate the engine gains for every input-output pair and the speed of response in each path.

A decoupled, stable response is desired which settles in one second with zero steady state error. Therefore a diagonal closed loop response matrix T(s) is chosen $t_{ii} = 1/(.25)\,(\bullet)$, for i = 1, 2, 3. With this choice of response matrix, the performance matrix Q(s) becomes a diagonal matrix $q_{ii} = 4/s\,(\bullet)$. An (.02) factor is included in q_{ii} to assure realizeability; this transmits an additional term of approximately (.019) to the denominators of T.

Synthesis equation (15), using actuator dynamics (25), generates controller

$$G = A^{-1}P_s^{-1}Q = \frac{\begin{bmatrix} .24(.02)(.36)(.55)(3.1)(.12) & 11(.02)(.34)(.5)(1.5)(.12) & 540(.02)(-.01)(.5)(1.3)(.12) \\ .003(.02)(-.05)(.50)(1.3)(.04) & .002(.02)(.29)(.5)(1.5)(.04) & -.27(.02)(.16)(.5)(1.3)(.04) \\ -.16(.02)(.20)(.50)(1.3)(.10) & .23(.007)(.20)(.5)(1.4)(.10) & -4.6(.02)(.03)(.5)(1.3)(.10) \end{bmatrix}}{S(.02)\,(.02)\,(.5)\,(1.3)} \tag{32}$$

This is an integral controller which produces the desired decoupled response essentially equal to $t_{ii} \cong 1/(.25)\,(.019)$, with zero steady state error.

Cancellations and approximations indicated by (32) reduce the controller matrix to

$$G = \frac{\begin{bmatrix} .24(.36)(.12)(3.1)/(1.3) & 11(.34)(.12) & 540(-.01)(.12) \\ .003(-.05)(.04) & .002(.29)(.04) & -.27(.16)(.04) \\ -.16(.20)(.10) & .23(.20)(.10) & -4.6(.03)(.10) \end{bmatrix}}{S\,(.02)} \tag{33}$$

Closed loop response transients for step inputs with controller (33) are shown in Figures 6 and 7. Desired response and decoupling of the sensed variables are achieved satisfactorily. Corresponding time responses of the outputs are shown in Figure 8.

To obtain decoupled responses essentially with time constants of .25, .33, and .50 one may choose $t_{11} \cong 1/(.25)\,(.02)$, $t_{22} \cong 1/(.33)\,(.02)$, $t_{33} \cong 1/(.50)\,(.02)$. For this choice of T the controller matrix is

$$G = \frac{\begin{bmatrix} .24(.36)(.12)(3.1)/(1.3) & 8.0(.34)(.12) & 270(-.01)(.12) \\ .003(-.05)(.04) & .0015(.29)(.04) & -.14(.16)(.04) \\ -.16(.20)(.10) & .18(.20)(.10) & -2.3(.03)(.10) \end{bmatrix}}{S(.02)} \tag{34}$$

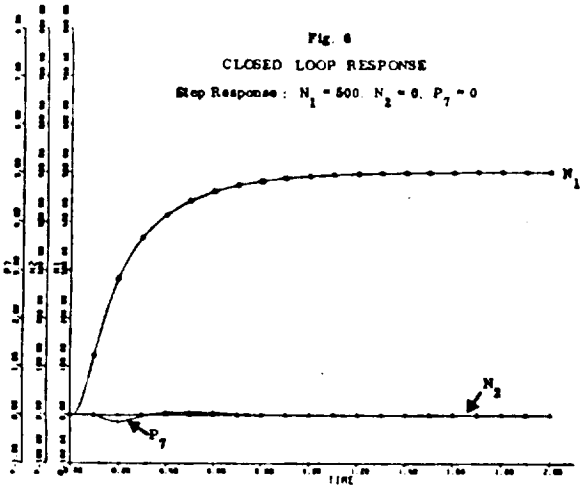

Fig. 6
CLOSED LOOP RESPONSE
Step Response : $N_1 = 500.$ $N_2 = 0.$ $P_7 = 0$

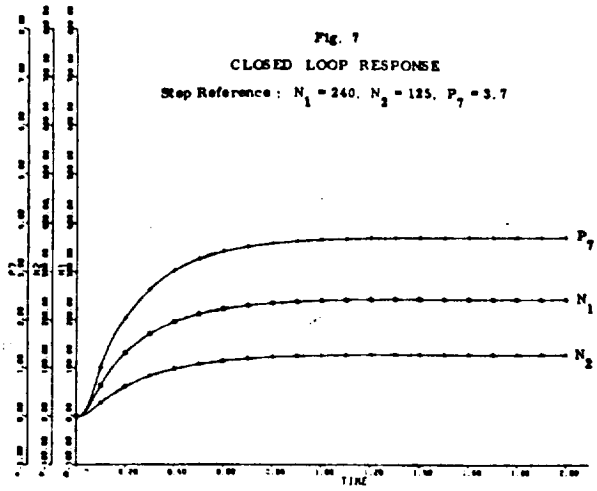

Fig. 7
CLOSED LOOP RESPONSE
Step Reference : $N_1 = 240.$ $N_2 = 125.$ $P_7 = 3.7$

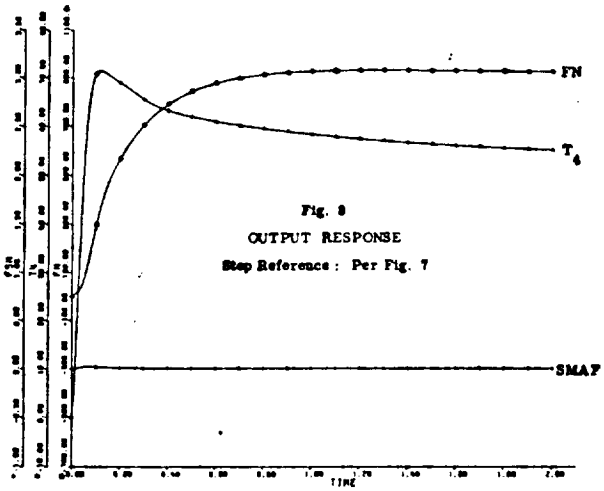

Fig. 8
OUTPUT RESPONSE
Step Reference : Per Fig. 7

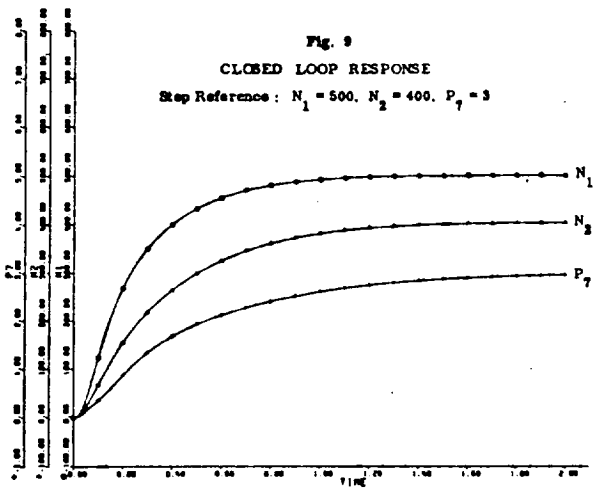

Fig. 9
CLOSED LOOP RESPONSE
Step Reference : $N_1 = 500.$ $N_2 = 400.$ $P_7 = 3$

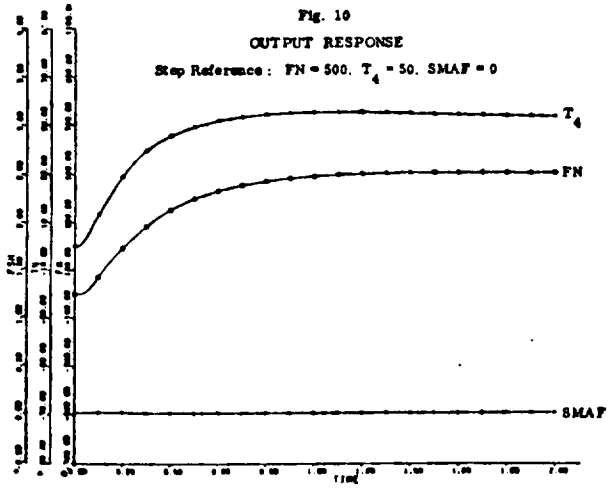

Fig. 10
OUTPUT RESPONSE
Step Reference : $FN = 500.$ $T_4 = 50.$ $SMAF = 0$

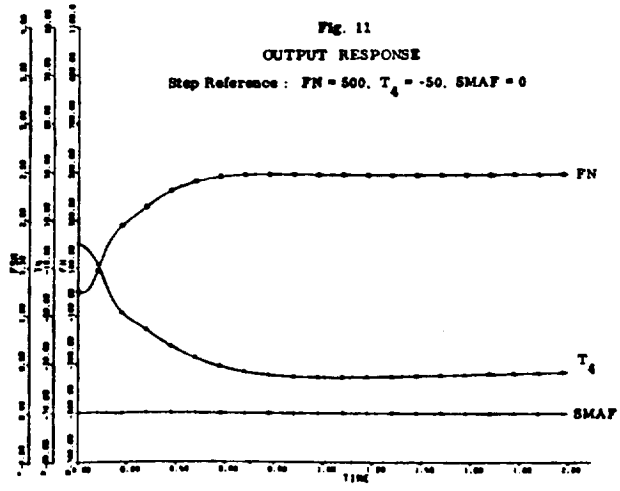

Fig. 11
OUTPUT RESPONSE
Step Reference : $FN = 500.$ $T_4 = -50.$ $SMAF = 0$

Step responses for the F100 engine with controller (34) are shown in Figure 9.

Shaping Output Response : Although satisfactory response of the sensed variables was achieved, the response of the outputs, particularly temperature T_4 in Figure 8, was not entirely satisfactory. Equation (19) is now applied to construct a prefilter matrix to shape the response of the inaccessible output variables to the form $t_{ii} = 1/(.25)(.02)$, similar to the closed loop response of the sensed variables.

$$F = \frac{\begin{bmatrix} .12(.02)(-.04)(.36)(.5)(1.5) & 2.2\ (.0004,.03)(.19)(.5)(1.4) & 3310(.02)(.005)(\ .37)(.5)(1.5) \\ -.009(.02)(\ .02)(-.3)(.5)(1.5) & 2.6\ (.02)(.017)(.13)(.5)(1.2) & -390(.02)(\ .02)(-.08)(.5)(1.5) \\ .0056(.02)(\ .15)(.33)(.5)(1.5) & -.03(.03)(\ .09)(.22)(.5)(1.4) & 18(.02)(\ .09,\ .55\ )(.5)(1.5) \end{bmatrix}}{(.017)(.02)(.13)(.33)(.5)(1.5)} \qquad (35)$$

Cancellations and simplifying assumptions reduce F to

$$F \cong \begin{bmatrix} .12/(\ .13) & 2.2\ /(.33) & 3310\ /(.13) \\ -.009\ (-.30)/(.13)(.33) & 2.6\ /(.33) & -390(-.03)/(.13)(.33) \\ .0056\ /(.02) & -.03/(.02) & 18(\ .28)/(.13) \end{bmatrix} \qquad (36)$$

The output responses of the F100 engine to step commands in thrust and temperature using controller G (33) and prefilter F (36) are shown in Figures 10 and 11.

Example 4 input - 4 output

This example proceeds in identical fashion to the preceeding 3 x 3 illustration. The input vector is $\underline{u}$ = (WFMB, A_j, CIVV, RCVV); the sensed variables are $\underline{x}_S$ = (N_1, N_2 , P_7, FTIT) , and the outputs are y = (FN, T_4 , SMAF, SMHC).

Decoupled response of the sensed variables with $t_{ii} \cong 1/\ (.25)\ (.02)$ is produced by the simplified controller

$$G = \frac{\begin{bmatrix} -1.0(-.29)(.12) & 2.6(\ .23)(.12) & 544(-.11)(.12) & 32(.22)(.12) \\ .0024(-.55)(.04) & .001(\ .14)(.04) & -.28(\ .16)(.04) & .004(.02)(.04) \\ -.20(\ .17)(.10) & .12(-.02)(.10) & -4.6(\ .02)(.10) & .48(.10) \\ -.016(-.04)(.03) & -.12(\ .37)(.03) & .04(\ .23)(.03) & .44(.02)(.03) \end{bmatrix}}{S\ (.02)} \qquad (37)$$

System transients to step references of the sensed variables are shown in Figures 12 and 13.

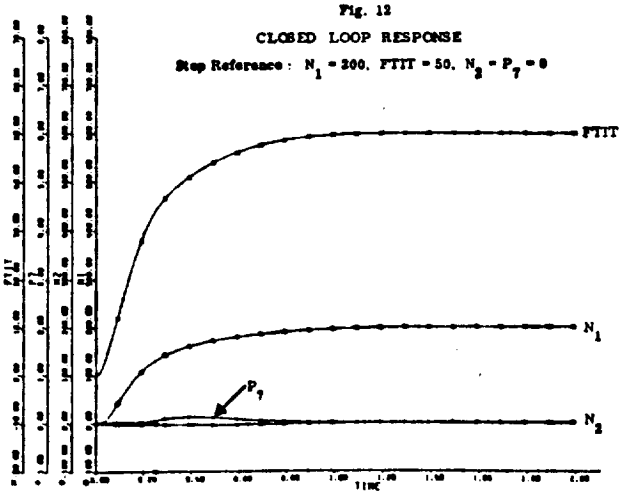

Fig. 12
CLOSED LOOP RESPONSE
Step Reference : N_1 = 200, FTIT = 50, N_2 = P_7 = 0

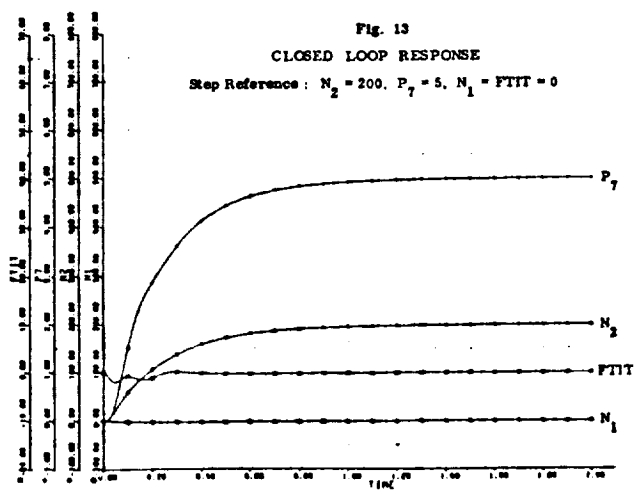

Fig. 13
CLOSED LOOP RESPONSE
Step Reference : N_2 = 200, P_7 = 5, N_1 = FTIT = 0

To shape the response of the outputs a prefilter matrix is designed using (19). A simplified prefilter matrix F is

$$F = \frac{\begin{bmatrix} .11(.30)(-.04) & 2.2(.13)(.02) & 3276(.30)(.02) & 2046(.02)(-.02) \\ -.02(.06)(-.17) & 2.7(.13)(.02) & 463(.02)(-.06) & 4948(.02)(.13) \\ .006(.13)(.30) & -.03(.19)(.13) & 18(.30)(.30) & -15(.07)(-.10) \\ .002(.30)(-.11)(.07) & .74(.13)(.30) & 29(.33)(-.06) & -29(.13)(.47) \end{bmatrix}}{(.02)(.13)(.30)} \qquad (38)$$

Response of the outputs to step commands with controllers (37) and (38) are shown in Figure 14 and 15.

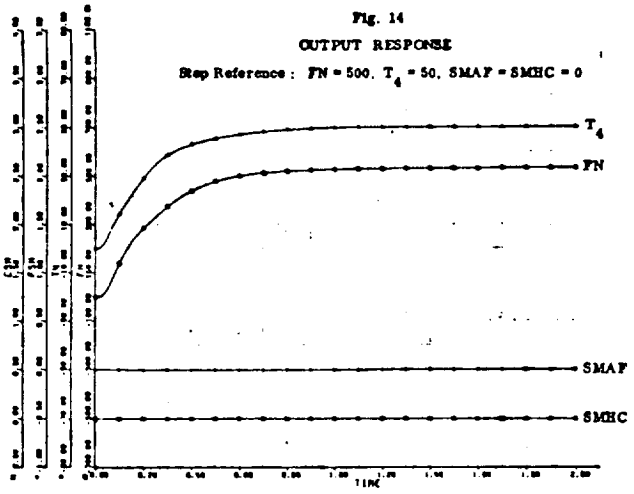

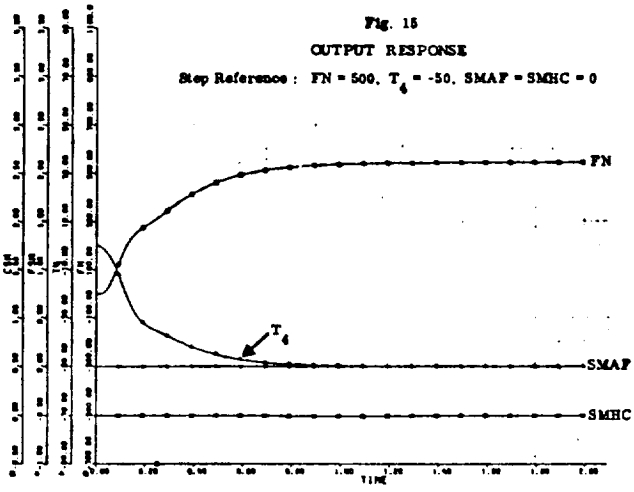

CONCLUSIONS

The authors believe that transfer functions offer a nontrivial, viable alternative for multivariable control synthesis.

The transfer function synthesis equation provides a unique, convenient format to the designer. The equation displays the salient characteristics of a plant to aid in selection of response, cancellations, approximations and realizeability. The plant inverse matrix plays a fundamental role in transfer function synthesis; it is the primary matrix in the controller equation and its existence assures output regulatability.

Some wisdom is useful in specifying desired closed loop response. Superlative response beyond the range of the plant model should be avoided. For regulatable plants, decoupled response is readily achieved, and happily, the diagonal matrix forms significantly enhance designer insight.

Verification of the design is recommended. There are two issues here : stability and final response. Verification of the final response by simulation is recommended to check the effects of assumptions and simplifications made by the designer. For stable, open loop plants and controllers, stability is determined by checking for right hand plane zeroes of the equation $|I + PAGHS| = 0$. For unstable plants or controllers, equation (22) is applied.

ACKNOWLEDGEMENT

It is a pleasure to acknowledge the analytical and programming assistance of Ms. Patrice Bridges and Mr. John Wildrick of the Bendix Energy Controls Division. The support and suggestions of Dr. R. J. Leake of Notre Dame also are gratefully acknowledged.

REFERENCES

1. Davison, E. J. and Wang, S. M., "Properties and Calculation of Transmission Zeroes of Linear Multivariable Systems," Automatica, Vol. 10, pp643-658, 1974.

2. MacFarlane, A.G.J., "The Role of Poles and Zeroes in Multivariable Feedback Theory," in Directions in Large-Scale Systems, Y.C. Ho and S.K. Mitter, eds., New York, Plenum Press, 1976, pp 325-338.

3. Wonham, W. M. and Francis, B. A., "The Role of Transmission Zeroes in Linear Multivariable Regulators," Report 7501, Dept. of Electrical Engineering, University of Toronto, Canada, February, 1975.

4. Michael, G. J. and Farrar, F. A. , "An Analytical Method for the Synthesis of Nonlinear Multivariable Feedback Control", Office of Naval Research Report M941338-2, June 1973.

5. DeHoff, R. L. and Hall, W. E., "Multivariable Control Design Principles with Application to the F100 Turbofan Engine", Proceedings JACC, July 1976, pp 113-116.

6. Beattie, E. C. and Spock, W. R., "Application of Multivariable Optimal Control Techniques to a Variable Area Turbine Engine,"Proceedings JACC, July 1976, pp 124 - 132.

7. Stone, C. R., Miller, N.E., Ward, M. D., Schmidt, R. D., Turbine Engine Control Synthesis, "Report AFAPL-TR-75, March 1975.

8. Rosenbrock, H. H., State Space and Multivariable Theory, John Wiley, New York, 1970.

9. MacFarlane, A.G.J., "Relationships Between Recent Developments in Linear Control Theory and Classical Design Techniques, "University of Manchester Institute of Science and Technology, Manchester M60 IQD, England.

10. Horowitz, I. M., Synthesis of Feedback Systems, Academic Press, New York, 1963.

11. Horowitz, I. M., and Shaked, U., "Superiority of Transfer Function Over State Variable Methods in Linear Time-Invariant Feedback System Design," IEEE Transaction on Automatic Control, Vol. AC-20, No. 1, February 1975.

12. Sain, M. K., "A Free-Modular Algorithm for Minimal Design of Linear Multivariable Systems, "Preprint, Sixth IFAC World Congress, Part 1B, paper No. 9.1 August 1975.

13. Leake, R. J., Peczkowski, J. L., Sain, M. K., "Output Regulatability of Linear Multivariable Plants," in preparation.

14. Freeman, H., A Synthesis Method for Multipole Control Systems, AIEE Trans. on Applications and Industry, Vol. 76, Pt. 11, pp 28-31, March 1957.

15. Kavanagh, R. J., "Noninteracting Controls in Linear Multivariable Systems," Trans. on Applications and Industry, Vol. 76, Pt. 11, pp 95-99, May 1957.

16. Freeman, H., "Stability and Physical Realizeability Considerations in the Synthesis of Multipole Control Systems", AIEE Trans. on Applications and Industry, Vol. 77, Pt. 11, pp 1-5, March 1958.

17. Kavanagh, R. J., "Multivariable Control System Synthesis", AIEE Trans. on Applications and Industry, Vol. 77, Pt. 11, pp 425 -429, November 1958.

18. Boksenbom, A. S. and Hood, R., "General Algebraic Method Applied to Central Analysis of Complex Engine Types", NACA Technical Note 1908, National Advisory Committee for Aeronautics, Washington, D. C., July 1949.

19. Feder, M. S., and Hood, R., " Analysis for Control Application of Dynamic Characteristics of Turbojet Engine with Tail-Pipe Burning", NACA Technical Note 2183, Washington, D. C., September 1950.

20. Sain, M. K., "The Growing Algebraic Presence in Systems Engineering: An Introduction," IEEE Proceedings, Vol. 64, No. 1, pp 96-111, January 1976.

21. Sain, M. K., "A Free-Modular Algorithm for Minimal Design of Linear Multivariable Systems," Proc. IFAC 6th World Congress, Part IB, pp 9.1 - 1 - 9.1-7, August 1975.

22. Gejji, R. R., and Sain, M. K., " Application of Polynomial Techniques to Multivariable Control of Jet Engines," Preprints 4th IFAC Symp. on Multivariable Technological Systems," pp 421-430, July 1977

23. Weinberg, M. S. and Adams, G. R., "Low Order Linearized Models of Turbine Engines", Technical Report ASD-TR-75-24, Aeronautical Systems Division, Wright-Patterson Air Force Base, Ohio, July 1975.

CARDIAD DESIGN: PROGRESS IN THE FOUR INPUT/OUTPUT CASE*

R.M. SCHAFER AND M.K. SAIN
Department of Electrical Engineering
University of Notre Dame
Notre Dame, Indiana 46556

ABSTRACT

The CARDIAD (Complex Acceptability Region for DIAgonal Dominance) plot has been shown to be a successful technique for achieving dominance in multivariable control systems with 2 and 3 inputs and outputs [1]. This note reports on success in applying the method to a 4 input-output jet engine model.

The CARDIAD plot is a graphical technique which achieves dominance using only input compensation. The form of the compensator used has 1's on the main diagonal and general complex entries off the diagonal. At a given frequency, a sufficient condition for dominance in a column of the system can be expressed as a quadratic function of the system evaluated at the frequency with the off-diagonal entries of the compensator as variables. To achieve dominance, the function must be made positive.

Two types of analysis are performed on the dominance function. Type 1 analysis maximizes the function assuming all but one of the off-diagonal entries in the compensator are zero. In this approach, it is attempted to achieve dominance using only one nonzero off-diagonal entry in the compensator. Type 2 analysis finds the gradient of the function, and all off-diagonal entries in the column are used to achieve dominance.

At each frequency of analysis, a solid circle, a dashed circle, or a triangle is plotted for each off-diagonal entry of the compensator. A solid circle is drawn when the acceptable choices of the entry lie inside the circle, and a dashed circle is drawn when the acceptable region is outside the circle. If a triangle is drawn, no value in the entry will achieve dominance at that frequency. The analysis is repeated over a range of frequencies, resulting in a CARDIAD plot.

If no triangles occur in the CARDIAD plot of an entry, that column of the system can be made dominant by choosing for that entry a function which lies inside the solid circles or outside the dashed circles at each frequency. If there exists a point on the real axis which is inside all solid circles and outside all dashed circles, constant compensation will achieve dominance. If no such point exists, the plot indicates the proper choice of the function by describing its path through the complex plane. In the case where all off-diagonal entries contain triangles, and hence no one entry is able to achieve dominance, all entries must be designed to fit the shape of the path through the complex plane described by the triangles in the type 2 analysis plots.

CARDIAD is a graphical technique which preserves much of the insight in the design procedure. The plots readily predict whether constant compensation can be used, what values work if it can, and what the frequency dependent compensation should look like if constant compensation won't work. Typical of this case is a plot which has solid circles forming a semi-circular plot in the complex plane. A function of the form $k_{ij}(s)=\{\alpha+\beta s\}/\{1+\delta s\}$ can be chosen by fitting the function at points on the plot.

*This work was supported by NASA Grant NSG 3048.

1. R.M. Schafer and M.K. Sain, "Input Compensation for Dominance of Turbofan Models", in Alternatives for Linear Multivariable Control, National Engineering Consortium, 1978, pp. 156-169.

+14515

NASA Conference Publication 2137

Propulsion Controls, 1979

Proceedings of a symposium held at Lewis Research Center Cleveland, Ohio May 17-19, 1979

NASA

ALTERNATIVES FOR JET ENGINE CONTROL*

Michael K. Sain and R. Michael Schafer**
University of Notre Dame

SUMMARY

The general purpose of these studies has been to evaluate alternatives to linear quadratic regulator theory in the linear case and to examine nonlinear modelling and optimization approaches for global control. Context for the studies has been set by the DYNGEN digital simulator and by models generated for various phases of the F100 Multivariable Control Synthesis Program. With respect to the linear alternatives, studies have stressed the multivariable frequency domain. Progress has been made in both the direct algebraic approach to exact model matching, by means of stimulating work on the basic computational issues, and in the indirect generalized Nyquist approach, with the development of a new design idea called the CARDIAD method. (The acronym stands for Complex Acceptability Region for DIAgonal Dominance.) With respect to nonlinear modelling and optimization, the emphasis has been twofold: to develop analytical nonlinear models of the jet engine and to use these models in conjunction with techniques of mathematical programming in order to study global control over non-incremental portions of the flight envelope. A hierarchy of models has been developed, with present work focused upon the possibility of using tensor methods. A number of these models have been used in time optimal control studies involving DYNGEN.

INTRODUCTION

The decade of the 1970s has coincided with the beginning of yet another round of substantial development in the jet engine industry. A notable factor involved with this stage of modern engine evolution has been the inevitable growing interest in better and better performance, which in turn placed more and more demands upon the application of classical hydromechanical control technique as the primary base technology for engine design. Fortunately, milestone developments in digital hardware began to offer realistic opportunities for onboard computation in ways not heretofore possible. The combination of these two events pointed the way to a concept of increasing the role of electronics in engine control. In turn, this created a variety of new possibili-

*This work was supported in part by the National Aeronautics and Space Administration under Grant NSG-3048.

**It is a pleasure to acknowledge the many hours contributed by our colleague, Dr. R. Jeffrey Leake, who is no longer associated with this effort.

ties for application of recent theories of control design. The F100 Multivariable Control Synthesis Program (ref. 1) sponsored by the National Aeronautics and Space Administration, Lewis Research Center, and the Air Force Aero-Propulsion Laboratory, Wright-Patterson Air Force Base, is a major example. In the linear case, the primary tool employed was linear quadratic regulator (LQR) theory; in the nonlinear case, optimal control methods were not directly applied.

The purpose of these studies has been to evaluate alternatives to LQR in the linear case and to examine nonlinear modelling and optimization for global control in the nonlinear case.

CONTEXT OF THE STUDIES

Evaluation of various theories for control alternatives has taken place using linearized models related to the F100 Multivariable Control Synthesis Program and using the DYNGEN digital simulator (ref. 2). DYNGEN has the combined capabilities of GENENG (ref. 3) and GENENG II (ref. 4), together with an added capability for calculating transient performance. The DYNGEN digital simulation is particularized to a given situation by a process of loading data for the various maps associated with a given engine. The maps for these studies have been provided by engineering personnel at Lewis Research Center. These maps correspond to a hypothetical engine which is not closely identified with any current engine. But the data do correspond in a broad, general sense to realistic two spool turbofan engines. The simulation provides for two essential controls, main burner fuel flow and jet exhaust area. Portions of the envelope which can be used for linear or nonlinear experimentation are a function of the convergence properties of the DYNGEN algorithm as interfaced with the given engine data load.

MULTIVARIABLE FREQUENCY DOMAIN STUDIES

Modern studies of control in the multivariable frequency domain display various faces in various contexts. Here it is convenient to classify these as "direct" or "indirect".

The direct approach can usually be recognized by its attention to achieving completely specified dynamic performance. The idea is classical (refs. 5-6). In fact, some of the earliest attempts to expand the direct approach to the multi-input, multi-output case involved work with jet engines (refs. 7-8). As is apparent from reference 7, there is an unfailing tendency to call these methods algebraic in nature. That tendency persists to this day, when direct approaches in multivariable applications typically involve solution for compensations described by matrices of transfer functions, with the solutions often requiring the algebra of modules over rings of polynomials or stable rational functions.

The indirect approaches are usually recognizable by their relation to the classic work of Nyquist. Here the key equation is often written in the manner

$$p_{CL}(s) = |M(s)|\, p_{OL}(s),$$

where $p_{CL}(s)$ is the closed loop characteristic polynomial, $p_{OL}(s)$ is the open loop characteristic polynomial, $M(s)$ is the matrix return difference, and $|\cdot|$ denotes determinant. This very fundamental equation permits an essential generalization of the classical Nyquist idea, for $p_{CL}(s)$ can be used to characterize the exponentials involved in closed loop control. Basically, a Nyquist plot of $|M(s)|$ tends to contain the same type of information which proved so useful in classical design. A great deal of the design effort centers upon the way in which dynamical compensation affects the determinant which acts on $M(s)$. There are three well recognized ways to study this effect. These are (1) direct construction of $|M(s)|$ by any of the known methods for determinant calculation; (2) construction of the eigenvalues of $M(s)$ as a function of s, and use of the idea that the determinant is equal to the product of its eigenvalues (ref. 9); and (3) design of compensation so that $M(s)$ is approximately diagonal, with concomitant development of a relation between the Nyquist plot of $|M(s)|$ and plots of the diagonal elements of $M(s)$, as in reference 10.

THE DIRECT APPROACH

With regard to the direct approach, a substantial case study of exact model mathcing (ref. 11) has been carried out.

The exact model matching problem can be phrased as follows. Let $R(s)$ denote the field of rational functions in s and with coefficients from the real number field R. Further, let V_1, V_2, and V_3 be finite-dimensional vector spaces over the field $R(s)$. Finally, let

$$G_1 : V_2 \to V_3$$

and

$$G_2 : V_1 \to V_3$$

be given linear transformations on one vector space to another. Then the exact model matching problem is to find linear transformations

$$G : V_1 \to V_2$$

of vector spaces, if they exist, such that

$$G_1 G = G_2.$$

In a control problem, G_1 and G_2 are functions of the plant, the complete

closed loop specifications, and the configuration chosen for the controller. The unknown G embodies the dynamics involved in the controller, relative to a fixed configuration of control.

The basic plant was a version of the F100 turbofan engine. Inputs were jet exhaust area and main burner fuel flow; states were fan inlet temperature, main burner pressure, fan speed, high compressor speed, and afterburner pressure; and outputs were thrust and high turbine inlet temperature. The linearized model approximated the small signal behavior of these engine variables in a neighborhood of 47° PLA.

Insofar as the authors are presently aware, this study represents one of the most elaborate exact model matching studies undertaken to date in the literature. Moreover, it is entirely in the spirit of the introductory work in references 7-8.

Technically, the mathematical framework was set up in terms of polynomial modules. The problem formulation itself has been recorded in reference 12, where it can serve as a comparison point for future algorithms. The computer algorithms implemented were those promulgated in the literature at that time (ref. 13).

These studies established several basic conclusions relative to the direct method:

(1) the direct method was of interest in jet engine control (indeed, had been proposed in industrial studies);

(2) the jet engine control problems typical of the 1970s were of sufficient size and complexity to overtax the routine solution procedures being mentioned in the literature at that time; and

(3) a substantial influx of ideas from the literature on numerical methods would be necessary before the direct method could be applied for jet engine control.

It is a pleasure to report that these results did indeed lead to the desired influx, so that computations of sufficient accuracy can now be made in seconds. Efforts involving the direct method are now being directed at the problem of making convenient specifications.

THE INDIRECT APPROACH

Though some efforts (ref. 14) were directed toward the evaluation of the eigenvalue approach (ref. 9) to $|M(s)|$, the major attention under the indirect approach classification in these studies was directed toward the idea of designing dynamical compensation so as to make $M(s)$ approximately diagonal in a way that would be useful in Nyquist studies.

Because of the indirect way in which compensation has an effect on $|M(s)|$, Nyquist analysis of $|M(s)|$ may be of little use to the designer for other than stability determination, for even the simplest systems. In the event that $M(s)$ is diagonal, design and stability considerations are reduced to a set of single input, single output problems, with net angular behavior of $|M(s)|$ being a consequence of summing the individual net behaviors of the diagonal entries.

Rosenbrock (ref. 10) has introduced the idea of diagonal dominance, which can be regarded as an approximate form of diagonality. An mxm matrix $Z(s)$ over $R(s)$ is said to be diagonally column dominant if for all $s \in D$ the Nyquist contour and for $i = 1,2,\ldots,m$

$$|z_{ii}(s)| > \sum_{\substack{j=1 \\ j \neq i}}^{m} |z_{ji}(s)|$$

Rosenbrock shows that, if a matrix $M(s)$ is diagonally column dominant, the net angular behavior of $|M(s)|$ on D can be inferred from that of $\{m_{ii}(s)\}$ on D. Thus the class of matrices for which design and stability analysis may be performed on only the diagonal entries is expanded from diagonal matrices to matrices which are diagonally dominant.

Efforts in these studies have focused upon methods to design compensation in order to achieve diagonal dominance.

The procedure which has been developed is called the CARDIAD method, where the acronym stands for Complex Acceptability Region for DIAgonal Dominance. The CARDIAD idea can be visualized as follows. Consider a unity negative feedback configuration with the mxm plant matrix $G(s)$ preceded by an mxm compensation matrix $K(s)$, both over $R(s)$. Except for renumbering of inputs, the design of $K(s)$ to achieve diagonal dominance may be restricted to $K(s)$ matrices having the unit transfer function 1 in each main diagonal position. This fact is an easy consequence of Rosenbrock's definition. In the CARDIAD approach, a sufficient condition for dominance in the ith column of

$$M(s) = I + G(s)K(s)$$

say, at a particular frequency $s \in D$, is expressed by a quadratic inequality of the type

$$f_i(v) = \langle v, Av \rangle + \langle v, b \rangle + c > 0$$

Here v is a vector in the real space R^{2m-2}, consisting of a list of the real and imaginary parts of the off-diagonal entries in the ith column of $K(s)$ at the particular frequency $s \in D$, $\langle \cdot, \cdot \rangle$ is the usual inner product, A is an Hermitian linear map, $b \in R^{2m-2}$, and $c \in R$. A, b, and c are functions of $G(s)$.

Several different approaches are used to choose v so that $f_i(v)$ is

positive. These are described in detail by references 15-22. References 15-17 deal primarily with engine models having two inputs and two outputs; reference 18 focuses on a three input/output case; and references 6-8 treat four input/output situations.

The basic idea of a CARDIAD plot is easy to understand in the two input/output case. The compensation takes a form

$$\begin{bmatrix} 1 & x_2(s) + jy_2(s) \\ x_1(s) + jy_1(s) & 1 \end{bmatrix}$$

where for $i = 1,2$

$$x_i : D \to R$$

$$y_i : D \to R$$

are the functions defining the real and imaginary parts of the off-diagonal entries in column i. The quadratic inequality can be set equal to its limiting value

$$f_i(x_i(s),y_i(s)) = 0 ,$$

which defines a circle on R^2 with coordinates (x_i,y_i). For a particular $s \in D$, a solid circle is drawn on R^2 if (x_i,y_i) pairs inside the circle satisfy the inequality; and a dashed circle is drawn on R^2 if (x_i,y_i) pairs outside the circle satisfy the inequality. As s traverses D, these circles generate a CARDIAD "plot" on R^2. The plot is essentially a set of requirements, in graphical form, which are necessary and sufficient for compensator design to achieve dominance in the configuration described above.

When $m > 2$, various additional strategies are brought into play. These are described in some detail in the references.

NONLINEAR MODELLING AND OPTIMIZATION

With respect to nonlinear modelling and optimization, the emphasis has been twofold; to develop analytical nonlinear models of the jet engine deck and to use these models in conjunction with techniques of mathematical programming in order to study global control over non-incremental reaches of the flight envelope. The context for such studies has been established by DYNGEN, as described above.

The first method of modelling which was considered was that of analytical construction of the equations from the basic physical principles. In this case, there were sixteen nonlinear differential equations, as well as a large number of nonlinear static functions which provided additional coupling among the

equations. Such a procedure then requires determination of parameters in the equations. A number of these parameters have very definite physical meanings, and these meanings were supplemented by simulation data when appropriate. Obtaining tractable models for the engine in this way, though promising from the point of view of physical insight, did not lead to very much mathematical insight. Subsequently, therefore, this method gave way to the following.

The second method of modelling placed increased emphasis upon the mathematical structure of the equations, with determination of parameters being done automatically from simulator data. A highlight of this part of the study was the development of the model class

$$\dot{x} = A(x)\ (x-g(u))$$

where $x \in R^n$, $u \in R^p$. The function g is arranged so as to satisfy the set-point or steady-state features of the engine deck, while the operator

$$A : R^n \to R^n$$

is useful to adjust the transient behavior of the model. The particulars of this idea were described in reference 23.

A number of possibilities exist for approaching the approximation of $A(x)$ and $g(u)$. One additional method and application has been presented in reference 24.

At this point in time, a new stage in the nonlinear modelling studies is being initiated. In this phase, extensive use will be made of the methods of multilinear algebra, specifically the theory of algebraic tensors.

Models of the types evolved in phases one and two have been used in time-optimal control studies. Results of these efforts have been written down in references 25-27.

CONCLUDING REMARKS

This brief paper has sketched a number of control alternatives which have been studied recently in the context of the DYNGEN digital engine simulator and of linear models deriving from the F100 Multivariable Control Synthesis Program. In the linear case, these studies have focused on alternatives to the linear quadratic regulator theory employed in that Program. In the nonlinear case, emphasis has been placed on nonlinear modelling and time-optimal control.

Principal results reported have been the case study on exact model matching, which has stimulated considerable new work in that problem area, the development of the CARDIAD plot as a design tool for generalized Nyquist work, and the introduction of a nonlinear model class which is proving to be helpful in recent engine design studies.

Present thrust in this work is toward the use of multilinear algebra for generalized nonlinear modelling.

Finally, the reader may be interested in the fact that the National Engineering Consortium sponsored an International Forum on Alternatives for Linear Multivariable Control in Chicago during October 1977. Authors in that meeting were asked to address a Theme Problem based upon F100 data. Two publications resulted, one a proceedings and one a hardbound book. Reference 23 is to the proceedings, while reference 18 is to the book. Much additional information may be found in those volumes.

REFERENCES

1. DeHoff, R.L.; Hall, W. Earl, Jr.; Adams, R.J.; and Gupta, N.K.: F100 Multivariable Control Synthesis Program. AFAPL-TR-77-35, June 1977.

2. Sellers, J.F.; and Daniele, C.J.: DYNGEN-A Program for Calculating Steady-State and Transient Performance of Turbojet and Turbofan Engines. NASA TN D-7901, April 1975.

3. Koenig, R.W.; and Fishbach, L.H.: GENENG-A Program for Calculating Design and Off-Design Performance for Turbojet and Turbofan Engines. NASA TN D-6552, February 1972.

4. Fishbach, L.H.; and Koenig, R.W.: GENENG II-A Program for Calculating Design and Off-Design Performance of Two and Three Spool Turbofans with as Many as Three Nozzles. NASA TN D-6553, February 1972.

5. Truxal, J.G.: Automatic Feedback Control Systems Synthesis. McGraw-Hill, 1955.

6. Horowitz, I.M.: Synthesis of Feedback Systems. Academic Press, 1963.

7. Boksenbom, A.S.; and Hood, R.: General Algebraic Method Applied to Control Analysis of Complex Engine Types. NACA TN 1908, July 1949.

8. Feder, M.S.; and Hood, R.: Analysis for Control Application of Dynamic Characteristics of a Turbojet Engine with Tail-Pipe Burning. NACA TN 2183, September 1950.

9. MacFarlane, A.G.J.; and Postlethwaite, I.: Characteristic Frequency Functions and Characteristic Gain Functions. Int. J. Control, vol. 26, 1977, pp. 265-278.

10. Rosenbrock, H.H.: Computer-Aided Control System Design. Academic Press, 1974.

11. Gejji, R.R.; and Sain, M.K.: Application of Polynomial Techniques to Multivariable Control of Jet Engines. 4th IFAC Symp. Mult. Tech. Syst.,

1977, pp. 421-429.

12. Gejji, R.R.; and Sain, M.K.: A Jet Engine Control Problem for Evaluating Minimal Design Software. Midwest Symp. Circuits & Syst., August 1976, pp. 238-243.

13. Gejji, R.R.: A Computer Program to Find the Kernel of a Polynomial Operator. 14th Allerton Conf., September 1976, pp. 1091-1100.

14. Seshadri, V.; and Sain, M.K.: Interaction Studies on a Jet Engine Model by Characteristic Methodologies. Midwest Symp. Circuits & Syst., August 1976, pp. 232-237.

15. Schafer, R.M.: A Graphical Approach to System Dominance. M.S. Thesis, Dept. Elec. Eng., Univ. Notre Dame, May 1977.

16. Schafer, R.M.; Gejji, R.R.; Hoppner, P.W.; Longenbaker, W.E.; and Sain, M.K.: Frequency Domain Compensation of a DYNGEN Turbofan Engine Model. 1977 JACC, pp. 1013-1018.

17. Gejji, R.R.; Schafer, R.M.; Sain, M.K.; and Hoppner, P.W.: A Comparison of Frequency Domain Techniques for Jet Engine Control. Midwest Symp. Circuits & Syst., August 1977, pp. 680-685.

18. Schafer, R.M.; and Sain, M.K.: Input Compensation for Dominance of Turbofan Models. Alternatives for Linear Multivariable Control (Sain, M.K.; Peczkowski, J.L.; and Melsa, J.L.; eds.), Nat'l. Eng. Consortium, 1977, pp. 156-159.

19. Schafer, R.M.; and Sain, M.K.: Some Features of CARDIAD Plots for System Dominance. 16th IEEE CDC, pp. 801-806.

20. Schafer, R.M.; and Sain, M.K.: CARDIAD Design: Progress in the Four Input/Output Case. 16th Allerton Conf., October 1978, p. 567.

21. Schafer, R.M.; and Sain, M.K.: Frequency Dependent Precompensation for Dominance in a Four Input/Output Theme Problem Model. 1979 JACC, pp. 348-353.

22. Schafer, R.M.; and Sain, M.K.: CARDIAD Approach to System Dominance with Application to Turbofan Engine Models. 13th Asilomar Conf., November 1979.

23. Leake, R.J.; and Comiskey, J.G.: A Direct Method for Obtaining Nonlinear Analytical Models of a Jet Engine. NEC Forum on Alternatives for Multivariable Control, pp. 203-212.

24. Rock, S.M.; and DeHoff, R.L.: Applications of Multivariable Control to Advanced Aircraft Turbine Engines. 1979 Propulsion Controls Symposium.

25. Basso, R.; and Leake, R.J.: Computational Alternatives to Obtain Time-Optimal Jet Engine Control. 14th Allerton Conf., September 1976, pp. 652-661.

26. Longenbaker, W.E.; and Leake, R.J.: Time Optimal Control of a Two-Spool Turbofan Jet Engine. M.S. Thesis, Univ. Notre Dame, September 1977.

27. Comiskey, J.G.: Time Optimal Control of a Jet Engine Using a Quasi-Hermite Interpolation Model. M.S. Thesis, Univ. Notre Dame, May 1979.

MULTIVARIABLE SYNTHESIS WITH INVERSES

J.L. Peczkowski
Energy Controls Division
Bendix Corporation
South Bend, Indiana 46620

M.K. Sain
Dept. Electrical Engineering
University of Notre Dame
Notre Dame, Indiana 46556

R.J. Leake
School of Engineering
California State University
Fresno, California 93740

Abstract

In this paper, we illustrate the application of total synthesis (TS) methods to the design of controller dynamics for linear multivariable models of realistic turbine engine simulations. TS methods provide the designer with a capability to specify thoroughly and directly the nominal dynamic relationship between command or request variables and controlled or response variables. Under reasonable assumptions, this capability can include transient response as well as limiting values, and of course internal stability. We place particular stress upon the inverse total synthesis problem (ITSP), which emphasizes the inverse of the plant input/output relation, expressed typically as a matrix of transfer functions. In numerous case studies, the ITS approach has shown an ability to preserve designer insight and influence, and has turned out to be relatively easy to understand——both properties of importance for general control applications.

INTRODUCTION

In this paper, we consider the design of controller dynamics for linear multivariable models of realistic turbine engine simulations. Our approach emphasizes the inverse of the plant input/output relation, expressed as a matrix of transfer functions.

Control system design methods in the frequency domain have traditionally been of two types. In the case of the first type, the designer does not progress directly from system performance specifications to a satisfactory control system. Instead, the designer works to modify and adjust open loop characteristics so that, when the loop is closed, an "acceptable" system results. In the case of the second type, the designer does proceed directly from the outside, closed loop specifications inward to the particular controller involved. A classical discussion of both methodologies may be read in Truxal [1]. We shall refer to the second type of method as a synthesis method.

INVERSE TOTAL SYNTHESIS

Synthesis methods have continued to receive study over the last quarter century. A brief indication of the main ideas can be sketched as follows. Consider Figure 1, where r denotes request, u denotes control action, and y denotes

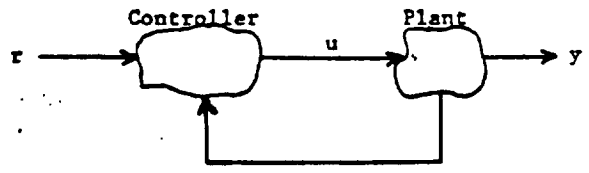

Figure 1. A General Control System.

response. Under broad assumptions, there exist linear operators $T : R \to Y$ and $M : R \to U$, where R, U, and Y may be understood as R(s)-vector spaces of finite dimension, such that

$$y = Tr \quad , \quad u = Mr.$$

The plant, in turn, can be understood in terms of an operator $P : U \to Y$, such that

$$y = Pu.$$

For internal stability of the loop in Figure 1, it is clear that M must be stable in the usual sense. Less immediately obvious but also true is the fact that M must be realizable as a linear dynamical system in order for the control system of Figure 1 to be realizable around P. The usual synthesis problem in recent years has been the exact model matching problem (EMMP), which is pictured in Figure 2a. In EMMP, T and P are given (solid lines) and

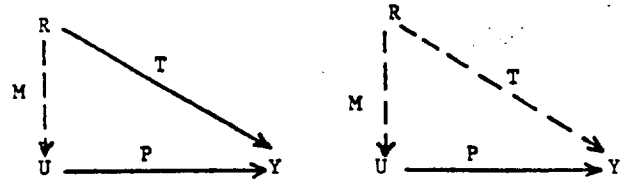

(a) EMMP (b) TSP

Figure 2. Synthesis Problems.

M is to be synthesized (dotted line) so that the diagram of Figure 2a commutes. This paper focuses upon TSP, the total synthesis problem, in which P is given, and T and M are to be found so that the diagram of Figure 2b commutes.

If a tracking requirement is present, as for example that y should asymptotically track arbitrary step requests, then P must be epic. If in addition it is assumed that the dimensions of U and Y are the same, as would occur if controls had been preconditioned, then P is monic also; and we can address the inverse total synthesis problem (ITSP), which is governed by the synthesis equation

$$M = P^{-1} T$$

and which is visualized in Figure 3. ITSP is particularly convenient as a synthesis tool because the multivariable zeros of P are the poles of P^{-1}.

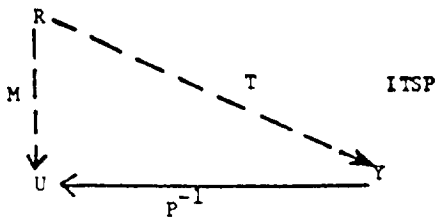

Figure 3. Inverse Total Synthesis Problem.

The idea is to select M and T so that the ITSP diagram commutes and so that M and T are proper and stable.

Feedback realizations of M, such as those indicated in Figures 4 and 11, can be obtained by performing the mapping $T \to Q$, where Q is PG in Figure 4 and is PAG in Figure 11. There are then counterparts

$$G = P^{-1} Q \quad , \quad G = A^{-1} P^{-1} Q$$

of the synthesis equation, which we call the controller dynamics design equation. We refer to Q as the performance matrix.

Though space is limited, we illustrate these ideas with four examples.

EXAMPLES

A single spool turbojet engine model is used in the next three examples to illustrate different aspects of transfer function design: decoupling, nondecoupling, and right half plane zeros. The engine model is due to Skira and DeHoff [2]. A state description of the turbojet is

$$\dot{x} = Ax + Bu$$
$$y = Cx + Du,$$

where

$$A = \begin{bmatrix} -1 & -.5 \\ 10 & -5 \end{bmatrix} \quad B = \begin{bmatrix} 2 & .5 \\ 0 & -1 \end{bmatrix} \quad C = \begin{bmatrix} .1 & 18 \\ .06 & 0 \end{bmatrix}$$

$$D = \begin{bmatrix} 0 & 0 \\ .46 & 0 \end{bmatrix}$$

u_1 = fuel flow rate, PPH
u_2 = exhaust nozzle area, IN^2
x_1 = rotor speed, RPM
x_2 = tailpipe pressure, PSI
y_1 = thrust, LBS
y_2 = turbine temperature, °R.

Example 1. Decoupled Response. A closed loop controller is desired to decouple the states x_1 - rotor speed and x_2 - tailpipe pressure. Response specifications require zero steady state error to step inputs and settling time in one second. Assume that fast sensors are available to measure the states. The problem may be pictured by the diagram in Figure 4 below.

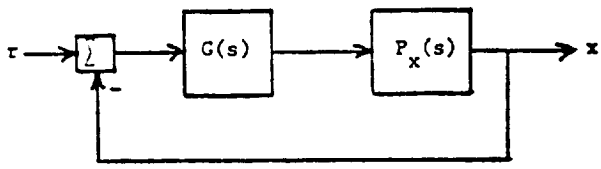

Figure 4. Unity Feedback Structure.

The transfer function matrix of the engine, in factored form, is

$$P_x = (sI-A)^{-1}B = \frac{\begin{bmatrix} 1.0(.2s+1) & .3(.17s+1) \\ 2.0 & .4(-.25s+1) \end{bmatrix}}{.1s^2+.6s+1}$$

The plant inverse matrix is

$$P_x^{-1} = \begin{bmatrix} -2.0(-.25s+1) & 1.5(.17s+1) \\ 10 & -5.0(.2s+1) \end{bmatrix}.$$

The plant has no zeros. Thus from P and P^{-1} is seen that the plant is stable and has no multivariable zeros; and it is possible to shape the response of the states.

From the response specifications, the response matrix T must produce:

- decoupled closed loop response (diagonal)
- response essentially equal to a.2 second time constant
- no steady state error (gain=1).

Thus a desired response matrix is assumed to be

$$T = \begin{bmatrix} \frac{1}{.2s+1} & 0 \\ 0 & \frac{1}{.2s+1} \end{bmatrix}.$$

Note that this simple form of T is consistent with the synthesis equation $M = P^{-1}T$ and the condition that M be stable and proper. For unity feedback, $Q = T(I-T)^{-1}$; thus if T is diagonal, Q is diagonal. The design equation $G = P^{-1}Q$ now displays the controller dynamics

$$G = P_x^{-1}Q = \begin{bmatrix} -2.0(-.25s+1) & q_{11}(s) & 1.5(.17s+1) & q_{22}(s) \\ 10 & q_{11}(s) & -5.0(.2s+1) & q_{22}(s) \end{bmatrix}$$

Since $q_{11}=q_{22}=5/s$, we immediately obtain the realizable, integral controller

$$G(s) = \begin{bmatrix} \frac{-10(-.25s+1)}{s} & \frac{7.5(.17s+1)}{s} \\ \frac{50}{s} & \frac{-25(.2s+1)}{s} \end{bmatrix}.$$

Computer simulation of the closed loop verifies the result. Figures 5 and 6 show the response of the closed loop system for step input requests of 500 RPM rotor speed and 5 PSI tail pipe pressure respectively.

Since Q is diagonal when T is diagonal, it is easy to alter the time constants of the response by adjusting of the gains in the columns of G(s). For example, if the desired response is

$$T(s) = \begin{bmatrix} \frac{1}{.4s+1} & 0 \\ 0 & \frac{1}{.3s+1} \end{bmatrix},$$

then $q_{11}=\frac{2.5}{s}$ and $q_{22}=\frac{3.33}{s}$; and

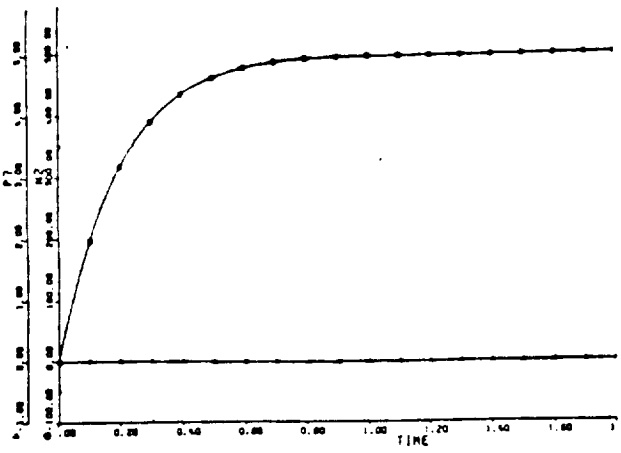

Figure 5. System Response to 500 RPM Step Request of Rotor Speed.

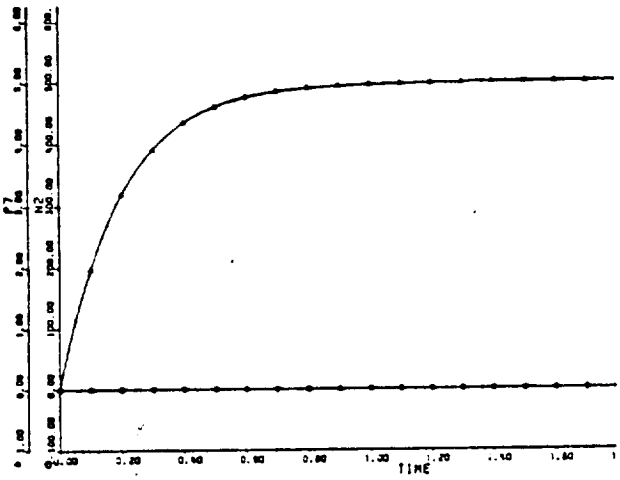

Figure 6. System Response to 5 PSI Step Request of Tailpipe Pressure.

$$G(s) = \begin{bmatrix} \frac{-5(-.25s+1)}{s} & \frac{5(.17s+1)}{s} \\ \frac{25}{s} & \frac{-16.7(.2s+1)}{s} \end{bmatrix} .$$

Many other response and controller possibilities are displayed for the designer by the design equation $G = P^{-1}Q$.

Example 2. Nondecoupled Response. This example illustrates that the synthesis method and design equation are not restricted only to decoupled systems. Suppose that the closed loop state response of the engine was required by design considerations to be

$$T = \begin{bmatrix} \frac{.6}{.2s+1} & \frac{40}{.2s+1} \\ 0 & \frac{.5}{.2s+1} \end{bmatrix} .$$

Also, assume that a unity feedback structure is desired as in Example 1.

First note that T satisfies the stability and properness conditions of the synthesis equation $M=P^{-1}T$. For unity feedback, we again have $Q=T(I-T)^{-1}$. The controller dynamics are given by the design equation $G = P_x^{-1}Q$

$$G = \begin{bmatrix} -2(-.25s+1) & 1.5(.17s+1) & \frac{1.5}{.5s+1} & \frac{200(.2s+1)}{(.4s+1)(.5s+1)} \\ 10 & -5(.2s+1) & 0 & \frac{1}{.4s+1} \end{bmatrix}$$

where P_x is taken from Example 1. Matrix multiplication gives

$$G = \begin{bmatrix} \frac{-3(-.25s+1)}{(.5s+1)} & \frac{-398.5(-.25s+1)(.2s+1)}{(.4s+1)(.5s+1)} \\ \frac{15}{(.5s+1)} & \frac{1995(.2s+1)(-.001s+1)}{(.4s+1)(.5s+1)} \end{bmatrix} .$$

Computer simulation of the closed loop verifies that the desired response T is achieved. Figure 7 shows the response of the closed loop to a step request of 500 RPM rotor speed. Note that the speed responds to 300 RPM (gain = .6) with a time constant of .2 seconds while the pressure response is zero as required by T. Figure 8 pictures the response of the system to a 5 PSI step request of tailpipe pressure. The responses match the dynamics corresponding to the second column of T.

This simple example demonstrates the utility of the design equation for a nondecoupled case.

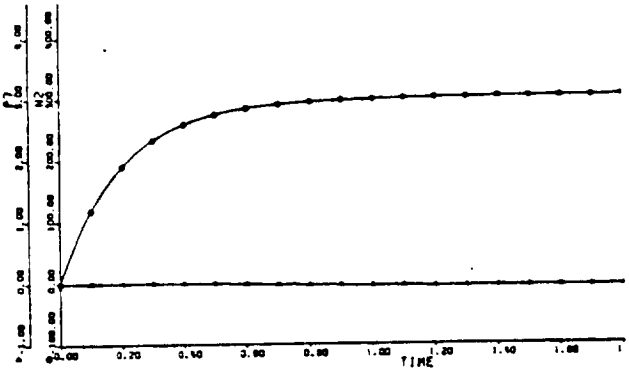

Figure 7. System Response to 500 RPM Step Request of Rotor Speed.

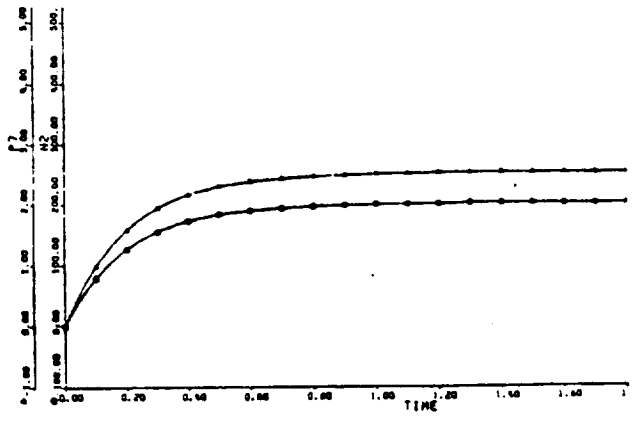

Figure 8. System Response to 5 PSI Step Request of Tailpipe Pressure.

Example 3. Plant rhp Zero. It is desired to control and to decouple the outputs of the turbojet

engine cited above. Response specifications require zero steady state error and settling time of 1.5 seconds. A unity feedback loop structure is desired. Assume that the outputs, y_1-thrust and y_2-turbine temperature, are sensed and available for feedback.

The problem may be pictured by the unity feedback structure in Figure 4 except that the controlled variables are the outputs y instead of the states x. The transfer function matrix of the engine is

$$P=C(sI-A)^{-1}B+D=\begin{bmatrix} 36(.0006s+1) & 7.2(-.25s+1) \\ \dfrac{.52(.088s^2+.55s+1)}{.1s^2+.6s+1} & \dfrac{.018(.17s+1)}{.1s^2+.6s+1} \end{bmatrix};$$

and the plant inverse matrix is

$$P^{-1}=\begin{bmatrix} -.006(.17s+1) & 2.3(-.25s+1) \\ \dfrac{.17(.088s^2+.55s+1)}{(-.27s+1)} & \dfrac{-11.6(.0006s+1)}{(-.27s+1)} \end{bmatrix}.$$

The factored forms of P and P^{-1} clearly indicate that the plant is stable, has a rhp zero at $s=3.7$ and is capable of shaping outputs.

The synthesis equation, $M=P^{-1}T$, requires that a decoupled response matrix T must have the form

$$T=\begin{bmatrix} \dfrac{K_1(-.27s+1)}{(T_1s+1)(T_2s+1)} & 0 \\ 0 & \dfrac{K_2(-.27s+1)}{(T_3s+1)(T_4s+1)} \end{bmatrix}$$

to render M stable and proper. Therefore we choose

$$T=\begin{bmatrix} \dfrac{(-.27s+1)}{(.3s+1)(.05s+1)} & 0 \\ 0 & \dfrac{(-.27s+1)}{(.3s+1)(.05s+1)} \end{bmatrix}.$$

Then the performance matrix is

$$Q(s)=\begin{bmatrix} \dfrac{1.61(-.27s+1)}{s(.02s+1)} & 0 \\ 0 & \dfrac{1.61(-.27s+1)}{s(.02s+1)} \end{bmatrix},$$

and the controller dynamics are given by

$$G=P^{-1}Q=\begin{bmatrix} \dfrac{-.01(.17s+1)}{s(.02s+1)} & \dfrac{3.70(-.25s+1)}{s(.02s+1)} \\ \dfrac{.27(.29s+1)(.29s+1)}{s(.02s+1)} & \dfrac{-18.7}{s(.02s+1)} \end{bmatrix}.$$

Computer simulation of the system verifies the decoupled, closed loop response. The rhp zero of the plant appears in the output response as shown in Figures 9 and 10. This is an inherent characteristic of decoupled systems which is predicted by the synthesis equation $M = P^{-1}T$.

Example 4. F100 Turbofan Engine. An extensive set of linear state descriptions of the F100 turbofan engine were given by Miller and Hackney [3]. The engine is described by the 16th order state models at 20 operating points. In this example a linear model at sea level, 67 degree power lever condition is controlled. The design objective is to decouple and to shape the transient response of sensed engine outputs. This example is given to illustrate a more realistic design situation including engine, actuators and sensors. The use of cancellation to simplify the controller is also illustrated.

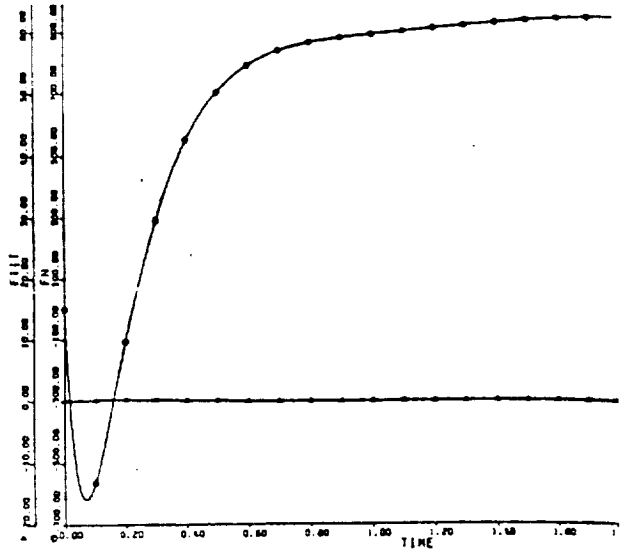

Figure 9. System Response to 1000 LB Step Request of Thrust.

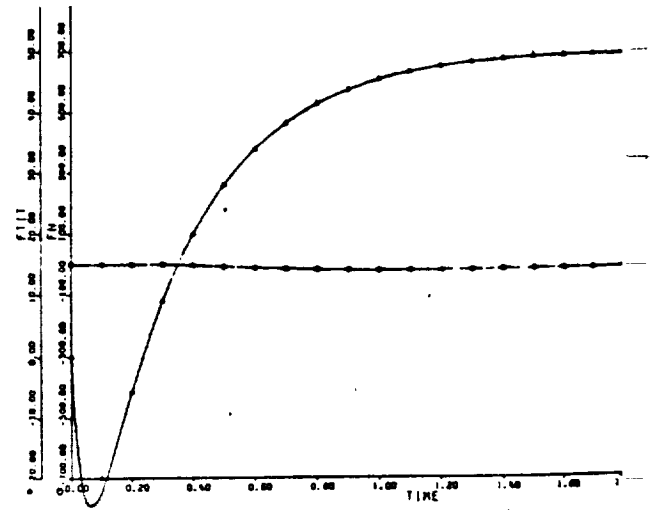

Figure 10. System Response to 50° Step Request of Temperature.

Four primary inputs were identified in the engine model; therefore, the transient responses of four sensed variables are controlled and shaped. A reduced six state engine model [4] is used in the problem. Because of the complexity of the plant, it was necessary to use machine computation for this example. A computer program which handles transfer matrix computations was available to the authors [5].

The reduced state description of the turbofan engine is

$$\dot{x} = Ax + Bu,$$

$$y = Cx + Du,$$

where

$$A = \begin{bmatrix} -4.064 & 3.895 & -470.8 & 7.971 & 8.294 & -3.005 \\ .03718 & -2.958 & -59.13 & .1727 & 2.08 & 12.48 \\ .03389 & .0067 & -4.442 & .0059 & .1474 & .0985 \\ 1.164 & -2.646 & -331.6 & -50.05 & -.473 & -11.36 \\ .05174 & -.1176 & -14.74 & -2.001 & -2.021 & -.505 \\ .00184 & .0036 & -.601 & .00008 & .0008 & -.666 \end{bmatrix}$$

$$B = \begin{bmatrix} .8686 & -14.51 & -96.14 & 9.246 \\ .8096 & -58.46 & -1.053 & -60.15 \\ -.007994 & -79.66 & 1.2 & .3673 \\ 1.643 & -112.2 & -18.23 & 41.53 \\ .2508 & -4.99 & -.8108 & 1.846 \\ .01 & -.3186 & -.02915 & .07426 \end{bmatrix}$$

$$C = \begin{bmatrix} 1 & 0 & 0 & 0 & 0 & 0 \\ 0 & 1 & 0 & 0 & 0 & 0 \\ 0 & 0 & 1 & 0 & 0 & 0 \\ 0 & 0 & 0 & 1 & 1 & 0 \end{bmatrix} \qquad D = \begin{bmatrix} 0 & \cdots & 0 \\ \vdots & \ddots & \vdots \\ 0 & & 0 \end{bmatrix}$$

The states, x, and inputs, u, and sensed outputs, y, are:

$x_1 = N_1$, fan speed, RPM

$x_2 = N_2$, compressor speed, RPM

$x_3 = P_7$, augmentor pressure, PSI

$x_4 = T_{h1}$, fan turbine temperature (fast), °F

$x_5 = T_{lo}$, fan turbine temperature (slow), °F

$x_6 = T$, burner temperature (slow), °F

$u_1 = WF$, fuel flow, PPH

$u_2 = AJ$, exhaust nozzle area, FT^2

$u_3 = CIVV$, inlet vane position, DEG

$u_4 = RCVV$, compressor vane position, DEG

$y_1 = N1$, fan speed, RPM

$y_2 = N_2$, compressor speed, RPM

$y_3 = P_7$, augmentor pressure, PSI

$y_4 = FTIT$, fan turbine inlet temperature, °F.

The system problem can be represented by the feedback structure shown in Figure 11 below.

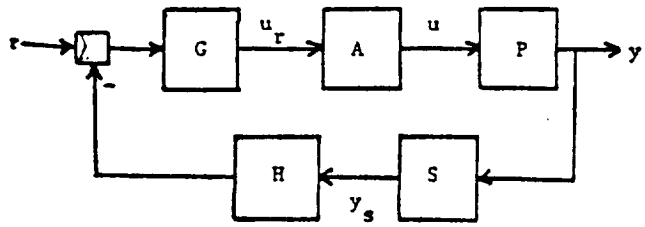

Figure 11. More General Feedback Structure.

The actuator dynamics are defined by $u = Au_r$, where

$$A = \begin{bmatrix} \frac{1}{.05s+1} & 0 & 0 & 0 \\ 0 & \frac{1}{.2s+1} & 0 & 0 \\ 0 & 0 & \frac{1}{.1s+1} & 0 \\ 0 & 0 & 0 & \frac{1}{.1s+1} \end{bmatrix};$$

and the sensor dynamics are defined by $y_s = S\,y$ where

$$S = \begin{bmatrix} \frac{1}{.02s+1} & 0 & 0 & 0 \\ 0 & \frac{1}{.02s+1} & 0 & 0 \\ 0 & 0 & \frac{1}{.02s+1} & 0 \\ 0 & 0 & 0 & \frac{1}{.5s+1} \end{bmatrix}.$$

The transfer matrix of the engine is $P=C(sI-A)^{-1}B+D$ and is shown in Figure 12. The plant inverse matrix is shown in Figure 13. In the figures the abbreviation $(Ts+1)\rightarrow(T)$ and $(a\,s^2+bs+1)\rightarrow(a,b)$ has been employed for simplicity.

The transfer function matrices P and P^{-1}, in factored form, indicate that the plant is stable, the plant has two lhp zeros, (although they both essentially cancel) and that the plant is capable of shaping the four chosen outputs.

Assume that the transient response specifications require that the output response, $y = Tr$, be decoupled, settle in one second and have zero steady state error. Thus T is a diagonal matrix and we shall choose the elements to have gain = 1 and response essentially equal to a .25 time constant. The synthesis equation, $M=A^{-1}P^{-1}T$, indicates that the simplest form for the elements of T is $1/(.25)(*)$ where the time constant of the denominator factor (*) does not significantly affect the one second settling time. We choose (.01); therefore, the response matrix is T=diag $1/(.25)(.01)$.

The controller dynamics design equation is $G=A^{-1}P^{-1}Q$ where $Q=T(I-HST)^{-1}$. Using the above T, A and S and choosing H=I, we find that G, simplified by cancellations and approximations, turns out to be

$$G(s) \approx \frac{\begin{bmatrix} -1.2(.11)(.05) & 3.2(.12)(.05) & 132(.05) & 10(.02)(.05)(.5)/(.16) \\ -.001(.66)(.02) & .002(-.17)(.02) & -.46(.14)(.02) & .004(.01)(.02)(.5)/(.16) \\ -.16(.24)(.1) & .16(-.01)(.1) & -16 (.1) & .21(.01)(.1)(.5)/(.16) \\ -.013(.06)(.1) & -.13(.40)(.1) & -.49(-.06)(.1) & .19(.02)(.1)(.5)/(.16) \end{bmatrix}}{s\,(.01)}.$$

System response using the above controller G and the given A, P, S and H=I matrices was verified by CSMP simulation. The dynamic response and decoupling is shown in Figures 14 and 15 for a step request of 4 PSI P_7 augmentor pressure and 50 degrees FTIT temperature respectively.

$$P = \begin{bmatrix} .409(1.45)(.501)(.301)(.132)(.009) & 1220(1.45)(.494)(.302)(.0175)(-.0064) & -30.6(1.45)(.493)(.302)(.094)(.019) & -10.8(1.41)(.464)(.300)(-.039)(.018 \\ .320(1.24)(.458)(.03,.265)(.019) & 198(1.19)(.486)(.253)(.019)(-.013) & -1.98(.927)(.200,1.08)(.021)(.012) & -10.1(1.50)(.493)(.027,.732)(.029 \\ .0025(1.32)(.483)(.224)(-.131)(021) & -7.80(1.47)(.501)(.341)(.256)(.02) & .024(1.95)(.990)(.475)(.329)(.05) & -.0160(1.63)(-1.41)(.51)(.122)(.02 \\ .095(1.56)(.470)(.377)(.028,.254) & 72.6(1.56)(.470)(.329)(.196)(-.004) & -1.23(1.55)(.470)(.088,.666)(.031) & 1.80(1.54)(.470)(.118)(.035,.144 \end{bmatrix}$$

$$(1.43)(.491)(.302)(.02)(.0297,.238)$$

Figure 12. Plant Matrix.

$$P^{-1} = \begin{bmatrix} -.334(1.55)(.470)(.109) & .897(1.55)(.470)(.119) & 42.0(1.55)(.470)(-.007) & 7.75(1.54)(.500)(.019) \\ -.000245(1.54)(.655)(.470) & .000505(1.54)(.470)(-.172) & -.129(1.55)(.470)(.097) & .00270(1.41)(.462)(.008 \\ -.046(1.55)(.470)(.235) & .0450(1.55)(.470)(-.010) & -4.50(1.55)(.470)(.0003) & .160(1.50)(.489)(.009 \\ -.00350(1.50)(.470)(.081) & -.0365(1.57)(.470)(.403) & -.138(1.50)(.470)(-.056) & .144(1.27)(.491)(.019 \end{bmatrix}$$

$$(1.85)(.470)$$

Figure 13. Plant Inverse Matrix.

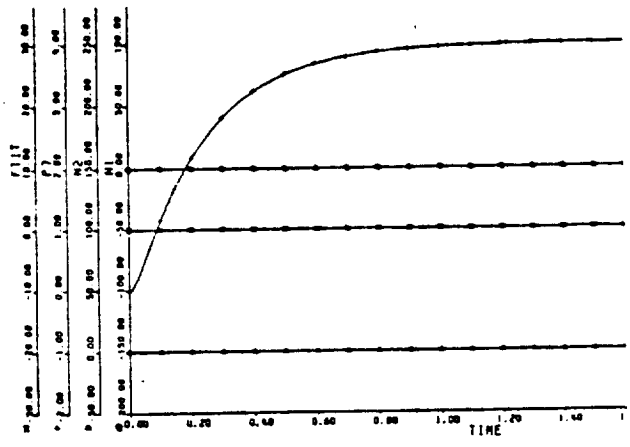

Figure 14. F100 Engine System Response to 4 PSI Step Request In P7 Pressure.

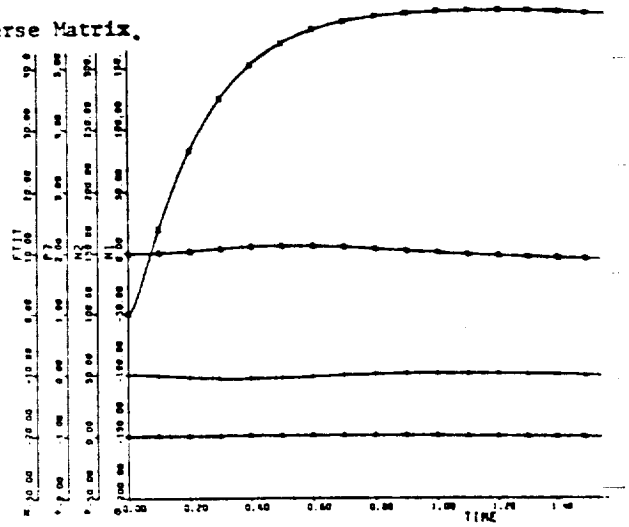

Figure 15. F100 Engine System Response to 50° Step Request in FTIT Temperatu

CONCLUSIONS

Multivariable synthesis methods based upon transfer functions appear to be feasible and practical. We have described a particular method to this end, based upon total synthesis of response and controller and stressing the inverse of the plant input/output relation. The inverse total synthesis (ITS) approach has been illustrated on four turbine engine examples, which include models from second to sixth order. Included have been coupled and decoupled cases, and even plants which are non-minimum phase.

ACKNOWLEDGMENT

It is a pleasure to acknowledge the computational support of Mr. S.A. Stopher and Mr. J.W. Wildrick, both of the Bendix Energy Controls Division.

REFERENCES

1. J.G. Truxal, Automatic Feedback Control Syste Synthesis. New York: McGraw-Hill, 1955.

2. C.A. Skira and R.L. DeHoff, "A Practical Approach to Linear Model Analysis for Multivariable Turbine Engine Control Design", in Alternatives for Linear Multivariable Control. M. Sain, J. Peczkowski, J. Melsa, Eds. Chicag NEC, 1978, pp. 31-46.

3. R.J. Miller and R.D. Hackney, "F100 Multivari Control System Engine Models/Design Criteria" Tech. Rept. AFAPL-TR-76-74, November 1976.

4. M.S. Weinberg and G.R. Adams, "Low Order Li ized Models of Turbine Engines", Tech. Rept. ASD-TR-75-24, July 1975.

5. J.W. Wildrick, "Transfer Function Arithmetic Package", Bendix Report ENCD-866-19438R, Au ust, 1978.

1/16
17

FREQUENCY DEPENDENT PRECOMPENSATION FOR DOMINANCE IN A FOUR INPUT/OUTPUT TURBINE PROBLEM MODEL

R. Michael Schafer and Michael K. Sain
Department of Electrical Engineering
University of Notre Dame
Notre Dame, Indiana 46556

Abstract

This paper reports on additional experience in applying the CARDIAD methodology to design of dynamical input compensation to achieve column dominance for linear multivariable models of realistic turbine engine simulations. In particular, the approach has been extended to models having four inputs and four outputs, and successful compensations have been achieved with an investment of about thirty minutes desk time.

INTRODUCTION

Control design methods based at least in part upon the frequency domain viewpoint have had a long and fruitful history [1], and interest in such approaches has continued into the present [2]. Generally speaking, in the more recent multivariable frequency domain work, the basic schools of thought tend to divide into two groups. These groups may be classified informally as "direct" and "indirect".

The direct approach can usually be recognized by its attention to achieving a completely specified dynamic performance. Such ideas have been discussed from the early days of organized control study; and a sampling of this thought may be found in [3,4]. The indirect approach is usually recognizable by its affinity to the classic works of Nyquist or Evans, involving, respectively, frequency response plots in the complex plane or versions of the root locus. The main focus of many indirect methods is the equation

$$p_c(s) = |M(s)|\, p_o(s),$$

where $p_o(s)$ is the open loop characteristic polynomial, $p_c(s)$ is the closed loop characteristic polynomial, $M(s)$ is the return difference matrix, and $|\cdot|$ denotes the determinant calculation. It is a fundamental consequence of this equation that Nyquist plots of the determinant of return difference have an import similar to that of the classical studies.

Methods discussed in this paper fall naturally into the "indirect" classification.

COLUMN DOMINANCE

One impediment to the making of a plot of the determinant of return difference is the loss of insight resulting from the way in which the columns of the return difference matrix pass through the alternating multilinear function created by the determinant. Consider Figure 1, where $G(s)$ represents the

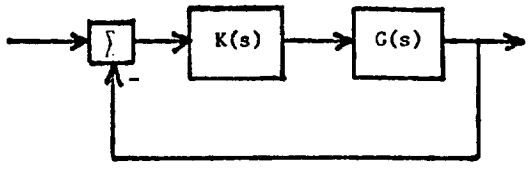

Figure 1.

plant, in this case a linear model based upon turbofan engine simulations, and $K(s)$ a matrix of precompensating dynamical elements. For this case,

$$|M(s)| = |I + G(s)\, K(s)|,$$

and the way in which the matrix $K(s)$ in the right member has influence upon the left member can be quite complicated.

When the matrix $M(s)$ is diagonal, of course, the determinant is equal to the product of its diagonal elements; and the winding number of the determinant can be determined from the winding numbers of the diagonal elements. A generalization of this idea is due to Rosenbrock [5]. Using the Gershgorin theorem, Rosenbrock was able to show that this property of the winding number was preserved in very general cases when $M(s)$ was not diagonal. To meet the conditions of Gershgorin, it was necessary to assume that the complex absolute value of the kth diagonal element in $M(s)$ was strictly greater than the sum of the complex absolute values of those elements in $M(s)$ which were in the kth column but not on the diagonal. This property was to be maintained for all complex frequencies on a classical Nyquist contour indented to include poles of the diagonal elements on the imaginary axis in the complex plane. Rosenbrock called this property column dominance.

For cases such as those shown in Figure 1, the determinant of return difference can be expressed as a ratio of two determinants: one of the closed loop transfer function matrix and one of the $G(s)\, K(s)$ product. Accordingly, there is considerable interest attached to the problem of designing $K(s)$ in such a way that the product $G(s)\, K(s)$ is column dominant. This is the fundamental problem considered in the present paper.

It is known that $K(s)$ over the field $R(s)$ can always be factored into the product of elementary column transformations. Moreover, it is easy to see by the Gershgorin test that scaling a column has no effect on column dominance. Thus the interest centers upon (1) column interchanges and (2) addition of scalar multiples of one column to another. Of these, the second can be normalized without loss, and in many ways seems to capture the essence of design to achieve dominance.

The CARDIAD method has been developed for the purpose of designing this normalized compensation. The acronym stands for Complex Acceptability Region for DIAgonal Dominance. An introduction to the basic ideas of CARDIAD plots may be found in [6].

In this paper, we discuss an application of CARDIAD plots to turbofan models having four inputs

and four outputs.

DESIGN EXAMPLE

As described above, the CARDIAD plot is a (graphical) method of choosing the entries of a precompensator K(s) such that G(s) K(s) is column dominant. The compensator is normalized to having 1's on the main diagonal, so that dominance is achieved in a given column of G(s) K(s) by appropriate choice of the off-diagonal entries of the corresponding column of K(s).

At a specific frequency, a sufficient condition for dominance can be expressed in a quadratic inequality of the form:

$$f(\underset{\sim}{x}) = \underset{\sim}{x}^T A \underset{\sim}{x} + \underset{\sim}{x}^T b + c > 0$$

where A, b, and c are respectively a matrix, a vector, and a scalar formed by evaluation of the plant transfer function matrix at the frequency being studied. $\underset{\sim}{x}$ is a vector of the real and imaginary parts of the off-diagonal entries of a column of the compensator. Dominance is achieved by choosing $\underset{\sim}{x}$ such that $f(\underset{\sim}{x})$ is positive.

Two approaches are used to choose $\underset{\sim}{x}$ such that $f(\underset{\sim}{x}) > 0$. Since it is desirable to achieve dominance with as simple a compensator as possible, the gradient of $f(\underset{\sim}{x})$ is taken with respect to each entry x_i assuming all other entries are zero. Here x_i may be understood as a pair (r_i, i_i) consisting of the real and imaginary part of some off-diagonal compensator entry. This approach, referred to as type 1 analysis, attempts to achieve dominance in a column using only one off-diagonal entry of the compensator. In the event that it is not possible to achieve dominance with only one off-diagonal entry, the gradient of $f(\underset{\sim}{x})$ with respect to all variables is taken. This approach is called type 2 analysis and utilizes all off-diagonal entries of the compensator to achieve dominance in a column.

The CARDIAD plot is a graphical representation of the results of the gradient analysis. Consider type 1 analysis of a given column. $f(0,\ldots 0,x_i,0..)$ is a paraboloid in 3-space, and the value found by the gradient analysis can be a positive maximum, a negative maximum, a positive minimum, or a negative minimum. In the positive maximum case, any value of x_i which lies inside the intersection of $f(\underset{\sim}{x})$ and the complex plane x_i will make $f(..0,x_i,0,..)$ positive; and dominance will be achieved at the frequency being studied. In the CARDIAD plot, this is represented by a solid circle which is the solution of $f(..0,x_i,0..)=0$, and a '+' at the value of x_i where the gradient vanishes, which is at the center of the circle. In the case of a negative minimum, all values of x_i lying outside the circle $f(\ldots 0,x_i,0..) = 0$ will make $f(..0,x_i,0\ldots)$ positive. In this case, an 'x' is drawn at the value where the gradient vanishes and a dashed circle at $f(\ldots 0,x_i,0..) = 0$. In the negative maximum case, no value of x_i will achieve dominance; and a 'Δ' is drawn. In the positive minimum case, any value of x_i will achieve dominance; in the column at this frequency, and a '$\square$' is drawn.

In type 2 analysis, the center symbols are drawn at the gradient values, but the center type and circle type are decided by making a worst case deviation from the gradient values of all but one of the entries of $\underset{\sim}{x}$; and then the remaining entry is analyzed in a fashion analogous to type 1 analysis.

A CARDIAD plot results when this graphical gradient information is plotted over a range of frequencies. Figures 4 and 5 are typical CARDIAD plots and will be used to describe compensator design.

Figure 4 is a type 1 analysis plot which contains only solid circles. In this case, there exist constant real values $(r_i,0)$ for x_i which lie inside all of the solid circles. Hence, to achieve dominance in this column at all frequencies, any such choice of x_i will suffice, since $f(..0,x_i,0..)$ will then be positive at all frequencies. In Figure 5, there exists no such constant real value, but a simple first order entry which as a function of frequency traces the centers of the circles can be used. Thus, if the CARDIAD plot indicates that no constant real value will achieve dominance, the shape of the plot guides the designer in determining a frequency dependent entry.

The model used in the following design example is taken from [7]. It is a sixth order, 4-input, 4-output description of a turbofan engine.

As a first step in the design procedure, the model was compensated with the inverse system evaluated at s=0. Figures 2-10 are the type 1 analysis plots of the first, second, and fourth columns of the system compensated by $G^{-1}(0)$. The type 1 analysis plots of the third column indicated that dominance could not be achieved by only one off-diagonal entry; so Figures 11-13 are the type 2 analysis plots of the third column with $G^{-1}(0)$ as a first compensator.

The fourth column of the system was dominant without further compensation. This can be seen from the fact that in each plot, Figures 8-10, the origin is included by all solid circles and excluded by all dashed circles; and no triangles occur. Hence, an acceptable choice for any one off-diagonal entry of the fourth column of the compensator, assuming that all other off diagonal entries in the column are zero, is zero. Thus, no further compensation is necessary.

The first column of the system required constant compensation in one off-diagonal entry to achieve dominance. Note that in the plot of the 2,1 entry, triangles occur, indicating that no value in the 2,1 entry will achieve dominance at the frequencies at which these triangles occur. However, in the 4,1 entry, Figure 4, only solid circles occur; and the value of -.034 is included by all the circles. Hence, with the 4,1 entry set at this value and the other off-diagonal entries of the compensator zero, dominance is achieved in this column.

The CARDIAD plots of the 3,2 and 4,2 entries, Figures 6 and 7, each have triangles occurring in them. Thus, if dominance is to be achieved in this column using only one off-diagonal entry, it will have to be the 1,2 entry, Figure 5. This plot contains only solid circles, but there is no point on the real axis which lies inside all of them. Hence, a frequency dependent entry was designed to trace the centers of the solid circles through the complex plane. The function chosen was

$$k_{1,2}(s) = \frac{-112.5s}{.178s + 1} .$$

This choice easily achieved dominance in this column.

The third column of the model was the most difficult to dominate. Figures 11-13 are the type 2 analysis of this column. Since type 2 analysis is necessary, all three off-diagonal entries must be designed. The simple shape of the centers of the plots aided in the design. It was possible to design a first order frequency dependent compensator for each entry. The three off-diagonal entries in the third column were chosen to be:

$$k_{1,3}(s) = \frac{-1.464s}{.0639s + 1}$$

$$k_{2,3}(s) = \frac{8.349\ E\text{-}04\ s}{.0639s + 1}$$

$$k_{4,3}(s) = \frac{.1159s}{.0639s + 1}\ .$$

The compensator which results from the above design is:

$$K(s) = \begin{bmatrix} 1. & \frac{-112.5s}{.178s + 1} & \frac{-1.4637s}{.0639s + 1} & 0. \\ 0. & 1. & \frac{8.349E\text{-}4s}{.0639s + 1} & 0. \\ 0. & 0. & 1. & 0. \\ -.034 & 0. & \frac{.1159s}{.0639s + 1} & 1. \end{bmatrix}$$

Figures 14-17 contain one type 1 analysis plot from each column of the system precompensated with $G^{-1}(0)*K(s)$. Note that it is possible to tell that the system is now dominant from the fact that in the type 1 analysis plot from each column, the origin lies inside all the solid circles, and only solid circles occur. Hence, zero is an acceptable choice for the entry of the compensator shown, and since type 1 analysis plots are drawn assuming that all other off-diagonal entries in the column are zero, the CARDIAD plots show that identity compensation will achieve dominance.

The overall design procedure took about thirty minutes of desk time to complete.

REMARKS

The turbofan engine model used in the design example above was derived from the Theme Problem [8] associated with the 1977 International Forum on Alternatives for Linear Multivariable Control, held in Chicago during October of that year. The Theme Problem itself is a 16 state, 5 input, 5 output model. In addition, five actuators were assumed, each with quadratic or cubic dynamics; and five sensors were included, four with first order delays and the other with a slow second order response. A lower order plant was determined by means of the approach of Weinberg and Adams [9]. The selection procedure involved elimination of all eigenvalues having real parts less than -17.8. In itself, this resulted in a fifth order model. However, inasmuch as FTIT is a sensed variable, the fast response eigenvalue -51 was also included. The resulting state variable correspondence was taken to be

fan speed
compressor speed
augmentor pressure
fan turbine inlet fast response
fan turbine inlet slow response
burner exit slow response.

Inputs were

main burner fuel flow
nozzle jet area
inlet guide vane position
high variable stator position
customer compressor bleed flow.

Outputs were

engine net thrust level
total engine airflow
turbine inlet temperature
fan stall margin
compressor stall margin.

The four input/output model is obtained by deleting customer compressor bleed flow as an input and total engine airflow as an output.

CONCLUSIONS

The CARDIAD plot is proving itself to be a useful and insightful design tool for achieving column dominance by means of dynamic precompensation. Originally applied to models having two input/output pairs, the method has progressed to three input/output pairs [6], and, in this paper, has been applied successfully to the case of four inputs and four outputs.

ACKNOWLEDGEMENT

This research has been supported by the National Aeronautics and Space Administration under Grant NSG-3048.

REFERENCES

1. A.G.J. MacFarlane, "Development of Frequency-Response Methods in Automatic Control", IEEE Transactions on Automatic Control, Vol. AC-24, No. 2, April 1979, pp. 250-265.

2. D. H. Owens, Feedback and Multivariable Systems. Herts. SG1 1HQ, England: Peter Peregrinus Ltd., 1978.

3. J.G. Truxal, Automatic Feedback Control System Synthesis. New York: McGraw-Hill, 1955.

4. I.M. Horowitz, Synthesis of Feedback Systems. New York: Academic Press, 1963.

5. H.H. Rosenbrock, Computer-Aided Control System Design. London: Academic Press, 1974.

6. R.M. Schafer and M.K. Sain, "Input Compensation for Dominance of Turbofan Models", in Alternatives for Linear Multivariable Control, M.K. Sain, J.L. Peczkowski, and J.L. Melsa, eds. Chicago: NEC, 1977, pp. 156-169.

7. J.L. Peczkowski and M.K. Sain, "Linear Multivariable Synthesis with Transfer Functions", in Alternatives for Linear Multivariable Control, M.K. Sain, J.L. Peczkowski, and J.L. Melsa, eds. Chicago: NEC, 1977, pp. 71-87.

8. M.K. Sain, "The Theme Problem", in Alternatives for Linear Multivariable Control, M.K. Sain,

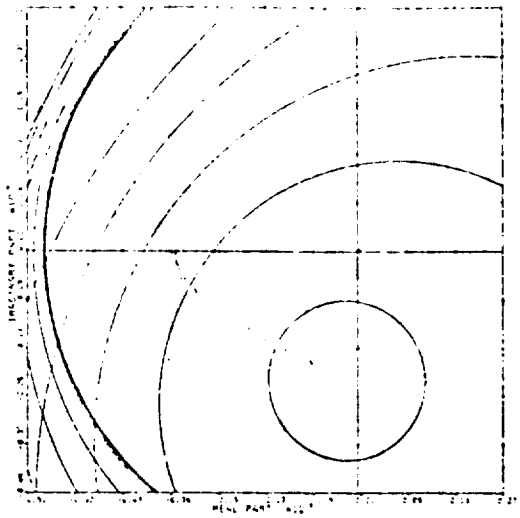

Figure 2. (2,1) Entry; Type 1 Analysis.

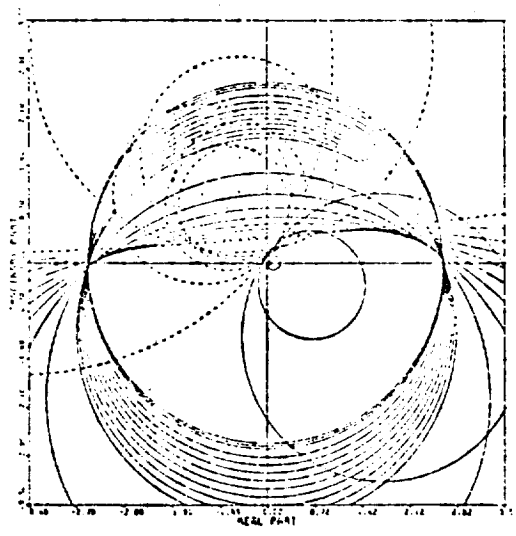

Figure 3. (3,1) Entry; Type 1 Analysis.

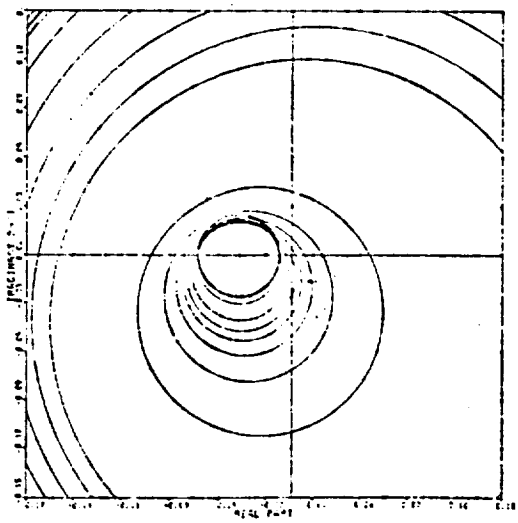

Figure 4. (4,1) Entry; Type 1 Analysis.

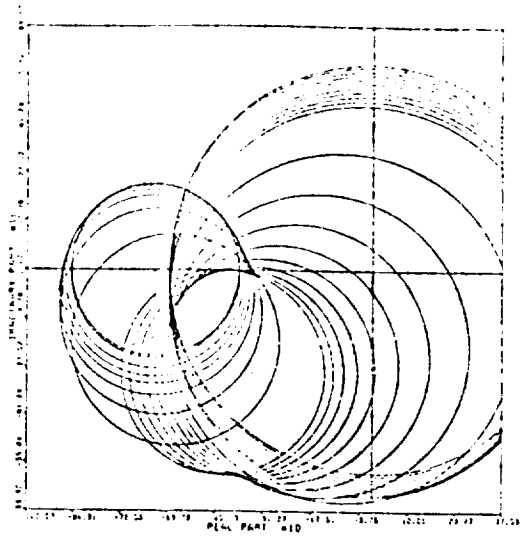

Figure 5. (1,2) Entry; Type 1 Analysis.

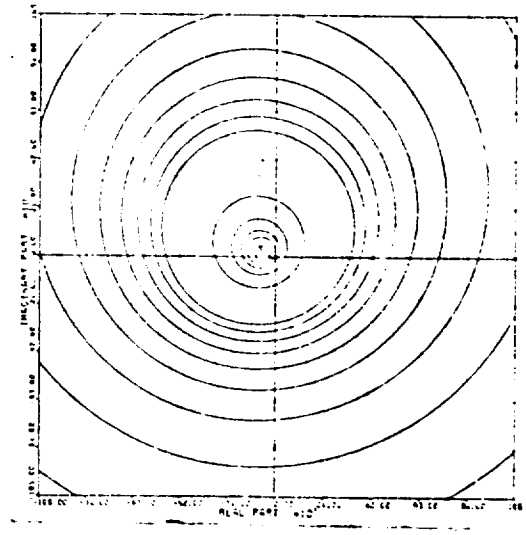

Figure 6. (3,2) Entry; Type 1 Analysis.

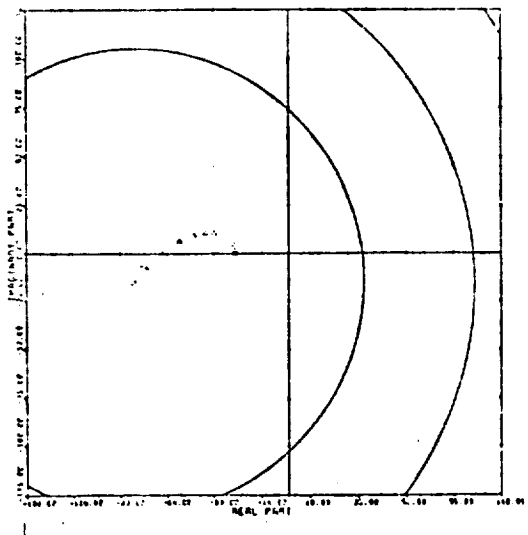

Figure 7. (4,2) Entry; Type 1 Analysis.

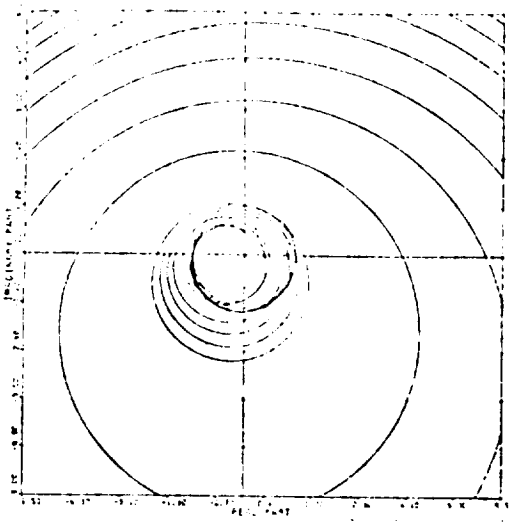

Figure 8. (1,4) Entry; Type 1 Analysis.

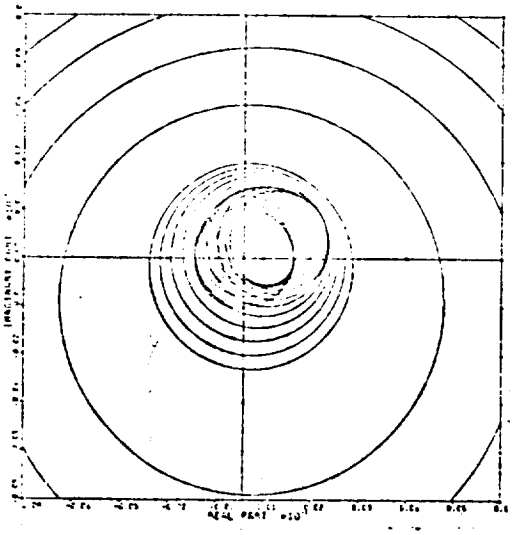

Figure 9. (2,4) Entry; Type 1 Analysis.

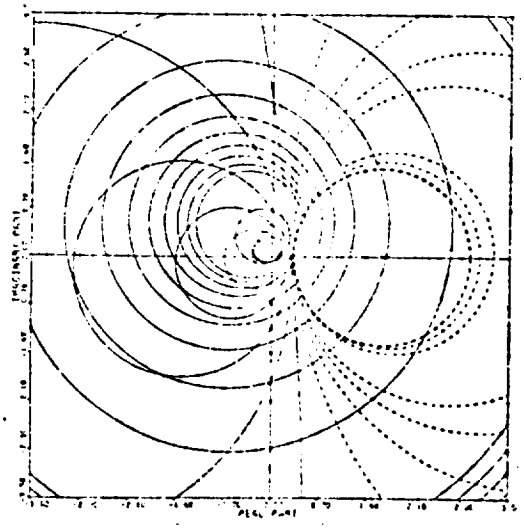

Figure 10. (3,4) Entry; Type 1 Analysis.

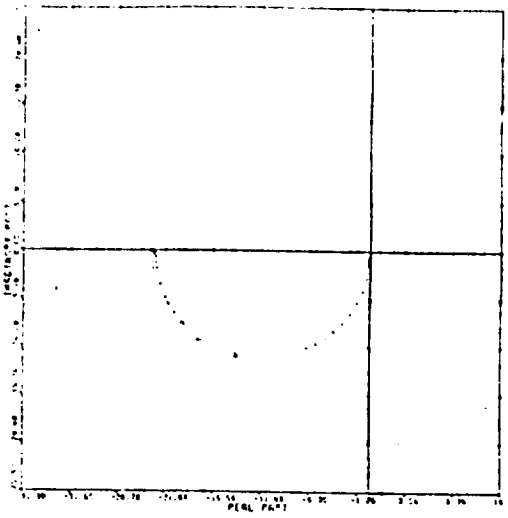

Figure 11. (1,3) Entry; Type 2 Analysis.

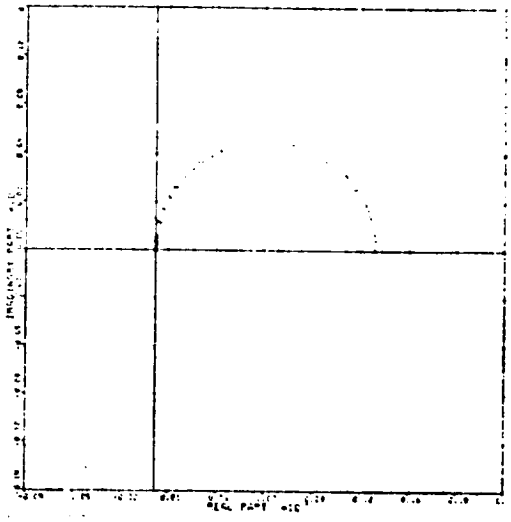

Figure 12, (2,3) Entry; Type 2 Analysis.

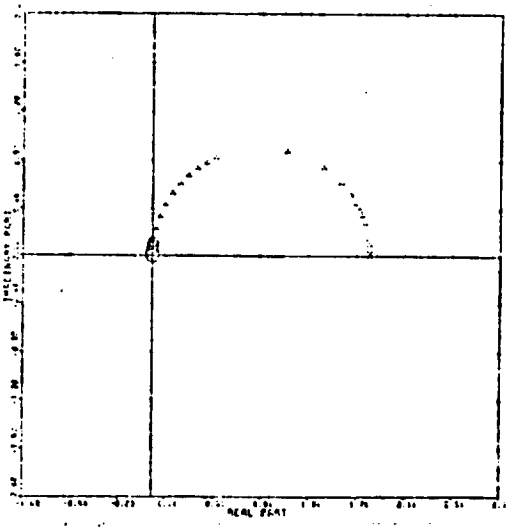

Figure 13. (4,3) Entry; Type 2 Analysis.

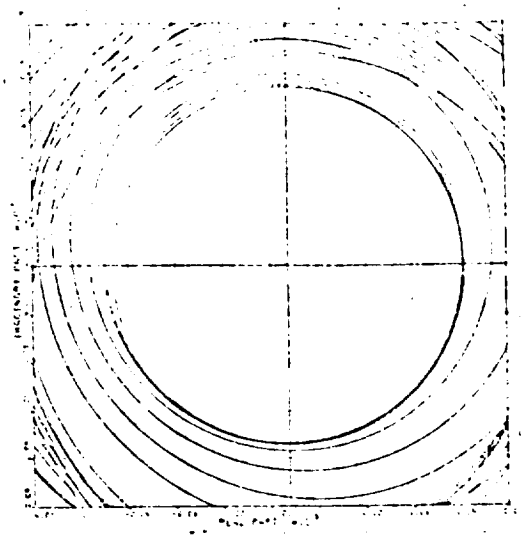

Figure 14. (2,1) Entry; Type 1; Compensated.

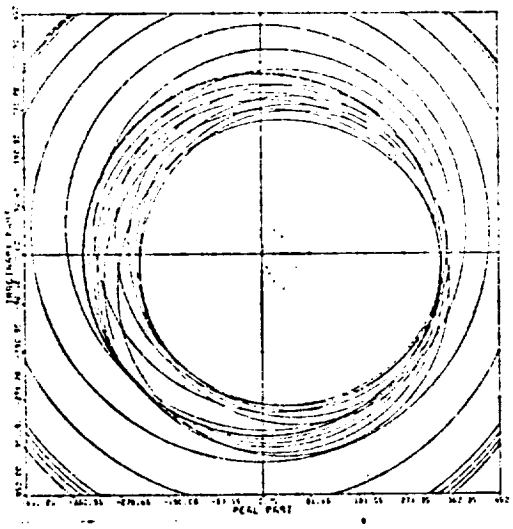

Figure 15. (1,2) Entry; Type 1; Compensated.

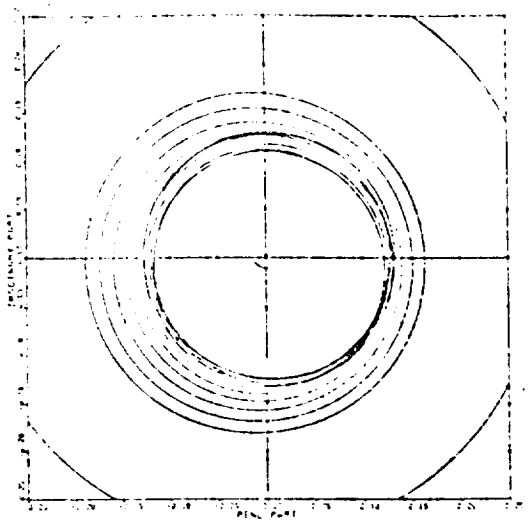

Figure 16. (1,3) Entry; Type 1; Compensated.

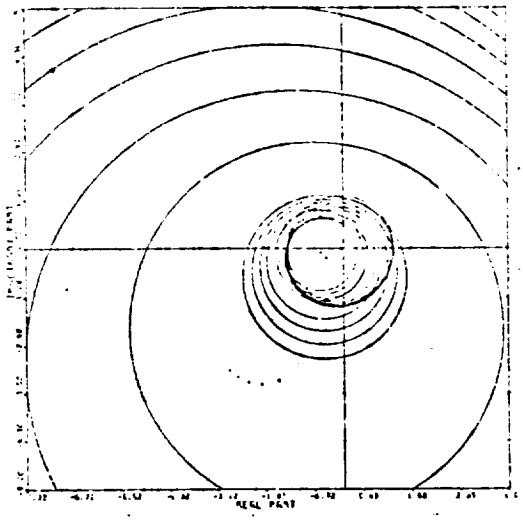

Figure 17. (1,4) Entry; Type 1; Compensated.

J.L. Peczkowksi, and J.L. Melsa, eds. Chicago: NEC, 1977, pp. 20-30.

9. M.S. Weinberg and G.R. Adams, "Low Order Linearized Models of Turbine Engines", Technical Report ASD-TR-75-24, Aeronautical Systems Division, Wright-Patterson Air Force Base, Ohio, July 1975.

D 17 18

CARDIAD APPROACH TO SYSTEM DOMINANCE WITH APPLICATION TO TURBOFAN ENGINE MODELS*

R. Michael Schafer and Michael K. Sain
Department of Electrical Engineering
University of Notre Dame
Notre Dame, Indiana
USA 46556

Summary

One of the features of present day research on linear multivariable systems has been a renewed interest in Nyquist methods. Based upon the determinant of return difference, these methods must develop procedures which interface with skew symmetric, multilinear forms. A well known interface has been made by Rosenbrock, who used a concept called diagonal dominance. This paper reports on a graphical, interactive way to achieve the concept.

Introduction

In recent years, increased attention has been paid to the use of frequency domain techniques for the design of multivariable control systems. Most of these techniques are based upon the equation

$$p_c(s) = |M(s)|\, p_0(s) \qquad (1)$$

which relates the zeros of the open loop characteristic polynomial $p_0(s)$ and the zeros of the closed loop characteristic polynomial $p_c(s)$ through the determinant of the return difference matrix $M(s)$. Given that the zeros of the open loop characteristic polynomial are known, stability of the closed loop characteristic polynomial can be determined by Nyquist analysis of $|M(s)|$. Unfortunately, direct Nyquist analysis of $|M(s)|$ yields little design insight. Therefore, alternate means of studying $|M(s)|$ have been devised.

In the Inverse Nyquist Array approach due to Rosenbrock, the system is first compensated to achieve diagonal dominance. An n x n matrix $Z(s)$ is said to be diagonally column dominant if for all s on the Nyquist contour D, and $i = 1,2,\ldots,n$,

$$|z_{ii}(s)| > \sum_{\substack{j=1 \\ j\neq i}}^{n} |z_{ji}(s)|. \qquad (2)$$

If this condition is satisfied, the usual net encirclements made by the Nyquist plot of $|M(s)|$ are equal to the sum of the net encirclements made by the diagonal entries of $M(s)$. Thus, stability can be determined by Nyquist analysis of the diagonal entries of $M(s)$.

The CARDIAD (Complex Acceptability Region for DIAgonal Dominance) method is a graphical technique for achieving this dominance condition.

CARDIAD Method

Consider the system of Figure 1. For the purposes of this paper, $G(s)$ represents a 4-input, 4-output model of a turbofan jet engine. It is desired to design the compensator $K(s)$ such that $G(s)\,K(s)$ is column dominant. The compensator is normalized to having 1's on the main diagonal, so that dominance is achieved in a given column of $G(s)\,K(s)$ by appropriate choice of the off-diagonal entries in the corresponding column of $K(s)$.

At a frequency, a sufficient condition for dominance can be expressed in a quadratic inequality of the form

$$f(x) = x^t A x + x^t b + c > 0, \qquad (3)$$

where A, b, and c are respectively a matrix, a vector, and a scalar formed by evaluation of the plant transfer function matrix at the frequency being studied, where x is a vector of the real and imaginary parts of the off-diagonal entries of a column of the compensator, and where superscript t denotes transpose. Dominance is achieved by choosing x such that $f(x)$ is positive.

Several approaches are used to choose x such that $f(x) > 0$. Since it is desirable to achieve dominance with as simple a compensator as possible, the gradient of $f(x)$ is taken with respect to each entry x_i assuming all other entries are zero. Here, x_i may be understood as a pair (r_i,i_i) consisting of the real and imaginary parts of some off-diagonal compensator entry. This approach, referred to as type 1 analysis, attempts to achieve dominance in a column by using only one nonzero, off-diagonal entry for the column of the compensator. In the event that it is impossible to achieve dominance with only one nonzero, off-diagonal entry, the gradient of $f(x)$ with respect to all variables is taken. This approach is referred to as type 2 analysis and utilizes all off-diagonal entries of the compensator to achieve dominance in a column. A third means of choosing the vector x is used in the event that the hessian in the type 2 analysis approach is indefinite. It is known that one solution to making $G(s)$ dominant is to compensate with the inverse system. Thus, a solution for the vector x is to choose the values of the inverse system at that frequency, normalized to 1 on the diagonal so as to fit the form of the compensator $K(s)$. In the case where the hessian is negative definite, this inverse system analysis, known as type 4 analysis, predicts the same solution as the type 2 analysis plots.

The CARDIAD plot is a graphical representation of the results of the gradient analysis. Consider type 1 analysis of a given column. $f(0,\ldots0,x_i,0..)$ is a paraboloid in 3-space, and the value found by the gradient analysis can be a positive maximum, a negative maximum, a positive minimum, or a negative minimum. In the positive maximum case, any value of x_i which lies inside the intersection of $f(x)$ and the complex plane x_i will make $f(..0,x_i,0,..)$ positive; and dominance will be achieved at the frequency being studied. In the CARDIAD plot, this is represented by a solid circle which is the solution of $f(..0,x_i,0..) = 0$, and a '+' at the value of x_i where the gradient vanishes, which is at the center of the circle. In the case of a negative minimum, all values of x_i lying outside the circle $f(...0,x_i,0..) = 0$ will make $f(..0,x_i,0...)$ positive. In this case, an 'x' is drawn at the value where the gradient vanishes and a dashed circle at $f(...0,x_i,0..) = 0$. In the negative maximum case, no value of x_i will achieve dominance; and a 'Δ' is drawn. In the positive minimum case, any value of x_i

*This work has been supported in part by the National Aeronautics and Space Administration under Grant NSG-3048.

will achieve dominance; in the column at this frequency, and a '□' is drawn.

In types 2 and 4 analyses, the center symbols are drawn at the gradient values, but the center type and circle type are decided by making a worst case deviation from the gradient values of all but one of the entries of x; and then the remaining entry is analyzed in a fashion analogous to type 1 analysis.

A CARDIAD plot results when this graphical gradient information is plotted over a range of frequencies. Figures 2 and 3 are typical CARDIAD plots and will be used to describe compensator design.

Figure 2 is a type 1 analysis plot which contains only solid circles. In this case, there exist constant real values $(x_1,0)$ for x_1 which lie inside all of the solid circles. Hence, to achieve dominance in this column at all frequencies, any such choice of x_1 will suffice, since $f(..0,x_1,0..)$ will then be positive at all frequencies. In Figure 3, there exists no such constant real value, but a simple first order entry which as a function of frequency traces the centers of the circles can be used. Thus, if the CARDIAD plot indicates that no constant real value will achieve dominance, the shape of the plot guides the designer in determing a frequency dependent entry.

Design Example

The model used in the following design example is taken from [1]. It is a sixth order, 4-input, 4-output description of a turbofan engine.

As a first step in the design procedure, the model was compensated with the inverse system evaluated at $s = 0$. Figures 4-8 are the type 1 analysis plots of the 4,2 entry, the 3,4 entry, and the entire first column. Type 1 analysis of the first column indicates that dominance cannot be achieved using only one nonzero, off-diagonal entry. The same was true for the third column. Figures 9-11 are the type 4 analysis plots for the first column; and Figures 12-14 are the type 2 analysis plots for the third column.

In both the second column and the fourth column, dominance was achievable using type 1 analysis and constant compensation as described in the discussion of Figure 2. Dominance was achieved in column 2 by choosing the 4,2 entry to be -880.8. Note that this value lies within all solid circles and outside all dashed circles. In like manner, the fourth column was made dominant by choosing the 3,4 entry to be -.59.

In the first and third columns, it was necessary to fit all three off-diagonal entries of the compensator to the shape of the centers of the type 4 and 2 plots, respectively. In each case, second order compensation was necessary to fit adequately the shapes. The three entries chosen for the first column were

$$k_{2,1}(s) = \frac{-.189E\text{-}3s^2 - .0129s}{.227E\text{-}2s^2 + .238s + 1},$$

$$k_{3,1}(s) = \frac{-.044s^2 - 2.30s}{.227E\text{-}2s^2 + .238s + 1},$$

$$k_{4,1}(s) = \frac{.146s^2 + 3.56s}{.227E\text{-}2s^2 + .238s + 1}.$$

The third column was made dominant with the following three off-diagonal entries

$$k_{1,3}(s) = \frac{-.175E\text{-}4s^2 + .263E\text{-}2s}{.198E\text{-}2s^2 + .0837s + 1},$$

$$k_{2,3}(s) = \frac{.333E\text{-}5s^2 - .274E\text{-}3s}{.198E\text{-}2s^2 + .0837s + 1},$$

$$k_{4,3}(s) = \frac{-.635E\text{-}2s^2 - .0188s}{.198E\text{-}2s^2 + .0837s + 1}.$$

It should be noted that, in each case, the denominator polynomial of the column is the same, thereby keeping the order of the resulting compensator small.

With compensation as described above, type 1 analysis was repeated to verify that dominance has been achieved. Figures 15-18 are a type 1 analysis plot from each column. Note that in every case, the plot predicts that an acceptable solution is the origin. Since type 1 analysis is drawn assuming all other off-diagonal entries are zero, this implies that the columns are now dominant, since the plots predict that identity compensation will achieve dominance.

Discussion

The tools associated with Nyquist analysis of (1) are often helpful in the analysis and design of multivariable systems in the frequency domain. One of the ways to approach the design of $|M(s)|$ in (1) is by means of the dominance ideas of Rosenbrock [2]. This paper describes a graphical, interactive procedure for attaining dominance. For other examples, see [3].

References

1. H.A. Spang III, "Insight into the Application of the Inverse Nyquist Array Method to Turbofan Engine Control", in Alternatives for Linear Multivariable Control, M.K. Sain, J.L. Peczkowski, and J.L. Melsa, eds., 1978, pp. 138-155.

2. H.H. Rosenbrock and N. Munro, "The Inverse Nyquist Array Method", ibid., pp. 101-137.

3. R.M. Schafer and M.K. Sain, "Input Compensation for Dominance of Turbofan Models", ibid., pp. 156-169.

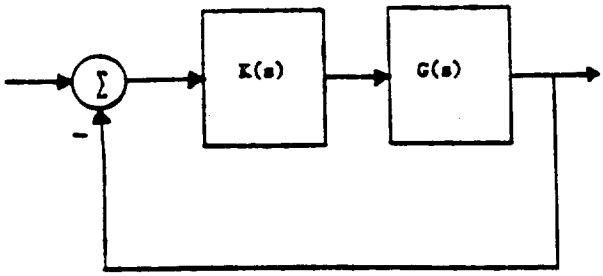

Figure 1

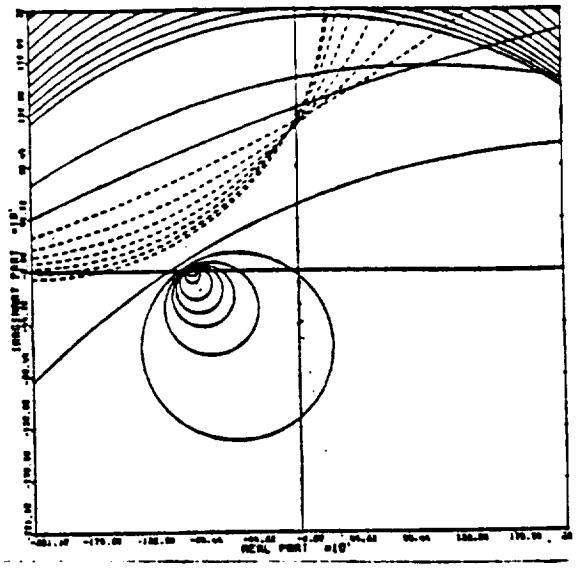

Figure 4

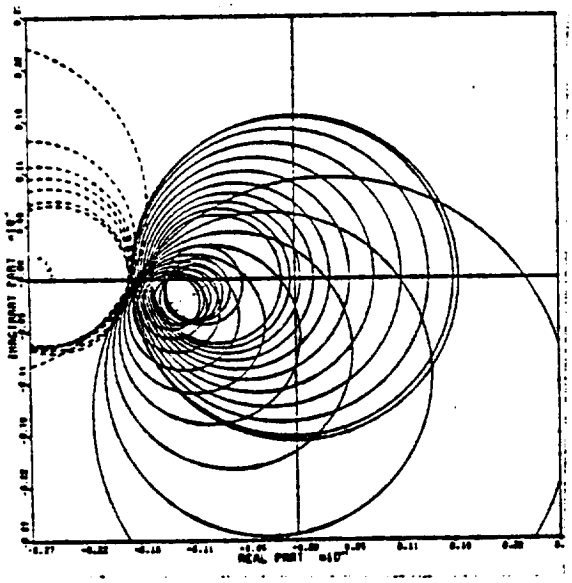

Figure 2

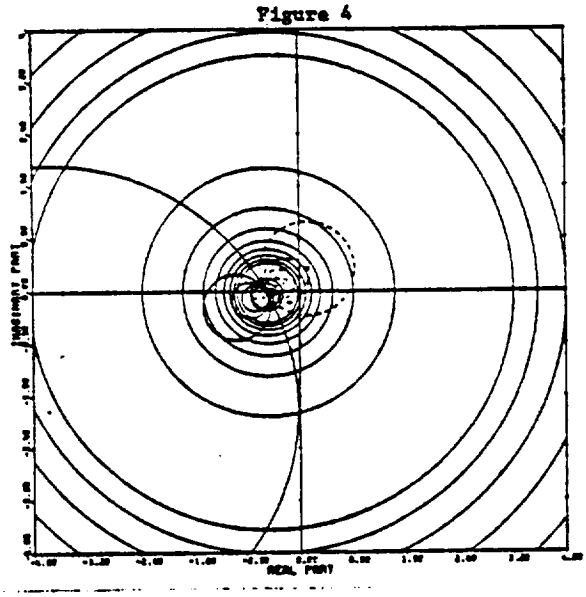

Figure 5

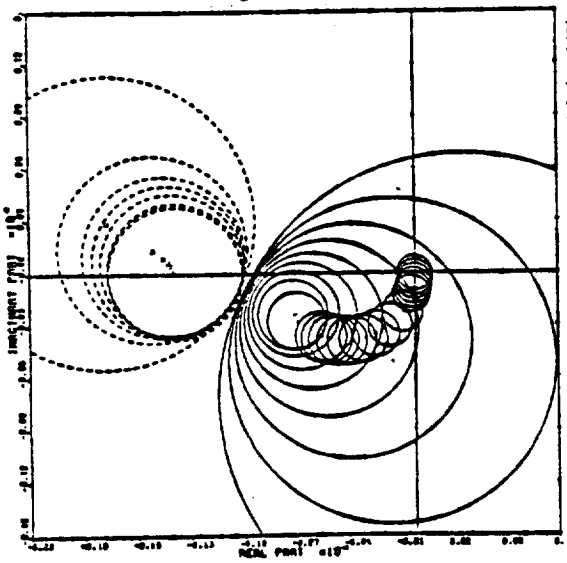

Figure 3

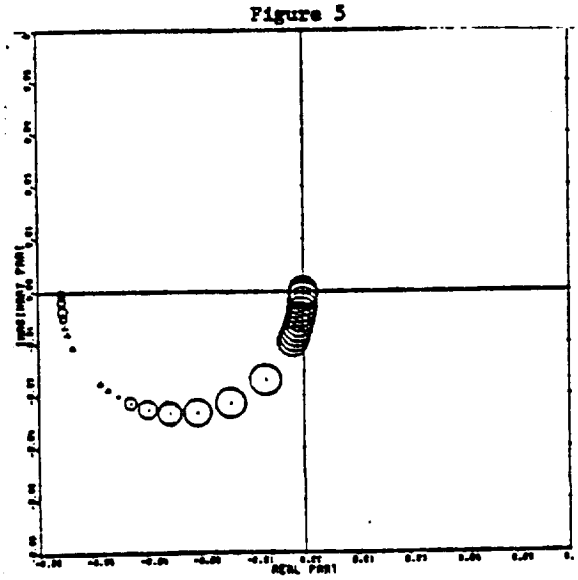

Figure 6

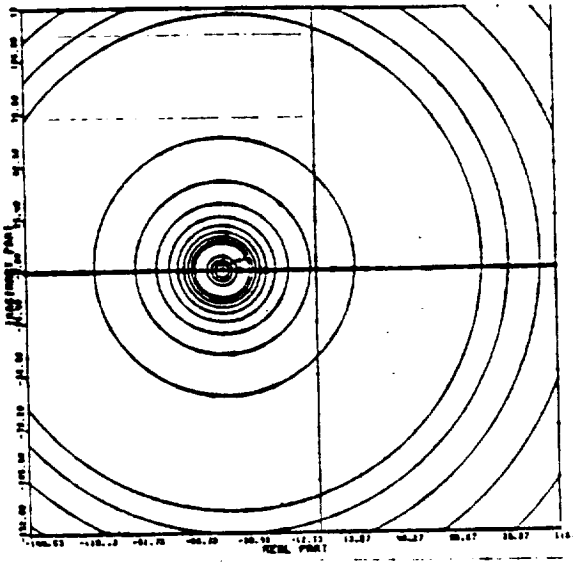

Figure 7

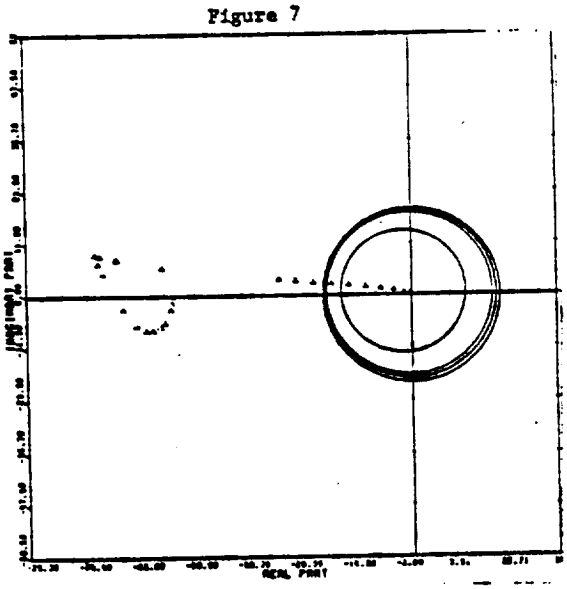

Figure 8

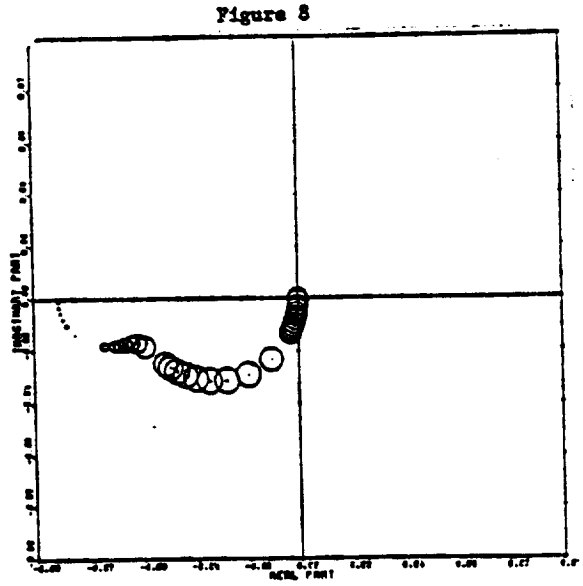

Figure 9

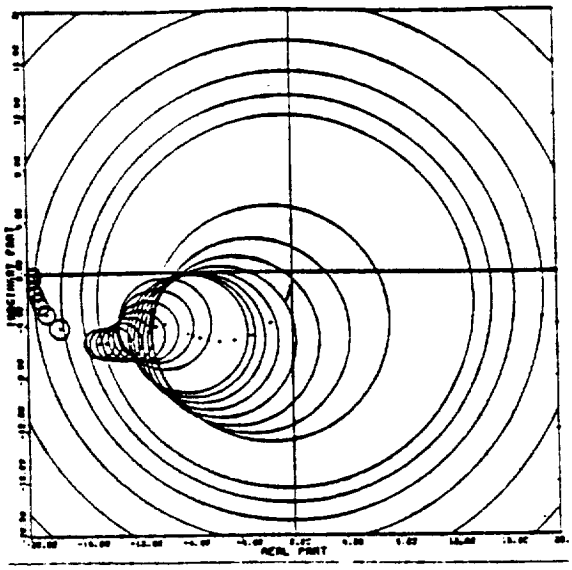

Figure 10

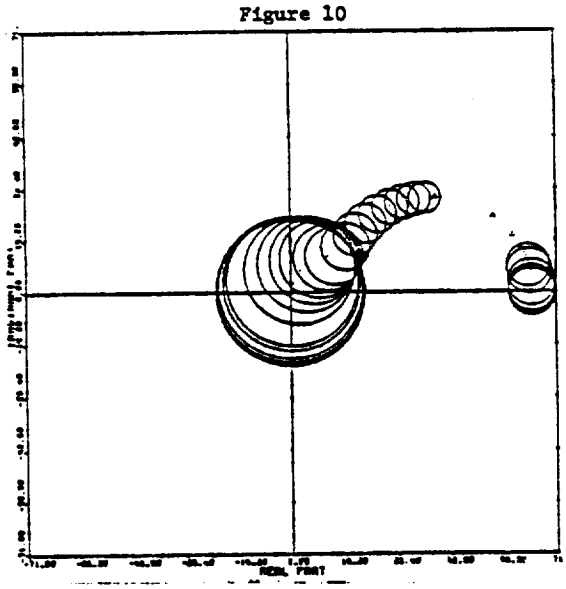

Figure 11

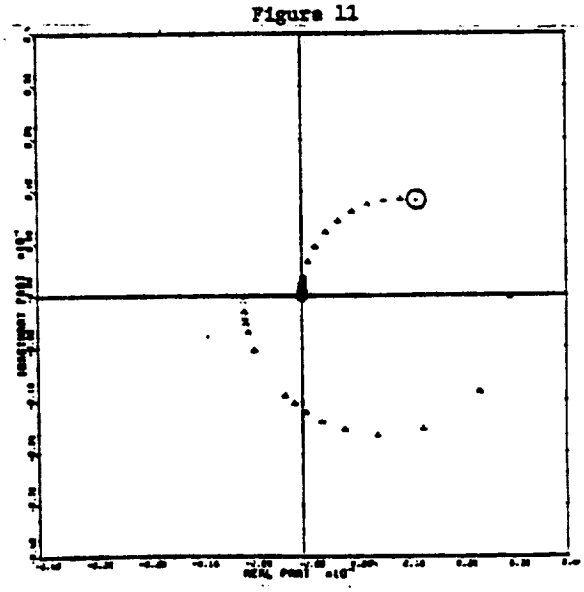

Figure 12

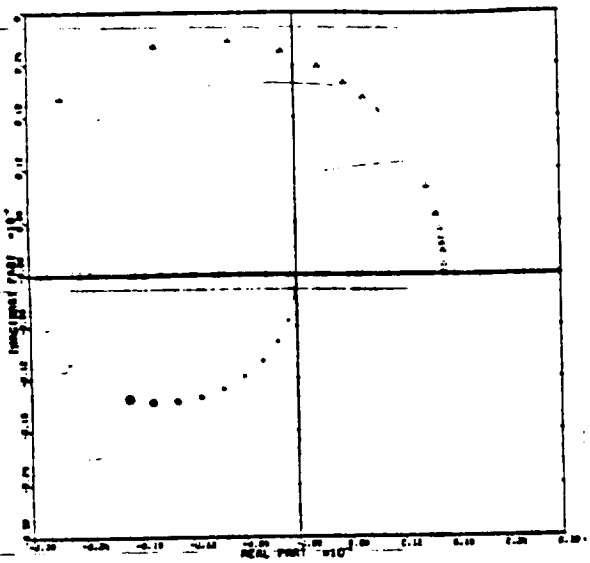

Figure 13

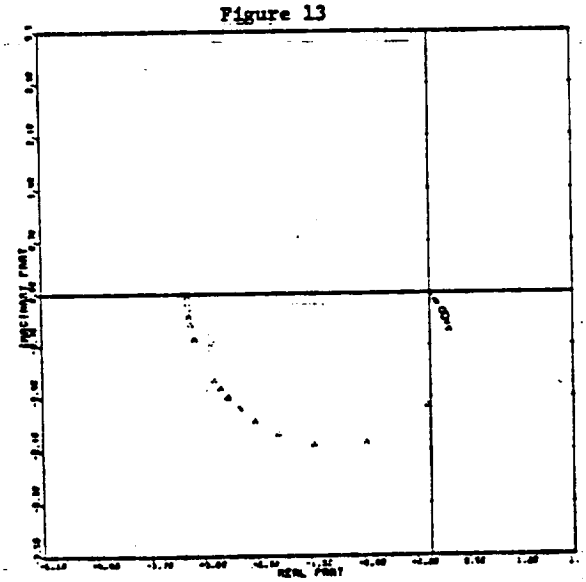

Figure 14

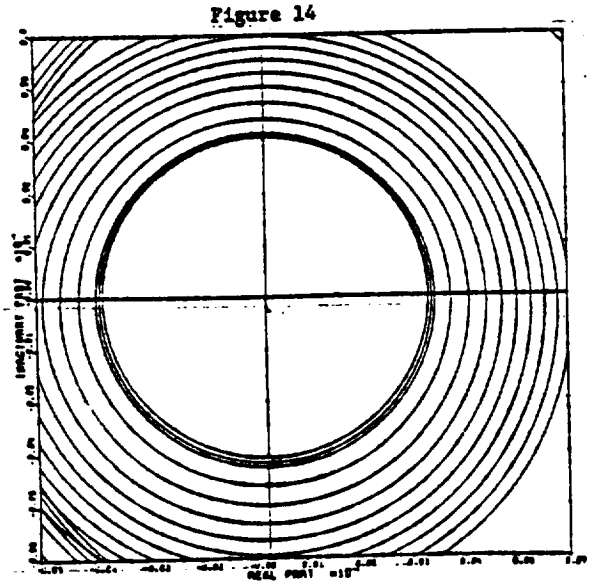

Figure 15

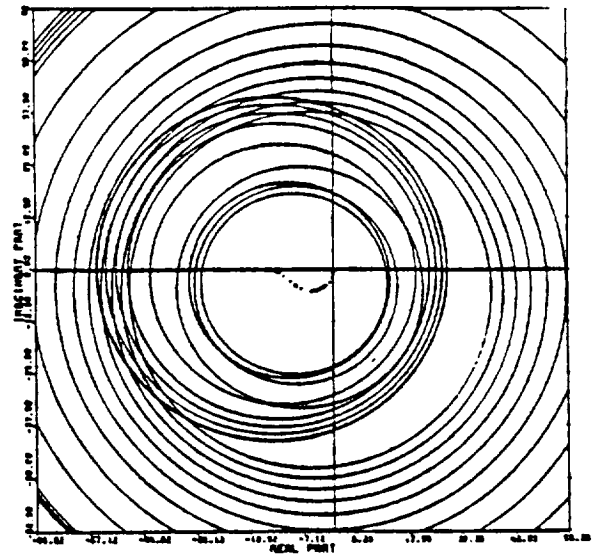

Figure 16

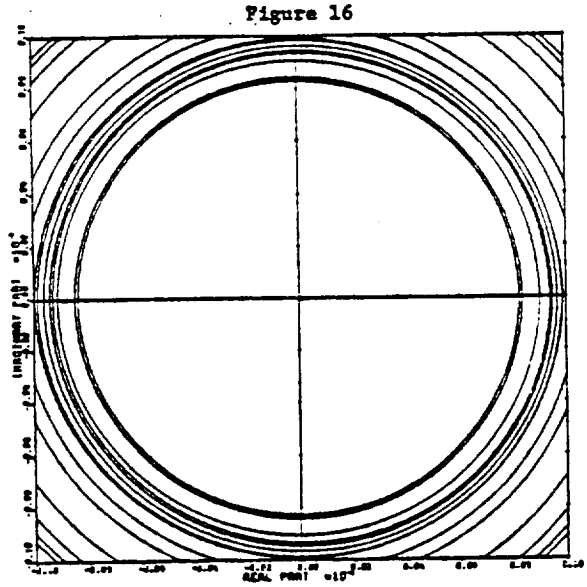

Figure 17

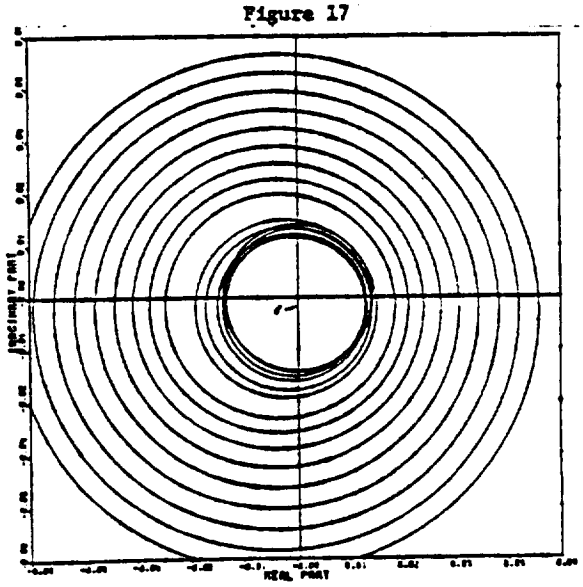

Figure 18

D19

D19

ON THE TOTAL SYNTHESIS PROBLEM OF LINEAR MULTIVARIABLE CONTROL

A Dissertation

Submitted to the Graduate School
University of Notre Dame in Partial Fullfillment
of the Requirements for the Degree of

Doctor of Philosophy

by

Raghvendra Ramchandra Gejji, M.S.E.E.

Michael K. Sain
Director

nt of Electrical Engineering
Notre Dame, Indiana

May, 1980

ON THE TOTAL SYNTHESIS PROBLEM
OF LINEAR MULTIVARIABLE CONTROL

Abstract

by

Raghvendra R. Gejji

New results in the theory of feedback system realizations and stable algorithms for solving the minimal design problem have provided a fresh impetus for designing linear multivariable control systems using algebraic methods for direct synthesis from a specified Closed-Loop Transfer Function Matrix (CLXFM). The Total Synthesis Problem (TSP) has been recently introduced in the literature as an approach which provides for simultaneous specification of plant output as well as plant input responses.

Introductory applications of TSP to jet engine control have stressed CLXFM's that are completely decoupled. In such cases, provision for internal stability leads to the appearance of any non-minimum-phase behavior of the plant explicitly in the closed-loop response. There is therefore interest in studying the non-decoupled CLXFM's in greater detail.

This study establishes the algebraic structure behind the basic TSP. The fundamental mapping of TSP is introduced and a characterization of the solution set of TSP is given as a rational vector space. It is shown that solutions that provide for internal stability must lie in a particular subset which is a free module over a ring of fractions formed from polynomials. Coefficients are considered as the field of reals in this study. Later, the utility of a minimal polynomial basis in characterizing the above subset is described. The problem of subjective criteria in calculation of minimal

bases is discussed, and a case study which leads to an empirical balancing rule for countering this problem is presented.

Design is approached as an approximation technique using least squares methods to select, among the feasible solutions, the nearest neighbor to a specified target performance. An interesting question arising as a result is whether control goals may be incorporated in the specified target performance. An example result on how tracking goals lead to constraints on the CLXFM is therefore included. A comprehensive example is included.

A discussion on the issue of internal stability in the error feedback structure has been included. Here there is special interest when the plant is unstable.

TABLE OF CONTENTS

ON THE DESIGN
OF DYNAMICAL COMPENSATION
FOR DIAGONAL DOMINANCE

A Dissertation

Submitted to the Graduate School
of the University of Notre Dame
in Partial Fulfillment of the Requirements
for the Degree of

Doctor of Philosophy

by

R. Michael Schafer, B.S.E.E., M.S.E.E.

Michael K. Sain
Director

Department of Electrical Engineering
Notre Dame, Indiana

May, 1980

D1920

ON THE DESIGN OF DYNAMICAL COMPENSATION FOR DIAGONAL DOMINANCE

Abstract

by

R. Michael Schafer

In recent years, increased attention has been given to the use of frequency domain techniques in the design of multivariable control systems. One class of methods currently under study are based on classical techniques such as those due to Evans and Nyquist. Fundamental to this class of methods is the relationship of the closed loop characteristic polynomial to the open loop characteristic polynomial through the determinant of the return difference matrix.

The Diagonal Dominance approach to the multivariable control system design problem is based on the classical Nyquist theory. It can be shown that if the return difference matrix has the property known as diagonal dominance, stability of the closed loop system can be determined from knowledge of the open loop characteristic polynomial and Nyquist analysis of the diagonal entries of the return difference matrix. Hence, if the system is first compensated so that the return difference matrix is diagonally dominant, the multivariable control design problem can be reduced to a set of single input, single output design problems and classical techniques may be applied. However, achieving diagonal dominance is not always easily accomplished.

This dissertation presents a graphical, frequency domain approach, called the CARDIAD (Complex Acceptability Region for DIAgonal Dominance)

method, to the problem of designing dynamical compensation to achieve diagonal dominance. In the CARDIAD method, a form of compensator having 1's on the main diagonal and general frequency dependent entries off the diagonal is assumed. Then a sufficient condition for dominance in a column of the system is expressed as a quadratic inequality in terms of the off-diagonal entries in the corresponding column of the compensator and the entries of the plant transfer function matrix.

Conditions for the existence of a compensator of the assumed form that achieves dominance are given, and the method is successfully demonstrated on jet engine models having 2, 3, 4, and 5 inputs and outputs.

TABLE OF CONTENTS

a 23rd Midwest Symposium on Circuits and Systems

CONTROL DESIGN WITH TRANSFER FUNCTIONS: AN APPLICATION ILLUSTRATION*

Joseph L. Peczkowski
Energy Controls Division
Bendix Corporation
South Bend, Indiana 46620

Michael K. Sain
Electrical Engineering Department
University of Notre Dame
Notre Dame, Indiana 46556

Abstract

In reference (1), a transfer function design theory for multivariable control design has been explained and applied to model data for the J-85 engine at sea level, 100% speed condition, and for the F100 engine at sea level, 67 degree power lever condition. Two basic relationships were highlighted: a synthesis equation and a design equation. In this paper, study of the J-85 model data is extended to include considerations of sensitivity with respect to model data. It is shown that the same synthesis equation is available for the extended design study, but that an additional design equation is implied by the use of a sensitivity specification. The synthesis equation displays all nominal, internally stable closed loop response possibilities. The design equations realize explicit forward and feedback controller dynamics. From an application viewpoint, the method has the advantage of being straightforward, easy to understand and easy to apply.

1. INTRODUCTION

Multivariable transfer function control design is not new. It was applied thirty years ago to jet engine control by Boksenbom, Hood and Feder (2,3) and was studied in 1957 by Freeman (4,5) and Kauanagh (6,7). Practical computation with transfer function matrices was a difficult issue at that time, and the issue of internal stability was a formidable problem. Also, discussion of classical transfer function control design techniques for single-input, single-output systems--which is related in spirit to the viewpoint of this paper--may be found in Truxal (8,pp. 302-310).

For purposes of this brief presentation, a design discussion format has been chosen. Numerous interesting and more theoretical questions arise from contexts such as these. Basically, these resolve into the nominal possibilities for command/control and command/response pairs of all types. To accommodate this question the authors (9) have defined the Total Synthesis Problem (TSP) of linear multivariable control as a study of the abstract module-theoretic kernel (10) associated with a fundamental homomorphism, defined on a natural product group describing command/control and command/response pairs. The module nature of TSP depends upon the particular subring of transfer functions chosen, as for example stable transfer functions or stable and proper transfer functions. For a more abstract discussion of these ideas, the reader is referred to (11), which also contains the results of a more complicated design example.

* This work was supported in part by the Office of Naval Research under Contract N00014-79-C-0475.

2. NOTATION AND BACKGROUND (9,12)

Consider Figure 1, a block diagram for a multivariable feedback structure with no disturbances. References, error, plant input and plant output are designated r, e, u and y respectively. Assume the plant has equal numbers of inputs and outputs, thus P(s) is a square matrix of transfer functions. This assumption is not nearly as restrictive as one

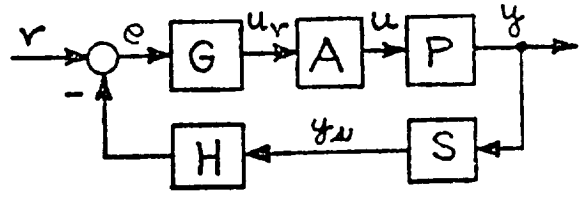

Figure 1. General Feedback Loop

later. The controllers G(s) and H(s) are also square.

The problem is, given plant P(s), to design controllers G and H to achieve desired, internally stable, closed loop response T(s) as indicated in Figure 2.

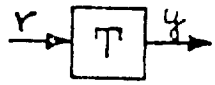

Figure 2. Desired Response

To effect control of a plant it is necessary to use actuators to drive inputs and to use sensors to measure outputs. Moreover, sensors and actuators can introduce significant dynamical effects into signal paths of the loop. Therefore A(s) and S(s) are diagonal actuator and sensor matrices. The output y is sensed and becomes y_s; the input request, u_r, commands the actuators to produce the plant input, u.

2.1 A DESIGN EQUATION

From Figure 1, the overall response of the loop is

$$y = (I + PAGHS)^{-1} PAG \quad r \qquad (1)$$

The desired response is

$$y = T r \qquad (2)$$

Combining equations (1) and (2) gives controller G

$$G = A^{-1} P^{-1} T (I - HST)^{-1} \qquad (3)$$

A performance matrix, which depends on the response T and feedback dynamics HS is identified

$$Q = T (I - HST)^{-1} \qquad (4)$$

Thus, a design equation for the forward controller dynamics G(s) becomes

$$G = A^{-1} P^{-1} Q \qquad (5)$$

Equation (5) is named a design equation for the forward controller. Forward controller dynamics are determined by the characteristics of the actuated plant inverse, $(PA)^{-1}$, and the performance matrix, Q. The plant inverse transfer function matrix is a key element in the design equation. What about the existence of the plant inverse? Is this a serious restriction to transfer function design?

2.2 THE PLANT INVERSE

Fortunately, the existence of the plant inverse turns out to be a very useful property for control synthesis. The plant inverse establishes and displays vital plant characteristics needed to effect successful closed loop control design. Four system and plant features, essential for design, are established and identified by the plant inverse transfer function:

1. meaningful multivariable control (13)
2. plant trackability (14).
3. multivariable plant zeros (15)
4. cancellations and simplifications.

Morse (6) and Wonham and Morse (7,8) have shown that if the number of plant inputs equals the numbers of its outputs and if $P(s)^{-1}$ exists, then one has both a meaningful multivariable control problem and necessary and sufficient conditions for existence of a physically realizable controller that decouples the system.

Leake, et.al.,(14) define a step trackable linear multivariable plant as one which can asymptotically achieve any constant steady-state output with a bounded control. It is shown that step trackability for proper rational continuous square plants is equivalent to the conditions that:

1. the plant is invertible and
2. it has no multivariable zeros at s=0.

The multivariable zeros of a plant, P(s), are the poles of the inverse, $P(s)^{-1}$, Wyman and Sain (15). Therefore, multivariable plant zeros are readily identified from the factored form of the inverse matrix. This is important for design, and especially so when a plant has hidden multivariable zeros in the right half plane (14).

Thus, existence of the plant inverse assures conditions needed to effect design, namely it provides essential design information about plant trackability, about plant multivariable zeros and about existence of meaningful and internally stable closed loop control realizations.

2.3 A SYNTHESIS EQUATION

From the foregoing discussion it is possible to design forward control dynamics G(s), by applying design equation (5) to achieve any specified closed loop output response. Surely some conditions and restrictions on the output response are needed if internal loop stability is to be assured. In this section, a synthesis equation is presented which displays all admissible output response transfer function matrices for which internally stable, feedback realizations exist (14).

Consider Figure 3, where r denotes request, u denotes control action, and y denotes response. Under broad assumptions, there exist linear operators T:R→Y and M: R→U, where R, U, Y may

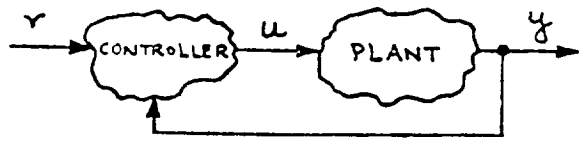

Figure 3. A General Control System

be understood as R(s)-vector spaces of finite dimension such that (9):

$$y = T r \text{ and } u = M r \qquad (6)$$

The plant can be understood in terms of an operator P: U→Y, such that

$$y = P u \qquad (7)$$

Combining equations (6) and (7) obtains the relationship

$T = PM$ (8)

More important than (8) is the equation which results when P is inverted

$$M = P^{-1}T \quad (9)$$

We highlight (9) and call it the synthesis equation.

Bengtsson (17) proves that internally stable feedback realizations of systems depicted by Figure 3 exist if and only if M is proper and stable and T is stable. Synthesis equation (9) will be used to choose responses T to guarantee that internally stable feedback realizations exist. The design problem is to find specific ones.

The question is will the specific control dynamics generated by the design equations produce internally stable feedback systems? The answer is yes provided that right hand plane cancellations by elements in the loop are avoided. From the application point of view, when a specific control is under design, internal stability would be easily verified by the usual computer simulations.

The foregoing ideas and use of the synthesis and design equation are illustrated by example 1 below.

3. SYSTEM DESIGN-RESPONSE AND SENSITIVITY

So far, multivariable design to achieve closed loop responses T(s) has been discussed. A synthesis equation, $M = P^{-1}T$, and a design equation, $G = A^{-1}P^{-1}Q$, have been highlighted. However, once a closed loop design with the desired response is obtained via the design equation and selected feedback dynamics, one may ask: how good is the design? Is there a better way to determine feedback dynamics? How sensitive is the loop response to parameter variations in the plant? Is it possible to impose a sensitivity requirement on the closed loop in addition to the response requirement and thus effect design of both response and sensitivity?

3.1 SENSITIVITY SYNTHESIS (19)

The main thrust of this section is to add closed loop sensitivity specifications for parameter variations in the plant to the foregoing multivariable control synthesis ideas for response.

Earlier, plant dynamics were written as a matrix of transfer functions P(s). This may have also been written as

$$P(s, a_1, a_2, \ldots a_n) = P(s,a) \quad (10)$$

where the a_i represent gains, time constants and coefficients in the plant transfer functions. The effect of the parameter vector a on control system performance is a most basic issue. The famous work of Bode (18) defined feedback in relation to its ability to reduce effects of parameter variations.

Typically there is a nominal parameter vector a_0 which results in the nominal plant $P(s)=P(s,a_0)$. In practise, control systems performance is usually specified at nominal conditions. Consider the feedback system diagram in Figure 4

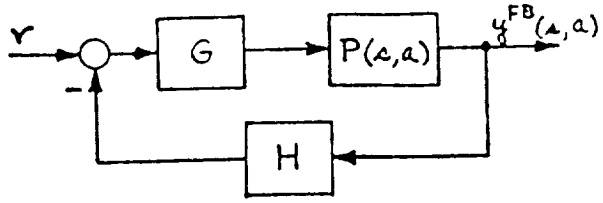

Figure 4. Output Feedback System

The output response is $y^{FB}(s,a) = T^{FB}(s,a)r$ where

$$T^{FB}(s,a) = (I + P(s,a)\,GH)^{-1}P(s,a,)\,G \quad (11)$$

Suppose now we demand that the desired response T be achieved by the parametrically uncertain plant at nominal conditions. We impose the requirement that $T^{FB}(s,a_0) = T(s)$. Next, a mechanism is needed to determine the effect of plant parameter vectors a not equal to the nominal a_0 upon the response. Thus $a \neq a_0$ implies that $T^{FB}(s,a) \neq T(s)$.

This question has been handled in the literature by Cruz and Perkins (19). The Cruz-Perkins idea is to compare the parametric variation effect on the response of the feedback system of Figure 4 with a corresponding effect of the same variation on an open loop system in Figure 5 which demands that $T^{OL}(s,a_0) = T(s)$. As before, if $a \neq a_0$,

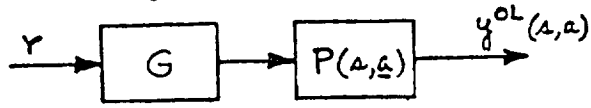

Figure 5. Open Loop System

$T^{OL}(s,a) \neq T(s)$.

When plant parameters are not equal to the nominal values, as is usually the case, both systems fail to meet the total synthesis response specification T(s). This situation produces two response error matrices: $E^{OL}(s,a) = T^{OL}(s,a) - T(s)$, the open loop response error and $E^{CL}(s,a) = T^{CL}(s,a) - T(s)$, the closed loop response error. A remarkable thing is that there exists a comparison sensitivity matrix (19) relating E^{CL} to E^{OL}

$$E^{CL} = S(s,a)\,E^{OL} \quad (12)$$

where

$$S(s,a) = (I + P(s,a)\,GH)^{-1} \quad (13)$$

We highlight (13) and refer to S (s,a) as the comparison sensitivity matrix.

The goal is to arrange the design so that the closed loop is more acceptable than the open loop.

Then the closed loop feedback configuration is said to "reduce" parameter sensitivity with respect to the open loop configuration, which is taken as the reference.

4. MULTIVARIABLE CONTROL DESIGN: RESPONSE AND SENSITIVITY

Equation (13) provides the link needed to specify both response and comparison sensitivity performance requirements simultaneously for multivariable

design of feedback systems. For the closed loop system in Figure 6 the following equations now

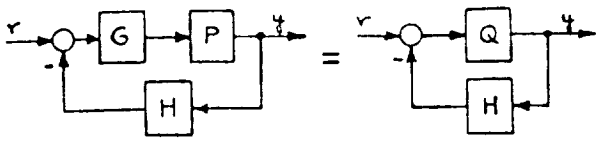

Figure 6 Output Feedback System

apply

$$T = (I + PGH)^{-1}PG \quad \text{response matrix} \quad (14)$$

$$S = (I + PGH)^{-1} \quad \text{sensitivity matrix} \quad (15)$$

$$Q = PG \quad \text{performance matrix} \quad (16)$$

Combining equations (14) and (15) obtains another relationship for the performance matrix:

$$Q = PG = S^{-1}T \quad (17)$$

Thus the performance matrix is a function of response T and comparison sensitivity S. Using (17) to solve for G and using in equation (15) to solve for H gives:

$$G(s) = P^{-1}S^{-1}T \quad (18)$$

$$H(s) = T^{-1} (I - S) \quad (19)$$

Equations (18) and (19) are highlighted as the forward and feedback controller dynamics design equations respectively for the output feedback structure in Figure 6. They express controller dynamics in terms of only the response matrix and comparison sensitivity matrix.

It is interesting to picture the controller dynamics design equations in a block diagram and note that the output feedback system in Figure 6 is transformed into a feedback system expressed only in terms of the response and sensitivity matrices. Figure 7 clearly shows that where T and S are specified, in effect,the dynamics of the forward and feedback paths are specified also.

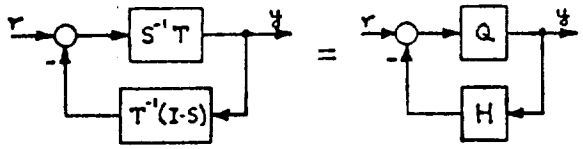

Figure 7. Output Feedback System in Terms of T and S

4.1 THREE BASIC EQUATIONS

In summary,three relationships form the basis for an approach to multivariable control synthesis and design with transfer function:

- o synthesis equation $M=P^{-1}T$ (13)
- o design equation $G=P^{-1}Q=P^{-1}S^{-1}T$ (18)
- o design equation $H=T^{-1} (I - S)$ (19)

Use of the basic equations and foregoing ideas are illustrated by examples of multivariable control design for a simple turbojet engine.

5. EXAMPLE

First, a unity feedback loop structure is used and a control design which achieves desired closed loop response is shown. Next, a general output feedback structure is used and controllers are designed which produce both desired closed loop response and comparison sensitivity. The authors are happy to acknowledge the assistance of Mr. Abraham Ma of the Bendix Energy Controls Division for computations and simulations of the examples.

Example 1. For a given multivariable turbojet engine, design a controller in a unity feedback structure so that the response is: 1. decoupled, 2. settles in one second and 3. attains zero steady state error. The engine, a GE J-85 turbojet at sea level 100% speed condition, is defined by $y = P(s)\, u$ where:

$$P(s) = \frac{\begin{bmatrix} 5.7(.18s + 1) & 56(.18s + 1) \\ .17(1.32s + 1) & -1.9(.005s + 1) \end{bmatrix}}{(.61s + 1)(.18s + 1)}$$

and $u_1 = W_f$ = fuel flow, PPH
$u_2 = A_j$ = exhaust area, IN^2
$y_1 = N^j$ = rotor speed, RPM
$y_2 = T$ = turbine temperature, ^oR

This is a multivariable plant with two inputs: fuel flow and exhaust area and two outputs: rotor speed and turbine temperature. The problem is pictured below:

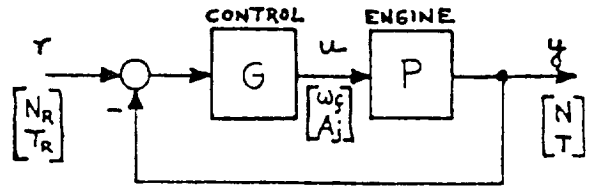

Figure 8. Unity Feedback Engine Control System

The first step in the design process is to apply $M = P^{-1}T$, to determine admissible responses T. Recall that for an admissible response, both M and T must be proper and stable (14). Calculating the plant inverse and taking a decoupled response (T diagonal) form, the synthesis equation becomes

$$M = P^{-1}T = \begin{bmatrix} .093(.005s + 1)t_{11} & 2.75(.18s + 1)t_{22} \\ .008(1.32s + 1)t_{11} & -.28(.18s + 1)t_{22} \end{bmatrix}$$

where t_{11} and t_{22} are the diagonal elements of T. It is clear that the matrix M is proper and stable if the diagonal elements of T are stable and the order of the denominator is at least one greater than the order of the numerator. Note the large range of choices for admissible response which are available. The simplest possible response form is taken namely, $t_{11} = t_{22} = K/(Ts+1)$.

To meet the other response requirements for 1 second settling time and zero steady state error, the time constant is selected to be .2 seconds and the gain K = 1. Thus the selected decoupled response T is a diagonal matrix where $t_{11} = t_{22} = 1/.2\ s + 1$. For this choice of response, the performance matrix, according to (4), is $Q = 5/s$. Design equation (5), $G=A^{-1}P^{-1}Q$, gives the control-

ler dynamics.

$$G = \frac{\begin{bmatrix} .47(.005s + 1) & 13.75(.18s + 1) \\ .04(1.32s + 1) & -1.4\ (.18s + 1) \end{bmatrix}}{s}$$

This is an integral controller, hence zero steady state error will be achieved. A digital simulation of the controller and engine showing the response of the close loop system to a step re-request in speed of 500 RPM is given in Figure 9. The desired response and decoupling are achieved for the nominal plant.

The effect of engine parameter variations (+ 30% on the gains of p_{11} and p_{22}) on the step response is also shown in Figure 9. The unity feedback system resists parameter variations but the effect on the step response is noticeable. Can the sensitivity be improved?

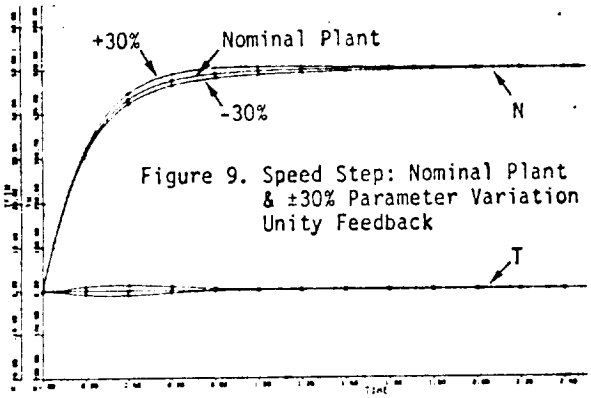

Figure 9. Speed Step: Nominal Plant & ±30% Parameter Variation Unity Feedback

Since a unity feedback structure was chosen: H=I; then equation (19) tells that the comparison sensitivity matrix is S = I - T. For the selected decoupled response. $t_{11} = t_{22} = 1/.2\ s + 1$, the comparison sensitivity is $s_{11} = s_{22} = .2s/(.2s+1)$. A plot of the magnitude of this transfer function versus frequency is shown at left in Figure 10.

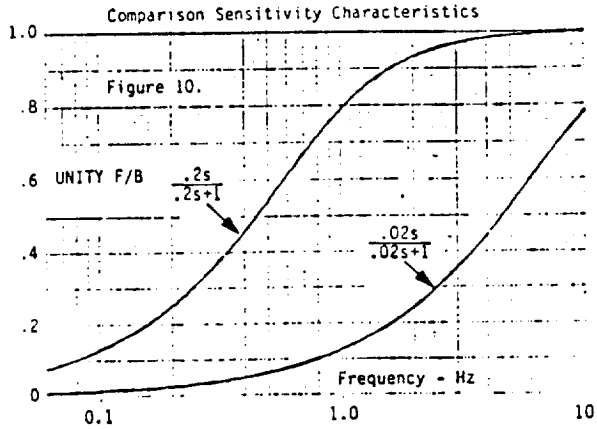

Example 2. Design a multivariable controller for the turbojet in example 1 with improved comparison sensitivity characteristics while maintaining the same overall system response.

Control design for both response and comparison sensitivity is accomplished by applying design equations (18) and (19). The comparison sensitivity characteristics of the unity feedback system S =diag (.2s/.2 s+1) shown in Figure 10 need to be improved. Comparison sensitivity is improved by a factor of 10 by, in effect, moving the curve to the right say by one decade in frequency. This results in a sensitivity transfer function matrix S = diag (.02s/.02s + 1). Thus the performance matrix, $Q = S^{-1}T$ = diag 50 (.02 s + 1)/s(.2s+1). Hence by equations (18) and (19) forward and feedback controller dynamics become:

$$G = \frac{(.02s + 1)\begin{bmatrix} 4.7(.005s + 1) & 137.5(.18s + 1) \\ .4(1.32s + 1) & -14\ (.18s + 1) \end{bmatrix}}{s(.2s + 1)}$$

$$H = T^{-1}(I - S) = \begin{bmatrix} \frac{.2s + 1}{.02s + 1} & 0 \\ 0 & \frac{.2s + 1}{.02s + 1} \end{bmatrix}$$

Three step responses of the system are shown in Figure 11: the nominal system and + 30% variation of p_{11} and p_{22}. Essentially no effect on response is discernable. This system has an improved parameter sensitivity performance and the desired overall response characteristics.

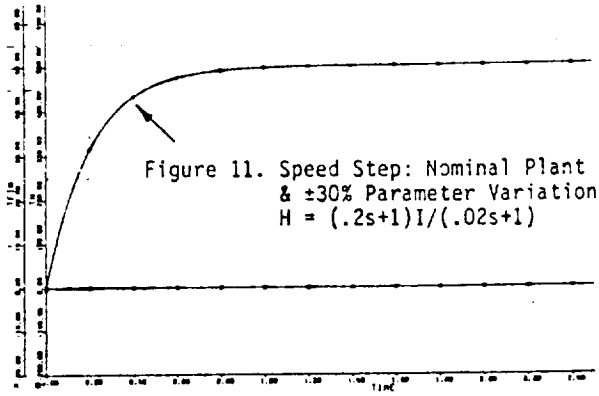

Figure 11. Speed Step: Nominal Plant & ±30% Parameter Variation H = (.2s+1)I/(.02s+1)

6. SUMMARY REMARKS

Linear multivariable control synthesis with transfer functions appears to be feasible and practical. A control design method, based on three fundamental equations, was described and illustrated.

Transfer function synthesis builds on classical transfer function concepts; it is easy to understand and contacts modern theory. Features include direct design of feedback systems to satisfy both response and comparison sensitivity with consideration of internal stability.

The plant inverse matrix is key in multivariable transfer function design. Its existence assures possibilities for plant trackability and decoupling.

in factored form, it indicates multivariable plant zeros, cancellations and potential performance trade-offs to simplify the controller.

7. REFERENCES

1. Peczkowski, J. L., "Multivariable Synthesis with Transfer Functions", Proceedings 1979 Propulsion Controls Symposium, NASA Lewis Research Center, NASA-CP-2137, August 1980.
2. Boksenbom, A.A. and Hood, R., "General Algebraic Method Applied to Control Analysis of Complex Engine Types", NACA Technical Note 1908, National Advisory Committee for Aeronautics, Washington, D.C., July 1949.
3. Feder, M. S. and Hood, R., "Analysis for Control Application of Dynamic Characteristics of Turbojet Engine with Tail Pipe Burning", NACA Technical Note 2183, Washington, D.C., September 1950.
4. Freeman, H., "A Synthesis Method for Multiple Control Systems", AIEE Transactions on Applications and Industry, Vol. 76, pp. 28-31, March 1957.
5. Freeman, H., "Stability and Physical Realizeability Considerations in the Synthesis of Multiple Control Systems", AIEE Transactions on Applications and Industry, Vol. 77, pp. 1-5, March 1958.
6. Kavanagh, R. J., "Noninteracting Controls in Linear Multivariable Systems", Transactions on Applications and Industry, Vol. 76,pp 95-99, May 1957.
7. Kavanagh, R. J., "Multivariable Control System Synthesis", AIEE Transactions on Applications and Industry, Vol. 77, pp. 425-429, November 1958.
8. Truxal, J. G., Automatic Feedback Control System Synthesis, McGraw-Hill, New York,1955.
9. Peczkowski, J. L., Sain, M. K., and Leake, R. J. "Multivariable Synthesis with Inverses", Proceedings, Joint Automatic Control Conference, June 1979, pp. 375-380.
10. R. R. Gejji, "On the Total Synthesis Problem of Linear Multivariable Control", Ph. Thesis, Department of Electrical Engineering, University of Notre Dame, Notre Dame, Indiana, January 1980.
11. Sain, M. K. and Ma, A., "Multivariable Synthesis with Reduced Comparison Sensitivity", Proceedings Joint Automatic Control Conference, August 1980, in Press.
12. Peczkowski, J. L. and Sain, M. K., "Linear Multivariable Synthesis with Transfer Functions", Proceedings, International Forum on Alternative for Multivariable Control, National Engineering Consortium, pp. 111-127, October 1977.
13. Rekasius, Z.V., "Linear Multivariable Control-A Problem of Specification", Proceedings, International Forum on Alternatives for Multivariable Control, National Engineering Consortium, pp. 101-110, October 1977.
14. Leake, R.J., Sain, M. K., and Peczkowski,J.L. "Step Trackable Linear Multivariable Plants", International Journal of Control, 1979.
15. Wyman, B. F. and Sain, M. K.,"Essential Right Inverses and System Zeros", Proceedings 18th IEEE Conference on Division and Control, pp. 23-33, December 1979.
16. Wonham, W. M. and Morse, A. S., "Decoupling and Pole Assignments in Linear Multivariable Systems: A Geometric Approach", SIAM Journal of Control, Vol. 8, pp. 317-337, 1970.
17. Bengtsson, Gunnar, "Feedback Realizations in Linear Multivariable Systems", IEEE Transactions on Automatic Control, Vol. AC-22, No.4, August 1977.
18. Bode, H. W., Network Analysis and Feedback Amplifier Design, Princeton, New Jersey: D. Van Nostraud Co., 1945.
19. Cruz, J. B. Jr., System Sensitivity Analysis, Dowden, Hutchinson and Ross, Inc.,Stroudsburg, Pennsylvania, 1973.

1980

Volume I

Joint Automatic Control Conference

August 13-15, San Francisco, California

MULTIVARIABLE SYNTHESIS WITH REDUCED COMPARISON SENSITIVITY

Michael K. Sain (IEEE)
Dept. Electrical Engineering
University of Notre Dame
Notre Dame, Indiana 46556

Abraham Ma (ASME)
Energy Controls Division
Bendix Corporation
South Bend, Indiana 46620

ABSTRACT

The idea of a total synthesis for a linear multivariable control system revolves around the simultaneous specification of the dynamical relationships of command/control and command/response. Though the practical motivation behind such specifications does not envision their exact achievement, it is nonetheless of interest to determine the way in which deviation from the specifications takes place as a function of changes in plant parameters. Moreover, should such deviation be unacceptably large, then procedures to accommodate the total synthesis are desirable. This paper initiates a study of the possible use of comparison sensitivity for such a purpose. A comprehensive illustration based upon realistic turbofan engine data is presented.

I. INTRODUCTION

Suppose that an object to be controlled is represented by the pair

$$\dot{x} = Ax + Bu, \tag{1a}$$

$$y = Cx + Du. \tag{1b}$$

Here we shall refer to y as the response of the object and to u as its control. Suppose also that control system goals can be expressed in terms of the dynamical relationship from a request r to the response and to the control. If $\hat{f}$ denotes the ordinary Laplace representation of a suitably smooth function $f : \mathbb{R} \to V$ for some real vector space V of finite dimension, then we may visualize these dynamical relationships in the manner

$$\hat{u} = M \hat{r}, \tag{2a}$$

$$\hat{y} = T \hat{r}, \tag{2b}$$

for

$$M : R(s) \to U(s) \tag{3a}$$

and

$$T : R(s) \to Y(s) \tag{3b}$$

morphisms of the rational vector spaces predicated upon finite-dimensional real vector spaces R, U, and Y associated with r, u, and y respectively.

For computation and for practical design, an appropriate choice of basis will yield matrices

$$[M] \tag{4a}$$

and

$$[T] \tag{4b}$$

over $\mathbb{R}(s)$, the field of real-coefficient rational functions; and specification can then be regarded in terms of the entries in the matrices (4). Relationships of command/control are embodied in $[M]$, while those of command/response are embodied in $[T]$.

As we shall see shortly, it would be unwise to attempt independent specification of $[M]$ and $[T]$, even in the case of an internally stable object of control. Momentarily, then, suppose that an acceptable pair $([M], [T])$ has been obtained. A controller driven by the request r and any measurements which are available from the object to be controlled will be said to achieve a total synthesis if its implementation results in (2) for the specified pair $([M], [T])$ and if the resulting loop is internally stable.

From the practical point of view, it is neither envisioned nor intended that the controller will achieve the total synthesis exactly. However, the degree to which the actual controlled system deviates from specifications when the object to be controlled deviates from its assumed description is always a practical matter. In particular, if these specification deviations are not acceptable, then the controller synthesis must be modified accordingly.

In [1] and [2], a synthesis procedure focused upon diagonal $[T]$ has been discussed in terms of its relevance to control design issues based upon modern turbofan engine data. Subsequently, these studies were extended to include the idea of $[M]$ and to illustrate applicability of the notion to controlled objects not of minimum phase [3]. As observed in simulations, the designs of [1-3] appeared to display adequate properties of robustness, at least for the application under study. Nonetheless, it seems appropriate to incorporate into the illustrated procedures a means of improving robustness. This paper makes a beginning along such lines, by placing specifications upon comparison sensitivity.

II. THE TOTAL SYNTHESIS PROBLEM (TSP)

The purpose of this section is to provide a num-

ber of basic algebraic remarks about the section preceding, in particular with regard to the question of simultaneous choice of [M] and [T].

Begin by inferring the traditional relationship

$$\dot{y} = P\,\dot{u} \tag{5}$$

from (1), where

$$P : U(s) \to Y(s) \tag{6}$$

is the morphism of rational vector spaces represented by

$$C(sI - A)^{-1}B + D. \tag{7}$$

Then the three equations (2a), (2b), and (5) combine to give

$$T = PM, \tag{8}$$

where the right member is traditional composition of P and M.

An equation of type (8) can also be described in diagrammatic form. Consider the triangle diagram of Figure 1. Each side of the triangle corresponds to one of the depictions (3a), (3b), and (6). Interpretation of Figure 1 may be made as follows. A group

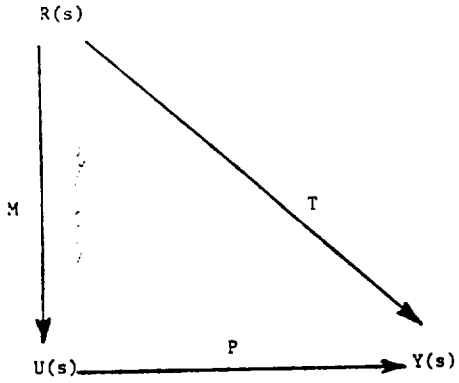

Figure 1. Diagram of (8).

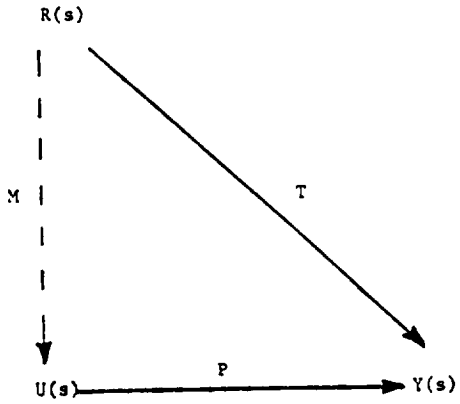

Figure 2. EMMP.

element in R(s) may be passed through T directly to produce an element in Y(s); or it may be passed through M to produce an element in U(s), with that element then being passed through P to give an element in Y(s). The assertion of (8), which is intended in Figure 1, is that the same element in Y(s) results in both cases. Then the diagram is said to commute, and is an alternate statement of (8).

In control problems, P is given as the object to be controlled. The classic question from linear equation theory may then be posed as follows. Given T and P, determine whether or not there exist solutions M to (8). If such solutions do exist, determine whether or not they are unique. Finally, if they exist and are not unique, characterize the collection of all solutions, as for example by an affine space. From the diagram point of view, the fact that T and P are given is ordinarily indicated by showing those sides of the triangle with solid arrows. Correspondingly, the fact that existence and uniqueness of M are to be determined is usually indicated by showing its side of the triangle with a dashed arrow. This convention has been used in Figure 2.

As a control problem, of course, Figure 2 portends full specification of command/response, with the controller synthesis indicated by M. Such problems have generally been included in the literature of model following; in particular, the problem of Figure 2 is often called the Exact Model Matching Problem (EMMP).

The idea of the Total Synthesis Problem (TSP) is then indicated in Figure 3. Here P is regarded as given, while both M and T are to be found. If P is an isomorphism of rational vector spaces, then its inverse is of type

$$P^{-1} : Y(s) \to U(s), \tag{9}$$

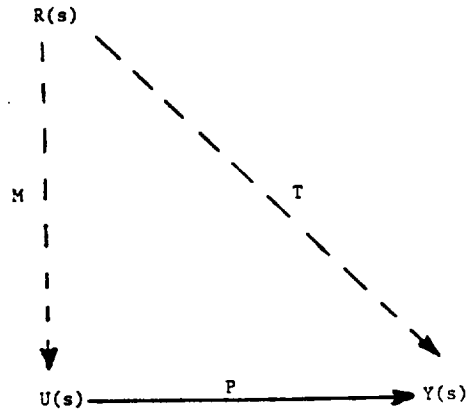

Figure 3. TSP.

and could be indicated in Figure 3 by reversing the arrow at the bottom of the triangle. An Inverse TSP is then obtained, with acronym (ITSP).

Because P (in TSP), or P^{-1} (in ITSP), serves as a constraint between M and T, it is not very realistic to regard their specification as two separate questions. Instead, we can proceed as follows

[3,4]. Denote by

$$\text{hom}\,(R(s),\ U(s)) \tag{10a}$$

the rational vector space of (homo) morphisms with domain $R(s)$ and codomain $U(s)$; and establish a counterpart notation

$$\text{hom}\,(R(s),\ Y(s)). \tag{10b}$$

Then define a morphism of rational vector spaces

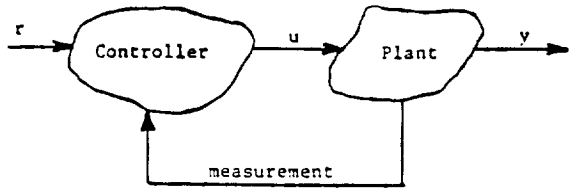

Figure 4.

$$\text{hom}(R(s),U(s))\text{x}\text{hom}(R(s),Y(s)) \to \text{hom}(R(s),Y(s)) \tag{11a}$$

by the action

$$(M,T) \mapsto PM-T. \tag{11b}$$

The kernel of the morphism (11) can be used to describe possible TSP designs. An analogous statement can be made for ITSP.

However, if the rational vector space format is applied to the indicated kernel study, then it would often happen in practical problems that internal loop stability would be difficult or impossible to achieve. To see this, consider the result of Bengtsson [5]. Here we have space only to sketch the general nature of the study. Consider Figure 4. The plant is of the type (1), with D the zero map, and with certain technical assumptions on the remaining maps. The controller structure is of quite general type, and can encompass most of the classical control configurations. For the structure class chosen, it is established in [5] that pairs (M,T) in the kernel of (11) can be realized along the lines of Figure 4 in an internally stable way if and only $[M]$ is a proper matrix and both $[M]$ and $[T]$ are stable matrices, in the usual sense. Of course, because $[P]$ is a strictly proper matrix, it follows that $[T]$ is (strictly) proper as well. For a discussion of one way to extend [5] to the case of nonzero D, see [6].

According to results such as these, it is appropriate to specialize the kernel study of (11) at least to the case in which the matrices $[M]$ and $[T]$ are proper and stable.

Considered as a field, the set of real-coefficient rational functions $\mathbb{R}(s)$ has various subrings. Among these are both the subring of proper rational functions and the subring of stable rational functions. Both of these subrings have interesting algebraic properties.

The intersection of these two subrings of $\mathbb{R}(s)$, namely the real-coefficient transfer functions which are both proper and stable, would be a very natural subring in which to study TSP or ITSP, at least from the conceptual point of view. But the intersection ring turns out to be more complicated from the algebraic standpoint. Accordingly, it is often desirable to begin by considering a total synthesis problem over the subring of stable transfer functions. The issue of properness can then be addressed by classical means, though the addition of adequate rolloff.

Adjusted to be a module kernel problem over the subring of stable transfer functions, computation of a kernel basis has become in recent years a more manageable problem. For a discussion, see [4,7].

III. USE OF A SENSITIVITY SPECIFICATION

After an acceptable (M,T) pair has been found, along the lines discussed in the section preceding, we may then turn our attention to the question of synthesizing the controller in such a way that it tends to maintain the command/response specification T even when small parameter variations occur in (1). For this purpose, we wish to consider the idea of comparison sensitivity [8,9].

In the use of comparison sensitivity, the comparison is made between open loop and feedback designs which achieve the same command/response specification when (1) does not deviate from its assumed or given form. With more detail, (6) may be regarded as depending upon a parameter vector α. This can be indicated by the notation $P(\alpha)$, which for $\alpha \in R^p$ would actually signify a construction

$$R^p \to \text{hom}(U(s),\ Y(s)). \tag{12}$$

The vector α is assumed to have a nominal value α_0 corresponding to (1). When α equals its nominal value, then (6) is replaced by

$$P_0 = P(\alpha_0) \tag{13}$$

in accordance with (12).

Now consider an open loop design to achieve the specified T. The open loop design is assumed to be achieved by series pre-compensation corresponding to a morphism

$$\tilde{G} : R(s) \to U(s). \tag{14}$$

The resulting design relationship is given by

$$T = P_0\tilde{G}. \tag{15}$$

Next, examine a feedback design to achieve the specified T. A number of configurations are realistic. For illustration, we choose the following. Establish a real space $E \overset{\sim}{=} R$, and regard E as the space of errors. Analogous to steps preceding, develop E into the rational vector space $E(s)$. Then the feedback design will make use of forward pre-compensation

$$G : E(s) \to U(s) \tag{16}$$

and parallel feedback compensation

$$H : Y(s) \to R(s), \tag{17}$$

together with the connection constraint

$$e = r - Hy. \tag{18}$$

The resulting design relationship is provided by the well known expression

$$T = (1 + P_0 G H)^{-1} P_0 G. \tag{19}$$

When α is not α_0, then (15) and (19) will generally fail to be satisfied. Thus,

$$T \neq P(\alpha) \overset{\alpha}{C}, \tag{20a}$$

$$T \neq (1+P(\alpha)GH)^{-1} P(\alpha)G. \tag{20b}$$

In (20a), denote by $E^{OL}(\alpha)$ the difference obtained by subtracting the left member from the right member. Similarly, in (20b), establish $E^{FB}(\alpha)$. Here the superscripts OL and FB refer respectively to open loop and feedback situations. Each of these morphisms is to be understood in the context

$$\text{hom } (R(s), Y(s)). \tag{21}$$

It has been shown, under minor technical assumptions, by Cruz and Perkins [8] that there exists a morphism

$$S(\alpha) : \text{hom}(R(s), Y(s)) \to \text{hom}(R(s), Y(s)) \tag{22}$$

relating these two error morphisms in the manner

$$E^{FB}(\alpha) = S(\alpha)\, E^{OL}(\alpha). \tag{23}$$

In fact, the comparison sensitivity morphism $S(\alpha)$ turns out to be the inverse of return difference, according to

$$S(\alpha) = (1 + P(\alpha)GH)^{-1}. \tag{24}$$

If a particular element $\hat{r}$ in $R(s)$ is chosen, then (23) infers a relationship

$$\Delta\hat{y}^{FB} = S(\alpha)\, \Delta\hat{y}^{OL}. \tag{25}$$

Moreover, in the time domain, the left member of (25) would have a counterpart

$$\Delta y^{FB}(t), \tag{26a}$$

while the right member would generate a corresponding

$$\Delta y^{OL}(t). \tag{26b}$$

The time vectors (26) can be sized in the manner

$$\int ||\Delta y||^2 \, dt \tag{27}$$

using Euclidean norm. Then Cruz and Perkins have established that, for superscript (*) denoting the conjugate transpose,

$$[1] - [S(\alpha)]^* [S(\alpha)] \tag{28}$$

positive semidefinite on the $j\omega$ - axis will lead to

$$\int_0^{t_1} ||\Delta y^{FB}||^2 \, dt \leq \int_0^{t} ||\Delta y^{OL}||^2 \, dt \tag{29}$$

for all $r(t)$ satisfying

$$\int_0^{t_1} ||r||^2 \, dt \tag{30}$$

finite and for all finite, nonnegative real t_1.

These remarks carry the practical implication that making the comparison sensitivity matrix $[S(\alpha)]$ "small" in an appropriate sense will tend to make the feedback design more effective in coping with changes in α than the open loop design.

It should also be noted that the comparison sensitivity morphism $S(\alpha)$ in (24) is defined in terms of $P(\alpha)$ rather than P_0. Because $P(\alpha)$ is rarely assumed to be known precisely, except when α equals α_0, there are practical questions to be decided in design. One accepted rule of thumb is to use $S(\alpha_0)$ for the purposes of design. One may then argue that this will give acceptable results for cases in which α is "close" to α_0. Or one may be quite conservative in the design of $S(\alpha_0)$ so as to "counter in advance" possible larger excursions in α. An example of such conservative design is given in [10].

Our approach here is to regard $S(\alpha_0)$ as an additional specification to be used in conjunction with M and T. Then [11] it is possible in principle to solve for the forward and feedback compensations G and H by means of basic relationships

$$G = P_0^{-1} S^{-1}(\alpha_0)\, T \tag{31a}$$

$$H = T^{-1} (I - S(\alpha_0)), \tag{31b}$$

under the assumption that P_0 is an isomorphism. It should be noted that such a condition on P_0 is taken in practice to be reasonable, in the sense that basic tracking conditions at fixed frequencies imply rank constraints on P_0.

IV. EXAMPLE

The purpose of this section is to illustrate the incorporation of a comparison sensitivity specification into the ITSP design procedure. For the illustration, we have chosen the turbofan engine data used in [3]. Relative to (1), the matrices of the quadruple (A, B, C, D) are shown in Figure 5, and correspond to a reduced order sea level, 67 degree power lever condition on the F100 engine. Figure 6 shows the control configuration. Actuators are represented by a diagonal matrix A_d, with nonzero elements

$$(1/.05s+1,\ 1/.2s+1,\ 1/.1s+1,\ 1/.1s+1); \tag{32}$$

and sensors are represented by a diagonal matrix S_m, with nonzero elements

$$(1/.02s+1,\ 1/.02s+1,\ 1/.02s+1,\ 1/.5s+1). \tag{33}$$

For the command/response specification, [3] chose a diagonal matrix

$$[T] = (1/.25s+1)(1/.01s+1)\ I. \tag{34}$$

Working from the ITSP viewpoint, design in [3] was achieved by choosing H to be the identity morphism. To simplify the presentation of $[P^{-1}]$, adopt the abbreviations

$$(as+1) \to (a) \quad ; \quad (as^2+bs+1) \to (a,b). \tag{35}$$

Then $[P^{-1}]$ is shown in Figure 7. It should be noted that its denominator time constants are positive, so that this object does not display nonminimum phase behavior. The forward compensator G chosen in [3] is given in Figure 8.

The response of this system design to a unit step command of 500 RPM in fan speed, with no command to the other channels is shown in Figure 9. This set of curves serves as a supplement of those of Figures 14 and 15 in [3]. It should be emphasized that this design already displayed a very favorable behavior to parameter variations of a physically reasonable nature. For the design, $S(\alpha_0)$ was diagonal, with nonzero entries

$$(S_2(s),\ S_2(s),\ S_2(s),\ S_1(s)), \tag{36}$$

where the nature of the $S_i(s)$, as well as plots of $|S_i(j\omega)|$, are shown in Figure 10. Nonetheless, in order to illustrate the use of a comparison sensitivity specification, we subjected the model (1) to a rather severe parameter variation according to the rule

$$A_{ii} \to 1.5\, A_{ii}. \tag{37}$$

The result of this parameter change is shown in Figure 11, for comparison with Figure 9.

To adjust for, and improve, this situation, a sensitivity specification range

$$S(\alpha_0) = S_i(s)I \quad , \quad i = 3,4,5, \tag{38}$$

was selected, with the three possible choices for S_i sketched in Figure 12. Of these possibilities, S_5 was selected for presentation here. With appropriate modification of the basic design equations of Section III, to account for actuators and sensors, a design for diagonal H was determined to be

$$(H_2,\ H_2,\ H_2,\ H_1) \tag{39}$$

with

$$H_1(s) = \frac{(.25)(.01)(.5)}{(.01331)(.001331)^2}, \tag{40}$$

$$H_2(s) = \frac{(.25)(.01)(.02)}{(.01331)(.001331)^2}, \tag{41}$$

and a corresponding G of the form

$$\frac{62.9(.01331)(.001331)^2}{s(.25)(.01)(1.476\times10^{-6},2.33\times10^{-3})}\,\bar{G}(s), \tag{42}$$

where $\bar{G}$ is given approximately in Figure 13.

Finally, Figure 14 indicates the effect achieved by the comparison sensitivity specification in reducing the influence of the abovementioned parameter change in A.

V. CONCLUSIONS

In this paper, we have explained the viewpoint of a total synthesis approach (TSP or ITSP) to linear multivariable control system design. To accommodate the effect of parameter variations, the use of an additional specification on comparison sensitivity has been introduced. The combined effect of these specifications has been illustrated on turbofan engine data originally studied in [3].

VI. ACKNOWLEDGMENTS

This work was supported by the Office of Naval Research under Contract N00014-79-C-0475.

REFERENCES

1. J.L. Peczkowski and M.K. Sain, "Linear Multivariable Synthesis with Transfer Functions", in Alternatives for Linear Multivariable Control, M.K. Sain, J.L. Peczkowski, and J.L. Melsa, eds. Chicago: National Engineering Consortium, 1978, pp. 71-87.
2. J.L. Peczkowski, "Multivariable Synthesis with Transfer Functions", Proceedings 1979 Propulsion Controls Symposium, to appear.
3. J.L. Peczkowski, M.K. Sain, and R.J. Leake, "Multivariable Synthesis with Inverses", Proceedings 1979 Joint Automatic Control Conference, pp. 375-380.
4. R.R. Gejji, "On the Total Synthesis Problem of Linear Multivariable Control", Ph.D. Dissertation, Department of Electrical Engineering, University of Notre Dame, Notre Dame, Indiana, May 1980.
5. G. Bengtsson, "Feedback Realizations in Linear Multivariable Systems", IEEE Transactions on Automatic Control, Vol. AC-22, No. 4, pp. 576-585, August 1977.
6. R.J. Leake, J.L. Peczkowski, and M.K. Sain, "Step Trackable Linear Multivariable Plants", International Journal of Control, Vol. 30, No. 6, pp. 1013-1022, 1979.
7. R.R. Gejji, "Reliable Floating Point Computation of Minimal Bases", Proceedings 1980 Joint Automatic Control Conference.
8. J.B. Cruz, Jr., Ed., Feedback Systems. New York: McGraw-Hill Book Co., 1972.
9. J.B. Cruz, Jr. and J.S. Freudenberg, "Comparison Sensitivity Criterion via a Singular Value Decomposition", Proceedings 1980 Joint Automatic Control Conference.
10. M.K. Sain, A. Ma, and D. Perkins, "Sensitivity Issues in Decoupled Control System Design", Proceedings 1980 Southeastern Symposium on System Theory.
11. V. Seshadri, "Compensation of Multivariable Control Systems", M.S. Thesis, Dept. of Electrical Engineering, University of Notre Dame, Notre Dame, Indiana, May 1976.

$$A = \begin{bmatrix} -4.064 & 3.895 & -470.5 & 7.971 & 5.294 & -3.005 \\ .03718 & -2.958 & -58.13 & .1727 & 2.08 & 12.48 \\ .03389 & .0067 & -4.642 & .0059 & .1474 & .0985 \\ 1.164 & -2.646 & -331.8 & -50.05 & -.473 & -11.36 \\ .05174 & -.1176 & -14.74 & -2.001 & -2.021 & -.505 \\ .00184 & .0038 & -.801 & .00008 & .0009 & -.666 \end{bmatrix}$$

$$B = \begin{bmatrix} .8686 & -14.51 & -98.14 & 9.246 \\ .9096 & -58.46 & -1.053 & -60.15 \\ -.007994 & -79.66 & 1.2 & .3673 \\ 5.643 & -112.2 & -18.23 & 41.53 \\ .2508 & -4.99 & -.8106 & 1.846 \\ .01 & -.3166 & -.02915 & .07426 \end{bmatrix}$$

$$C = \begin{bmatrix} 1 & 0 & 0 & 0 & 0 & 0 \\ 0 & 1 & 0 & 0 & 0 & 0 \\ 0 & 0 & 1 & 0 & 0 & 0 \\ 0 & 0 & 0 & 1 & 1 & 0 \end{bmatrix} \qquad D = \begin{bmatrix} 0 & \cdots & 0 \\ \vdots & \ddots & \vdots \\ 0 & & 0 \end{bmatrix}$$

Figure 5

$$\begin{bmatrix} -.334(1.55)(.470)(.109) & .897(1.55)(.470)(.119) & 42.6(1.55)(.470)(-.007) & 7.75(1.56)(.500)(.019) \\ -.000245(1.54)(.655)(.470) & .000505(1.54)(.470)(-.172) & -.129(1.553)(.470)(.097) & .00220(1.41)(.462)(.008) \\ -.046(1.55)(.470)(.235) & .045(1.55)(.470)(-.010) & -6.50(1.553)(.470)(.0003) & .160(1.563)(.480)(.009) \\ -.0035(1.50)(.470)(.061) & -.0365(1.52)(.470)(.403) & -.138(1.50)(.470)(-.056) & .144(1.27)(.491)(.019) \end{bmatrix}$$

Figure 7

$$P^{-1} \approx$$

$$(1.55)(.470)$$

Figure 8

$$G(s) \approx \frac{\begin{bmatrix} -1.2(.11)(.05) & 3.2(.12)(.05) & 152(.05) & 10(.02)(.05)(.5)/(.16) \\ -.001(.66)(.02) & .002(-.17)(.02) & -.46(.1)(.02) & .004(.01)(.02)(.5)/(.16) \\ -.16(.24)(.1) & .16(-.01)(.1) & -16(.1) & .21(.01)(.1)(.5)/(.16) \\ -.013(.06)(.1) & -.13(.40)(.1) & -.49(-.06)(.1) & .19(.02)(.1)(.5)/(.16) \end{bmatrix}}{s\ (.01)}$$

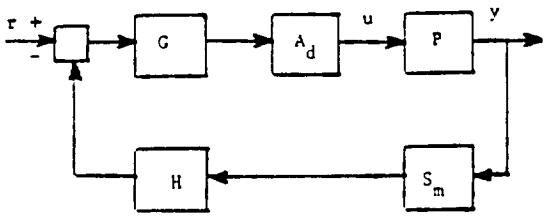

Figure 6

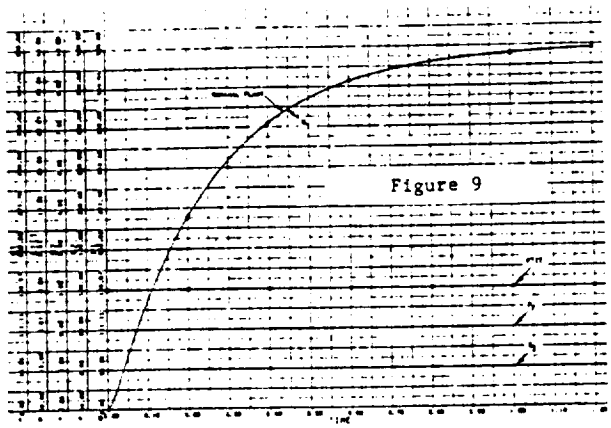

Figure 9

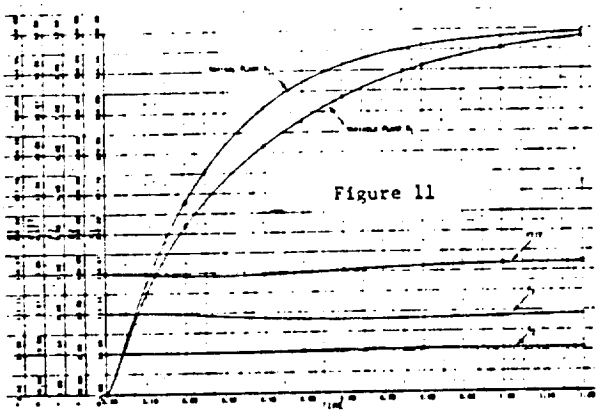

Figure 11

Figure 10

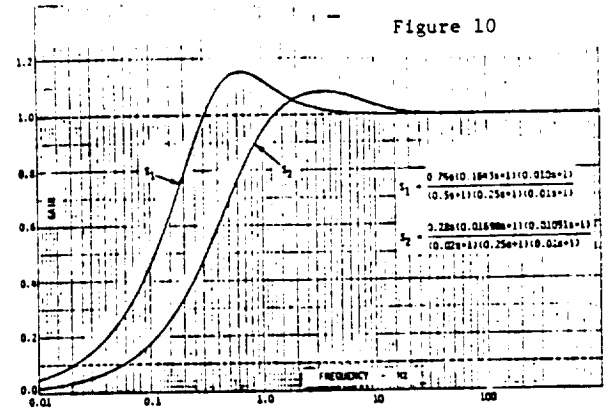

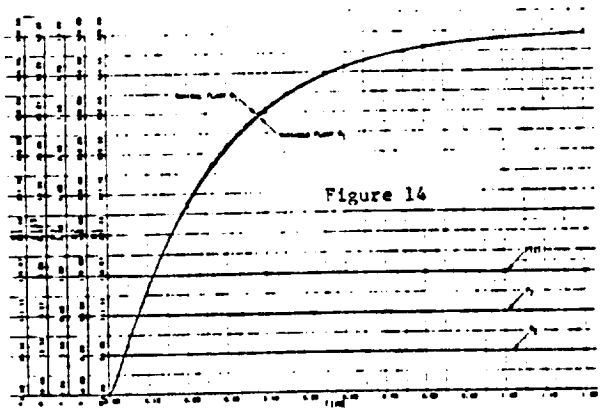

Figure 14

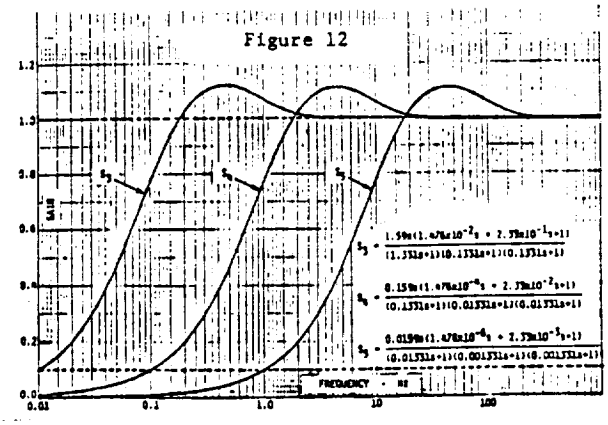

Figure 12

$$\bar{G}(s) \approx \begin{bmatrix} -.334(.109)(.05) & .897(.119)(.05) & 42.6(-.00713)(.05) & 7.75(.0193)(.05) \\ -.000245(.655)(.2) & .000505(-.172)(.2) & -.129(.0972)(.2) & .0027(.00822)(.2) \\ -.0456(.235)(.1) & .045(-.0102)(.1) & -4.5(.0000308)(.1) & .16(.00929)(.1) \\ -.0035(.061)(.1) & -.0365(.403)(.1) & -.138(-.0562)(.1) & .144(.0191)(.1) \end{bmatrix}$$

Figure 13

1980

Volume I

Joint Automatic Control Conference

August 13-15, San Francisco, California

RELIABLE FLOATING POINT COMPUTATION OF MINIMAL BASES

R.R. Gejji
Western Michigan University
Kalamazoo, Michigan

ABSTRACT

Minimal bases are of great interest in linear multivariable control due to their use in characterizing solutions to the minimal design problem (MDP), an important idea in multivariable control. Only recently has the literature seen procedures of adequate practical advantage in solving the MDP in floating point arithmetic. A survey of recent techniques for performing the floating point arithmetic shows a link to the problem of rank determination in real matrices. Such rank decisions are usually based upon a user chosen threshold. The magnitude of some calculated quantity, termed the decision criterion, needs to be compared to the threshold. Accurate calculation of the decision criterion itself may depend on the conditioning of the raw data. In this paper we see the reason why considerations of conditioning are particularly central for MDP calculations. MDP solutions arise only out of the linear dependency existing in the columns of the real matrix. It is this same linear dependency which also leads to difficulty with data conditioning. A comprehensive case study is given. It comprises a least squares and a singular value decision criterion, combined with two existing methods of converting the problem to a real matrix. As a note on complexity, the problem for the case study is taken from the literature and leads to a 20x27 matrix of reals. The original MDP has seven first degree basis elements in its solution. The case study leads to a heuristic balancing rule for reliable computation. The importantance of balancing becomes explicit by consideration of the underlying premultiplication by a matrix of polynomials. Such premultiplication routinely occurs in numerous methods of MDP solution. Although this does not change the essential MDP, it can radically alter the balance structure of the resulting real matrix.

I. TECHNIQUES FOR SOLVING THE MINIMAL DESIGN PROBLEM IN FLOATING POINT

In this work R(s) denotes the field of rational functions in 's' with real coefficients; R[s] is the ring of polynominals in s with real coefficients, R is the field of reals. Our motivation for this work came from a study of the Total Synthesis Problem (TSP) [Refs. 1,2] which led to a problem of kernel computation in free R[s]-modules. The solution structure arises from its being associated with a more fundamental problem of linear multivariable control, viz. the Minimal Design Problem (MDP) [Refs. 3,4]. The MDP states that two R(s)-matrices of size pxq and pxr are given. Let these be denoted by $B_1(s)$ and $B_2(s)$ respectively. Then it is required to find a proper R(s)-matrix B(s) of minimal order (McMillan degree) such that

$$B_1(s)\, B(s) = B_2(s) \qquad (1)$$

The natural approach to solution of MDP leads to the construction of the matrix.

$$B_3(s) = [B_1(s) \;\vdots\; -B_2(s)] \qquad (2)$$

Then the solution can be reduced to a search for the minimal basis [4] for the R[s]-module Ker $B_3(s)$ $R^{q+r}[s]$. Ker denotes kernel. Various authors have used essentially different forms of the matrix $B_3(s)$, obtained by premultiplication by suitable square nonsingular R[s]-matrices. This does not change the structure of its kernel, as noted in [1]. From a computational viewpoint, we will see, such changes can be crucial. In particular, the polynomial matrix form of $B_3(s)$ is of interest. This may be obtained by suitably multiplying each row of $B_3(s)$ to clear out all denominators. Let this be denoted by $B_{3p}[s]$.

Another computational matter we wish to emphasize concerns the appearance of a subjective element in the computation whenever floating point arithmetic is used. This generally appears in the form of a user defined threshold or parameter which determines a machine epsilon, or computationally insignificant "zero".

Next, we address a few remarks to some earlier efforts in this area. A method to solve MDP was given by Sain [5] incorporating some of the ideas of [3,4]. The algorithm proceeds in two district segments. From the first step an R[s]-vector basis in obtained for Ker $B_3(s)$. It is possible to specify a degree for each element of such a basis by expanding into a polynomial with R-vector coefficients. The second step systematically reduces the sum total of degrees of the basis elements to the minimum achievable.

FORTRAN and PL/I language implementations of Sain's algorithm [6] and later reprogramming in exact rational arithmetic using FORMAC [7] taught two major lessions. The prime difficulty in using floating point software is in recognizing a zero calculated during computation. Second, the reduction step involved the bulk of the computation.

Recent methods by Foster [8] and Kung and Kailath

[9] completely eliminate the reduction step, going directly to a minimal basis. The key idea that carries both the methods is remarkably similar.

Let the integer μ equal or exceed the maximum column degree among all elements of a minimal basis. Let $t_0(s), t_1(s), \ldots, t_\mu(s)$ denote polynomials of degree $0, 1, \ldots, \mu$ respectively. Then the following matrix contains all the information necessary to calculate a minimal basis. $B_4(s) = [t_0(s)B_3(s) \quad t_1(s)B_3(s) \quad \ldots, \quad t_\mu(s)B_3(s)]$ (3)

Eq. (3) is the essence of Foster's technique. Foster has suggested a Chebysheff polynomial approach to selecting $t_0(s), \ldots, t_\mu(s)$. This is described in the reference [8] in greater detail. The claim remains true if $B_3(s)$ is a polynomial matrix $B_{3p}[s]$. This is used in the Kung-Kailath method with the polynomials $t_0(s), t_1(s), \ldots, t_\mu(s)$ taken to be $1, s, s^2, \ldots, s^\mu$ respectively. The minimal basis is calculated by successively checking each column of $B_4(s)$ for R-linear dependence on the preceding ones.

The problem is converted into an R-matrix problem by replacing $B_4(s)$ with an equivalent real matrix. Foster does this by assuming for proper $B_3(s)$, ν to be the observability index of $B_3(s)$ and N any integer greater than $\mu+\nu$. Then for arbitrary numbers in R $\lambda_1, \ldots, \lambda_N$ which are not poles of $B_3(s)$, the matrix $B_4(s)$ can be replaced by the real matrix

$$RF = \begin{bmatrix} t_0(\lambda_1)B_3(\lambda_1) & t_1(\lambda_1)B_3(\lambda_1) & \ldots & t_\mu(\lambda_1)B_3(\lambda_1) \\ t_0(\lambda_2)B_3(\lambda_2) & & \ldots & t_\mu(\lambda_2)B_3(\lambda_2) \\ \vdots & \vdots & & \vdots \\ t_0(\lambda_N)B_3(\lambda_N) & & \ldots & t_\mu(\lambda_N)B_3(\lambda_N) \end{bmatrix} \quad (4)$$

In the spirit of the King-Kailath method, a different real matrix may be used in place of $B_4(s)$. The polynomial matrix $B_{3p}[s]$ is expanded in powers of s as, $B_{3p}[s] = RM_0 + RM_1 s + \ldots + RM_K s^K$ (5)

where K denotes the maximum degree occurring in $B_{3p}[s]$, and RM_0 through RM_K are real matrices of the same size as $B_{3p}[s]$. Then the following is the required real matrix; it has $\mu+1$ block columns. (See below.)

$$RK = \begin{bmatrix} RM_0 & 0 & \ldots & 0 \\ RM_1 & RM_0 & & \vdots \\ \vdots & RM_1 & \ddots & 0 \\ RM_K & \vdots & \ddots & RM_0 \\ 0 & RM_K & \ddots & \vdots \\ \vdots & 0 & & \\ 0 & 0 & \ldots & RM_K \end{bmatrix} \quad (6)$$

II. METHODS FOR RANK CALCULATION IN REAL MATRICES

Once the problem of finding a minimal basis is reduced to determining linear dependencies in a real matrix, a relatively wide range of methods become available for completing the solution. In calculating a minimal basis from the kernel of either the real matrix RK or the matrix RF, the method is exactly identical. Since both have $\mu+1$ block columns, each containing as many columns as in $B_3(s)$, i.e., $q+r$, then the total number of columns in the matrix is $(\mu+1) \times (q+r)$. Suppose w is a real vector of size $(\mu+1)\times(q+r)$ determined to be in the kernel of RF or RK, it may be partitioned into $\mu+1$ block rows of $q+r$ elements each. Let $w^T = (w_0^T, w_1^T, \ldots, w_\mu^T)$. Then the polynomial vector $w_0 t_0(s) + w_1 t_1(s) + \ldots + w_\mu t_\mu(s)$ is an element of the minimal basis, if w has been generated according to the following strategy (explained by both Foster [8] and Kung, Kailath [9]).

Each column of the matrix, from left to right, is successively checked for linear dependency on the preceding columns. If such dependency exists, it is easy to see then that the last column considered may be written as an R-linear combination of the preceding ones. Excluding some cases that yield redundant solutions, it is true that every time a linear dependency is encountered, it then indicates the existence of a suitable real vector w which may be used to generate an element of the minimal basis. Let us denote by H, the matrix we are working with, be it RF or RK. The technique used by Foster in his work is now explained. At any point in the computation, let H_k denote the matrix formed by the linearly independent columns encountered up to that point, and let h_k denote the column being considered for linear dependency on the columns of H_k. The following linear least squares problem is solved for $\hat{w}_k$,

$$\text{minimize} \quad \| H_k \hat{w}_k + h_k \| \quad (7)$$

The criterion for a linear dependency decision is calculated as

$$\epsilon_k = \| H_k \hat{w}_k + h_k \| \; / \; M_k \quad (8)$$

The quantity M_k has been recommended by Foster to be most appropriate as

$$M_k = M \cdot \| (\hat{w}_k, 1) \| \quad (9)$$

Here, M denotes the maximum of the Euclidean norms of all the columns of H. $\|\cdot\|$ denotes the Euclidean norm $\|\cdot\|$ denotes the Euclidean norm, and $(\hat{w}_k, 1)$ denotes a vector of dimension one larger than $\hat{w}_k$, with elements of $\hat{w}_k$ followed by unity. In practice, as in earlier work done by Foster [8], M_k may also be taken as $\| H_k \|$, where for $\|\cdot\|$, a matrix norm is used. The usual row sum is norm is adequate.

Kung and Kailath have suggested a scheme of residuals. First, working with block columns, the residual for each block column is calculated by subtracting its projections on all the preceding block columns. Whenever a residual vanishes, it indicates a dependent column. Now the problem of calculating residuals is in fact a least squares problem. For purposes of calculation, the residuals are replaced by so-called orthonormal residuals. These serve the same purpose but are capable of being calculated by Householder type orthogonal transformations. Kung-Kailath have not specifically addressed the question of when a residual may be treated as zero, from

practical considerations. Moreover, there is a useful recursion in the Foster least squares procedure which offers a significant benefit in terms of programming simplification. In view of these considerations, we have not studied a computer level implementation of the Kung-Kailath projection procedure.

The two techniques we have implemented are the Foster least squares technique and a singular value technique which is still to be described in the text that follows.

The singular value decomposition is first introduced with a Theorem.

Theorem 1: (from Laub [10] Let A be an mxn real matrix of rank r. Then there exist orthogonal real matrices U and V of sizes mxm and nxn respectively, such that

$$A = U \Sigma V^T \tag{10}$$

where

$$\Sigma = \begin{bmatrix} S & 0 \\ 0 & 0 \end{bmatrix}, \text{ and}$$

$S = \text{diag}(\sigma_1, \sigma_2, \ldots, \sigma_r)$ with $\sigma_i > 0$, $1 \leq i \leq r$, and $\sigma_i \geq \sigma_{i+1}$, $1 \leq i \leq r-1$

The set of numbers $\sigma_1, \ldots, \sigma_r$ together with the definition $\sigma_{r+1} = \ldots = \sigma_n = 0$ are called the singular values of A. In fact, these are the positive square roots of the eigenvalues of the symmetric matrix A^TA.

The true importance of singular value decompositions springs from the following theorem which has important implications for the problem in determining rank by numerical methods. This is because, in actual applications, almost never will a zero singular value appear in computation, because of roundoff errors in floating point representations. There can be real difficulty in determining when a singular value may be considered zero. The result included here as a theorem is taken from Laub's work, but was originally proved elsewhere by Golub, Klema and Stewart.

Theorem 2: Let A be an mxn real matrix of rank r, and assume distances to be defined by spectral norms. Let $\sigma_1, \ldots, \sigma_r$ be the non-zero singular values of A. Then all matrices lying strictly inside the σ_r ball around A have rank $\geq r$.

In practice, where floating point data represents an approximation $\hat{A}$ to the actual matrix A, one may be able to make a statement that A lies within a ball of $\hat{A}$. Here may, for instance, correspond to the zero threshold, multiplied by the norm of A. Then if $\delta < \sigma_r$, it can definitively be said that A has rank at least r. But if $\delta > \sigma_r$, no definitive statement may be made, and it is left to the judgment of the user whether or not to consider A to have rank less than r. To assume so would correspond to assuming that singular value σ_r is in fact, zero, from a numerical viewpoint. It is interesting to consider the relationship of this remark to the statement made in Section I about the user's choice in determining a zero threshold. It appears that the assumption of rank deficiency always implies the exercise of subjective judgment on the user's part.

Since the norm of A, $\|A\| = \sigma_1$ and since σ_r is clearly sensitive to data scaling the quantity of interest is always σ_r/σ_1. This quantity turns out to be important in its own right in numerical linear algebra. It is the reciprocal of the number $\text{cond}(A) = \|A\| \cdot \|A^+\|$, the so-called "condition number of A with respect to pseudo-inversion", where A^+ denotes the well-known Moore-Penrose pseudo inverse of A.

Let us return to the problem of calculating a minimal basis. Typically, it is necessary to determine whether a particular column b is linearly dependent on the column set of a matrix A. It may be assumed without loss of generality that the columns of A have been previously determined to form a linearly independent set. Now define the matrix

$$E = [A \mid b] \tag{11}$$

Singular value analysis can now be used to determine whether or not matrix E is rank deficient. This involves calculating the ratio of the smallest singular value of E to the largest. If the ratio is exceeded by the zero threshold, E may be considered to be rank deficient.

While it was mentioned before that the singular values of a matrix A are related to the eigenvalues of A^TA, it is hardly advisable to compute them this way. The least squares as well as the singular value method have been programmed using SPEAKEZY language; this involves a procedure using stable Householder transformations.

III. CONSIDERATIONS FOR ACTUAL USE

In the prior sections, we have seen ways in which the MDP problem may be reduced to one of finding linear dependencies among the columns of a real matrix, and also some techniques of performing this computation. For calculations done with perfect accuracy, there is little to choose among the alternatives available. But a consideration of the vagaries of finite precision arithmetic on computers mandates a careful selection of the method to be used.

Anyone attempting to apply the techniques of the two previous sections to solving MDP-type problems will immediately be faced with some uncertain issues. Some of the questions that might arise are, whether to use the matrix RF or RK, how to select the various parameters in forming the matrix RF, whether to use a singular values or a Foster-type least squares approach, how to formulate the decision criterion, and how to choose a zero threshold. The main purpose of this work is to provide some sort of guidelines by which a user may proceed in this numerical maze with some degree of confidence. We also provide a technique by which a user may be confident that the correct solution has been obtained. Nevertheless, it is as well to note that our conclusions are strictly empirical. A process of experimentation and gaining experience over a period of time has led to the notions recorded here. We mention that only an exhaustive numerical analysis bounding the error in the solutions obtained by the proposed technique would firmly establish its validity. A related analysis has been performed by Foster, whereby a bound is placed on the condition number of the matrix whose pseudo-inversion is necessary for solving the least-squares problems in this technique. But Foster's bound contains the chosen zero threshold as a quantity in the denominator [8,

Eq. 3.23], and this reduces the usefulness of the bound.

In the next section we will take up a detailed case study of the effects of attempting to solve the same problem by a variety of different lines chosen within the constraints of the techniques of Secs. I and II. Here, we first present a discussion of these questions which pertain to the success of the calculation. It is best to define at the outset, what we mean by a good solution. On the basis of working with an example for which the solution was known in advance, we may state the following. The primary area of difficulty for any solution procedure is in correctly identifying the dependent columns of the real matrix. All procedures which were able to do this correctly, led to solutions of adequate accuracy for engineering purposes, e.g., at least three decimal digits. So the crucial issue in determining success or failure of the procedure is not its ability to accurately calculate the vectors w in the kernel, but the ability to correctly deduce whether a particular column is a dependent column.

Another related consideration is that of resolution. This arises because for each column under consideration, the decision of whether it is a dependent column is going to be based on some computed quantity in comparision to the zero threshold. The decision will be made easier if the decision criterion is significantly above the threshold for columns which are not dependent coluns, and is significantly below it for dependent columns.

The question of choosing the zero threshold is next considered. We believe the zero threshold to be an expression of the user's confidence in the data that comes from the program. For example, if the real matrix has been calculated to an accuracy of sixteen decimal digits, and no further loss of significance is expected in performing the linear dependency calculation, then this would be expressed by setting the value of the zero threshold at 10^{-16} . However, in typical applications, neither of the above situations is likely to hold. If the real matrix has been calculated using double precision floating point arithmetic on a modern computer, one may expect somewhat less than sixteen significant digits. Moreover, the additional loss of accuracy while performing the linear dependency calculations depends on the conditioning of the matrix, and hence is a function of the actual numbers involved. This is the most critical issue which makes the success of the solution process so unpredictable.

To understand the relevance of conditioning to the techniques we are using, it may be said that conditioning is a measure of how far from the actual solution the computed solution may be. If we are using a least squares procedure, conditioning dictates the accuracy of the solution to the least squares problems. If we are using a singular value approach, conditioning dictates the extent to which the calculated singular values may be significant. Pseudo-inversion of matrices with large condition numbers is akin to division by a very small quantity, and the process causes the smallest errors to be greatly magnified. The condition number is the ratio of the largest to the smallest singular values of the matrix, but this measure is useless in practice, since ill-conditioning may preclude an accurate calculation of the singular values.

The relation of conditioning to matrix rank is obvious from singular value considerations. The closer the matrix is to being rank-deficient, the higher its condition number, and hence the more the difficulty to compute with it. Since our problem assumes the existence of rank deficiencies, the difficulty of dealing with an ill-conditioned matrix is unavoidable. To put it pessimistically, the very fact that a rank deficiency exists, makes it difficult for us to discover it.

We would like to remark here about whether the problem of ill-conditioning affects both the least-squares and the singular value procedures in the same way. Consider our problem of determining whether the matrix $[A|b]$ is rank deficient. The matrix A represents the submatrix formed by columns of RF or RK , known to be linearly independent and the vector b represents the column under consideration. Assume the matrix $[A|b]$ is rank deficient. The accuracy to which a least-squares solution to the problem $Ax + b = 0$ may be obtained is governed by the conditioning of the matrix A. On the other hand, the accuracy of singular values, if we use the singular value approach, is governed by the conditioning of the matrix $[A|b]$. Since the matrix A is full rank. it is likely to be much better conditioned than the matrix $[A|b]$, which is rank-deficient. This would tempt us to conclude that the least-squares solution would, in every case, be more favorable. But actual computational experience failed to bear this out. In every case, the least-squares and singular value approaches were both equally effective (or ineffective.) This may be because the decision criterion in the least-squares technique requires us to calculate the vanishingly small quantity $Ax + b$. The accuracy with which the decision criterion may be calculated would again be governed by the conditioning of the matrix $[A|b]$. Thus, accuracy of the least squares solution alone does not guarantee a correct decision on rank-deficiency, a more important issue by far.

We propose that the way out of the dilemma is to observe that ill-conditioning does not necessarily mean that erroneous solutions will always result. It means that a possibility of relatively large errors does exist. Our strategy begins with the observation that on certain kinds of examples the above procedures to lead to successful solutions. We then carried out a study to attempt to discover some pattern among the cases which yielded good solutions. If we are able to adapt every problem in order to fit such a pattern, then we have a heuristic rule for effective use of these computational techniques.

The pattern we discovered is simplicity itself, although considerable amount of experimentation and trial-and-error procedures were necessary to arrive at it. Briefly, it was found that when the structure of the real matrix is such that there is a great deal of variation in the norms of the rows of the matrix, it leads to serious computational errors. Meanwhile, with matrices which demonstrated a balance in the row norms, the software was able to arrive at the correct solution without any serious difficulties, e.g., poor resolution. In solving MDP problems, a lack of row norm balance (RNB) can arise from the structure of original matrix $B_3(s)$.

IV. CASE STUDY OF EXAMPLE WITH KNOWN SOLUTION

In this section we consider a more detailed study of the factors which go into deciding how successful the solution process is going to be. For this, we consider an example which demonstrates the complexity of features that leads to difficulty in solutions. With reference to Eq. (1), our example, taken from the work by Gejji and Sain [7], has $B_1(s)$ as a 2 X 7 matrix of rational functions. The physical origins of the problem are described in reference [7].

The matrix $B_2(s)$ is the 2 x 2 identity. This leads to a matrix $B_3(s)$ of size 2 x 9. $B_{3p}[s]$ has maximum degree 13 in its entries. When converted to the form $B_{3p}[s]$, the common denominator polynomial of $B_1(s)$ appears in the submatrix formed by the last two of the nine columns. We point this out, because the entries in $B_1(s)$ are such that the nemerator and denominator degrees are quite close. Furthermore, the leading coefficients are also of the same order. This fact, coupled with the identity matrix of the last two columns, leads to a $B_3(s)$ which does not vary a great deal when evaluated over a range of real values for s . This leads to a built-in RNB when the matrix RF is calculated from $B_3(s)$. If, on the other hand, one uses the matrix $B_{3p}[s]$, a steady increase in magnitudes of the coefficients with decreasing degree leads to a highly unbalanced matrix RK .

The problem was first solved by Gejji using exact rational arithmetic software. This procedure carried calculations to all significant digits and took up an inordinate amount of computer time. Later Foster gave a solution to this problem using the technique of the matrix RF . This solution was performed in floating point arithmetic on the PDP-10 computer and reduced CPU time to a reasonable range. Six cases are presented in our study here.

First, the matrix RF was formulated directly from the rational matrix $B_3(s)$ for the problem. From Foster's work, we know that a value of N = 6 is adequate. We chose N = 10 , μ= 2. This is exactly as is done in Foster's paper. The lues for the real numbers $\lambda_1, \lambda_2, \ldots, \lambda_N$ were taken to be 5, 10, 20, 30, 40, 50, 100, 200, 500, and 1000. The zero threshold was taken as 10^{-10}. For convenience, the polynomials $t_0(s)$, $t_1(s)$, $t_2(s)$ were taken to be 1, s, s^2 . This leads to a 20 x 27 real matrix.

Next, the polynomial matrix $B_{3p}[s]$ corresponding to our problem was used to form the matrix RK. The coefficients for this were taken from existing data calculated to an accuracy of fifteen digits. μ was again taken to be 2 . This led to a 28 x 32 real matrix.

To set up the third approach, we used experience to achieve RNB for the second case. In this particular problem, because of the graded variation of coefficients with degree, it is possible to achieve RNB by simply scaling the frequency down by a factor of 10. Such a scaling was applied to the polynomial matrix $B_{3p}[s]$, and the resulting polynomial matrix was again expanded to yield a new formulation of the matrix RK. This one has RNB. The frequency scaling does not change the problem, except that solution vectors in the minimal basis have to be interpreted with the scaling in mind.

The three approaches given above were implemented using both the singular values as well as the least squares techniques for rank determination. Thus the six cases. The important issue here is not the vectors appearing in the minimal basis solution; it is the correct determination of rank dependencies in the columns of the matrix. When ever this happened, our solution was the same in Foster's work, up to the three significant digits recoreded by Foster. Table 1 summarizes the cases tried. All solutions are judged by the standard set by Case I. This shows that the first eleven columns are linearly independent; and columns 12 through 18 are all dependent.

Here we notice that all the procedures stop when seven depe dent columns have been found.

Now we give the results one by one. In Case I, the first eleven columns were found independent and columns 12 through 18 were determined as dependent.

Table 1: The Cases

Case	Matrix Formulation	Rank-finding Technique
I	RF	LS (Least Squares)
II	RF	SV (Singular Values)
III	RK (Unbalanced)	LS
IV	RK	SV
V	RK (Balanced)	LS
VI	RK	SV

The values of the decision criterions for columns 2 through 18 are given in the Table 2. Note that we consider this resolution adequate.

In Case II again, we see that the column dependencies are correctly identified. The decision criterion for column 11 is quite close to the threshold. The resolution is still quite good.

In Case III, the dependent columns were found to be columns 13 through 16 and columns 18 and 26. The dashes in Table 2 indicate that corresponding columns were not considered because of the selection rule to eliminate redundant solutions. Notice that only six dependent solumns were encountered before all 27 columns in the real matrix had been considered. Normally this would indicate that μ was not chosen large enough. But in this case, we know that the solution process is in error. Here, we call attention to the poor resolution.

In Case IV, the real matrix is the same as that used in Case III. In spite of the lack of RNB, the column dependencies were correctly identified and the correct solution was obtained. A closer examination reveals that this case suffers from rather poor resolution. The largest magnitude of the decision criterion for a dependent column is only one order of magnitude away from the smallest magnitude obtained for an independent column.

The results of Case V and VI are essentially similar. Case V yields somewhat better resolution. In these cases a modified RK was used, which displayed RNB due to frequency scalling of the original problem.

Finally, we include the result of an interesting case that occurred. As we have mentioned, the formulation of the matrix RF holds for polynomial matrices also, since these come under the heading of rational matrices. Our problem was converted to a matrix of polynomials and frequency scaling then applied as in Case IV. Instead of embedding the resulting matrix into the structure RK , the matrix RF was then formed, using values for $\lambda_1, \lambda_2, \ldots, \lambda_{10}$ as 0.1, 0.2, 0.4, 0.8, 1.6, 3.2, 6.4, 12.8, 25.6 and 51.2 . The real matrix thus formed was highly unbalanced and both the

Table 2: The Results

Column \ Case	I	II	III	IV	V	VI
2	3.96	0.220	0.800	0.21	2.84	0.176
3	1.1×10^{-3}	2.10×10^{-3}	0.330	0.173	0.294×10^{-1}	0.045
4	1.95×10^{-4}	2.45×10^{-4}	0.060	0.0506	4.76×10^{-3}	7.44×10^{-3}
5	1.91×10^{-4}	1.72×10^{-4}	0.040	0.212	4.54×10^{-3}	4.74×10^{-3}
6	8.80×10^{-6}	1.59×10^{-5}	2.72×10^{-3}	6.68×10^{-3}	1.13×10^{-4}	1.39×10^{-4}
7	8.21×10^{-5}	1.42×10^{-5}	4.01×10^{-5}	1.72×10^{-6}	$8.86 \times 10^{-}$	2.40×10^{-4}
8	1.02×10^{-3}	1.26×10^{-6}	2.25×10^{-4}	4.18×10^{-8}	0.0135	1.57×10^{-5}
9	2.76×10^{-4}	7.83×10^{-8}	7.41×10^{-8}	3.30×10^{-8}	6.25×10^{-5}	1.27×10^{-5}
10	23.4	3.71×10^{-9}	6.19×10^{-4}	2.26×10^{-10}	0.0399	1.09×10^{-6}
11	0.204	$5.17 \times 10^{-}$	6.97×10^{-6}	$3.28 \times 10^{-}$	6.94×10^{-3}	1.04×10^{-6}
12	5.49×10^{-15}	3.39×10^{-18}	1.90×10^{-10}	5.33×10^{-12}	7.64×10^{-12}	1.79×10^{-12}
13	1.28×10^{-15}	1.19×10^{-18}	4.45×10^{-12}	8.36×10^{-12}	2.29×10^{-12}	5.46×10^{-13}
14	3.89×10^{-17}	4.89×10^{-19}	5.94×10^{-12}	1.28×10^{-11}	3.95×10^{-13}	5.99×10^{-13}
15	1.35×10^{-16}	8.04×10^{-19}	5.47×10^{-11}	1.72×10^{-11}	4.23×10^{-13}	7.34×10^{-13}
16	1.35×10^{-17}	8.55×10^{-18}	6.79×10^{-10}	2.69×10^{-11}	4.23×10^{-13}	6.67×10^{-12}
17	2.20×10^{-15}	3.30×10^{-18}	1.33×10^{-11}	1.90×10^{-12}	3.97×10^{-12}	2.37×10^{-12}
18	1.10×10^{-14}	3.32×10^{-18}	4.36×10^{-4}	7.72×10^{-12}	1.63×10^{-11}	$1.89 \times 10^{-}$
19	-	-	4.32×10^{-6}	-	-	-
20	-	-	5.67×10^{-10}	-	-	-
21	-	-	$9.14 \times 10^{-}$	-	-	-
22	-	-	-	-	-	-
23	-	-	-	-	-	-
24	-	-	-	-	-	-
25	-	-	-	-	-	-
26	-	-	5.09×10^{-11}	-	-	-
27	-	-	-	-	-	-

LS and SV methods failed due to problems of real number overflow. We then performed a "brute-force" normalization of this real matrix. Each row of the matrix was scaled by the inverse of its norm. The singular value criterion was then used to perform the linear dependency checking. This led to the following values of the decision criterion for columns 2 through 11, 0.424, 0.132, 0.0263, 0.0116, 3.67×10^{-5}, 7.33×10^{-6}, 2.65×10^{-5}, 3.38×10^{-6}, 2.89×10^{-6}, 1.26×10^{-6}, and for columns 12 through 18 the following, 2.10×10^{-11}, 1.58×10^{-11}, 9.18×10^{-12}, 5.23×10^{-12}, 2.64×10^{-11}, 1.85×10^{-11}, 1.86×10^{-11}. Thus, this technique offered results comparable to Cases V and VI. For the correct floating point solution first obtained by Foster please see [8]. This shows that there are seven vectors in the minimal basis, and the maximum degree occurring in each is one. Each vector is therefore considered of first degree.

It is observed from the above case study that a convenient and useful method to get reliable solutions using the techniques of Foster and Kung-Kailath is to aim for RNB.

V. ACKNOWLEDGEMENTS

Thanks are due to Dr. L.V. Foster for his cooperation in our efforts to build a software library. This research was supported in part by the Office of Naval Research under Contract N-0014-79-C-0475. Special appreciation is due to Dr. M.K. Sain for providing the motivation for this research.

VI. REFERENCES

[1] Peczkowski, J.L. et al., "Multivariable Synthesis with Inverses," Proc. JACC, Denver, Colo., 1979, pp. 375-380.

[2] Gejji, R.R., "On the Total Synthesis Problem of Linear Multivariable Control," Ph.D. Diss., Univ. Notre Dame, Notre Dame, Ind., 1980.

[3] Wang, S.H. et al., "A Minimization Algorithm for the Design of Linear Multivariable Systems," IEEE Trans. Aut. Contr., Vol. AC-18, 1973. PP. 220-225.

[4] Forney, Jr., G.D., "Minimal Bases of Rational Vector Spaces," SIAM J. of Contr., Vol. 13, 1975 pp. 493-520.

[5] Sain, M.K., "A Free-Modular Algorithm for Minimal Design of Linear Multivariable Systems," Preprint 1975 IFAC Congr., 1975.

[6] Gejji, R.R., "A Computer Program to find the Kernel of a Polynomial Operator," Proc. 14th Allerton Conf. Circuits Syst., Urbana, Ill., 19 pp. 1013-1018.

[7] Gejji, R.R. et al., "Application of Polynomial Techniques to Multivariable Contr. Jet Engines," Proc. 4th IFAC MVTS Symp., Fredericton, Canada 1977, pp. 47.1-47.9.

[8] Foster, L.V., "A Practical Solution to the Minim Design Problem," IEEE Trans. Aut. Contr., Vol. AC-24, 1979, pp. 449-454.

[9] Kung, S. et al., "Fast and Stable Algorithms fo Minimal Design," Proc. 4th IFAC Symp. MVTS, Fredericton, Canada, 1977.

[10] Laub, AJ., "Linear Multivariable Control, Numerical Considerations," M.I.T. Electronic Syst. La Report ESL-p-833, Cambridge, Mass., 1978.

AN APPLICATION OF TOTAL SYNTHESIS TO ROBUST COUPLED DESIGN*

M.K. SAIN, R.M. SCHAFER, AND K.P. DUDEK
Department of Electrical Engineering
University of Notre Dame
Notre Dame, Indiana 46556

ABSTRACT

Total synthesis techniques for the control of linear multivariable systems are module theoretic methods aimed at bottom line design, wherein the designer selects at the outset the control action and system response characteristics which will be attained. This selection is made from the class having associated with it the possibility of an internally stable feedback realization. In practice, however, such realizations are normally carried out with decentralized dynamics---or fixed structure. Moreover, they must be achieved in such a way that plant parameter variation does not materially inhibit the nominal filter responses. This paper reports on the extension of the Total Synthesis Problem (TSP) concept to robust feedback realizations of fixed structure. An example from turbojet engine data illustrates the concepts.

INTRODUCTION

In the following discussion, the object of control is understood to satisfy the state equations

$$\dot{x} = Ax + Bu \tag{1a}$$

$$y = Cx + Du \ , \tag{1b}$$

for x, u, and y members of the n, m, and p dimensional real vector spaces X, U, and Y, respectively. This brief exposition will assume that control goals include a command/response relationship between an exogenous signal r, which takes its values in a p dimensional real vector space R, and the pair (u,y).

Consider now the expression of such a relationship in the frequency domain. Denote the field of real numbers by $\mathbb{R}$, the principal ideal domain ring generated from $\mathbb{R}$---considered as a commutative ring---and the indeterminate element s by $\mathbb{R}[s]$, and the quotient field of $\mathbb{R}[s]$ by $\mathbb{R}(s)$. Then the constructions [1]

$$U[s] = U \otimes_{\mathbb{R}} \mathbb{R}[s] \ , \tag{2a}$$

$$X[s] = X \otimes_{\mathbb{R}} \mathbb{R}[s] \ , \tag{2b}$$

$$Y[s] = Y \otimes_{\mathbb{R}} \mathbb{R}[s] \ , \tag{2c}$$

$$R[s] = R \otimes_{\mathbb{R}} \mathbb{R}[s] \tag{2d}$$

establish free $\mathbb{R}[s]$-modules $U[s]$, $X[s]$, $Y[s]$, and $R[s]$, respectively. In turn, these imbed naturally into the $\mathbb{R}(s)$-vector spaces

$$U(s) = U \otimes_{\mathbb{R}} \mathbb{R}(s) \ , \tag{3a}$$

*This work was supported by the Office of Naval Research under Contract N00014-79-C-0475.

$$X(s) = X \otimes_{\mathbb{R}} \mathbb{R}(s) , \tag{3b}$$

$$Y(s) = Y \otimes_{\mathbb{R}} \mathbb{R}(s) , \tag{3c}$$

$$R(s) = R \otimes_{\mathbb{R}} \mathbb{R}(s) , \tag{3d}$$

in the manner

$$U[s] \subset U(s) , \tag{4a}$$

$$X[s] \subset X(s) , \tag{4b}$$

$$Y[s] \subset Y(s) , \tag{4c}$$

$$R[s] \subset R(s) . \tag{4d}$$

In this context, the plant appears as a morphism

$$P : U(s) \to Y(s) . \tag{5}$$

It is further assumed that there exists a morphism

$$M : R(s) \to U(s) , \tag{6}$$

which embodies the command/control action relationship, and that there exists a morphism

$$T : R(s) \to Y(s) , \tag{7}$$

which characterizes the command/system response relationship. Broadly speaking, the assumptions reflected in (6) and (7) mean that the discussion is in focus on linear feedback control systems.

Practical design and computation can be carried out through a process of basis selection in U, X, Y, and R. Understood as elements of U[s], X[s], Y[s], and R[s], these basis vectors become free generators of their associated $\mathbb{R}[s]$-modules. In like manner, understood as elements of U(s), X(s), Y(s), and R(s), they comprise a basis for their associated $\mathbb{R}(s)$-vector spaces as well. Denote by [L] the matrix of a morphism

$$L : V_1 \to V_2 \tag{8}$$

of F-vector spaces V_i, $i = 1,2$. Then (5), (6), and (7) have their counterparts

$$[P] : \mathbb{R}(s)^m \to \mathbb{R}(s)^p , \tag{9}$$

$$[M] : \mathbb{R}(s)^p \to \mathbb{R}(s)^m , \tag{10}$$

$$[T] : \mathbb{R}(s)^p \to \mathbb{R}(s)^p . \tag{11}$$

These ideas and notations are now applied to define and elaborate the idea of total synthesis.

THE TOTAL SYNTHESIS PROBLEM

The idea of total synthesis revolves around the commutative diagram of Figure 1, which points out the basic feature that any pair (M,T) brought about by a feedback control system must coexist with the plant or object of

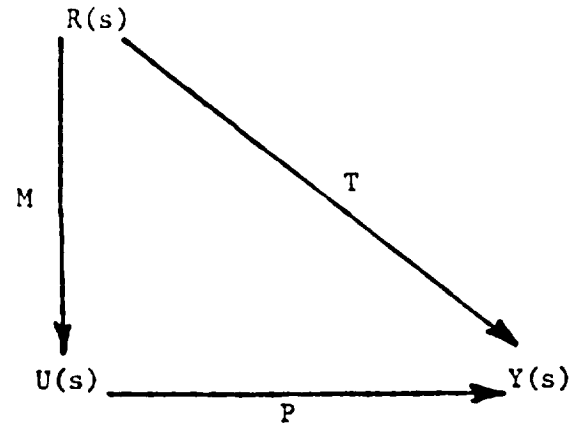

Figure 1.

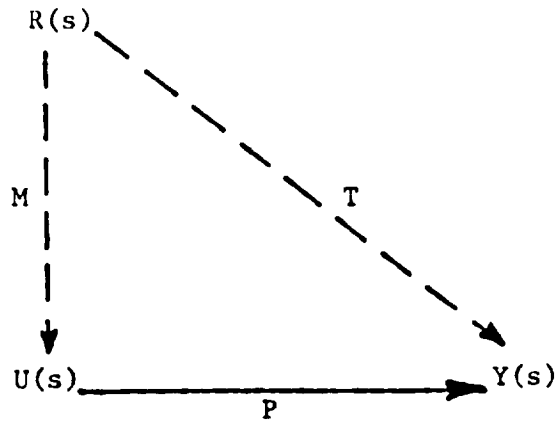

Figure 2.

control. In other words, with

$$P = C(sI_X - A)^{-1} B + D \ , \tag{12}$$

the pair (M,T) must satisfy

$$T = P \circ M \ . \tag{13}$$

The Total Synthesis Problem (TSP) is brought about through a study of the possible pairs (M,T) which can satisfy (13) for a given P. TSP may be conceptualized as follows. Denote by

$$\hom (R(s), Y(s)) \tag{14}$$

The $\mathbb{R}(s)$-vector space of morphisms with domain R(s) and codomain Y(s). In like manner, establish

$$\hom (R(s), U(s)) \ , \tag{15}$$

with the alternative codomain U(s). Then the action

$$(M,T) \mapsto P \circ M - T \tag{16}$$

establishes a morphism

$$\hom (R(s), U(s)) \times \hom (R(s), Y(s)) \to \hom (R(s), Y(s)) \ . \tag{17}$$

Denote this morphism by F; then Ker F is an appropriate setting within which to begin a study of TSP.

It is important to realize at the outset, however, that the rational subspace Ker F is much too capacious a place in general within which to design control systems. Indeed, arbitrary pairs (M,T) taken from Ker F may not be feedback realizable in an internally stable way. It is easy to see why this is the case. Suppose that [M] contained unstable elements of $\mathbb{R}(s)$. Then a command r would generate unstable control action u, a situation which is at odds with the notion of internal stability. Moreover, internal stability would also require that [T] have stable elements from $\mathbb{R}(s)$ as well. Accordingly, the pair ([M], [T]) must have its $\mathbb{R}(s)$-elements in the stable subring of $\mathbb{R}(s)$. Beyond this natural condition, it is clearly desirable from the practical point of view to require each entry in [M] and in [T] to be proper. Failure to do so would create unacceptable

transients in response to fast commands.

When D is the zero morphism, Bengtsson [2] established in 1977 the results which could be used to show that $\mathbb{R}(s)$-elements in [M] and [T] being stable and proper was both necessary and sufficient for the pair (M, T) to admit an internally stable feedback realization. However, Bengtsson's working assumptions involved centralized controller dynamics, whereas many applications require the distribution of dynamics in the controller to more than one site. Stated in other words, the Bengtsson configuration places little constraint upon the connections within the controller, whereas many applications have such constraints.

If connection constraints within the controller make it useful to distribute the controller dynamics to more than one location, then the stable and proper conditions on ([M], [T]), while still necessary, may not be sufficient for internal stability.

COMPUTATIONAL ASPECTS

As discussed in the section preceding, TSP studies of possible pairs (M,T) are located generally within Ker F. In particular, however, conditions of internally stable feedback realizability require that the study be localized to pairs (M,T) whose matrices ([M],[T]) are proper and stable. Because the subring of proper and stable elements in $\mathbb{R}(s)$ fails to achieve the status of a field---the multiplicative inverse of a stable transfer function need not be stable---it is appropriate to examine Ker F from a module theoretic, as opposed to a vector space theoretic, point of view. A practical approach to computing the stable and proper part of Ker F is to suppress, temporarily, the properness condition and to calculate a basis for the stable part of Ker F. Because transfer functions without denominators may be regarded as stable in this sense, polynomials can serve as such basis elements. Once the polynomials are obtained, properness can be restored by dividing basis elements with Hurwitz polynomials of appropriate degree, such operations being just basis transformations within the stable kernel. The idea can be seen in the following first step of the turbojet example.

Turbojet Example: Step 1

Consider the single spool turbojet engine model due to Skira and DeHoff [3]. For this model, the plant state description is given by

$$[A] = \begin{bmatrix} -1 & -.5 \\ 10 & -5 \end{bmatrix}; \quad [B] = \begin{bmatrix} 2 & .5 \\ 0 & -1 \end{bmatrix};$$
$$[C] = \begin{bmatrix} .1 & 18 \\ .06 & 0 \end{bmatrix}; \quad [D] = \begin{bmatrix} 0 & 0 \\ .46 & 0 \end{bmatrix}. \tag{18}$$

Then a brief calculation establishes that

$$[P] = \frac{\begin{bmatrix} 36.1(.000554s + 1) & 7.23(-.248s + 1) \\ .52(.0884s^2 + .554s + 1) & .018(.1667s + 1) \end{bmatrix}}{(.1s^2 + .6s + 1)}. \tag{19}$$

Let

$$d_P(s) = .1s^2 + .6s + 1 \ , \tag{20}$$

and denote by N_P the numerator matrix in (19). The kernel problem can be understood in the manner

$$[N_P \ | \ - d_P(s)I] \begin{bmatrix} N_M \\ \hline N_T \end{bmatrix} = 0 \ , \tag{21}$$

where the representations

$$[M] = \frac{N_M}{d_M(s)} \ , \tag{22}$$

$$[T] = \frac{N_T}{d_T(s)} \ , \tag{23}$$

have been employed. Columns of the matrix

$$\begin{bmatrix} N_M \\ \hline N_T \end{bmatrix} \tag{24}$$

are computed so that they constitute a basis for the stable part of Ker F. In this example, they were found to be

$$\begin{bmatrix} -2.5 & 2.17s - 8.70 \\ s + 10 & 43.5 \\ -17.95 & .435 \\ -1.12 & s - 3.74 \end{bmatrix} , \tag{25}$$

so that a base choice for N_M and N_T is

$$N_M = \begin{bmatrix} -2.5 & 2.17s - 8.70 \\ s + 10 & 43.5 \end{bmatrix} , \tag{26}$$

$$N_T = \begin{bmatrix} -17.95 & .435 \\ -1.12 & s - 3.74 \end{bmatrix} . \tag{27}$$

However, it would be rare indeed if the choices (26) and (27) turned out to be physically satisfactory, inasmuch as they represent an arbitrary choice of basis. What is needed next in the design process is a manipulation of the basis (25) so as to move toward a desirable practical design. One approach to this goal is to adjust the zeros and gains of [P] so as to reach an alternate pattern. Notice that the given gain matrix of [P] is just

$$[P]\big|_{s = 0} = \begin{bmatrix} 36.1 & 7.23 \\ .52 & .018 \end{bmatrix} . \tag{28}$$

The signs and magnitudes of the individual entries in (28) may be taken as an indication of the natural propensities of the plant. While changes in the pattern of (28) may reflect interesting design goals, it is necessary to bear in mind that gross changes may tend to invalidate the original plant data or may result in the plant operating locally in a manner which is not in keeping with its global features. Notice also that the 11-element of [P] has a rather large left half plane zero, and that the 12-element of

[P] has a right half plane zero. As an example design strategy, suppose that it is chosen to

i) move the zero of the 11-element farther out in the left half plane;

ii) reduce the gain in the 21-element;

iii) remove the zero of the 12-element from the right half plane.

A least squares procedure can be applied in order to pick polynomic entries in Ker F which are in the aggregate as close as possible to matrices N_T which would have the three properties listed above. The result of one such calculation is given by

$$\begin{bmatrix} .0291s + .0223 & -.289s + 2.3 \\ -2.79 \times 10^{-5}s^2 - .0557s + .0271 & -.0531s^2 - .775s - 10.9 \\ 5.00 \times 10^{-4}s + 1 & .953s + 4.31 \\ .0134s + .0121 & -.135s + 1 \end{bmatrix}, \quad (29)$$

where N_M appears in the top two rows and N_T in the bottom two rows. Here

$$N_T|_{s=0} = \begin{bmatrix} 1 & 4.31 \\ .0121 & 1 \end{bmatrix}; \quad (30)$$

under the choice

$$d_T(s) = d_M(s) = (.2s+1)(.04s+1), \quad (31)$$

(30) may be compared with (28). The sign pattern in the gain matrix has been maintained, with some readjustment of relative gain magnitudes in the second channel, as well as near normalization in the first channel. The zero of the 11-element has moved to -2,000 from its original position; the gain in the 21-element has decreased from .52 to .0121; and the zero in the 12-element has migrated from 4.03 in the right half plane to -4.52 in the left half plane. As is usually the case, this adjustment must be traded off against other changes which occur consequentially. Of particular importance is the creation of a right half plane zero in the 22-element. Also worthy of mention is the use of second degree elements in the kernel; these are seen in the upper two rows of (29). Second degree elements were employed in order to achieve more satisfactorily the three design goals elaborated above. The consequence is greater complexity in the controller.

Remark 1

The use of (21) to define the kernel problem permits interpretation of the calculation in terms of free $\mathbb{R}[s]$-modules along the lines of (2). This way of thinking has been presented in [4]. However, the infinite precision algorithms discussed in [4] are not useful in the case of finite precision [5]. Instead, it is convenient to retain the free-modular viewpoint while constructing a minimal (sum of column degrees) basis with the aid of ideas of Foster [6] or of Kung and Kailath (see [7]).

Remark 2

Second degree elements, as appearing in (29), may connote one of two events. If only free $\mathbb{R}[s]$-modular basis changing isomorphisms are used to construct (29) from (25), then the solution indicates a non-minimal (sum of column degrees) basis. If (25) is adjusted in the larger class of monic, rank two morphisms to reach (29), then attention in Ker F has been specialized to a submodule. The latter case is ordinarily to be avoided because it increases the number of closed loop system multivariable zeros beyond the required minimum quantity present in (25).

ROBUST FEEDBACK REALIZATION

Suppose next that feedback realization of the pair (M,T) is to be achieved within the fixed configuration of Figure 3. Regard T, as determined in the preceding discussion---cf. (29) and (31)---as given; and recall that the plant of the turbojet example is stable. Then G and H : $Y(s) \to R(s)$ will be chosen so as to realize the pair (M,T) and to reach a given level of comparison sensitivity to inaccuracies in the plant. According to the results of Cruz and Perkins [8], it is a straightforward derivation to show that $S : Y(s) \to Y(s)$, the comparison sensitivity operator, satisfies the pair of equations

$$S \circ P \circ G = T \ , \tag{32}$$

$$T \circ H = 1_{Y(s)} - S \ . \tag{33}$$

Because S is an isomorphism, (32) can be expressed

$$P \circ G = S^{-1} \circ T \ . \tag{34}$$

For this brief treatment, suppose that P is monic and that

$$[S] = \frac{n(s)}{d(s)} I \ , \tag{35}$$

with $(n(s),d(s)) \in \mathbb{R}[s]^2$ and $d(s) \neq 0$. Then

$$G = S^{-1} \circ M \ , \tag{36}$$

which is unstable only if n(s) is unstable. Moreover, (33) may be regarded as an equation for pairs (H,S), in which case it has an especially interesting particular solution

$$(0, 1_{Y(s)}) \ . \tag{37}$$

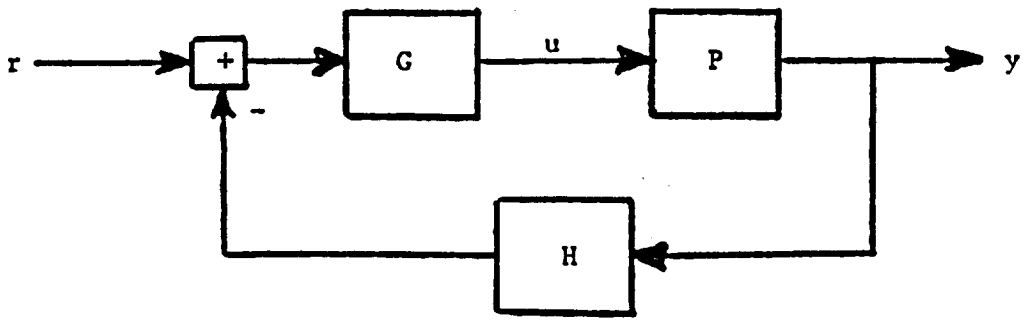

Figure 3. Fixed Structure Feedback Realization.

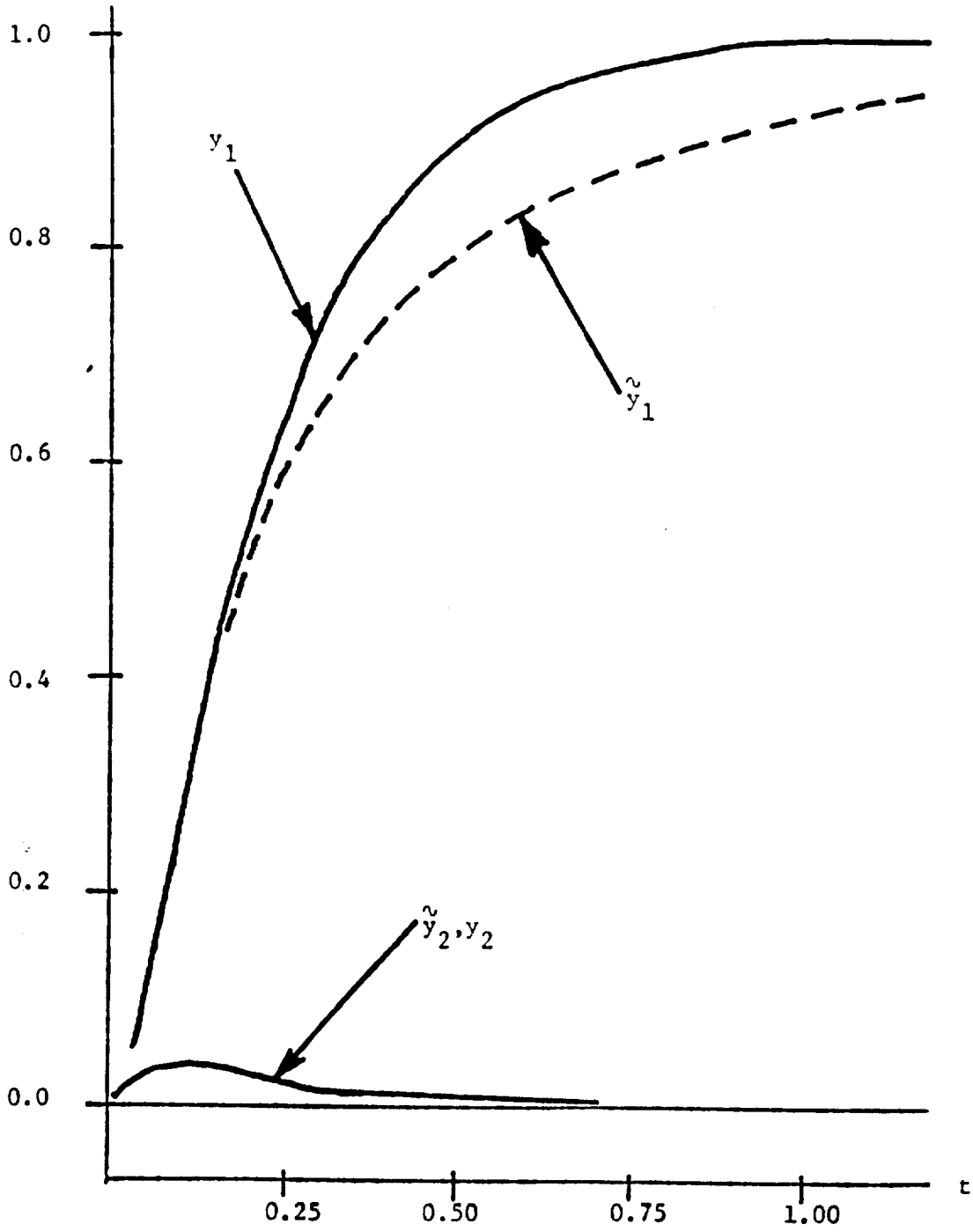

Figure 4. Unit Step in First Channel.

The complementary solutions can be found from another kernel problem

$$[T \mid I]\begin{bmatrix} -H \\ \hline S \end{bmatrix} = 0 \; ; \tag{38}$$

because [S] must be stable in order to ensure internal loop stability, and because instabilities in [H] would be undesirable from the viewpoint of multivariable zeros in the closed loop, the same module theoretic and computational ideas described above for (M,T) pairs may be applied here to (H,S) pairs. To accommodate the sort of assumption (35), softwares of the Foster or Kung-Kailath type can be appropriately modified.

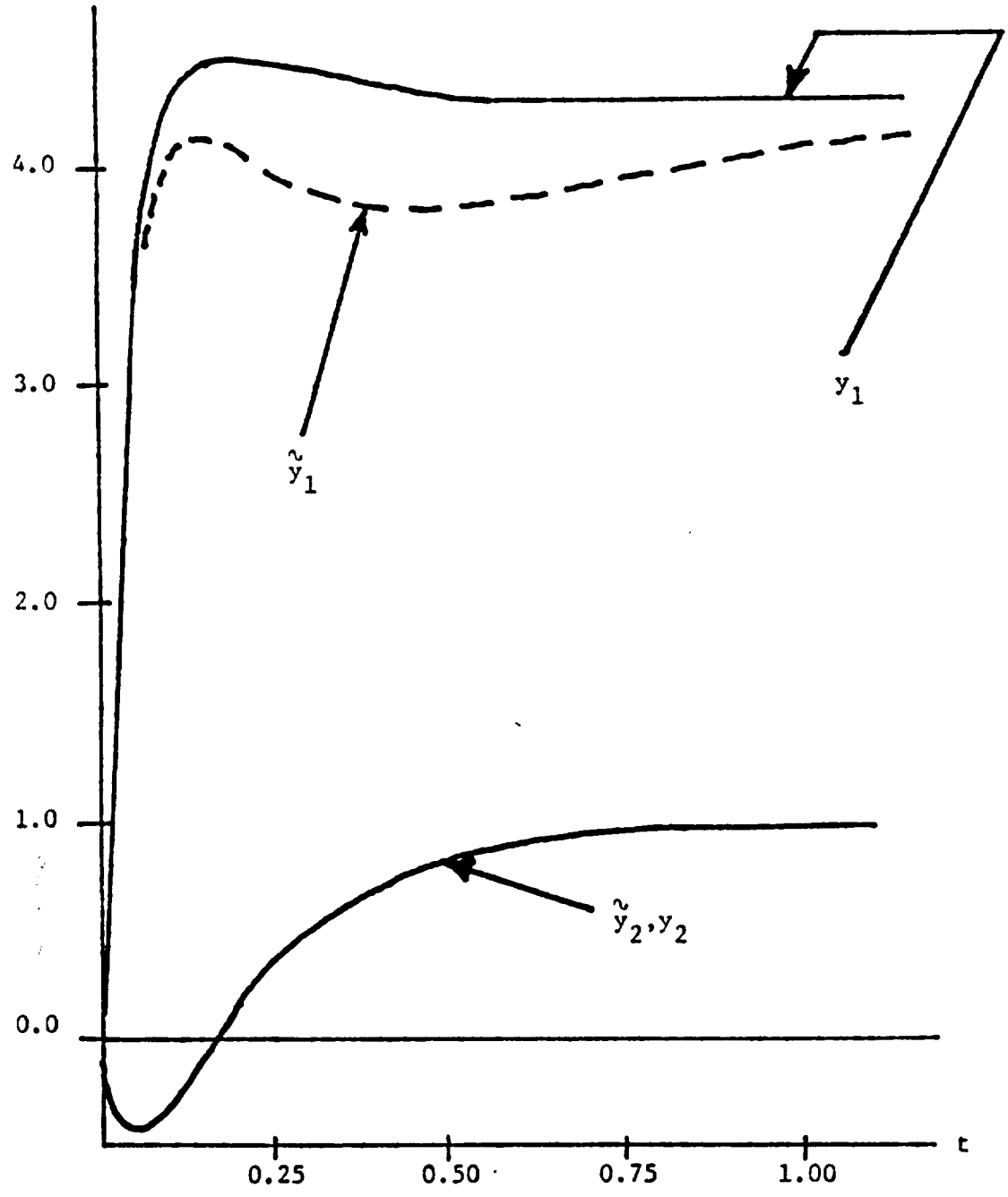

Figure 5. Unit Step in Second Channel.

Taken all together, [T] stable, [G] stable, [P] stable, and [H] stable preclude internal instabilities.

Turbojet Example: Step 2

Calculation of a basis for stable complementary solutions in (38), under the constraint (35), yields the result

$$\begin{bmatrix} N_H \\ \hline \tilde{n}(s)I \end{bmatrix}, \tag{39}$$

where $\tilde{n}(s)$ has its zeros equal to the multivariable zeros of the [T], and where N_H is of degree three---a consequence of the constraint (35).

A choice of degree three for Hurwitz d(s) assures [H] and [S] proper and stable. The particulars of d(s) may be established by root-locus or Bode analysis. Final choice for (35) was determined to be

$$\frac{n(s)}{d(s)} = \frac{.0001s^2 + .2855s}{.0001s^2 + .02s + 1} \tag{40}$$

the form of which places integrators in G.

Figures 4 and 5 show the nominal step responses y_i and the step responses $\tilde{y}_i$ which result from the change of A_{12} to -.9. Steady state behavior is preserved. This large parameter change increases the oscillatory plant behavior while leaving it stable.

Bibliographical Remark

The origins of the TSP concept are cited in [9]. For the unity feedback case, an extension to a larger class of plants is given in [10].

REFERENCES

1. S. MacLane and G. Birkhoff, Algebra. London: The MacMillan Co., 1967.
2. G. Bengtsson, "Feedback Realizations in Linear Multivariable Systems", IEEE Trans. Automatic Control, Vol. AC-22, pp. 576-585, August 1977.
3. C.A. Skira and R.L. DeHoff, "A Practical Approach to Linear Model Analysis for Multivariable Turbine Engine Control Design", in Alternatives for Linear Multivariable Control, M.K. Sain, J.L. Peczkowski, and J.L. Melsa, eds. Chicago: NEC, 1978, pp. 31-46.
4. M.K. Sain, "A Free-Modular Algorithm for Minimal Design of Linear Multivariable Systems", Proc. 6th IFAC World Congress, Part IB, Section 9.1.
5. R.R. Gejji and M.K. Sain, "Application of Polynomial Techniques to Multivariable Control of Jet Engines", Proc. 4th IFAC Symposium on Multivariable Technological Systems, pp. 421-429, July 1977.
6. L.V. Foster, "A Practical Solution to the Minimal Design Problem", IEEE Trans. on Automatic Control, Vol. AC-24, pp. 449-454, 1979.
7. R.R. Gejji, "On the Total Synthesis Problem of Linear Multivariable Control", Ph.D. Dissertation, Dept. Electrical Engineering, University of Notre Dame, May 1980.
8. J.B. Cruz, Jr. and W.R. Perkins, "A New Approach to the Sensitivity Problem in Multivariable Feedback System Design", IEEE Trans. on Automatic Control, Vol. AC-9, pp. 216-223, July 1964.
9. M.K. Sain and A. Ma, "Multivariable Synthesis with Reduced Comparison Sensitivity", Proc. 1980 Joint Automatic Control Conference, Part WP8-B.
10. C.A. Desoer and M.J. Chen, "Algebraic Design of Unity Feedback Systems with Stable Plant", Proc. 1980 Joint Automatic Control Conference, Part TA8-E.

SCHEDULED NONLINEAR CONTROL DESIGN FOR A TURBOJET ENGINE

Joseph L. Peczkowski

The Bendix Corporation
Energy Controls Division
South Bend, Indiana

Michael K. Sain

Electrical Engineering Department
University of Notre Dame
Notre Dame, Indiana

ABSTRACT

The last decade has witnessed a general maturing of theoretical thought on linear multivariable control system design; and, movements are now afoot to imbed certain of these thoughts into the bigger area of nonlinear design. As all this has transpired, however, nonlinear design has been proceeding apace in industrial applications. The present paper is part of an effort by the authors to formulate some theoretical views about current practical design procedures in the nonlinear domain.

I. INTRODUCTION

The spirit of nonlinear control system design can vary somewhat from one application area to another. Remarks made herein are influenced strongly by current practice in aircraft gas turbine control systems. In this case, the plant is a highly sophisticated piece of hardware, whose best available model is a digital simulation supplied by the manufacturer. Models of the form $\dot{x} = f(x,u), y=g(x,u)$ are not explicitly available; and, even if an approximation of such type could be determined, its complexity would be formidable. Nonetheless, control systems for such cases must be, and are, successfully designed. An example of such a system is given in the next section, and this paper briefly describes a typical design procedure.

Basically, the control philosophy is to linearize the simulation at a finite number of points in a flight envelope involving engine speed, mach number and altitude. Linear philosophy is applied at each point, and the resulting compensations are scheduled over the envelope, within a broad, nonlinear model following strategy.

The design viewpoint employed here is based upon the prior work [1,2,3,4,5]. A concept of Total Synthesis Problem is put into place for the nonlinear control situation, and a beginning is made on relating it to the scheduled designs typically used in practice.

II. NONLINEAR TURBOJET MODEL FEATURES

A nonlinear engine model is depicted in Figure 1. It is representative of the nonlinear objects designers of turbine engine controls currently deal with in practice. A nonlinear engine model typically is constructed by engine manufacturers and provided to control manufacturers in the form of a digital or hybrid computer simulation.

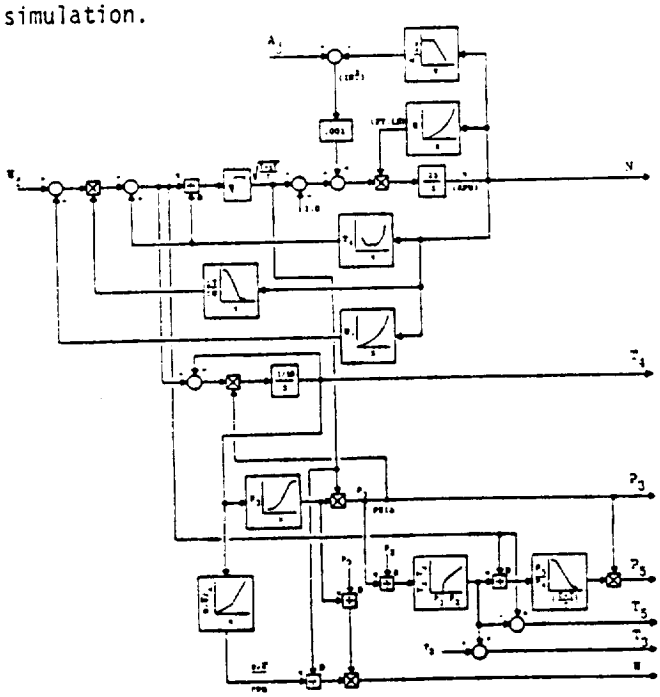

Figure 1

The simplified J-85 engine model in Figure 1 consists of only two integrators but includes nine nonlinear functions, eleven multipliers and dividers and eight summing junctions. The model describes the nonlinear dynamical and steady state relationships between two inputs u: fuel flow, W_f, and exhaust nozzle area, A_j, and seven outputs y: engine speed, N; turbine inlet temperature, T_4; and five other outputs. One can think of the plant simulation as a nonlinear function p which takes inputs to outputs, namely $p(u) = y$. A local snapshot of the nonlinear plant should give the small signal behavior and a linear description P such that $P(\Delta u) = \Delta y$. The underlying notion in

this paper is that linear descriptions, obtained from local action, may be combined to produce global nonlinear action with sufficient integrity to effect closed loop control design.

III. A TOTAL SYNTHESIS PROBLEM

In reference [4], the authors have discussed the concept of a Total Synthesis Problem (TSP) for linear multivariable control. This section relaxes some of those concepts from the homomorphism case to the function case, thereby introducing the possibility of nonlinearity. Of necessity, the treatment is merely an introductory glimpse.

Consider Figure 2. For simplicity, assume

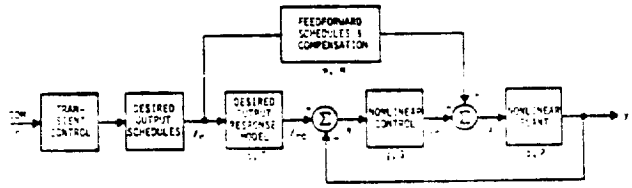

Figure 2

that the control u and output y are elements of commutative groups (U,+,0) and(Y,+,0) respectively. As functions, then, p: U→Y is the plant, g: Y→U is feedback compensation, m: Y→U is feedforward compensation, and t: Y→Y is desired output request/response. For the case of nominal design, in which the plant is stable, it is desired to have the relationship.

$$t = p \circ m, \qquad (1)$$

where the symbol ∘ denotes function composition. The Total Synthesis Problem is then to find pairs (t,m) satisfying this relationship, for given p. Pictorially, TSP can be visualized in the manner of Figure 3. Locally, the nature of the pair (t, m) can frequently be directly studied. Suppose that the plant has internal representation $\dot{x}_p = f(x_p,u), y = g(x_p,u)$; and consider a fixed $(\tilde{x},\tilde{u})$ such that $f(\tilde{x},\tilde{u}) = 0$. Then suitable technicalities imply that the actions of f and g may be represented locally by

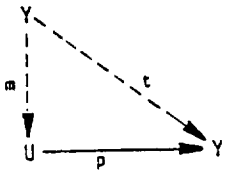

Figure 3

$$f(x,u) = \tilde{A}(x-\tilde{x})+\tilde{B}(u-\tilde{u})+\ldots = \tilde{A}\,\Delta x+B\,\Delta u+\ldots$$

$$g(x,u) = \tilde{C}(x-\tilde{x})+\tilde{D}(u-\tilde{u})+\ldots = \tilde{C}\,\Delta x+D\,\Delta u+\ldots \qquad (2)$$

In the transform domain, with $\Delta y = y-g(\tilde{x},\tilde{u})$, p has local character

$$\mathcal{L}\{\Delta y\} = \tilde{P}(s)\,\mathcal{L}\{\Delta u\}, \quad \tilde{P}(s)=\tilde{C}(sI-\tilde{A})^{-1}\tilde{B}+\tilde{D}. \qquad (3)$$

$\tilde{P}(s)$, of course, depends upon $(\tilde{x},\tilde{u})$. The idea is to achieve local designs for $\tilde{M}(s)$, $\tilde{T}(s)$, and $\tilde{G}(s)$ and then to schedule them into global control by selecting explicit matrix functions of the form $M(x,u,s)$; $T(x,u,s)$; $G(x,u,s)$ where $M(\tilde{x},\tilde{u},s) = \tilde{M}(s)$, $T(\tilde{x},\tilde{u},s)=\tilde{T}(s)$, and $G(\tilde{x},\tilde{u},s) = \tilde{G}(s)$. At no time is f or g explicitly determined, except locally through $(\tilde{A}, \tilde{B}, \tilde{C}, \tilde{D})$; moreover, the resulting global controller is tested by computer simulation.

IV. LOCAL DESIGN EQUATIONS

In references [2,3,4,5] the authors have discussed and illustrated linear multivariable control synthesis methods using the input-output viewpoint. These methods give a capability, locally, to design internally stable feedback controllers which achieve prespecified output response.

Briefly, the above established that for a unity feedback system as in Figure 4: If a stable

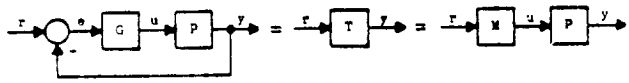

Figure 4

square plant P(s) is given, a controller G(s) produces internally stable, feedback realizable closed loop response T(s) only if:

$$M = P^{-1}T \quad , \ M \text{ proper \& stable} \qquad (4)$$

and

$$G = P^{-1}Q = P^{-1}T(I-T)^{-1} \qquad (5)$$

Equation (4) is called the synthesis equation because it displays all admissible responses T(s) and M(s). Equation (5) is the control dynamics design equation. The synthesis equation is used to assure acceptable response choices T and M ; the design equation then gives controller dynamics G. The relationships are pictured by the block diagrams in Figure 4.

Since the controller G is linear, to use it in a nonlinear system, steady state information lost in linearization must be restored. One way to do this (1) is to supply appropriate input, u_r, and request, y_{rc} levels to the control loop. An augmented control loop conforming locally to the Total Synthesis Problem discussed in Section III

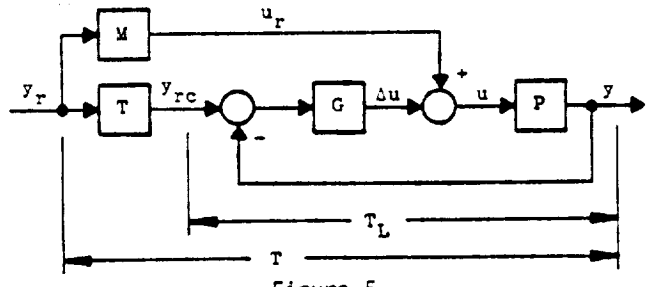

Figure 5

is shown in Figure 5. The approach provides coordinated input requests u_r and output requests y_{rc} with the closed loop in balance. The overall response is T; the closed loop response may be T_L. This structure organizes and realizes control action in terms of significant system characteristics: the desired response T, the synthesis matrix M and the controller G. This is considered an extension of [1].

V. CONTROLLER SCHEDULING

A nonlinear plant p such as that shown in Figure 1 has local character, and identification methods can provide a local state space or frequency domain description from which a local plant transfer function P(s) can be obtained. If a desired local response T(s) is selected, the foregoing equations (4) and (5) give M(s) and G(s) respectively. This can be repeated at any desired number of locations to obtain a set of T,M and G matrices. These may be linked together as a function of plant condition to form nonlinear control elements. Thus {T}→t, {M}→m, {G}→g and of course {P}→p.

For a practical nonlinear turbojet control, the foregoing is not sufficient by itself; desired output schedules, transient control means and plant protection functions are also necessary. The control structure in Figure 2 adapted to the J-85 engine model becomes Figure 6.

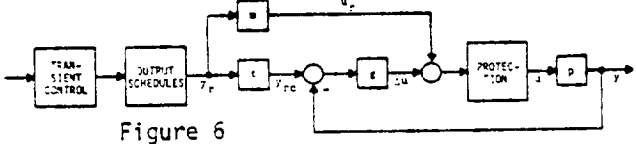

Figure 6

This scheme provides the basic features needed for nonlinear turbojet engine control. It is the structure used in the design example which follows.

VI. DESIGN EXAMPLE

The process to design a nonlinear control for the J-85 turbojet engine shown in Figure 1 was as follows:

1. Identified local engine dynamics at selected points.
2. Chose desired local responses: T overall and T_L closed loop.
3. Designed local matrices M and G.
4. Linked local matrices by scheduling as a function of engine speed to obtain nonlinear controller elements t, m and g.
5. Established desired steady state output schedules, transient control and protection logic.
6. Simulated and examined local and full range performance.

Since two inputs (fuel flow W_f and nozzle area A_j) are available, only two outputs may be independently controlled at any one time [3,2]. Engine speed, N, and turbine temperature, T_4, were selected for control.

The nonlinear engine model was identified at four local conditions: 50,72, 85, and 100 speed levels. At 100% speed condition the local characteristics of the engine are by defined by

$$P(s)=\frac{\begin{bmatrix}5.67\ (.18s+1) & 56\ (.18s+1\\ .17\ (1.3s+1) & -1.9\ (.005s+1)\end{bmatrix}}{(.62s+1)\qquad(.18s+1\ )} \tag{6}$$

A nonlinear, decoupled response function t was selected where the time constant for the speed and temperature response varied smoothly from .4 sec @ 72% N to .2 sec @ 100% N. Thus 100% N, the local system response matrix T is T = diag (1/.2s+1)). The loop response matrix is T_L=diag (1/(.1s+1)) for the entire operating range.

For the given P(s) and the chosen T(s), the synthesis matrix M(s) and the control dynamics G(s) a+ 100% speed are

$$M(s) = P^{-1}T = \frac{\begin{bmatrix}.095\ (.005s+1) & 2.8\ (.18s+1)\\ .008\ (1.32s+1) & -.28\ (.18s+1)\end{bmatrix}}{(.2s+1)} \tag{7}$$

$$G(s)=P^{-1}T(I-T)^{-1} =\frac{\begin{bmatrix}.95\ (.005s+1) & 28\ (.18s+1)\\ .08\ (1.32s+1) & -2.8\ (.18s+1)\end{bmatrix}}{s} \tag{8}$$

Of course, M, G and T are dependent on local condition; therefore, the M, G and T matrices were scheduled as a function of engine speed and formed the nonlinear controller elements m, g and t. The form of the nonlinear control g is shown in Figure 7.

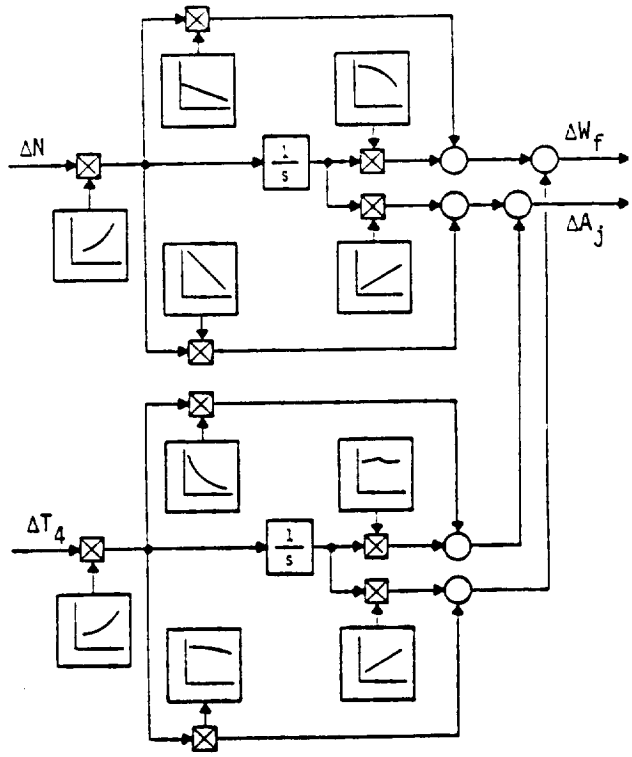

Figure 7 Nonlinear Controller

The nonlinear system was assembled in accordance with Figure 6 and simulated on a hybrid computer. The authors are happy to gratefully acknowledge the contribution of Mr. Ben Jacobs of The Bendix Corporation for the expert simulation

of the system. The operating range of interest was from 70% N to 100% N.

Figure 8 shows the response of speed N and turbine temperature T_4 relative to their requested values for a series of 5% step commands over the operating range. The outputs follow the requests satisfactorily recalling that the desired response time constant at 70% was .4 seconds and at 100% was .2 seconds. The system is stable over the entire range and performs essentially as desired. Figure 9 shows the response of the inputs, fuel flow W_f and nozzle area A_j, corresponding.

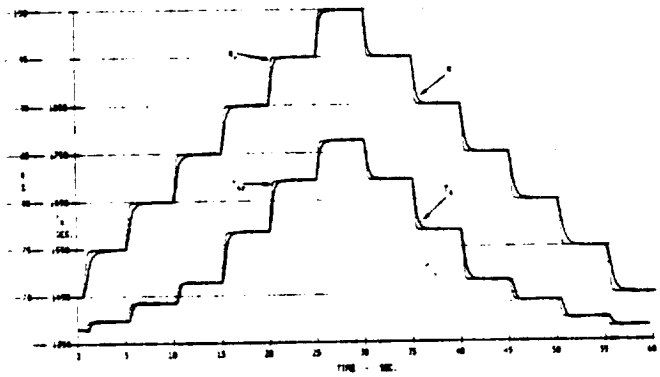

Figure 8

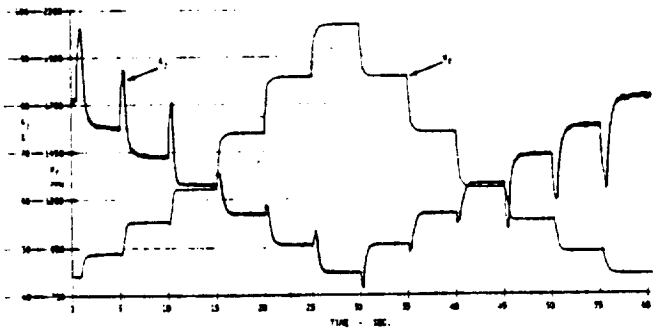

Figure 9

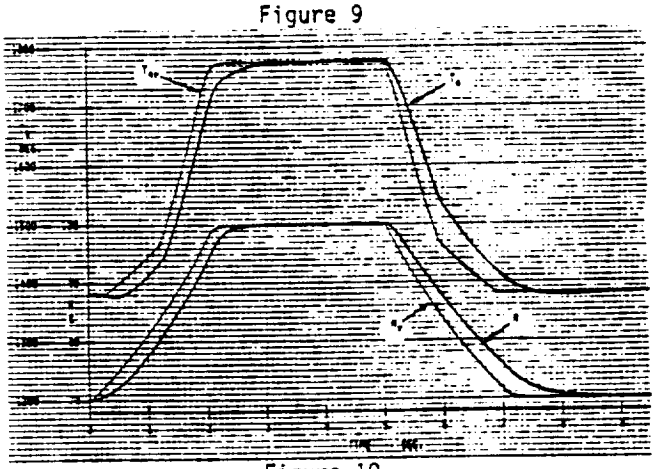

Figure 10

Full range acceleration and deceleration transients are shown in Figures 10 and 11. The outputs track the requests without overshoot and the transient time is less than three seconds. Corresponding response of the inputs is shown in Figure 11. The input responses are reasonable and within limits.

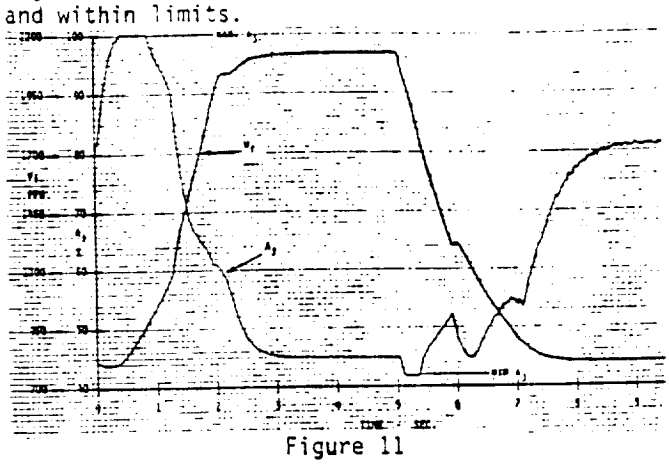

Figure 11

VII. SUMMARY REMARKS

A nonlinear control synthesis method was described. It extends and generalizes earlier work [1] and establishes connections with prior linear theory and concepts of local response, synthesis and controller matrices. The ideas are chosen to be compatible with practice in aircraft turbine control, and to illustrate the viewpoint of a major type of application thinking.

A concept of Total Synthesis Problem was introduced for the nonlinear domain, building on prior linear theory and ideas.

VIII. REFERENCES

1. J. L. Peczkowski and S. A. Stopher,"Nonlinear Multivariable Synthesis with Transfer Functions," Proceedings 1980 Joint Automatic Controls Conference, Paper WA8-D, August 1980.
2. J. L. Peczkowski and M. K. Sain, "Control Design with Transfer Functions, an Application illustration," Proceedings Twenty-Third Midwest Symposium on Circuits and Systems, pp. 47-52, August 1980.
3. R. J. Leake, J. L. Peczkowski, and M. K. Sain, "Step Trackable Linear Multivariable Plants," International Journal of Control, Vol. 30, No. 6 pp. 1013-1022, December 1979.
4. J. L. Peczkowski, M. K. Sain, and R. J. Leake, "Multivariable Synthesis with Inverses," "Proceedings Eighteenth Joint Automatic Control Conference, pp. 375-380, June 1979.
5. J. L. Peczkowski and M. K. Sain, "Linear Multivariable Synthesis with Transfer Function, in Alternatives for Linear Multivariable Control, M. K. Sain, J. L. Peczkowski and J. L. Melsa, Eds. Chicago: National Engineering Consortium, 1977, pp. 71-87.

TENSOR IDEAS FOR NONLINEAR MODELING OF A TURBOFAN JET ENGINE: PRELIMINARY STUDIES*

Stephen Yurkovich, Thomas A. Klingler, and Michael K. Sain
Department of Electrical Engineering
University of Notre Dame
Notre Dame, IN 46556

ABSTRACT

The importance of nonlinear models for model following methods so prevalent in the modern turbofan engine industry dictates the need for reliable techniques for nonlinear model generation. This paper reports upon a continuing investigation aimed at developing nonlinear differential models utilizing the notions of power series and algebraic tensors. Emphasis of the study is on an application of these ideas in nonlinear model generation using a real-time digital turbofan engine simulation.

INTRODUCTION

Model following control systems constitute a solid backbone for much of the control work in modern aviation. Basically, one has the plant, which may be an airframe or an engine---or both the airframe and the engine regarded as an integrated whole. Under certain conditions, such as temperatures, pressures, and compressor speeds, the plant may be said to satisfy certain nonlinear differential equations. Moreover, many of the variables in these equations are related to one another through complicated nonlinear maps. It is within this range of acceptable conditions that any realistic control system must carry on its work. Accordingly, when a control system receives a request to change important physical quantities within the plant, it must arrange to do so in such a way that the plant moves to the new condition without violating its identity, that is, without leaving the acceptable region of conditions anywhere along the way. For example, if altitude is to be changed, then this must be accomplished without stall. Or, if thrust is to be changed, it must be changed without permitting excessive increases in turbine inlet temperature.

The reason that model following control thinking is so useful in such situations is due to the fact that the models may be used to prescribe behaviors which are in consonance with the region of acceptable plant conditions. Scheduled over an operating envelope, such models can absorb a large part of control stress, and can free the feedback loop for its primary task of achieving accuracy in the presence of parametric uncertainties and disturbances.

This paper deals with studies on the use of algebraic tensors [1] for generating a family of nonlinear models. The main feature of the algebraic tensor involves the way that it gives ground on dimensionality in order to gain advantages of linearity. This provides an organized way of looking at expansion formula and provides a direct line with parameter identification techniques for linear equations. Basically, one has to design initial conditions and control signals in order to assure that the nonlinear model will outperform the linear model locally, as well as arranging that it yield a larger region of acceptable modeling. Such modeling exercises have been exhibited in [2] and [3] for representative off-simulator examples. Our purpose here, then, is to apply the techniques to nonlinear model generation using a real-time digital turbofan engine simulation, and to present some preliminary representative results.

ALGEBRAIC TENSORS IN MODELING

We illustrate now the use of algebraic tensors in nonlinear model building, utilizing ideas of power series and truncation approximations. To this end, let $x \in X$ be the n-vector of states and $u \in U$ be the m-vector of inputs, where X and U are real vector spaces. Consider the nonlinear ordinary differential equation

*This work was supported by the National Aeronautics and Space Administration under Grant NSG 3048.

$$\dot{x} = f(x,u); \tag{1}$$

we will assume without loss that the origin is an equilibrium point of (1). The function $f : X \times U \to X$, under certain technical assumptions such as analyticity in a neighborhood of $(0,0)$ in $X \times U$, may be expressed in a power series expansion of two variables. Due to the notational complexity of higher order mixed partial derivatives, only the first few terms of such an expansion may be easily recorded. However, if we employ the universal bilinear tensor product function $\otimes : X \times U \to X \otimes U$ [4,5], where the nm-dimensional real vector space $X \otimes U$ is the tensor product of X with U, we can express the right side of (1) in the compact form

$$f(x,u) = \sum_{j=0}^{\infty} \sum_{k=0}^{\infty} \frac{1}{j!k!} M_{jk} \left(\underbrace{x \otimes x \otimes \cdots \otimes x}_{j \text{ times}} \otimes \underbrace{u \otimes u \otimes \cdots \otimes u}_{k \text{ times}} \right) . \tag{2}$$

The main feature of (2) lies in the fact that the M_{jk} are linear maps, facilitating an orderly treatment of higher order terms in the expansion. Such elements are built up by iteration, as for example $(X \otimes (X \otimes U)) \otimes U$.

A nonlinear model of (1) can be obtained by truncation of (2). To allow for this (2) may be simplified by introducing the new linear map L_{jk} whose action is that of M_{jk} followed by the scalar multiplication by $1/j!k!$. Thus, a linear identification problem may be formulated via the equation

$$\dot{x} = [L_{10}\ L_{01}\ L_{20}\ L_{11}\ L_{02}\ L_{30}\ \cdots]\ x_T \tag{3}$$

where x_T is a vector partitioned into tensor product terms in an appropriate order, given by $(x, u, x \otimes x, x \otimes u, u \otimes u, x \otimes x \otimes x, \ldots)$. Consider the tensor product associated with the L_{12} map which is generated by elements in $X \otimes U \otimes U$. For the case of $n = 3$ and $m = 2$, the 12 monimals of $x \otimes u \otimes u$ consist of terms such as $x_1u_1^2$, $x_1u_1u_2$, $x_1u_2u_1$, and so on. But due to the commutativity of scalar multiplication in the field there exist three redundant terms; elimination of these terms results in an object of dimension 9. In general, the number of distinct elements from each product is given by the combinatorial expression

$$p = \binom{n+q-1}{q} \cdot \binom{m+r-1}{r} \tag{4}$$

for q copies of x and r copies of u in the product. Construction of the system consists of stacking these monomials in the vector x_T to give a reduced-size version of (3), which amounts to a use of the symmetric tensor algebra [5]. It is important to note that now the matrix L_{jk} is of reduced size, corresponding to the reduced order structure.

To complete the construction of our approximate system, sinuosidal inputs are applied to (1), and the state solutions are sampled at h selected time points. These sampled values are loaded into the $p \times h$ matrix X_T. The first $n+m$ rows of X_T are determined from the sampled values of x and u; the remaining $p-(n+m)$ rows contain monomials which are multiplies of the entries of those first $n+m$ rows. The $n \times h$ matrix $\dot{X}$ is formed by loading derivatives estimates for $\dot{x}_1, \dot{x}_2, \ldots, \dot{x}_n$ at the h time points. As an illustration, for an approximation retaining up to third degree tensor product terms we have

$$\dot{X} = [L_{10}\ L_{01}\ L_{20}\ L_{11}\ L_{02}\ L_{30}\ L_{21}\ L_{12}\ L_{03}]\ X_T . \tag{5}$$

The method employed here in solving for the coefficient matrix uses a singular value decomposition of the transpose of X_T to solve the minimal least-squares problem, returning the $n \times p$ partitioned matrix of the L_{jk}.

APPLICATION: JET ENGINE SIMULATOR

In the modeling discussions to follow attention will center around NASA's QCSEE ("Quixie")---Quiet, Clean, Short-haul Experimental Engine [6]. Following in the evolution of turbojet to turbofan engines in aircraft propulsion, the QCSE engine is an advanced turbofan designed specifically for powered-lift, short-haul aircraft. The engine incorporates several new concepts not all currently used on turbofans to achieve optimal efficiency as well as quiet, clean operation. Primary uses of QCSEE-type engines will be on short take off and landing (STOL) aircraft, promising brighter prospects for compact metropolitan airports.

An ideal of any propulsion simulation is to achieve absolute realism for use in flight simulators. To approach this ideal requires very detailed digital simulations in the form of complex computer programs. The goal of the QCSEE simulator program employed in this study has been to achieve real time propulsion simulation to be used in aircraft simulators with

under-the-wing engine application.

For the analytical model to be discussed, the states and controls employed are as follows. Engine states are the combustor exit temperature and rotor dynamics in the form of the fan speed and compressor speed. Control inputs are the fuel metering valve position (which determines main burner fuel flow), nozzle area setting, and a fan pitch angle parameter for control of the variable pitch fan. Thus a three-state, three-control model will be formulated. Model formulations using more than three states are currently under investigation.

Engine operation for the model identification can take two basic approaches. The engine simulator may be run with the loop closed, that is, with the digital controller segment fully operative, while simply varying the power demand (or, equivalently, the "throttle") about some equilibrium point. Figure 1 illustrates this scheme where we represent the engine dynamics in terms of the states and their derivatives. The reference input power demand (PWRX) is depicted as a sinusoidal perturbation which in turn, with plant measurements y_m, determines the controller dynamics. An alternative approach for the simulator operation involves opening the loop, effectively deactivating the controller and independently inserting the individual control inputs. This situation is portrayed in Figure 2 where we insert a constant power demand and "turn-off" the controller by equating the controller state derivatives with zero. In this way sinusoidal inputs, u, may be inserted and engine states observed.

In the second approach mentioned above, which we will adopt here, nonlinearities of the plant are excited which might otherwise have been less pronounced had the controller been in the loop. For both operations the engine simulator is run into the steady state prior to any perturbations in order to establish an operating point. The initial conditions thus generated form the point of expansion for the series truncation approximation in the model formulation.

SAMPLE RESULTS

In this final section we offer an overview of the procedure for an identification using the QCSEE simulator. As mentioned in the preceding section, the operation of QCSEE for purposes of model generation in this study is of the type depicted in Figure 2. The simulator is run with a 100% power demand for several seconds to settle all transients. This produces some equilibrium value (x_o,u_o) where x and u each consist of three elements. Within the digital simulation program the control variables are manipulated so that a sinusoidal input with some amplitude and frequency is inserted into each input channel. Likewise, the state variables are perturbed from their equilibrium values and then sampled over some interval at evenly spaced points in time. The difference between these sampled values and the corresponding equilibrium values form the block of observed data for the identification procedure. The derivative values are also extracted directly from the simulator at the given sample times so that a truncation approximation, such as that given in (5), may be formulated. Ordering of the elements in x_T is of critical import for identification as well as simulation of the model; a complete algorithm for such an ordering procedure may be found in [2].

Validation studies of a model consist of comparing model responses to true responses of the state variables to perturbations in the initial states and input signal parameters about the point at which the model is identified. Moreover, a standard linear approximation model is normally identified by another method and also used in the comparison studies. All simulations here are done in the open loop. For example, observe the response curves given in Figures 3-5. The first plot represents a sample response for perturbations in the initial state values; Figure 3 shows the behavior of the compressor speed for a decrease to 25% of the perturbation used in the identification. Figure 4 represents the response of the compressor speed for a downward perturbation in the control signal amplitudes. Finally, Figure 5 exhibits the fan speed behavior for a 20% increase in frequencies in each signal.

Preliminary studies have resulted in several nonlinear models for specific identification points. To illustrate the type of simulations which result from such models, representative response curves have been presented with various input parameter sets for one such model. A final identification, that is, one with full validation studies, is currently under investigation.

REFERENCES

1. M.K. Sain, "The Growing Algebraic Presence in Systems Engineering: An Introduction", Proceedings of the IEEE, Volume 64, No. 1, pp. 96-111, January 1976.
2. S. Yurkovich, "Application of Tensor Ideas to Nonlinear Modeling and Control", M.S. Thesis, Department of Electrical Engineering, University of Notre Dame, Notre Dame, Indiana, January 1981.
3. S. Yurkovich and M.K. Sain, "A Tensor Approach to Modeling of Nonhomogeneous Nonlinear Systems", Proceedings Eighteenth Allerton Conference on Communication, Control, and Com-

puting, October 1980.
4. S. MacLane and G. Birkhoff, Algebra. London: Macmillan, 1967, Chapters 9 and 16.
5. W.H. Greub, Multilinear Algebra. New York: Springer-Verlag, 1967.
6. J.R. Mihaloew and C.E. Hart, "Real Time Digital Propulsion System Simulation for Manned Flight Simulators", NASA TM-78958, Lewis Research Center, Cleveland, Ohio, 1978.

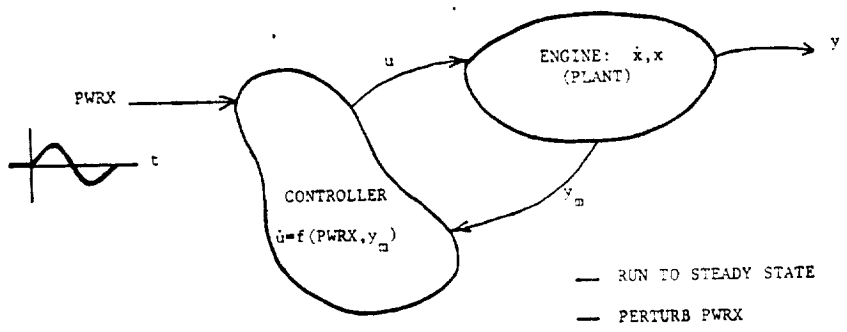

Figure 1 Closed Loop Identification

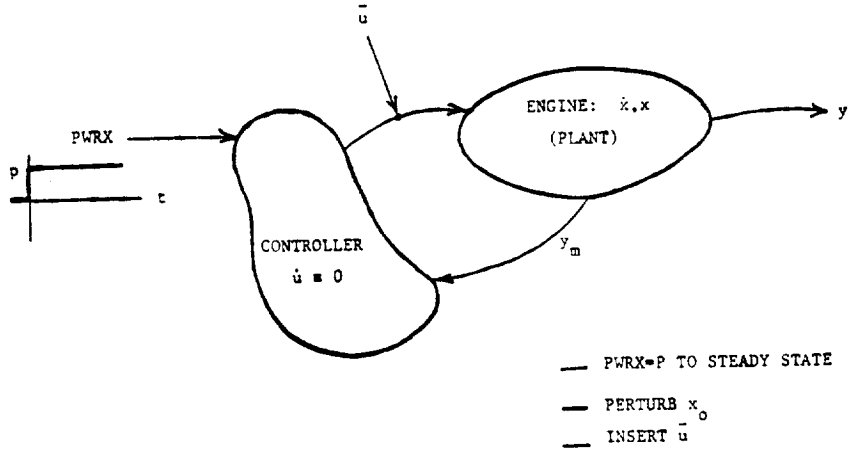

Figure 2 Open Loop Identification

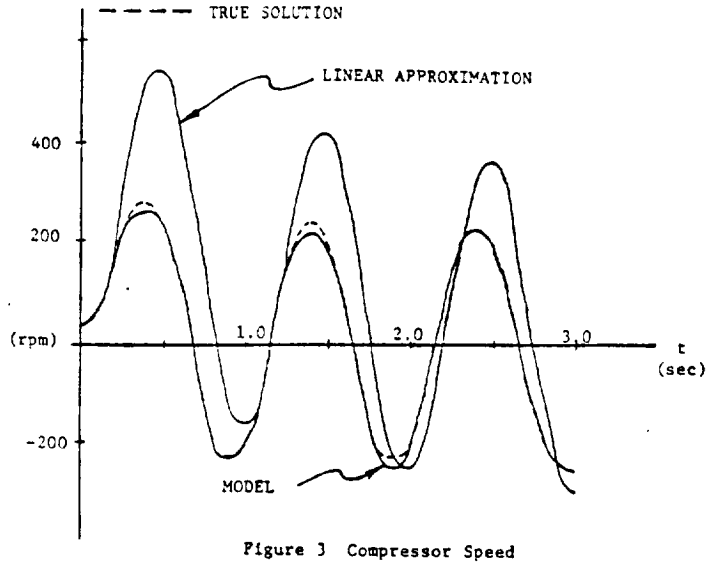

Figure 3 Compressor Speed

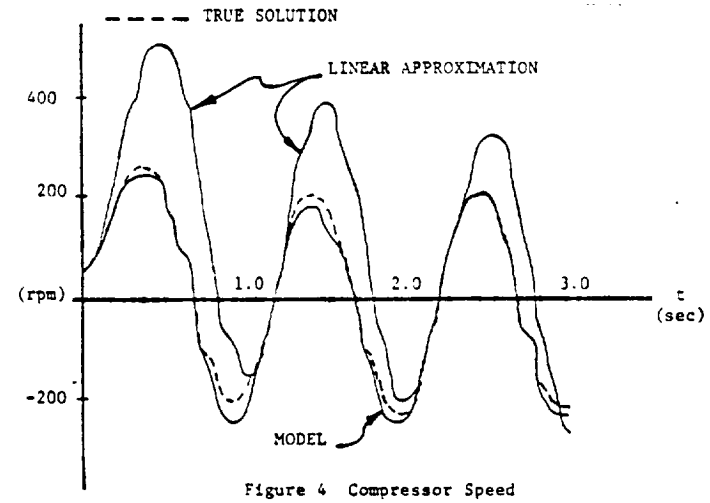

Figure 4 Compressor Speed

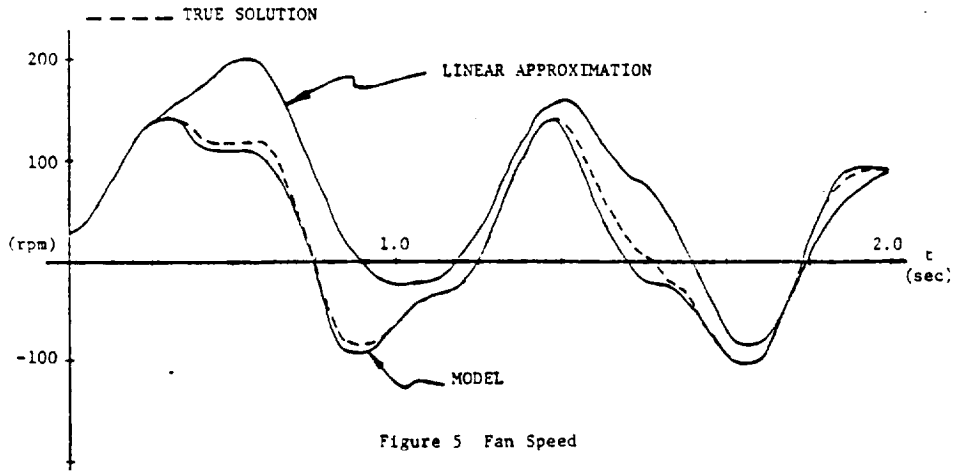

Figure 5 Fan Speed

D576

AN APPROACH TO ROBUST NONLINEAR CONTROL DESIGN

Michael K. Sain
Department of Electrical Engineering
University of Notre Dame
Notre Dame, Indiana 46556

Joseph L. Peczkowski
Energy Controls Division
The Bendix Corporation
South Bend, Indiana 46620

ABSTRACT

When the plant is a highly sophisticated piece of hardware, whose best available model is a digital or hybrid computer simulation provided by the manufacturer, a common nonlinear control design philosophy is to linearize the simulation at a finite number of points in the operation envelope, to apply linear design strategy at each point, and to schedule the resulting compensations over the envelope, within a broad, nonlinear, model following scheme. This study is part of a continuing effort by the authors to articulate some theoretical views of this method. Included is a new local extension of comparison sensitivity to the model following case. Nonlinear turbojet engine illustrations are also given.

I. INTRODUCTION

The theory of nonlinear automatic control systems presents a difficult challenge to the intellectual community. On the one hand, considerable progress has been made, as in the topical areas of optimal control, feedback stabilization, and algorithms. On the other hand, a great deal of industrial design still seems to proceed without the explicit use of such ideas. Some leading theoreticians have suggested that more effort needs to be spent upon communicating existing theoretical concepts to control design engineers. Others have opined that the ideas are not in use because they are not in demand. However the truth may be distributed among these camps, we can certainly point out that optimal control theory is an indirect way of viewing the problem, a sort of technologically advanced version of "putting all the eggs in one basket"; and we can see that certain applications may require a more direct design insight. Moreover, we can recognize that stability is necessary, but not sufficient, for practical design---and that the stability issue is frequently resolved in practice by local and full range simulations and tests.

Classroom models of the form

$$\dot{x} = f(x,u)$$

$$y = g(x,u)$$

may not be explicitly available. Though approximate versions of such models can be contemplated, they may turn out to be formidably complex---or worse, intractable. These remarks can be motivated by the area of aircraft gas turbine control systems. In this case, the plant is a highly sophisticated piece of hardware, whose best available model is a digital or hybrid simulation supplied by the manufacturer. Even in such cases, however, control systems must be, and are, designed. The nonlinear turbojet engine model used in this paper falls into such a category, and we hope that it illustrates the point.

The work reported here is part of a continuing effort [1,2] by the authors to formulate some theoretical views concerning current practical design procedures in these cases. We recognize that nonlinear control design varies from one application area to another; and we point out that our remarks are certainly influenced by current practice for aircraft gas turbines. However, we believe that many practical situations are quite similar in spirit. Thus, we hope to further the theory/application dialogue.

We will discuss the control philosophy which linearizes the simulation at a finite number of points over the envelope of operation, which applies linear design technique locally about each such point, and which strings all the local designs together into a global design by scheduling the resulting compensations over the envelope, as a function of key physical variables, and within a broad, nonlinear model following strategy.

The sections following contain a review of relevant local model following ideas, an extension of the local comparison sensitivity concept to the model following situation, a presentation of the global model following concept, and a complete illustration based upon a realistic nonlinear turbojet engine simulation.

II. LOCAL THEORY

Let F be a field. Then $F[s]$ is the principal ideal domain of polynomials in s with coefficients in F, and $F(s)$ is its quotient field [3]. Let V be an F-vector space of finite dimension. Define the F-vector spaces

$$F[s] \otimes_F V \qquad (1)$$

and

$$F(s) \otimes_F V \qquad (2)$$

respectively, using the conventional tensor product [3]. It is not difficult to see that (1) admits the structure of an F[s]-module, denoted V[s], and that (2) admits the structure of an F(s)-vector space, denoted V(s).

Next, let R, U, and Y be F-vector spaces of finite dimension. We think of R as a space of constant, exogenous request vectors, of U as a space of constant control inputs, and of Y as a space of constant plant responses. To make these spaces dynamical, we form the F[s]-modules R[s], U[s], and Y[s] and the F(s)-vector spaces R(s), U(s), and Y(s), respectively.

The plant, in an input/output sense, is then defined by a morphism

$$P(s) : U(s) \to Y(s)$$

of F(s)-vector spaces. The matrix [P(s)] of the morphism P(s), for suitable basis choices in U(s) and Y(s), has its elements in F(s).

Each such morphism of finite-dimensional F(s)-vector spaces has associated with it a pole module [4]; and this pole module has a unique monic minimal polynomial m(P) associated with it. Plants can be classified according to the properties of m(P). For example, if $F = \mathbb{R}$, the real numbers, we can say that the plant is stable whenever m(P) is strictly Hurwitz. More generally, let $S_g \subset F[s]$ be closed under multiplication, exclude the zero polynomial, and include the polynomial 1. We then say that the plant P(s) is good if $m(P) \in S_g$.

By the Nominal Design Problem (NDP), we shall mean the selection of a pair (M(s),T(s)) of good morphisms

$$M(s) : R(s) \to U(s)$$

and

$$T(s) : R(s) \to Y(s)$$

such that the diagram of Figure 1 commutes.

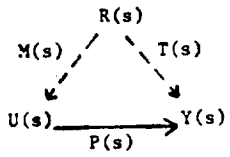

Figure 1. Nominal Design Problem.

The condition that (M(s),T(s)) be a good pair is motivated by the concept of internal stability in feedback realizations of the controller. Notice that M(s) represents the action of the controller, which abstractly can be understood as a morphism

$$C(s) : R(s) \times Y(s) \to U(s) \qquad (3)$$

of F(s)-vector spaces, in the output feedback case. T(s) represents the input/output response of the control system to dynamical, exogenous signals. Notice also that NDP is not the Model Matching Problem (MMP), as for example in [5], because T(s) is not regarded as given. In MMP, the diagram of Figure 1 would have to be modified so that the T(s) arrow is solid, and not dashed.

To accommodate the idea of achieving M(s) with feedback, we introduce the notion of the Feedback Synthesis Problem (FSP), which is to determine a morphism C(s), as in (3), in such a way that, combined with P(s), a well defined mapping R(s) → Y(s) results and is equal to T(s). By itself, FSP offers little challenge, unless the plant is not good. In such situations, and indeed in the general feedback control problem, we are led to look at an internal, instead of an input/output, description of the system which generates T(s). Indeed, the system also has a pole module, whenever C(s) generates a well defined mapping R(s) → Y(s); and we can speak of the Good Feedback Synthesis Problem (GFSP), which is just FSP with the minimal polynomial of the system being good. Again, if $F = \mathbb{R}$, one version of GFSP is FSP with internal stabilization. See, for example, the work of Bengtsson and Pernebo [6,7].

We define the Total Synthesis Problem (TSP) as the combination of NDP and GFSP. Notice that this represents a generalization and refinement of the original TSP notion in [8]. Examples of the TSP way of thinking may be found in [8,9,10].

From both a conceptual and a numerical point of view, it turns out to be very convenient [11,12] to consider TSP in terms of coprime factorizations of P(s), for example

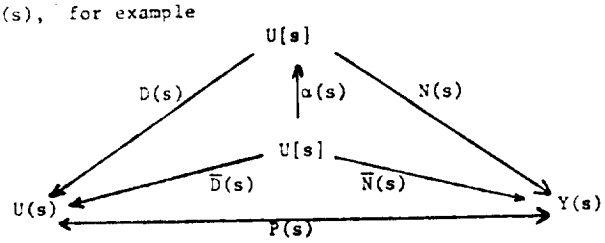

Figure 2. Right Coprime Factorization.

the right coprime case of Figure 2, in which D(s) is a monomorphism of F[s]-modules, in which N(s) is a morphism of F[s]-modules, and in which any other such pair $(\bar{D}(s),\bar{N}(s))$ is related to (D(s),N(s)) by the morphism α(s) indicated.

III. TSP AND COMPARISON SENSITIVITY

To insert a notion of robustness into the design procedure, we build upon the classic idea of comparison sensitivity, originated by Cruz and Perkins [13] in 1964. Recently, Cruz, Freudenberg, and Looze [14] have shown that the comparison sensitivity matrix relates not only to perturbations in the plant but also to the important issue of stability robustness. For a detailed example of this utility, see Sain, Ma, and Perkins [15].

For purposes of this section, we shall suppose that FSP is carried out within the structure of Figure 3. In this configuration, the feedback loop produces

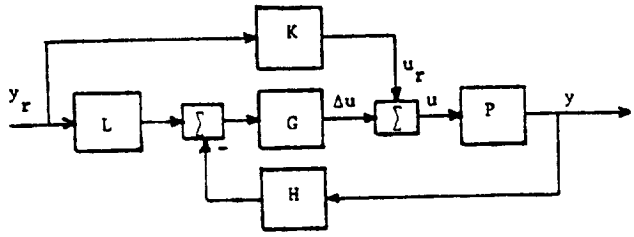

Figure 3. FSP Structure.

incremental control action Δu, while $K(s)$ produces a control action request u_r. The plant response request y_r is in $R(s)$, which in many cases may be taken equal to $Y(s)$.

The Cruz-Perkins viewpoint [13,14] considers and compares two solutions $(G(s),H(s),K(s),L(s))$ to FSP. The feedforward solution is given by $(M(s),0,0,1)$, and the feedback solution is of the form $(G(s),H(s),0,1)$. It is assumed that NDP has been solved when $P(s) = P^\circ(s)$, the nominal plant. When $P(s) \neq P^\circ(s)$, the feedforward solution gives an error

$$E_{ff} = P(s)M(s) - T(s),$$

and the feedback solution gives an error

$$E_{fb} = (1 + P(s)G(s)H(s))^{-1}P(s)G(s) - T(s).$$

The central observation is that

$$E_{fb} = S(s)E_{ff},$$

where

$$S(s) : Y(s) \to Y(s)$$

has action given by

$$S(s) = (1 + P(s)G(s)H(s))^{-1}.$$

$S(s)$ is called the comparison sensitivity morphism. Other solutions, such as $(G(s),1,0,L(s))$ have been considered; but it is believed that the following discussion is novel.

Consider the error E_{mf}, when $P(s) \neq P^\circ(s)$ in Figure 3. The subscript (mf) stands for model following, the implication of which should soon become clear. Then, with (s) suppressed,

$$\begin{aligned} E_{mf} &= (1+PGH)^{-1}P(GL+K) - T \\ &= (1+PGH)^{-1}P(GL+K) - (1+P^\circ GH)^{-1}P^\circ(GL+K) \\ &= S\,\{P - (1+PGH)\,S^\circ P^\circ\}\,(GL+K)\,. \end{aligned}$$

Now regard the perturbation in P as additive, namely $P = P^\circ + \Delta P$; then

$$\begin{aligned} E_{mf} &= S\,\Delta P\,\{1 - GH\,S^\circ P^\circ\}\,(GL+K) \\ &= S\,\Delta P\,(1+GHP^\circ)^{-1}(GL+K) \end{aligned}$$

the last step following from [16]. Next write $L = HT + \Delta L$, $K = M + \Delta K$. With these, and the commutative diagram of Figure 1, we have

$$\begin{aligned} E_{mf} = S\,\{&\Delta PM + \Delta P(1+GHP^\circ)^{-1}G\Delta L \\ &+ \Delta P(1+GHP^\circ)^{-1}\,\Delta K\}\,. \end{aligned}$$

Notice that ΔPM is E_{ff}. In the second term, $(1 + GHP^\circ)^{-1}G$ might be called M_{loop}, because it generates Δu from the loop request Ly_r. M_{loop} must be of reasonable gain-bandwidth product, so that the loop is effective. Thus it is natural to propose choosing ΔL small, or even zero, in order to reduce the effect of the second term. Therefore, choose $\Delta L = 0$; then the fact that Figure 3 realizes M implies the relation

$$(1 + GHP^\circ)^{-1}\,(GHT + K) = M\,.$$

This can be rewritten in the manner

$$(1+GHP^\circ)^{-1}(GHP^\circ M+M+\Delta K) = M,$$

from which

$$(1+GHP^\circ)^{-1}\Delta K = 0.$$

Thus, $\Delta K = 0$, and we have the diagram of Figure 4. For this case, we have shown that

$$E_{mf} = SE_{ff}\,,$$

a result in the Cruz-Perkins tradition. Notice that

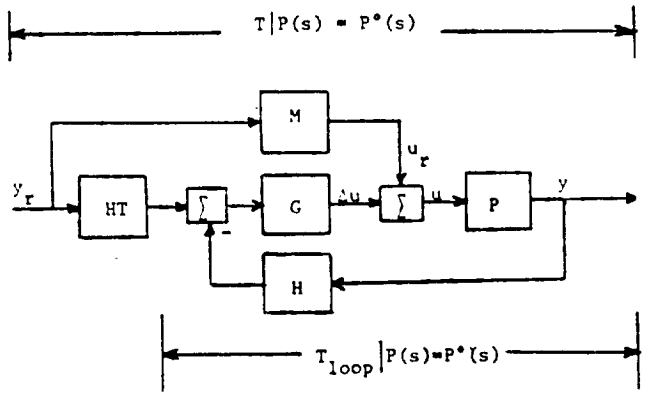

Figure 4. Natural Version of Figure 3.

the zero choice for ΔL in the expression for E_{mf} occurs naturally, inasmuch as ΔP is not a controllable quantity and M_{loop} must be of reasonable action. Notice further that the loop is active only when P is not equal to P°.

IV. A NONLINEAR NDP

The ideas of NDP can be extended to the nonlinear case [2]. We sketch them briefly here. Assume that the request r, the control u, and the response y are elements of commutative groups $(\hat{R},+,0)$, $(\hat{U},+,0)$, and $(\hat{Y},+,0)$ respectively. As functions, then, $p : \hat{U} \to \hat{Y}$ is the plant, $t : \hat{R} \to \hat{Y}$ gives control system response, and $m : \hat{R} \to \hat{U}$ provides control action. The diagram of Figure 1 can be redrawn as in Figure 5.

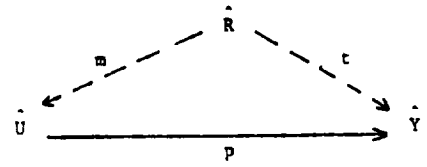

Figure 5. Nonlinear NDP.

The idea is to solve TSP locally at a finite number of points in the envelope of operation and schedule these solutions into a family

$$\{(G(s),\ H(s),\ K(s),\ L(s))\}$$

which then infers functions g, h, k, and l respectively.

V. TURBOJET MODEL

The J-85 engine model in Figure 6 consists of two integrators, nine nonlinear functions, eleven multipliers and dividers, and eight summing junctions. The model describes the nonlinear dynamical and steady state relationships between the inputs u : fuel flow W_f and exhaust nozzle area A_j, and seven outputs y : including engine speed N, turbine inlet temperature T_4. This model is, on a small scale, representative of the nonlinear objects seen by turbine engine control designers in practice.

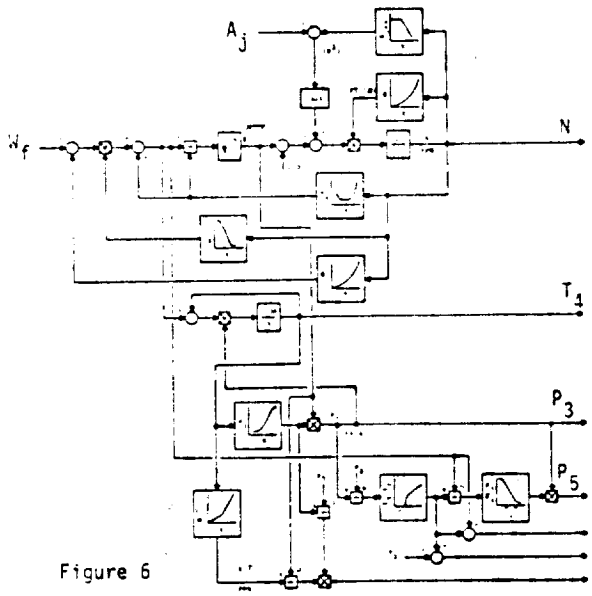

Figure 6

VI. LOCAL DESIGN EQUATIONS

In references [1,2,8,9,10,15,17,18] the authors have presented and illustrated linear and nonlinear multivariable control design methods using the input-output transfer function point of view. In this paper, earlier ideas are extended to include closed-loop sensitivity specifications together with response specifications.

A linear control structure which embodies the Total Synthesis Problem including sensitivity is shown in Figure 4. The system response matrix is T; the closed-loop response matrix is T_{loop}; the closed-loop sensitivity matrix is S; and all may be selected by the designer to suit applications, as outlined briefly in Section VIII.

Four key equations define controller dynamics in terms of response and sensitivity specifications:

$$M = P^{-1} T; \text{ M proper \& stable} \quad (4)$$

$$M_{loop} = P^{-1} T_{loop}; \ M_{loop} \text{ proper \& stable} \quad (5)$$

$$G = P^{-1} S^{-1} T_{loop} \quad (6)$$

$$H = T_{loop}^{-1} (I-S) \quad (7)$$

Equations (4) and (5) are called synthesis equations because they display all possible responses T, T_{loop} and M, M_{loop}. Equations (6) and (7) are design equations for the forward and feedback dynamics respectively. These equations allow for specification of both response and sensitivity performance of the system at the outset and throughout the design process.

VII. LOCAL TO NONLINEAR CONTROL

Nonlinear plant models p, as shown in Figure 6, almost always exhibit linear dynamical behavior in a neighborhood of an operating point. Hence, identification methods can provide state space or frequency domain characterization from which the local plant transfer function matrix P(s) can be obtained. This process, repeated at desired operating conditions, obtains a set of plant transfer functions {P(s)}.

A linear philosophy applied at desired operating points for selected sets of system responses {T}, closed-loop responses $\{T_{loop}\}$ and sensitivities {S} generates the sets of controller matrices {M}, {G}, {H} via the key equations (4) through (7). These sets may be linked or scheduled as functions of plant operating conditions to form nonlinear control system elements. Thus {T} → t, {M} → m, {G} → g, {H} → h.

Desired steady state operating schedules, transient control means and plant protection limit functions are also necessary to establish a basic nonlinear turbojet control system. These transform the linear system in Figure 4 to the nonlinear system in Figure 7.

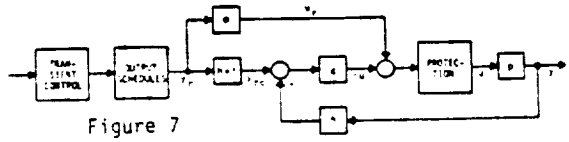
Figure 7

VIII. DESIGN PROCEDURE

Briefly, the steps to design a nonlinear control for the J-85 turbojet engine model are as follows:

1. Select available engine inputs and outputs. Establish desired operating schedules.
2. Identify local engine dynamics. Check plant invertibility.
3. Choose desired local response T, T_{loop} and sensitivity S.
4. Design local matrices M, G, H.
5. Schedule local matrices with engine speed. Obtain nonlinear controller elements m, g, h, h ∘ t.
6. Check local and full range performance by simulation.

Two inputs (fuel flow W_f, PPH, and nozzle area A_j, IN^2) are available on the J-85 engine; therefore, only two outputs may be independently controlled at any given time [1]. Engine speed N, RPM, and turbine temperature T_4, °R, were selected for control. The nonlinear engine model was identified at five sea level conditions: 50, 72, 85, 100 and 110% speed levels. The transfer function matrix of the engine is defined by P(s). The engine output vector is $[N,T_4]$ and the engine input vector is $[W_f,A_j]$. At 100% speed conditions the plant transfer function was identified to be

$$P = \frac{\begin{matrix} 5.67(.18s+1) & 56(.180s+1) \\ .17(1.30s+1) & -1.9(.005s+1) \end{matrix}}{(.62s+1)(.18s+1)}$$

The plant inverse matrix is

$$P^{-1} = \frac{\begin{matrix} .009(.005s+1) & 2.80(.18s+1) \\ .008(1.320s+1) & -.28(.18s+1) \end{matrix}}{1}$$

Performance goals for the system can be established and selected, for example:

- perfect steady state tracking of output schedules.
- system response of turbine temperature: no overshoot and .4 second lag between requested and engine temperature for smooth action at all conditions.
- system response of speed: no overshoot and .2 second lag at 100% conditions increasing smoothly to a .4 second lag at 72% conditions.
- closed-loop response at all conditions equal to .2 second lag and zero steady state error.
- sensitivity of the closed-loop of same form as unity feedback configuration and 8 times better than unity feedback for improved performance under plant parameter variation.

The above performance goals translate into the following response and sensitivity matrices at 100% speed conditions:

$$T = \begin{bmatrix} \frac{1}{.2s+1} & 0 \\ 0 & \frac{1}{.4s+1} \end{bmatrix} \qquad T_{loop} = \begin{bmatrix} \frac{1}{.2s+1} & 0 \\ 0 & \frac{1}{.2s+1} \end{bmatrix}$$

$$S = \left(\frac{.2s}{.2s+1}\right) I \text{ (Unity F/B)} \qquad S = \left(\frac{.025s}{.025s+1}\right) I$$

Note that sensitivity matrices are $S = [0]$ at $s = 0$. This specification on the closed-loop produces steady state tracking results. The controller matrices M, G, and H can now be calculated at 100% speed conditions; and in similar manner, at other engine operating conditions. The sets of controller matrices are scheduled as a function of engine speed to form the nonlinear control system elements m, g, h and $h \cdot t$. The form of the nonlinear control element g is shown in Figure 8 below.

The nonlinear system, Figure 7, was simulated on a hybrid computer. The operating range of interest was from 70%N to 100%N. The authors gratefully acknowledge the assistance and contributions of Mr. Ben Jacobs of the Bendix Corporation for the expert simulation of the system.

Full range acceleration and deceleration transients of the feedback system are shown in Figure 9 and 10. The outputs track the requests without overshoot and the transient time is less than 3 seconds. Corresponding response of the inputs is shown in Figure 10. The input responses are reasonable and within limits.

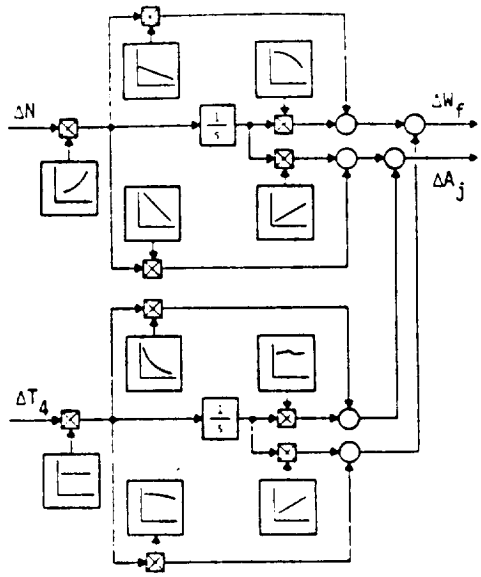

Figure 8 Nonlinear Controller g

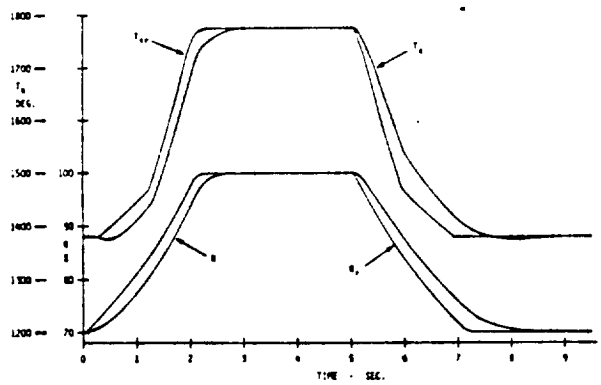

Figure 9

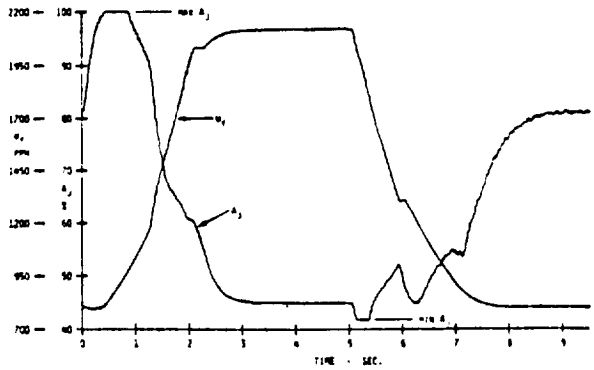

Figure 10

REFERENCES

1. J.L. Peczkowski and S.A. Stopher, "Nonlinear Multivariable Synthesis with Transfer Functions", Proceedings 1980 Joint Automatic Control Conference, Volume 1, Part WA8-D.

2. J.L. Peczkowski and M.K. Sain, "Scheduled Nonlinear Control Design for a Turbojet Engine", Proceedings 1981 IEEE International Symposium on Circuits and Systems, in press.
3. S. MacLane and G. Birkhoff, Algebra. New York: The Macmillan Company, 1967.
4. B.F. Wyman and M.K. Sain, "The Zero Module and Essential Inverse Systems", IEEE Transactions on Circuits and Systems, Volume 28, Number 2, pp. 112-126, February 1981.
5. A.S. Morse, "Structure and Design of Linear Model Following Systems", IEEE Transactions on Automatic Control, Volume 18, Number 4, pp. 346-353, August 1973.
6. G. Bengtsson, "Feedback Realizations in Linear Multivariable Systems", IEEE Transactions on Automatic Control, Volume 22, Number 4, pp. 576-585, August 1977.
7. L. Pernebo, "An Algebraic Theory for the Design of Controllers for Linear Multivariable Systems", Parts I and II, IEEE Transactions on Automatic Control, Volume 26, Number 1, pp. 171-194, February 1981.
8. J.L. Peczkowski, M.K. Sain, and R.J. Leake, "Multivariable Synthesis with Inverses", Proceedings 1979 Joint Automatic Control Conference, pp. 375-380.
9. J.L. Peczkowski and M.K. Sain, "Linear Multivariable Synthesis with Transfer Functions", in Alternatives for Linear Multivariable Control, M.K. Sain, J.L. Peczkowski, and J.L. Melsa, Eds. Chicago: National Engineering Consortium, 1977, pp. 71-87.
10. R.J. Leake, J.L. Peczkowski, and M.K. Sain, "Step Trackable Linear Multivariable Plants", International Journal of Control, Volume 30, Number 6, pp. 1013-1022, December 1979.
11. M.K. Sain, P.J. Antsaklis, B.F. Wyman, R.R. Gejji, and J.L. Peczkowski, "Total Synthesis of Linear Multivariable Control Systems, Part I", Proceedings 1981 Joint Automatic Control Conference.
12. R.R. Gejji, "On the Total Synthesis Problem of Linear Multivariable Control", Ph.D. Thesis, University of Notre Dame, 1980.
13. J.B. Cruz, Jr. and W.R. Perkins, "A New Approach to the Sensitivity Problem in Multivariable Feedback Design", IEEE Transactions on Automatic Control, Volume 9, pp. 216-223, July 1964.
14. J.B. Cruz, Jr., J.S. Freudenberg, and D.P. Looze, "A Relationship between Sensitivity and Stability of Multivariable Feedback Systems", IEEE Transactions on Automatic Control, Volume 26, Number 1, pp. 66-74, February 1981.
15. M.K. Sain, A. Ma, and D. Perkins, "Sensitivity Issues in Decoupled Control System Design", Proceedings Twelfth Southeastern Symposium on System Theory, pp. 25-29, May 1980.
16. M.K. Sain, "Matrix Identities", IEEE Transactions on Automatic Control, Volume 15, Number 2, p. 282, April 1970.
17. M.K. Sain and A. Ma, "Multivariable Synthesis with Reduced Comparison Sensitivity", Proceedings 1980 Joint Automatic Control Conference, Volume 1, Part WP8-B.
18. M.K. Sain, R.M. Schafer, and K.P. Dudek, "An Application of Total Synthesis to Robust Coupled Design", Proceedings Eighteenth Annual Allerton Conference on Communication, Control, and Computing, pp. 386-395, October 1980.

D-7

AN APPLICATION OF TENSOR IDEAS TO NONLINEAR MODELING OF A TURBOFAN JET ENGINE*

Thomas A. Klingler, Stephen Yurkovich, and Michael K. Sain
Department of Electrical Engineering
University of Notre Dame
Notre Dame, IN 46556

ABSTRACT

The design of nonlinear control systems for gas turbine engines frequently involves a combination of feedforward scheduling and local, dynamic feedback regulation on the desired final responses. Scheduling the feedback dynamics, or adding dynamical tuning to the feedforward schedules, creates a class of nonlinear dynamical controllers which is often classical in nature, as for example the first few terms in a series expansion. Tensor algebra provides a universal setting within which to parameterize such representations. Moreover, if such models are available for the engine itself, then there exist feedback control theories based upon them. In this paper, a model of tensor type is computed and tested locally on a digital simulation of the QCSE gas turbine engine.

INTRODUCTION

The use of local, linear dynamical models in control of gas turbine engines has received a great deal of attention in the last ten years. While the lion's share of control action for such engines tends to be the result of feedforward schedules, the local feedback applied to reach desired response points along these schedules is of great importance. In particular, careful choice of the local controller dynamics can achieve quick, smooth settling, without undesirable overshoots in crucial variables, as for example temperatures in the vicinity of turbines.

Such local dynamics are frequently scheduled also, as a function of a smoothly changing physical variable, such as a speed. When this is accomplished, the local control dynamics become nonlinear in nature; and key examples can be viewed in terms of vector fields created by polynomic functions of state and control, or, more generally, in terms of power series. Tensor algebra provides a universal parameterization within which to represent such schemes. Moreover, there exist feedback theories designed to accommodate plant models based upon such representations.

Accordingly, there is interest in application studies of tensor models. In this paper, we provide one such study, on a QCSE engine simulator.

For background, we consider briefly some tensor ideas and issues associated with nonlinear modeling. A short description of the QCSE engine itself is given, and then the application is discussed in detail.

TENSOR IDEAS

We begin our discussion with a brief description of the tools to be employed in the nonlinear model formulation. Let V and W be real vector spaces and let $(\otimes^r V, \otimes^r)$ be a tensor product for r copies of V, where each integer r is two or greater. For convenience we define $\otimes^1 V = V$ and $\otimes^0 = \mathbb{R}$. Then by the unique factorization property of the tensor product [1], for every r-linear mapping

$$\psi : V^r \to W \tag{1}$$

there exists a unique linear mapping

*This work was supported by the National Aeronautics and Space Administration under Grant NSG 3048.

$$\lambda : \otimes^r V \to W \tag{2}$$

such that $\psi = \lambda \circ \otimes^r$ for the r-linear mapping $\otimes^r : V^r \to \otimes^r V$. If $L(V^r;W)$ denotes the real vector space of r-linear mappings from V^r to W, and $L(\otimes^r V,W)$ denotes the real vector space of linear mappings from $\otimes^r V$ to W, the implication is that

$$L(\otimes^r V,W) \to L(V^r;W) \tag{3}$$

is a vector space isomorphism.

These notions may be tied to the discussion of abstract derivatives and the calculus on normed vector spaces. As an introduction, equip V and W with norms and let Z be open in V. Suppose that the mapping $f : Z \to W$ is differentiable at a point p in Z, in the usual sense (see, for example, [2,3]). We denote the derivative of $f : Z \to W$ at p by

$$(Df)(p) : V \to W, \tag{4}$$

and note that

$$Df : Z \to L(V,W); \tag{5}$$

that is, the derivative mapping (4) is a linear mapping, an element of $L(V,W)$. The notion extends for higher derivatives, defined in a recursive fashion as

$$(D^r f)(p) = (D(D^{r-1}f))(p) \tag{6}$$

provided the (r-1)st derivative is differentiable, since

$$\begin{aligned} D^2 f(p) &\in L(V,L(V,W)), \\ D^3 f(p) &\in L(V,L(V,L(V,W))), \end{aligned} \tag{7}$$

and so on. It can be shown that there exist isomorphisms

$$\begin{aligned} L(V^2;W) &\to L(V,L(V,W)), \\ L(V^3;W) &\to L(V,L(V,L(V,W))), \\ &\vdots \qquad\qquad \vdots \end{aligned} \tag{8}$$

so that $D^r f(p)$ can be regarded as an r-linear mapping $V^r \to W$, up to isomorphism. We suppress this isomorphism and think of $D^r f(p)$ as just such a mapping.

It is now straightforward to establish a connection with the tensor ideas expressed above. The r-linear mapping (1), for our purposes given by $D^r f(p) : V^r \to W$, can be composed from a linear mapping $\otimes^r V \to W$ and the universal r-linear tensor product mapping $\otimes^r : V^r \to \otimes^r V$. This connection, facilitated by the isomorphisms (3) and (8), is explored in the section following for the case of dynamical system representation.

MODEL STRUCTURE

Suppose that the dynamical system which we wish to model is described by the nonlinear ordinary differential equation

$$\dot{x} = f(x,u) \tag{9}$$

for $f : X \times U \to X$, where X and U are normed real vector spaces of states and controls, respectively. Using the notation of the preceding section, let $(\bar{x},\bar{u})$ be a fixed point in Z open in $X \times U$, and suppose that $f : X \times U \to X$ is of sufficient smoothness on Z. Then, formally,

$$f(\bar{x} + x, \bar{u} + u) = \sum_{k=0}^{\infty} \frac{1}{k!} (D^k f)(\bar{x},\bar{u})(x,u)^{(k)}, \tag{10}$$

where $(x,u)^{(k)} = ((x,u),(x,u),\ldots,(x,u))$ k times. We note that the series in (10) could be represented by a finite number of terms together with a remainder term in a standard application of Taylor's formula. Indeed, for practical applications, such as the present paper, a truncation approximation of (10) is considered. Unfortunately, limitations of space forbid discussions concerning such issues as existence of solutions to (9) or questions related to the convergence of (10).

We now make use of the fact that $(D^k f)(\bar{x},\bar{u})$ in (10) is a k-linear mapping, which suggests a means of applying tensor product ideas. Let $(\otimes^k(X \times U), \otimes^k)$ be a tensor product for k copies of $X \times U$. Then we may make the unique factorization

$$D^k f(\bar{x},\bar{u}) = L_k(\bar{x},\bar{u}) \circ \otimes^k, \tag{11}$$

where $L_k(\bar{x},\bar{u}) : \otimes^k(X \times U) \to X$ is a linear mapping. Now let the notation $(x,u)^k$ denote the k-fold tensor product of (x,u) with itself. Then upon substitution of (11) into (10) we have

$$f(\bar{x}+x,\bar{u}+u) = \sum_{k=0}^{\infty} \frac{1}{k!} L_k(\bar{x},\bar{u})(x,u)^k. \tag{12}$$

It is shown in [4] that the individual terms of (12) may be rewritten as, for example,

$$\frac{1}{2!} L_2(\bar{x},\bar{u})(x,u)^2 = L_{20}(\bar{x},\bar{u})x\otimes x + L_{11}(\bar{x},\bar{u})x\otimes u + L_{02}(\bar{x},\bar{u})u\otimes u. \tag{13}$$

In this way the formal expansion (10) becomes

$$f(\bar{x}+x,\bar{u}+u) = \sum_{i=0}^{\infty} \sum_{j=0}^{\infty} L_{ij}(\bar{x},\bar{u})x^i \otimes u^j, \tag{14}$$

which forms the structure for the nonlinear model.

As alluded to earlier, in practice the series (14) may be truncated in an approximation of (9). The task in the model building scheme, then, is to identify the parameters contained in matrix representations of the $L_{ij}(\bar{x},\bar{u})$, once ordered bases for the spaces in question are chosen. For more discussion of the details involved in such an exercise, the reader may wish to consult [5,6].

QCSE ENGINE

The intent of this section is to supply a brief introduction to NASA's QCSEE ("Quixie")---Quiet, Clean, Shorthaul Experimental Engine---prior to discussing an application of the modeling methodology described above. The QCSE engine is an advanced turbofan designed specifically for powered-lift, short-haul aircraft, and combines several innovative concepts to achieve optimal efficiency with quiet, clean operation [7,8]. The eight physical quantities chosen as state variables for the system include two fan speeds, four pressures, and two temperatures. A digital controller is incorporated into the overall design [9], and the control inputs are the main burner fuel flow, the fan pitch angle, and the fan nozzle area.

For the modeling exercises of this study, a detailed digital simulation developed for the QCSE engine [10] is employed. The primary input variable to be manipulated in the digital program is the percentage power demand, PWRX, for testing performance over the entire envelope of operation. Values of individual internal variables are extracted and inserted at various locations within the program.

APPLICATION

Attention in the following discussion will center around the formulation of a reduced order four-state, three-control analytical model. The engine states chosen are the combustor discharge pressure (P4GS), the core nozzle total pressure (P8GS), and the rotor dynamics in the form of fan speed (NL), and compressor speed (NH). All three engine control inputs are employed, namely, the main burner fuel flow (WFM), the exhaust nozzle area (A18) and the fan pitch angle (BETAF).

Appropriate engine operation for the model identification involves opening the loop by deactiviting the controller and independently inserting the individual control inputs. In this strategy, nonlinearities of the plant exist---which might otherwise be less noticeable had the controller been present in the loop. A further explanation of this strategy as well as an alternate one are presented in [11]. An important point to note is that, in the open loop situation, the choice of input control signals is critical. This is due to the fact that the engine itself has certain physical limits, which in turn have been incorporated into the simulator. In reality, exceeding these limits could cause severe damage to the engine, an example of which is turbine melt down.

To aid in the selection of input signals, a family of parametric plots have been constructed using QCSEE steady state data from idle (62.5% PWRX) to maximum power (100% PWRX). Figure 1 contains an example of one such steady state plot. From these plots a set of acceptable input signals can be selected. Acceptable state perturbations can be selected in a similar

fashion. Another important feature of these steady state plots is that they suggest regions of nonlinearity. From Figure 1 it appears that in the locality of 92% power demand the engine is nonlinear due to the abrupt changes in exhaust nozzle area and fan pitch angle. With this in mind, we shall establish 92% as the operating point of the present study. Model formulations at other operating points are currently under investigation.

The following is an overview of the identification procedure. The QCSEE simulator is run, closed loop, with a 92% power demand for ten seconds to settle all transients. This produces the equilibrium value $(\bar{x},\bar{u})$, where $\bar{x}$ is a four-tuple and $\bar{u}$ is a three-tuple. The initial conditions thus generated form the point of expansion for the series truncation approximation in the model formulation. Within the digital simulation program the controller is disconnected by setting the control derivatives to zero. From the steady state plots a point $(\hat{x},\hat{u})$ is chosen on the engine operating line at 93% power demand. The state variables are perturbed x from their equilibrium values where

$$x = \hat{x} - \bar{x}.$$

Furthermore, the control variables are manipulated so that a cosinusoidal input of amplitude a is inserted, where a is a three-tuple given by the expression

$$a = \hat{u} - \bar{u}.$$

The observed states and inputs are sampled over a six second interval; 100 samples are evenly spaced at .06 seconds, and the difference between these values and the corresponding equilibrium values, together with the ordered monomials from the tensor product terms (see [5]) comprise one of two blocks of data necessary for the identification. The second block of data consists of the state derivative values which are extracted directly from the simulator at the given sample rate. Through use of these data blocks, the parameters contained in matrix representations of the $L_{ij}(\bar{x},\bar{u})$ can be identified via a least squares minimization technique.

Using the above procedure, two models have been identified: a second-degree nonlinear model, and a first-degree linear model. The linear model has been identified for use in comparison studies. The second-degree approximation keeps second degree tensor products which are associated with quadratic terms. Accordingly, such a nonlinear model is expected to outperform the linear model in a region about the point of expansion.

A simple error comparison criterion is used in testing the performance of the nonlinear model versus that of the linear model. Let ε_i^N denote the absolute maximum error in the nonlinear model solution, as compared to the true simulation solution, over the time range of simulation for the ith state variable. Similarly, we define ε_i^L for the linear model error. Then ε_i is the comparison $\varepsilon_i^N - \varepsilon_i^L$. Thus, if ε_i is negative, the nonlinear model has exhibited a smaller maximum absolute error in the ith state, and in that sense has outperformed the linear model. Table 1 contains a list of the state variables, their corresponding QCSEE variable name, their unit of measure, as well as their corresponding state notation x_i. Samples of the error comparison for various initial conditions, input amplitudes and frequencies are presented in Table 2. All input frequencies are in Hertz.

The error criterion in Table 2 clearly indicates that the nonlinear model outperforms the linear model in a region about the equilibrium point; however, there exists a better method for revealing model performance, namely, trajectory comparison. Consequently, a representative number of comparative solution plots have been included in Figures 2-10. Figure 2 offers a simulation of pressure P8GS for a step response, whereas Figures 3-4 illustrate P8GS and NL respectively for the frequency set $\omega = (.25, 0., .5)$. A simulation of P4GS is shown in Figure 5 for an excursion away from the typical engine line of operation, and likewise Figure 6 depicts NH. Figures 7-8 illustrate the speeds NL and NH for a 1% amplitude control signal, and finally P4GS and NL are seen in Figures 9-10 with initial conditions of approximately 1%.

COMPUTING ENVIRONMENT

The software package, developed using the extensive capabilities of the IBM and DEC Command Procedure Languages and the strengths of FORTRAN and SPEAKEZY, is divided into two segments and tailored to utilize effectively existent computer hardware. The interactive nonlinear model generation segment is implemented on a Time Sharing Option (TSO) of the IBM 370-168 computer system, where the memory dependent, and highly computational routines of the package can benefit from use of the virtual memory and floating point hardware.

Once a nonlinear model is identified on the IBM 370-168, it is transferred to a DEC PDP 11/60, where, in an interative environment, it can be analyzed and compared to a linear model and the true solution. This is accomplished through use of the nonlinear simulation segment

of the package. In this manner, the routines can use both the graphics capabilities of a Tektronix 4025 video terminal, and a Versatec electrostatic printer/plotter for the display of data and comparative trajectories.

CONCLUSIONS

This paper has presented an application illustration of tensor modeling to a digital simulation of the QCSE engine. For plant modeling prior to feedback control, or for representing scheduled controllers over an operating line, the tensor algebra offers a universal parameterization which is helpful in conceptualization and identification. The case studied in this paper offers support to these conclusions. Further work is in progress.

ACKNOWLEDGEMENT

The authors are pleased to thank Mr. Daniel Bugajski for his assistance in certain of the computer studies associated with these results. Dan is a senior in the Department of Electrical Engineering.

REFERENCES

1. W.H. Greub, Multilinear Algebra. New York: Springer-Verlag, 1967.
2. J. Dieudonne, Foundations of Modern Analysis. New York: Academic Press, 1960.
3. S. Lang, Analysis. Vols. I and II, Reading: Addison-Wesley, 1969.
4. M. Sain and S. Yurkovich, "Controller Scheduling: A Possible Algebraic Viewpoint", Proc. 1982 American Control Conf., June 14-16, 1982, to appear.
5. S. Yurkovich and M.K. Sain, "A Tensor Approach to Modeling of Nonhomogeneous Nonlinear Systems", Proc. Eighteenth Allerton Conf. on Communication, Control, and Computing, October 1980, pp. 604-613.
6. S. Yurkovich, "Application of Tensor Ideas to Nonlinear Modeling and Control", M.S. Thesis, Electrical Engineering Dept., Univ. of Notre Dame, Notre Dame, Indiana, Jan. 1981.
7. C.E. Wise, "Turbofan of the Future", Machine Design, Aug. 22, 1974, pp. 20-25.
8. "Quiet Clean Short-haul Experimental Engine (QCSEE) Under-the-Wing (UTW) Simulation Report", NASA CR-134914, July 1977.
9. "Quiet Clean Short-haul Experimental Engine (QCSEE) Under-the-Wing (UTW) Engine Digital Control System Design Report", NASA CR-134920, January 1978.
10. J.R. Mihaloew, "A Nonlinear Propulsion System Simulation Technique for Piloted Simulators", Proc. Twelfth Pittsburgh Conf. on Modeling and Simulation, April 1981, pp. 1407-1417.
11. S. Yurkovich, T.A. Klingler, and M.K. Sain, "Tensor Ideas for Nonlinear Modeling of a Turbofan Jet Engine: Preliminary Studies", Proc. Twelfth Pittsburgh Conf. on Modeling and Simulation, April 1981, pp. 1423-1427.

TABLE 1 Variable Ledger for Figures 2-10

○ : True Engine Response	∆ : Linear Model Response	* : Nonlinear Model Response	
x_1: P4GS (psi) x_2: P8GS (psi)	x_3: NL (rpm) x_4: NH (rpm)	u_1: WFM (lb_m/hr) u_2: A18 (in^2)	u_3: BETAF (degrees)

TABLE 2 Comparison Studies

Initial State Conditions				Input Amplitudes			Input Freq.			Error			
x_1	x_2	x_3	x_4	a_1	a_2	a_3	ϕ_1	ϕ_2	ϕ_3	ε_1	ε_2	ε_3	ε_4
0.000	0.000	0.000	0.000	18.92	0.000	-0.111	0.0	0.0	0.0	-1.040	-0.018	-10.40	-14.00
0.000	0.000	0.000	0.000	18.92	0.000	-0.111	0.3	0.0	0.5	-0.668	-0.012	- 7.04	- 8.49
0.000	0.000	0.000	0.000	74.29	-21.20	-0.239	1.9	0.9	1.2	-0.259	-0.004	- 4.62	- 8.11
0.010	0.001	0.010	0.100	17.00	-2.000	-0.050	0.0	0.0	0.0	-0.947	-0.017	- 7.48	-11.50
0.010	0.001	0.010	0.100	18.92	0.000	-0.111	0.0	0.0	0.0	-1.070	-0.019	-10.60	-14.20
0.010	0.001	0.010	0.100	19.00	-2.000	-0.159	1.0	0.8	0.5	-0.198	-0.003	- 2.49	- 3.16
0.010	0.001	0.010	0.500	18.92	0.000	-0.111	0.3	0.0	0.5	-0.642	-0.012	- 6.88	- 8.22
0.010	0.001	-0.010	0.500	40.00	-5.000	-0.150	1.5	1.0	1.3	-0.354	-0.006	- 1.96	- 6.69
0.010	-0.001	0.010	-0.750	-18.80	0.000	0.115	2.0	0.0	1.5	-0.307	-0.005	- 1.71	- 4.89
-0.010	-0.001	-0.010	-0.750	-37.46	0.000	0.228	1.9	0.0	1.3	-0.202	-0.004	- 1.59	- 3.42
-0.010	0.001	-0.010	0.750	74.29	-21.20	-0.239	1.9	1.1	1.3	-0.293	-0.005	- 5.89	- 6.55
0.075	0.001	20.00	10.00	-18.80	0.000	0.000	1.9	0.0	0.0	-0.343	-0.007	- 3.36	- 3.43
0.110	0.001	-20.00	12.00	55.78	-14.03	-0.198	1.8	1.1	1.4	-0.447	-0.008	- 4.98	- 5.51
0.120	0.002	50.00	10.00	37.35	-6.830	-0.159	2.1	1.0	1.3	-0.435	-0.008	- 5.06	- 4.91
0.100	0.002	75.00	5.00	54.00	-12.00	-0.200	1.8	1.0	1.3	-0.401	-0.007	- 9.80	- 8.80

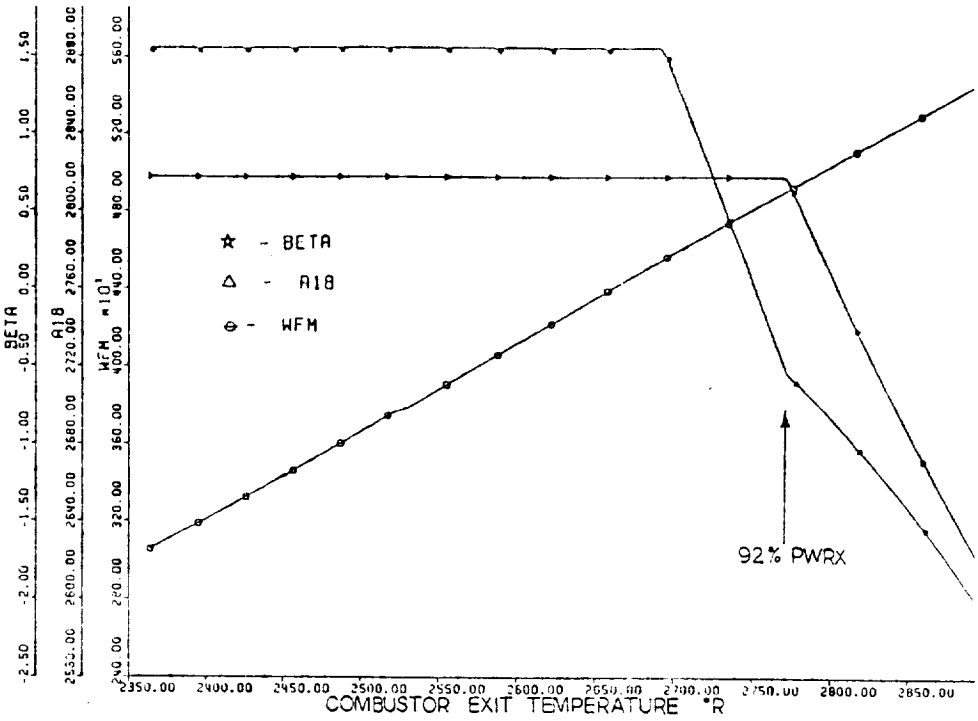

Figure 1 Example Steady State Response: Parameterization with PWRX

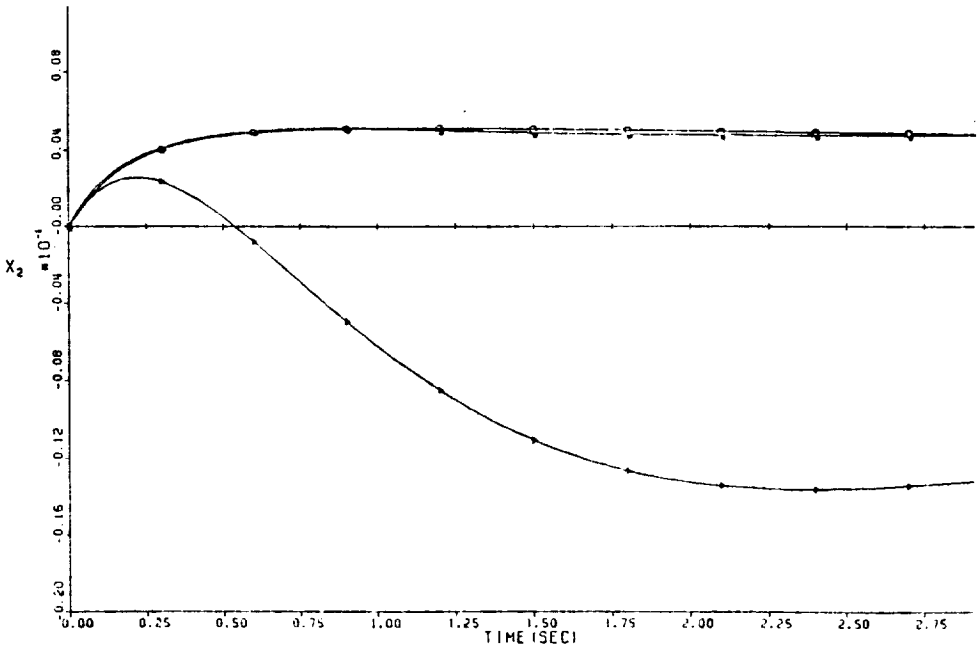

Figure 2 Table 2, Line 1

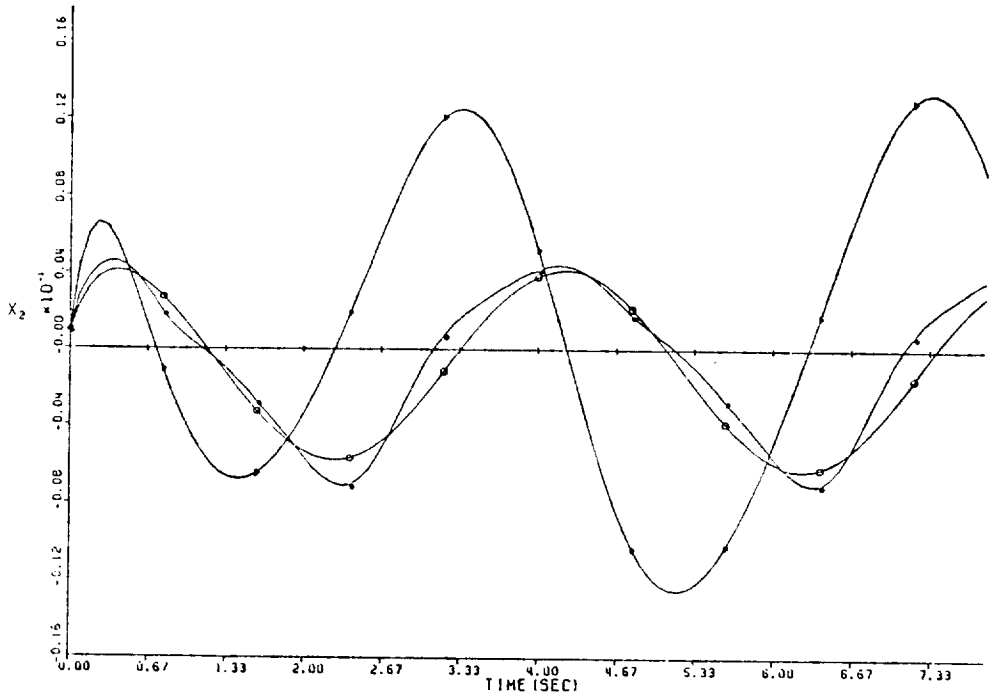

Figure 3 Table 2, Line 7

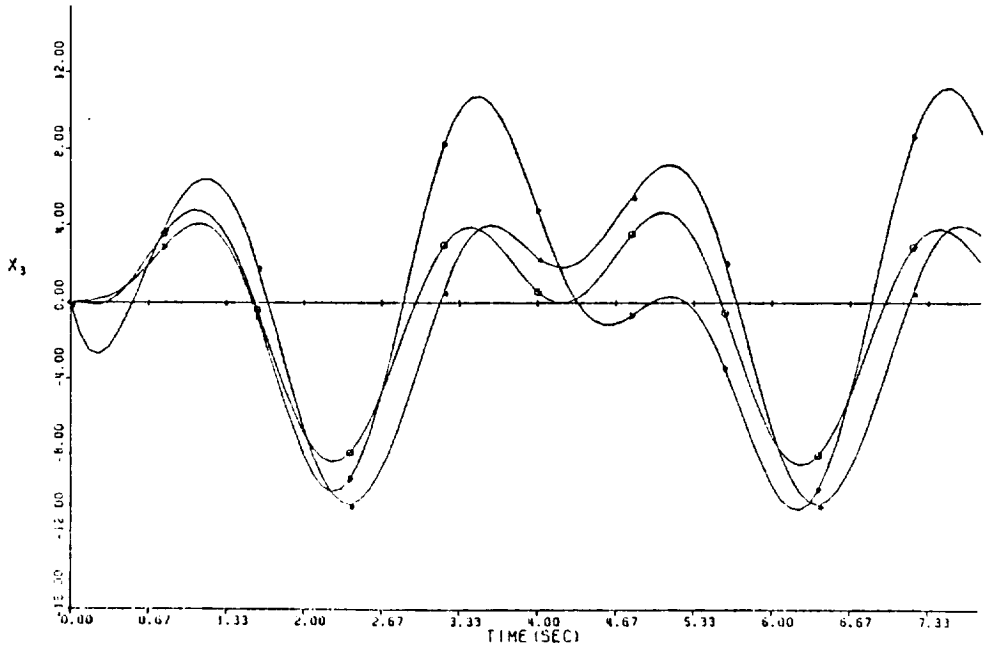

Figure 4 Table 2, Line 7

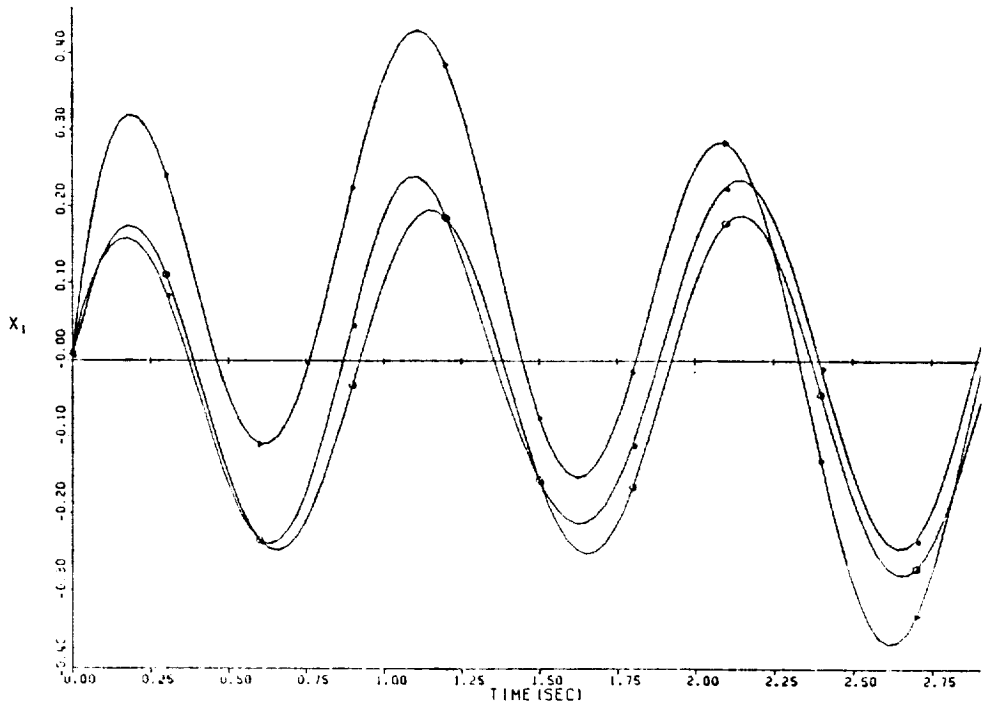

Figure 5 Table 2, Line 6

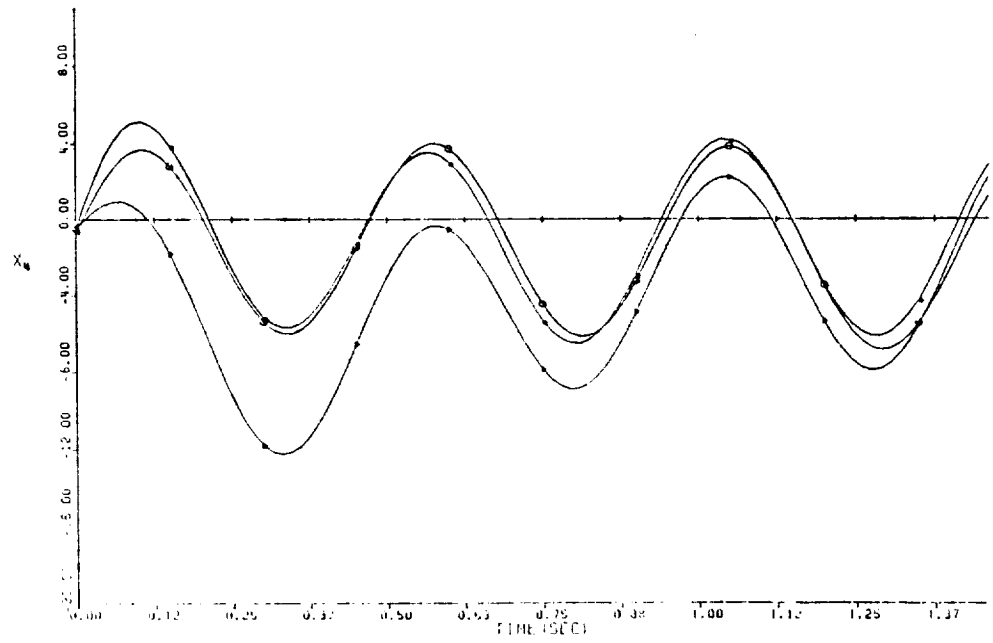

Figure 6 Off the Operating Line at 1/2%

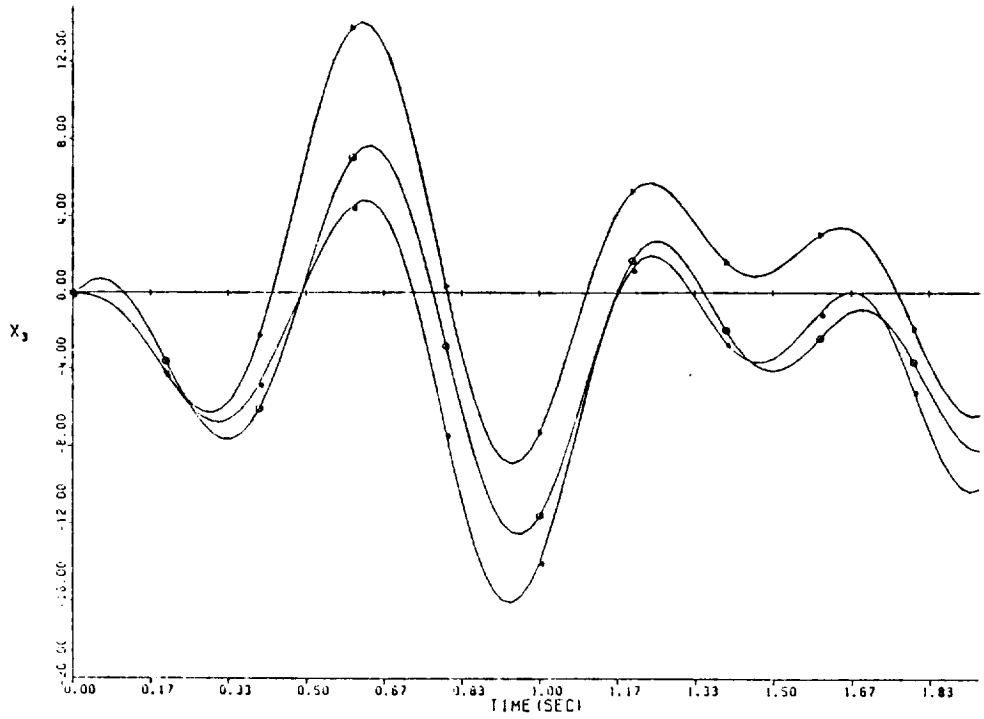

Figure 7 Table 2, Line 11

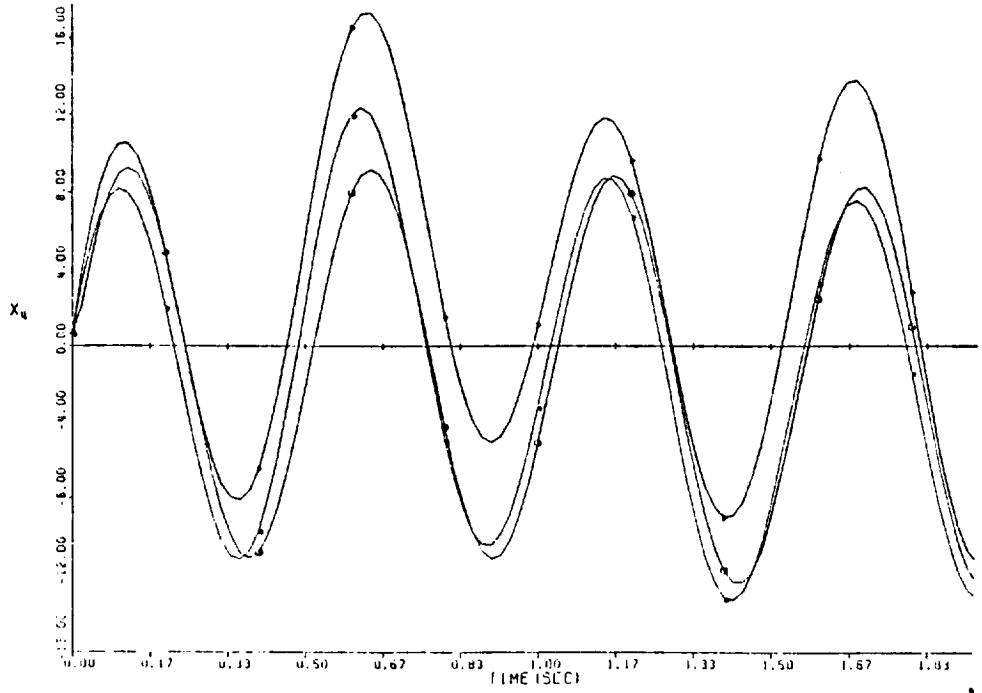

Figure 8 Table 2, Line 11

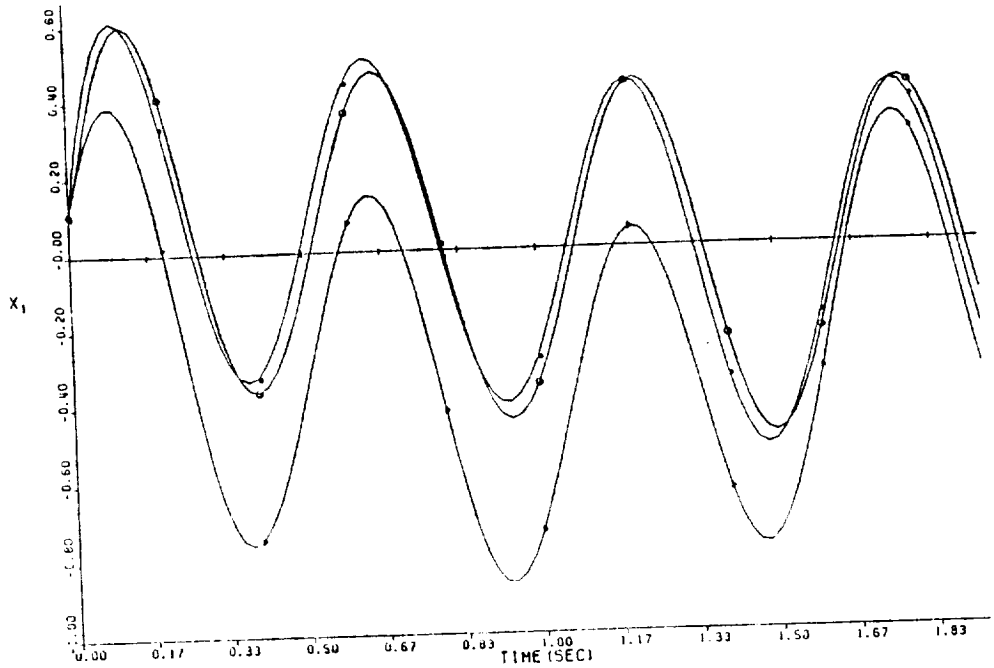

Figure 9 Table 2, Line 13

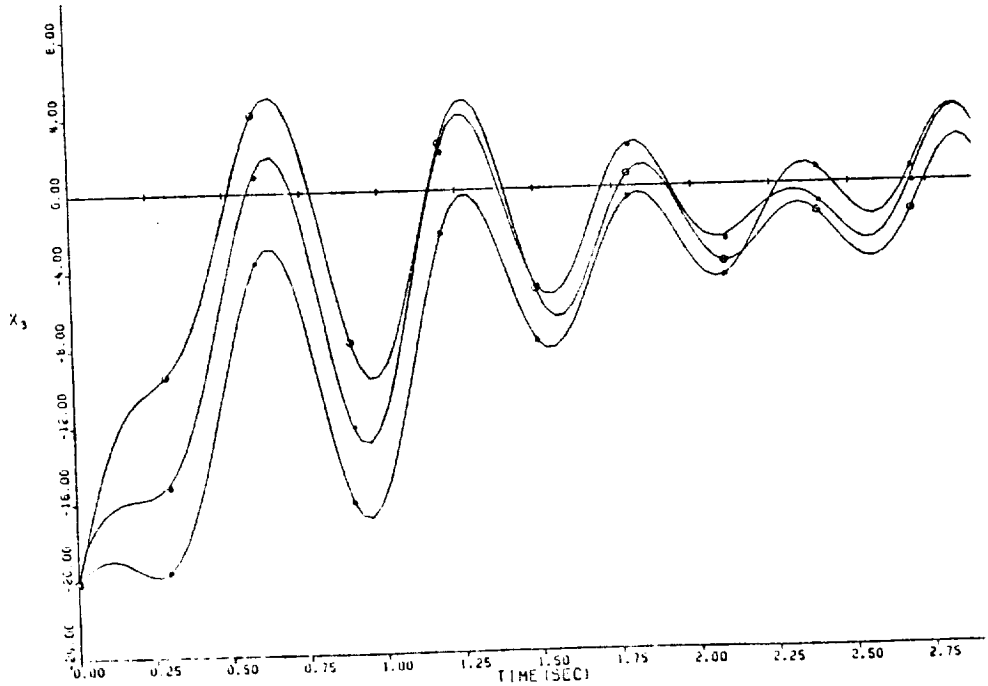

Figure 10 Table 2, Line 13

NONLINEAR MULTIVARIABLE DESIGN BY TOTAL SYNTHESIS

Michael K. Sain
Electrical Engineering Department
University of Notre Dame
Notre Dame, Indiana 46556

Joseph L. Peczkowski
Energy Controls Division
The Bendix Corporation
South Bend, Indiana 46620

Abstract

In a recent publication [1], Bristol has presented an application theorist's view of process control design as it really exists and has challenged others to do likewise for areas within their own purview. This paper continues just such an effort [2,3,4] by the authors within the domain of nonlinear multivariable control of gas turbine engines. Under examination is the fundamental notion that linear controller descriptions, obtained from local actions of nonlinear objects, may be recombined to produce global nonlinear control action, with sufficient integrity to effect closed loop design. Total Synthesis refers to a top-down strategy of Nominal Design and Feedback Synthesis. This paper extends the study of the Nominal Design Problem (NDP) to nonlinear cases, and presents a new case study of robust feedback synthesis for gas turbine control design.

Introduction

The idea of describing families of curves by their tangents has a rich history in mathematics, in science, and in engineering. Consider, by way of example, the ubiquitous differential equation. More generally, the notions of manifold, tangent spaces, and geometry are very much a part of modern multivariable systems research.

Not surprisingly, the same notions permeate a great deal of control design in various applications. Intuitively, one linearizes a nonlinear dynamical system at a sequence of points along lines of operation considered desirable by the plant manufacturer. A suitably rich sequence of points can lead to a correspondingly valuable sequence of linear multivariable systems describing local gains and transient behavior of the plant along these operating lines. From such a sequence of systems one may construct a sequence of controllers which effect desirable local motions along the lines. Smooth global control is then a function of appropriately scheduled feedforward and feedback requests, as well as scheduling of local controller gains and dynamics which determine the approach to such requests.

Bristol [1] believes that experience and intuition are the crucial requisites for efficacious design, and that the best of design-flavored control theories can serve only as an introduction to the path followed by engineers with experience. Accordingly, Bristol also suggests that one should seek theories which extend one's intuition and which do not presuppose its replacement.

The local control theory employed by the authors in this paper was proposed [5] in 1979 by Peczkowski, Sain, and Leake, with just such a view in mind. Conceptually, the method is founded upon the idea of a Nominal Design Problem (NDP), which is independent of controller structure and which is intended as the first step in a top-down design procedure. A thorough discussion is given in [6]. This paper treats an extension of NDP to the nonlinear case. Completion of step one in NDP is followed by a second step, called the Feedback Synthesis Problem (FSP) [6]. A case study of this step may be found in [7], which also contains a full list of references. An alliance of NDP with FSP is called a Total Synthesis Problem (TSP). The case study following in this paper is part of a continuing assault of FSP for the nonlinear case, from the view of design practice in gas turbine engine control.

The section following provides mathematical preliminaries which precede a discussion of NDP for the nonlinear plant. Beyond that, nonlinear nominal design is defined and characterized, after which the paper progresses to design of local controllers for a turbojet case, and the scheduling of these local controls into a global control.

Mathematical Preliminaries

In this section, we consider a bijection $b : S \to T$ from a set S onto a set T, with T admitting the structure of an F-vector space. As a result of the fact that b is bijective, each vector t in T can be represented uniquely in the manner $b(s)$ for an s in S; and each element s in S can be represented uniquely by $b^{-1}(t)$ for a t in T. Here, we have denoted the inverse of b in the usual way, $b^{-1} : T \to S$.

The commutative group structure $(T, +, 0)$ on our F-vector space T can be used, together with b, to induce a commutative group structure $(S, \boxdot, e)$ on the set S. The first step in this construction is to define the binary operation $\boxdot : S \times S \to S$. We do this as follows. Let $(s_1, s_2) \in S \times S$; then

$$s_1 \boxdot s_2 = b^{-1}(b(s_1) + b(s_2)) ,$$

where the binary operation $+$ in the right member is that on $T \times T$ to T. Associativity of the new operation can be demonstrated. Indeed,

$$(s_1 \boxdot s_2) \boxdot s_3 = b^{-1}(b \circ b^{-1}(bs_1 + bs_2) + bs_3)$$

$$= b^{-1}((bs_1 + bs_2) + bs_3)$$
$$= b^{-1}(bs_1 + (bs_2 + bs_3))$$
$$= b^{-1}(bs_1 + b \circ b^{-1}(bs_2 + bs_3))$$
$$= s_1 \square (s_2 \square s_3) .$$

The unit e can be chosen to be $b^{-1}(0)$, as is apparent from the calculation

$$s \square b^{-1}(0) = b^{-1}(bs + b \circ b^{-1}(0))$$
$$= b^{-1}(bs + 0)$$
$$= s .$$

For commutativity of the operation, we exhibit the steps

$$s_1 \square s_2 = b^{-1}(b(s_1) + b(s_2))$$
$$= b^{-1}(b(s_2) + b(s_1))$$
$$= s_2 \square s_1 .$$

Finally, for an element s in S, we define an additive inverse $\hat{s}$ in S to be $b^{-1}(-b(s))$, and verify it by

$$s \square \hat{s} = b^{-1}(bs + b \circ b^{-1}(-b(s)))$$
$$= b^{-1}(0)$$
$$= e ,$$

as desired. Accordingly, $(S, \square, b^{-1}(0))$ is a commutative group.

Next, we can use the scalar multiplication operation $F \times T \to T$ on the F-vector space T to induce a scalar multiplication $F \times S \to S$. To do this, we define the scalar multiple fs of s by f to be

$$fs = b^{-1}(fb(s)) ,$$

for a pair (f,s) in $F \times X$. Notice that

$$f(s_1 \square s_2) = b^{-1}(fb(s_1 \square s_2))$$
$$= b^{-1}(fb \circ b^{-1}(bs_1 + bs_2))$$
$$= b^{-1}(fbs_1 + fbs_2)$$
$$= b^{-1}(b \circ b^{-1}fbs_1 + b \circ b^{-1}fbs_2)$$
$$= b^{-1}(b(fs_1) + b(fs_2))$$
$$= (fs_1) \square (fs_2) .$$

Moreover, we can also see that

$$(f_1 + f_2)s = b^{-1}((f_1 + f_2)b(s))$$
$$= b^{-1}(f_1b(s) + f_2b(s))$$
$$= b^{-1}(b \circ b^{-1}f_1bs + b \circ b^{-1}f_2bs)$$
$$= b^{-1}(b(f_1s) + b(f_2s))$$
$$= (f_1s) \square (f_2s) .$$

Next, observe the property

$$(f_1f_2)s = b^{-1}((f_1f_2)bs)$$
$$= b^{-1}(f_1(f_2bs))$$
$$= b^{-1}(f_1(b \circ b^{-1}f_2bs))$$
$$= b^{-1}(f_1b(f_2s))$$
$$= f_1(f_2s) .$$

Finally,

$$1s = b^{-1}(1b(s))$$
$$= b^{-1}(b(s))$$
$$= s .$$

Thus, $(S, \square, b^{-1}(0))$ has been developed into an F-vector space S. We summarize this fact as a theorem.

Theorem 1.

Let $b : S \to T$ be a bijection onto the F-vector space $(T, +, 0)$. Then $(S, \square, b^{-1}(0))$ is also an F-vector space, with addition

$$s_1 \square s_2 = b^{-1}(b(s_1) + b(s_2)) ,$$

with additive inverse

$$b^{-1}(-b(s))$$

for a vector s, and with scalar multiplication

$$fs = b^{-1}(fb(s)) .$$

Remark

Frequently, S may be given as an F-vector space on a commutative group $(S, +, 0)$. Though the set S is common to these structures, the binary operations + and $\square$ are distinct, as well as the units 0 and $b^{-1}(0)$ and the scalar multiplications.

Relative to the induced space, the bijection and its inverse assume desirable properties.

Corollary 2.

Regarded as a function

$$b : (S, \square, b^{-1}(0)) \to (T, +, 0) ,$$

the bijection b is a morphism of F-vector spaces, as is its inverse

$$b^{-1} : (T, +, 0) \to (S, \square, b^{-1}(0)) .$$

Proof: We have only to examine the defining constructions

$$b(s_1 \square s_2) = b \circ b^{-1}(b(s_1) + b(s_2))$$
$$= b(s_1) + b(s_2) ;$$
$$b(fs) = b \circ b^{-1}(fb(s))$$
$$= fb(s) ;$$

moreover, for each t_i in T, we have a unique s_i in S such that $t_i = b(s_i)$; and so we have also

$$b^{-1}(t_1 + t_2) = b^{-1}(b(s_1) + b(s_2))$$
$$= b^{-1} \circ b(s_1 \square s_2)$$
$$= s_1 \square s_2$$
$$= (b^{-1}(t_1)) \square (b^{-1}(t_2)) ;$$
$$b^{-1}(ft) = b^{-1}(fb(s))$$
$$= fs$$
$$= fb^{-1}(t) .$$

Remark

If R is a ring with identity, then all the discussions above generalize to R-modules.

Next, denote by S^R the set of all functions from a set R to the F-vector space $(S, \square, e)$. Under pointwise conventions,

$$(g_1 \square g_2)(r) = (g_1(r)) \square (g_2(r)) ,$$
$$(fg)(r) = fg(r) ,$$

S^R becomes an F-vector space also [8], as does T^R under the corresponding operations induced from T.

The following section defines the NDP for nonlinear plants, and uses the properties above to characterize its structure.

Nonlinear NDP

The concept of a nonlinear NDP was outlined in [3] by the authors for functions on commutative groups. Here we extend the idea. Let R, U, and Y denote F-vector spaces of requests to the system, controls to the plant, and responses from the plant. It is useful to visualize these, for example, as function spaces, predicated perhaps on time sets. Let $p : U \to Y$ denote the plant. If the feedback action of the controller is well defined, then there will be a function $m : R \to U$ generating control actions from requests and a function $t : R \to Y$ describing plant responses to requests. These three functions must then be related by the equation

$$t = p \circ m ,$$

which is presented as a commutative diagram in Figure 1. The nonlinear Nominal Design Problem is to find pairs (m,t) in (U^R, Y^R) such that the diagram of Figure 1 commutes. As usual, we point out

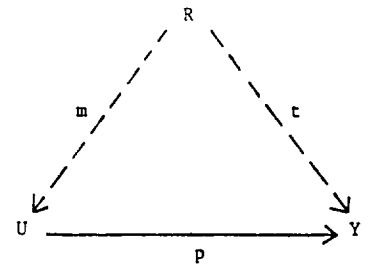

Figure 1. Nonlinear NDP.

that NDP is not a model matching problem, in which t would also be given and in which only m in Figure 1 would appear on a dashed line.

Now consider a pair (m_i,t_i) of solutions to NDP. Characterization of the set $\{(m_\alpha,t_\alpha)\}$ of all solutions to NDP is severely hindered by the fact that

$$p \circ (m_1 + m_2) \neq (p \circ m_1) + (p \circ m_2) .$$

With the ideas of the section preceding, however, this difficulty can be addressed.

Let $(Y, +, 0)$ denote the F-vector space of plant responses, and let $(R, +, 0)$ denote the given F-vector space of requests. If p is a bijection, we can develop on U the F-vector space structure $(U, \square, p^{-1}(0))$ of Theorem 1. Relative to this structure, p and $p^{-1} : Y \to U$ become$_R$ isomorphisms of F-vector spaces. Moreover, $(U^R, \square, e_{U^R})$ and $(T^R, +, 0)$ become F-vector spaces, with

$$e_{U^R}(r) = p^{-1}(0)$$

for all r in R; and $0(r) = 0$ in T for all r in R. We can then define the F-linear map $F : U^R \times T^R \to T^R$ by setting the action

$$F(m,t) = p \circ m - t .$$

This leads to the following result.

Theorem 3.

Let $p : U \to Y$ be a bijection onto the F-vector space $(Y, +, 0)$. Then a pair (m,t) is a solution to the nonlinear Nominal Design Problem if and only if

$$(m,t) \in \text{Ker } F .$$

Proof: The assertion is immediate. It may be worthwhile, however, to point out the F-vector product group structure on $U^R \times T^R$ defined by the operation

$$(m_1,t_1) * (m_2,t_2) = (m_1 \square m_2,\ t_1 + t_2) .$$

Remark

If one wished, he or she could assume vector space structure on U, and define a special binary operation $\square$ on $T \times T$ by $p(p^{-1}(t_1) + p^{-1}(t_2))$.

Remark

An Inverse nonlinear NDP, denoted INDP, can be defined from the equation

$$m = p^{-1} \circ t \ .$$

Remark

Suppose that p were only surjective. It follows that p induces natural equivalence classes on U; and a projection $\pi : U \to U/\equiv$ can be defined. Then one has the universal factorization

$$p = \bar{p} \circ \pi$$

for a unique $\bar{p} : U/\equiv \to \underline{Y}_1$ which is a bijection. The structure $(U/\equiv, \square, p^{-1}(0))$ can be developed, and NDP pursued again. Only equivalence classes of controls are determined.

The existence of plant inverses is of the first importance both in theory and in application design. In the next section, we examine briefly the turbojet engine model which will be used for our case study.

Nonlinear Turbojet Model

A nonlinear model of a simple turbojet engine is shown in Figure 2. It is representative, on a small scale, of the kind of nonlinear plant with which designers of turbine engines and turbine controls deal currently in practice. In essence, it is a computer simulation, typically constructed by engine manufacturers and provided to control manufacturers. The nonlinear turbojet model consists of three integrators, nine nonlinear functions, including five bi-variant functions, nine multipliers and dividers, and nine summing junctions. The model describes nonlinear dynamical and steady state relationships between three inputs: fuel flow, W_f, exhaust nozzle area, A_j, and turbine vane position, B, and six outputs: engine speed, N, turbine temperature, T4, engine thrust, FN, tailpipe pressure, P5, and two other outputs. We propose to think of the nonlinear simulation model as a nonlinear function p from a real vector space of control functions of time to a real vector space of plant response functions of time.

Locally, with appropriate technical assumptions, the nonlinear plant function can be approximated by a linear map $P : U \to Y$, in the neighborhood of a pair $(\bar{u},\bar{y})$ in the relation defined by p. When the plant function p is a linear map P, the transformation

$$P^{-1}(P(u_1) + P(u_2)) = u_1 + u_2 \ ,$$

for the usual vector space structure $(U, +, 0)$. Locally, then, the operation $\square : U \times U \to U$ can be replaced by $+ : U \times U \to U$.

Suppose next that the plant has an internal representation

$$\dot{x} = f(x,u) \quad , \quad y = g(x,u) \ ,$$

with appropriate smoothness conditions associated with the functions $f : X \times U \to X$ and $g : X \times U \to Y$. Let $\bar{x}$ be such that

$$f(\bar{x},\bar{u}) = 0 \ ,$$

and define

$$\Delta y = y - g(\bar{x},\bar{u}) \quad , \quad \Delta u = u - \bar{u} \ .$$

Then p may be assumed to have a local representation given by an impulse response operator

$$C\, e^{At} B + D$$

or by its transform, say $P(s)$, in the usual way.

The idea is to use these $P(s)$ to determine corresponding local descriptions of the parts of the controller, and then to schedule these parts together into a global whole.

Remark

In addition to the case study which follows, an accompanying paper [9] discusses some additional conceptual issues associated with such schedules.

For the following case study, three outputs have been selected for control: engine speed, N, turbine temperature, T4, and engine thrust, FN. The nonlinear engine model was identified locally at five conditions corresponding to 70%, 80%, 90%, 100%, and 110% speed levels. The engine input is given by

$$u = (W_f, A_j, B) \ ,$$

and the selected engine response vector is

$$y = (N, T4, FN) \ .$$

By way of illustration, at 100% speed conditions, the plant transfer function $P(s)$ and its inverse were found to be:

$$P(s) = \frac{\begin{bmatrix} 5.4(.01s+1) & 56.1(.01s+1) & -2704(.01s+1) \\ .13(1.5s+1) & -2.7(.50s+1)(.01s+1) & 336(.31s+1) \\ 2.4(.29s+1) & 68.3(.42s+1)(.01s+1) & 951(.01s+1) \end{bmatrix}}{(.50s+1)(.01s+1)}$$

$$P(s)^{-1} = \frac{\begin{bmatrix} .18(.23s+1)(.01s+1) & 1.7(.01s+1)(.007s+1) & -.083(.01s+1) \\ -.005(-.2s+1) & -.08(.01s+1) & .015(.01s+1) \\ -.0001(.74s+1)(.01s+1) & .0017(.01s+1)(.013s+1) & .00015(.01s+1) \end{bmatrix}}{(.009s+1)}$$

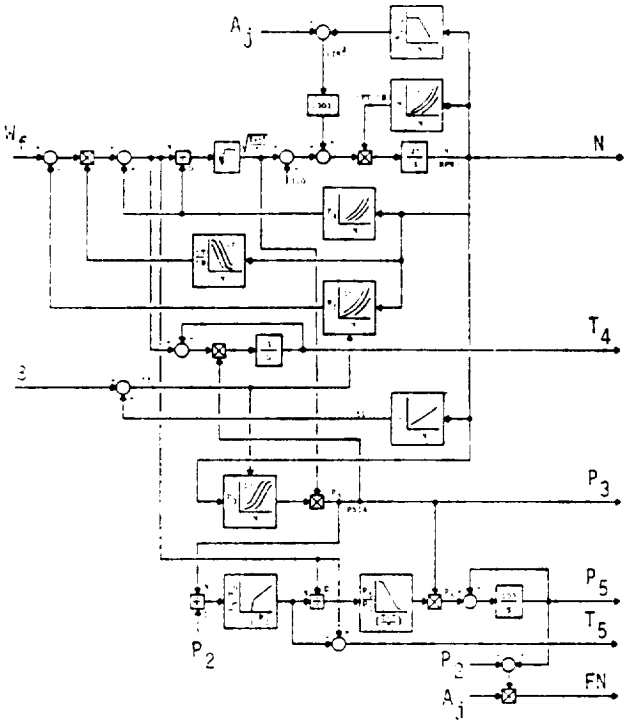

Figure 2. Nonlinear Turbojet Model.

Multivariable Design

A nonlinear multivariable design method, based on Total Synthesis ideas, is described and illustrated. Features of the design method include:

1. an input-output viewpoint;
2. design for desired response performance; control performance, and sensitivity;
3. a relatively general system structure;
4. a systematic way to synthesize the nonlinear controller.

Starting point for the design procedure is a nonlinear plant model or simulation such as the turbojet engine model shown in Figure 2. First, it is necessary to establish the desired steady state operating conditions of the plant and determine available plant inputs and plant outputs. Identification of the nonlinear plant along selected operating lines then can provide local plant dynamics and a set of plant transfer function matrices $P(s)$ relating inputs and outputs.

Possibilities for control of plant outputs using available inputs can be checked by choosing subsets of square matrices of the plant transfer function matrix and determining the existence and condition of the corresponding plant inverse matrices. Existence of the plant inverse with good condition is necessary and vital to obtain reliable, independent control of selected outputs with available inputs [10-15].

Linear Design

A general linear system structure which combines TSP ideas with the idea of Comparison Sensitivity was presented and discussed in [4] and is shown in Figure 3. This system structure provides coordinated feedforward inputs u_r and loop command requests y_{rc}

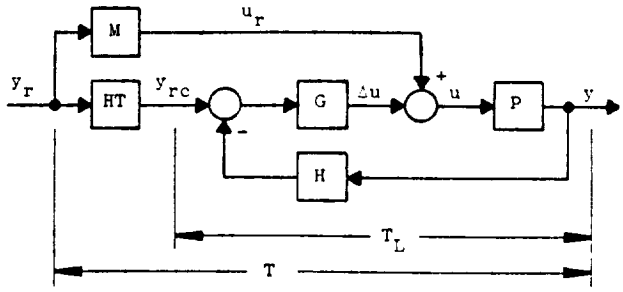

Figure 3. Robust Controller Structure.

to a closed loop control system. The feedforward elements coordinate request commands y_r; the closed loop assures steady state tracking and robustness of the outputs, y. The desired overall system response is designated by T. The chosen response of the loop is denoted by T_L.

Important controller elements of the structure are G, H, and M, which must be designed in an acceptable way so as to produce T and T_L within specifications. It turns out that three key equations govern local design:

$$M = P^{-1}T \qquad (I)$$

$$G = P^{-1}S_L^{-1}T_L \qquad (II)$$

$$H = T_L^{-1}(1-S_L) \qquad (III)$$

Equation (I) is called the synthesis equation. It is used to display all admissible responses (T,M) and (T_L,M_L). Equations (II) and (III) are design equations for the forward dynamics G and the feedback dynamics H, respectively. Note that all control dynamics are defined by selection of M, T, T_L and the comparison sensitivity S_L. The sensitivity S_L is defined [16,4] by $(1 + PGH)^{-1}$. These equations provide a basis to design linear control systems directly by specifying local response and sensitivity performance.

Nonlinear Design

As observed in the Introduction, the idea of describing families of curves by their tangents has a rich history in mathematics, in science, and in engineering. The method of phase plane portraits was already well developed more than two decades ago [17]. In more modern terms, we say today that

state space descriptions, by ordinary differential equations, coincide with vector fields on manifolds [18]. Solutions on the manifold are curves tangent to the vectors of the field.

What about nonlinear design? The fundamental notion used in this paper is that linear descriptions, obtained from local actions of nonlinear objects, may be combined to produce nonlinear action, with sufficient integrity to effect closed loop control. For example, if a set of local designs has given rise to a family $\{G(s)\}$ of forward dynamics in the loop, then the goal is to link members of the family together so as to produce a nonlinear function g, that is $\{G\} \rightarrow g$. Now each G may be regarded as giving a local approximation to a part of the vector field. Under reasonable conditions of smoothness, and with enough members in the family, a careful linking could indeed lead to useful g, over regions of interest.

To extend this notion, one can consider choosing, along an operating line, sets of desired system responses $\{M,T\}$, loop responses $\{M_L, T_L\}$, and sensitivities $\{S_L\}$. From these performance choices, sets of controller matrices $\{M\}$, $\{G\}$, $\{H\}$, and $\{HT\}$ can be generated via equations (I), (II), and (III). All of the linear sets may be linked and scheduled as a function of plant condition to form nonlinear control elements. Thus $\{T\} \rightarrow t$, $\{M\} \rightarrow m$, $\{G\} \rightarrow g$, $\{H\} \rightarrow h$, $\{HT\} \rightarrow h \circ t$.

Desired steady state operating schedules, transient control means and protection limits are also needed to provide other practical and functional features for a nonlinear turbojet engine control system. These features transform the linear system structure in Figure 3 to the nonlinear system structure shown below, in Figure 4.

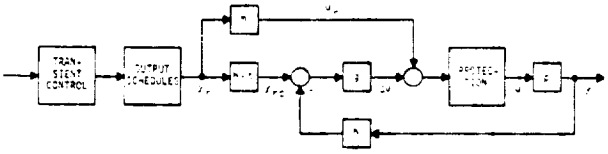

Figure 4. Nonlinear Control System.

The structure embodies key relationships of the Total Synthesis viewpoint and provides other basic features needed for full range, nonlinear control. It is used in the design examples which follow.

Design Examples

In this section we illustrate the foregoing synthesis ideas by designing a control system for the nonlinear turbojet engine described in Figure 2. Recall that the turbojet has three inputs: fuel flow, W_f, nozzle area, A_j, and turbine vane angle B; therefore, three outputs: engine speed, N, turbine temperature, T4, and engine thrust, FN were selected for control. We want to execute designs to achieve specific, beneficial output response strategies and show the effect that sensitivity specifications have in resisting plant parameter variations. Results are illustrated by time response traces for small step commands and by full range acceleration and deceleration transients.

Performance Specifications

Design a multivariable control system for full range acceleration and deceleration capability along the steady state schedules so that complete transients are completed in less than three seconds. Small signal responses of the system are desired to produce: 1) fast thrust response; 2) smooth, gentle temperature response; and 3) convenient speed response. All should take place without overshoot and without steady state error.

These requirements translate into the following kinds of response and sensitivity specifications:

1. Track output schedules with zero steady state error.
2. Accelerate or decelerate from 70% to 100% speed levels in less than 3 seconds.
3. Local System Responses (T) - Decoupled
   - Speed - .5 second lag @ 70% speed
   - Speed - .2 second lag @ 100% speed
   - Temp. - .5 second lag - constant
   - Thrust - .2 second lag - constant.
4. Local Closed Loop Response (T_L) - Decoupled .2 second lag constant for all outputs.
5. Local Sensitivity (S_L)
   a) Unity feedback: $S_L = (I-T_L)$;
   b) Ten times better than unity feedback.

The following response and sensitivity matrices at 100% speed condition were obtained:

$$T = \text{diag}\left(\frac{1}{.2s+1}, \frac{1}{.5s+1}, \frac{1}{.2s+1}\right)$$

$$T_L = \text{diag}\left(\frac{1}{.2s+1}, \frac{1}{.2s+1}, \frac{1}{.2s+1}\right)$$

$$S_L = \text{diag}\left(\frac{.2s}{.2s+1}, \frac{.2s}{.2s+1}, \frac{.2s}{.2s+1}\right) \quad (H=I)$$

$$S_L = \text{diag}\left(\frac{.02s}{.02s+1}, \frac{.02s}{.02s+1}, \frac{.02s}{.02s+1}\right)$$

The forward control dynamics G(s) at 100% speed condition with unity feedback are:

$$G(s) = \frac{\begin{bmatrix} .90(.23s+1) & 8.5(.01s+1) & -.42(.01s+1) \\ -.025(-.2s+1) & -.40(.01s+1) & .075(.01s+1) \\ -.0005(.74s+1) & .0085(.013s+1) & .0008(.01s+1) \end{bmatrix}}{s(.01s+1)}$$

Controller elements M, G, H and HT were calculated at five engine speed conditions. These sets were scheduled as a function of engine speed

to form nonlinear control system elements m, g, h and h ∘ t. For example, the form of the nonlinear controller g so constructed is shown in Figure 5 below.

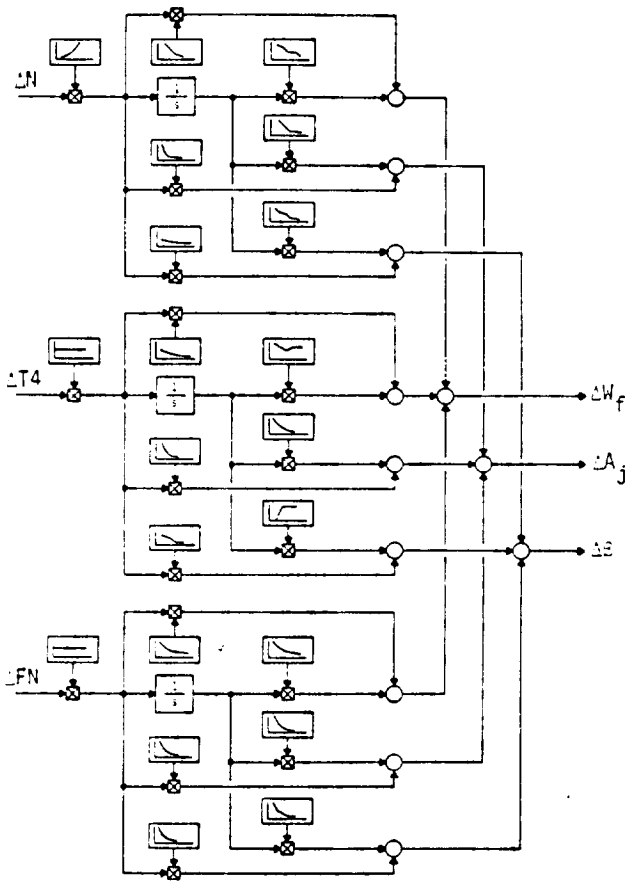

Figure 5. Nonlinear g.

Simulation Results

Small step transients of the nominal engine with sensitivity feedback system are shown in Figure 6. The output responses verify desired small signal performance: thrust response is fast (.2 second lag); temperature response is smooth (.5 second lag), and speed response varies from .5 second lag at 70% to .2 second lag at 100% speed condition. Corresponding input responses are shown in Figure 7.

Full range acceleration and deceleration transients of the nominal engine with sensitivity feedback system are shown in Figure 8. The outputs track the requests without overshoot and the transient time is less than three seconds. Corresponding input responses are shown in Figure 9. All inputs are within desired limits.

To show the effect of sensitivity specification on plant parameter variations, the time constants of the engine affecting speed, temperature

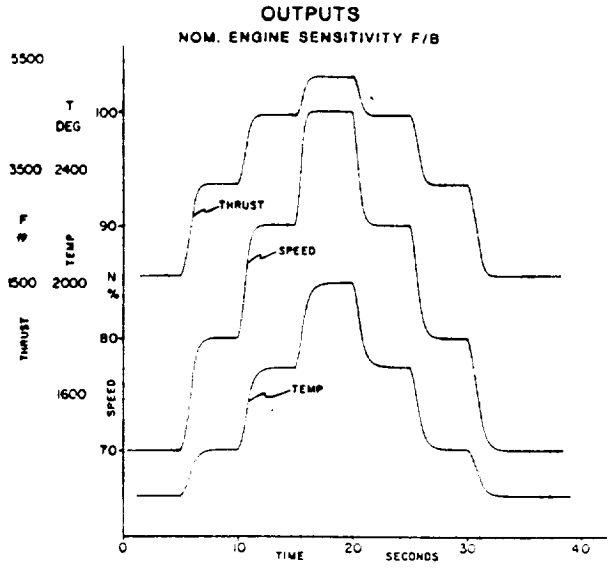

Figure 6. Outputs.
Nominal Engine; Sensitivity F/B.

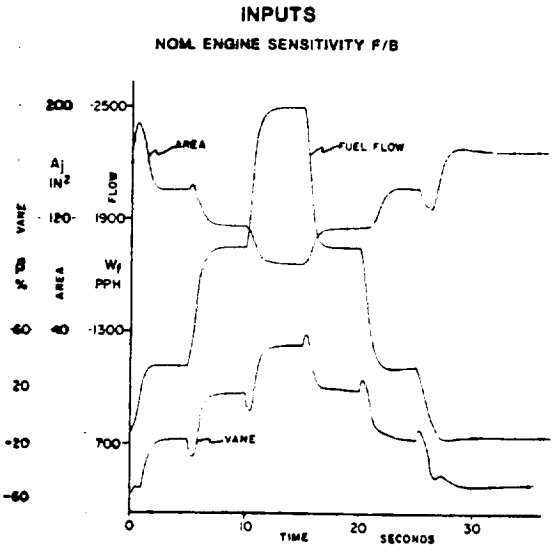

Figure 7. Inputs.
Nominal Engine; Sensitivity F/B.

and tail pipe pressure response were all doubled. This produced a nonnominal engine.

Small step responses of a nominal and nonnominal engine with unity feedback control are pictured in Figure 10. Deviations from desired output responses are caused by the engine parameter variations.

Imposing a sensitivity specification which is effectively ten times better than the unity feedback design produced feedback dynamics H = diag ((.2s+1)/(.02s+1)). Step responses for the sensi-

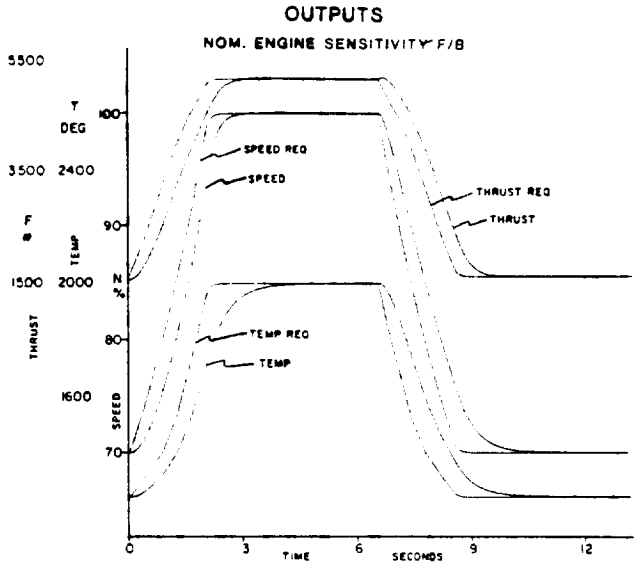

Figure 8. Outputs.
Nominal Engine ; Sensitivity F/B.

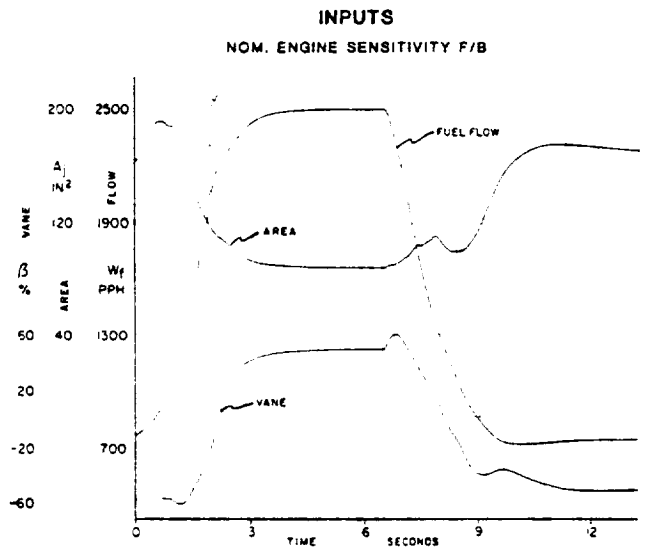

Figure 9. Inputs.
Nominal Engine; Sensitivity F/B.

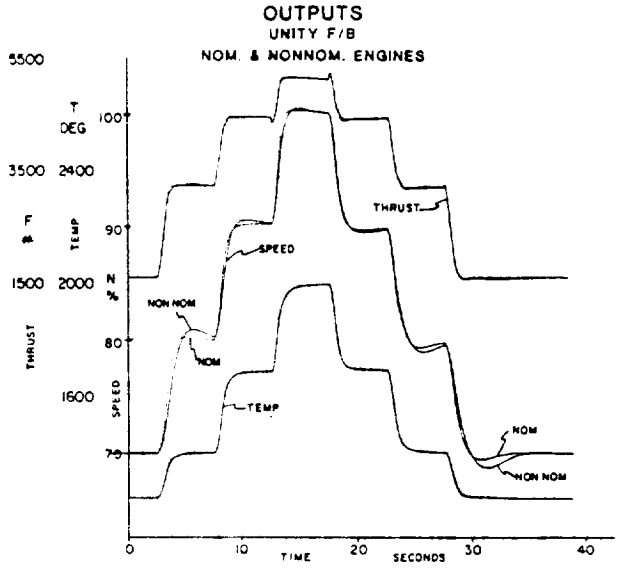

Figure 10. Outputs; Unity F/B.
Nominal and Nonnominal Engines.

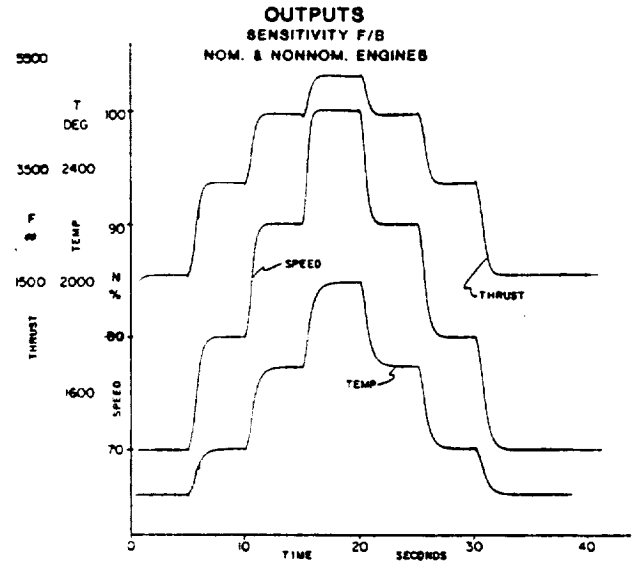

Figure 11. Outputs; Sensitivity F/B.
Nominal and Nonnominal Engines.

tivity feedback design with both the nominal and nonnominal engines are shown in Figure 11. Deviations due to engine parameter variations are virtually eliminated.

Full range acceleration and deceleration transients of the sensitivity feedback controller with both nominal and nonnominal engines are shown in Figure 12. The sensitivity design feedback controller maintains full range output transients essentially at nominal conditions, successfully handling plant parameter variations.

Summary Remarks

A nonlinear control synthesis method based on TSP viewpoint was discussed and illustrated. A three input/three output turbojet engine example demonstrated a feasibility to achieve desired system response and sensitivity specifications.

A concept of the nonlinear Nominal Design Problem (NDP) was presented and discussed, extending and building on earlier Total Synthesis Problem (TSP) theory and ideas. Additive structure was ob-

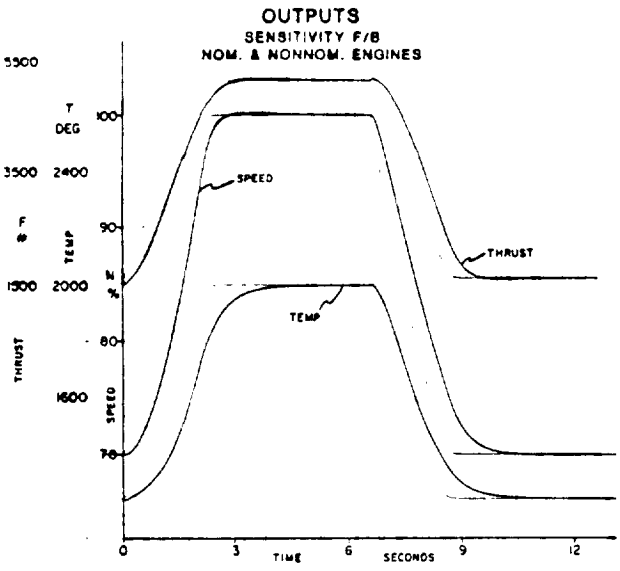

Figure 12. Outputs; Sensitivity F/B. Nominal and Nonnominal Engines.

tained by a process of inducing a special binary operation on the control input space. Though not a new mathematical idea [18], this concept seems to fit constructively into current design developments in nonlinear control.

Research to develop nonlinear control synthesis methods is needed. It is felt that the input-output TSP viewpoint offers possibilities to develop useful, systematic and straightforward methods for nonlinear multivariable control synthesis.

Acknowledgments

The support and extraordinary contribution of Mr. Ben Jacobs in simulation and verification of the design on our AD-10 hybrid computer is gratefully acknowledged. The assistance of Betty Raven in identification of the engine model is also gratefully acknowledged. Ben and Betty are both with the Bendix Energy Controls Division.

This work also benefited in part from support extended to the first author by the National Aeronautics and Space Administration under Grant NSG-3048.

References

1. E. Bristol, "Process Control: An Application Theorist's View of Control", IEEE Control Systems Magazine, Vol. 2, No. 1, pp. 3-8, March 1982.
2. J.L. Peczkowski and S.A. Stopher, "Nonlinear Multivariable Synthesis with Transfer Functions", Proc. 1980 Joint Automatic Control Conf., Vol. 1, Pt. WA8-D.
3. J.L. Peczkowski and M.K. Sain, "Scheduled Nonlinear Control Design for a Turbojet Engine", Proc. 1981 IEEE Int. Symp. on Circuits and Systems, pp. 248-251, April 1981.
4. M.K. Sain and J.L. Peczkowski, "An Approach to Robust Nonlinear Control Design", Proc. 1981 Joint Automatic Control Conf., Vol. 2, Pt. FA-3D.
5. J.L. Peczkowski, M.K. Sain, and R.J. Leake, "Multivariable Synthesis with Inverses", Proc. 1979 Joint Automatic Control Conf., pp. 375-380.
6. M.K. Sain, B.F. Wyman, R.R. Gejji, P.J. Antsaklis, and J.L. Peczkowski, "The Total Synthesis Problem of Linear Multivariable Control, Part I: Nominal Design", Proc. 1981 Joint Automatic Control Conf., Paper WP-4A.
7. M.K. Sain, P.J. Antsaklis, B.F. Wyman, R.R. Gejji, and J.L. Peczkowski, "The Total Synthesis Problem of Linear Multivariable Control, Part II: Unity Feedback and the Design Morphism", Proc. 1981 IEEE Conf. on Decision and Control, pp. 875-884.
8. M.K. Sain, Introduction to Algebraic System Theory. New York: Academic Press, 1981.
9. M.K. Sain and S. Yurkovich, "Controller Scheduling: A Possible Algebraic Viewpoint", Proc. 1982 American Control Conference.
10. L.M. Silverman and H.J. Payne, "Input-Output Structure of Linear Systems with Application to the Decoupling Problem" SIAM J. on Control, Vol. 9, pp. 199-233, May 1971.
11. B.C. Moore and L.M. Silverman, "Exact Model Matching by State Feedback and Dynamic Compensation", IEEE Trans. on Automatic Control, Vol. AC-17, pp. 491-497, August 1972.
12. S.-H. Wang and E.J. Davison, "A Minimization Algorithm for the Design of Linear Multivariable Systems", IEEE Trans. on Automatic Control, Vol. AC-18, pp. 220-225, April 1973.
13. W.M. Wonham and A.S. Morse, "Decoupling and Pole Assignment in Linear Multivariable Systems: A Geometric Approach", SIAM J. on Control, Vol. 8, pp. 317-337, 1970.
14. Z.V. Rekasius, "Linear Multivariable Control: A Problem of Specification", Proc. Int. Forum on Alternatives for Linear Multivariable Control, National Engineering Consortium, pp. 101-110, October 1977.
15. B.F. Wyman and M.K. Sain, "The Zero Module and Essential Inverse Systems", IEEE Trans. on Circuits and Systems, Vol. CAS-28, pp. 112-126, February 1981.
16. J.B. Cruz, Jr. and W.R. Perkins, "A New Approach to the Sensitivity Problem in Multivariable Feedback Design", IEEE Trans. on Automatic Control, Vol. AC-9, pp. 216-223, July 1964.
17. G.J. Thaler and M.P. Pastel, Analysis and Design of Nonlinear Feedback Control Systems. New York: McGraw-Hill, 1962.
18. W.M. Boothby, An Introduction to Differentiable Manifolds and Riemannian Geometry. New York: Academic Press, 1975.

D.1930

NONLINEAR MODELING OF A TURBOFAN JET ENGINE: A TENSOR METHOD APPLICATION

A Thesis

Submitted to the Graduate School
of the University of Notre Dame
in Partial Fulfillment of the Requirements
for the Degree of

Master of Science in Electrical Engineering

by

Thomas Anthony Klingler, B.S.E.E.

Michael K. Sain
Director

Department of Electrical Engineering
Notre Dame, Indiana

August, 1982

NONLINEAR MODELING OF A TURBOFAN JET ENGINE:

A TENSOR METHOD APPLICATION

Abstract

by

Thomas A. Klingler

Demand for reliable nonlinear model generating techniques in industry has risen in recent years, in part because of increasing plant complexity and in part because of requirements in control system design. Practical examples of the use of nonlinear models are provided by gas turbine engine control systems, which are inherently nonlinear. This thesis summarizes an investigation focused on the use of one such modeling technique which incorporates algebraic tensors in power series truncation approximations. Emphasis is placed on the application of these ideas in nonlinear model generation using a real-time digital turbofan engine simulation. Included in the discussion is an interactive computer-aided design package for the generation of such models. This package, which uses two independent computing systems, is designed to accommodate the overall process of model formulation, identification, and validation for any particular nonlinear modeling problem when developed within the framework of the tensor scheme.

TABLE OF CONTENTS

A COMPUTER-AIDED DESIGN PACKAGE FOR NONLINEAR MODEL APPLICATIONS*

T.A. Klingler, S. Yurkovich, and M.K. Sain

Department of Electrical Engineering, University of Notre Dame, Notre Dame, Indiana 46556

Abstract. An important aspect of multivariable control system design involves the formulation of reliable mathematical models. Gas turbine engine control systems, with their inherent nonlinearities, provide common practical examples of the need for nonlinear models. In this paper we discuss a computer-aided design package for generation of such nonlinear models, using an approach involving notions of power series and algebraic tensors. Two independent computing systems are employed interactively in the overall process of model formulation, identification, and validation. The package is sufficiently generalized to accommodate any particular nonlinear modeling problem when formulated within the framework of the algebraic tensor scheme.

Keywords. Computer-aided system design; multivariable control systems; modelling; tensor algebra; nonlinear systems; algebraic system theory.

INTRODUCTION

Models have always been an important aspect of applications engineering in the area of multivariable control system design. See for example the work of Kreindler and Rothchild (1976). Practical and industrial examples of the use of models are provided by gas turbine engine control systems, which commonly use models to generate control and response trajectories for various power demands. These models, when scheduled over the operating envelope, can reduce the compensation normally required of the controller, and thus provide the feedback loop with an opportunity to achieve better accuracy in the presence of noise and parametric uncertainties.

The scheduling of feedforward models and feedback compensation typically produces nonlinearities, even if the local models are linear. Accordingly, there is basic interest in fundamental approaches which incorporate nonlinearity at the outset. Such approaches should (1) reduce to the earlier linear schemes for variables with small excursions, (2) be amenable to scheduling, and (3) offer opportunities for determination of parameters from simulation data.

One such approach, investigated by Yurkovich and Sain (1980) and Klingler, Yurkovich, and Sain (1982), uses the notions of power series and algebraic tensors (Sain, 1976) to generate a class of nonlinear models. The important feature of the algebraic tensor is that it provides an organized way of describing the power series expansion formula, lending itself with relative ease to programming on a digital computer. Furthermore, its use allows for the implementation of linear parameter identification techniques.

This paper reports on the development of an interactive computer-aided design package for the formulation, identification, and validation of one particular model structure which uses the above-mentioned tensor approach. The software package, developed using the extensive capabilities of the IBM and DEC Command Procedure Languages with the strengths of FORTRAN and SPEAKEASY, is divided into two segments and tailored to utilize existing computer hardware effectively, as well as to provide the fastest possible user turnaround time. The interactive nonlinear model generation segment is implemented on a Time Sharing Option (TSO) of the IBM 370-168 computer system, where the memory dependent and highly computational routines of the package can benefit from use of the virtual memory and floating point hardware. Once a structured nonlinear model is identified, it is then transfered to the DEC PDP 11/60, where in an interactive environment it can be analyzed and compared to a linear model as well as the true system. In this manner, the user has at his disposal both the graphics capabilities of the video terminal and an electrostatic printer/plotter for the immediate display of data and comparative trajectories.

The remainder of the paper is outlined as follows. First, we briefly discuss notions from analysis and algebra which form the foundation for the tensor approach used in the model formulation. A detailed discussion of the interactive design package is

*This work was supported by the National Aeronautics and Space Administration under Grant NSG 3048.

then given, followed by a brief discussion of the computational aspects regarding floating point operations in the model simulation phase. We close with an example problem from a turbofan jet engine simulation.

NONLINEAR MODEL FORMULATION

Prior to proceeding to the description of the computer-aided design procedure in the modeling scheme, we outline here some of the prerequisite mathematical issues in a coordinate-free development. Since the treatment is brief, the reader may wish to consult Dieudonne (1960) and Greub (1967) for complete expositions of the topics discussed herein.

Tensor Ideas

We begin with a discussion of abstract derivatives and the calculus of normed vector spaces. Let V and W be normed vector spaces and let Z be open in V. Suppose that $f : Z \to W$ is differentiable at a fixed point p in Z. Then the derivative of $f : Z \to W$ at p is a mapping

$$(Df)(p) : V \to W \tag{1}$$

where

$$Df : Z \to L(V,W) ; \tag{2}$$

that is, the derivative mapping in Eq. (1) is an element of the real vector space of *linear* mappings from V to W. Higher order derivatives are defined recursively as

$$(D^r f)(p) = (D(D^{r-1}f))(p) , \tag{3}$$

for the positive integer r, provided that the $(r-1)$st derivative is differentiable. Moreover, higher order derivatives are themselves linear mappings according to

$$\begin{aligned} D^2 f(p) &\in L(V,L(V,W)) , \\ D^3 f(p) &\in L(V,L(V,L(V,W))) , \\ &\vdots \qquad\qquad \vdots \end{aligned} \tag{4}$$

If $L(V^r;W)$ denotes the real vector space of r-linear mappings from V^r to W, it can be shown that there exist isomorphisms

$$\begin{aligned} L(V^2;W) &\to L(V,L(V,W)) , \\ L(V^3;W) &\to L(V,L(V,L(V,W))) , \\ &\vdots \qquad\qquad \vdots \end{aligned} \tag{5}$$

so that the rth derivative of f at p can be regarded as a mapping from V^r to W. We suppress this isomorphism and consider $D^r f(p)$ as an element of $L(V^r;W)$.

We now use this multilinearity of the derivative mapping to make a connection with notions from algebraic tensors. Let $(\otimes^r V, \otimes^r)$ be a tensor product for r copies of V. Recall that by the unique factorization property of the tensor product, for every mapping $\psi : V^r \to W$ in $L(V^r;W)$ there exists a mapping $\lambda : \otimes^r V \to W$ in $L(\otimes^r V, W)$ such that $\psi = \lambda \circ \otimes^r$ for $\otimes^r : V^r \to \otimes^r V$ in $L(V^r;\otimes^r V)$. Furthermore, the implication of the unique factorization property is that

$$L(\otimes^r V, W) \to L(V^r;W) \tag{6}$$

is a vector space isomorphism. Thus, via the isomorphisms of Eqs. (5) and (6), the r-linear mapping $D^r f(p) : V^r \to W$ can be composed from a linear mapping $\otimes^r V \to W$ and the universal r-linear tensor product mapping $\otimes^r : V^r \to \otimes^r V$.

State Description

The ideas discussed above are now used to formulate the model structure for a given nonlinear system. We consider systems whose states and inputs are elements of the normed real vector spaces X and U, respectively, and which may be described by the nonlinear ordinary differential equation

$$\dot{x} = f(x,u) \tag{7}$$

for $f : X \times U \to X$. Let $(\bar{x},\bar{u})$ be a fixed point in Z open in $X \times U$, and suppose that $f : X \times U \to X$ is of sufficient smoothness on Z. Formally,

$$f(\bar{x}+x,\bar{u}+u) = \sum_{k=0}^{\infty} \frac{1}{k!} (D^k f)(\bar{x},\bar{u})(x,u)^{(k)} , \tag{8}$$

where $(x,u)^{(k)} = ((x,u),(x,u),\ldots,(x,u))$ k times. Due to space limitations we cannot address existence or convergence questions relative to Eq. (8). We note, however, that this series could be replaced by a finite number of terms together with a remainder term in a standard application of Taylor's formula.

According to the preceding discussions we now make the unique factorization

$$D^k f(\bar{x},\bar{u}) = L_k(\bar{x},\bar{u}) \circ \otimes^k , \tag{9}$$

where $L_k(\bar{x},\bar{u}) : \otimes^k(X \times U) \to X$ is linear. Denote the k-fold tensor product of (x,u) with itself by $(x,u)^k$ so that, with Eq. (9), we have

$$f(\bar{x}+x,\bar{u}+u) = \sum_{k=0}^{\infty} \frac{1}{k!} L_k(\bar{x},\bar{u})(x,u)^k . \tag{10}$$

Sain and Yurkovich (1982) have shown that the individual terms in the series of Eq. (10) may be rewritten as, for example in the case of $k = 2$,

$$\frac{1}{2!} L_2(\bar{x},\bar{u})(x,u)^2 = L_{20}\, x \otimes x + L_{11}\, x \otimes u + L_{02}\, u \otimes u , \tag{11}$$

where we have suppressed the notation of $(\bar{x},\bar{u})$ on the right side of Eq. (11). In this way Eq. (8) becomes

$$f(\bar{x}+x,\bar{u}+u) = \sum_{i=0}^{\infty}\sum_{j=0}^{\infty} L_{ij}\, x^{i} \otimes u^{j} , \qquad (12)$$

forming the structure for the nonlinear model.

Application

In practical applications a truncation approximation of the series in Eq. (12) is considered. In terms of computing, then, the task in the model building scheme is to identify the parameters contained in matrix representations of the L_{ij}. Ordered bases in X, U, X ⊗ X, X ⊗ U, and so on, are chosen a priori to be used in constructing a linear least squares identification problem. The ordering algorithm (Yurkovich, 1981) which facilitates this procedure, used in the interactive software package described herein, is easily implemented on a digital computer.

In practice, a differential equation description of the nonlinear system may or may not be available. In either case, the basic strategy involves initial condition and control signal design so that, through data sampling and derivative estimation, a model of the original system of Eq. (7) may be identified. The nonlinear model is required not only to outperform a standard linear model locally about an expansion point, but to establish a larger region of model validity as well.

CATNAP

The intent of this section is to present a detailed discussion of the Computer-Aided Tensor Nonlinear Modeling Applications Package (CATNAP) currently used as a development tool in the formulation, identification, and validation of nonlinear models of the type mentioned above. The structure of CATNAP is based upon ideas from distributed processing and local networking (Tanenbaum, 1981) in which computations are spread over multiple machines. More specifically CATNAP is divided into two segments, each of which is implemented on an independent computing system. These segments are entitled GENERATE and SIMULATE. GENERATE is implemented on a Time Sharing Option (IBM, 1975) of the IBM 370-168 mainframe computer and is used to formulate and identify models, whereas SIMULATE is implemented on the DEC PDP 11/60 computer system and is used to study model validity and performance. Furthermore, both of these segments are highly interactive and contain straightforward input prompts as well as informative error messages.

GENERATE

The GENERATE segment of CATNAP is primarily made up of three routines governed by a higher level supervisor. Figure 1 contains a block diagram depicting the structure of GENERATE.

GENERATE Supervisory. This supervisory level is written using the command procedure language CLIST (IBM, 1976) and performs the following main functions in sequence:

(1) prompts the user for the name of the desired loader routine to be executed;

(2) passes control to the loader routine defined in (1);

(3) passes control to IDENTIFY; and,

(4) upon user request, passes control to TRANSFER.

In addition to these main functions, certain maintenance roles such as file creation, allocation and deletion are handled by this supervisor.

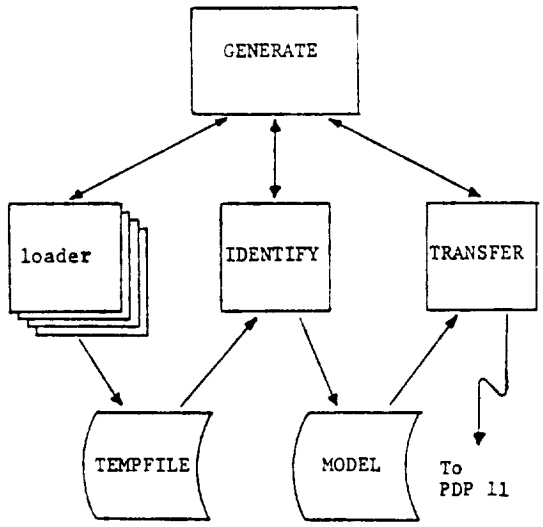

Fig. 1. Block diagram for the CATNAP segment GENERATE.

Loader Routine. Associated with each nonlinear system to be modeled, there exists a loader routine which performs the model formulation task. These routines are stored in a library and are typically written in double precision FORTRAN.

The purpose of any loader routine is to excite the given nonlinear system via initial condition and control input perturbations and to sample the states, inputs and derivative estimates over h selected points in time. The system is then represented by the matrix equation

$$\underset{nxh}{\dot{X}} = \underset{nxp}{[L_{10}\ L_{01}\ L_{20}\ L_{11}\ L_{02}\ L_{30}\ \ldots]}\ \underset{pxh}{X_T} . \qquad (13)$$

The first $n+m$ rows of the matrix X_T are formed from the sampled values of x and u; the remaining $p-(n+m)$ rows are formed according to the ordering algorithm previously mentioned, which minimizes the number of computations. X is formed by loading derivative estimates for $\dot{x}_1, \dot{x}_2, \ldots, \dot{x}_n$ at the h time points. The number p depends on n and m, and the degree of the truncation approximation. All this data is then stored in TEMPFILE for later use.

Using this approach, CATNAP can accommodate any particular nonlinear modeling problem since the problem specifics are transparent to the remainder of the package. The only requirement is that TEMPFILE contains the appropriate data.

IDENTIFY. After the completion of any chosen loader routine, the program IDENTIFY is executed. IDENTIFY reads the interim data from TEMPFILE and forms a least squares minimization problem which is solved for the partitioned matrix containing the desired L_{ij} parameters. These L_{ij} parameters are recorded at the terminal as well as entered into the MODEL data file.

It should be noted here that IDENTIFY is written in the high level language SPEAKEASY, which is based on the concepts of arrays and matrices and processes these as entities. This results in the elimination of the many loops necessary in other programming languages. See the work of Cohen and Pieper (1979). The main reason for employing SPEAKEASY here is that the highly efficient routine SIMEQUAT can be easily used to solve the least squares problem via singular value decomposition, thus reducing the apparent complexity of the problem to a minimum.

TRANSFER. Upon a yes response to a supervisory prompt, the program TRANSFER is submitted batch to the IBM 370-168. TRANSFER is merely a Job Control Language (JCL) deck which sends a copy of the file MODEL, containing the L_{ij} parameters, to the DEC PDP 11/60 computing system by the way of a Remote Job Entry port, and stores it in the nonlinear model library. An excellent account of JCL can be found in Brown (1977).

SIMULATE

Shifting our concern away from the discussion of GENERATE, we now focus our attention on the SIMULATE segment of CATNAP. Basically, two routines plus a supervisor comprise the structure of SIMULATE. Figure 2 offers an illustration of this structure to supplement the following presentation.

SIMULATE Supervisory. Written in the form of an Indirect Command File (DEC, 1979), this supervisor allows the user to:

(1) create new simulator routines;

(2) execute existing simulator routines; and,

(3) execute VERSATEC which produces hardcopy plots.

As earlier, this supervisor performs a number of file maintenance duties in addition to the above functions.

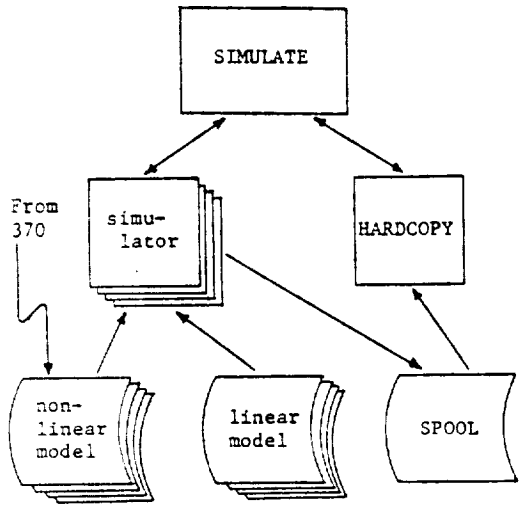

Fig. 2. Block diagram for the CATNAP segment SIMULATE.

Simulator Routine. A FORTRAN simulator routine usually exists for each nonlinear modeling problem studied; however, only one subroutine in that program is altered among versions, and that is the application subroutine TRUES. The remainder of the program stays unchanged. TRUES contains the true system representation of the nonlinear system being modeled, and is used extensively in comparison studies. Because of the number of TRUES subroutines that exist, a library has been created to store the various simulator routines.

The execution of a particular simulator routine can be divided into three steps: (1) problem configuration; (2) systems integration; and (3) solution display.

The first of these steps requires the user to decide which of the available systems, true solution, linear model and/or nonlinear model, should be included in the session configuration. When a model is chosen, the user is asked to enter the name of the desired model. That model is then read into the simulator from the appropriate library. The linear models used in CATNAP are generally identified by standard techniques and are available for use in comparison studies.

Next, the user is prompted for various integration parameters such as stepsize and upper time limit as well as initial condi-

tions, input amplitudes and frequencies. The configured systems are then integrated and the solutions are sampled at 100 points, evenly spaced in time.

Finally, to assist in the data analysis, a number of options are available to the user. They include:

(1) printing the solutions on the Versatec;

(2) displaying the comparative trajectories on the Tektronix graphics terminal;

(3) writing the trajectory solutions to SPOOL for hardcopy plotting at a later time; and,

(4) solving the configuration for another set of initial conditions and control inputs.

The use of these options provides a powerful yet flexible capability for the study of model performance and validity. Furthermore, when all three systems are included in the configuration, an additional error criterion is generated and used in testing the performance of the nonlinear model versus that of the linear model.

Let ε_i^N denote the absolute maximum error in the nonlinear model solution, as compared to the true simulation solution, over the time range of simulation for the ith state variable. Similarly, we define ε_i^L for the linear model error. Then ε_i is the comparison $\varepsilon_i^N - \varepsilon_i^L$. Thus, if ε_i is negative, the nonlinear model has exhibited a smaller maximum absolute error in the ith state, and in that sense has outperformed the linear model.

VERSATEC. The routine VERSATEC, written in FORTRAN, reads the trajectory solutions from SPOOL and records at the Versatec printer/plotter, a data sheet corresponding to each plot set which follows. The comparative trajectories themselves are then plotted.

MODEL SIMULATION

In this section we comment on the efficiency of the model structure discussed above by studying the number of floating point operations (FLOPs) necessary in typical simulations. It is common practice in computer architecture to design processors which require no extra time for floating point additions calculated simultaneously with multiplications. Thus, we concern ourselves primarily with the latter, and by FLOPs we will mean multiplies. Since the largest burden of the computer in the simulation process is the actual numerical integration of model differential equations, we will analyze only that portion of the simulation.

The system to be considered takes the form of Eq. (13), or

$$\dot{x} = Lz \ ,$$

where x is the n-vector of states, L the parameter matrix, and z the p-vector of ordered monomial terms derived from the various symmetric products of x and u, the m-vector of inputs (Yurkovich and Sain, 1980). The least number of multiplications required to construct z is merely p-n+m, or the total number of terms which involve products. This number is given by

$$p-(n+m) = \sum_{i=2}^{d} \left\{ \binom{n+i-1}{i} + \binom{m+i-1}{i} + \left[\sum_{j=1}^{i-1} \binom{n+(i-j)-1}{(i-j)} \binom{m+j-1}{j} \right] \right\} ,$$

where d is the model degree.

Assuming the use of a fourth-order integration routine, the number of FLOPs necessary to formulate and integrate the system as embodied by the model, across one integration time step, is $4(n)(p)$. As an illustration consider a four-state, three-input model.[1] Suppose, for simplicity, that 100 integration time steps is the equivalent of one second in real time. This translates roughly to 0.25 million FLOPs per second for a degree-3 model (an approximation which retains terms up to and including the third degree). While there are many other obvious considerations involved in real time simulation, this number is well within the bounds dictated by state-of-the-art computation speeds of ten million FLOPs per second.

EXAMPLE

In the example to follow attention will center around NASA's QCSEE ("Quixie")---Quiet, Clean, Shorthaul Experimental Engine. Wise (1974) provides an excellent overview of the QCSE engine program. QCSEE is designed specifically for powered-lift, short-haul aircraft, and incorporates several new concepts not all currently used on turbofans to achieve operational efficiency in a quiet, clean manner.

QCSEE APPLICATION

For this nonlinear modeling problem, a complex eight-state, three-control digital simulation of the QCSE engine is employed (Mihaloew, 1981). Using this digital deck as the system representation, a loader routine, QCSELOAD, is constructed to formulate a reduced order four-state, three-control analytical model. The engine states chosen are the combustor discharge pressure (P4GS), the core nozzle pressure (P8GS), the fan speed (NL), and the compressor speed (NH). The control inputs used are the fuel flow

[1] This represents a typical model as investigated by Klingler, Yurkovich, and Sain (1982).

(WFM), the exhaust nozzle area (A18) and the fan pitch angle (BETAF). In a similar way, the simulator routine QIXSIM is built using QCSEE as the true system in the subroutine TRUES.

For the results presented herein, two models have been formulated using QCSELOAD at 92% power demand: a second-degree nonlinear model, and a first-degree linear model. Both formulations are made using 1% steady state perturbations in the state and control variables. Furthermore, the control inputs are manipulated so that cosinusoidal signals are inserted. The observed states and inputs are sampled over a six second interval, and the difference between these values and the corresponding equilibrium values, together with the ordered tensor product terms and state derivative values comprise the data necessary for the identification. The model parameters are easily computed from IDENTIFY and then sent to the PDP 11/60 via TRANSFER.

Using the capabilities of QIXSIM and VERSATEC, several validation studies have been completed to date, all yielding satisfactory results. Figures 3-7 contain a representative plot set from VERSATEC illustrating the model performance for a particular input set, as well as the graphical capabilities of CATNAP. Table 1 contains a variable ledger for Figures 3-7.

CONCLUSION

The importance of nonlinear modeling in multivariable control systems could hardly be overemphasized. And the applications side of the problem has benefited greatly with the advent of expanded and more versatile computing environments.

Rarely does it happen, though, that one computing system can accommodate all requirements placed on it, particularly when plagued by multiple users demanding unlimited access. It often happens, however, that the capabilities of several computing systems are at ones disposal, each with various features to offer. In this case schemes employing the notions of distributed processing and local networking become extremely useful.

We have presented one such scheme in the form of an interactive computer-aided design package for a specific nonlinear modeling problem. The software package facilitates the analysis of complex problems, with relative ease to the user, from the initial model formulation and identification stage through to the model testing and validation studies. Series ideas and algebraic tensors are the main vehicles in the model formulation. The importance of the tensor approach lies in its parametric possibilities, and ongoing research is currently underway to exploit further the richness of such structures.

REFERENCES

Brown, G.D. (1977). System 370 Job Control Language. John Wiley and Sons, New York.

Cohen, S., and S. Pieper (1979). The Speakeasy III Reference Manual. Speakeasy Computing Corporation, Chicago.

DEC (1979). RSX-11M/M-Plus MCR Operations Manual, AA-H263A-TC. Chapter 5, Digital Equipment Corp., Maynard, MA.

Dieudonne, J. (1960). Foundations of Modern Analysis. Academic Press, New York.

Greub, W.H. (1967). Multilinear Algebra. Springer-Verlag, New York.

IBM (1975). OS/VS2 TSO Terminal User's Guide, GC28-0645-2, IBM Corporation, Poughkeepsie, N.Y.

IBM (1976). OS/VS2 TSO Command Language Reference, GC28-0646-3. IBM Corporation, Poughkeepsie, N.Y.

Klingler, T.A., S. Yurkovich, and M.K. Sain (1982). An Application of Tensor Ideas to Nonlinear Modeling of a Turbofan Jet Engine. Proc. Thirteenth Pittsburgh Conf. on Modeling and Simulation, to appear.

Kreindler, E., and D. Rothchild (1976). Model Following in Linear Quadratic Optimization. AIAA J., 14, pp. 835-842.

Mihaloew, J.R. (1981). A Nonlinear Propulsion System Simulation Technique for Piloted Simulators. Proc. Twelfth Pittsburgh Conf. on Modeling and Simulation, pp. 1423-1427.

Sain, M.K. (1976). The Growing Algebraic Presence in Systems Engineering: An Introduction. Proc. IEEE, 64, pp. 96-111.

Sain, M.K., and S. Yurkovich (1982). Controller Scheduling: A Possible Algebraic Viewpoint. Proc. 1982 American Control Conf., to appear.

Tanenbaum, A.S. (1981). Computer Networks. Prentice-Hall, Inc., Englewood Cliffs, N.J.

Wise, C.E. (1974). Turbofan of the Future. Machine Design, pp. 20-25.

Yurkovich, S. (1981). Application of Tensor Ideas to Nonlinear Modeling and Control. M.S. Thesis, Elec. Engrg. Dept., Univ. of Notre Dame, Notre Dame, IN.

Yurkovich, S., and M.K. Sain (1980). A Tensor Approach to Modeling of Nonhomogeneous Nonlinear Systems. Proc. Eighteenth Allerton Conf. on Communication, Control, and Computing, pp. 604-613.

TABLE 1 Variable Ledger for Figures 3-7

○ : True Engine Response △ : Linear Model Response * : Nonlinear Model Response	
x_1: P4GS (psi) x_2: P8GS (psi) x_3: NL (rpm) x_4: NH (rpm)	u_1: WFM (lb_m/hr) u_2: A18 (in^2) u_3: BETAF (deg.)

```
********** PROBLEM SUMMARY **********
    CONFIGURATION:  TRUE, LINEAR & NONLINEAR
    NUMBER OF STATES:  4
    NUMBER OF CONTROLS:  3
    LENGTH OF TENSOR TERM VECTOR:  35
    DEGREE OF APPROXIMATION:  2
*************************************

SOLUTION PARAMETERS:
********************

    INTEGRATION STEPSIZE:  0.010
    UPPER TIME LIMIT OF INTEGRATION:  2.000
    NUMBER OF PLOT POINTS: 100
    SPACING BETWEEN PLOT POINTS:  0.020
```

STATE NUMBER	INITIAL CONDITION	ERROR CRITERION
1	-0.075	-0.533E+00
2	0.001	-0.915E-02
3	-0.250	-0.698E+01
4	0.500	-0.111E+02

CONTROL NUMBER	AMPLITUDE	FREQUENCY (CYCLES/SEC)
1	74.290	2.100
2	-21.200	1.000
3	-0.239	1.500

Fig. 3. Sample data sheet for the QCSEE example

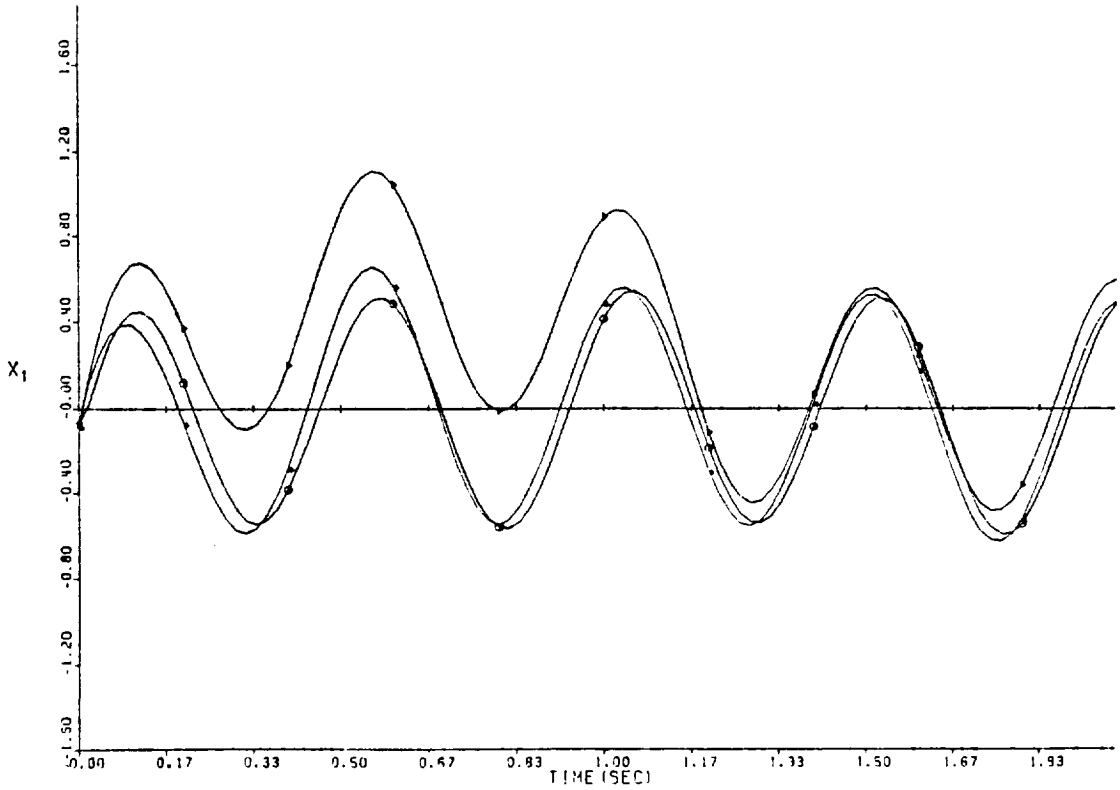

Fig. 4. Comparative solutions: Fig. 3, state 1.

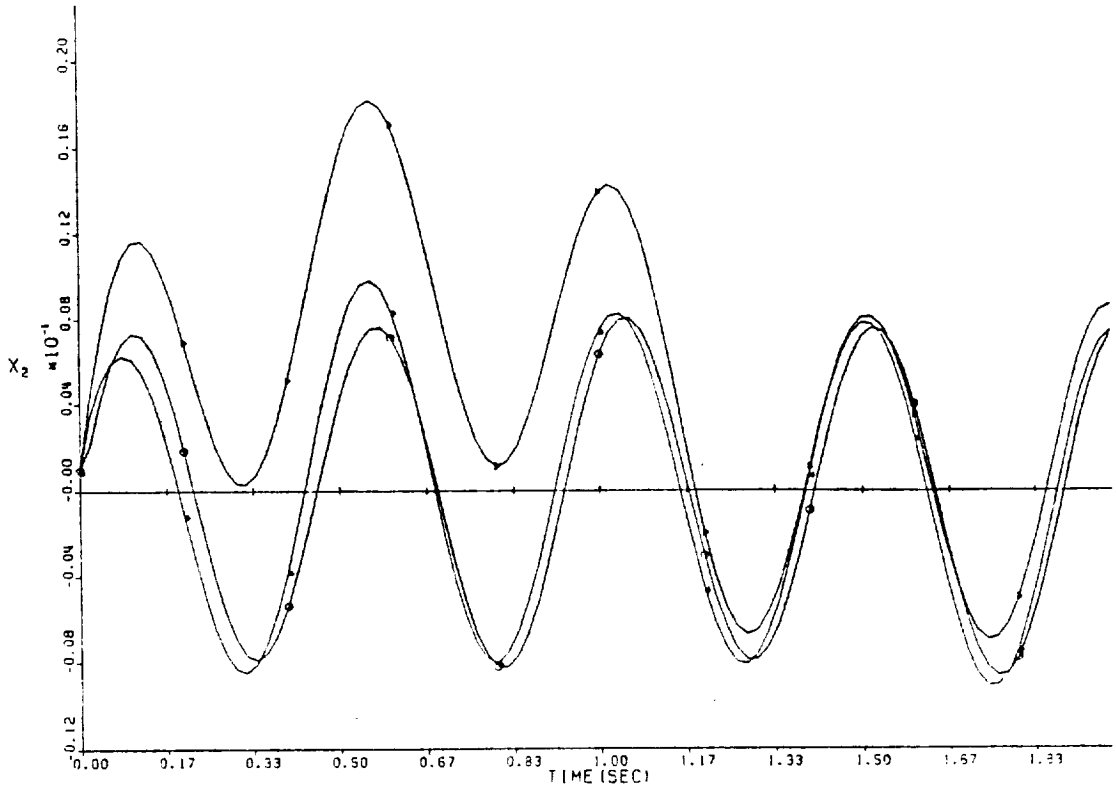

Fig. 5. Comparative solutions: Fig. 3, state 2.

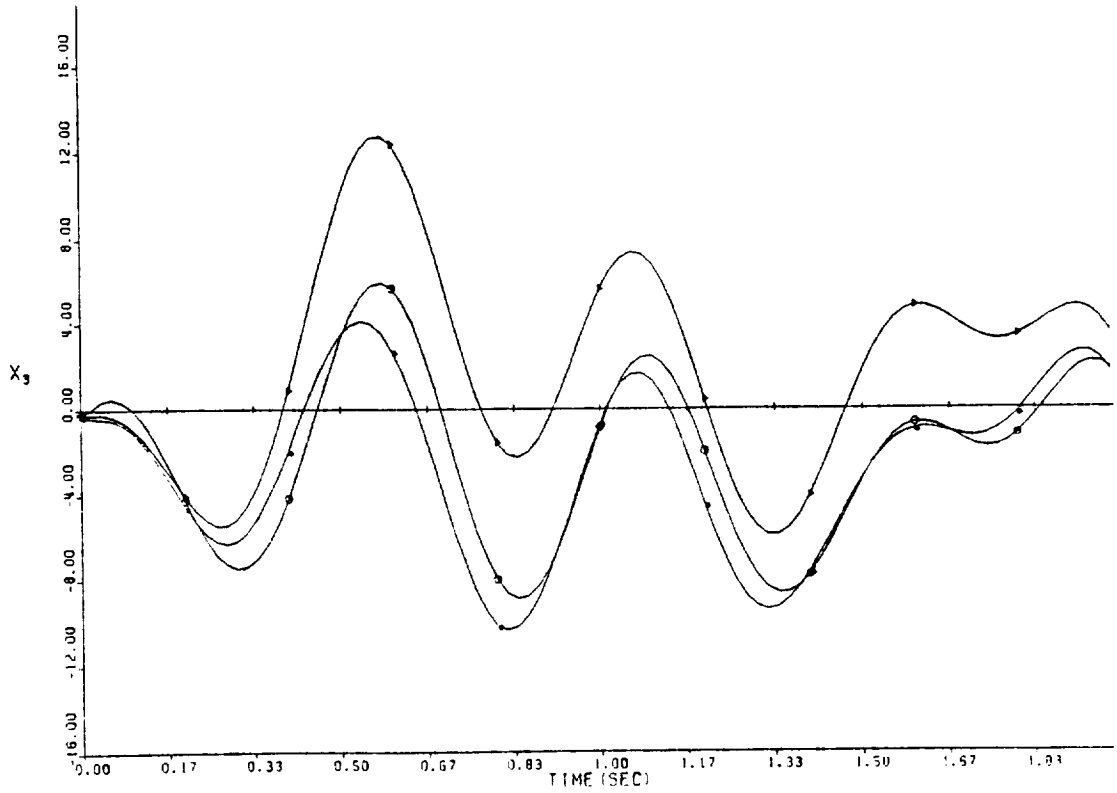

Fig. 6. Comparative solutions: Fig. 3, state 3.

-21 (OUTP)

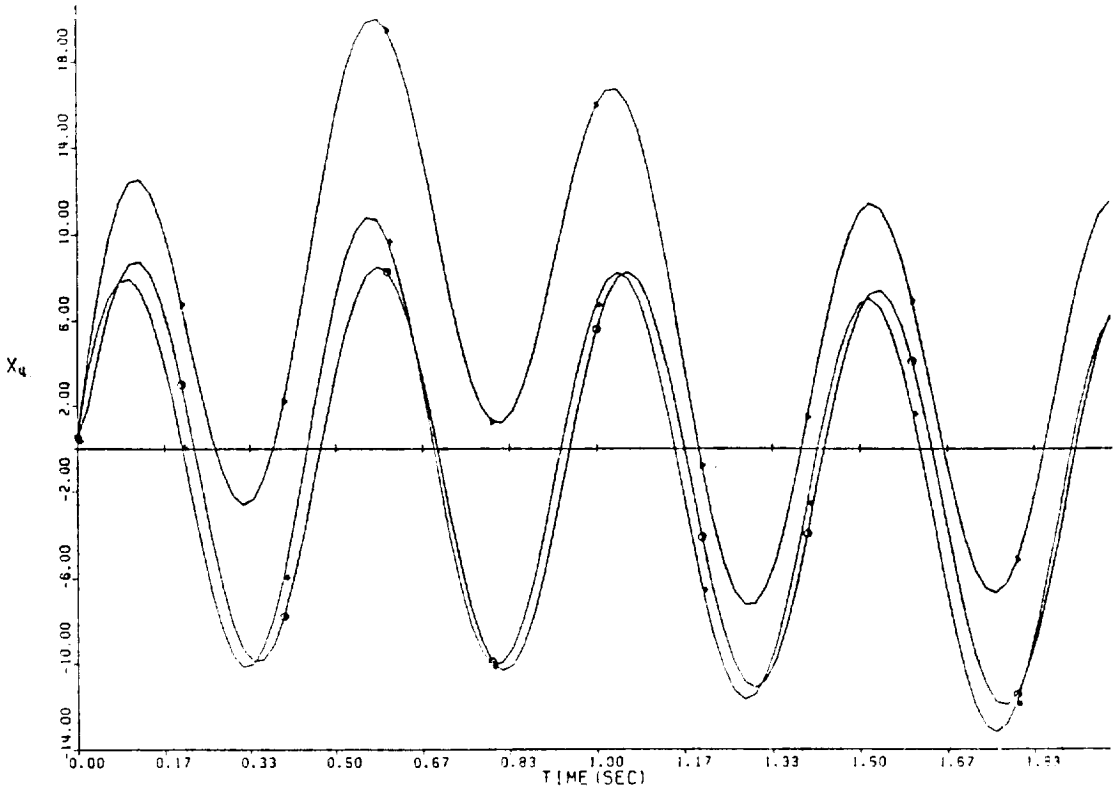

Fig. 7. Comparative solutions: Fig. 3, state 4.

THE TOTAL SYNTHESIS PROBLEM FOR LINEAR MULTIVARIABLE SYSTEMS WITH DISTURBANCES

A Dissertation

Submitted to the Graduate School
of the University of Notre Dame
in Partial Fulfillment of the Requirements
for the Degree of

Doctor of Philosophy

by

Kenneth Paul Dudek, B.S.E.E., M.S.E.E.

Michael K. Sain
Director

Department of Electrical Engineering
Notre Dame, Indiana

May 1984

D30
32

The Total Synthesis Problem for Linear Multivariable Systems with Disturbances

Abstract
by
Kenneth Paul Dudek

The Total Synthesis Problem for Linear Multivariable Systems with Disturbances (TSD) is an extension of the Total Synthesis Problem (TSP) to include systems whose plants and sensors are subject to external disturbances. TSP provides an algebraic method for the direct frequency domain design and synthesis of a system's response to commands and the control actions needed to produce those responses under the fundamental constraint imposed by the plant.

Analogous to TSP, we define TSD to be the composite of the Nominal Design Problem for TSD (NDP/TSD) and the Good Feedback Synthesis Problem for TSD (GFSP/TSD). Here, NDP/TSD is the problem of simultaneously characterizing all outputs and controls a linear multivariable system can produce in response to exogenous commands, plant disturbances, and sensor disturbances. GFSP/TSD is the problem of finding a good feedback synthesis for a NDP/TSD solution.

We separate NDP/TSD into command and disturbance parts, the former being the Nominal Design Problem for Command Responses (NDP/CR) and the latter being the Nominal Design Problem for Disturbance Responses (NDP/DR). Similarly, we separate GFSP/TSD into the Good Feedback Synthesis Problem for Command Responses (GFSP/CR) and the Good Feedback Synthesis Problem for Disturbance Responses (GFSP/DR). The solutions to NDP/CR and NDP/DR may be specified independently. Furthermore, solutions to GFSP/CR exist whenever solutions to GFSP/DR exist. Hence, TSD readily separates into two subproblems: the Command Part of TSD (TSD/CR) and the Disturbance Part of TSD (TSD/DR) where

TSD/CR is the composite of NDP/CR and GFSP/CR and TSD/DR is the composite of NDP/DR and GFSP/DR. As NDP/CR and NDP/DR are completely independent and GFSP/CR and GFSP/DR are "consecutively" independent, it follows that TSD/CR and TSD/DR are "consecutively" independent. This is important since TSD/CR has already been solved in earlier works where it is called the Total Synthesis Problem. As such, the primary contribution of this work is the solution to TSD/DR.

We recognize NDP/DR as an abstract kernel problem whose solutions are effectively parameterized in terms of a single morphism. By placing conditions on this morphism, we can guarantee the existence of solutions to GFSP/DR, thereby solving TSD/DR.

D32 over

TABLE OF CONTENTS

DBT33

DESIGN OF NONLINEAR MULTIVARIABLE FEEDBACK CONTROLS BY TOTAL SYNTHESIS

Joseph L. Peczkowski
Energy Controls Division
The Bendix Corporation
South Bend, Indiana 46620

Michael K. Sain
Electrical Engineering Department
University of Notre Dame
Notre Dame, Indiana 46556

Abstract

Total Synthesis (TS) ideas for nonlinear, multivariable control design are based upon the Total Synthesis Problem introduced in 1979 [2]. Motivation for the TS approach, which originated in gas turbine studies [1], is the development of an application based, user oriented design theory for nonlinear, multivariable feedback controller synthesis. This paper continues the evaluation of TS techniques, in an illustrative way, by means of multiple examples founded upon a realistic digital simulation for a gas turbine engine. Emphasis is placed upon the application viewpoint.

Introduction

This paper is about synthesis of nonlinear multivariable feedback control systems. More specifically it concerns the application of Total Synthesis (TS) ideas to nonlinear, multivariable control design. The Total Synthesis Problem (TSP) was introduced in 1979 by Peczkowski, Sain, and Leake [2] and has continued under study [3-24], with the motivation to develop a comprehensive and useful, application based, design method for multivariable feedback controller synthesis.

The primary aim of the paper is to illustrate, by example, the utility of TS relationships and the input-output viewpoint, and to show how these ideas, employing transfer function matrices, lead to a useful, application oriented, multivariable design method. The TS approach allows designers to choose, at the outset, specific, desired system responses and then to realize them with feedback control structures having acceptable control action. Because many nonlinear plants and systems are locally linear in nature, linear methods must pertain to a significant part of many nonlinear problems. The linear properties, however, must be appropriately linked and scheduled to produce proper nonlinear action.

Total Synthesis

Total Synthesis ideas refer to a top-down strategy of Nominal Design and Feedback Synthesis [19]. Nominal Design depends on plant characteristics only, is independent of controller structure, and is the first step in the design procedure [16]. Feedback Synthesis depends on the controller structure and is the second step in the design procedure. Discussion of Feedback Synthesis for unity feedback is given in [18] and for several other structures in [23] and in [24].

For applications, the significance of Nominal Design is that this first step defines for the designer, up front, acceptable system responses which the plant can produce. Or saying it another way, it outlines the performance which the plant can deliver. This is important because then one knows what responses may be requested.

The fundamental approach and thrust we take here in application of Total Synthesis is to design feedback controllers to produce specific, desired plant output responses, y = Tr, and acceptable control action, u = Mr, in the manner illustrated by Figure 1. The objective is to give the

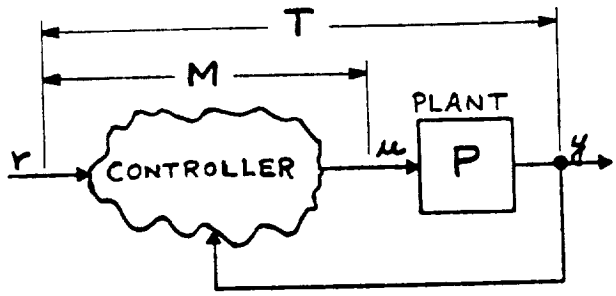

Figure 1.

designer, at the beginning, direct selection of desired responses (M,T) of the closed loop system, and to provide insights into the performance choices available so that the designer is able to influence directly the final outcome.

Nominal Design

Using the general control structure shown in Figure 1, the Nominal Design Problem (NDP) can be summarized in the following way [16]:

When P is given, find stable and proper pairs M,T such that T = PM, so the diagram at the left of Equation (1) commutes.

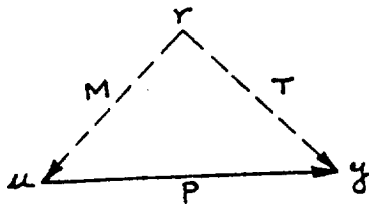

$$y = Pu \qquad (1a)$$

$$u = Mr \qquad (1b)$$

$$y = Tr \qquad (1c)$$

It is known [16] that when $P = ND^{-1}$, with N and D having no zeros in common (right coprime), pairs (M,T) must be of the form:

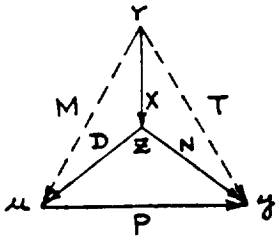

$$u = Mr = DXr \qquad (2a)$$

$$y = Tr = NXr \qquad (2b)$$

$$u = Dz;\ y = Nz \qquad (2c)$$

These equations lead to a relationship between the pairs M, T and the plant coprime factors N and D:

$$(T,M) = (NX,DX) \qquad (3)$$

where X is a transfer function design matrix. Relationships (2) and (3) are independent of controller structure. Equation (3) shows that there is only a single transfer function design matrix, X, governing Nominal Design.

In practice, designers need to establish how a plant must be controlled and, having established that, verify that the plant can indeed be so controlled. In this paper we want to control output responses (y) of the plant independently with uniquely available plant inputs (u). The condition to do this is that the plant inverse, P^{-1}, must exist. As an additional practical consideration, the plant inverse should exist with good condition so that reasonable margin for control is available. The existence of plant inverses is of paramount importance in both theory and applications and relates closely to characteristics which directly affect successful design, as for example meaningful multivariable control [2], plant trackability [4], multivariable zeros [12], and cancellations and simplifications [2].

When P^{-1} exists, Equation (1a) may be written

$$u = P^{-1}y. \qquad (1a')$$

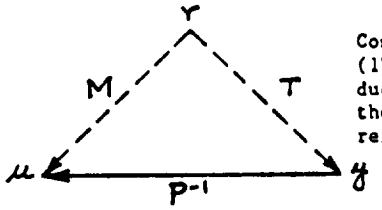

Combining (1a') with (1b) and (1c) produces the diagram on the left and a useful relationship

$$M = P^{-1}T. \qquad (4)$$

Equation (4) is called the synthesis equation. For M and T proper and stable, it displays internally stable causal responses [7]. The synthesis equation is independent of controller structure.

Feedback Synthesis

The Feedback Synthesis problem is concerned with realizations of M, T pairs by specific control dynamics in a specific structure. We take a unity feedback case for our purpose here [18] and omit discussion on feedback path dynamics and sensitivity specifications [23-24]. A unity feedback structure is shown in Figure 2.

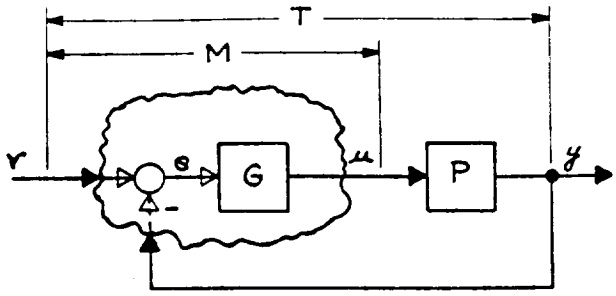

Figure 2.

The overall response of the unity feedback loop is

$$y = (I + PG)^{-1}\, PG\, r. \qquad (5)$$

The desired response is $y = Tr$. Combining these relationships and solving for the controller dynamics matrix G infers

$$G = P^{-1}T(I-T)^{-1} = P^{-1}Q \qquad (6)$$

where Q is a performance matrix defined by $Q = T(I-T)^{-1} = PG$.

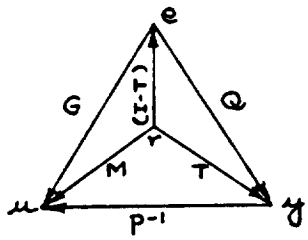

Equation (6) is a design equation. Relationships between design equation (6) and synthesis equation (4) for unity feedback are pictured in the diagram.

A basic question is: Will the specific dynamics generated by the design equation produce internally stable feedback systems? Sain, et. al [18] and Antsaklis and Sain [23-24] have studied and answered this question for unity feedback and for various other systems. In practice, internal stability is checked readily by thorough computer simulations of specific closed loop realizations, which simulations are required anyway to verify performance. For Figure 2, the principal considerations are that M be stable and that no right-half-plane cancellations occur in PG or in GP.

Nonlinear Multivariable Design

A nonlinear multivariable design method, based on TS ideas, is now described and illustrated. Features of the design method include:

1. Input-Output Viewpoint
2. Nominal Design
   - plant evaluation
   - a synthesis equation
   - preselected output response T and control response M
3. Feedback Synthesis
   - unity feedback structure using M and T
   - a design equation
4. Synthesis of Nonlinear Controllers

Nominal Design

The design process begins with identification and evaluation of a given nonlinear plant, such as the turbojet model shown in Figure 5, and follows with Nominal Design. It is necessary to know or to establish the desired steady state operating conditions of the plant and to determine available plant inputs and plant outputs. Then, identification of the nonlinear plant along the selected operating lines provides local plant dynamics and a set of plant transfer function matrices {P(s)} relating inputs and outputs.

The capability of the plant to produce independent output performances using uniquely available inputs can be checked by choosing subsets of square matrices of the plant transfer function matrix and determining the existence and condition of the corresponding set of plant inverse matrices $\{P^{-1}(s)\}$. Now the Nominal Design step can be addressed, using the synthesis equation $M = P^{-1}T$, to display the response possibilities available via M, T pairs. In this paper, we will select output responses, T, and check acceptability of corresponding control responses, M.

Feedback Synthesis

Consider the dynamic behavior of a given, nonlinear plant near its steady state points. More generally, consider a class of nonlinear plants whose dynamic action near steady state points is smooth enough so that the action can be identified or described, essentially, by linear dynamic considerations. An example of such a nonlinear plant is a turbojet engine model shown in Figure 5. We discuss and illustrate a nonlinear control synthesis method for nonlinear plants with the characteristics described above.

A relatively general linear unity feedback system structure which uses the M and T dynamic response concepts of Total Synthesis is shown in Figure 3. This feedback structure provides coordinated feedforward plant inputs, u_r, and plant

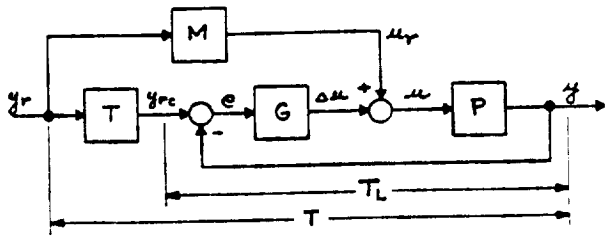

Figure 3.

output reference requests, y_{rc}, to a closed loop control system. The feedforward elements M and T coordinate the request command, y_r; and the closed loop provides accurate steady state tracking and robustness of the plant outputs, y. The chosen and desired system response is designated by T. The selected response of the feedback loop is denoted by T_L.

The salient dynamic elements of the control structure are T, M and G which must be designed to produce desired, designer specified, T and T_L responses. It turns out that two key equations govern local design:

$$M = P^{-1}T, \tag{4}$$

$$G = P^{-1}T_L(I-T_L)^{-1} \tag{7a}$$

$$= P^{-1}Q_L. \tag{7b}$$

Equation (4) is the synthesis equation. It is used to display all admissible (internally stable and causal) responses (T,M) and (T_L,M_L).

Equation (7) is the design equation defining the loop controller dynamics, G, for the control structure in Figure 3. All controller dynamics M, T and G are defined by the synthesis and design equations when a designer selects specific responses T and T_L. Thus two Total Synthesis relationships provide a basis for design of linear multivariable control systems. For other discussion and useful relationships see [1,23-24]. What about nonlinear design?

Nonlinear Synthesis

The fundamental idea for synthesis of nonlinear controller elements to be illustrated here is essentially simple and straightforward. The idea is that families of local linear dynamic descriptions, taken along desired steady state conditions, may be linked and scheduled, as a function of operation conditions, to produce accurate full range nonlinear dynamic action. For example, if a set of linear controllers, obtained by repeated application of design equation (7), gives rise to a family {G} of forward dynamics in the loop, then the goal is to link members of the family together to produce a nonlinear dynamical function g, that is {G} → g. Now each G may be regarded as giving accurate dynamic behavior in some local region of a steady state point. Under reasonable conditions of smoothness, and with enough members in the family, a careful linking must lead to accurate and useful g, over operating regions of interest, which emphasize behavior along lines of setpoints.

To extend this notion, one can choose, along an operating line, sets of desired system output responses {M,T} and loop responses $\{M_L,T_L\}$. From these performance choices, sets of controller matrices {T}, {M}, and {G} can be generated via the synthesis and design equations. All of the linear sets may then be linked and scheduled, as a function of plant condition, to form nonlinear control elements. Thus {T} → t, {M} → m, and {G} → g.

Other functional features needed to structure a nonlinear turbojet engine control system include means to achieve desired steady state operating schedules and means to effect transient control. These features transform the linear system structure in Figure 3 to the nonlinear, unity feedback system structure shown in Figure 4. This unity feedback structure embodies key variables of the Total Synthesis viewpoint, namely t, m, and g, and

provides basic features needed for full-range, nonlinear control. It is used in the turbojet engine design examples which follow.

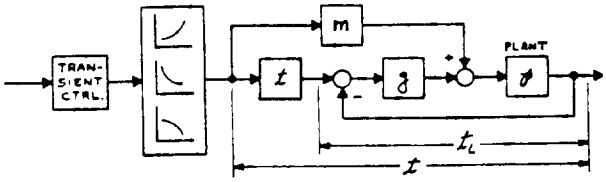

Figure 4.

Nonlinear Design Examples

We illustrate the foregoing synthesis by designing a nonlinear control system for a turbojet engine. In the design examples, unique, independent control of the engine outputs will be demonstrated. Utility of independent control is shown by designs which produce desired and specific output response strategies, with unique, acceptable control inputs. Robustness of the control system to significant plant parameter variations is illustrated also. Performance results are presented by time traces, from hybrid simulations, of system responses for small step commands and for full range step commands.

Nonlinear Turbojet Engine

A nonlinear model of a simple turbojet engine is described by Figure 5. In essence, it is a full range computer simulation constructed by engine manufacturers and provided to engine control designers. The turbojet model consists of three integrators, nine nonlinear functions including five bi-variant functions, nine multipliers and dividers and nine summing junctions. The model describes nonlinear dynamical and steady state relationships between three input variables: fuel flow, W_f, exhaust nozzle area, A_j, and turbine vane position, β, and six outputs: engine speed, N, turbine temperature T, engine thrust, FN, and three other variables. We regard the nonlinear simulation model as a nonlinear function p from a real vector space of control functions of time to a real vector space of plant output response functions of time, y = pu.

For the design examples, three outputs: speed, temperature, and thrust were selected for control by three inputs, fuel flow, nozzle area, and turbine vane. The engine input vector is

$$u' = [W_f, A_j, \beta]$$

and the engine output vector is

$$y' = [N, T, FN].$$

The nonlinear engine model was identified locally at five sea level, standard conditions corresponding to 70%, 80%, 90%, 100% and 110%

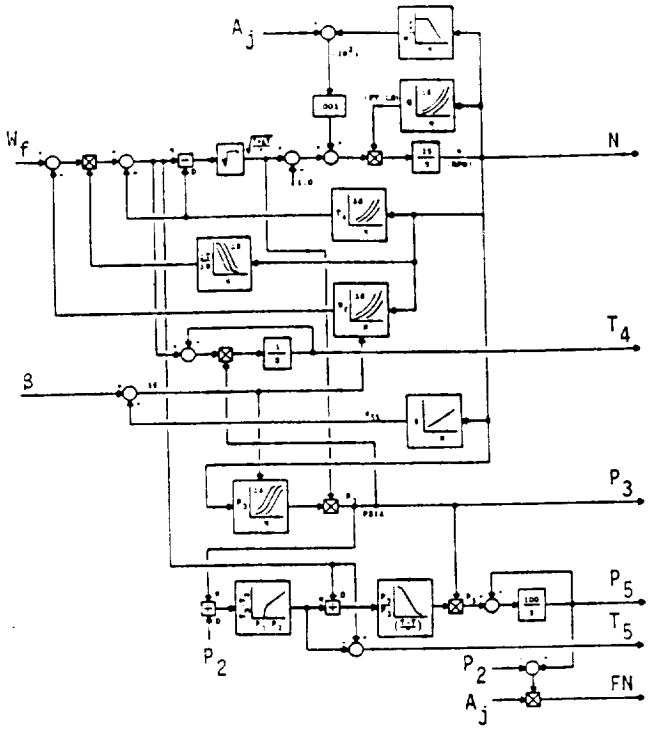

Figure 5.

speed levels. Thus from the nonlinear engine p, a set of five transfer function matrices, {P}, was identified. At 100% speed conditions, the plant transfer function and its inverse were found to be:

$$P(s) = \frac{\begin{bmatrix} 5.4(.01s+1) & 58.1(.01s+1) & -2704(.01s+1) \\ .13(1.5s+1) & -2.7(.50s+1)(.01s+1) & 336(.31s+1) \\ 2.4(.29s+1) & 68.3(.42s+1)(.01s+1) & 951(.01s+1) \end{bmatrix}}{(.50s+1)(.01s+1)}$$

$$P(s)^{-1} = \frac{\begin{bmatrix} .18(.23s+1)(.01s+1) & 1.7(.01s+1)(.007s+1) & -.083(.01s+1) \\ -.005(-.2s+1) & -.08(.01s+1) & .015(.01s+1) \\ -.0001(.74s+1)(.01s+1) & .0017(.01s+1)(.013s+1) & .00015(.01s+1) \end{bmatrix}}{(.009s+1)}$$

Design Strategy

For a turbojet engine, a nice strategy for control is: 1. fast thrust response, 2. smooth temperature response, 3. varied speed response. To be able to influence the engine output response directly and independently, the system is decoupled by specifying T as a diagonal matrix. Plant inverses, $(P(s)^{-1})$, exist with good condition. Therefore, decoupling and independent control of the selected output with the available inputs is possible.

Nominal Design using synthesis equation (4), $M = P^{-1}T$, requires that M be proper and stable. To satisfy this requirement, it turns out, the simplest response form in the elements of T is $t_{ii} = 1/(\tau s+1)$, first order lags. To achieve the control strategy cited above, over the engine operating range from 70% speed to 100% speed, the following local output response elements of T are chosen:

Thrust: $t_{33} = \frac{1}{.2s+1}$ (fast)

Temperature: $t_{22} = \frac{1}{1s+1}$ (smooth)

Speed: $t_{11} = \frac{1}{.5s+1}$ at 70% + $\frac{1}{.2s+1}$ at 100%

These sets of {T} lead to a nonlinear t, {T} → t, of the form shown in Figure 6. This will be the response specification for Example 1.

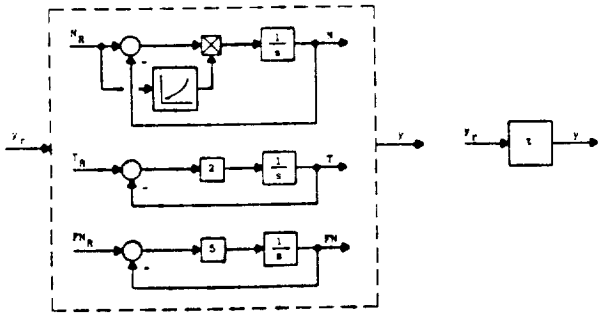

Figure 6.

The response of the closed loop is designed to produce T_L. It is assumed that T_L is a diagonal matrix and the local response of each element is $t_{ii} = 1/(.02s+1)$ over the entire operating range. Thus the closed loop is decoupled and fast acting. Feedback Synthesis of the controller g is accomplished by repeated use of design equation (7), $G = P^{-1}T_L(I-T_L)^{-1} = P^{-1}Q_L$. This obtains the set {G} and then {G} is scheduled to form g. This process produced a nonlinear controller g of the form shown in Figure 7. It will be used in all of the examples.

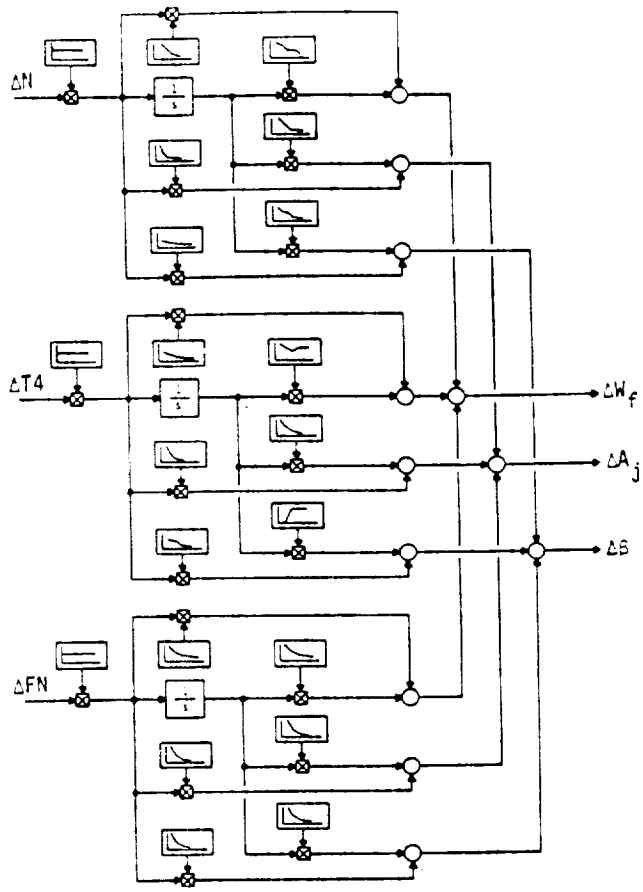

Figure 7.

Design Examples

Performance of control systems (Figure 4) are illustrated by time traces of plant output and plant input responses for small and full range step commands.

Example 1. The engine performance strategy desired is: fast thrust response, smooth temperature response, and a varied speed response. The specified nonlinear output response, t, is given by Figure 6. Plant output and control action re-

sponses for small step commands are shown in Figures 8 and 9 respectively. The output response performance is achieved with reasonable control action. Full range acceleration and deceleration transients are shown in Figures 10 and 11.

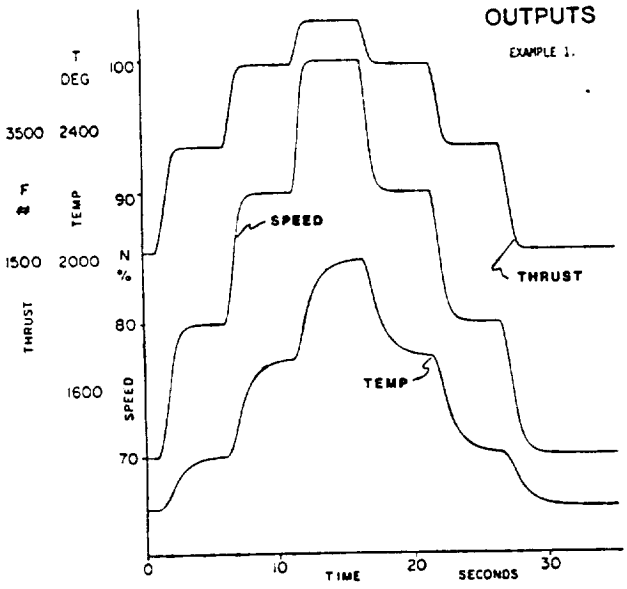

Figure 8.

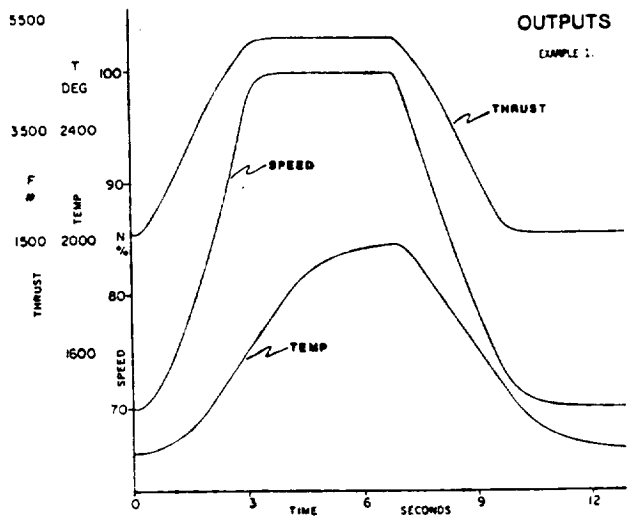

Figure 10.

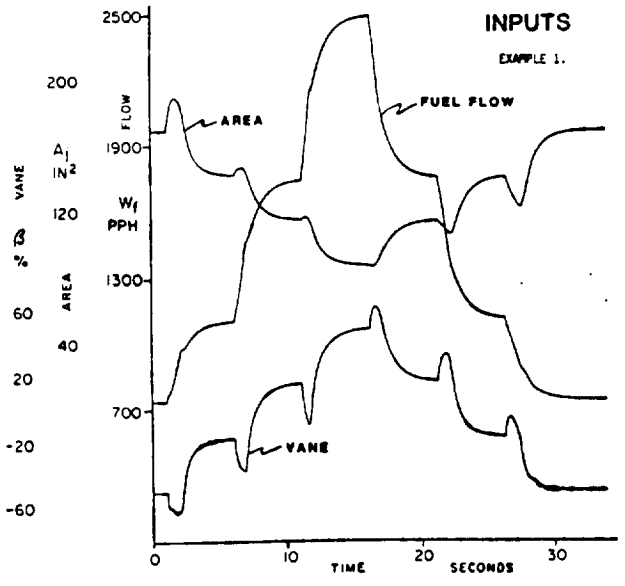

Figure 9.

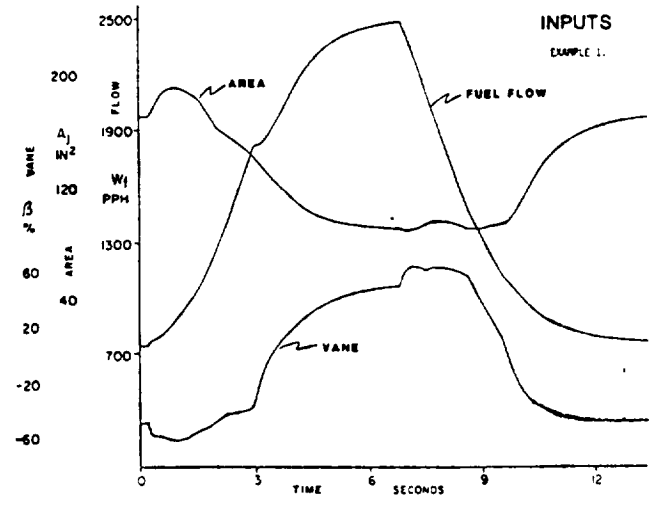

Figure 11.

Example 2. At this point the designer may choose many other response options. For instance, instead of varying the speed response as in Example 1, choose the speed response to be constant over the range such that $t_{11} = 1/(.3s+1)$. Keep $t_{22} = 1/(1s+1)$ and $t_{33} = 1/(.2s+1)$. Thus the response strategy is the same except that the local speed response is constant over the full range. Output response performance is shown in Figure 12.

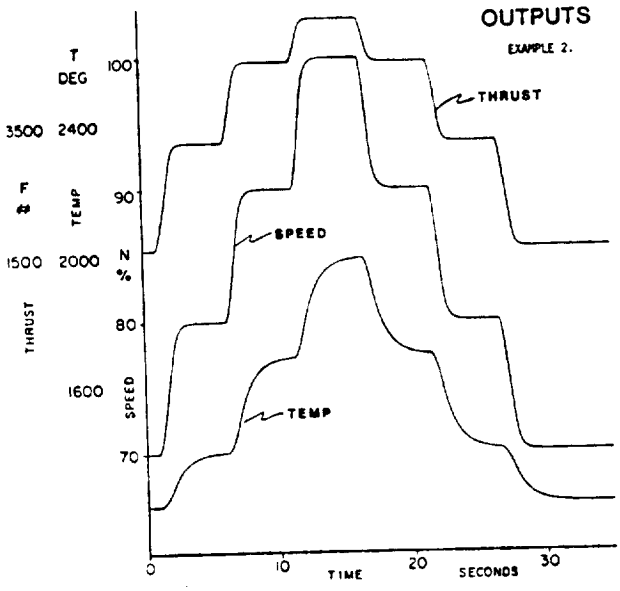

Figure 12.

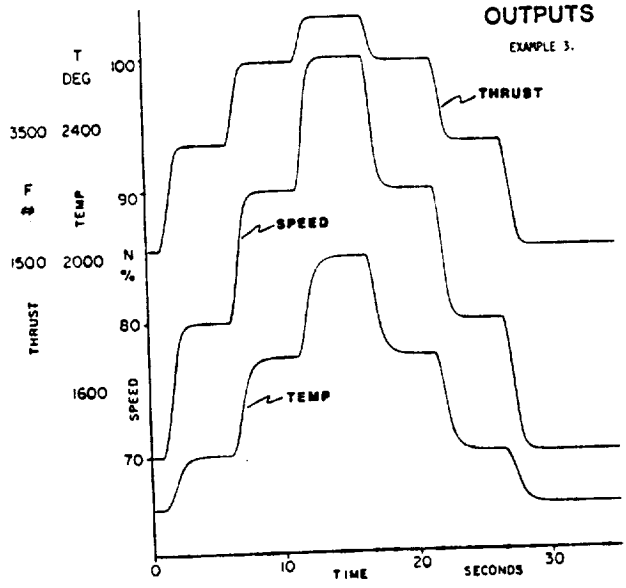

Figure 13.

Example 3. Keep the strategy in Example 2, but speed up the relative response of the temperature to $t_{22} = 1/(.5s+1)$ from $1/(1s+1)$. Small step command output response is shown in Figure 13.

Example 4. To show versatility, we imagine that the designer wishes to "flick carbon off the turbine blades" and selects the speed response to be oscillatory at 5 radians per second with a damping ratio of .25, $t_{11} = 1/(.04s^2 + 10s+1)$. The temperature and thrust responses need to be maintained as 1 second and .2 second lags respectively. The output transients are shown in Figure 14. Control action performance is shown in Figure 15.

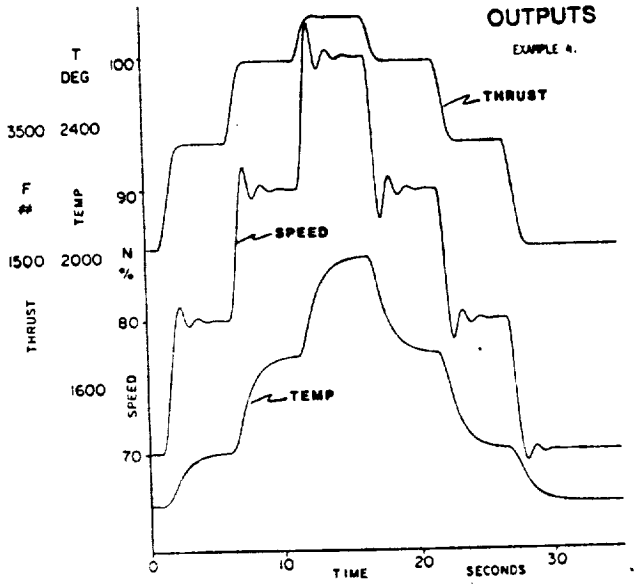

Figure 14.

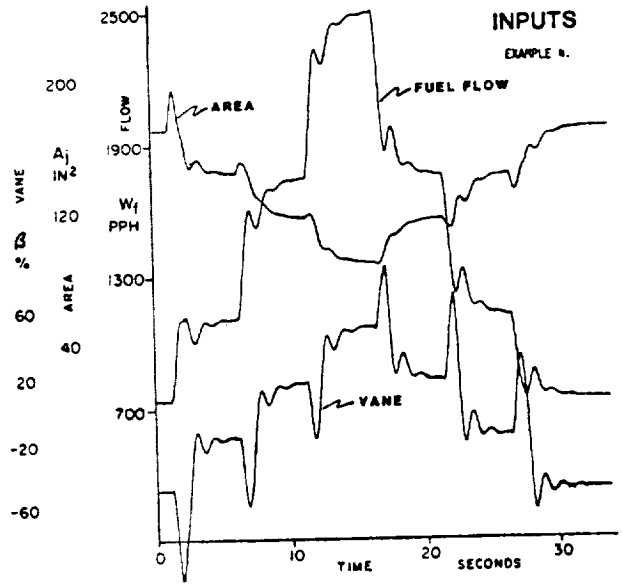

Figure 15.

Example 5. Robustness of the controller relative to engine parameter variation is shown. The engine time constants on speed, temperature and tailpipe pressure were slowed by a factor of 2. This is a large variation of jet engine parameters and is a good test of control robustness. The response strategy from Example 2 is chosen as the desired output response performance. Time transients comparing the plant output responses for the nominal engine and the slow engine are shown in Figures 16 and 17. Note that the controller maintains output performance at the desired conditions. Corresponding responses of the control action are shown in Figures 18 and 19. The controller keeps output responses at the desired condition but produces substantially different control action for the slow engine, as needed.

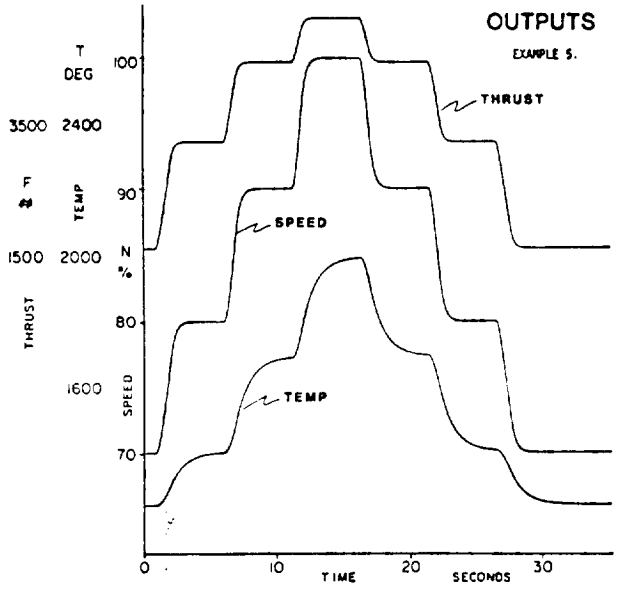

Figure 16.

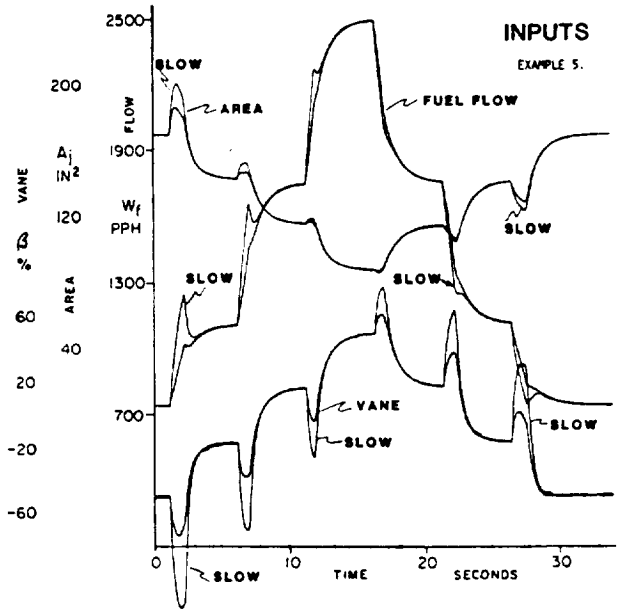

Figure 18.

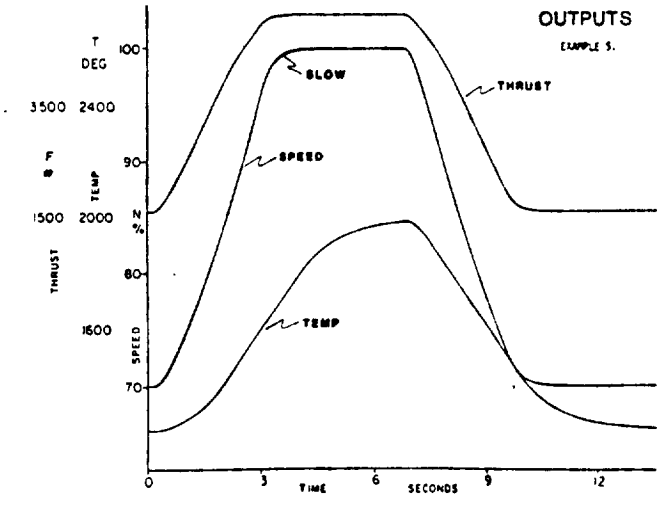

Figure 17.

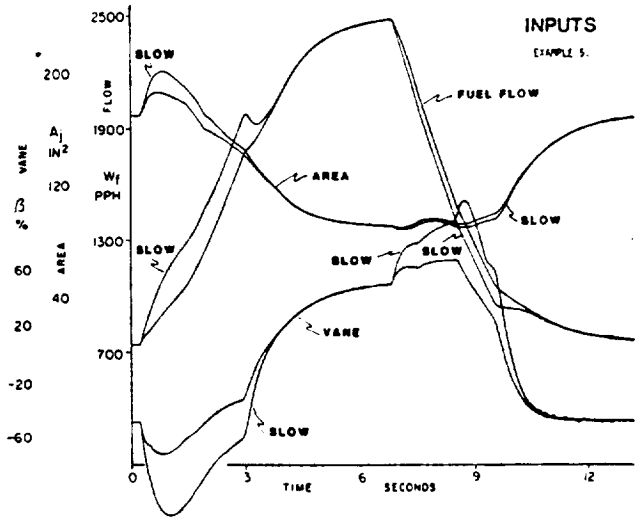

Figure 19.

Example 6. Here we change the strategy and choose to specify all output responses to be fast to match the thrust. Thus t is a diagonal matrix with all first order lags and the time constants are .2 seconds over the full range. The response of the system to small step inputs is shown in Figures 20 and 21. The responses of the system to full range transients are pictured in Figures 22 and 23.

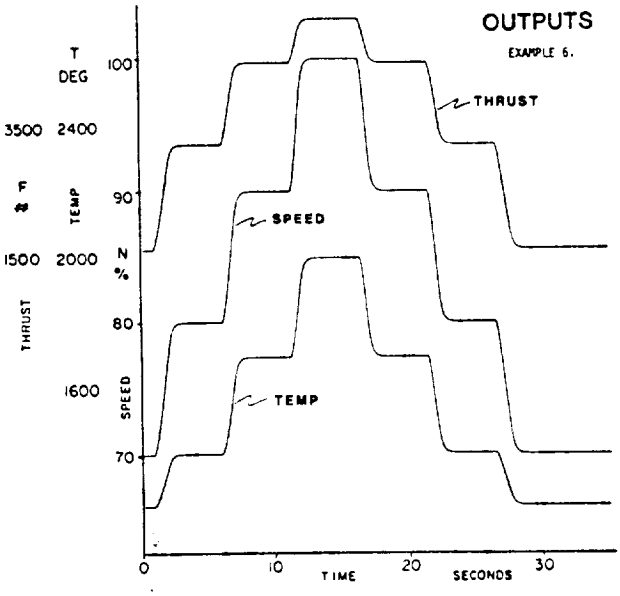

Figure 20.

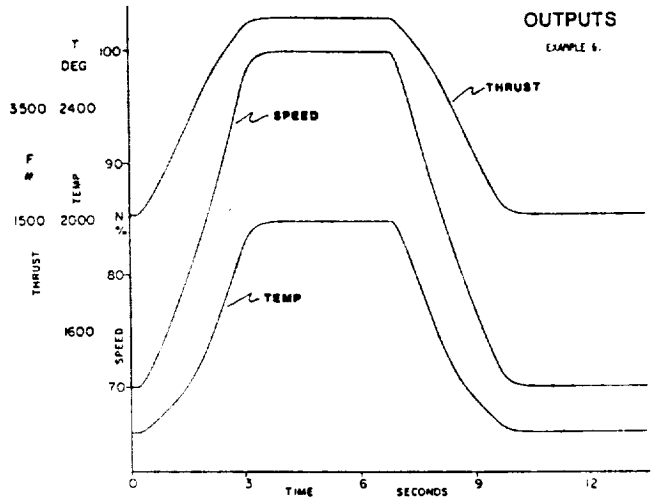

Figure 22.

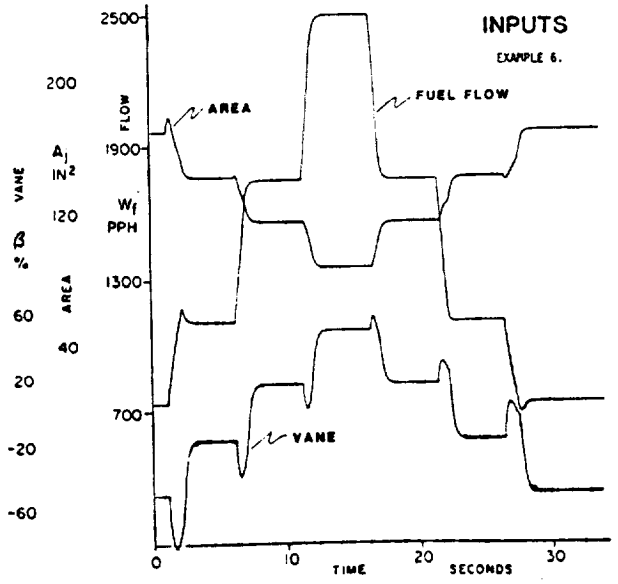

Figure 21.

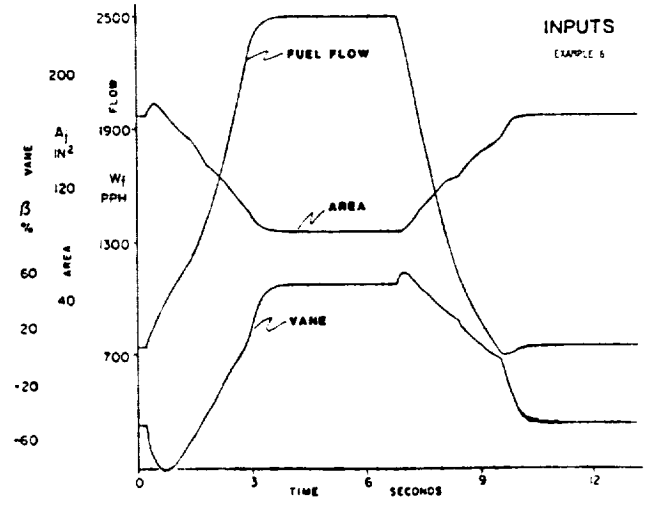

Figure 23.

D 33 (over)

Summary Remarks

A nonlinear, multivariable control design method, based on Total Synthesis ideas, was discussed and illustrated. Emphasis was placed on application viewpoint and a nonlinear synthesis technique which produced designer specified response performance.

Total Synthesis is a top-down strategy of Nominal Design and Feedback Synthesis. Nominal Design, the first step in the design process, depends on plant characteristics only. Feedback Synthesis, the second step in the design process, depends on controller structure. Unity feedback structure was highlighted in this paper.

Control systems were designed for six illustrative examples to demonstrate various, desired nonlinear output response strategies and selected, local output response performance.

Acknowledgment

The authors acknowledge the support and contribution of Mr. Ben Jacobs, Allied-Bendix Energy Controls Division, for simulation of the design examples on an AD-10 hybrid computer.

References

1. J.L. Peczkowski and M.K. Sain, "Linear Multivariable Synthesis with Transfer Functions", in Alternatives for Linear Multivariable Control, M.K. Sain, J.L. Peczkowski, and J.L. Melsa, Eds. Chicago: National Engineering Consortium, 1978, pp. 71-87.
2. J.L. Peczkowski, M.K. Sain, and R.J. Leake, "Multivariable Synthesis with Inverses", Proceedings Joint Automatic Control Conference, pp. 375-380, 1979.
3. J.L. Peczkowski, "Multivariable Synthesis with Transfer Functions", Proceedings Propulsion Controls Symposium, NASA Conference Publication 2137, pp. 111-128, May 1979.
4. R.J. Leake, J.L. Peczkowski, and M.K. Sain, "Step Trackable Linear Multivariable Plants", International Journal on Control, Volume 30, Number 6, pp. 1013-1022, December 1979.
5. J.L. Peczkowski, "Total Multivariable Synthesis with Transfer Functions", Proceedings Bendix Controls and Control Theory Symposium, pp. 109-126, April 1980.
6. M.K. Sain, A. Ma, and D. Perkins, "Sensitivity Issues in Decoupled Control System Design", Proceedings Southeastern Symposium on System Theory, pp. 25-29, May 1980.
7. R.R. Gejji, "On the Total Synthesis Problem of Linear Multivariable Control", Ph.D. Thesis, Department of Electrical Engineering, University of Notre Dame, May 1980.
8. J.L. Peczkowski and M.K. Sain, "Control Design with Transfer Functions, An Application Illustration", Proceedings Midwest Symposium on Circuits and Systems, pp. 47-52, August 1980.
9. M.K. Sain and A. Ma, "Multivariable Synthesis with Reduced Comparison Sensitivity", Proceedings Joint Automatic Control Conference, Paper WP-8B, August 1980.
10. J.L. Peczkowski and S.A. Stopher, "Nonlinear Multivariable Synthesis with Transfer Functions", Proceedings Joint Automatic Control Conference, Paper WA-8D, August 1980.
11. M.K. Sain, R.M. Schafer, and K.P. Dudek, "An Application of Total Synthesis to Robust Coupled Design", Proceedings Allerton Conference on Communication, Control, and Computing, pp. 386-395, October 1980.
12. B.F. Wyman and M.K. Sain, "The Zero Module and Essential Inverse System", IEEE Transactions on Circuits and Systems, Volume CAS-27, Number 2, pp. 112-126, February 1981.
13. J.L. Peczkowski and M.K. Sain, "Scheduled Nonlinear Control Design for a Turbojet Engine", Proceedings IEEE International Symposium on Circuits and Systems, pp. 248-251, April 1981.
14. B.A. Jacobs and J.L. Peczkowski, "Nonlinear Multivariable Systems Simulation", Proceedings 12th Annual Pittsburgh Conference on Modeling and Simulation, May 1981.
15. M.K. Sain and J.L. Peczkowski, "An Approach to Robust Nonlinear Control Design", Proceedings Joint Automatic Control Conference, Paper FA-3D, June 1981.
16. M.K. Sain, B.F. Wyman, R.R. Gejji, P.J. Antsaklis, and J.L. Peczkowski, "The Total Synthesis Problem of Linear Multivariable Control, Part I: Nominal Design", Proceedings Joint Automatic Control Conference, Paper WP-4A, June 1981.
17. P.J. Antsaklis and M.K. Sain, "Unity Feedback Compensation of Unstable Plants", Proceedings IEEE Conference on Decision and Control, pp. 305-308, December 1981.
18. M.K. Sain, P.J. Antsaklis, B.F. Wyman, R.R. Gejji, and J.L. Peczkowski, "The Total Synthesis Problem of Linear Multivariable Control, Part II: Unity Feedback and the Design Morphism", Proceedings 20th IEEE Conference on Decision and Control, pp. 875-884, December 1981.
19. J.L. Peczkowski and M.K. Sain, "Nonlinear Multivariable Design by Total Synthesis", Proceedings American Control Conference, pp. 252-260, June 1982.
20. M.K. Sain and R.M. Schafer, "A Computer-Assisted Approach to Total Feedback Synthesis", Proceedings American Control Conference, pp. 195-196, June 1982.
21. M. Sain and S. Yurkovich, "Controller Scheduling: A Possible Algebraic Viewpoint", Proceedings American Control Conference, pp. 261-269, June 1982.
22. K.P. Dudek, M.K. Sain, and B.F. Wyman, "Module Considerations for Feedback Synthesis of Sensitivity Comparisons", Proceedings Allerton Conference on Communication, Control, and Computing, October 1983.
23. P.J. Antsaklis and M.K. Sain, "Feedback Controller Parameterizations: Finite Hidden Modes and Causality", in Multivariable Control: New Concepts and Tools, S. Tzafestas, Ed. Dordrecht, Holland: D. Reidel, 1984.
24. P.J. Antsaklis and M.K. Sain, "Feedback Synthesis with Two Degrees of Freedom: {G,H;P} Controller", 9th IFAC Triennial World Congress, June 1984.

SYNTHESIS OF SYSTEM RESPONSES: A NONLINEAR MULTIVARIABLE CONTROL DESIGN APPROACH

Joseph L. Peczkowski
Energy Controls Division
Allied-Bendix Aerospace
South Bend, Indiana 46620

Michael K. Sain
Electrical Engineering Department
University of Notre Dame
Notre Dame, Indiana 46556

ABSTRACT

The idea of specifying desired system responses has resulted in a new approach for design of multivariable control systems. A unique feedback controller structure, using coordinated feedforward and feedback dynamics, is presented and discussed. The method offers designer insight into plant dynamics and offers influence and choices over system responses. Responses are specified and control dynamics are obtained at local conditions along desired steady state control paths. Linear designs are linked to form nonlinear control law dynamics. The method is illustrated by simulations.

INTRODUCTION

Acceptable response is a hallmark of successful design for multivariable control systems. The work reported here is part of a continuing effort [1-9] by the authors to formulate theoretical and practical views concerning nonlinear multivariable synthesis and design.

This paper discusses a multivariable control design approach with emphasis on application aspects of system response. A companion paper by the authors in these Proceedings, titled "Nonlinear Control by Coordinated Feedback Synthesis, with Gas Turbine Applications", discusses theoretical and other aspects of nonlinear synthesis.

Here we discuss a control approach and philosophy which linearizes the plant at a finite number of points over the envelope of operation, which applies linear transfer function synthesis techniques about each point to obtain desired output responses and acceptable control responses, which systematically links and schedules all local designs together into a global design over the envelope as a function of key plant variables within a broad nonlinear design strategy. The synthesis approach is based on three matrix design equations which show how a controller is related to the given plant, the desired response performance and the selected controller structure.

LINEAR SYNTHESIS

In this section we describe and illustrate a design method called Total Synthesis [6, 7, 8, 9] which consists of two basic parts and steps: 1. Nominal Design and 2. Feedback Synthesis. Nominal Design, the first step, depends on plant characteristics only and is independent of controller structure. Feedback Synthesis, the second step, depends on the specific controller structure chosen for realizing the feedback loop.

The purpose here is to apply Total Synthesis to design linear feedback controllers which achieve preselected, attainable plant output responses, $y = Tr$, and acceptable control responses, $u = Mr$, in the manner illustrated by Figure 1 below.

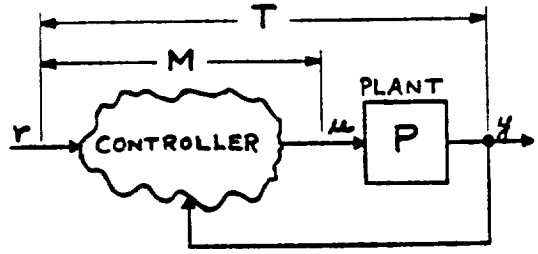

Figure 1.

The objective is to obtain a design method which allows the designer, at the outset, choices for selection of attainable responses (M, T) for the closed loop system, and provides insight into the performance choices available so that the designer may directly influence the desired performance outcome.

The significance of Nominal Design is that the first step evaluates the plant and defines the attainable system responses which the plant can produce. This is vital for design because when the classes of attainable plant responses are known at the outset, then one can more successfully ask for, and get, acceptable system performance. The second step, Feedback Synthesis, is concerned with realizations of (M, T) pairs by control dynamics with specific feedback configurations.

Synthesis for Output Response

The basic notion of multivariable control synthesis to obtain desired output response is straightforward and easy to understand. Consider Figure 2, a block diagram for a negative feedback multivariable structure with no disturbances. References, error, plant input and plant output are designated r, e, u and y respectively. Assume the plant has equal numbers of inputs and outputs; thus

D3.2.3

P(s) is a square matrix of transfer functions. The assumption is not nearly as restrictive as one might suppose at the outset: more on this later. The controller G(s) is also square.

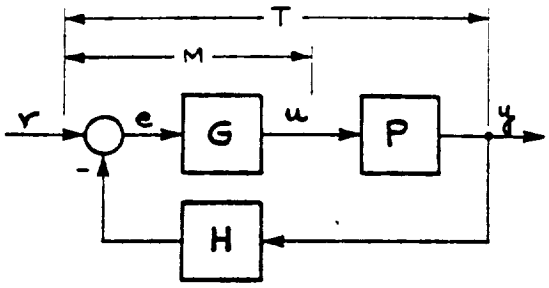

Figure 2.

The problem, given plant P(s), is to design a controller G(s) to achieve desired, internally stable, closed loop response T(s) as indicated in Figure 2. The objective is to design G(s) so that closed loop response T(s) is achieved in such a way that designer choices, insight and influence are available and accessible. References [1-4] can provide more details for the interested reader.

A Design Equation

From Figure 2, the total response of the unity feedback loop is

$$y = (I + PGH)^{-1}PGr. \qquad (1)$$

The desired response is

$$y = Tr. \qquad (2)$$

Combining equations (1) and (2) and solving for G gives the controller

$$G = P^{-1}T(I - HT)^{-1}. \qquad (3)$$

This equation may be written in a convenient, compact form

$$G = P^{-1}Q \qquad (4)$$

where Q, a performance matrix, is defined by $Q = T(I - HT)^{-1}$. Equation (4) is named the design equation for the feedback structure of Figure 2. The design equation simply and clearly indicates that controller design focuses upon the properties of the plant inverse and how they interact with Q(s), the performance matrix. Does the existence of the plant inverse pose a serious restriction for transfer function design?

The Plant Inverse

Fortunately, the need for existence of the plant inverse turns out to be a very useful property for control synthesis. The plant inverse establishes and displays vital plant characteristics needed to effect successful closed loop control design. Four system and plant features are established and identified by the plant inverse transfer function:

1. meaningful multivariable control [10].
2. plant trackability [11].
3. multivariable plant zeros [12].
4. cancellations and simplifications [1-4].

Existence of the plant inverse assures conditions needed to effect synthesis and design.

Feedback Synthesis

From the foregoing discussion it appears to be possible to design control dynamics G(s), by applying design equation (4) so that desired closed loop output response is achieved. Some conditions and restrictions on the output response are needed if internal loop stability is to be assured. In this section, a synthesis equation is developed which displays all attainable control response and output response transfer function matrices for which internally stable, feedback realizations exist [11].

Consider Figure 3 where r denotes request, u denotes control action, and y denotes response. Under broad assumptions, there exist linear operators T : R -> Y

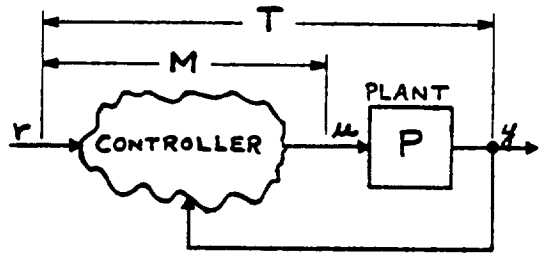

Figure 3.

and M : R -> U, where R, U, and Y may be understood as R(s)-vector spaces of finite dimension such that:

$$y = Tr \text{ and } u = Mr. \qquad (5)$$

The plant can be understood in terms of an operator P : U -> Y, such that

$$y = Pu\ . \qquad (6)$$

Combining equations (5) and (6) obtains the relationship

$$T = PM\ . \qquad (7)$$

Bengtsson [13] proved that internally stable feedback realizations of systems depicted by Figure 3 exist if and only if M is proper and stable and T is proper and stable.

More important than (7) is the equation which results when P is inverted, namely

$$M = P^{-1}T\ . \qquad (8)$$

We highlight (8) and call it the synthesis equation.

The idea is, for given plant P, to select proper and stable T so that M is also proper and stable. This insures existence of internally stable controllers. The synthesis equation displays all possible responses T which have internally stable feedback realizations. When T is selected, design equation (4) may be applied. What about the choice for the feedback dynamics H(s)? Is it possible to impose a sensitivity requirement on the closed loop in addition to the response requirements and thus synthesize both response and sensitivity?

Synthesis for Response and Sensitivity

This section is based on ideas and concepts reported by Perkins & Cruz [14] & Sain & Ma [15]. The purpose of this section is to obtain design equations to achieve both desired dynamic response, T, and desired sensitivity, S. The specification of T has to do with tracking, regulation, transient response, decoupling or nondecoupling and steady state values. The specification of S involves the extent to which the specification, T, is to deviate from nominal conditions under parametric variation in the plant.

The Perkins-Cruz idea is to compare the parametric variation effect on the response of a feedback system with a corresponding effect of the same variation on an open loop system, where both are designed to achieve the same nominal response. This means that when plant parameters are not equal to the nominal values, as is usually the case, both the open loop and closed loop systems fail to meet the total synthesis response specification T(s). This situation produces two response error matrices: the open loop error, EOL, and a closed loop error, ECL.

A remarkable thing is that there exists a comparison sensitivity matrix relating closed loop error to open loop error:

$$ECL = S(s, a)\, EOL \tag{9}$$

where

$$S(s, a) = (I + P(s, a)GH)^{-1} . \tag{10}$$

We highlight (10) and refer to S as the comparison sensitivity matrix.

The goal is to arrange the design so that the closed loop error, ECL, is more acceptable than the open loop error EOL. Then the feedback configuration is said to "reduce" parameter sensitivity with respect to the open loop configuration, which is taken as the reference.

Equation (10) provides the link needed to specify both output response and comparison sensitivity performance requirements simultaneously for synthesis of multivariable feedback systems. For the closed loop system in Figure 4, the following equations now apply:

$T = (I + PGH)^{-1}PG$ response matrix (11)

$S = (I + PGH)^{-1}$ comparison sensitivity (12)

$Q = PG$ performance matrix (13)

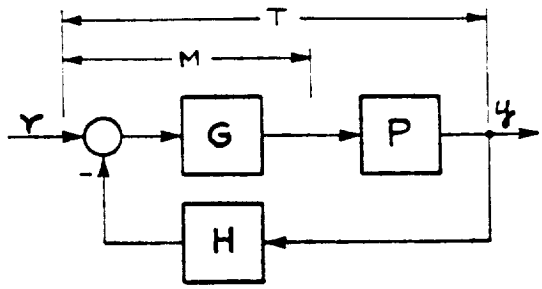

Figure 4.

Combining equations (11), (12) and (13) obtains a new relationship for the performance matrix.

$$Q = PG = S^{-1}T . \tag{14}$$

Thus the performance matrix is a function of response T and comparison sensitivity S. Using (14) to solve for G and H gives:

$$G = P^{-1}S^{-1}T \tag{15}$$

and

$$H = T^{-1}(I - S) . \tag{16}$$

Equations (15) and 16) are highlighted as the design equations for the forward and feedback controller dynamics respectively for the output feedback structure in Figure 4. They express controller dynamics in terms of the response matrix and comparison sensitivity matrix only.

It is interesting to picture these design equations in a block diagram and note that the feedback system in Figure 4 is transformed into a feedback system expressed only in terms of the response and sensitivity matrices. This diagram, Figure 5, clearly shows that when T and S are specified, in effect, the dynamics of the forward and feedback paths are determined explicitly.

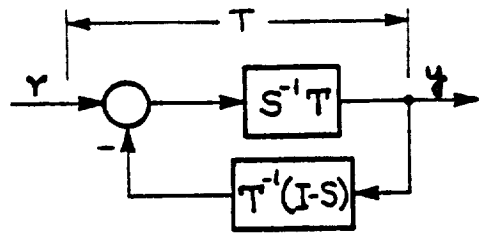

Figure 5.

Three Basic Equations

In summary, three relationships form the basis for an approach to synthesize multivariable controls:

- synthesis equation $M = P^{-1}T$ (8)

- design equation $G = P^{-1}Q = P^{-1}S^{-1}T$ (15)

- design equation $H = T^{-1}(I - S)$ (16)

These ideas are next extended to nonlinear design.

NONLINEAR SYNTHESIS

As we have seen, Total Synthesis, for the linear multivariable case, gives the capability to design internally stable feedback control systems which achieve prescribed control and output responses and also specified sensitivity. In this Section we apply and extend the Total Synthesis concepts for global, nonlinear control. The goal is to design nonlinear multivariable controllers to obtain prescribed performance.

Feedforward-Feedback Synthesis

Consider the dynamic behavior of a nonlinear plant near its steady state points. Real, physical plants are generally nonlinear, but almost always exhibit linear dynamic behavior in neighborhoods of operating lines. We consider such classes of nonlinear plants in this paper. An example on this class is the nonlinear turbojet engine model described in Figure 8. Our objective is to apply Total Synthesis ideas to design nonlinear control systems.

For small signal action of the nonlinear control system, the following feedforward-feedback structure is proposed:

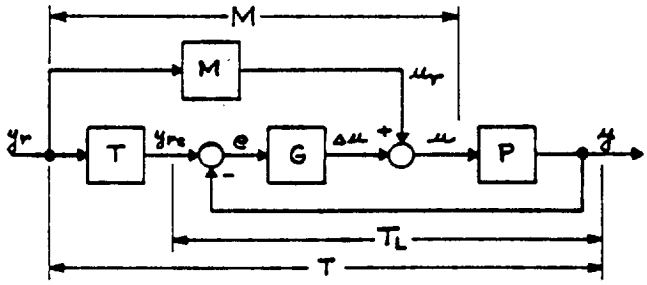

Figure 6.

The controller configuration is arranged so that feedforward, open loop controllers M and T act to produce M and T response action directly and the feedback controller loop action trims any errors which are generated. A separation principle is imposed on the feedforward and feedback actions. That is to say, the feedforward elements are required to produce directly the desired (M, T) response pair and the feedback loop is required to track the y_r command signal.

This control configuration defines separated, unique, coordinated feedforward and feedback controllers. Moreover, the dynamics of the feedforward elements are exactly the dynamics of the desired control response, M(s), and the desired output response, T(s). Also, the independence of the feedback loop response, T_L, due to the separation principle,is an added beneficial feature for robust design. We extend these ideas to the nonlinear case in the following.

Nonlinear Synthesis

Assume a given nonlinear plant p, and assume that identification of its dynamics in local neighborhoods along steady state operating lines gives rise to a set of plant transfer function matrices {P(s)}. That is p -> {P} and from {P} -> $\{P^{-1}\}$, the set of plant inverses is calculated. The question is do the sets {P} and $\{P^{-1}\}$ contain sufficient information to define accurately and to reconstruct the dynamic action of the nonlinear plant and the inverse along its operating line? When the answer is yes, nonlinear controller dynamics can be designed systematically using Total Synthesis concepts.

If repeated application of design equation (15) leads to a family {G} of forward dynamics, the goal is to link members of the family together to produce a nonlinear controller g, that is {G} -> g. Now each G is regarded as giving accurate dynamic behavior in some local region of a steady state point. Therefore, under reasonable conditions of smoothness, and with sufficient members in the family, a careful linking of the set must lead to accurate and useful g over operating regions of interest.

Continuing this notion, one chooses, along the operating line, sets of desired system responses {M, T} and desired loop responses $\{M_L, T_L\}$. From these performance choices, sets of linear controller matrices {T}, {M}, {G} and {H} can be generated via synthesis equation (8) and design equations (15) and (16). Then, all of the linear control sets may be linked and scheduled, as a function of plant condition, to form nonlinear control elements: {T} -> t, {M} -> m, and {G} -> g.

Using the foregoing philosophy, the linear feedforward-feedback structure in Figure 6 may be extended to the nonlinear case. Adding features needed to achieve desired steady state output schedules, and means to effect transient control, transforms the linear structure in Figure 6 to the nonlinear structure shown in Figure 7. The structure embodies key variables and concepts of the Total Synthesis viewpoint, namely: t, m and g, and provides support features needed for full-range, nonlinear control. This structure will be used in the turbojet engine design examples which follow.

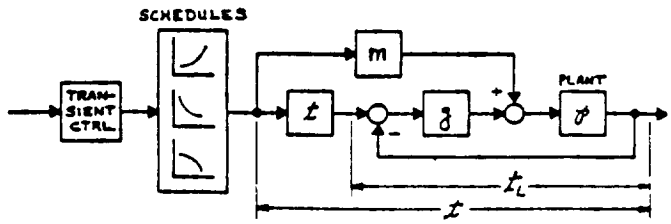

Figure 7.

NONLINEAR EXAMPLES

We illustrate the foregoing synthesis by designing nonlinear control systems for a turbojet engine. Unique, independent control of the engine outputs is demonstrated. Utility of independent control is shown by designs which produce desired and specific output response strategies, with unique, acceptable control inputs. Robustness of the control system to significant plant parameter variations is illustrated also. Performance results are presented by time traces, from hybrid simulations, of system responses for small step commands and for full range step commands.

Nonlinear Turbojet Engine

A nonlinear model of a simple turbojet engine is described by Figure 8. The model describes nonlinear dynamical and steady state relationships between three input variables: fuel flow, W_f, exhaust nozzle area, A_j, and turbine vane position, β, and six outputs: engine speed, N, turbine temperature, T, engine thrust, FN, and three other variables. We regard the nonlinear simulation model as a nonlinear function p from a real vector space of control functions of time to a real vector space of plant output response functions of time, y = pu.

For the design examples, three outputs: speed, temperature, and thrust were selected for control by three inputs. The engine input vector is $u' = [W_f, A_j, \beta]$ and the engine output vector is $y' = [N, T, FN]$.

The nonlinear engine model was identified locally at five sea level, standard conditions corresponding to 70%, 80%, 90%, 100, and 110% speed levels. At 100% speed conditions, the plant transfer function and its inverse were found to be:

$$P(s) = \frac{\begin{bmatrix} 5.4(.01s+1) & 56.1(.01s+1) & -2704(.01s+1) \\ .13(1.5s+1) & -2.7 & 336(.31s+1) \\ 2.4(.29s+1) & 68.3(.42s+1)(.01s+1) & 951(.78s+1) \end{bmatrix}}{(.50s+1)(.01s+1)}$$

$$P(s)^{-1} = \frac{\begin{bmatrix} .18(.23s+1)(.01s+1) & 1.7(.01s+1)(.007s+1) & -.063(.01s+1) \\ -.005(-.2s+1) & -.08(.01s+1) & .015(.01s+1) \\ -.0001(.74s+1)(.01s+1) & .0017(.01s+1)(.013s+1) & .00015(.01s+1) \end{bmatrix}}{(.009s+1)}$$

Synthesis Strategy

For a turbojet engine we consider two possible response strategies: 1. fast thrust response, smooth temperature response, varied speed response, and 2. uniform response of all engine outputs to keep system transients near the steady state. We shall demonstrate both strategies. Plant inverses, $\{P^{-1}\}$, at all steady states exist with good condition; therefore, independent control of the selected outputs is attainable. To be able to influence the response of each output separately, we shall specify T as a diagonal matrix.

Nominal design using synthesis equation (8), $M = P^{-1}T$, requires that M be proper and stable. To satisfy this requirement, the simplest response forms for the elements of T may be chosen as first order lags, $t_{ii} = 1/Ts+1$. This may be seen by noting the form of the plant inverse transfer function given above. To achieve control strategy 1 cited above, over the operating range from 70% speed to 100% speed, the following dynamics for the output elements of T are chosen:

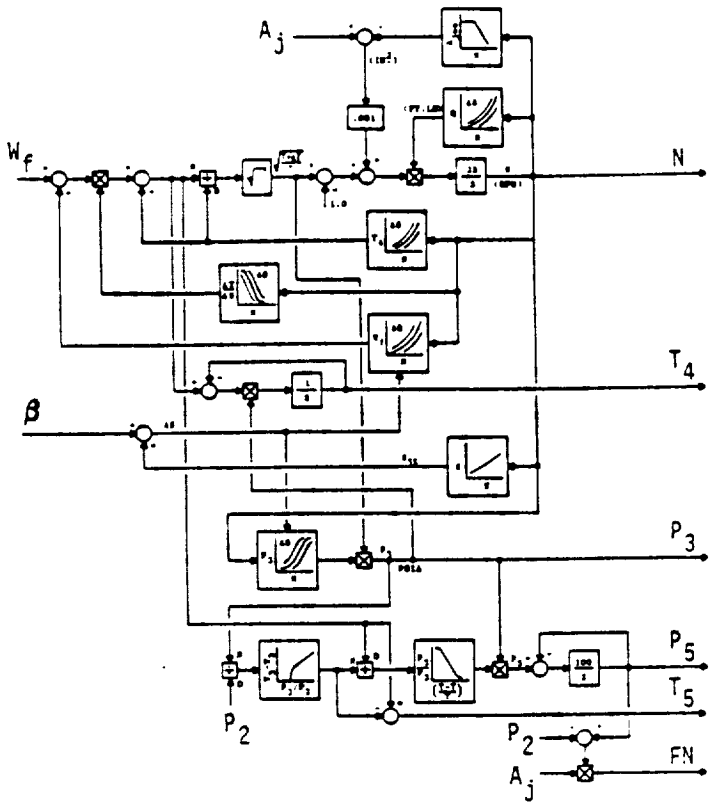

Figure 8.

Speed:(varied) $t_{11} = \frac{1}{.6s+1}$ @70% to $\frac{1}{.3s+1}$ @100% N

Temperature:(smooth) $t_{22} = \frac{1}{1s+1}$

Thrust:(fast & varied) $t_{33} = \frac{1}{.4s+1}$ @70% to $\frac{1}{.2s+1}$ @100% N

These specifications form a set of responses {T} which lead to a nonlinear, diagonal t shown in Figure 9. This will be the response specification for Example 1 using the control structure in Figure 7.

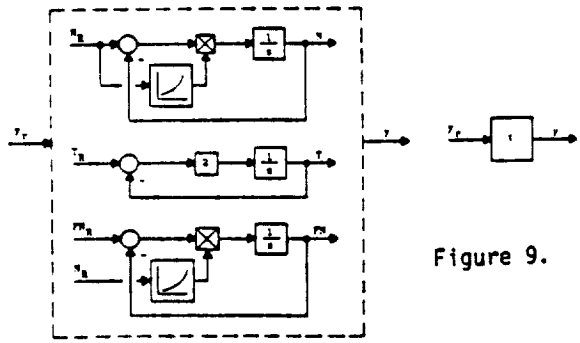

Figure 9.

The response of the closed loop in Figure 7 is designed to produce t_L. We choose to make T_L a diagonal matrix and we set the response of each element to be 1/(.02s+1) over the entire operating range. This unity feedback loop is fast acting and has diagonal sensitivity S_L whose elements are $s_{ii} = .02s/(.02s+1)$ in accordance with design equation (16).

Synthesis of the nonlinear controller g is accomplished by repeated use of design equation (15). This obtains a set {G} which is scheduled to make a g of the form shown in Figure 10.

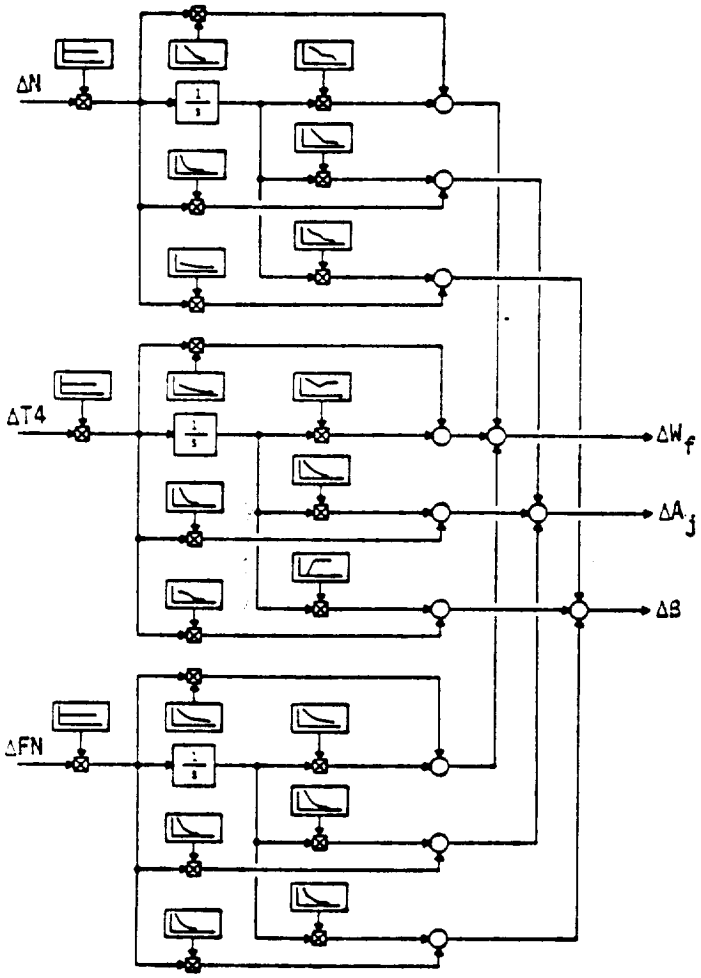

Figure 10.

Design Examples

Performance of the nonlinear control systems (Figure 7) are illustrated by time traces of plant output and plant input responses for small and full range step commands.

Example 1. Execute engine performance strategy 1, namely: fast, varied thrust response, smooth, constant temperature response and nominal, varied speed response. The specifications for this nonlinear response, t, are given by Figure 9. Engine output and control action responses for small step commands are shown in Figures 11 and 12 respectively. Full range acceleration and deceleration transients are shown in Figures 13 and 14. Desired output response performance is achieved with acceptable control action.

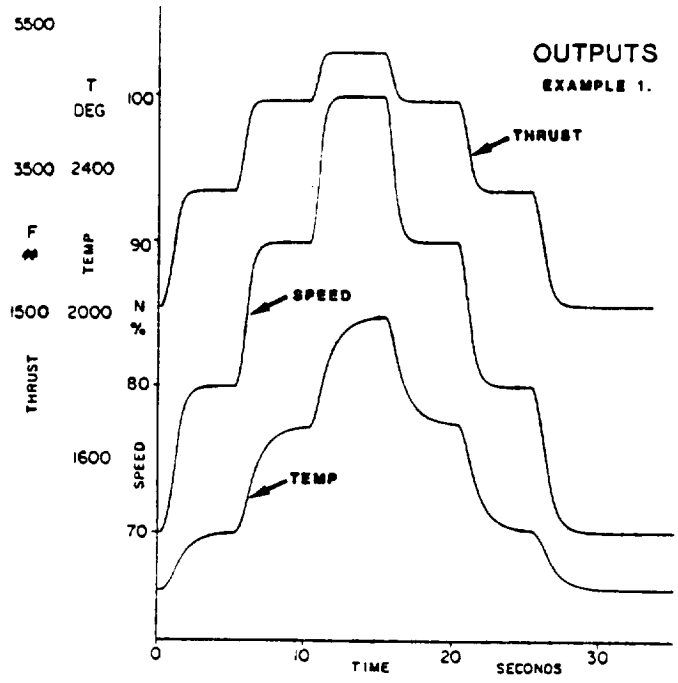

Figure 11.

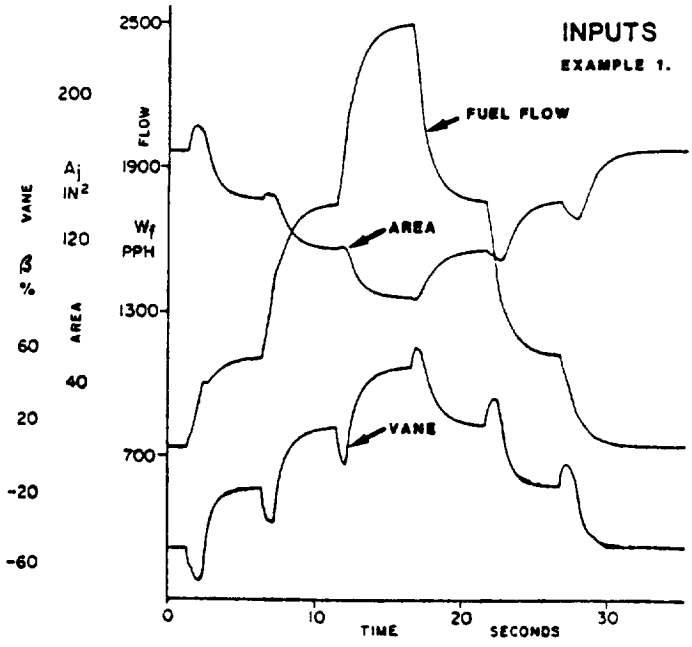

Figure 12.

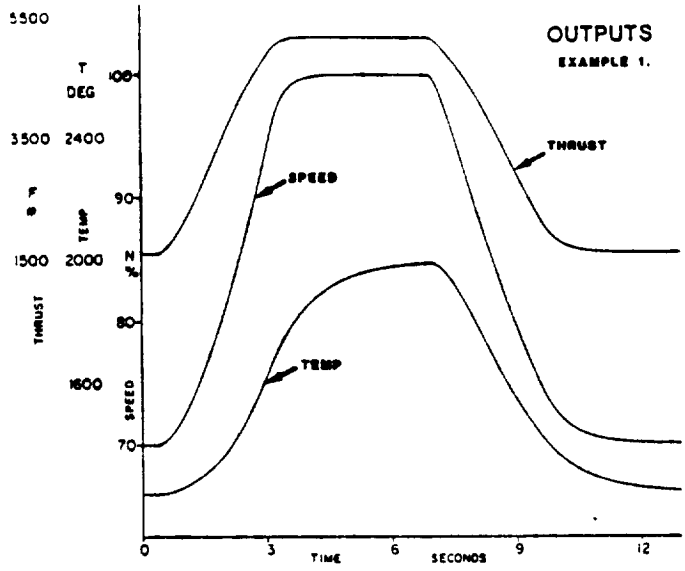

Figure 13.

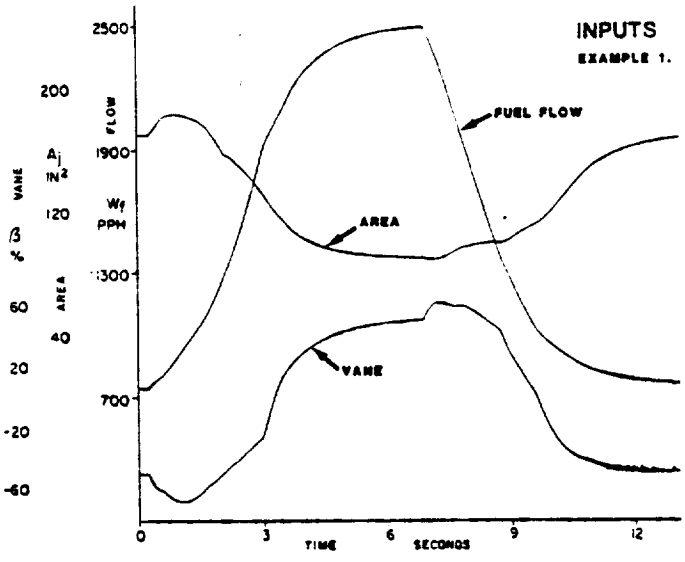

Figure 14.

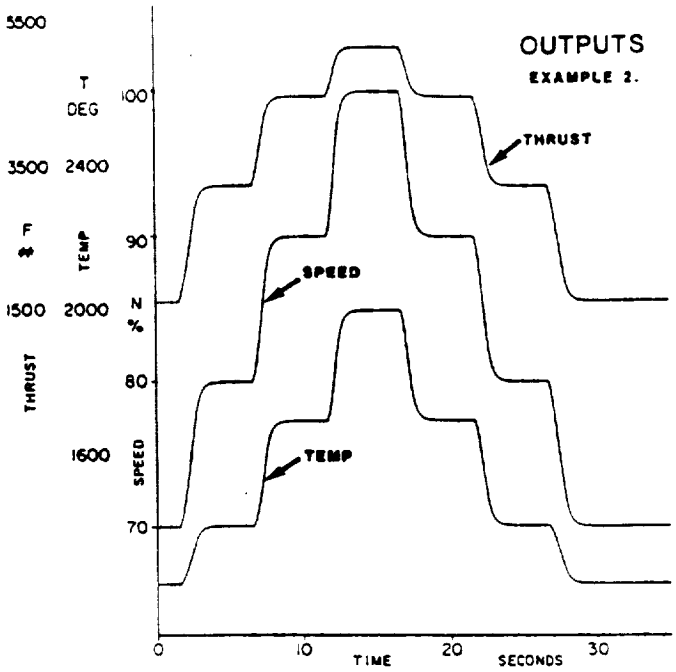

Figure 15.

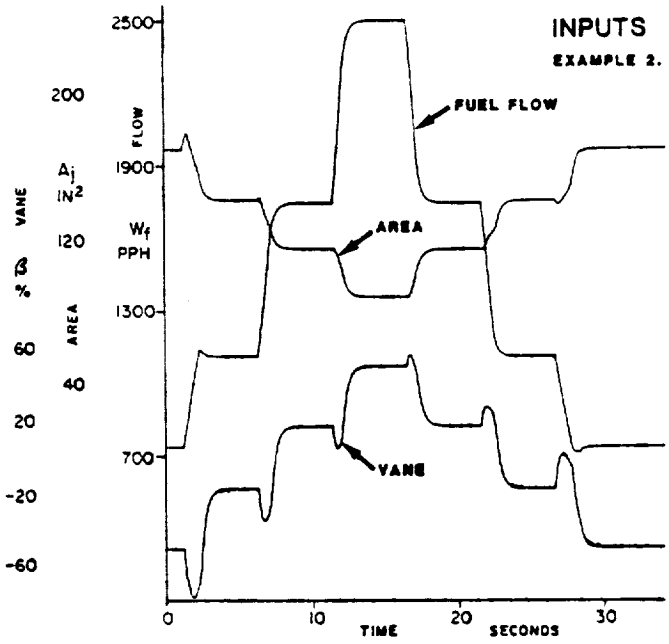

Figure 16.

Example 2. Demonstrate strategy 2. We choose the dynamic response of every output to be identical and we choose to fit this response over the speed range. This strategy is used to keep the system nearer to the steady state operating line during transients. Decoupled output response is chosen and the elements of the diagonal matrix were selected 1/(.3s+1). The response of the system for small step inputs is shown in Figures 15 and 16.

V33 over

Example 3. Demonstrate robustness of the controller relative to engine parameter variation. Response strategy 1 from Example 1 is chosen as the desired performance. The engine time constants on speed, temperature and pressure were slowed by a factor of 2. This is a large variation of engine parameters and a good test of control robustness. Step transients comparing engine output and input responses for the nominal engine and the slow engine are shown in Figures 17 and 18. The controller maintains output response at desired conditions and produces different control response action for the slow engine, as needed.

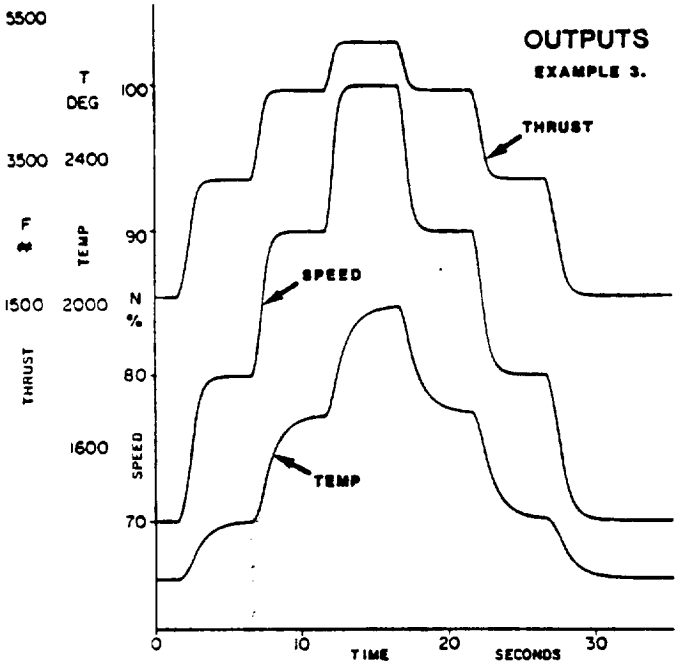

Figure 17.

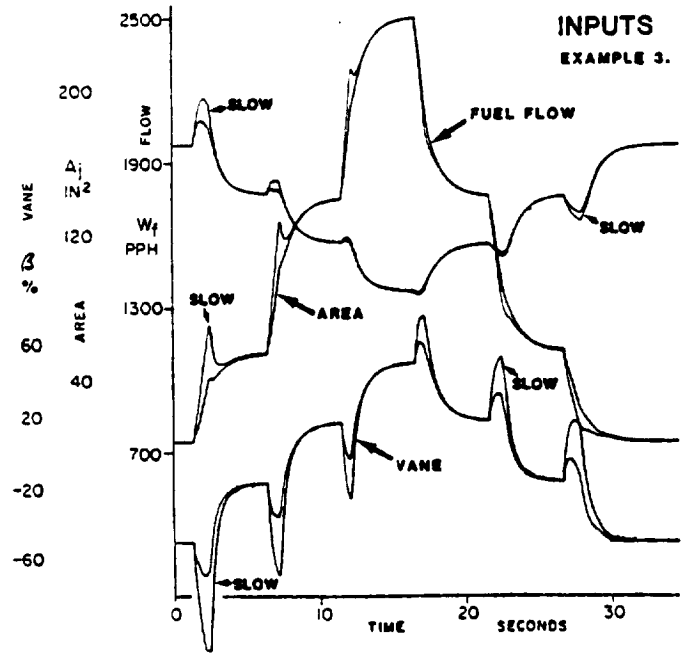

Figure 18.

SUMMARY

A synthesis approach for nonlinear multivariable systems was discussed. Features of the approach include the capability to synthesize nonlinear feedback control systems directly to produce desired response and desired sensitivity performance. Emphasis was placed on application viewpoint.

ACKNOWLEDGMENT

The authors acknowledge the significant contribution of Mr. Ben Jacobs, Allied-Bendix Energy Controls Division, for simulation of the design examples on an AD-10 hybrid computer.

REFERENCES

1. J.L.Peczkowski and M.K.Sain, "Linear Multivariable Synthesis with Transfer Functions, "Alternatives for Linear Multivariable Control, M.K. Sain, J.L. Peczkowski, and J.L. Melsa, Editors, National Engineering Consortium, 1977, Pages 71-87.
2. J.L. Peczkowski, "Multivariable Synsthesis With Transfer Functions", Proceedings NASA Propulsion Controls Symposium, NASA CP-2137 Pages 111-128, May 1979.
3. J.L. Peczkowski, M.K. Sain, and R.J. Leake, "Multivariable Synthesis with Inverses", Proceedings Eighteenth Joint Automatic Control Conference, Pages 375-380, June 1979.
4. Joseph L. Peczkowski and Micahel K. Sain, "Control Design with Transfer Functions,an Application Illustration" Proceedings Twenty-Third Midwest Symposium on Circuits and Systems", Pages 47-52, August 1980.
5. Joseph L. Peczkowski and Michael K. Sain, "Scheduled Nonlinear Control Design for a Turbojet Engine", Proceedings IEEE International Symposium on Circuits and Systems, Pages 248-251, April 1981.
6. Michael K. Sain, Bostwick F. Wyman, R.R. Gejji, P.J. Antsaklis, and Joseph L. Peczkowski, "The Total Synthesis Problem of Linear Multivariable Control, Part I: Nominal Design", Proceedings Twentieth Joint Automatic Control Conference, Paper WP-4A, June 1981.
7. Michael K. Sain, P.J. Antsaklis, Bostwick F. Wyman, R.R. Gejji, and Joseph L. Peczkowski, "The Total Synthesis Problem of Linear Multivariable Control, Part II: Unity Feedback and the Design Morphism", Proceedings IEEE Conference on Decision and Control, Pages 875-884, December 1981.
8. Michel K. Sain and Joseph L. Peczkowski, "Nonlinear Multivariable Design by Total Synthesis", Proceedings American Control Conference, pages 252-260, June 1982.
9. Joseph L. Peczkowski and Michael K. Sain, "Design of Nonlinear Multivariable Feedback Controls by Total Synthesis", Proceedings American Control Conference, 1984
10. Rekasius, Z. V., "Linear Multivariable Control - A Problem of Specification," Proceedings, International Forum on Alternatives for Multivariable Control, National Engineering Consortium, pp.101-110, October 1979.
11. R.J. Leake, J.L. Peczkowski, and M.K. Sain, "Step Trackable Linear Multivariable Plants", International Journal of Control, Volume 30, Number 6, pages 1013-1022, December 1979.
12. Wyman, B.F. and Sain, M.K., "Essential Right Inverses and System Zeros", Proceedings 18th IEEE Conference on Decision and Control, pp.23-28, December 1979.
13. Bengtsson, Gunnar, "Feedback Realizations in Linear Multivariable Systems," IEEE Transactions on Automatic Control, Vol. AC-22, No.4, August 1977.
14. Cruz, J.B. Jr. (ed.), Feedback Systems, McGraw-Hill, New York, 1972.
15. Michael K. Sain and Abraham Ma, "Multivariable Synthesis with Reduced Comparison Sensitivity", Proceedings Nineteenth Joint Automatic Control Conference, Paper WP-8B, August 1980.

D34

D35

NONLINEAR CONTROL BY COORDINATED FEEDBACK SYNTHESIS WITH GAS TURBINE APPLICATIONS

Michael K. Sain
Electrical Engineering Department
University of Notre Dame
Notre Dame, Indiana 46556

Joseph L. Peczkowski
Energy Controls Division
Allied-Bendix Aerospace
South Bend, Indiana 46620

ABSTRACT

Broadly understood, the tasks of a feedback controller are to close loops and to inject signals into those loops. The performance of a feedback control system depends upon both of these tasks, which are interdependent. In this paper, we study conditions under which the tasks may be separated. In a most general setting, we define separation in terms of the assumption that a match between desired and actual loop responses implies zero feedback action. It is then shown that such a feature implies what may be termed feedforward signal coordination; moreover, under slightly stronger assumptions, such signal coordination implies separation. All the ideas are illustrated in terms of a three-input, three-output gas turbine simulation.

I. INTRODUCTION

The work reported here is part of a continuing effort [1 - 26] by the authors to formulate some theoretical and some practical views concerning current nonlinear design procedures in aircraft gas turbine engines. We illustrate our ideas in the context of a three-input, three-output gas turbine simulation.

Acceptable response, simple controllers and clear insight are hallmarks of successful design for multivariable control systems. Even when perfect plant knowledge is available and there are no system disturbances, the development of reasonable response specifications, and their achievement in practice, is not a trivial matter. When the plant is uncertain, or acted upon by disturbances, or unstable, the choice of feedback realization of the controller may place the response goals in competition with new goals such as internal stability, sensitivity suppression, and disturbance rejection. It is important to reduce the effects of such competition. One way to approach this goal is to eliminate the competition when plants are accurately described and disturbances are inconsequential. Then, when such is not the case, the loop activity may be directed to suppression and rejection.

This paper discusses such a possibility. A companion paper in this proceedings, entitled "Synthesis of System Response: A Nonlinear Multivariable Control Design Approach", examines the design implementation of such ideas, down to controller construction and system simulation.

II. PRELIMINARIES

It is a relatively rare thing for a control engineer to be given a plant description in terms of explicit differential equations expressed in terms of textbook special functions. Instead, plant differential equations must ordinarily be inferred implicitly from a digital simulation supplied by the manufacturer. We view the textbook differential equation as a compact symbolism with which to describe simulations; and we shall endeavor to describe as much of the design process as possible in these terms.

By a system we shall mean a set of n ordinary differential equations,

$$\dot{x}_i = f_i(x_1, x_2, \ldots, x_n, u_1, u_2, \ldots, u_m)$$

for $i = 1,2,3, \ldots, n$, together with a list of p functions

$$y_j = g_j(x_1, x_2, \ldots, x_n, u_1, u_2, \ldots, u_m)$$

for $j = 1,2,3, \ldots, p$. The system state x is $(x_1, x_2, \ldots, x_n)$; the system input u is $(u_1, u_2, \ldots, u_m)$; and the system output y is $(y_1, y_2, \ldots, y_p)$. We shall regard (x, u, y) as being resident in a function subset $S \subset X \times U \times Y$, where X, U, and Y are real vector function spaces and $X \times U \times Y$ is the product of X with U with Y. Such a subset S is called a relation. If we agree upon the conventions $f = (f_1, f_2, \ldots, f_n)$, $g = (g_1, g_2, \ldots, g_p)$, $\dot{x} = (\dot{x}_1, \dot{x}_2, \ldots, \dot{x}_n)$, then we have the textbook description

$$\dot{x} = f(x,u) \; ; \quad y = g(x,u) \; ;$$

briefly, we may refer to (f, g) as the system. By itself, without the subset S, it is typically the case that (f, g) has little engineering significance.

With the plant simulation being provided by the manufacturer, it is reasonable to assume that S is a feature of that simulation. With regard to controller simulation, we shall assume that appropriate (f, g) and S are indicated implicitly and constructively by the design process. It is sometimes useful to project S upon X, U, and Y to obtain S_X, S_U, and S_Y, respectively. However, care must be used in interpreting these "factor" sets.

Feedback systems make use of interconnections; and each component system which participates in the connection is identified by some functions, as for example (f, g). It is natural, therefore, that the designer will become involved with certain questions which depend upon the relationships between and among functions. In many cases, such relationships can be pictured concisely by arrow diagrams.

D33

Begin with the functions f and g. Each operates on pairs (x, u) in X x U. If we assume that X contains first derivatives of its elements x, then f and g have arrow diagram representations:

$$X \times U \xrightarrow{f} X \; ; \quad X \times U \xrightarrow{g} Y \; .$$

The set at the arrowhead is called the codomain of the function, while the other set is called its domain. Domains and codomains may also be indicated, in line, by the notations $f : X \times U \to X$ and $g : X \times U \to Y$.

To illustrate the study of relationships by diagrams, we make use of the fact that X and U are real vector spaces, so that we can write

$$r(x, u) = (rx, ru) \; ; \quad (x, u) = (x, 0) + (0, u).$$

With these operations X x U is a direct sum, denoted by $X \oplus U$. Such spaces have projections and injections defined as follows:

$$p_X : X \oplus U \to X \; ; \quad p_X(x, u) = x \; ;$$

$$p_U : X \oplus U \to U \; ; \quad p_U(x, u) = u \; ;$$

$$i_X : X \to X \oplus U \; ; \quad i_X(x) = (x, 0) \; ;$$

$$i_U : U \to X \oplus U \; ; \quad i_U(u) = (0, u) \; .$$

In Figure 1, we have drawn in solid arrows for the functions f, i_X, and i_U; we have drawn in dashed arrows for two new functions $a : X \to X$ and $b : U \to X$. The solid arrows refer to given functions;

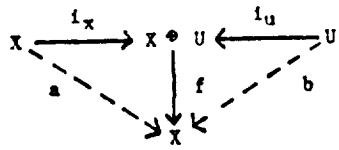

Figure 1.

the dashed arrows indicate possible new functions. In order to be able to change the dashed arrows to solid arrows, we must define a and b so that the diagram "commutes". A diagram commutes when alternate paths from the same begin set to the same end set give the same result for each element in the begin set. By way of example, define $a(x) = f(x, 0)$; then the left triangle in Figure 1 commutes because $f(i_X(x)) = f(x, 0) = a(x)$. We write this as $a = f \circ i_X$, where $\circ$ denotes function composition. No other definition for a is possible. In like manner, we must choose $b = f \circ i_U$ to make the diagram commute. In case f is a linear function, then $f(x, u) = a(x) + b(u)$ where a and b are linear as well, by calculations such as

$$f(x, u) = f\big((x, 0) + (0, u)\big) = f(x, 0) + f(0, u).$$

In the next section we can make immediate application of a counterpart of Figure 1, even when the function fails to be linear. Consider a function $c : V \to W \oplus Z$, as in Figure 2. Along the

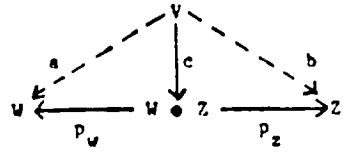

Figure 2.

lines just discussed, the choices $a = p_W \circ c$ and $b = p_Z \circ c$ make the diagram commute. Moreover

$$c = i_W \circ a + i_Z \circ b$$

even though a, b, and c are nonlinear functions. Proof rests upon the calculation

$$\begin{aligned} c(v) &= i_W\big(a(v)\big) + i_Z\big(b(v)\big) \\ &= i_W\big(p_W(c(v))\big) + i_Z\big(p_Z(c(v))\big) \\ &= i_W(w) + i_Z(z) \end{aligned}$$

when $c(v) = (w, z)$. This important result states that nonlinear systems with two outputs split naturally into a pair of nonlinear systems, each of which produces one output.

One other concept which is also helpful in Section III is the generalized derivative.

Let V and W be normed real vector spaces with $Z \subset V$ an open subset. A function $f : Z \to W$ is differentiable at a point p in Z if there exists a continuous linear map $F : V \to W$ such that, for $(p + h)$ in Z and h in V,

$$\lim_{||h|| \to 0} \frac{|| \; f(p + h) - f(p) - Fh \; ||}{|| \; h \; ||} = 0 \; .$$

If F exists, then it is unique and is called the derivative of f at p, and is denoted by $(Df)(p) : V \to W$. In case f is differentiable on Z, then we have a construction $Df : Z \to L(V, W)$, where the right member denotes the real vector space of real linear maps $V \to W$.

With the notion of generalized differentiation comes the associated idea of Taylor representation. For the present, we wish only to observe that the expansion

$$f(z) = f(p + h) = f(p) + (Df)(p)h + \ldots$$

is available when the required smoothness conditions hold.

III. STRUCTURE SEPARATION

The feedback system is comprised of a plant and a controller. The plant will be described by a function $p : S_u \to S_y$ induced by the system (f, g) explained in Section II. We assume that the value of x at the left support point is fixed for the problem and that the system has finite time horizon. Relative to the feedback controller, we choose to control the entire system from a point of reference r, which is an element of the function set $S_r \subset R$, also a real vector function space.

General equations for the controller are of the form

$$\dot{x}_c = f_c(x_c, r, y), \quad u = g_c(x_c, r, y)$$

on a suitably designed subset $S_c \subset X_c \times R \times Y \times U$, with X_c a real vector function space. Analogously, we introduce the function $c : (S_c)_r \times (S_c)_y \to (S_c)_u$ and summarize these features in Figure 3. We must arrange in our design process that the feedback system of Figure 3 is properly posed, in the sense that x_c and x, at their left support points, together with r in $(S_c)_r$ determine (x, x_c, r, u, y) in a subset $S_{fb} \subset X \times X_c \times R \times U \times Y$ associated with an overall feedback system (f_{fb}, g_{fb}).

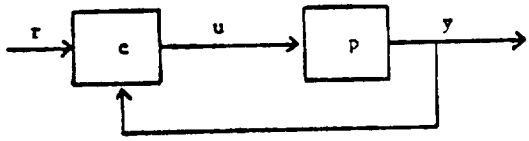

Figure 3.

Technically, on a finite time interval, we may not with acceptable control action achieve a steady state in Figure 3, unless such steady state matches the system variables at the left time support. In practice, however, we may not only achieve one steady state, but several. The idea may be approached as follows. Let $(\bar{x}, \bar{x}_c, \bar{r}, \bar{u}, \bar{y})$ be a quintuple of constant functions which satisfy the system equations in Figure 3:

$$f(\bar{x}, \bar{u}) = 0 \; ; \quad \bar{y} = g(\bar{x}, \bar{u}) \; ;$$

$$f_c(\bar{x}_c, \bar{r}, \bar{y}) = 0 \; ; \quad \bar{u} = g_c(\bar{x}_c, \bar{r}, \bar{y}) \; .$$

We shall assume that, whenever this is the case, the reference point $\bar{r}$ infers $\bar{u}$ and $\bar{y}$. Clearly, such a quintuple need not lie in S_{fb}, because $\bar{x}$ and $\bar{x}_c$ need not match left support values for x and x_c, respectively. But it may happen that $(\bar{x}, \bar{x}_c, \bar{r}, \bar{u}, \bar{y})$ is approached quite closely by some (x, x_c, r, u, y) which is in S_{fb}, over some subset of the time support.

To make this notion precise, introduce the ideas that X, X_c, R, U, and Y are spaces which, at any point of time support, contain functions whose values are vectors in appropriate finite dimensional real spaces. Establish norms on these last five spaces, and develop a norm on their product in the usual way. Close approach of (x, x_c, r, u, y) to $(\bar{x}, \bar{x}_c, \bar{r}, \bar{u}, \bar{y})$ means that, for prespecified (ε, δ), there exist times $t_1(\varepsilon, \delta) < t_1(\varepsilon, \delta) + \delta < t_2(\varepsilon, \delta)$ such that

$$(x(t)-\bar{x}, x_c(t)-\bar{x}_c, r(t)-\bar{r}, u(t)-\bar{u}, y(t)-\bar{y})$$

is less than ε in norm for $t_1(\varepsilon, \delta) < t < t_2(\varepsilon, \delta)$. To get the practical result, we choose ε very small and δ of reasonable size. In practice, the value of ε may be conveniently inferred from the resolving capability of available sensors.

Denote by $\bar{S}_{fb}$ the set of such $(\bar{x}, \bar{x}_c, \bar{r}, \bar{u}, \bar{y})$ which can be approached closely by elements of S_{fb}. We wish to extend the definition of p to include such steady inputs and outputs. For any point in $\bar{S}_{fb}$, select the associated pair $(\bar{u}, \bar{y})$ and define $\bar{p} : (\bar{S}_{fb})_u \to (\bar{S}_{fb})_y$ by $\bar{y} = \bar{p}(\bar{u})$. For this definition to be sound, we cannot allow two points in $\bar{S}_{fb}$ with associated pairs $(\bar{u}, \bar{y}_1)$ and $(\bar{u}, \bar{y}_2)$, unless $\bar{y}_1 = \bar{y}_2$. One way to assure this feature is to require that two points in $\bar{S}_{fb}$ with associated pairs $(\bar{x}_1, \bar{u})$ and $(\bar{x}_2, \bar{u})$ satisfy $\bar{x}_1 = \bar{x}_2$. We shall make this assumption for the plant, and refer to $\bar{p}$ as the plant steady-state input-output map. Along the same lines, we construct

$$\bar{c} : (\bar{S}_{fb})_r \times (\bar{S}_{fb})_y \to (\bar{S}_{fb})_u .$$

With these maps in place, we have Figure 4.

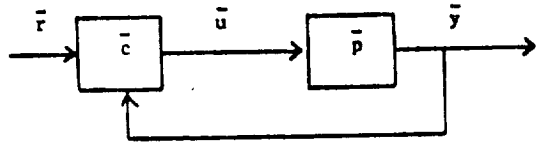

Figure 4.

The equations for Figure 4 are $\bar{y} = \bar{p}(\bar{u})$, $\bar{u} = \bar{c}(\bar{r}, \bar{y})$. We shall require that $\bar{r}$ in these equations implies $\bar{u}$ and $\bar{y}$.

The role of the controller c is twofold: to close the loop and to inject suitable command signals into the loop. Generally, the task of a controller is to produce desired plant outputs with the aid of acceptable plant inputs. In keeping with control practice, we shall inject one signal, y_r, corresponding to desirable plant output behavior, and another signal, u_r, corresponding to acceptable plant input behavior. Both signals to be injected are assumed to be generated by r alone. With these steps, we have Figure 5. The function

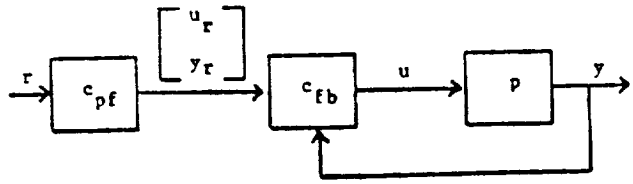

Figure 5.

$c_{pf} : (S_{fb})_r \to U \times Y$ is the input/output function of a prefilter. The function $c_{fb} : (U \times Y) \times (S_{fb})_y \to (S_{fb})_u$ is the input/output function of the feedback part of the controller, namely that part which closes the loop and executes command injection.

Because $U \times Y$ admits the direct sum structure $U \oplus Y$, we see that the function prefilter c_{pf} can play the role of c in Figure 2, Section II. Simply identify $V = (S_{fb})_r$, $W = U$, and $Z = Y$. Note carefully that V need not be a vector space. The result is that

$$c_{pf} = i_u \circ a + i_y \circ b,$$

which can be diagrammed as in Figure 6. Clearly,

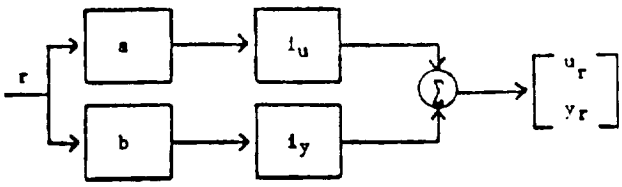

Figure 6.

the essential part of c_{pf} in Figure 6 is the pair of functions (a, b). We show these explicitly in Figure 7 while incorporating the functions i_u, i_y, and the sum junction into c_{fb}, without loss of generality.

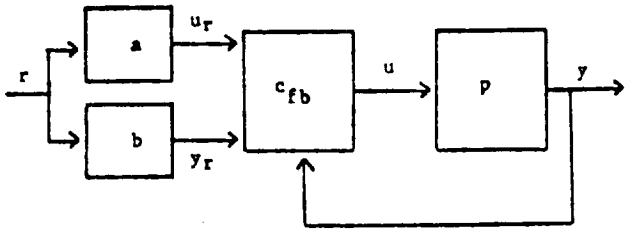

Figure 7.

Controller Separation

Next we wish to place a single constraint upon c_{fb}. Notice that $u = c_{fb}(u_r, y_r, y)$, from Figure 7. Make the following assumption: When $y = y_r$, then $c_{fb}(u_r, y_r, y) = u_r$. Intuitively, this means that a balance of the desirable plant output behavior with the actual plant output behavior implies the feedback controller producing plant input behavior equal to that desired. This assumption, in the context of Figure 7, would require $y_r = p(u_r)$. Because of the way u_r and y_r are generated, we have as a consequence that $b(r) = p(a(r))$ or $b = p \circ a$. When a pair (a, b) satisfies this condition, we shall use the notation $a = m$, $b = t$ and the terminology that (m, t) constitutes a coordinated synthesis of the prefilter. Such (m, t) satisfy the commutative diagram of Figure 8.

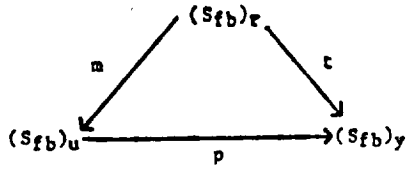

Figure 8.

Moreover, the choice (a, b) = (m, t), with (m, t) as shown in Figure 8, has the corresponding converse property if the plant satisfies an invertibility condition $u = p^{-1}(y)$ on S_{fp}. Indeed, when $y = y_r$, we find

$$p^{-1}(y) = p^{-1}(y_r) = p^{-1}(t(r))$$

$$= p^{-1}(p \circ m)(r) = m(r) = u_r$$

which, in the system of Figure 7 means that $c_{fb}(u_r, y_r, y_r) = u_r$.

With reference to the last subsection of Section II, we observe that, under appropriate conditions,

$$c_{fb}(u_r, y_r, y) = c_{fb}(u_r, y_r, y_r + (y - y_r))$$

$$= c_{fb}(u_r, y_r, y_r) + (Dc_{fb})(u_r, y_r, y_r)(y - y_r)$$

to a first order approximation. The first term in the right member is, under our assumption on c_{fb}, just u_r. If we simplify the notation by

$$c_{fb}(u_r, y_r, y) = u_r - g_r(y - y_r),$$

then we can further develop Figure 7 into Figure 9.

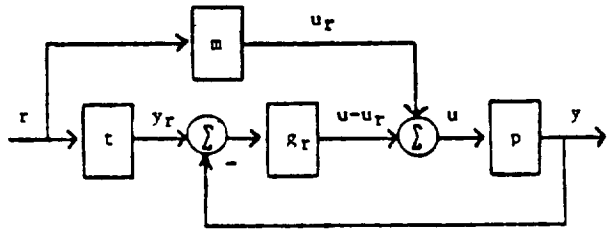

Figure 9.

Inasmuch as g_r is a linear map, $y = y_r$ implies $u = u_r$, as assumed. Under such circumstances, the loop is closed, but the output of g_r is zero. We call this separation of prefilter signal injection from feedback filter action a coordination of feedforward control.

Notice that, with the configuration of Figure 9, (a, b) equal to (m, t), with (m, t) as in Figure 8, is a necessary and sufficient condition for separation, even if p fails to invert.

The above ideas on separation may be carried through to the steady state case, with the agreements described earlier in this section. In this event, one introduces the diagram of Figure 10.

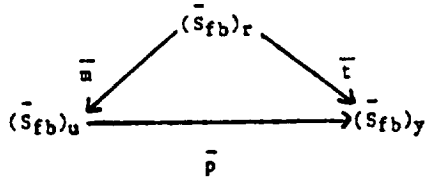

Figure 10.

The analysis above indicates that, under very modest assumptions, feedforward coordination by means of the prefilter pair (m, t) in Figure 8 is virtually inevitable in the design process. In the remainder of this paper, we relate $(\bar{m}, \bar{t})$ in Figure 10 to the real-world design process, with the aid of the simulation of Section IV. In the companion paper, described in Section I, we address the design issues associated with Figure 8. As a practical matter, it is also desirable to separate the portion of the controller which realizes $(\bar{m}, \bar{t})$ from that which completes (m, t). In this way, if specified steady state operating conditions change, only one feature of the controller has to be modi-

fied. Conceptually, we can accomplish this by factoring $(\bar{m}, \bar{t})$ out of (m, t). The result of this factorization is a sort of "unit gain" pair $(\bar{m}, \bar{t})$, which is used in the companion paper without tildes.

IV. GAS TURBINE ENGINE

A nonlinear simulation of a turbojet engine is shown in Figure 11. It is representative, on a small scale, of the kind of nonlinear plant which we have mentioned above and with which designers of turbine engines and turbine controls currently deal in practice. In essence, it is a computer simulation, typically constructed by engine manufacturers and provided to control designers.

The model describes nonlinear steady state and dynamical relationships between three plant inputs and six plant outputs. The nonlinear simulation consists of three integrators, nine nonlinear functions or schedules (including five bivariant schedules), six multiplications, three divisions, and nine additive junctions. The plant inputs are W_f, fuel flow, A_j, exhaust nozzle area, and β, turbine vane position; and the six outputs are N, engine speed, T_4, turbine temperature, P_3, compressor pressure, P_5, tailpipe pressure, T_5, tailpipe temperature, and FN, engine thrust. The set of nonlinear functions used to describe the dynamics of the turbine engine are included as Figures 12 through 20. This way of describing nonlinear relationships is typical of current practice for turbine engines, as also for other nonlinear, physical plant descriptions. Note that they are relatively smooth and not easily described by textbook special functions.

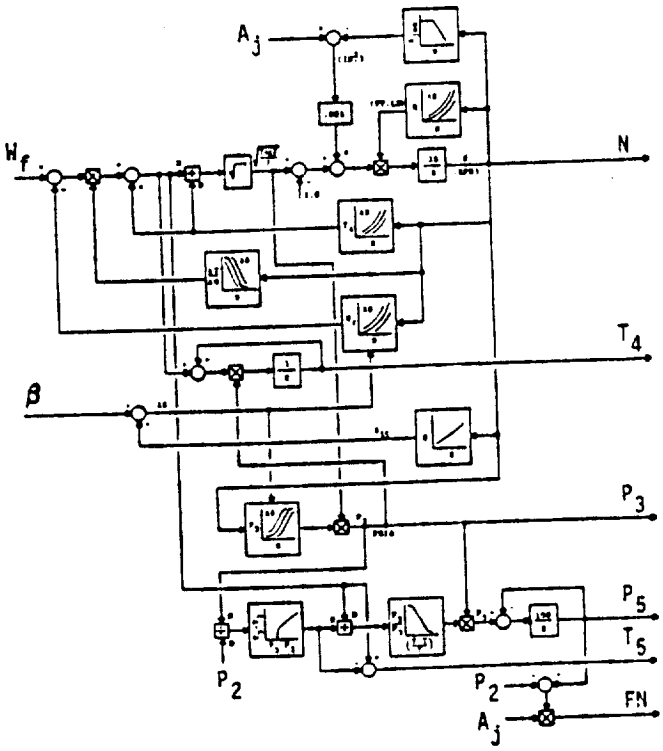

Figure 11.

V. OPERATING LINE

Refer now to Figure 7 in Section III. By an operating point, we shall mean the component $\bar{y}$ in any fivetuple $(\bar{r}, \bar{u}_r, \bar{y}_r, \bar{u}, \bar{y})$ which satisfies the system equations $\bar{u}_r = \bar{a}(\bar{r})$, $\bar{y}_r = \bar{b}(\bar{r})$, $\bar{u} = \bar{c}_{fb}(\bar{u}_r, \bar{y}_r, \bar{y})$, $\bar{y} = \bar{p}(\bar{u})$ and which can be approached closely by an element in S_{fb}. For the turbojet engine simulation of Section IV, such an operating point is given by N = 10,200 RPM, T_4 = 1,157.6 °R, and FN = 758.6 LBS, if we choose N, T4, and FN as the three outputs to be controlled. Inasmuch as all functions involved in the definition of an operating point are constant with time, and because all these functions take their values at any time in a finite dimensional real vector space, it is always possible to regard an operating point as such a list of real numbers. In other words, $\bar{Y} = \mathbb{R}^p$, where $\bar{Y} \subset Y$ is the subspace of constant functions.

It is straightforward to depict operating points for Section IV in $\mathbb{R}^3$. For the numeric example above, the operating point can be shown as in Figure 21.

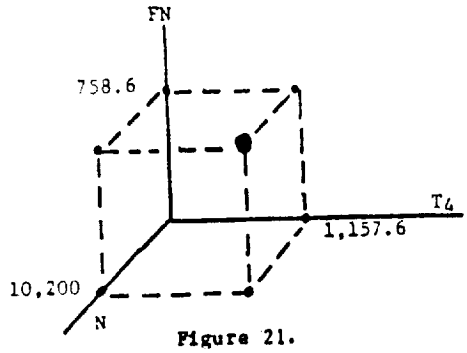

Figure 21.

We next introduce a family of such points:

N	T_4	FN
10,200	1,157.6	758.6
11,900	1,242,4	1,603.2
13,600	1,403.5	3,213.0
15,300	1,693.7	4,439.0
17,000	1,996.5	5,110.0
18,700	2,241.2	5,434.0

with units in RPM, °R, and LBS, respectively, as before. Note that our previous example of an operating point is just the first of these. We sketch the operating points in Figure 22, where we have joined them with a smooth curve.

An operating line is then a smooth curve of operating points $\bar{y}$ through which we wish our feedback system to be able to pass, that is, to which we wish the solution y of our feedback system to be able to approach closely. Discussion of theoretical features of operating lines has not received much attention in the literature. The dynamic characteristics of nonlinear control design, the numerical conditioning of control algorithms, and the sensitivity of feedback systems may be greatly affected by operating line design.

We shall define an operating line as a function. To see the idea behind this, we have only

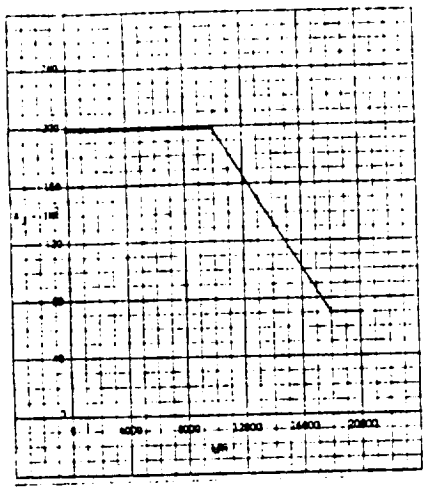

Figure 12.

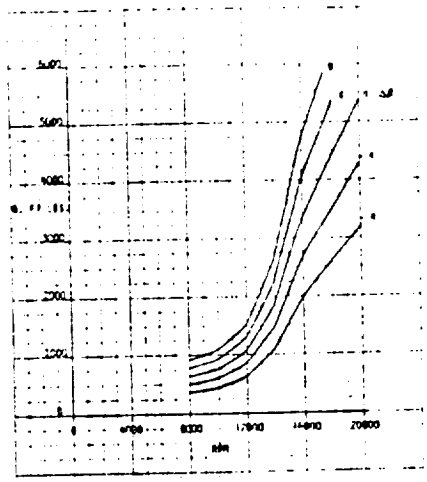

Figure 13.

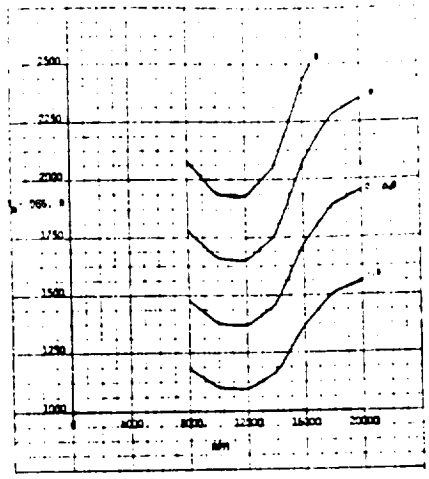

Figure 14.

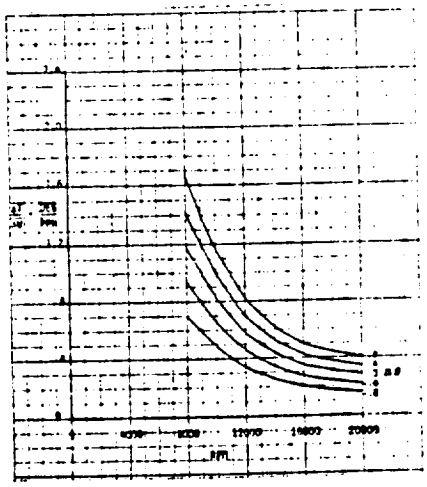

Figure 15.

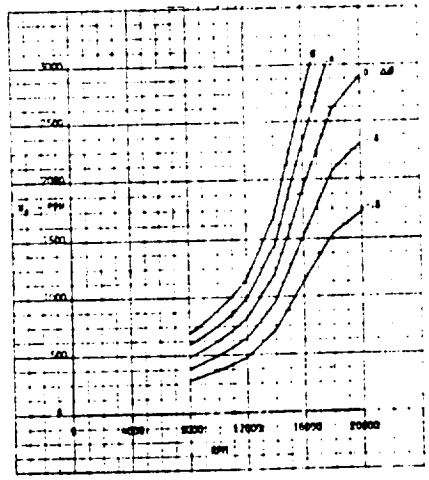

Figure 16.

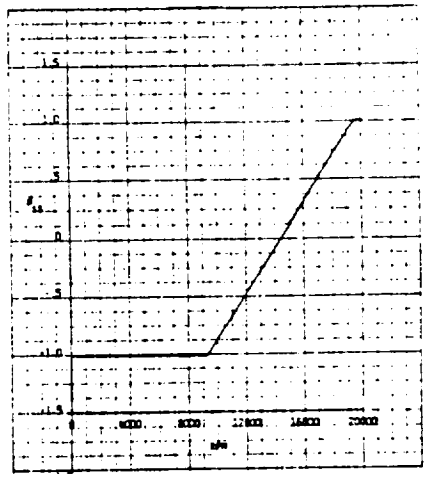

Figure 17.

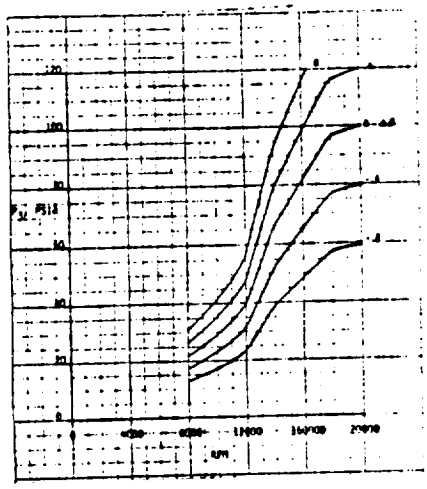

Figure 18.

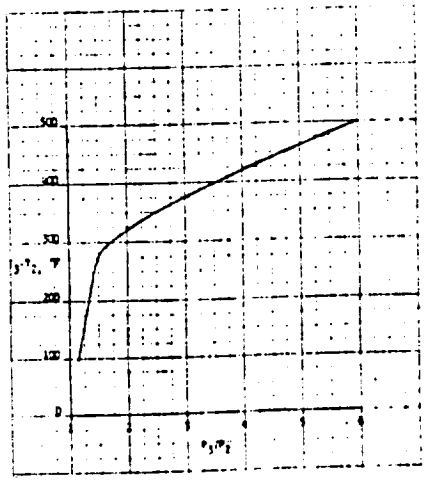

Figure 19.

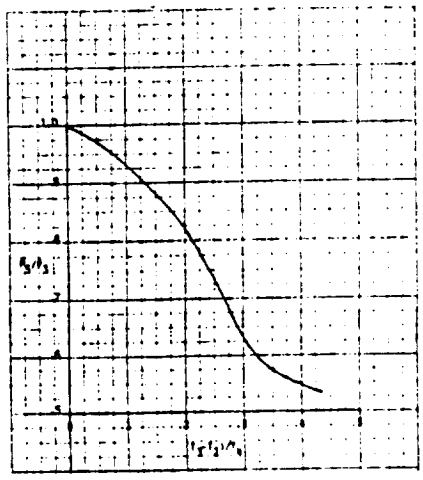

Figure 20.

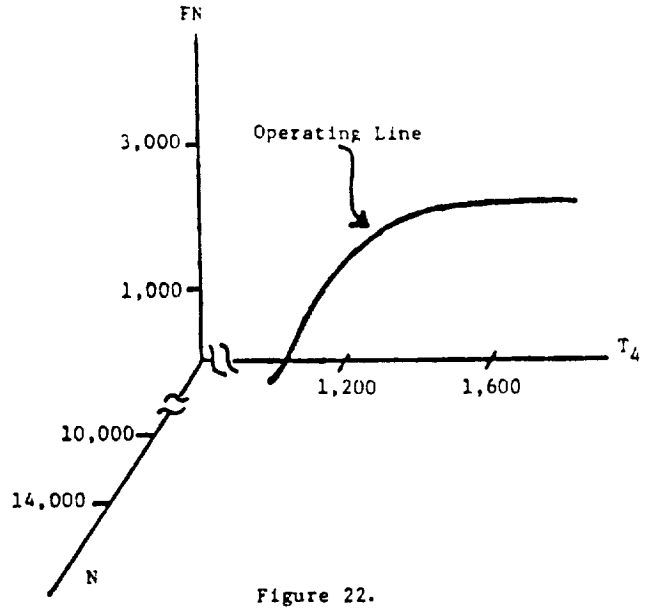

Figure 22.

to examine Figure 23, where the abscissa has been chosen as the "number" of the operating point.

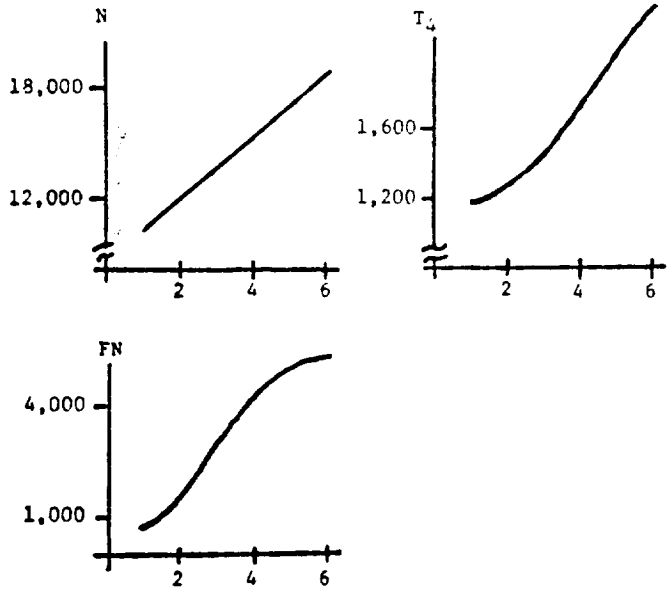

Figure 23.

These three graphs define a function from the set of numbered points to $\bar{Y}$ for the turbojet simulation. Frequently, the operating point number may be associated with some tangible "dial setting" variable associated with the controller. For the turbojet of Section IV, this variable is Power Lever Angle (PLA) which is given in degrees. Typical PLA settings for Figure 23 are listed below:

Operating Point	1	2	3	4	5	6
PLA(°)	60	70	80	90	100	110

Intuitively, PLA can be described as a throttle setting for the engine. Certain percentage settings may be associated with engine idle, engine cruise, and so forth. In our illustration, then, the operating line is a function $\bar{\alpha} : (PLA) \to R^3 = \bar{Y}$ from the indicated set of power lever angles into triples of real numbers corresponding to engine speeds, turbine temperatures, and thrust.

In general, we shall understand an operating line as a function $\bar{\alpha}$ from a set of references to RP. Each point in the image of α is an operating point for the feedback system. The image of $\bar{\alpha}$ produces a curve in $\bar{Y}$, with its argument acting as a parameter on the curve. Since a single parameter suffices to locate a point on such a curve, the set of references may be imbedded in a one-dimensional real vector space R.

VI. SCHEDULE DESIGN

Schedules provide a convenient, versatile and pictorial way to represent nonlinear function relationships associated with abstract functions and operators. In effect, the control designer constructs schedules which then imply the functions. Schedules serve to maintain designer insight and influence. Moreover, schedules provide a concrete way in which to deliver abstract functions to the customer. Refer to Section II.

Our objective is to use these kinds of nonlinear plant descriptions in a systematic manner to design nonlinear controllers. In this section, we address steady state schedules. These schedules may be regarded as steady state instructions to the controller. We shall define them in this section, and give illustrations for our gas turbine engine application.

The treatment which follows assumes that an operating line has been completed. See Section V.

Recall the definition of an operating line as a function $\bar{\alpha}$ from a set of references R to RP. We select $(\bar{S}_{fb})_r$ as the set of references. See Section III. Thus $\bar{\alpha} : (\bar{S}_{fb})_r \to RP$ is the numeric context for our discussion.

In Section V, Figure 23 and the PLA table can be used to construct a representation of $\bar{\alpha}$. First choose $(\bar{S}_{fb})_r = \{60, 70, 80, 90, 100, 110\}$, the set of six real numbers. Joining the points, as in Figure 23, with an appropriately smooth curve would then extend $(\bar{S}_{fb})_r$ to $[60, 110]$, the closed interval.

For the purposes explained in Section III, we shall assume that the plant is steady-state invertible. In terms of Figure 8, this means that we have the commutative diagram of Figure 24. A table

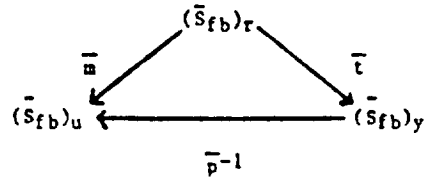

Figure 24.

can be drawn for $\bar{p}^{-1}$ in the case of each operating point shown in Figure 22. We list this table below, making use of the calculation

$$(W_f, A_j, \beta) = \bar{u} = \bar{p}^{-1}(\bar{y}) = \bar{p}^{-1}(N, T4, FN).$$

To save space, for $\bar{y}$ we list only N:

N	W_f	β	A_j
10,200	557.5	-.833	194.8
11,900	747.5	-.5	168.1
13,600	1,114	-.167	141.4
15,300	1,748	.167	114.7
17,000	2,497	.5	88.0
18,700	3,156	.833	72.28

W_f is in pounds per minute; Aj is in square inches; and β is a normalized degree variable. We can use this information to define a function $\bar{\beta}$: [60, 110] $\rightarrow R^3$ as in Figure 25.

So constructed, $\bar{p} \circ \bar{\beta} = \bar{\alpha}$, which means that the choice $(\bar{\beta}, \bar{\alpha}) = (\bar{m}, \bar{t})$ is possible, and $(\bar{\beta}, \bar{\alpha})$ is a coordinated, steady state, feedforward synthesis, in the sense of Figure 8. For realization, it is useful to construct $\bar{m}$ in the form $\bar{p}^{-1} \circ \bar{t}$, as shown in Figure 26.

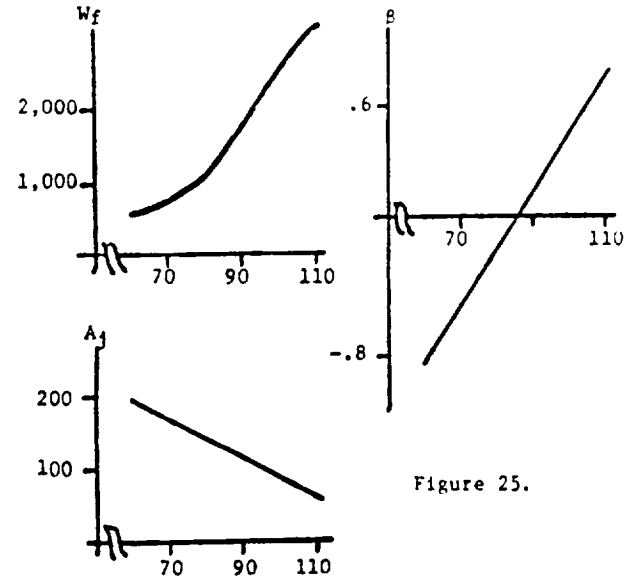

Figure 25.

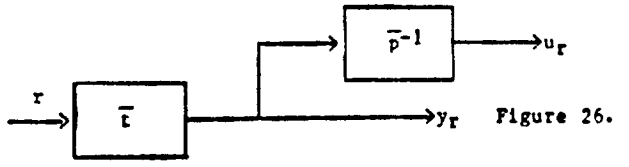

Figure 26.

VII. CONCLUSIONS

The tasks of a feedback controller are to close loops and inject signals into those loops. Under broad assumptions, in this paper we have studied a condition under which these tasks may be separated. In simplest terms, we have assumed that the controller is to produce acceptable control action when the plant is producing desirable responses. Then the prefilter must be a pair of functions (m, t) related by p, what we call a coordinated synthesis. For a realistic gas turbine model, we have illustrated the construction of (m, t) in the steady state. A companion paper in this proceedings illustrates the rest of the design process. Refer to Section I.

REFERENCES

1. M.K. Sain, "The Theme Problem," Alternatives for Linear Multivariable Control, M.K. Sain, J.L. Peczkowski, and J.L. Melsa, Editors, National Engineering Consortium, 1977, Pages 20-30
2. J.L. Peczkowski and M.K. Sain, "Linear Multivariable Synthesis with Transfer Functions," Alternatives for Linear Multivariable Control, M.K. Sain, J.L. Peczkowski, and J.L. Melsa, Editors, National Engineering Consortium, 1977, Pages 71-87
3. J.L. Peczkowski, "Multivariable Synthesis With Transfer Functions", Proceedings NASA Propulsion Controls Symposium, Pages 111-128, May 1979
4. J.L. Peczkowski, M.K. Sain, and R.J. Leake, "Multivariable Synthesis with Inverses", Proceedings Eighteenth Joint Automatic Control Conference, Pages 375-380, June 1979
5. R.J. Leake, J.L. Peczkowski, and M.K. Sain, "Step Trackable Linear Multivariable Plants", International Journal of Control, Volume 30, Number 6, Pages 1013-1022, December 1979
6. J.L. Peczkowski, "Total Multivariable Synthesis With Transfer Functions", Proceedings Bendix Controls and Control Theory Symposium, Pages 107-126, April 1980
7. A.F. Gejji, Ph.D. Thesis, "On the Total Synthesis Problem of Linear Multivariable Control", May 1980
8. Joseph L. Peczkowski and Michael K. Sain, "Control Design with Transfer Functions, an Application Illustration", Proceedings Twenty-Third Midwest Symposium on Circuits and Systems, Pages [illegible], August 198[illegible]
9. Michael K. Sain and Abraham Ma [illegible], "Multivariable Synthesis with Reduced Comparison Sensitivity", Proceedings Nineteenth Joint Automatic Control Conference, Paper WP-8A, August 198[illegible]
10. J.L. Peczkowski and S.A. Stopher, "Nonlinear Multivariable Synthesis With Transfer Functions", Proceedings Nineteenth Joint Automatic Control Conference, Paper WA-9D, August 198[illegible]
11. M.K. Sain, R.M. Schafer, and R.P. Dudek, "An Application of Total Synthesis to Robust Coupled Design", Proceedings Eighteenth Annual Allerton Conference on Communication, Control, and Computing, Pages 386-396, October 1980
12. Joseph L. Peczkowski and Michael K. Sain, "Scheduled Nonlinear Control Design for a Turbojet Engine", Proceedings IEEE International Symposium on Circuits and Systems, Pages 248-251, April 1981
13. Michael K. Sain and Joseph L. Peczkowski, "An Approach to Robust Nonlinear Control Design", Proceedings Twentieth Joint Automatic Control Conference, Paper FA-3D, June 1981
14. Michael K. Sain, Bostwick F. Wyman, A.R. Gejji, P.J. Antsaklis, and Joseph L. Peczkowski, "The Total Synthesis Problem of Linear Multivariable Control, Part I: Nominal Design", Proceedings Twentieth Joint Automatic Control Conference, Paper WP-4A, June 1981
15. P.J. Antsaklis and M.K. Sain, "Unity Feedback Compensation of Unstable Plants", Proceedings IEEE Conference on Decision and Control, Pages 309-310, December 1981
16. Michael K. Sain, P.J. Antsaklis, Bostwick F. Wyman, A.R. Gejji, and Joseph L. Peczkowski, "The Total Synthesis Problem of Linear Multivariable Control, Part II: Unity Feedback and the Design Morphism", Proceedings IEEE Conference on Decision and Control, Pages 875-884, December 1981
17. Michael Sain and Stephen Yurkovich, "Controller Scheduling: A Possible Algebraic Viewpoint", Proceedings American Control Conference, Pages 241-260, June 1982
18. Michael K. Sain and Joseph L. Peczkowski, "Nonlinear Multivariable Design by Total Synthesis", Proceedings American Control Conference, Pages 252-260, June 1982
19. Michael K. Sain and R. Michael Schafer, "A Computer-Assisted Approach to Total Feedback Synthesis", Proceedings American Control Conference, Pages 195-196, June 1982
20. P.J. Antsaklis and Michael K. Sain, "Feedback Controller Parameterizations: Causality and Hidden Modes", Proceedings Sixth International Symposium on Measurement and Control, International Association of Science and Technology for Development, August 1983
21. Kenneth P. Dudek, Michael K. Sain, and Bostwick F. Wyman, "Module Considerations for Feedback Synthesis of Sensitivity Comparisons", Proceedings Twenty-First Annual Allerton Conference on Communication, Control, and Computing, October 1983
22. P.J. Antsaklis and M.K. Sain, "Feedback Controller Parameterizations: Finite Hidden Modes and Causality", in Multivariable Control: New Concepts and Tools, S.G. Tzafestas, Editor, Dordrecht, Holland: D. Reidel Publisher, 1984
23. K.P. Dudek, Ph.D. Thesis, "The Total Synthesis Problem for Linear Multivariable Systems with Disturbances", May 1984
24. Joseph L. Peczkowski and Michael K. Sain, "Design of Nonlinear Multivariable Feedback Controls by Total Synthesis", Proceedings American Control Conference, 1984
25. R. Michael Schafer and Michael K. Sain, "Computer Aided Design Package for the Total Synthesis Problem", Proceedings Ninth Triennial World Congress, International Federation of Automatic Control, July 1984
26. P.J. Antsaklis and M.K. Sain, "Feedback Synthesis with Two Degrees of Freedom: (G,H:P) Controller", Proceedings Ninth Triennial World Congress, International Federation of Automatic Control, July 1984